Green Energetic Materials

Green Energetic Materials

Editor

TORE BRINCK
School of Chemical Science and Engineering,
KTH Royal Institute of Technology, Sweden

WILEY

This edition first published 2014

Registered office
John Wiley & Sons Ltd, The Atrium, Southern Gate, Chichester, West Sussex, PO19 8SQ, United Kingdom

Library of Congress Cataloging-in-Publication Data

Green energetic materials / [compiled by] Tore Brinck.
pages cm
Includes bibliographical references and index.
ISBN 978-1-119-94129-3 (cloth)
1. Fuel. 2. Explosives. 3. Green chemistry. I. Brinck, Tore, editor of compilation.
TP318.G74 2014
662.6–dc23 2013034800

A catalogue record for this book is available from the British Library.

HB ISBN: 9781119941293

Set in 10/12pt, Times-Roman by Thomson Digital, Noida, India

1 2014

Contents

List of Contributors

Tore Brinck, Applied Physical Chemistry, School of Chemical Science and Engineering, KTH Royal Institute of Technology, Sweden

David E. Chavez, WX Division, Los Alamos National Laboratory, USA

Carina Eldsäter, Swedish Defence Research Agency, FOI, Sweden

Thomas M. Klapötke, Department of Chemistry and Biochemistry, Energetic Materials Research, Ludwig-Maximilian University of Munich, Germany

Eva Malmström, School of Chemical Science and Engineering, KTH Royal Institute of Technology, Sweden

Jane S. Murray, Department of Chemistry, University of New Orleans, USA and CleveTheoComp, USA

Karl D. Oyler, U.S. Army Armament Research, Development and Engineering Center (ARDEC) Picatinny Arsenal, USA

Peter Politzer, Department of Chemistry, University of New Orleans, USA and CleveTheoComp, USA

Martin Rahm, Loker Hydrocarbon Research Institute and Department of Chemistry, University of Southern California, USA

Jesse J. Sabatini, US Army RDECOM-ARDEC, Pyrotechnics Technology & Prototyping Division, Pyrotechnics Research, Development & Pilot Plant Branch, USA

Jörg Stierstorfer, Department of Chemistry and Biochemistry, Energetic Materials Research, Ludwig-Maximilian University of Munich, Germany

Lynne Wallace, UNSW Canberra, University of New South Wales at the Australian Defence Force Academy, Canberra, Australia

Preface

It has become increasingly apparent that the use, or production, of many common energetic materials leads to the release of substances that accumulate in nature and can be harmful to humans or to the environment. As a consequence, the use of several important compounds has already been restricted or banned, and many more are expected to face restrictions in the near future. This has resulted in considerable research efforts aimed at developing sustainable alternatives with preserved performance. This book is an attempt to review the current status of the field of green energetic materials. My objective has been to cover the entire process in the development of a new energetic material, from the initial theoretical design to the optimization of the manufacturing process. In addition, the aim has been to consider all different types of energetic materials, including propellants, explosives and pyrotechnics, and both military and civilian applications. To ensure the quality and relevance of the description, I have invited active scientists that are all highly regarded experts in their respective fields to write the individual chapters.

The book is intended as a reference and an inspiration for academic, industrial, and government researchers active in the field of energetic materials. It should also find use as a textbook for courses at the graduate level.

In the first chapter I introduce the concept of green energetic materials and define it in the context of the principles of green chemistry. The particular issues that separate the production and use of energetic materials from other chemical products are highlighted and discussed. Furthermore, the development of green propellants for civil space travel is used as a case study to analyze the problems of taking an energetic material from the initial design phase to its final application.

In the subsequent chapter, Martin Rahm and I discuss the use of quantum chemical methods to design green energetic materials with targeted properties. We show that, while such procedures are very effective for identifying compounds with extreme performance levels, the real challenge often lies in devising routes for their synthesis and large-scale production. The focus of Chapter 3 is on the sensitivity for detonation of energetic materials. Peter Politzer and Jane Murray describe the current understanding of sensitivity at the molecular level, and identify molecular and crystalline features that can be used to design compounds with decreased risks of unintended detonations.

The advances in the development of green pyrotechnics are impressive, considering the diversity of the applications and the large number of toxic chemicals that traditionally have been used to achieve the special effects. Jesse Sabatini reviews the efforts that have been made to remove perchlorates, toxic heavy metals, and harmful organic compounds from pyrotechnic applications. In the subsequent chapter, Karl Oyler writes about similar developments in the field of primary explosives. Here, the main challenge has been to find replacements for lead azide and lead styphnate. Thomas Klapötke and Jörg Stierstorfer describe current efforts to develop greener secondary explosives. Their chapter focuses on

the synthesis and properties of tetrazole *N*-oxides; a class of compounds that shows great promise to hold a green alternative for the most common military explosive, RDX.

The following two chapters turn attention to the development of green propellants. In Chapter 7, Martin Rahm and I discuss recent advances in the understanding of ammonium dinitramide (ADN). This oxidizer, first synthesized in the 1970s in the former Soviet Union, has long been considered a potential green replacement for ammonium perchlorate in solid propellants. However, its implementation in solid formulations has been plagued with stability and compatibility issues. Due to new knowledge, gathered from theoretical and spectroscopic analyses, the chemical rationale behind these issues has been resolved and the potential for designing stable ADN-propellants has improved. In the following chapter, Carina Eldsäter and Eva Malmström discuss binder materials for green solid composite and homogeneous rocket propellants. They consider propellants based on ADN as well as other green oxidizers. This chapter highlights the many factors that need to be optimized in order to obtain a functional propellant formulation.

David Chavez reviews the development of sustainable manufacturing technologies for energetic materials in Chapter 9. According to the principles of green chemistry, it is not sufficient that the end product is benign, the entire manufacturing process should be environmentally friendly and make efficient use of natural resources. Challenges that are discussed include minimization of waste, reduced use of organic solvents, and the introduction of energy efficient synthesis procedures. Electrochemical synthesis is one such procedure that is discussed in more detail in Chapter 10. In this chapter, Lynne Wallace also describes the use of electrochemical methods for remediation of wastewater arising from the use and manufacture of energetic materials.

I am very grateful to all the authors that have contributed to this book. My hope is that you will appreciate their chapters as much as I have, and that you will find this book useful for your future endeavors in the exciting field of green energetic materials.

Tore Brinck
Sweden

1

Introduction to Green Energetic Materials

Tore Brinck

Applied Physical Chemistry, School of Chemical Science and Engineering,
KTH Royal Institute of Technology, Sweden

1.1 Introduction

The first energetic materials were developed in ancient China. Around 200 BC, Chinese alchemists were already starting to experiment with heating mixtures of saltpeter and sulfur. In the seventh century, saltpeter and sulfur were combined with charcoal to create an explosive material resembling what we today refer to as gunpowder. It was originally used for fireworks but soon became increasingly important for a range of military applications. The use of gunpowder in mining and civil engineering did not begin until the seventeenth century. Gunpowder remained the base for all energetic materials in practical use until the isolation of mercury(II) fulminate in 1799 by Edward Charles Howard. However, the first revolution in the development of energetic materials since the discovery of gunpowder started with the inventions of nitrocellulose (NC) in 1846 and nitroglycerine (NG) in 1847. NC was used as a propellant, whereas NG was mainly an explosive. Both these compounds had greatly enhanced performance compared to gunpowder. In 1866, Alfred Nobel introduced the original dynamite, a mixture of 75% NG with 25% kiselguhr, with a minor addition of sodium carbonate. It had much reduced sensitivity compared to pure NG and was, in contrast to NG, relatively safe to handle and transport. Nobel later developed gelatinous dynamite by combining NG with NC in a jelly. This material performed considerably better than the original

Green Energetic Materials, First Edition. Edited by Tore Brinck.

dynamite and additionally improved safety. These examples illustrate the two main objectives, to improve performance and safety, that have traditionally driven research on energetic materials. It is important to remember that, in the wider definition of energetic materials – which include propellants, explosives, and the large area of pyrotechnics – the definition of performance depends largely on the purpose of the intended device. For example, in the area of pyrotechnics, performance can relate to light intensity, gas generation or smoke production.

Since the end of the twentieth century it has been increasingly realized that the use, or production, of many energetic materials leads to the release of substances that are harmful to human health or to the environment. In some instances the use of certain compounds has been restricted, or even banned, as a consequence of legislative actions. The result is that new objectives have been enforced on the development of energetic materials. Today, almost all research in the area is focused on designing new materials that can be considered "green." This book intends to summarize the most recent developments in the area of green energetic materials, and to introduce the reader to some tools that are used in the research. However, before we embark on this journey, it may be valuable to try to define "green", and how this extra requirement relates to the objectives of maximizing performance and safety of handling.

1.2 Green Chemistry and Energetic Materials

The concept of "green chemistry" was first introduced in 1990s by the US Environmental Agency (EPA), and is briefly defined on their web site as [1]:

> To promote innovative chemical technologies that reduce or eliminate the use or generation of hazardous substances in the design, manufacture, and use of chemical products.

Since its first appearance, green chemistry has gradually evolved due to organized efforts in both Europe and the USA, and has been widely adopted within the chemical industry as a method to promote sustainability in the design and manufacturing of new chemicals. The basic ideas behind green chemistry were concretized in 1998 by Anastas and Warner by their definition of the Twelve Principles of Green Chemistry [2]:

The Twelve Principles of Green Chemistry

1. **Prevention**
   It is better to prevent waste than to treat or clean up waste after it has been created.
2. **Atom Economy**
   Synthetic methods should be designed to maximize the incorporation of all materials used in the process into the final product.
3. **Less Hazardous Chemical Syntheses**

Wherever practicable, synthetic methods should be designed to use and generate substances that possess little or no toxicity to human health and the environment.

4. **Designing Safer Chemicals**
   Chemical products should be designed to affect their desired function while minimizing their toxicity.
5. **Safer Solvents and Auxiliaries**
   The use of auxiliary substances (e.g. solvents, separation agents, etc.) should be made unnecessary wherever possible and innocuous when used.
6. **Design for Energy Efficiency**
   Energy requirements of chemical processes should be recognized for their environmental and economic impacts and should be minimized. If possible, synthetic methods should be conducted at ambient temperature and pressure.
7. **Use of Renewable Feedstocks**
   A raw material or feedstock should be renewable rather than depleting whenever technically and economically practicable.
8. **Reduce Derivatives**
   Unnecessary derivatization (use of blocking groups, protection/deprotection, temporary modification of physical/chemical processes) should be minimized or avoided if possible, because such steps require additional reagents and can generate waste.
9. **Catalysis**
   Catalytic reagents (as selective as possible) are superior to stoichiometric reagents.
10. **Design for Degradation**
    Chemical products should be designed so that at the end of their function they break down into innocuous degradation products and do not persist in the environment.
11. **Real-time analysis for Pollution Prevention**
    Analytical methodologies need to be further developed to allow for real-time, in-process monitoring and control prior to the formation of hazardous substances.
12. **Inherently Safer Chemistry for Accident Prevention**
    Substances and the form of a substance used in a chemical process should be chosen to minimize the potential for chemical accidents, including releases, explosions, and fires.

The principles of green chemistry are largely geared towards guiding the design of the manufacturing process, since for many chemicals the manufacturing has the largest impact on human health and the environment. Energetic materials are to some extent different, in that their use prohibits recycling and proper waste disposal; they disintegrate, and the decomposition or combustion products are directly released into the environment. It is, therefore, particularly important to consider the health and environmental effects of the final product and its usage. With this aspect in mind, the principles of green chemistry can be applied to the design of energetic materials and their manufacturing. It may seem very

difficult to adhere to some of the principles, such as 2, 5, 8, and 9. After all, most energetic materials are complex structures that are very high in energy. Energy and complexity are often afforded by employing reactive reagents, specialized solvents, extreme reaction conditions, and through the use of protecting groups or other derivatization. However, most drugs are of equal or larger complexity, and therefore it is encouraging that green chemistry has been very successfully implemented in the pharmaceutical industry [3,4]. It is also obvious from reading Chapter 9 that great progress is currently being made in adopting green chemistry principles to the design of manufacturing processes for energetic materials. In some cases the achievements are clearly at the forefront of sustainable manufacturing, such as the use of biocatalysts or the implementation of continuous processes. The implementation of electrochemical methods is also likely to become of increased importance. Electrochemical processes often constitute energy efficient approaches for synthesis and for remediation of chemical waste. The use of water as the prevalent solvent in many such processes is an added advantage.

The principles of green chemistry provide no direct indication of how to determine the sustainability of a chemical or manufacturing process. One attempt to remedy this deficiency is the E-factor, which has been introduced as a method for quantifying the greenness of processes and products [5–7]. It is defined as the quotient of mass of waste over the mass of product, that is, $m_{\text{waste}}/m_{\text{product}}$. The waste is often considered to include all compounds formed during the process, including gases and water. It is generally a better measure for comparing different processes for making the same product than for comparing products, since it does not explicitly consider the constitution of the waste or its toxicity. Even if the E-factor is a relatively blunt tool, it provides a rapid and often very revealing method for assessing different process alternatives from an environmental perspective. A lifecycle assessment (LSA) is a much preferred approach as it attempts to give an assessment of the overall environmental impact of a product. It considers the entire process from the extraction and acquisition of the raw material, via the manufacturing and use of the product, to the end-of-life management [5,8]. There are also methods that attempt to combine LSA with lifecycle cost analysis to get a total assessment of the costs for a product. Such a technique was recently used to analyse the life-cost of a toxic monopropellant (hydrazine) propellant versus a green one [9]. The analysis demonstrated that replacing the toxic propellant would give large cost reductions, even though the actual manufacturing cost for the green replacement is higher. It is a common observation that it pays off, from a direct cost perspective, to replace old products with greener alternatives. This also holds for the manufacturing of chemical products; converting to processes that adhere to the green principles of chemistry is often cost effective.

Reduction of costs can actually be considered one of main forces that drive the implementation of green products and manufacturing technologies; the others are societal pressure due to public awareness and government legislation. In Europe, chemicals and their use are regulated through the European Community regulation REACH (**R**egistration, **E**valuation, **A**uthorization and Restriction of **Ch**emical substances) [10]. REACH was introduced in 2007 and will be gradually phased in over 11 years. “The aim of REACH is to improve the protection of human health and the environment through the better and earlier identification of the intrinsic properties of chemical substances” [10]. REACH significantly increases the responsibilities of

manufacturers and importers of chemicals. They are required to gather information on the properties of their chemical substances and provide safety information that ensures their safe handling. The Regulation further calls for the progressive substitution of the most dangerous chemicals when suitable alternatives have been identified. This also has implications for the energetic materials industry. It is becoming increasingly important to identify early on energetic materials that are in danger of being phased out, and to begin the development of green replacements.

So far we have not touched on the subject of whether the considerations according to the principles of green chemistry should be prioritized over performance and safety of handling when designing green energetic materials. Safety of handling is partly considered in principle 12. However, the potential consequence of an accident in the case of an energetic material is often of such magnitude that safety of handling must take precedence over other priorities. The prioritization of performance is a slightly more complicated matter, and is somewhat dependent on the application. It is obvious that the performance of a product will affect its atom-economy, for example, if a new material has half the performance of an old material, we need to use twice the amount of the new material to accomplish the same task. However, for some applications the consequence of lowered performance can be detrimental. In the case of rockets for space exploration, the mass of the propellant can easily be up to 90% of the total weight, whereas the payload typically constitutes only a few percent; even a minor reduction in performance (specific impulse) will significantly reduce the size of the payload. Thus, high performance is essential for efficient energy utilization and is often needed for mission completion. There are many other applications of energetic materials where high performance is also of great importance.

With this discussion in mind we can attempt to define the concept of a green energetic material:

> A green energetic material is a material designed and manufactured in accordance with the principles of green chemistry, with the minimum requirement to preserve the performance level, and safety of handling, of the energetic material it is intended to replace.

It is important to remember that it is not always possible to design a material that fully satisfies this definition and, if the need to replace an old composition is sufficiently urgent, it may be necessary to settle for something that is not entirely green, just greener. In many cases, such an approach can lead to a significant improvement over the existing situation.

1.3 Green Propellants in Civil Space Travel

We are facing environmental challenges related to the use of energetic materials in many areas of society. In the following section, we will use the civil space sector as an example, and discuss some past and present attempts to develop and implement green propulsion technology. This is not intended to be a comprehensive survey, but rather to indicate some of the challenges associated with taking a green material from the initial development state to its final application.

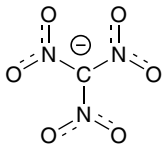

$H_2N—NH_3^+$

HNF

Scheme 1.1

1.3.1 Green Oxidizers to Replace Ammonium Perchlorate

Ammonium perchlorate (AP, NH_4ClO_4, Scheme 1.1) is the most common oxidizer in solid propellants. Its use extends from civil pyrotechnics, via a range of military applications, to the large booster engines in space shuttles and heavy-lift launchers. One of the environmental concerns relating to AP is its high chlorine content, which is converted to hydrochloric acid (HCl) upon combustion. As an example, it is easy to calculate that each launch of the European heavy-lift launcher, Ariane 5, produces HCl corresponding to 270 metric tons of concentrated hydrochloric acid at full conversion [11,12]. The large amount of HCl released into the atmosphere as consequence of the extensive use of AP may contribute to acidic rain and ozone depletion. The direct release of perchlorates into the environment, either due to incomplete combustion, or leakage from undisposed material, is considered to be an even bigger problem. It is estimated that drinking water in at least 35 of the states in the USA is contaminated by perchlorates [13]. This is a matter of concern since it has been suggested that high intakes of perchlorates may lead to an increase in thyroid disorders [14]. The EPA published in 2009 an interim health advisory with a maximum limit of 15 ppb for drinking water, and announced in 2011 that they are moving forward with regulations [15,16].

Hydrazinium nitroformate (HNF) has been considered as a potential green oxidizer in solid booster propellants. HNF was discovered already in 1951 [17]. However, the real interest in HNF as a replacement for AP started in the late 1980s, when the European Space Agency (ESA) began to realize the potential environmental problems associated with acid release from AP combustion. The ESA initiated a large research program with the aim of developing a green solid propellant for use in space applications. This included the establishment of a production plant for producing HNF at a scale of 300 kg per year [17]. HNF is not considered to be entirely green, since one of the reactants used to manufacture HNF is hydrazine, which is a highly toxic and carcinogenic compound. Still, HNF is chlorine free, and the burning is clean and without acid release. It was soon realized that HNF has severe compatibility issues with common binder systems. However, HNF was later shown to be compatible with the energetic binder glycidyl azide polymer (GAP), and a propellant based on HNF, aluminum (Al), and GAP has been developed [18]. The performance, in terms of specific impulse, is reported to be 2–7% higher than for a standard formulation of AP-Al with hydroxyl-terminated polybutadiene (HTPB) as the binder [19]. This increase would, according to some estimates, translate into a reduction in the cost/kg payload of a launch system of 5–50% [19]. In spite of these very encouraging results, and the large investments made, ESA seems to have largely lost interest in the

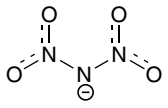

ADN

Scheme 1.2

development of an HNF-based propellant; the research has almost halted and there are no indications of industrialization in the near future. We can only speculate about the reasons. However, it may be connected to problems with the thermal stability and sensitivity of HNF [17]. In addition, the manufacturing costs of both HNF and GAP are high and it is expected that a HNF propellant would be too expensive to use on a larger scale. This should be added to the large costs associated with the development of a new engine system and the related infrastructure.

Ammonium dinitramide (ADN, Scheme 1.2) is another oxidizer that has received considerable interest as a potential green replacement for AP. ADN was first prepared in 1971 in Moscow, and is believed to have been used for propulsion of Soviet intercontinental missiles during the Cold War [11]. Reportedly, the main advantage of the propellant was the smokeless signature (a consequence of the clean burning of ADN), which prevented radar detection of the missiles. ADN was rediscovered in the late 1980s by US scientists. Since then, it has been the focus of intense research efforts worldwide. Like HNF it is chlorine free, and combustion of pure ADN without a fuel leads to formation of N_2, H_2O, and O_2 as the thermodynamic products. ADN is today produced on a large scale in a relatively green process at the SNPE Eurenco plant in Karlskoga, Sweden.

ADN is very hygroscopic in nature. Although it is relatively stable in pure form, it has, like HNF, been found to be incompatible with a number of binder and curing systems, most notably the common isocyanate curing system [17,20] (see Chapter 8 for details). The reactivity of ADN has been very difficult to understand and anomalous solid state decomposition behavior has been reported [17,20]. As described in Chapter 7, many of the issues with ADN are now finally beginning to be resolved. New compatible binder systems have also recently been presented [11,21] (see also Chapter 8). Although they need considerable optimization before a working solid ADN propellant can be realized, the preliminary results are promising. Theoretical calculations indicate that an optimized ADN-propellant would have a high performance and increase the specific impulse over a standard AP-Al propellant by up to 5–7% (see Chapter 2).

Even though ADN-based solid propulsion is on the verge of becoming a mature propulsion technology, we do not see any initiative that in the near future is likely to lead to the implementation of ADN in a larger propulsion system. In 2008, NASA signed an agreement with the Swedish Defence Research Agency (FOI) with the title *Initial evaluation of ADN as oxidizer in solid propellants for large spacelauncher boosters* [22], and it was rumored that ADN was considered for the next-generation ARES booster. However, NASA, in an unoffical statement, denounced this rumor and explained that ADN needed further evaluation and development before eventual implementation [23]. The reason for the current relatively low interest in an ADN-based launch system from private investors and space agencies is not obvious. However, the answer is probably connected to the size of the

investment and the large risk associated with such a project. It would not only involve the development of the propellant, but also of the engine system, and the accompanying infrastructure, and would take many years from start until an eventual first launch. In addition, considering the large quantities of propellant used at each launch, it must be possible to produce the propellant at a relatively low cost.

1.3.2 Green Liquid Propellants to Replace Hydrazine

For obvious reasons, it is easier to attract funding for the development of propellants for smaller engine systems, where the costs and risks are lower. One such area has been finding a replacement for the hydrazine monopropellant, which is mainly used for satellite station-keeping motors. Hydrazine is highly toxic and carcinogenic and cannot be handled without stringent safety precautions. Researchers at the FOI had already realized in the late 1990s the potential of ADN to be used in monopropellant formulations because of its high solubility in polar solvents [11]. This led the Swedish National Space Board to fund the first attempt to develop a liquid ADN monopropellant; the project was a collaboration between the FOI and the Swedish Space Corporation (SSC). This investigation found compositions of ADN, methanol and water (AMW) to be particularly promising for replacing hydrazine [11]. ECAPS, a subsidiary of the SSC, subsequently continued the development of an AMW propellant and an associated rocket engine. In the final design the 1N thruster system was demonstrated to provide a specific impulse that was 5% higher than a corresponding hydrazine thruster [24]. The improvement in density impulse was even larger due to the 24% higher density of the developed propellant, LMP-103S. The first in-flight demonstration came in 2010, when the system was tested for rendezvous and formation-flying satellite maneuvers on the PRISMA technology demonstration mission [25].

ECAPS today claims to be the market leader in green propulsion technology, and LMP-103S is marketed worldwide. Their ADN-based technology is one of the first examples of a green propellant that has made the full journey from the initial development stage to finally reaching the commercial market. In this context it is interesting to note the time span of nearly 15 years from the initial research project in 1997 to the market release in 2012. This is similar to the development time in drug design, where it typically takes up to 15 years from the initial discovery phase to market release. The pharmaceutical industry is normally considered, of all technology industries, to hold the record for long development times. The significance of the development time for LMP-103S is difficult to estimate, considering we only have this example. However, one can only hope that ECAPS has broken the ice and that new and improved propellants will soon be ready for commercialization. There are some candidates that have already shown great promise. The FOI has their own ADN-based liquid propellant, which is reported to provide a significantly higher density impulse than the ECAPS propellant [11]. A green propellant with even better performance has been developed by the US Air Force Division [26]. It is an ionic liquid formulation of hydroxyl ammonium nitrate (HAN, Scheme 1.3). This propellant is set to be tested on a satellite on the 2015 GPIM mission [27].

At this point, it may be relevant to reflect upon how green an ADN-based propellant, like LMP-103S, really is. It should first be realized that ADN is considerably less toxic than hydrazine, as indicated by the LD50 values for oral intake in rats, which are 823 mg/kg [11]

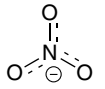

$^{+}H_3N—OH$

HAN

Scheme 1.3

and 59 mg/kg, respectively. In reality the difference in health hazard is much larger due to the carcinogenicity of hydrazine and its higher vapor pressure. It is actually argued that the methanol is the reason for the hazard symbol labeling of LMP-103S as being toxic [24]. In any case, the safety precautions for handling the propellant are similar to most organic solvents. This should be compared to the handling of hydrazine, which requires the use of an advanced protective suit. All the subcomponents of LMP-103S are biodegradable and it is considered environmentally benign [24]. The propellant is insensitive to impact and friction, and it has even been approved for transportation on commercial aircrafts [24]. Thus, it seems like LMP-103S fulfills many of the criteria for being considered green.

In this context, it is also relevant to evaluate the manufacturing of ADN from a green perspective. ADN is currently produced at the SNPE Eurenco plant in Karlskoga. Beginning in the mid 2000s, substantial efforts were made to optimize the process for capacity, reduction of impurities, recirculation of chemicals, and reduction of chemical waste. Some of the results have been published and are discussed in Chapter 9 of this book [28,29]. The optimized process is described in a company newsletter from 2004 [30]:

> Dinitramide is synthesized with a mixed acid nitration of a sulphamic acid salt. The dinitramide is then precipitated as GUDN (guanylurea dinitramide) from a water solution by adding guanylurea. The spent nitration acids are regenerated by using standard procedures. In a following step GUDN is transformed to ADN in two separate ion exchange reactions. First, GUDN is changed to potassium dinitramide (KDN) using potassium hydroxide. Finally, KDN is transformed to ADN in an ion exchange reaction with ammonium sulphate. ADN is crystallized from the solution and potassium sulphate is generated as a waste. The solvents used in all steps are recycled.

The process for manufacturing ADN seems to be a very good example of the advances in adopting green chemistry and engineering to energetic materials production.

At this stage, we can safely conclude that replacing hydrazine with a monopropellant based on ADN, such as LMP-103S, is also a significant improvement in sustainability if the propellants' entire lifecycle is considered. This has also been verified by a lifecycle cost analysis, which in addition showed a 66% reduction in the operational mission cost for LMP-103S compared with hydrazine [9]. The largest improvements where found in environmental costs, mainly associated with facility operations and maintenance, and costs associated with health and human safety protection. Thus, this example clearly illustrates that the implementation of a green energetic material can also be advantageous from a direct cost perspective.

1.3.3 Electric Propulsion

Another major step towards greener propulsion is related to the recent advances in the development and implementation of electric propulsion. The basic idea behind electric propulsion is to use electrical rather than chemical energy to accelerate the propellant. Thrusters for electric propulsion can be divided into three categories: electrothermal, electrostatic, and electromagnetic. The first is most similar to a conventional thruster, in that the electric energy is used to heat the propellant and the thermal energy is converted to kinetic energy. In the two latter approaches the propellant is ionized and the resulting ions are accelerated in an electromagnetic field; the most common propellant is xenon, as it combines a relatively low ionization potential with high atomic mass. Electric thrusters are characterized by a much higher specific impulse, and therefore much lower propellant consumption, compared to conventional thrusters. Their disadvantage is the low thrust, which means that the time taken to accomplish a particular maneuver will be much longer. Typical applications of electric propulsion include station keeping, and the transfer of satellites from the geostationary transfer orbit (GTO) to their geostationary earth orbit (GEO); maneuvers that are traditionally performed using chemical thrusters driven by a hydrazine monopropellant or toxic bipropellants based on methylhydrazine and nitrogen tetroxide.

Electric propulsion is particularly advantageous when combined with solar energy. For example, for transferring a satellite to GEO, it may be possible to use electric power from solar panels that are otherwise not in use during that phase. The potential of solar-driven electric propulsion was demonstrated by the ESA SMART-1 mission to the Moon in September 2003 [31]. The 370 kg satellite built by SSC used a solar-powered Hall effect thruster for the entire transfer from the GTO to the lunar orbit. It was kept in orbit using the same propulsion system until September 2006, when it was finally crashed into the Moon's surface. At the end of the mission, the thruster had been operating 5000 h and had used only 82 kg of xenon propellant in total. This is a very impressive example of the advantages of solar-driven electric propulsion. A system based on traditional chemical propulsion would have required a much heavier propulsion system, and the total cost of the mission would have been substantially higher. From a green perspective the advantages are considerable.

Xenon cannot be considered an energetic material in its traditional form. However, in a wider definition, it could be designated as a green energetic material, or at least a green propellant. Xenon is commercially produced as a byproduct of the separation of air into oxygen and nitrogen. It is relatively chemically inert, and nontoxic. Its disadvantage is a relatively high price due to its low natural abundance; a price that is rising because of the increased usage of xenon, in particular in lightning devices. Recent research shows that more traditional energetic materials, like those based on ADN, could potentially be used for electric propulsion too [32]. In addition to lower propellant cost, this could also have other benefits, in particular in terms of saving weight, since systems for electrical and chemical propulsion could share the same fuel system.

1.4 Conclusions

We can safely conclude that the time when energetic materials could be developed with the sole aims of improving performance and safety of handling is now gone. It is becoming increasingly important to also consider the potential health and environmental effects of a

new material during its entire lifetime. In this respect, the principles of green chemistry can be a great aid to the design of new products and their manufacturing processes. This type of approach serves not only to improve the sustainability of the product but can also often lead to reduced costs. Lifecycle assessment is another tool that can be very effective in the process. We have further suggested a definition of a green energetic material from the principles of green chemistry.

We have analyzed some of the past and present attempts to develop green propulsion technologies for civil space travel. Our limited analysis shows that the entire development process, from the initial discovery of a new propellant component to the implementation of the final propellant in an engine system, is a lengthy journey full of potential risks of failure. The costs, and the chances of succeeding, seem to largely depend on the size and type of the engine system. The development of green solid propellants to replace ammonium perchlorate formulations for heavy-launch systems has not yet reached the stage where new propellants are ready to be implemented. On the other hand, there have been significant advances in green technologies aimed at replacing smaller engines that use liquid propellants based on hydrazine or hydrazine derivatives. The recent development and implementation of a green liquid propellant based on ADN is one obvious example. This propellant has recently been tested for formation flying of satellites, and has been released on the commercial market. Electric propulsion is another green alternative that is advancing. The great potential of this technology was demonstrated in 2003 by the SMART-1 mission to the Moon.

Finally, we note that the relatively slow progress of introducing green propulsion technologies to civil space travel is not representative of the impact of green energetic materials in other areas. Despite many challenges, particularly large advances have been made in the area of green pyrotechnics. Here, the development has largely been driven by military research. However, the new materials are being increasingly implemented in civilian pyrotechnics. Similar progress is also being made in other areas of energetic materials, but at different rates. Overall, the future of energetic materials seems bright and green.

References

1. US Environmental Protection Agency, (last updated September 13, 2013), http://www.epa.gov/p2/pubs/partnerships.htm (last accessed in September, 2013).
2. Anastas, P.T. and Warner, J.C. (1998) *Green Chemistry: Theory and Practice*, Oxford University Press, Oxford.
3. Dunn, P.J. (2012) The importance of green chemistry in process research and development. *Chemical Society Reviews*, **41** (4), 1452–1461.
4. Bandichhor, R., Bhattacharya, A., Diorazio, L. *et al.* (2013) Green chemistry articles of interest to the pharmaceutical industry. *Organic Process Research & Development*, **17** (4), 615–626.
5. Rothenberg, G. (2008) *Catalysis: Concept and Green Applications*, Wiley-VCH Verlag GmbH & Co., Weinheim, Germany.
6. Sheldon, R.A. (1994) Consider the environmental quotient. *Chemtech;(US)*, **24** (3) 38–47
7. Sheldon, R.A. (1997) Catalysis: The key to waste minimization. *Journal of Chemical Technology and Biotechnology (Oxford, Oxfordshire: 1986)*, **24** (3), 381–388.
8. Lankey, R.L. and Anastas, P.T. (2002) Life-cycle approaches for assessing green chemistry technologies. *Industrial & Engineering Chemistry Research*, **41** (18), 4498–4502.

9. Johnson, C.C. and Duffey, M.R. (2013) Environmental life cycle criteria for propellant selection decision-making. *International Journal of Space Technology Management and Innovation (IJSTMI)*, **2** (1), 16–29.
10. European Commission, REACH - Environment - European Commission, (last updated September 12, 2013) http://ec.europa.eu/environment/chemicals/reach/reach_en.htm, (last accessed in September, 2013).
11. Larsson, A. and Wingborg, N. (2011) Green propellants based on ammonium dinitramide (ADN), in *Advances in Spacecraft Technologies* (ed. J. Hall), InTech, Available from http://cdn.intechweb.org/pdfs/13473.pdf.
12. Arianespace (2013) http://www.arianespace.com/launch-services-ariane5/ariane-5-intro.asp (last accessed in July 2013).
13. Schor, E. (2010) As EPA Moves to Regulate Perchlorate, Groups Await Pentagon Response, *The New York Times*http://www.nytimes.com/gwire/2010/10/04/04greenwire-as-epa-moves-to-regulate-perchlorate-groups-aw-43754.html (last accessed July 6, 2013).
14. Sellers, K., Weeks, K., Alsop, W., and Clough and, H.M. (2007) *Perchlorate Environmental Problems and Solutions*, CRC Press – Taylor & Francis Group, Boca Raton, FL, US.
15. US Environmental Protection Agency (January, 2009) Revised Assessment Guidance for Perchlorates: http://www.epa.gov/fedfac/documents/perchlorate_memo_01-08-09.pdf (last accessed in July 2013).
16. US Environmental Protection Agency (February 2011) Fact Sheet: Final Regulatory Determination for Perchlorate - US Environmental Protection Agency http://water.epa.gov/drink/contaminants/unregulated/upload/FactSheet_PerchlorateDetermination.pdf (last accessed in July 8, 2013).
17. Agrawal, J.P. (2010) *High Energy Materials - Propellants, Explosives, Pyrotechnics*, Wiley-VCH Verlag GmbH & Co., Weinheim, Germany.
18. Gadiot, G.M.H.J.L., Mul, J.M., Meulenbrugge, J.J. *et al.* (1993) New solid propellants based on energetic binders and HNF. *Acta Astronautica*, **29** (10), 771–779.
19. APP Aerospace Propulsion Products B.V., HNF (2006–2012) http://www.appbv.nl/index.asp?grp_id=3&sub_id=23 (last accessed in July 6, 2013).
20. Rahm, M. (2010) Green Propellants, PhD thesis, Physical Chemistry, KTH The Royal Institute of Technology, Stockholm, Sweden.
21. Rahm, M., Malmstrom, E., and Eldsater, C. (2011) Design of an ammonium dinitramide compatible polymer matrix. *Journal of Applied Polymer Science*, **122** (1), 1–11.
22. A–Initial evaluation of ADN as oxidizer in solid propellants for large spacelauncher boosters, NASA Presolicitation December 2008, http://www.fbo.gov/?s=opportunity&mode=form&id=6e876911f91a4be2cc6bfc8314b39242&tab=core&_cview=1 (last accessed in 2013).
23. Flightglobal/Blogs, December 2008, NASA denies imminent Ares I first-stage oxidiser change, http://www.flightglobal.com/blogs/hyperbola/2008/12/nasa-denies-ares-i-crew-launch.html (last accessed in 2013).
24. Anflo, K. and Möllerberg, R. (2009) Flight demonstration of new thruster and green propellant technology on the PRISMA satellite. *Acta Astronautica*, **65** (9–10), 1238–1249.
25. D'Amico, S., Ardaens, J.S., and Larsson, R. (2012) Spaceborne autonomous formation-flying experiment on the PRISMA mission. *Journal of Guidance Control and Dynamics*, **35** (3), 834–850.
26. Masse, R., Overly, J., Allen, M., and Spore, R. (2012) A New State-of-The-Art in AF-M315E Thruster Technologies 48th AIAA/ASME/SAE/ASEE, Joint Propulsion Conference and Exhibits, American Institute of Aeronautics and Astronautics.
27. Green Propellant Infusion Mission (GPIM), (last updated November 6, 2012) http://www.nasa.gov/mission_pages/tdm/green/gpim_overview.html (last accessed in 2013).

28. Skifs, H., Stenmark, H., and Thormahlen, P. (2012) Development and scale-up of a new process for production of high purity ADN, International Conference of ICT, 43rd (Energetic Materials) 6/1-6/4, Karlsruhe, Germany.
29. Stenmark, H., Skifs, H., and Voerde, C. (2010) Environmental improvements in the dinitramide production process, International Conference of ICT, 41st (Energetic Materials: for High Performance, Insensitive Munitions and Zero Pollution) 1/1-1/5, Karlsruhe, Germany.
30. EURENCO Group SNPE (October, 2004) Dinitramide News, http://www.eurenco.com/en/high_explosives/newsletters/Dinitramide_oct_2004.pdf_ (last accessed in 2013).
31. Estublier, D., Soccoccia, G., and delAmo, J.G. (2007) Electronic propulsion on SMART-1 - A technology milestone. *ESA BULL-EUR Space*, **129**, 40–46.
32. Kleimark, J., Delanoë, R., Demairé, A., and Brinck, T. (2013) Ionization of ammonium dinitramide: decomposition pathways and ionization products, Theoretical Chemistry Accounts, **132** (12), 1412.

2

Theoretical Design of Green Energetic Materials: Predicting Stability, Detection, Synthesis and Performance

Tore Brinck[1] *and Martin Rahm*[2]

[1]*Applied Physical Chemistry, School of Chemical Science and Engineering, KTH Royal Institute of Technology, Sweden*
[2]*Loker Hydrocarbon Research Institute and Department of Chemistry, University of Southern California, USA*

2.1 Introduction

This book is a testament to the need for development of greener energetic materials. However, to be considered truly green, the material properties must be refined at many levels. For example, a potential replacement for today's solid propellant compositions should not only produce substantially less toxic waste during combustion, but also be perform better or on par with today's solutions. Reduced performance would lower payloads and increase propellant consumption, and thereby have a negative impact on the environment. There are also numerous other issues to consider. The complexity of the design problem, together with the inherit safety issues associated with the synthesis and handling of energetic materials, makes the road to progress much slower to travel without invoking rational design based on modeling and theoretical considerations. The energetic materials community has also been ground breaking in the employment of computational chemistry methods in general, and quantum chemical techniques in particular, for the design of new materials with optimized properties. However, it must be emphasized that chemical

Green Energetic Materials, First Edition. Edited by Tore Brinck.

knowledge and intuition are necessary inputs to the design process, and without the contribution of chemists experienced in synthesis new compounds will never materialize.

In this chapter our main focus is on the use of computational techniques for the development of new propellant components. However, not only the techniques, but also the basic considerations, are to a great extent similar to those employed when designing other energetic materials, such as explosives and pyrotechnics.

Most propellant compositions combine an oxidizer with one or more fuel components. For example, the typical solid propellant consists of ammonium perchlorate and solid aluminum in a hydroxyl-terminated polybutadiene binder. Most common oxidizers have a rather low energy content by themselves. It is instead through the combustion of fuels, and particularly metal fuels, that a rocket motor can release energy. The combustion temperature rapidly becomes a concern with increased metal loadings, as state of the art materials used in throat and nozzles of rocket engines fail at approximately 2500 K [1]. Some modern highly aluminized propellants exhibit combustion temperatures up towards 3600 K and can only be employed together with engine designs that employ techniques such as, regenerative cooling, film cooling, or ablative protection [1,2]. Further performance increases cannot rely much further on improved engine designs and larger metal loadings, as combustion temperatures above 5000 K are considered unrealistic for practical applications. Maintaining high performance, while reducing combustion temperatures through reduced metal loadings, will require new oxidizers with higher internal energy, for example compounds with highly energetic bonds. Compounds that are able to combust themselves entirely, without the addition of a fuel, are for many purposes desirable, as they can be used with lighter and less expensive engines. We will refer to such compounds as having a neutral oxygen balance.

Good candidate compounds for green high performance propulsion are generally high in nitrogen, have a positive or neutral oxygen balance, and are free of halogens. Nitrogen-rich compounds are desirable as they release large amounts of energy upon decomposition when forming the exceedingly stable N−N triple bond of molecular nitrogen from the much weaker single and double N−N bonds of the parent molecules. Average bond energies for the triple, double, and single bonds of nitrogen are 226, 98, and 39 kcal/mol, respectively. The extraordinary relative stability of the N_2 triple bond is easily realized when comparing it to the same energies for C−C bonds, which have the values 230, 146, and 83 kcal/mol.

Whereas compounds featuring a large number of N−N single bonds are desirable for their high internal energy, they generally have problems with low kinetic stability. Fundamental theory, such as the Bell–Evans–Polanyi principle [3], clearly shows that there is a general correlation between thermodynamic and kinetic stability. From a more simplistic perspective, it can be realized that the activation barrier towards dissociation is not likely to exceed the energy of the weakest bond of the molecule. A common design objective is therefore to strengthen weak N−N and N−O single bonds by invoking resonance delocalization to attain a partial double bond character. Common strategies include resonance stabilization between sp^2 hybridized nitrogen and oxygen, and aromatic stabilization in ring systems with $4n + 2$ π-electrons [4]. Resonance stabilization is generally a prerequisite of planar molecules. This is also of interest from a stability perspective, as planar molecules and ions are more likely to crystalize in sheet-like structures, a structure type that is believed to reduce the impact sensitivity.

Another alternative design strategy for combining high energy content (low thermodynamic stability) with sufficient kinetic stability is to utilize caged structures. Besides invoking single bonds that are high in energy, for example N−N bonds, such structures often benefit thermodynamically from strain energy. Despite the fact that a caged structure often is made up of seemingly weak bonds, the kinetic stability can be relatively high. The reason for the high decomposition barrier is usually that it is not possible to form a thermodynamically favored intermediate by breaking only one bond. Instead, the main dissociation pathway either involves several bonds breaking in one step, or passes via a high lying intermediate; both types of transformations are often associated with a high barrier. This should be taken as a general consideration for identifying energetic compounds with high kinetic stability, that is, molecules that cannot decompose to a stable intermediate via a single simple chemical transformation are likely to have a larger kinetic stability than can be anticipated from the strengths of their individual chemical bonds. In the following discussion we will provide several examples where this is the case.

It is obvious that predicting performance and stability is key to the design of green energetic materials. Traditionally, it is also in these areas that computational chemistry has played its most important role. Enthalpies of formation for gaseous molecules are readily obtained by quantum chemical methods. However, as most energetic materials are used in solid or liquid phases, methods have been developed to also calculate phase transition energetics and condensed phase densities. The kinetic stability is first approximated by evaluating the potential decomposition pathways and their barriers in the gas phase by quantum chemistry. Invoking the effects of interactions with neighboring molecules in condensed phases increases the complexity considerably, but significant progress has been made in this area too. However, the true bottleneck in obtaining new functional energetic materials has been devising synthetic routes. Here, we believe that computational chemistry has the potential to play a more important role. Potential synthetic routes can be evaluated by a similar analysis to that used for evaluating stability and decomposition pathways. Finally, we note that detection and characterization often are key issues in the discovery of highly energetic molecules of high symmetry and low molecular weight. Theoretically predicted spectra for different spectroscopies can be great aids to the process.

2.2 Computational Methods

Kohn–Sham density functional theory (KS-DFT) is today the standard quantum chemical method for the optimization of molecular geometries and calculation of vibrational frequencies. It is generally used to probe potential energy surfaces and characterize transition states. The widely used B3LYP exchange-correlation functional has also been quite successful for energetic molecules and their reactions. In general, B3LYP geometries are more accurate than energies. However, there are examples of nitro-group rich systems where B3LYP produces both erroneous geometries and energies, and for some of these the more recent M06-2X functional [5] of Truhlar and coworkers performs considerably better. A general observation is that when the two functionals give geometries in consensus, these can be trusted for energy calculations at higher level. Double zeta basis sets augmented by

diffuse and polarization functions, for example 6–31+G(d,p), are recommended for geometry optimizations of energetic molecules.

In order to obtain energies that are close to chemical accuracy, post-Hartree Fock methods are generally needed. In particular, methods such as CBS-QB3 [6,7] and G3MP2 [8], that combine coupled cluster [CCSD(T)] calculations with smaller basis sets and basis set extrapolation at the MP2 level, are recommended for small and medium sized energetic molecules. Heats of formation (ΔH_f^o) of new systems should not be computed via atomization energies, but rather from hypothetical reactions involving molecules with well-defined experimental gas phase heats of formations. For larger molecules, it may be necessary to resort to DFT-methods. We note that the B3LYP-based atom-equivalent parameterizations of Rice and coworkers often provide accurate ΔH_f^o for energetic molecules at a very modest computational cost [9,10]. However, for novel compounds whose structures deviate from the parameterization set, or for computing activation energies, we recommend direct calculations using some modern, more accurate, functionals, such as M06-2X and the double hybrid functional B2-PLYP of Grimme *et al.* [11].

For probing decomposition reactions and analyzing synthetic routes, it is often necessary to account for the effects of neighboring molecules in the liquid environment. Solvation models based on a continuum description of the liquid state, such as the polarizable continuum model (PCM) [12] and the conductor like screening model (COSMO) [13], are surprisingly accurate for correcting geometries and energies. However, for computing barriers of reactions where a neighboring molecule takes active part, such as in solvent-assisted catalysis, incorporation of explicit molecules from the environment is necessary.

Most energetic compounds are either liquids or solids, and computed gas phase heats of formation need to be corrected by computational estimates of heats of vaporization (ΔH_{vap}) or sublimation (ΔH_{sub}). Parameterized methods that utilize descriptors obtained from quantum chemical calculations produce reliable estimates for reasonable computational effort. These methods are generally based on a statistical analysis of the surface electrostatic potential together with descriptors that describe molecular size, such as surface area or molecular volume. The methodology stems from original work by Brinck, Murray, and Politzer [14–16]. Recent developments for the prediction of molecular (non-ionic) compounds are due to Politzer *et al.* [17,18] and Rice *et al.* [9,10]. It is important to remember that these methods are only reliable for compounds similar to those used in the parameterization. In this respect, the recently developed parameters of Politzer *et al.* [18] are more generally applicable than those of Rice *et al.* [9,10]. There are also methods for predicting lattice enthalpies of molecular salts based on electrostatic considerations and estimates of molecular size. Rice and coworkers have recently analyzed the accuracy of several such methods for the prediction of solid phase heats of formation of energetic salts [19].

In addition to heats of formation, computational estimates of liquid and solid densities are necessary to compute the performance of propellants and explosives. These can be estimated from molecular volumes determined by quantum chemical calculations [20–22]. Whereas such estimates often are sufficiently accurate for rocket performance calculations, these methods provide no structural information. Crystal structure prediction is extremely difficult, and one of the current frontiers in development of computational chemistry. The challenge lies in that there are usually millions of possible structures, and hundreds to thousands of these may lie within a few kcal/mol of the global minimum. In energetic materials research, Herman Ammon has been the most prominent pioneer [23].

His approach, which is also being used in pharmaceutical research, involves initial large-scale packing simulations, followed by structure optimization with specially tuned force fields. In recent years, it has been shown that more accurate predictions can be obtained by invoking optimizations of the lowest energy structures with periodic DFT calculations. This methodology was pioneered by Neumann and Perrin [24], and has been further refined and introduced into the area of energetic materials by Rice and coworkers [25–27]. The obtained structures are generally more than adequate for evaluating sensitivity issues, and provide starting points for computational analysis of solid state decomposition pathways. Presently, the accuracy of the free energy predictions is not sufficient to analyze potential issues due to polymorphism or predict transition temperatures between different crystal phases.

Prediction of spectral properties to guide the experimental identification of new compounds is attainable by quantum chemical methods. Vibrational spectra, including both IR and Raman intensities, are often well predicted by standard DFT methods. Since the computations generally are conducted within the harmonic approximation, and do not account for anharmonicity effects, the computed frequencies have to be scaled before comparison with experiment. Solvation normally has very small effects on the frequencies, and gas phase calculations are usually sufficient to estimate liquid spectra. UV-Vis spectra can readily be computed using time-dependent DFT, which also has been implemented in the major quantum chemistry codes. However, the transition energies are sensitive to the choice of exchange-correlation functional and, especially for analyzing charge-transfer bands, long-range corrected functionals, such as CAM-B3LYP [28] or ωB97X [29], are highly recommended. Even better accuracy can be obtained using equation of motion (EOM) or linear response (LR) coupled-cluster calculations [30]. The most exact methods, EOM-CCSD and LR-CC3, can only be used for smaller systems. In contrast, LR-CC2 is tractable even for larger systems and is in most cases sufficiently accurate. Solvent effects sometimes induce large shifts in spectral bands. The molecular interactions behind these shifts are often complex, and although continuum solvation effects can be included in TD-DFT calculations, the predicted shifts are not seldom in the wrong direction.

Additionally, NMR-spectra can be predicted using quantum chemical methods. Comparison with computed spectra is indeed often necessary for experimental identification of energetic compounds that mainly consist of nitrogen and oxygen, since the spectra often only have a few bands and spin–spin coupling patterns can seldom be used for characterization. High level post-Hartree Fock methods, in particular coupled-cluster methods, are recommended for more exotic compounds. However, in practice one often has to resort to DFT-calculations as solvent effects can have a large influence on spectral shifts, and solvent corrections by means of continuum models have not yet been implemented for coupled-cluster techniques in standard quantum chemical codes.

Once heats of formation and densities have been obtained, expected performances of new compounds for different applications can be predicted by thermodynamic calculations. The NASA CEA code is still the standard for computing propulsion performance data, such as the expected specific impulse (I_{sp}) for complex propellant compositions [31,32]. There are several newer codes available that employ the same basic theory. The recently developed RPA program should be mentioned, as it is very user friendly, and exists in a fully functional variant that can be used free of charge [33]. For prediction of detonation properties, there are only a few alternatives available and most of these are commercial. The CEA code, which

also is freely available, computes detonation properties using Chapman–Jouguet analysis, but the input is cumbersome and requires heat capacity estimates. The simplified method of Kamlet and Jacob for CHON compounds, and its revision and extension to also include halogens, is quite reliable for initial estimates of detonation properties [34–36]. It can be easily implemented without the need for extensive programming.

2.3 Green Propellant Components

We will discuss a number of energetic compounds that has the potential to fulfill the basic criteria for being considered in the green category. All of these have been thoroughly characterized by quantum chemical calculations, and most show great promises for use in propellants. In two cases, experimental detection has followed after theoretical characterization, but none of the compounds has yet been synthesized at a larger scale.

2.3.1 Trinitramide

Trinitramide (TNA, $N(NO_2)_3$, **1**), or trinitroamine, which is the systematic name, was first prepared and detected in 2010 by Rahm *et al.* after a thorough computational analysis [37]. It is one of only nine nitrogen oxides that have been observed experimentally, and by far the largest to date. The first theoretical study on TNA was published in 1987 [38], but after that only a few studies appeared in the 1990s [39,40] before the 2010 detection. The reason for the loss of interest in TNA was probably that the bonding of this molecule is poorly described by standard DFT methods [37]. The common B3LYP method predicts a bond dissociation enthalpy (BDE) for the N−N bond of only 20 kcal/mol; a value that would render TNA much too unstable to be of interest for any application. Our original interest in this molecule stemmed from its proposed role in the decomposition of dinitraminic acid. However, as we were investigating the molecule by the gold standard of quantum chemistry methods, CCSD(T), within the CBS-QB3 scheme, we were surprised to see that the BDE went up to more than 28 kcal/mol [37]. This led to a more thorough analysis of the kinetic stability of TNA, and Figure 2.1 shows our current best estimate of the gas phase decomposition energetics for this molecule [37] (Brinck, T. and Rahm, M., 2013, unpublished results). Compared to our 2011 study [37], some of the energies have been corrected for the effect of optimizing geometries using coupled-cluster (CCSD) instead of B3LYP. In addition to the homolytic N−N bond cleavage, there is a second decomposition channel that involves a transfer of a NO_2-group to form the higher lying intermediate **4**. In the gas phase also this pathway has activation barrier close to 29 kcal/mol. This corresponds to a decomposition half-life of around 15 years at 20 °C, which should be sufficient to make TNA of applied interest.

The barrier for the NO_2-group transfer pathway is very sensitive to solvation effects. Whereas the transformation can be characterized as a NO_2-radical transfer in the gas phase, the character is gradually altered into NO_2-cation transfer with increasing solvent polarity. This results in significant reductions of the activation barrier, and in the only moderately polar solvent THF, we estimate that the barrier is reduced by 5–8 kcal/mol [37]. The effect is larger in polar solvents, and in acetonitrile the reduction is estimated to be more than 10 kcal/mol (Brinck, T. and Rahm, M., 2013, unpublished results).

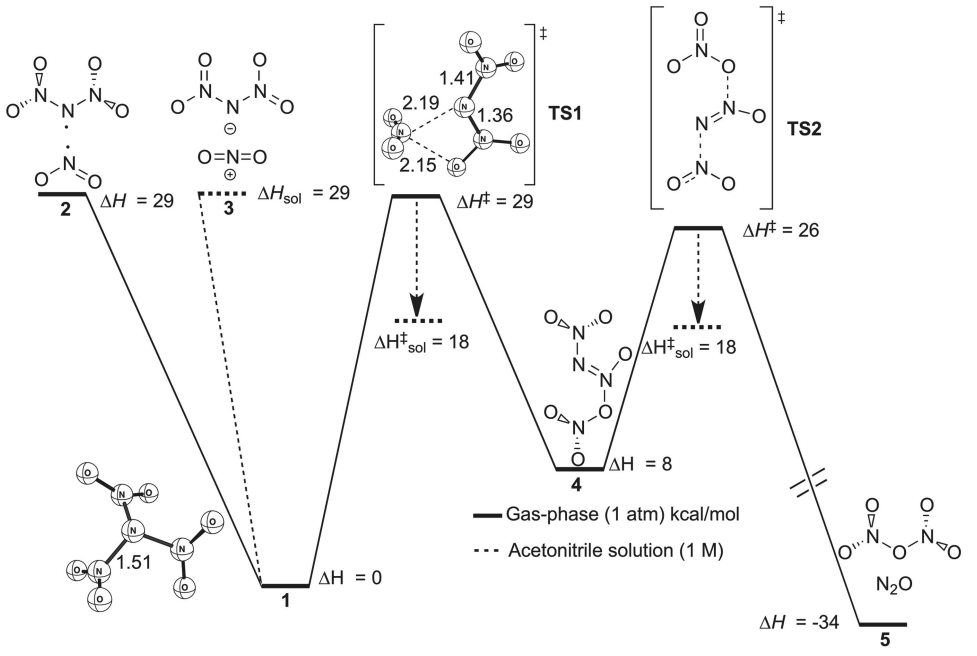

Figure 2.1 *The potential energy surface in kcal/mol for decomposition and formation of TNA (**1**) computed at the CBS-QB3 level [37]. Energies and geometries for TNA and its initial decomposition steps have been revised based on geometry optimizations at the CCSD/6-311G(d) level (Brinck, T. and Rahm, M., 2013, unpublished results). Dashed lines refer to conditions in acetonitrile solution. Adapted with permission from [37] © 2011 WILEY-VCH Verlag GmbH & Co. KGaA, Weinheim.*

2.3.1.1 Synthesis and Detection

On the basis of the quantum chemical analysis, we decided to attempt the synthesis of TNA. Two different routes were considered as shown in Eqs. (2.1) and (2.2) [37].

$$N(NO_2)_2^- \xrightarrow{-e^-} N(NO_2)_2 \xrightarrow{NO_2} N(NO_2)_3 \tag{2.1}$$

$$N(NO_2)_2^- \xrightarrow{NO_2^+} N(NO_2)_3 \tag{2.2}$$

An earlier theoretical analysis [41] had indicated that the dinitramide radical ($N(NO_2)_2$) should be sufficiently stable to be considered a potential intermediate for the synthesis of TNA. The ionization potential of the dinitramide anion is close to 4.4 eV, and it should be feasible to generate TNA by electrochemical oxidation of a dinitramide in the presence of dinitrogen tetroxide at low temperatures. The second route involves direct nitration of the dinitramide anion (DN, $N(NO_2)_2^-$) by NO_2^+ in free form. The selectivity of this reaction is difficult to assess from computational analysis; the electrostatic potential associated with

oxygen is lower than that of the central nitrogen, whereas there is a greater thermodynamic driving force for forming TNA compared to the oxygen bonded intermediate.

Despite the potential selectivity issue, the second route was chosen for our initial attempts to synthesize TNA. Using NO_2BF_4 as the nitrating agent, direct nitration of both $KN(NO_2)_2$ and $NH_4N(NO_2)_2$ in acetonitrile was attempted. The production of TNA was detected by ^{14}N-NMR and *in situ* IR-spectroscopy and the characterization was aided by predicted spectra from quantum chemical calculations [37]. In the NMR-measurements, a peak at −65 ppm relative nitromethane was attributed to the NO_2-group of TNA. This value is within 2.7 ppm of the theoretical estimate at 62.3 ppm. Similarly to $N(NO_2)_2^-$, the signal of the central nitrogen cannot be observed at low temperatures due to extensive line broadening arising from quadrupolar relaxation. This effect was rationalized from the magnitude of the computed electric gradient at the nucleus. TNA was observed to decompose to HNO_3, N_2O_4, and N_2O as the temperature was increased towards room temperature, in agreement with the theoretical predictions. The detection was strengthened by the IR-spectra in which all theoretically predicted IR bands were observed. Additionally, the build-up of decomposition products was observed as the temperature was increased.

It is clear that the detection and verification of TNA could not have been conclusive without the aid of quantum chemical calculations. In particular, the NMR-spectrum provides very little information without comparison with the theoretical counterpart, and also the interpretation of the IR-spectrum would have been very difficult. Under very harsh reaction conditions and in the relatively polar medium, TNA decomposed rapidly and isolation was not possible. We believe that a properly optimized electrochemical procedure following Eq. (2.1) may provide gentler preparation and potentially enable isolation.

2.3.1.2 Properties and Performance

The theoretical thermochemical and physical properties of TNA are listed in Table 2.1. It has a very high predicted gas phase heat of formation that was obtained from high level quantum chemical calculations on a set of reference reactions. The vaporization enthalpy ($\Delta H_{vap} = 7.3$ kcal/mol) was determined from the computed surface area and electrostatic potential distribution using the relationship of Politzer *et al*. [18]. The parameterization of Rice *et al*. gives a very similar value of 7.6 kcal/mol [9]. In contrast, only Politzer's method gives a reasonable estimate for ΔH_{sub} (10.3 kcal/mol); the method of Rice predicts ΔH_{sub} to a value (6.6 kcal/mol) lower than the ΔH_{vap}. A value (9.4 kcal/mol) close to that obtained with Politzer's method was predicted from a preliminary optimization (Ammon, H.I., 2011,

Table 2.1 *Predicted properties of TNA (**1**).*

Molecular weight (MW)	152.02 g/mol
Heat of formation ($\Delta H_f^o(g)$)[a]	54.8 ± 1 kcal/mol
Heat of sublimation (ΔH_{sub})[b]	10.3 (9.4) kcal/mol
Heat of vaporization (ΔH_{vap})[b]	7.3 kcal/mol
Melting point (mp)[b]	ca 10 °C
Density of solid (25 °C)[a]	2.0 g/cm
Oxygen balance	+63.15%

[a] Computed value from Ref. [37].
[b] This work (Brinck, T. and Rahm, M., 2013, unpublished results).

personal communication) of the crystal structure using the procedure of Aammon *et al*. [23], followed by a periodic DFT optimization (Brinck, T. and Rahm, M., 2013, unpublished results). We estimate the melting point to 10 °C from a comparison with compounds that have similar vaporization and sublimation enthalpies. As an example, the structurally similar compound trinitromethane, with a vaporization enthalpy of 7.8 kcal/mol and a sublimation enthalpy of 10.3 kcal/mol, has a melting point of 15 °C [42,43]. Although the melting point prediction is very approximate, it may be concluded that TNA most likely is a liquid under ambient conditions. We have estimated the density to circa 2.0 g/cm^3 based on several procedures, including the crystal structure prediction and an estimate based on the molecular volume determined from the 0.001 electron density contour [37].

The main problem with TNA lies in its limited kinetic stability. At room temperature the computed half-life of gaseous TNA is 15 years. However, liquid TNA is expected to provide a similar environment as a moderately polar solvent, and this will reduce the half-life to days or weeks. Thus, we anticipate that TNA would have to be used at subzero temperatures and then in solid form. At a temperature of −10 °C, the half-life of solid TNA is expected to be in the order of years. Providing such conditions can be maintained, TNA would perform very well as an oxidizer for space propulsion. The strength of TNA lies in the combination of a high energy and a highly positive oxygen balance. In Table 2.2 we list the predicted performance of a number of hypothetical propellants with TNA (Brinck, T. and Rahm, M., 2013 unpublished results). One option would be to use TNA in liquid–solid hybrid formulations. For propellants with hydrazine [$N_2H_4(l)$] as fuel, it is noted that TNA provides a slightly lower I_{sp} than liquid oxygen [$O_2(l)$] but slightly higher than nitrogen tetroxide [$N_2O_4(l)$]. The much higher density of TNA compared to $O_2(l)$ leads to a nearly 30% higher I_d. Compared to $N_2O_4(l)$ the difference in density is smaller, but the resulting density impulse (I_d) is still 20% higher. A similar trend is seen for propellant mixtures using liquid hydrogen [$H_2(l)$] as fuel. Again, TNA loses to $O_2(l)$ in I_{sp}, but provides a much higher I_d than both $O_2(l)$ and $N_2O_4(l)$. TNA could potentially also replace ammonium perchlorate [AP, $NH_4ClO_4(s)$] in solid formulations. Here we have looked at propellants with aluminum

Table 2.2 *Computed propulsion performance of TNA-based propellants compared to propellants based on common oxidizers and fuels.*[a]

Oxidizer (O)	Fuel (F)	O : F ratio at maximum I_{sp}	Specific impulse, (I_{sp}) (s)	Density impulse (I_d) (kg, s/L)	Combustion temperature (T_c) (K)
$O_2(l)$	$N_2H_4(l)$	48 : 52	313	333	3392
$N_2O_4(l)$	$N_2H_4(l)$	57 : 43	293	356	3250
TNA(s)	$N_2H_4(l)$	59 : 41	300	427	3375
$O_2(l)$	$H_2(l)$	80 : 20	390	107	2947
$N_2O_4(l)$	$H_2(l)$	85 : 15	342	122	2762
TNA(s)	$H_2(l)$	86 : 14	350	141	2891
$NH_4ClO_4(s)$	$AlH_3(s)$	58 : 42	293	505	3637
TNA(s)	$AlH_3(s)$	57 : 43	302	526	4156

[a] The RPA Lite edition 1.2.8 was used for all performance computations [33]. A chamber pressure of 7 MPa and a nozzle expansion to atmospheric pressure (0.1 MPa) was assumed (Brinck, T. and Rahm, M., 2013, unpublished results). ΔH_f^o values were taken as provided in the RPA software. 44.8 kcal/mol was used for TNA. Density impulses were calculated using the following densities (in g/cm^3): $\rho(TNA) = 2.0$, $\rho(O_2) = 1.141$, $\rho(N_2O_4) = 1.443$, $\rho(N_2H_4) = 1.005$, $\rho(H_2) = 0.0678$, $\rho(AlH_3) = 1.486$, $\rho(NH_4ClO_4) = 1.95$.

hydride [$AlH_3(s)$] as the fuel. Replacing AP with TNA results in slight increases in both I_{sp} and I_d.

2.3.2 Energetic Anions Rich in Oxygen and Nitrogen

Salt-based energetic materials have some general advantages over nonionic materials, such as better thermal stability, higher melting point, and lower vapor pressure. In particular, ionic oxidizers are of great importance for solid propellants. One promising green alternative is ammonium dinitramide (ADN, $NH_4N(NO_2)_2$), which is the focus of Chapter 7 of this book. However, as noted there, ADN has some stability and compatibility issues and the design of alternative oxidizers is of great interest. One strategy to increase the stability of dinitramide-based propellants has been to search for alternative counterions to replace the ammonium ion. Some examples of the outcome of this strategy are discussed in the chapter on ADN. Here we will instead focus on the attempts to design and characterize negative ions that are rich in nitrogen and oxygen.

2.3.2.1 Trinitrogen Dioxide Anion

One interesting candidate for green propulsion is the trinitrogen dioxide anion (TNO, $N(NO)_2^-$), **6**). It has been identified in the gas phase by mass spectrometry in several independent experiments [44–47], but the experimental estimates of its kinetic and thermodynamic stability differ greatly. We have demonstrated that the potential energy surface is extremely complex. The most probable pathway for decomposition is dissociation into N_2O and NO^- via a spin-forbidden transition, see Figure 2.2 [48].

This dissociation is computed to be endothermic by 28 kcal mol in the gas phase and exothermic by 4 kcal/mol in solution. We have characterized the minimum energy crossing point (MECP) of the singlet and triplet surfaces along the dissociation pathway using density functional theory at the B3LYP level. Energy calculations using both DFT and coupled-cluster theory indicate that the MECP lies a few kcal/mol above the gas phase dissociation limit. Thus, we have estimated that the effective activation enthalpy for the gas phase decomposition is at least 28 kcal/mol. Since the MECP lies early along the dissociation pathway, the solvation effect on the MECP barrier is small and 28 kcal/mol is also a good estimate in solution. Furthermore, it has been estimated that spin-forbidden transitions are slower than spin-allowed by a factor of 1 to 4 orders of magnitude. This corresponds to an increase in an adiabatic reaction barrier by 1.4–5.5 kcal/mol at room temperature. It should be noted that more accurate characterization of the minimum energy

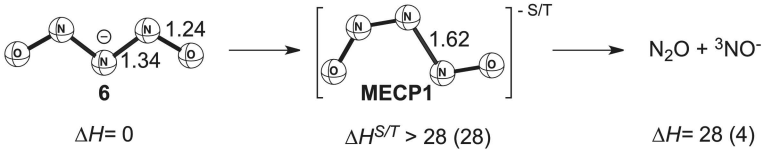

Figure 2.2 *The lowest energy decomposition pathway (in kcal/mol) of TNO (**6**) [48]. Geometries, including the minimum energy crossing point (**MECP1**), optimized at B3LYP/6-31 + G(d) level. Energies based on CCSD(T) computations. Enthalpies in parentheses refer to THF solution. Bond lengths are in Å.*

Table 2.3 *Computed properties of the energetic anions, DN, TNO, and NOAT and their corresponding ammonium salts.*

Compound	DN	TNO (**6**)	NOAT (**7**)
$\Delta H_f^o(anion, g)$ (kcal/mol)[a]	−31.2	13.0	32.9[b]
$\Delta H_f^o(s)$ (kcal/mol)[a,c]	−36.2 (−35.4)[d]	2.9	32.6[b]
$IP_{ad.}$ (eV)[a]	4.4	3.1	3.3[b]
A_{max} (nm)[a,e]	279 (0.11)	271 (0.40)	—
Density (g/cm^3)[a,c]	1.8	1.6	1.7[b]
Oxygen balance (%)[c]	25.8	0.0	0.0
(I_{sp}) (s)[f] of monoprop.	203 (2062)	269 (3015)	284 (3242)
(I_{sp}) (s)[f] (Ox-Al prop.)[g]	267 (4114)	283 (3780)	292 (3818)
% oxidizer in propellant[g]	75	79	83

[a] Computed value from Ref. [48].
[b] Value from Ref. [49].
[c] Value for the corresponding ammonium salt.
[d] Experimental value from Ref. [50].
[e] Vertical excitation energy with oscillator strength in parenthesis. The RPA Lite edition 1.2.8 was used for all performance computations [33].
[f] Combustion temperatures within parentheses. A chamber pressure of 7 MPa and a nozzle expansion to atmospheric pressure (0.1 MPa) was assumed.
[g] Propellant composition (oxidizer and aluminum) optimized for maximum I_{sp}.

crossing point and the calculation of the transition probability would require multireference methods, such as CAS-SCF or preferably MR-CI. However, our estimate of the kinetic stability is sufficient to indicate that TNO should be at least as stable as the pentazolate ion (*vid. infra*), and render it of interest for propulsion applications.

The adiabatic ionization potential has been experimentally estimated to 3.1 eV, which is in excellent agreement with our computed value (Table 2.3). This suggests that TNO should form stable salts with standard cations, such as NH_4^+. The computed absorption spectra of TNO has a strong band at 271 nm. This transition could be used as an important fingerprint for identification of TNO by UV-Vis spectroscopy. Unfortunately, experimental studies [46], as well as our computational characterization [48], indicate that the excited state is dissociative and that irradiation at this wavelength region leads to photodissociation with NO, N_2, and O^- as the most probable products. Thus, salts of TNO are likely to be photosensitive, and this could become a serious drawback for their use in propellant compositions.

Different routes can be envisioned for the synthesis of TNO. In a similar manner as for the gas phase production, reduced nitrous oxide in solution can be expected to react with nitrogen monoxide.

$$N_2O^- + NO \rightarrow \mathbf{6} \tag{2.3}$$

This reaction is exothermic by 25 kcal/mol in THF [48]. The main difficulty will be the reduction of nitrous oxide and the inherent instability of N_2O^- towards dissociation into O^- and N_2. An alternative pathway would be the exothermic reaction ($\Delta H = -4$ kcal/mol in THF) between the hyponitrite anion and nitrous oxide [48].

$$N_2O + NO^- \rightarrow \mathbf{6} \tag{2.4}$$

The ammonium salt of TNO (ATNO) has a computed $\Delta H_f^o(s)$ of 2.9 kcal/mol, a value that is significantly higher than the −35.4 kcal/mol of ADN. Our analysis also indicates that ATNO performs considerably better than ADN in propellant formulations with aluminum (Table 2.3). At the optimal Al loading of 21%, the I_{sp} is 6% higher than for an optimized ADN-Al propellant with 75% oxidizer. Compared to a 73 : 23 AP-Al propellant the performance gain is 14%. Since ATNO has a perfect oxygen balance, the compound would also perform very well as a monopropellant. Pure ATNO has a computed I_{sp} that is almost identical to the ADN-Al propellant. From an environmental perspective, it would be of great value to omit the aluminum from the propellant. To summarize, TNO has many attractive features for propulsion applications. However, there are still some questions regarding its stability, and particularly photosensitivity. Furthermore, potential pathways for synthesis are yet to be explored.

2.3.2.2 1-Nitro-2-oxo-3-Amino-Triazene Anion

The 1-nitro-2-oxo-3-amino-triazene anion (NOAT, **7**) is another interesting candidate anion for green propulsion. NOAT has the summation formula $N_5O_3H_3$, and was identified during an organized effort to computationally characterize a number of potential green oxidizers [4,51]. Similarly to TNO, the ammonium salt of NOAT (ANOAT) has a perfect oxygen balance. However, NOAT has the advantage of a much higher decomposition barrier. We have explored a large number of potential decomposition mechanisms by computations [49]. According to our most recent results, shown in Figure 2.3, the initial decomposition step involves the concerted dissociation of the H_2N–N(O)N bond to form isodiazene and a high energy conformer of $(ONNNO_2)^-$ (Brinck, T. and Rahm, M., 2013, unpublished results).

This dissociation has an activation enthalpy of 38 and 42 kcal/mol in gas phase and THF, respectively. Furthermore, the reaction is endothermic by 31 and 29 kcal/mol, respectively, in the two media. The apparent high kinetic stability stems from the fact that it is not possible to break up the molecule into stable products in a single reaction step. Instead, the initial reaction step results in high energy species, which inevitably also drives up the activation barrier. This is a feature that should always be considered when attempting the design of high energy materials with high kinetic stability.

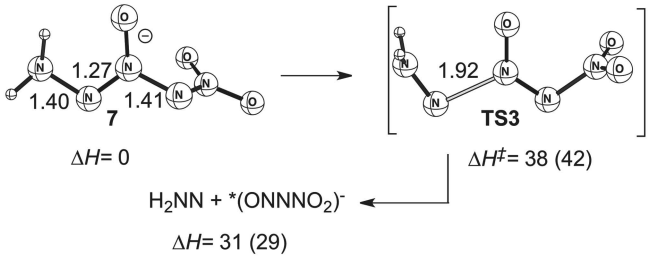

Figure 2.3 *The initial step of the lowest energy decomposition pathway (in kcal/mol) of NOAT (**6**). The asterisk (*) denotes a high-energy isomer. Energies obtained at the CBS-QB3 level but with geometries obtained at the M06-2X/6-31 + G(d,p) level. Enthalpies in parentheses refer to THF solution. Bond lengths are in Å.*

Identification of NOAT by absorption or fluorescence spectroscopy does not seem feasible, since we have not been able to identify any transitions of significant intensity in the visible or near-UV region [49]. The lack of active absorption bands in these regions has the advantage that the compound should not be sensitive to photodecomposition. In addition, due to the size and lack of symmetry, there are a number of other spectroscopies that can be used for identification and characterization. These include NMR as well as IR and Raman. In particular, the vibrational spectra will include a wealth of information, and can be compared to accurate theoretical spectra.

The ammonium salt of NOAT (ANOAT) has a very high $\Delta H_f^o(s)$, and the predicted performance in solid formulations is the highest of all the ammonium salts that we have studied, see Table 2.3 [49]. Due to the perfect oxygen balance (0%), it performs very well as a monopropellant; in fact, the predicted I_{sp} is 6% higher than for the optimum ADN-Al blend. Compared to ATNO, the performance gain is 6% for a monopropellant but only 2–3% for propellants with Al. More importantly, ANOAT has a much higher kinetic stability, and photodecomposition is not expected to pose a problem. The main problem rather lies in how to synthesize this compound. It is difficult to envision any realistic pathway for large-scale synthesis.

2.3.3 The Pentazolate Anion and its Oxy-Derivatives

For a long time there has been a great interest in nitrogen clusters as potential components of high energy density materials (HEDM). The elusive pentazolate anion (PZ, cyc-N_5^-, **8**) is one of the species that has received the most attention. Ugi and Huisgen synthesized and studied arylpentazoles (ArN_5) in the 1950s [52,53]. They also used these compounds as starting materials in the first serious attempts to isolate PZ [54]. The synthesis of the open-chain N_5^+ cation in 1999 resulted in renewed interest in nitrogen cluster chemistry and particularly in PZ [55]. Finally, in 2002 and 2003, after extensive theoretical studies, the PZ was detected in two independent mass spectrometry experiments [56,57]. The detection in solution was reported in 2003 [58], but the NMR-assignment was subsequently questioned [59]. Although a recent theoretical study has provided support for the original assignment [60], it is clear that PZ at best was generated as a transient species [61]. Thus, the quest for its synthesis and isolation goes on. Recently some of the focus has been turned to the oxo-derivatives of PZ, the oxopentazolate (OPZ, **9**) and the 1,3-dioxopentazolate (DPZ, **10**). They are expected to perform better in propulsion applications, have higher kinetic stabilities, and be easier to detect and characterize by spectroscopic techniques [48,49].

2.3.3.1 Kinetic Stability

The dominating decomposition mechanism of PZ is well established from numerous theoretical studies. It proceeds via a concerted dissociation into molecular nitrogen and the azide anion, see Figure 2.4. We have computed the activation enthalpy to 28 kcal/mol, which is in good agreement with other theoretical studies [48]. The initial state is slightly better solvated than the transition state, and this raises the predicted barrier in THF by circa 1 kcal/mol. The reaction is exothermic by 9 kcal/mol in gas phase, and increases to 14 kcal/mol in THF due to the strong solvation of the azide anion.

The potential energy surface of OPZ is much more complex than that of PZ and there are a number of potential decomposition pathways [48]. However, according to our analysis, the

initial and rate-determining step of the dominating pathway involves the concerted dissociation into molecular nitrogen and the energetic intermediate $(N_3O)^-$. The latter will subsequently decompose into N_2 and NO^-, see Figure 2.4. The first reaction is endothermic by 8 kcal/mol in gas phase and 2 kcal/mol in THF. However it is exergonic in both media, due to the release of nitrogen gas. Compared to PZ, the endothermicity of the initial step results in a raised activation enthalpy of more than 2 kcal/mol in gas phase as well as THF. This again highlights the advantage from the viewpoint of kinetic stability of molecules that cannot decompose to stable species in a single step. The relevance of this principle is enforced by considering the decomposition of DPZ, where the initial step again is exothermic and results in the formation of N_2 and TNO; DPZ has a theoretical activation enthalpy that is almost identical to that of PZ in both gas phase and solution [49]. Interestingly, the NN bonds initially broken in the three species, PZ, OPZ, and DPZ, are very similar in length, see Figure 2.4. Thus, the larger decomposition barrier of OPZ cannot be anticipated from the ground-state geometric structure. As a final point on kinetic stabilization of the pentazolates, we note that DPZ has a lower activation entropy and therefore larger preexponential factor than PZ, and as a consequence DPZ should be slightly more stable than PZ [49].

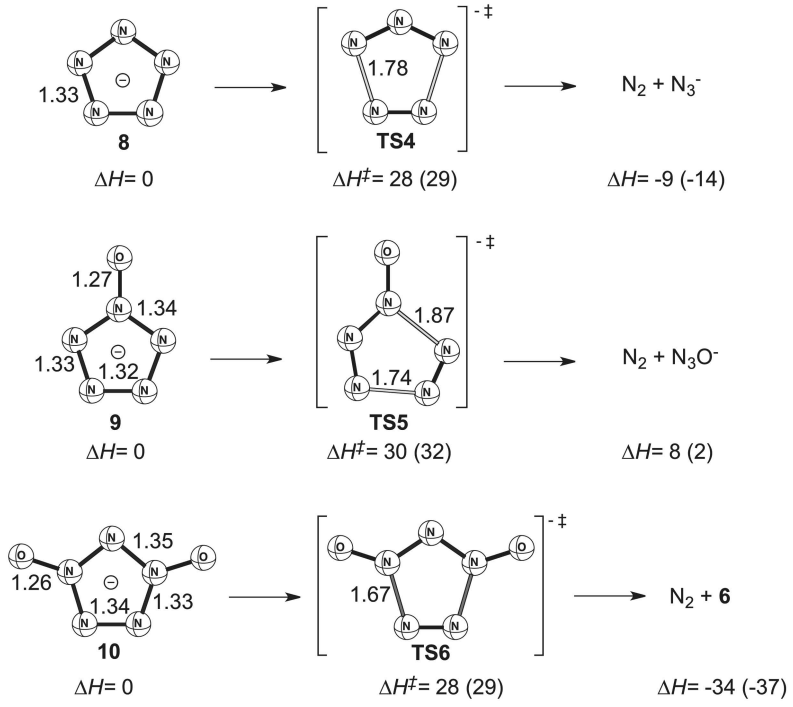

Figure 2.4 *The initial step of the lowest energy decomposition pathway (in kcal/mol) of PZ (**8**), OPZ (**9**), and DPZ (**10**). Energies obtained at the CBS-QB3 level [48,49]. Enthalpies in parentheses refer to THF solution. Bond lengths are in Å.*

2.3.3.2 Spectroscopic Detection

The high symmetry of PZ renders the molecule difficult to detect and characterize by spectroscopical methods. The IR-spectrum has only one weak band. Bartlett computed the Raman spectrum using the accurate CCSD method and found that although there are three allowed bands, only the fully symmetric stretch with a harmonic frequency of $1222\,cm^{-1}$ has an intensity that is sufficient for detection and characterization [62]. The NMR spectrum, whether it is ^{14}N or ^{15}N, also consists of a single peak. The frequency of this peak is difficult to predict accurately by theoretical methods and is sensitive to the solvent [60]. As mentioned, the use of the NMR-shift for fingerprinting has already stirred up a controversy in the case of Butler's attempted synthesis of PZ. To further complicate the issue of detection, we have not been able to identify any allowed transition in the UV-Vis spectral region. Studies by Frenking and coworkers indicate that PZ can be stabilized by bonding to Fe(II) in a ferrocene-like complex, that is $Fe(\eta^5\text{-}N_5)_2$ [63]. We have found that this compound has a distinct absorption spectrum in the UV-Vis region (Brinck, T. and Carlqvist, P. unpublished results).

The matter of detection and characterization should be less of an issue in any attempts to prepare the oxo-derivatives, OPZ and DPZ. In both cases, the vibrational spectra provide a wealth of information for fingerprinting. Also ^{14}N- or ^{15}N-NMR may be of great use for identification as both species have three unique nitrogens that should result in distinct spectra. In these cases, comparison with computed NMR-shifts could significantly aid the identification. Finally, we note that both species have a relatively strong absorption band in the near-UV region, with absorption maxima at 240 nm and 284 nm for OPZ and DPZ, respectively, according to calculations at the CC2/aug-cc-pVTZ level [48,49]. We have not yet explored whether these transitions could render the compounds photosensitive.

2.3.3.3 Synthesis

In contrast to the case for most other nitrogen clusters, there exists a class of potentially useful starting materials for synthesis of PZ, namely the arylpentazoles. This was recognized by Huigi and coworkers in the late 1950s, and they made several attempts at preparing PZ [53,54]. Considering the difficulties in detecting PZ, even with modern spectroscopical methods, it is tempting to speculate that some of their experiments actually resulted in the desired product. Butler and coworkers used Ceric ammonium nitrate (CAN) in methanol–water at $-40\,°C$ for *N*-dearylation of 1-*p*-methoxyphenylpentazole to produce benzoquinone [58,61]. They suggest that the reaction afforded pentazole (HN_5), which was held in solution as PZ complexed to Zn^{2+}. The outcome of this experiment has been under scrutiny, and rather than going into the details we refer the interested reader to the relevant literature [59,60]. In any case, it seems clear that the experimental protocol will not enable isolation of PZ without significant modifications. We have investigated two other routes of synthesis by quantum chemical theory (Scheme 2.1). The first is inspired by a reaction used

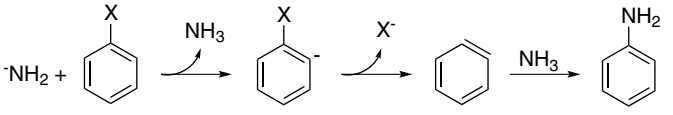

Scheme 2.1 *The classical amination reaction.*

Table 2.4 *Computed standard free energies in liquid ammonia for the two first reaction steps in the amination of halobenzenes and phenylpentazole [64].*

Arylpentazole	Proton abstration		Benzyne formation
X	ΔG°_{sol} [a]	ΔG°_{sol}	ΔG°_{sol} [a]
Br	15.7	7.9	2.9
Cl	16.6	7.8	5.4
F	16.6	7.1	29.0
cyclo-N_5	16.4	4.7	25.3 (19.2)[b]

[a] Standard free energy of activation.
[b] Phenylpentazole in complex with Zn^{2+}.

for amination of halobenzenes. In its classical form halobenzenes are treated with excess sodium or potassium amide in liquid ammonia at −33 °C to produce anilines.

Our hypothesis was that the first two reaction steps might be applicable to arylpentazoles and generate free PZ [64]. In order to validate the computational approach, we studied the original reaction in parallel. Standard Gibbs free energies in solution for the different reaction steps are presented in Table 2.4. The data for the halobenzenes is in agreement, at least qualitatively, with experimentally observed trends of reactivity. The initial step, the deprotonation, is slightly more favored for the phenylpentazole than for the halobenzenes. The second step is known to proceed only for Br and Cl and not F. This is confirmed by our computed energetics, which show low barriers for the two former and an exceedingly high activation free energy for the fluoro-derivative. The barrier for the phenylpentazole is lower than that for fluorobenzene, but still too high to make the reaction feasible. Inspired by the work of Butler and coworkers [58], we investigated the effect of complexation of Zn^{2+} to the N_5 ring. This reduces the barrier for the dissociation by 6 kcal/mol. The resulting activation energy is still slightly too high, but the effect of metal-ion complexation needs to be investigated further. With proper optimization of the reaction conditions and the metal ion this reaction could potentially produce PZ. Using a metal ion, however, may be a dead end if the objective is to prepare an energetic salt, such as ammonium pentazolate (APZ).

Another approach that we have studied in more detail is based on electrochemical reduction of arylpentazoles. In 2003, we reported the detection of PZ by laser desorption ionization mass spectrometry in a collaborative study with the group of Östmark and coworkers [57]. As a part of that study we also investigated the molecular mechanism for the formation of PZ from the starting material, *p*-dimethylaminophenylpentazole. Our analysis showed that the most plausible pathway is the direct dissociation of the reduced arylpentazole into the *p*-dimethylaminophenyl radical and PZ. This pathway has a dissociation barrier that is very similar to the dissociation of the arylpentazole into the corresponding azide and N_2. The fact that such a mechanism is able to produce PZ in the gas phase is very promising for the prospect of electrochemical synthesis in solution. It is known that the kinetic stabilities of arylpentazoles increase with increasing polarity of the solvent [65]. The same behavior is predicted for PZ according to our calculations. On the other hand, the barrier for the productive dissociation of the reduced arylpentazole is expected to decrease with increasing solvent polarity. The relevant reactions of the neutral and reduced arylpentazoles are given in Scheme 2.2.

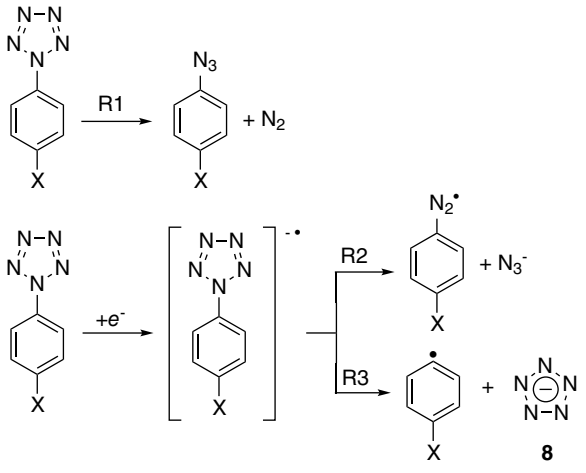

Scheme 2.2 *Reactions relevant for electrochemical synthesis of PZ (**8**).*

As seen in Table 2.5, the productive dissociation (R3) of the reduced arylpentazole becomes kinetically favored over the neutral arylpentazole decomposition (R1) in relatively polar solvents, such as acetonitrile and methanol. Unfortunately, the nonproductive dissociation of the reduced form (R2) has a similar solvent effect as the desired reaction. The difference between the two activation barriers is found to increase with the resonance electron-donating effect of the substituent, and for reduced arylpentazoles with strong electron-donating substituents the nonproductive dissociation dominates over the productive dissociation. This effect is particularly apparent when comparing the phenylpentazole to the *p*-dimethylaminophenylpentazole. The methoxy-substituted arylpentazole looks to be

Table 2.5 *Computed standard free energies of activation for the relevant reactions in the electrochemical reduction of arylpentazoles to produce the pentazolate anion, and computed reduction potentials of the arylpentazoles.*

	R1		R2		R3		Red.
X	ΔG°_g [a,b]	ΔG°_{sol} [b,c]	ΔG°_g [a,d]	ΔG°_{sol} [d,e]	ΔG°_g [a,d]	ΔG°_{sol} [d,e]	E^{red} (V)[f]
Cl	16.4	19.5 (19.6)[g]	23.2	21.5	23.4	21.7	−1.66
H	16.5	19.5 (19.8)[g]	23.3	21.5	23.4	21.5	−1.74
OCH_3	[17.7][h]	[20.8][h]	23.0	19.6	22.8	20.3	−2.08
$N(CH_3)_2$	18.3	21.3 (20.7)[g]	23.2	18.7	24.0	20.9	−2.02
O^-	20.8	22.0 (21.0)[g]	17.0	17.5	17.0	18.4	−2.38

[a] Value in gas phase (1 atm).
[b] From Ref. [65].
[c] In methanol solution (1 M).
[d] From Ref. (Brinck, T. and Carlqvist, P. unpublished results).
[e] In acetonitrile solution (1 M). The solvent effect is expected to be similar to that of a methanol solution.
[f] Computed reduction potential in acetonitrile relative the standard calomel electrode (Brinck, T. and Carlqvist, P. unpublished results).
[g] Experimental value [53].
[h] Estimated value based on the for value *p*-hydroxy-phenylpentazole.

a good compromise in terms of the activation of the different dissociation pathways. A better approach may be to first reduce the relatively unstable phenylpentazole at a very low temperature and then let the solution slowly heat to form the desired product. There is also potential for optimizing the conditions with respect to solvent polarity and other factors. In any case, we feel that the theoretical results, in conjunction with the favorable outcome of the mass-spectrometry experiment, are promising enough to encourage attempts to synthesize PZ by this approach. We have included the computed reduction potentials in acetonitrile of the arylpentazoles as a reference for the reader interested in pursuing such an activity. These have been computed using an approach that has been very successful for predicting reduction potentials for substituted aromatics, and are expected to have an accuracy of 0.2 eV [66,67].

Frison *et al*. recently used quantum chemical methods (B3LYP and CCSD(T)) to investigate the prospect of preparing OPZ and DPZ by ozonolysis of PZ [68]. They found a barrier of 20 kcal/mol for the initial step to form OPZ, and 26 kcal/mol for forming DPZ from OPZ. These results suggest that the synthesis of OPZ should be feasible once PZ has been produced in pure form; the barrier for ozonlysis is lower than the decomposition barriers of PZ and OPZ, and with proper experimental conditions the reaction will not proceed to form DPZ. The preparation of DPZ from OPZ appears more difficult as the reaction is exothermic by 37 kcal/mol and the barrier is close to the decomposition barrier of DPZ. An alternative procedure for preparing OPZ and DPZ would be the ozonolysis of an arylpentazole followed by the cleavage of the C−N bond in a subsequent step. However, the ozonolysis of phenylpentazole has a barrier of more than 40 kcal/mol, which renders the reaction impossible for preparative purposes.

2.3.3.4 Performance

The $\Delta H_f^o(g)$ of PZ has theoretically been estimated to 58 kcal/mol [48]. This high value is a manifest over the much lower bond energy of an aromatic N−N bond compared to the triple bond in N_2. Addition of one and two oxygen atoms to form OPZ and DPZ decreases the $\Delta H_f^o(g)$ by 5 and 4 kcal/mol respectively [48,49]. There are smaller differences in the $\Delta H_f^o(s)$ values of the corresponding ammonium salts, see Table 2.6. The ammonium pentazolate (APZ) has a relatively poor predicted performance as a monopropellant due to its negative oxygen balance. Together with an oxygen rich counterion or additive, PZ has the potential to perform much better. Another alternative would be to combine APZ with a green oxidizer, such as ADN, for example a 50 : 50 mix of ADN and APZ performs almost as well as an ADN-Al propellant, but has the advantage of a much reduced combustion temperature. The AOPZ salt reaches a similar performance level as monopropellant, and the I_{sp} can be further increased with the addition of up to 40% ADN. ADPZ has an oxygen balance of zero and performs very well both as a monopropellant and in compositions with up to 20% Al. Overall, the performance is marginally higher than for ATNO, but does not reach the full level of ANOAT.

Despite the better predicted performance of ADPZ compared to AOPZ, we believe the chances of seeing the former in future propellant compositions to be much lower; AOPZ has a higher kinetic stability and the prospects for preparing this compound in large quantities is better. The performance level is also more than sufficient to make this compound an interesting alternative for the future.

Table 2.6 *Computed properties of the pentazolate anion (PZ) and its oxo-derivatives (OPZ and DPZ) and their corresponding ammonium salts.*

Compound	PZ	OPZ	DPZ
$\Delta H_f^o(anion, g)$ (kcal/mol)	58.2[a]	53.1[a]	49.3[b]
$\Delta H_f^o(s)$ (kcal/mol)[c]	47.9[a]	45.6[a]	44.3[b]
$I_{ad.}$ (eV)	2.1[d]	3.8[a]	3.7[b]
A_{max} (nm)[e]	—	240 (0.20)[a]	284 (0.16)[b]
Density (g/cm^3)[a,c]	1.5[a]	1.6[a]	1.7[b]
Oxygen balance (%)[c]	−36.4	−15.3	0.0
(I_{sp}) (s)[f] of monoprop.	200 (1576))	250 (2675)	273 (3205)
(I_{sp}) (s)[f] (opt. prop.)[g]	257 (2909)	263 (3022)	285 (3845)
Composition (O : F)[g]	58 : 42 (ADN : APZ)	36 : 64 (ADN : AOPZ)	82 : 18 (ADPZ : Al)

[a] From Ref. [48].
[b] From Ref. [49].
[c] Value for the corresponding ammonium salt.
[d] From Ref. [69].
[e] Vertical excitation energy with oscillator strength in parenthesis.
[f] The RPA Lite edition 1.2.8 was used for all performance computations [33]. A chamber pressure of 7 MPa and a nozzle expansion to atmospheric pressure (0.1 MPa) was assumed. Combustion temperatures within parentheses.
[g] Propellant composition (oxidizer : fuel) optimized for maximum I_{sp}.

2.3.4 Tetrahedral N_4

There has been a considerable interest in allotropes of nitrogen as potential sources for new HEDMs. Such materials would not only be highly energetic but also green, as molecular nitrogen (N_2) would be the only product of the energy releasing reaction. However, despite extensive theoretical and experimental efforts, N_2 remains the only form of nitrogen that has been isolated at room temperature. Linear and cyclic N_3, as well as an open-chain form of N_4, have been detected experimentally, but they are too unstable to be of any direct interest for applications [70–72]. The synthesis of N_5^+ and the subsequent detection of N_5^- [55–57], spawned interest in N_8 and N_{10} in the form of molecular salts. Bartlett and coworkers arrived at the conclusion that $N_5^+N_3^-$ cannot exist but that $N_5^+N_5^-$ is likely to be kinetically stable [73]. Dixon *et al.* questioned the stability of the N_{10} salt based on a Haber–Bosch analysis [69]. Their study indicates that the salt would spontaneously dissociate into N_3 radicals and N_2 due to the dissociative nature of the open-chain and cyclic N_5 radicals. Other forms of N_8 and N_{10} have been investigated, but were found to have relatively low kinetic stabilities [74]. Tetraazatetrahedrane ($N_4(T_d)$, **11**) is probably the nitrogen allotrope compound with the best prospect for use as a HEDM.

2.3.4.1 Potential Energy Surface

The potential energy surface of N_4 has been the focus of intense theoretical studies [75]. It is very sensitive to the theoretical level and many of its features can only be properly described with high-level multi-configurational *ab initio* methods. There are two kinetically stable forms of N_4 of almost identical energy, namely $N_4(T_d)$ and a cyclic form ($N_4(D_{2h})$, **12**), see Figure 2.5. The latter has a low barrier for dissociation into two N_2, which we have estimated to *circa* 7 kcal/mol based on MR-CI and CCSD(T) computations [76]. Thus, this isomer can only exist at very low temperatures. In

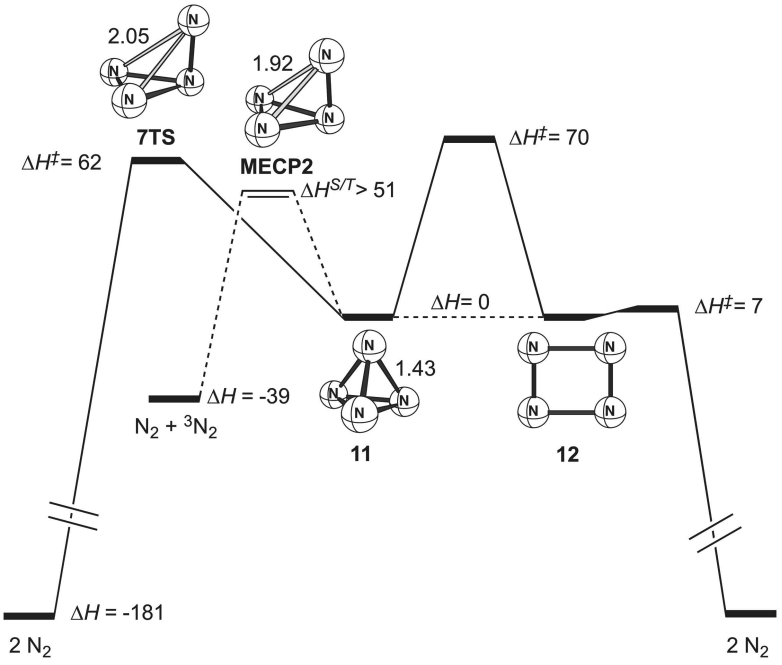

Figure 2.5 *Enthalpies (in kcal/mol) for stationary points on the N_4 potential energy surface. The spin-forbidden dissociation pathway that passes via the singlet-triplet minimum energy crossing point* ***MECP2*** *is included. The enthalpies have been estimated from CCSD(T), MR-CI and CAS-SCF calculations reported in Ref. [75,77–79]. Selected bond lengths in Å. Adapted with permission from [75] © 2003 Elsevier B.V., The Amsterdam, NL.*

contrast, $N_4(T_d)$ has a very high lying transition state for dissociation due to an avoided crossing. Such a process cannot be described by a single reference method, and to our knowledge the best estimate of this barrier is *circa* 62 kcal/mol, which was obtained from a MR-CI calculation at a CAS-SCF optimized geometry [77]. This dissociation is highly exothermic and the dissociation energy at 0 K has been estimated to a staggering −182.2 kcal/mol using the very accurate W1 theory [78]. Thus, $N_4(T_d)$ seems like a contradiction to the thesis of this chapter that compounds that can decompose to stable products in a single exothermic step have low kinetic stabilities. However, this is a special case, since the molecule needs to change its electron configuration during the process.

A second pathway for decomposition involves the interconversion to $N_4(D_{2h})$ in the initial step [76]. Also in this case the barrier stems from an avoided crossing, and we have estimated it to be of similar or higher magnitude as the barrier for the direct dissocation into two N_2. It was long considered that the kinetic stability of $N_4(T_d)$ would be governed by the spin-forbidden dissociation into one ground-state N_2 and one triplet-state $N_2[N_2(^3\Sigma_u^+)]$. The minimum crossing point had been estimated to lie only 28 kcal/mol above the ground state based on a structure determined at the CI-SD level [80]. However,

we have shown that this structure is not valid at higher levels of theory. Furthermore, the structure is clearly post-dissociative, that is, the molecule would have to pass the transition state on the singlet surface before reaching this point. We have located the minimum energy crossing point by state-averaged CAS-SCF computations, and estimated the barrier for the spin-forbidden transition to at least 51 kcal/mol based on CAS-SCF and CCSD(T) single points [75]. This value is sufficiently large to confirm the very high kinetic stability of $N_4(T_d)$. In many ways $N_4(T_d)$ seems to be the ideal energetic molecule; it combines high stability with excellent energetics and green burning. There are only two "minor" problems left: detection and synthesis.

2.3.4.2 Spectroscopic Detection

In a similar manner as for the pentazolate anion, the high symmetry of the molecule complicates the detection of $N_4(T_d)$. The IR spectrum has only one line of weak intensity. This transition can still be used for identification if isotopic labeling is employed. The Raman spectrum is more informative, and consists of three relatively strong bands. Identification by IR or Raman would benefit from the very accurate quartic force-field obtained at the CCSD(T) level by Lee and Martin [78]. IR and Raman intensities determined at the same level but within the harmonic approximation have been published by Pereira and Bartlett [62]. Raman is a relatively sensitive technique, and the detection limit of $N_4(T_d)$ has been determined to be in the order of 10^2 ppm in liquid and solid nitrogen with a standard setup [81]. We have performed EOM-CCSD and QR-CCSD computations to determine the one- and two-photon absorption spectra [75,82]. The first excited state has a vertical excitation energy as high as 9.65 eV, and zero oscillator strength. The first allowed transition with a sizeable oscillator strength lies at 10.65 eV (116 nm). This state can also be reached by two-photon absorption. It would be preferable to excite the molecule by two-photon absorption and then detect it by the fluorescence. However, it is uncertain if this excitation will generate any sizeable fluorescence and the fluorescence wavelength is very hard to predict.

2.3.4.3 Synthesis

Although the detection of $N_4(T_d)$ will be problematic, the real problem lies in the synthesis. The very high energy of the molecule renders it almost impossible to prepare from ground-state molecules. Essentially, two types of approaches have been proposed for the synthesis. The first is based on the collision of excited-state N_2 molecules. High concentrations of excited-state N_2 molecules can be generated in liquid or solid nitrogen by laser irradiation, ion bombardment, r.f. excitation or in a hollow-cathode discharge. One requirement for such a reaction to be productive is that the starting material must be higher in energy than the transition state for the dissociation. In reality, this requirement is not the limiting factor, the real problem lies in the necessity of the interacting N_2 molecules to have electron configurations that can facilitate the formation of $N_4(T_d)$, that is, as argued by Lee and Dateo, the interacting N_2 should have single bonds and the remaining *p*-electrons should be unpaired for the formation of the new N−N bonds [83]. Furthermore, the N_2 molecules need to be excited to quintet states as singlet and triplet excited states of this character have extremely short lifetimes. The relevant quintet states are very high in energy and hard to generate. Their high energies have the significant drawback that any $N_4(T_d)$ formed will be in a highly excited vibrational state and likely to dissociate within a few vibrations.

The second type of approach utilizes nitrogen atoms to furnish the necessary energy. The hypothetical reaction between two ground-state nitrogen atoms and N_2 to form $N_4(T_d)$ is exothermic by 46 kcal/mol. However, also for this type of reaction, it is not sufficient to fulfill the energy requirement, as the interacting species need to be in electronic configurations that can facilitate the bond formation. We have shown that $N_4(T_d)$ could potentially be prepared from ground-state N_2 and nitrogen atoms in their ^2D state in a two-step process [79].

The first step involves the formation of a cyclic isomer of the azide radical ($N_3(C_{2v})$, **13**). This isomer was first indicated to be stable by Wasilewski on the basis of MR-CISD calculations with a relatively small active space [84]. We later performed a more elaborate investigation of the potential surface at a higher level of theory, that is MR-CISD(Q)/cc-pVTZ calculations on CAS(15,12)/cc-pVTZ geometries [79]. The isomerization to the ground-state N_3 radical is exothermic by 31 kcal/mol, but has a large barrier of 32 kcal/mol. The dissociation into N_2 and $N(^2D)$ is endothermic by 26 kcal/mol with a barrier of 32 kcal/mol. These results show that this species will have a very long lifetime under collision-free conditions even at ambient temperatures. However, its radical character makes it highly reactive in bimolecular interactions. $N_3(C_{2v})$ could potentially be formed from the direct reaction between N_2 and $N(^2D)$, that is, the reverse of the dissociation. The interacting fragments need to possess sufficient internal energy to overcome the barrier and collide in such a manner that the two bonds can be formed symmetrically. The probability of forming $N_3(C_{2v})$ will be reduced by a number of competing reactions, in particular the formation of the ground-state N_3 in a near barrierless process [79].

The first experimental evidence of the $N_3(C_{2v})$ came in 2003 from Hansen and Wodtke [71]. They studied the photodissociation of chlorine azide (ClN_3) near 235 nm under collision-free conditions, and were able to demonstrate the formation of two isomers of N_3, that is linear and cyclic N_3. On the basis of derived kinetic energy distributions of the state selected $Cl(^2P_J)$, the energy difference between the two isomers was determined to 1.35 ± 0.1 eV. The almost perfect agreement with our computed value of 1.34 eV (30.8 kcal/mol) provided a strong indication that the high energy isomer indeed is $N_3(C_{2v})$. This experiment of Hansen and Wodtke is very interesting since it has not only demonstrated the existence of $N_3(C_{2v})$, but also provided an alternative approach for generating this species [85].

The second step in the synthesis is the reaction between $N(^2D)$ and $N_3(C_{2v})$. A scan of the potential energy surface at the CAS(12,12) level, followed by MR-CISD(Q) at selected points, has shown that a perpendicular approach of $N(^2D)$ towards the molecular plane of $N_3(C_{2v})$ will generate $N_4(T_d)$ in a nearly barrierless process [79]. However, the reaction channel is rather narrow and there is a competing reaction that generates two N_2 molecules.

Both reaction steps require access to nitrogen atoms in the ^2D state. $N(^2D)$ can be generated by $N(^4S)$ quenching of N_2 in the triplet state $[N_2(^3\Sigma_u^+)]$ [79]. This can, for example, be performed under cryogenic conditions in nitrogen matrices. Thus, one can envision a potential set up for small-scale preparation of $N_4(T_d)$ according to the route shown in Figure 2.6. However, even if the experiment proves to be successful, it is very difficult to see how such a procedure could be scaled-up for production of N_4 in larger quantities.

2.3.4.4 Thermodynamic Stability and Performance

As already stated, the energy for dissociating $N_4(T_d)$ to two N_2 molecules is as high as 182 kcal/mol at 0 K. This corresponds to a $\Delta H_f^o(g)$ of 181 kcal/mol at 298 K. The small size

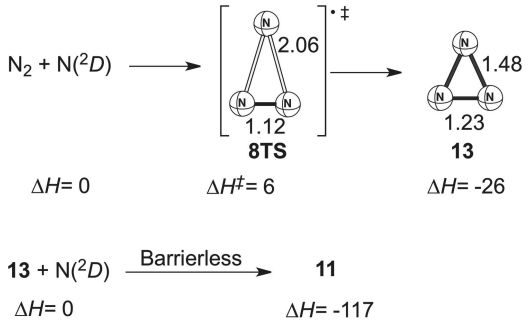

Figure 2.6 *Two-step mechanism for forming $N_4(T_d)$ from N_2 and excited N-atoms in the ^2D state. Enthalpies (in kcal/mol) have been obtained from MR-CISD(Q) energies computed at CAS-SCF geometries [79]. Bond lengths in Å.*

and low polarity of the molecule suggest that N_4 should be a gas at standard conditions. We have attempted to predict the crystal structure of $N_4(T_d)$ by means of periodic DFT calculation with the PBE0 functional and a Gaussian basis set (Brinck, T. and Rahm, M., 2013, unpublished results). This crystal prediction assumed a similar packing arrangement as white phosphorous and included Grimme's D-potential to correct for the improper treatment of dispersion interactions in the correlation-exchange functional [86]. On the basis of these calculations, the sublimation enthalpy is estimated to 8.0 kcal/mol and the crystal density to 1.76 g/cm^3. The density may be somewhat overestimated due to the lack of correction for the basis set superposition error (BSSE) in the structure optimization. Estimating the density from the molecular volume defined by the 0.001 electron density contour gives a value of 1.63 g/cm^3. The computed sublimation enthalpy, which has been corrected for the BSSE, is surprisingly large and indicates that $N_4(T_d)$ is a liquid at ambient temperatures. This would be favorable compared to other high performing propellant components, such as a liquid oxygen and hydrogen, which have to be stored and used under cryogenic conditions.

The predicted performance of $N_4(T_d)(s)$[1] as a monopropellant is 3.5% higher in I_{sp} than a regular 80 : 20 O_2 : H_2 propellant, see Table 2.7. However, the highly exothermic decomposition of $N_4(T_d)$ results in a very high combustion temperature of almost 7500 K. This energy is better utilized for acceleration of light molecules or atoms, and the introduction of 20% H_2 reduces the temperature to 2660 K and increases the I_{sp} by 14%. At the optimum composition with respect to I_{sp}, that is 11% $H_2(l)$, the combustion temperature is still moderate (3700 K) and the I_{sp} is more than 20% higher than for O_2+H_2. The density impulse (I_d) is more than twice that of the standard propellant. It is of further interest to note that the gas exiting the nozzle would be a pure mixture of N_2 and H_2; the total molfraction of the other components, mainly hydrogen atoms and ammonia, is less than 100 ppm.

In many ways, a proper combination of $N_4(T_d)$ and H_2 seems like the ideal green propellant, with extreme performance and very clean burning. In addition, the high stability

[1] Due to the availability of estimates for the sublimation enthalpy and density, all performance computations have been performed for $N_4(T_d)$ in the solid state. However, the changes in performance going to liquid state are expected to very small, and mainly lead to slight improvements in I_{sp} and slight reductions in I_d.

Table 2.7 *Computed propulsion performance of propellants based on $N_4(T_d)$(s) and $H_2(l)$ compared to a standard $O_2(l) + H_2(l)$ propellant.*[a,b]

Compound (C)	Additive (H)	C : A ratio	Specific impulse, (I_{sp}) (s)	Density impulse (I_d) (kg, s/L)	Combustion temperature (T_c) (K)
$O_2(l)$	$H_2(l)$	80 : 20	390	107	2947
$N_4(T_d)(s)$	$H_2(l)$	80 : 20	458	134	2659
$N_4(T_d)(s)$	$H_2(l)$	89 : 11	474	221	3700
$N_4(T_d)(s)$	$H_2(l)$	92 : 8	460	267	4099
$N_4(T_d)(s)$	—	100 : 0	404	686	7475

[a] The RPA Lite edition 1.2.8 was used for all performance computations. [33] A chamber pressure of 7 MPa and a nozzle expansion to atmospheric pressure (0.1 MPa) was assumed. [b] ΔH_f^o values were taken as provided in the RPA software. 172 kcal/mol was used for $N_4(T_d)(s)$. Density impulses were calculated using the following densities (in g/cm^3): $\rho(O_2) = 1.141$, $\rho(H_2) = 0.0678$, $\rho(N_4) = 1.7$.

of $N_4(T_d)$ would make this compound safe and easy to handle. Another advantage is the predicted condensed phase properties, which suggest that $N_4(T_d)$, rather surprisingly, is a liquid at ambient temperatures. This would allow for lighter rocket motors and increases performance and payloads further. Unfortunately, it is very hard to imagine large-scale production of $N_4(T_d)$ in the foreseeable future.

2.4 Conclusions

We have tried to illustrate that modern quantum chemical methods can be an invaluable tool in the rational design of energetic materials with targeted properties. Traditionally, such methods have mainly been used for prediction of thermochemical data, and for analysis of decomposition pathways and kinetic stabilities of new compounds. However, as shown in this chapter, prediction of spectral data and analysis of synthetic pathways are equally important tasks in order to facilitate the synthesis and characterization of novel energetic materials. It is also in these areas that computational analysis has the greatest potential for future improvements.

We have given a few examples of the theoretical characterization of compounds with promising properties for use in green propellants. Three of these compounds have so far been observed experimentally, and for two of them the detection followed intense computational studies. In the case of trinitramide (TNA), the preparation and detection was a direct consequence of the theoretical analysis. None of the compounds has yet been isolated, or prepared on a larger scale. A stronger emphasis on investigating synthetic routes, and closer collaboration between theoreticians and synthetic chemists, may be needed to increase the success rate.

Two of the studied compounds have properties that make them particularly interesting. The first is the ammonium salt of 1-nitro-2-oxo-3-amino-triazene (ANOAT). This compound has a high kinetic stability combined with excellent performance characteristics as a monopropellant. However, so far we have not been able to identify any realistic route for its synthesis. The second compound, tetraazatetrahedrane [$N_4(T_d)$], is in many aspects even more promising. Formulations of $N_4(T_d)$ and $H_2(l)$ are predicted to have

extreme performance levels for propulsion, while producing only N_2 and H_2 as exhaust. The kinetic stability of $N_4(T_d)$ is high, and according to the latest computations $N_4(T_d)$ is expected to be in liquid form under standard conditions. A potential pathway for preparing $N_4(T_d)$ from N_2 and excited-state nitrogen atoms in a two-step process has been analyzed. This reaction may allow for small-scale preparation of $N_4(T_d)$ in matrix isolation experiments. It is very hard to envisage any method that would allow for the preparation of $N_4(T_d)$ on a larger scale.

References

1. Davenas, A. (1993) *Solid Rocket Propulsion Technology*, Pergamon Press, New York.
2. Naumann, K.W. (2010) New Trends and Developments in Rocket Motor Propulsion Technology. Int. Annu. Conf. ICT. 41st (Energetic Materials), **9**, 1.
3. Jensen, F. (1999) *Introduction to Computational Chemistry*, John Wiley & Sons, New York.
4. Rahm, M. (2010) Green Propellants, PhD thesis, Physical Chemistry, KTH The Royal Institute of Technology, Stockholm, Sweden.
5. Zhao, Y. and Truhlar, D. (2008) The M06 suite of density functionals for main group thermochemistry, thermochemical kinetics, noncovalent interactions, excited states, and transition elements: two new functionals and systematic testing of four M06-class functionals and 12 other functionals. *Theoretical Chemistry Accounts*, **120** (1–3), 215–241.
6. Montgomery, J.A., Frisch, M.J., Ochterski, J.W. and Petersson, G.A. (1999) A complete basis set model chemistry. VI. Use of density functional geometries and frequencies. *Journal of Chemical Physics*, **110** (6), 2822–2827.
7. Montgomery, J.A., Frisch, M.J., Ochterski, J.W. and Petersson, G.A. (2000) A complete basis set model chemistry. VII. Use of the minimum population localization method. *Journal of Chemical Physics*, **112** (15), 6532–6542.
8. Curtiss, L.A., Redfern, P.C., Raghavachari, K. *et al*. (1999) Gaussian-3 theory using reduced Moller-Plesset order. *Journal of Chemical Physics*, **110** (10), 4703–4709.
9. Rice, B.M., Pai, S.V. and Hare, J. (1999) Predicting heats of formation of energetic materials using quantum mechanical calculations. *Combustion and Flame*, **118** (3), 445–458.
10. Byrd, E.F.C. and Rice, B.M. (2006) Improved prediction of heats of formation of energetic materials using quantum mechanical calculations. *Journal of Physical Chemistry A*, **110** (3), 1005–1013.
11. Grimme, S. (2006) Semiempirical hybrid density functional with perturbative second-order correlation. *Journal of Chemical Physics*, **124** (3), 034108.
12. Cances, E., Mennucci, B. and Tomasi, J. (1997) A new integral equation formalism for the polarizable continuum model: Theoretical background and applications to isotropic and anisotropic dielectrics. *Journal of Chemical Physics*, **107** (8), 3032–3041.
13. Klamt, A. and Schuurmann, G. (1993) COSMO - A new approach to dielectric screening in solvents with explicit expressions for the screening energy and its gradient. *Journal of the Chemical Society, Perkin Transactions 2* (5), 799–805.
14. Brinck, T., Murray, J.S. and Politzer, P. (1992) Quantitative-determination of the total local polarity (charge separation) in molecules. *Molecular Physics*, **76** (3), 609–617.
15. Murray, J.S., Lane, P., Brinck, T. *et al*. (1993) Relationships of critical constants and boiling points to computed molecular-surface properties. *The Journal of Physical Chemistry*, **97** (37), 9369–9373.
16. Murray, J.S., Brinck, T. and Politzer, P. (1996) Relationships of molecular surface electrostatic potentials to some macroscopic properties. *Chemical Physics*, **204** (2–3), 289–299.

17. Politzer, P., Murray, J.S., Grice, M.E. *et al*. (1997) Calculation of heats of sublimation and solid phase heats of formation. *Molecular Physics*, **91** (5), 923–928.
18. Politzer, P., Ma, Y.G., Lane, P. and Concha, M.C. (2005) Computational prediction of standard gas, liquid, and solid-phase heats of formation and heats of vaporization and sublimation. *International Journal of Quantum Chemistry*, **105** (4), 341–347.
19. Byrd, E.F.C. and Rice, B.M. (2009) A comparison of methods to predict solid phase heats of formation of molecular energetic salts. *Journal of Physical Chemistry A*, **113** (1), 345–352.
20. Politzer, P., Martinez, J., Murray, J.S. *et al*. (2009) An electrostatic interaction correction for improved crystal density prediction. *Molecular Physics*, **107** (19), 2095–2101.
21. Politzer, P., Martinez, J., Murray, J.S. and Concha, M.C. (2010) An electrostatic correction for improved crystal density predictions of energetic ionic compounds. *Molecular Physics*, **108** (10), 1391–1396.
22. Rice, B.M., Hare, J.J. and Byrd, E.F.C. (2007) Accurate predictions of crystal densities using quantum mechanical molecular volumes. *Journal of Physical Chemistry A*, **111** (42), 10874–10879.
23. Holden, J.R., Du, Z.Y. and Ammon, H.I. (1993) Prediction of possible crystal-structures for C-containing, H-containing, N-containing, O-containing and F-containing organic-compounds. *Journal of Computational Chemistry*, **14** (4), 422–437.
24. Neumann, M.A. and Perrin, M.A. (2005) Energy ranking of molecular crystals using density functional theory calculations and an empirical van der Waals correction. *Journal of Physical Chemistry A*, **109** (32), 15531–15541.
25. Balu, R., Byrd, E.F.C. and Rice, B.M. (2011) Assessment of dispersion corrected atom centered pseudopotentials: application to energetic molecular crystals. *The Journal of Physical Chemistry. B*, **115** (5), 803–810.
26. Podeszwa, R., Rice, B.M. and Szalewicz, K. (2008) Predicting structure of molecular crystals from first principles. *Physical Review Letters*, **101** (11), 115503.
27. Sorescu, D.C. and Rice, B.M. (2010) Theoretical predictions of energetic molecular crystals at ambient and hydrostatic compression conditions using dispersion corrections to conventional density functionals (DFT-D). *The Journal of Physical Chemistry C*, **114** (14), 6734–6748.
28. Yanai, T., Tew, D.P. and Handy, N.C. (2004) A new hybrid exchange-correlation functional using the Coulomb-attenuating method(CAM-B3LYP). *Chemical Physics Letters*, **393** (1–3), 51–57.
29. Chai, J.D. and Head-Gordon, M. (2008) Long-range corrected hybrid density functionals with damped atom-atom dispersion corrections. *Physical Chemistry Chemical Physics*, **10** (44), 6615–6620.
30. Dreuw, A. and Head-Gordon, M. (2005) Single-reference ab initio methods for the calculation of excited states of large molecules. *Chemical Reviews*, **105** (11), 4009–4037.
31. Gordon, S. and McBride, B.J. (1994) Computer Program for Calculation of Complex Chemical Equilibrium Compositions and Applications. I. Analysis, NASA.
32. McBride, B.J. and Gordon, S. (1996) Computer Program for Calculation of Complex Chemical Equilibrium Compositions and Applications. II. Users Manual and Program Description, NASA.
33. Ponomarenko, A. (2013) RPA: Tool for Rocket Propulsion Analysis, RPA Lite v1.2.8, www.propulsion-analysis.com, (last accessed in July 2013).
34. Kamlet, M.J. and Jacobs, S.J. (1968) Chemistry of detonations I. A simple method for calculating detonation properties of C-H-N-O explosives. *Journal of Chemical Physics*, **48** (1), 23–35.
35. Kamlet, M.J. and Hurwitz, H. (1968) Chemistry of detonations. IV. Evaluation of a simple predictional method for detonation velocities of C-H-N-O explosives. *Journal of Chemical Physics*, **48** (8), 3685–3692.
36. Keshavarz, M.H. and Pouretedal, H.R. (2004) An empirical method for predicting detonation pressure of CHNOFCl explosives. *Thermochimica Acta*, **414**, 203–208.

37. Rahm, M., Dvinskikh, S.V., Furo, I. and Brinck, T. (2011) Experimental detection of trinitramide, $N(NO_2)_3$. *Angewandte Chemie-International Edition in English*, **50** (5), 1145–1148.
38. Miroshnichenko, E.A. *et al*. (1987) The thermochemistry of methyldinitramine and the enthalpies of formation of methylnitramine radical. *Doklady Akademii Nauk SSSR*, **295** (2), 419–423.
39. Montgomery, J.A. and Michels, H.H. (1993) Structure and stability of trinitramide. *The Journal of Physical Chemistry*, **97** (26), 6774–6775.
40. Chen, Z. and Hamilton, T.P. (1999) Ab initio calculation of the heats of formation of nitrosamides: Comparison with nitramides. *Journal of Physical Chemistry A*, **103** (50), 11026–11033.
41. Rahm, M. and Brinck, T. (2010) On the Anomalous Decomposition and Reactivity of Ammonium and Potassium Dinitramide. *Journal of Physical Chemistry A*, **114** (8), 2845–2854.
42. Chickos, J.S. and Acree, W.E. (2002) Enthalpies of sublimation of organic and organometallic compounds. 1910-2001. *Journal of Physical and Chemical Reference Data*, **31** (2), 537–698.
43. Chickos, J.S. and Acree, W.E. (2003) Enthalpies of vaporization of organic and organometallic compounds, 1880–2002. *Journal of Physical and Chemical Reference Data*, **32** (2), 519–878.
44. Hiraoka, K., Fujimaki, S., Aruga, K. and Yamabe, S. (1994) Gas-phase clustering reactions of O_2^-, NO^-, And O^- With N_2O^- isomeric structures for ($NO^-N_2O^-$). *The Journal of Physical Chemistry*, **98** (34), 8295–8301.
45. Moruzzi, J.L. and Dakin, J.T. (1968) Negative-ion–molecule reactions in N_2O. *Journal of Chemical Physics*, **49**, 5000–5006.
46. Resat, M.S., Zengin, V., Garner, M.C. and Continetti, R.E. (1998) Dissociative photodetachment dynamics of isomeric forms of $N_3O_2^-$. *Journal of Physical Chemistry A*, **102** (10), 1719–1724.
47. Torchia, J.W., Sullivan, K.O. and Sunderlin, L.S. (1999) Thermochemistry of N_3O_2-. *Journal of Physical Chemistry A*, **103** (50), 11109–11114.
48. Rahm, M. and Brinck, T. (2010) Kinetic stability and propellant performance of green energetic materials. *Chemistry - A European Journal*, **16** (22), 6590–6600.
49. Rahm, M., Trinchero, A. and Brinck, T. (2010) Envisioning new high energy density materials: stability, detection and performance. Int. Annu. Conf. ICT 41st (Energetic Materials), **9**, 1.
50. Venkatachalam, S., Santhosh, G. and Ninan, K.N. (2004) An overview on the synthetic routes and properties of ammonium dinitramide (ADN) and other dinitramide salts. *Propellants, Explosives and Pyrotechnics*, **29** (3), 178–187.
51. Trinchero, A. (2010) Quantum Chemical Study of the Stability of Novel Energetic Materials, MSc thesis, Physical Chemistry, KTH The Royal Institute of Technology, Stockholm.
52. Huisgen, R., Ugi, I. and Pentazole, I. (1957) Die Lösung Eines Klassischen Problems der Organischen Stickstoffchemie. *Chemische Berichte*, **90** (12), 2914–2927.
53. Ugi, I. and Huisgen, R. (1958) Pentazole, II. Die Zerfallsgeschwindigkeit der Aryl-pentazole. *Chemische Berichte*, **91** (3), 531–537.
54. Ugi, I. (1961) GDCh-Ortsverband Aachen am 9. January 1961. *Angewandte Chemie*, **73**, 172.
55. Christe, K.O., Wilson, W.W., Sheehy, J.A. and Boatz, J.A. (1999) N_5^+: A novel homoleptic polynitrogen ion as a high energy density material. *Angewandte Chemie-International Edition in English*, **38** (13–14), 2004–2009.
56. Vij, A., Pavlovich, J.G., Wilson, W.W. *et al*. (2002) Experimental detection of the pentaaza-cyclopentadienide (pentazolate) anion, *cyclo*-N_5^-. *Angewandte Chemie-International Edition in English*, **41** (16), 3051–3054.
57. Östmark, H., Wallin, S., Brinck, T. *et al*. (2003) Detection of pentazolate anion (cyclo-N-5(-)) from laser ionization and decomposition of solid *p*-dimethylaminophenylpentazole. *Chemical Physics Letters*, **379** (5–6), 539–546.
58. Butler, R.N., Stephens, J.C. and Burke, L.A. (2003) First generation of pentazole (HN_5, pentazolic acid), the final azole, and a zinc pentazolate salt in solution: A new N-dearylation of 1-(*p*-methoxyphenyl) pyrazoles, a 2-(p-methoxyphenyl) tetrazole and application of the methodology to 1-(*p*-methoxyphenyl) pentazole. *Chemical Communications*, (8), 1016–1017.

59. Schroer, T., Haiges, R., Schneider, S. and Christe, K.O. (2005) The race for the first generation of the pentazolate anion in solution is far from over. *Chemical Communications*, (12), 1607–1609.
60. Perera, S.A., Gregusova, A. and Bartlett, R.J. (2009) First calculations of ^{15}N-^{15}N J values and new calculations of chemical shifts for high nitrogen systems: a comment on the long search for HN5 and its pentazole anion. *Journal of Physical Chemistry A*, **113** (13), 3197–3201.
61. Butler, R.N., Hanniffy, J.M., Stephens, J.C. and Burke, L.A. (2008) A ceric ammonium nitrate N-dearylation of N-p-anisylazoles applied to pyrazole, triazole, tetrazole, and pentazole rings: Release of parent azoles. Generation of unstable pentazole, HN_5/N_5^-, in solution. *The Journal of Organic Chemistry*, **73** (4), 1354–1364.
62. Perera, S.A. and Bartlett, R.J. (1999) Coupled-cluster calculations of Raman intensities and their application to N_4 and N_5^-. *Chemical Physics Letters*, **314** (3–4), 381–387.
63. Lein, M., Frunzke, J., Timoshkin, A. and Frenking, G. (2001) Iron bispentazole $Fe(\eta^5\text{-}N_5)_2$, a theoretically predicted high-energy compound: Structure, bonding analysis, metal-ligand bond strength and a comparison with the isoelectronic ferrocene. *Chemistry - A European Journal*, **7** (19), 4155–4163.
64. Carlqvist, P., Ostmark, H. and Brinck, T. (2004) Computational study of the amination of halobenzenes and phenylpentazole. A viable route to isolate the pentazolate anion? *The Journal of Organic Chemistry*, **69** (9), 3222–3225.
65. Carlqvist, P., Ostmark, H. and Brinck, T. (2004) The stability of arylpentazoles. *Journal of Physical Chemistry A*, **108** (36), 7463–7467.
66. Brinck, T., Carlqvist, P., Holm, A.H. and Daasbjerg, K. (2002) Solvation of sulfur-centered cations and anions in acetonitrile. *Journal of Physical Chemistry A*, **106** (37), 8827–8833.
67. Holm, A.H., Yusta, L., Carlqvist, P. *et al*. (2003) Thermochemistry of arylselanyl radicals and the pertinent ions in acetonitrile. *Journal of the American Chemical Society*, **125** (8), 2148–2157.
68. Frison, G., Jacob, G. and Ohanessian, G. (2013) Guiding the synthesis of pentazole derivatives and their mono- and di-oxides with quantum modeling. *New Journal of Chemistry*, **37** (3), 611–618.
69. Dixon, D.A., Feller, D., Christe, K.O. *et al*. (2004) Enthalpies of formation of gas-phase N_3, N_3^-, N_5^+, and N_5^- from ab initio molecular orbital theory, stability predictions for $N_5^+N_3^-$ and $N_5^+N_5^-$, and experimental evidence for the instability of $N_5^+N_3^-$. *Journal of the American Chemical Society*, **126** (3), 834–843.
70. Cacace, F., dePetris, G. and Troiani, A. (2002) Experimental detection of tetranitrogen. *Science*, **295** (5554), 480–481.
71. Hansen, N. and Wodtke, A.M. (2003) Velocity map ion imaging of chlorine azide photolysis: Evidence for photolytic production of *cyclic*-N_3. *Journal of Physical Chemistry A*, **107** (49), 10608–10614.
72. Trush, B.A. (1956) The detection of free radicals in the high intensity photolysis of hydrogen azide. *Proceedings of the Royal Society of London A*, **235**, 143.
73. Fau, S., Wilson, K.J. and Bartlett, R.J. (2002) On the stability of $N_5^+N_5^-$. *Journal of Physical Chemistry A*, **106** (18), 4639–4644.
74. Samartzis, P.C. and Wodtke, A.M. (2006) All-nitrogen chemistry: how far are we from N-60? *International Reviews in Physical Chemistry*, **25** (4), 527–552.
75. Brinck, T., Bittererova, M. and Ostmark, H. (2003) Electronic structure calculations as a tool in the quest for experimental verification of N_4, in *Energetic Materials Part 1: Initiation, Decomposition and Combustion, Theoretical and Computational Chemistry 12* (ed. P. Politzer), Elsevier B.V., Amsterdam, The Netherlands, pp. 421–437.
76. Bittererova, M., Ostmark, H. and Brinck, T. (2001) Ab initio study of the ground state and the first excited state of the rectangular (D_{2h}) N_4 molecule. *Chemical Physics Letters*, **347** (1–3), 220–228.

77. Dunn, K.M. and Morokuma, K. (1995) Transition-state for the dissociation of tetrahedral N_4. *Journal of Chemical Physics*, **102** (12), 4904–4908.
78. Lee, T.J. and Martin, J.M.L. (2002) An accurate quartic force field, fundamental frequencies, and binding energy for the high energy density material $T_d N_4$. *Chemical Physics Letters*, **357** (3–4), 319–325.
79. Bittererova, M., Ostmark, H. and Brinck, T. (2002) A theoretical study of the azide (N_3) doublet states. A new route to tetraazatetrahedrane (N_4): $N+N_3 \rightarrow N_4$. *Journal of Chemical Physics*, **116** (22), 9740–9748.
80. Yarkony, D.R. (1992) Theoretical-studies of spin-forbidden radiationless decay in polyatomic systems - insights from recently developed computational methods. *Journal of the American Chemical Society*, **114** (13), 5406–5411.
81. Ostmark, H., Launila, O., Wallin, S. and Tryman, R. (2001) On the possibility of detecting tetraazatetrahedrane (N_4) in liquid or solid nitrogen by Fourier transform Raman spectroscopy. *Journal of Raman Spectroscopy*, **32** (3), 195–199.
82. Bittererova, M., Brinck, T. and Ostmark, H. (2001) Theoretical study of the singlet electronically excited states of N_4. *Chemical Physics Letters*, **340** (5–6), 597–603.
83. Lee, T.J. and Dateo, C.E. (2001) Towards the synthesis of the high energy density material $T_d N_4$: excited electronic states. *Chemical Physics Letters*, **345** (3–4), 295–302.
84. Wasilewski, J. (1996) Stationary points on the lowest doublet and quartet hypersurfaces of the N_3 radical: A comparison of molecular orbital and density functional approaches. *Journal of Chemical Physics*, **105** (24), 10969–10982.
85. Samartzis, P.C. and Wodtke, A.M. (2007) Casting a new light on azide photochemistry: photolytic production of *cyclic*-N_3. *Physical Chemistry Chemical Physics*, **9** (24), 3054–3066.
86. Grimme, S. (2006) Semiempirical GGA-type density functional constructed with a long-range dispersion correction. *Journal of Computational Chemistry*, **27** (15), 1787–1799.

3

Some Perspectives on Sensitivity to Initiation of Detonation

Peter Politzer and Jane S. Murray

Department of Chemistry, University of New Orleans, USA and CleveTheoComp, USA

3.1 Energetic Materials and Green Chemistry

In designing and evaluating potential explosives, two of the prime considerations are detonation performance and sensitivity – the latter referring to the vulnerability of the compound to accidental detonation caused by an unintended stimulus, such as impact, shock, friction, and so on. A long-standing and continuing goal is to maximize detonation performance while minimizing sensitivity. The challenge is that factors that promote one of these objectives often oppose the other. An optimum balance must be sought.

In recent years, another consideration has entered the picture: the concept of "green chemistry" [1–6]. While definitions and interpretations of this term may vary [7], in general it seems to represent a focus upon decreasing the hazards associated with chemical processes and products. Anastas and Warner have stated 12 principles of green chemistry [8]. To a large extent, these are simply what any good industrial chemist or chemical engineer would view as desirable from a purely economic standpoint, for example, prevent waste, minimize energy requirements and byproducts, simplify processes as much as possible, exploit catalysts, avoid hazardous reactants and products if possible, and so on.

Particularly relevant in the present context is the rule, "Substances and the form of a substance used in a chemical process should be chosen so as to minimize the potential for chemical accidents, including releases, explosions, and fires" [7,8]. Thus, efforts to develop less sensitive explosives coincide with one of the stated goals of green chemistry!

Green Energetic Materials, First Edition. Edited by Tore Brinck.

The emphasis upon "greenness" can also be quite compatible with designing compounds with improved detonation performance. For example, greenness urges high nitrogen content at the expense of carbon, since carbon can lead to CO_2 as a detonation product, viewed as environmentally undesirable, while nitrogen goes to N_2, which is (at present) regarded as relatively benign. Replacing carbons by nitrogens typically increases the crystal density of the compound and also its heat of formation, both of which improve detonation performance [9,10]. The greater density can be understood as resulting from the nitrogen atom being smaller and heavier than C−H; the increased heat of formation reflects the general weakness of the N−N bonds in high-nitrogen molecules, compared to C−N and C−C [11], which makes the molecules less stable. Thus, such compounds may combine greenness with improved detonation performance. On the other hand, the diminished stability can result in greater sensitivity!

In this chapter, we will focus upon sensitivity. We will look at some factors that may be related to it, and which may be useful to consider in trying to design new energetic compounds with reduced sensitivity. However, we must also examine the effects of such factors upon detonation performance. There is always the need for balance.

3.2 Sensitivity: Some Background

A variety of stimuli can initiate accidental detonation: impact, shock, friction, electric sparks, heat, and so on. A given energetic material may respond more readily to some of these than to others. Storm *et al*. did find relationships between some measured shock and impact sensitivities [12], but this is not always the case [13].

The ease of initiating detonation (i.e., sensitivity) depends upon a combination of factors: molecular features, crystal structure, physical state of the compound, environmental conditions, and so on [14–17]. The number of variables makes it notoriously difficult to obtain reproducible measurements of sensitivity. The key, of course, is to keep the variables as uniform as possible [13–15].

In this chapter, we shall deal primarily with impact sensitivity. This is commonly measured by the height, h_{50}, from which a mass m dropped on the compound produces detonation 50% of the time [12,18]. The sensitivity is then expressed as either the drop height h_{50} (usually in cm) or as the impact energy mgh_{50}, where g is the acceleration due to gravity. The larger are the drop height and the impact energy required to initiate detonation, the less sensitive is the compound. For a 2.5 kg mass, a drop height h_{50} of 100 cm corresponds to an impact energy of 24.5 J.

The initiation of detonation is usually viewed as involving the formation of "hot spots," which are small regions of the crystal lattice in which is localized some portion of the energy introduced by the external stimulus, for example, impact or shock [19–24]. If enough hot spot energy, which is in lattice vibrations, is channeled into appropriate molecular vibrational modes, the result may be bond scission and/or other steps that lead to self-sustaining exothermal chemical decomposition [25–27]. Energy and gaseous products are released and a high pressure shock front may be created, which propagates through the compound at supersonic velocity (detonation) [18,27,28].

Hot spots are commonly linked to the presence of lattice defects (voids, interstitial occupancy, dislocations, etc.) [20–23,29]. One interpretation of this is that the defect induces strain in the

lattice, which is relieved by the externally-introduced energy, resulting in its disproportionate localization in the neighborhood of the defect, that is, a hot spot [21,29].

It is believed that certain types of bonds are particularly likely to be the ones broken by the input of hot spot energy, their ruptures then "triggering" further decomposition that is exothermic and self-sustaining [14,15]. Some proposed trigger bonds are $C-NO_2$ in nitroaromatics, nitroaliphatics, and nitroheterocycles, $N-NO_2$ in nitramines, $O-NO_2$ in nitrate esters, and $N-N_2$ in organic azides [16,19,24,30]. However breaking one of these bonds is by no means the only way in which detonation may be initiated, as shall be discussed.

The brief comments above only touch upon the complex topic of detonation initiation. For more extensive discussions, see, for example, Armstrong *et al.* [21,29], Tarver *et al.* [22], Dlott *et al.* [25,27], McNesby and Coffey [26], Holmes *et al.* [31], Coffey *et al.* [32,33], and so on.

3.3 Sensitivity Relationships

Over the years, there have been numerous attempts to relate sensitivity to some specific molecular or crystal property (usually for a given class of compounds, e.g., nitroaromatics). Such efforts have sometimes been received skeptically because of the variety of factors that are known to affect sensitivity [16,27], mentioned earlier. Nevertheless, relationships have been proposed between experimental sensitivities and a remarkable array of molecular and crystal properties, including the energies or lengths of $C-NO_2$ or $N-NO_2$ bonds [34–36], NMR chemical shifts [30], electrostatic potentials [37,38], bond polarities [39], electronic energy levels [40], atomic charges [41], molecular multipoles [42], band gaps [43–45], heats of fusion [30], stoichiometry [14,15], and so on. There have been several overviews of this work [16,24,30,42,46].

Such relationships can be valuable predictive tools, the practical importance of which should not be underestimated. However, they do not necessarily explicitly identify factors that govern sensitivity; as noted by Brill and James [16], they are often likely to be symptomatic rather than causal. (We prefer to use the term "relationship" rather than "correlation" because the latter may be taken to imply a degree of statistical verifiability and cause-and-effect that are unrealistic in the context of sensitivity.)

If a key step in the initiation of detonation in a particular group of compounds is the rupture of a particular trigger bond, then their sensitivities may be approximately related to a property that is a measure of the strength of that bond. For example, an unusual feature of $C-NO_2$ bonds is a buildup of positive electrostatic potential above and below the bond region. This was observed first in nitroaromatics [47,48] and subsequently in nitroheterocycles [49] and nitroalkanes [50]. It was further found that measured impact sensitivities of nitroaromatics and nitroheterocycles, separately, could be related to these positive potential buildups [37,50–52]. This is not something that would necessarily be anticipated. What is the basis for it? The explanation appears to be that the magnitudes of the positive potentials in $C-NO_2$ bond regions can be related inversely to the strengths of these bonds [49,50]. (This will be further discussed in a later section.) Thus, for nitroaromatics and nitroheterocycles that have a $C-NO_2$ trigger mechanism for detonation initiation, the electrostatic potentials in the $C-NO_2$ bond regions may be *symptomatic* of relative sensitivities.

It must be emphasized, however, that initiation may often involve a mechanism other than breaking one of the expected trigger bonds, such as $C-NO_2$, $N-NO_2$, and so on. There are a number of other possibilities, as has been discussed in detail for nitroaromatics by Brill and James [16]. In general, nitro groups can undergo a variety of reactions with neighboring substituents [16,53], such as nitro/aci tautomerization [54–56] and furazan/furoxan formation [57,58]. Nitro/nitrite isomerizations can occur [16,59]. 1,2,3-Triazoles may release N_2 [60,61]. Thus while sensitivity can sometimes be related, to a limited extent, to the strengths of certain bonds, this certainly cannot be generally assumed.

The concept that hot spot energy is transferred to low-lying ("doorway") molecular vibrational modes and thence to higher ones ("up-pumping") provides another route to estimating relative sensitivities. Fried and Ruggiero [62] and McNesby and Coffey [26] used experimental data to predict the rates of these energy transfers for small groups of compounds, and found that they relate quite well to measured impact sensitivities. Analogous results have also been obtained with just the number of doorway modes alone [63].

Any sensitivity relationship should be viewed as, at best, somewhat indicative of relative trends. There can be many complicating issues. For instance, crystalline shock sensitivity can differ from one lattice direction to another [64]. Several initiating mechanisms may be operating simultaneously [16,65]. The dissociation energy of a bond may change significantly between the gas phase (the typically computed value) and the solid [66–68]. For example, for an axial $N-NO_2$ bond in HMX (1,3,5,7-tetranitro-1,3,5,7-tetraazacyclooctane), it has been computed to be 38.1 kcal/mol in the gas phase, 43.7 kcal/mol in the bulk crystal, 37.4 kcal/mol at a surface, and 36.5 kcal/mol at a vacancy [68].

3.4 Sensitivity: Some Relevant Factors

In this section we shall try to identify some molecular and crystalline features that appear to be related to sensitivity. As shall be seen, understanding the basis for such relationships can be a challenge.

3.4.1 Amino Substituents

There is empirical evidence that the introduction of amino groups, NH_2, diminishes sensitivity; note, for instance, the effects of successive amino groups upon the sensitivities of the trinitrobenzenes and dinitrobenzofuroxans in Table 3.1. There are several possible explanations for this:

Table 3.1 *Experimental impact sensitivities, showing desensitizing effect of amino groups.*

Compound	Drop height, h_{50}, cm[a]	Impact energy, J
1,3,5-trinitrobenzene (TNB)	71	17
2-amino-1,3,5-trinitrobenzene	141	34.5
2,4-diamino-1,3,5-trinitrobenzene (DATB)	320	78.4
2,4,6-triamino-1,3,5-trinitrobenzene (TATB)	490	120
4,6-dinitrobenzofuroxan	76	19
7-amino-4,6-dinitrobenzofuroxan	100	24.5
5,7-diamino-4,6-dinitrobenzofuroxan	120	29.4
1,1-diamino-2,2-dinitroethene (FOX-7)	126	30.9

[a] Ref. [69].

1. Donation of electronic charge by an amino group may be strengthening the $C-NO_2$ bonds [70], as shown for example in **1**. If these bonds are triggers for detonation initiation (which is not necessarily the case), then strengthening them would be likely to diminish sensitivity.

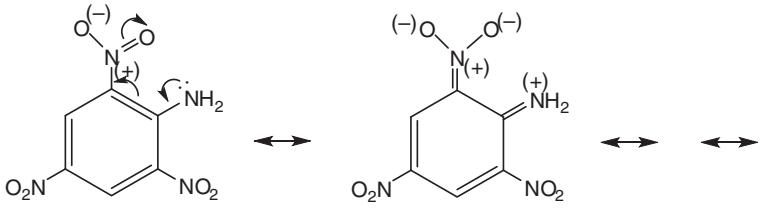

1

2. Inter- or intramolecular hydrogen bonding, 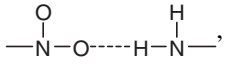 , stabilizes the system.
3. An intermolecular hydrogen bonding network may increase thermal conductivity, allowing the diffusion and dissipation of hot spot energy [22].
4. Hydrogen bonding may cause closer packing and thereby diminish the amount of free space in the crystal lattice. As shall be seen later, this is sometimes linked to decreased impact sensitivity [71].

The lowering of sensitivity by amino groups may be due to one or more of these factors, or perhaps all of them, and there may be yet some other reason. But whatever the basis for it is, amino groups do tend to diminish sensitivity. It should be noted, however, that the stabilizing effects of amino groups reduce the heat of formation. For instance, in going from 1,3,5-trinitrobenzene to its mono- and triamino derivatives, the heat of formation drops from -10.4 to -20.1 to -28.06 kcal/mol [18]. This results in less heat release upon detonation and decreased detonation velocity and pressure [9,10]. On the other hand, hydrogen bonding is likely to increase the crystal density, and thereby the detonation velocity and pressure, which depend upon the density [9,10].

3.4.2 Layered (Graphite-Like) Crystal Lattice

Parallel planar layers, which can more easily slip or slide past each other, reduce the shear strain caused by shock or impact; this strain can create hot spots and facilitate initiation [72,73]. This factor has been invoked in several instances to explain why some compounds are less sensitive than others with similar molecular structures [72–74]. The likelihood of a layered lattice is enhanced by planar molecules with the possibility of intermolecular hydrogen bonding. However, 1,1-diamino-2,2-dinitroethene (FOX-7) satisfies both of these criteria, and while it is indeed relatively insensitive (Table 3.1), it is much more sensitive than TATB. This has been attributed, at least in part, to the FOX-7 lattice having zig-zag layers whereas TATB has planar ones [73]. Planar molecules may also pack better in the crystal lattice, resulting in a higher crystal density and improved detonation properties [9,10].

3.4.3 Free Space in the Crystal Lattice

When an energetic solid is subjected to shock or impact, it undergoes rapid compression accompanied by local heating (hot spots) [21,27]. This suggests a link between compressibility and sensitivity. Indeed Dick found the sensitivity of PETN (pentaerythritol tetranitrate) to shock to differ from one crystallographic direction to another [64]; the direction of greater sensitivity is that of higher compressibility [75].

Since compressibility should be related to the amount of free space in the crystal lattice, impact and shock sensitivity might be as well, at least to some degree. We have tested this possibility [71], taking the free space per molecule in the unit cell, labeled ΔV, to be given by the formula,

$$\Delta V = V_{\text{eff}} - V_{\text{int}} \tag{3.1}$$

V_{eff} is the effective volume per molecule that would completely fill the unit cell,

$$V_{\text{eff}} = (M/d) \tag{3.2}$$

where M is the molecular mass and d is the crystal density. V_{int} is the intrinsic gas phase volume of the molecule. This was taken to be the space enclosed by the 0.003 au (electrons/bohr^3) contour of the molecular electronic density; V_{int} defined in this manner reproduces well the range and average value of the crystallographic packing coefficients of a group of 38 energetic compounds [76].

We have evaluated ΔV for a series of energetic compounds of different chemical types, using their experimental crystal densities to find V_{eff}, Eq. (3.2), and computing V_{int} [71]. We found a general tendency for the compounds having larger ΔV (more free space in the lattice) to have smaller h_{50} (greater impact sensitivity). This is consistent with a link to compressibility, and with evidence that free space in the crystal (e.g., surfaces, voids, vacancies) facilitates bond homolysis [68].

One of the largest subsets within the series consisted of the nitramines, and these show an interesting feature: While their sensitivities do follow the overall trend of increasing with ΔV, the dependence is relatively weak. Nearly all of them are quite sensitive, as is indeed typical of nitramines [12]. ΔV appears to play only a minor role. One interpretation of this is that the detonation initiation of most nitramines is governed by some common dominating factor [77] – this could be the weak $N-NO_2$ bond acting as a trigger. This will be further discussed in the next section.

In general, there does appear to be a very rough relationship, impact sensitivity increasing as there is more free space available in the crystal lattice. However this is certainly not the only factor.

3.4.4 Weak Trigger Bonds

In cases in which detonation initiation centers upon the rupture of a particular bond, a trigger, sensitivity can be expected to increase as that bond is weaker. Four types of bonds are often mentioned as possible triggers: $C-NO_2$, $N-NO_2$, $O-NO_2$, and $N-N_2$ [16,19,24,30]. The last three – $N-NO_2$, $O-NO_2$, and $N-N_2$ – are normally quite weak; their dissociation energies are usually in the neighborhood of 40 kcal/mol [11].

(To put this in perspective, the dissociation energy of the extremely reactive F_2 molecule is 37.923 kcal/mol.) It is not surprising, therefore, that nitramines, nitrate esters, and organic azides are frequently very sensitive. In the extensive compilation of measured impact sensitivities by Storm *et al*. [12], 49 of the 61 nitramines have $h_{50} < 40$ cm (impact energy <9.8 J); six of the seven nitrate esters have $h_{50} \leq 21$ cm (impact energy ≤ 5.1 J). The extremely high sensitivity of organic azides is well known; see, for example, Klapötke *et al*. [78].

In contrast, $C-NO_2$ dissociation energies tend to be in the 60–70 kcal/mol range [11]. (Both the $C-NO_2$ and the $N-NO_2$ decrease considerably if there are more than one NO_2 on the same carbon or nitrogen [11,77].) C−NO bonds are weaker than $C-NO_2$, roughly 30–50 kcal/mol.

In recent years, interest has developed in another means of introducing oxygens into energetic molecules besides NO_2 and ONO_2 groups. This involves forming *N*-oxides, that is, introducing $N \rightarrow O$ coordinate covalent bonds [79–83]. If the $N \rightarrow O$ bonds serve as triggers for some of these compounds, it is relevant that they are likely to be as strong or stronger than the $C-NO_2$, approximately 60–80 kcal/mol [11]. However we caution again against trying to relate sensitivity to any one factor.

3.4.5 Molecular Electrostatic Potentials

So far in this chapter, we have discussed specific molecular and crystal features that appear to influence sensitivity in some manner. Now we wish to adopt a broader perspective, and look at a property that characterizes a molecule as a whole as well as its interactions with its environment.

This property is the electrostatic potential $V(\mathbf{r})$ that the electrons and nuclei of the molecule create at any point $\mathbf{r}$ in the surrounding space. $V(\mathbf{r})$ is given by,

$$V(\mathbf{r}) = \sum_{\mathrm{A}} \frac{Z_{\mathrm{A}}}{|\boldsymbol{R}_{\mathrm{A}} - \mathbf{r}|} - \int \frac{\rho(\mathbf{r}')d\mathbf{r}'}{|\mathbf{r}' - \mathbf{r}|} \tag{3.3}$$

In Eq. (3.3), Z_{A} is the charge on nucleus A, located at $\boldsymbol{R}_{\mathrm{A}}$, and $\rho(\mathbf{r})$ is the electronic density of the molecule. The sign of $V(\mathbf{r})$ in any region depends upon whether the positive contribution of the nuclei or the negative one of the electrons is dominant there.

The electrostatic potential is a real physical property, an observable, which can be obtained experimentally by diffraction methods [84,85] as well as computationally. While it has often been used to interpret and predict reactive behavior [85–93], it is in fact of much more general and fundamental significance [92–94]. Like the electronic density, *the electrostatic potential can serve as the basic determinant of all molecular properties* [95]. For example, atomic and molecular energies can be expressed rigorously in terms of the electrostatic potentials at their nuclei [93,96].

In the present discussion, we will follow the common practice of looking at $V(\mathbf{r})$ computed on the "surface" of the molecule, which is taken to be the 0.001 au (electrons/bohr^3) contour of its electronic density, as proposed by Bader *et al*. [97]. Such surface $V(\mathbf{r})$ are labeled $V_{\mathrm{S}}(\mathbf{r})$. The $V_{\mathrm{S}}(\mathbf{r})$ can be characterized in terms of certain statistical quantities: (i) the local most positive and most negative values, $V_{\mathrm{S,max}}$ and $V_{\mathrm{S,min}}$ (of which there may be several), (ii) the averages of the positive and negative surface potentials,

(iii) the positive and negative variances, and (iv) the average deviations. In a series of studies, summarized by Politzer and Murray [91], it was shown that a variety of condensed phase physical properties that depend upon noncovalent interactions can be related analytically to various subsets of these quantities; these properties include heats of sublimation and vaporization, solubilities and solvation energies, partition coefficients, viscosities, diffusion constants, boiling points and critical constants, and so on. What is particularly notable is that these properties pertain to condensed phases, yet they can be represented empirically as functions of quantities evaluated for a single (i.e., gas phase) molecule. Evidently the surface potential is able to account satisfactorily for the molecule's noncovalent interactions in solid, liquid, and solution phases.

A particularly good illustration of this arises in predicting the densities of C,H,N,O-containing energetic solids. Qiu *et al*. [98] and later Rice *et al*. [99] showed that reasonable results can usually be obtained simply by dividing the molecular mass by the volume enclosed within the 0.001 au contour of the molecule's electronic density. That this approach is overall fairly successful is surprising, since it considers only a single molecule and takes no account of intermolecular interactions. In some instances, however, quite significant errors are obtained. It has been demonstrated that these can be greatly reduced by introducing an electrostatic interaction term based upon the positive and negative variances of $V(\mathbf{r})$ over the molecular surface [100,101].

For organic molecules in general, the most positive surface potentials are likely to be associated with acidic hydrogens and sometimes with σ-holes of Group IV–VII atoms [102] and π-holes [103], for example, of some carbonyls. Hydrocarbon portions of molecules are typically weakly positive. Negative potentials are normally produced by lone pairs, π electrons and strained C−C bonds [87,92–94]. As an example, Figure 3.1 displays $V_S(\mathbf{r})$ for

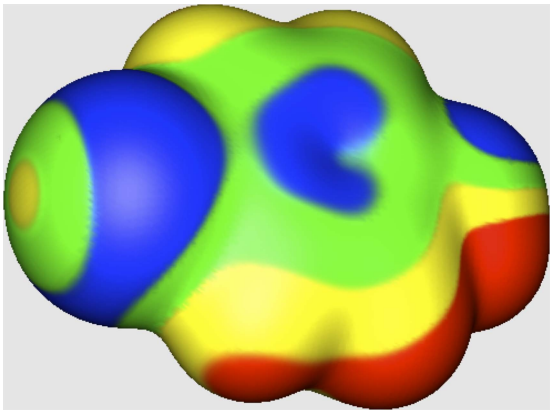

Figure 3.1 *Calculated (B3PW91/6-31G**) electrostatic potential on the 0.001 au molecular surface of* p*-chlorophenol. The chlorine is at the left, the hydroxyl group at the right. Color ranges, in kcal/mol: red, greater than 15; yellow, between 15 and 0; green, between 0 and −10; blue, more negative than −10. The most positive potentials ($V_{S,max}$) are 59.0 kcal/mol associated with the hydroxyl hydrogen and 15–18 kcal/mol for the other hydrogens. The chlorine has a positive σ-hole on the extension of the C−Cl bond, with $V_{S,max} = 2.6$ kcal/mol. The most negative potentials ($V_{S,min}$) are −21.4 kcal/mol (oxygen), −15.4 kcal/mol (chlorine), and −12.1 kcal/mol above and below the aromatic ring.*

p-chlorophenol. The hydrogens have positive potentials, with the hydroxyl one having by far the highest $V_{S,max}$. The chlorine σ-hole is only very weakly positive. There are negative regions due to the lone pairs of the oxygen and the chlorine, as well as the π electrons of the ring.

Energetic molecules characteristically have markedly less balanced surface potentials, with more distinct charge separations. They commonly have highly electron-withdrawing components on their peripheries, such as nitro groups, aza nitrogens, and so on. The effect of these is to deplete the electronic densities in the central portions of the molecules, making them strongly positive and highly variable, often with $V_{S,max}$ above certain bonds, such as $C-NO_2$ and $N-NO_2$. Negative potentials are largely on the outsides of the molecules, near lone pairs of nitro oxygens and/or aza nitrogens, and so on. These features can be seen for 1,3,5-trinitrobenzene (TNB) in Figure 3.2; the entire central part of the molecular surface is positive, with local $V_{S,max}$ over the $C-NO_2$ bonds and the ring (as well as the ring hydrogens). The negative potential typical of aromatic π electrons is completely gone.

Qualitatively, the same pattern is found in 1,3-diamino-2,4,6-trinitrobenzene (DATB), Figure 3.3; the central region is strongly positive and variable, and negative potentials are only along parts of the periphery, by the nitro oxygens. The central positive potential is somewhat weaker than in TNB (Figure 3.2) because of the two electron-donating amino groups. More examples of the surface electrostatic potentials of energetic molecules are in Murray *et al*. [24,37,77] and Rice and Hare [69].

Clearly, many energetic molecules show an anomalous imbalance and separation (compared to most typical organic molecules) between the very dominant positive central

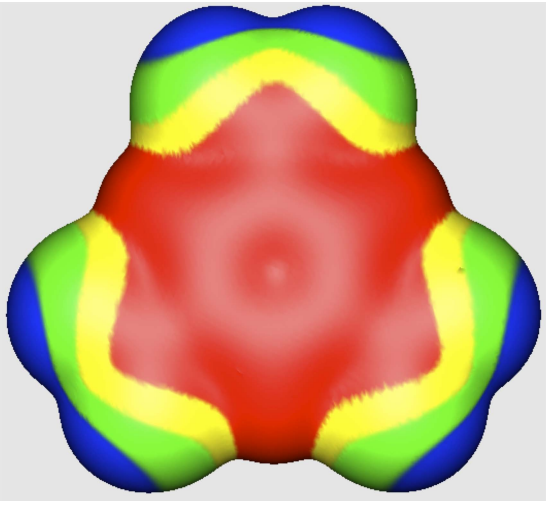

Figure 3.2 *Calculated (B3PW91/6-31G**) electrostatic potential on the 0.001 au molecular surface of 1,3,5-trinitrobenzene. Color ranges, in kcal/mol: red, greater than 15; yellow, between 15 and 0; green, between 0 and −10; blue, more negative than −10. The most positive potentials ($V_{S,max}$) are 31.8 kcal/mol above and below the $C-NO_2$ bonds, 29.2 kcal/mol above and below the center of the ring, and 27.1 kcal/mol associated with the hydrogens. The most negative potentials ($V_{S,min}$) are −19.5 kcal/mol (oxygens).*

portion, with its maxima over certain bonds, and the outer negative periphery. Is this imbalance somehow linked to sensitivity? Pauling postulated an "electroneutrality rule" [104,105], according to which " . . . the electronic structure of substances is such as to cause each atom to have essentially zero resultant electrical charge" [104]. This implies a tendency for the electrostatic potential to be as uniform and close to neutral as possible, with deviations from this promoting instability. Thus the strong charge imbalance/separation that characterizes the electrostatic potentials on energetic molecular surfaces may be at least symptomatic of their metastabilities and perhaps sensitivities.

Within a given category of compounds, for example, nitroaromatics, sensitivity does generally increase as $V_S(\mathbf{r})$ over the inner part of the molecule becomes more positive and more variable. This can be seen, for example, in comparing the $V_S(\mathbf{r})$ of DATB (Figure 3.3) and TNB (Figure 3.2); the latter is considerably more sensitive to impact (Table 3.1). Analogous qualitative comparisons have correctly identified relative trends in sensitivity in earlier work [24,69,77,106–108].

It has even proven to be possible to put this on a more quantitative level. It was mentioned earlier that the impact sensitivities of nitroaromatics and nitroheterocycles, separately, had been related empirically to the maxima of the electrostatic potentials, the local $V_{S,max}$, above and below the $C-NO_2$ bonds [37,50]. These relationships were subsequently expanded to describe more fully the molecular surface charge imbalance/separation, expressed in terms of the maxima, variances, and averages of $V_S(\mathbf{r})$ [38], and one was developed for nitramines as well. It should be pointed out, however, that for molecules having extended three-dimensional frameworks, the electrostatic potentials on their surfaces will not fully reflect

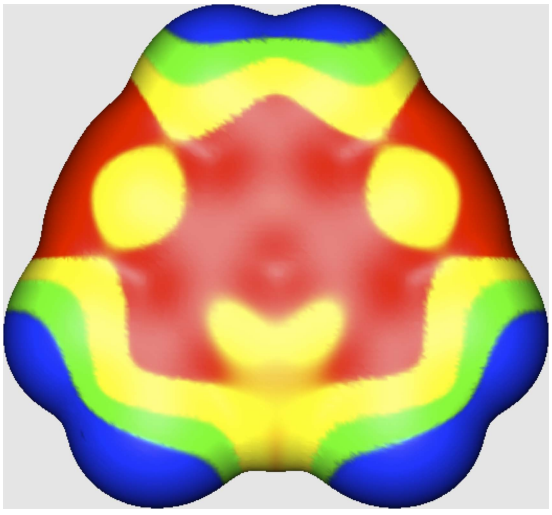

Figure 3.3 *Calculated (B3PW91/6-31G**) electrostatic potential on the 0.001 au molecular surface of 1,3-diamino-2,4,6-trinitrobenzene. Color ranges, in kcal/mol: red, greater than 15; yellow, between 15 and 0; green, between 0 and −10; blue, more negative than −10. The most positive potentials ($V_{S,max}$) are associated with the amino hydrogens, 38–40 kcal/mol, and above and below the ring, 23–24 kcal/mol. The most negative potentials ($V_{S,min}$) are −22 to −26 kcal/mol (oxygens).*

the charge imbalances/separations in their interiors, which are not visible. An example is the extremely sensitive compound PETN (pentaerythritol tetranitrate), $C(CH_2ONO_2)_4$, for which $V_S(\mathbf{r})$ is not nearly as positive as would be anticipated from its high sensitivity ($h_{50} = 12$–16 cm, impact energy = 3–4 J [69]).

The distinctive charge imbalance and separation that characterize energetic molecules is caused by the strongly electron-withdrawing components on their peripheries – nitro groups, aza nitrogens, and so on. These deplete the electronic densities in the central portions of the molecules and weaken some bonds. It was already mentioned that the strengths of C−NO_2 bonds vary inversely with the magnitudes of the positive maxima ($V_{S,max}$) associated with these bonds [49,50,77].

This can be seen in Table 3.2, which demonstrates the same to be true for N−NO_2 bonds. Table 3.2 shows that: (i) as the number of nitro groups in a molecule increases, so do their $V_{S,max}$, and (ii) the increasing $V_{S,max}$ are accompanied by weakening of the C−NO_2 and/or N−NO_2 bonds. Note the marked decrease in the C−NO_2 dissociation enthalpy when a second nitro group is introduced on the same carbon. This is true as well for N−NO_2 bonds; for instance the N-NO_2 dissociation energy in trinitramide, $N(NO_2)_3$, which was recently detected [109], has been calculated to be 26 kcal/mol [110] and 28.2 kcal/mol [109], well below the roughly 40 kcal/mol for a single NO_2 on a nitrogen [11] (Table 3.2).

Accordingly, the charge imbalance and separation reflect electronic depletion in the central portion of the molecule and concomitant weakening of C−NO_2 and N−NO_2 bonds. To the extent that these are triggers for detonation initiation, the degree of charge imbalance/separation may be symptomatic of the sensitivity.

Table 3.2 *Computed $V_{S,max}$ and gas phase dissociation enthalpies ΔH of C–NO_2 and N−NO_2 bonds.*[a]

Molecule	C−NO_2 bonds		N−NO_2 bonds	
	$V_{S,max}$[b]	ΔH(298 K)[c]	$V_{S,max}$[b]	ΔH(298 K)[c]
CH_3NO_2	23.2	56.9		
$CH_2(NO_2)_2$	43.8	43.3		
$CH(NO_2)_3$	56.4	37.5		
nitrobenzene	11.5	68.9		
1,3-dinitrobenzene	22.3	66.2		
1,3,5-trinitrobenzene	31.8	63.9		
2-nitroimidazole	18.2	71.2		
2,4,5-trinitroimidazole	42.2	64.7		
1-nitroazetidine			2.1	45.8
3-nitroazetidine	24.6	56.3		
1,3-dinitroazetidine	31.8	53.2	10.5	41.7
1,3,3-trinitroazetidine	43.0, 44.1	39.8	17.3	39.9
1-nitro-1,3-diazacyclobutane			5.4	40.9
1,3-dinitro-1,3-diazacyclobutane			16.9	37.8
H_2N-$(CH_2)_2$-NH-NO_2			6.0	46.7
O_2N-NH-$(CH_2)_2$-NH-NO_2			13.6	44.2

[a] Data are from reference [77]. The C–NO_2 $V_{S,max}$ are above the bond; the N–NO_2 $V_{S,max}$ are near the amine nitrogen.
[b] Computational level: B3PW91/6-31G(d,p)//B3PW91/6-31++G(3d,2p). Units: kcal/mol.
[c] Computational level: B3PW91/6-31++G(3d,2p). Units: kcal/mol.

Amino substituents counter the electronic depletion, as can be seen by comparing Figures 3.2 and 3.3. This may strengthen $C-NO_2$ and/or $N-NO_2$ bonds, as is depicted in structure **1**, and thus help to account for their desensitizing effect. In 1,1-diamino-2,2-dinitroethene (FOX-7), the amino groups produce a gradient of electrostatic potential from strongly positive at the amino end to negative at the nitro.

When initiation does not involve $C-NO_2$ or $N-NO_2$ triggers, then the anomalous surface charge imbalance/separation may reflect the weakening of some other key bond, or may be indicative of factors that promote some alternative initiation mechanism, such as nitro/nitrite isomerization, $C-NO_2 \rightarrow C-ONO$ [59,65]. This involves the interaction of a nitro oxygen with the carbon, which should certainly be promoted by the typically strongly positive electrostatic potentials around $C-NO_2$ carbons (see, for example, Figures 3.2 and 3.3).

3.5 Summary

Designing new energetic compounds that maximize detonation performance while minimizing sensitivity is a continuous struggle to deal with two somewhat conflicting objectives. For example, it could be argued that nitramines should be avoided because they tend to be quite sensitive, presumably because of the weakness of the $N-NO_2$ bond. However the fact is that our two standards of excellent performance are HMX (tetranitrotetraazacyclooctane) and CL-20 (hexanitrohexaazaisowurtzitane), both of which are nitramines.

Nevertheless, some cautious generalizations may be in order:

1. The advantages of some hydrogen bonding in lowering sensitivity and increasing crystal density probably outweigh its negative effect upon the heat of formation.
2. Planar molecules, especially with hydrogen bonding possibilities, may promote the formation of layered (graphite-like) crystal lattices, reducing sensitivity caused by shear strain. They may also increase crystal density.
3. High density is desirable not only because of its effect upon detonation properties but also because it reduces the apparently sensitizing free space in the crystal lattice.
4. Substitutes for weak trigger bonds should be further explored, for example, *N*-oxides. These are of particular interest given the current emphasis upon high-nitrogen compounds arising from both performance and green chemistry considerations. There is evidence that *N*-oxides can stabilize nitrogen catenation [82,111].
5. Avenues for reducing the charge imbalance/separation in energetic molecules should be considered, for example, appropriate selection of substituents.

Finally, efforts to identify molecular and crystalline features that appear to be related to sensitivity should be continued.

Acknowledgments

We appreciate the support of this work by the Office of Naval Research, contract number N00014-12-1-0535, Program Officer Dr. Clifford Bedford.

References

1. Klapötke, T.M. and Holl, G. (2001) The greening of explosives and propellants using high energy nitrogen chemistry. *Green Chemistry*, **3**, G75–G77.
2. Giles, J. (2004) Collateral damage. *Nature*, **427**, 580–581.
3. Ding, Y.H. and Inagaki, X. (2005) Silanes/oxygen/water: green high-energy-density materials. *European Journal of Inorganic Chemistry*, 3131–3134.
4. Talawar, M.B., Sivabalan, R., Mukundan, T. *et al*. (2009) Experimentally compatible next generation green energetic materials (GEMs). *Journal of Hazardous Materials*, **161**, 589–607.
5. Rahm, M. and Brinck, T. (2010) Kinetic stability and propellant performances of green energetic materials. *Chemistry - A European Journal*, **16**, 6590–6600.
6. Klapötke, T.M. (2012) *Chemistry of High-Energy Materials*, de Gruyter, Berlin.
7. Linthorst, J.A. (2010) An overview: origins and development of green chemistry. *Foundations of Chemical*, **12**, 55–68.
8. Anastas, P.T. and Warner, J.C. (1998) *Green Chemistry: Theory and Practice*, Oxford University Press, New York.
9. Kamlet, M.J. and Jacobs, S.J. (1968) Chemistry of detonation. I. A simple method for calculating detonation properties of C,H,N,O explosives. *Journal of Chemical Physics*, **48**, 23–35.
10. Politzer, P. and Murray, J.S. (2011) Some perspectives on estimating detonation properties of C, H,N,O compounds. *Central European Journal of Energetic Materials*, **8**, 209–220.
11. Luo, Y.-R. (2007) *Comprehensive Handbook of Chemical Bond Energies*, CRC Press, Boca Raton, FL.
12. Storm, C.B., Stine, J.R., and Kramer, J.F. (1990) Sensitivity relationships in energetic materials, in *Chemistry and Physics of Energetic Materials* (ed. S.N. Bulusu), Kluwer, Dordrecht, The Netherlands, Chapter 27, pp. 605–639.
13. Doherty, R.M. and Watt, D.S. (2008) Relationship between RDX properties and sensitivity. *Propellants, Explosives, Pyrotechnics*, **33**, 4–13.
14. Kamlet, M.J. (1976) The relationship of impact sensitivity with structure of organic high explosives. I. Polynitroaliphatic explosives, in Proceedings of the 6th Symposium (International) on Detonation, San Diego, CA, Report No. ACR 221, Office of Naval Research, Arlington, VA pp. 312–322.
15. Kamlet, M.J. and Adolph, H.G. (1979) The relationship of impact sensitivity with structure of organic high explosives. II. Polynitroaromatic explosives. *Propellants, Explosives*, **4**, 30–34.
16. Brill, T.B. and James, K.J. (1993) Kinetics and mechanisms of thermal decompositions of nitroaromatic explosives. *Chemical Reviews*, **93**, 2667–2692.
17. Sučeska, M. (1995) *Test Methods for Explosives*, Springer-Verlag, New York.
18. Meyer, R., Köhler, J., and Homburg, A. (2007) *Explosives*, 6th edn, Wiley-VCH, Weinheim.
19. Kamlet, M.J. and Adolph, H.G. (1981) Some comments regarding the sensitivities, thermal stabilities, and explosive performance characteristics of fluorodinitromethyl compounds, Proceedings of the Seventh Symposium (International) on Detonation, Naval Surface Warfare Center, Silver Springs, MD, Report No. NSWCMP-82-334, 60–67.
20. Field, J.E. (1992) Hot spot ignition mechanisms for explosives. *Accounts of Chemical Research*, **25**, 489–496.
21. Tsai, D.H. and Armstrong, R.W. (1994) Defect-enhanced structural relaxation mechanism for the evolution of hot spots in rapidly compressed crystals. *The Journal of Physical Chemistry*, **98**, 10997–11000.
22. Tarver, C.M., Chidester, S.K., and Nichols, A.L. III (1996) Critical conditions for impact- and shock-induced hot spots in solid explosives. *The Journal of Physical Chemistry*, **100**, 5794–5799.

23. Politzer, P. and Boyd, S. (2002) Molecular dynamics simulations of energetic solids. *Structural Chemistry*, **13**, 105–113, and references cited.
24. Politzer, P. and Murray, J.S. (2003) Sensitivity correlations, in *Energetic Materials. Part 2. Detonation, Combustion* (eds P. Politzer and J.S. Murray), Elsevier, Amsterdam, Chapter 1, pp. 5–23.
25. Chen, S., Tolbert, W.A., and Dlott, D.D. (1994) Direct measurement of ultrafast multiphonon up-pumping in high explosives. *The Journal of Physical Chemistry*, **98**, 7759–7766.
26. McNesby, K.L. and Coffey, C.S. (1997) Spectroscopic determination of impact-sensitivities of explosives. *The Journal of Physical Chemistry. B*, **101**, 3097–3104.
27. Dlott, D.D. (2003) Fast molecular processes in energetic materials, in *Energetic Materials. Part 2. Detonation, Combustion* (eds P. Politzer and J.S. Murray), Elsevier, Amsterdam, Chapter 6, pp. 125–191.
28. Mader, C.L. (1998) *Numerical Modeling of Explosives and Propellants*, 2nd edn, CRC Press, New York.
29. Armstrong, R.W., Coffey, C.S., DeVost, V.F., and Elban, W.L. (1990) Energy transfer rates in primary, secondary and insensitive explosives. *Journal of Applied Physiology*, **68** (1–6), 979.
30. Zeman, S. (2007) Sensitivities of high energy compounds. *Structure and Bonding*, **125**, 195–271.
31. Holmes, W., Francis, R.S., and Fayer, M.D. (1999) Crack propagation induced heating in crystalline energetic materials. *Journal of Chemical Physics*, **110**, 3576–3583.
32. Coffey, C.S. and Sharma, J. (1999) Plastic deformation, energy dissipation, and initiation of crystalline explosives. *Physical Review B-Condensed Matter*, **60**, 9365–9371.
33. Coffey, C.S. (2003) Initiation due to plastic deformation from shock or impact, in *Energetic Materials. Part 2. Detonation, Combustion* (eds P. Politzer and J.S. Murray), Elsevier, Amsterdam, Chapter 5, pp. 101–123.
34. Owens, F.J. (1996) Calculation of energy barriers for bond rupture in some energetic molecules. *Journal of Molecular Structure: Theochem*, **370**, 11–16.
35. Politzer, P., Murray, J.S., Lane, P. *et al*. (1991) Shock sensitivity relationships for nitramines and nitroaliphatics. *Chemical Physics Letters*, **181**, 78–82.
36. Kohno, Y., Maekawa, K., Tsuchioka, T. *et al*. (1994) A relationship between the impact sensitivity and the electronic structures for the unique N−N bond in the HMX polymorphs. *Combustion and Flame*, **96**, 343–350.
37. Murray, J.S., Lane, P., and Politzer, P. (1995) Relationships between impact sensitivities and molecular surface electrostatic potentials of nitroaromatic and nitroheterocyclic molecules. *Molecular Physics*, **85**, 1–8.
38. Murray, J.S., Lane, P., and Politzer, P. (1998) Effects of strongly electron-attracting components in molecular surface electrostatic potentials; application to predicting impact sensitivities of energetic molecules. *Molecular Physics*, **93**, 187–194.
39. Delpuech, A. and Cherville, J. (1978) Relation entre la structure electronique et la sensibilité an choc des explosifs secondaires nitrè-critère moléculaire de sensibilité. *Propellants Explosives*, **3**, 169–175.
40. Sharma, J., Beard, B.C., and Chaykovsky, M. (1991) Correlation of impact sensitivity with electronic levels and structures of molecules. *The Journal of Physical Chemistry*, **95**, 1209–1213.
41. Zhang, C. (2009) Review of the establishment of nitro group charge method and its applications. *Journal of Hazardous Materials*, **161**, 21–28.
42. Anders, G. and Borges, I. Jr. (2011) Topological analysis of the molecular charge density and impact sensitivity models of energetic molecules. *Journal of Physical Chemistry A*, **115**, 9055–9068.

43. Kuklja, M.M., Stefanovich, E.V., and Kunz, A.B. (2000) An exitonic mechanism of detonation initiation in explosives. *Journal of Chemical Physics*, **112**, 3417–3423.
44. Zhang, H., Cheung, F., Zhao, F., and Cheng, X.-L. (2009) Band gaps and the possible effect on impact sensitivity for some nitroaromatic explosive materials. *International Journal of Quantum Chemistry*, **109**, 1547–1552.
45. Zhu, W. and Xiao, H. (2010) First-principles band gap criterion for impact sensitivity of energetic crystals: a review. *Structural Chemistry*, **21**, 657–665.
46. Shackelford, S.A. (2008) Role of thermochemical decomposition in energetic material initiation sensitivity and explosive performance. *Central European Journal of Energetic Materials*, **5**, 75–101.
47. Politzer, P., Abrahmsen, L., and Sjoberg, P. (1984) Effects of amino and nitro groups upon the electrostatic potential of an aromatic ring. *Journal of the American Chemical Society*, **106**, 855–860.
48. Politzer, P., Laurence, P.R., Abrahmsen, L. *et al*. (1984) The aromatic $C-NO_2$ bond as a site for nucleophilic attack. *Chemical Physics Letters*, **111**, 75–78.
49. Politzer, P. and Murray, J.S. (1995) C-NO_2 dissociation energies and surface electrostatic potential maxima in relation to the impact sensitivities of some nitroheterocyclic molecules. *Molecular Physics*, **86**, 251–255.
50. Politzer, P. and Murray, J.S. (1996) Relationships between dissociation energies and electrostatic potentials of $C-NO_2$ bonds: applications to impact sensitivities. *Journal of Molecular Structure*, **376**, 419–424.
51. Owens, F.J., Jayasuriya, K., Abrahmsen, L., and Politzer, P. (1985) Computational analysis of some properties associated with the nitro group in polynitroaromatic molecules. *Chemical Physics Letters*, **116**, 434–438.
52. Murray, J.S., Lane, P., Politzer, P., and Bolduc, P.R. (1990) A relationship between the impact sensitivity and the electrostatic potentials at the midpoints of $C-NO_2$ bonds in nitroaromatics. *Chemical Physics Letters*, **168**, 135–139.
53. Zeman, S. (2003) A study of chemical micro-mechanisms of initiation of organic polynitro compounds, in *Energetic Materials. Part 2. Detonation, Combustion* (eds P. Politzer and J.S. Murray), Elsevier, Amsterdam, Chapter 2, pp. 25–52.
54. Politzer, P., Seminario, J.M., and Bolduc, P.R. (1989) A proposed interpretation of the destabilizing effect of hydroxyl groups on nitroaromatic molecules. *Chemical Physics Letters*, **158**, 463–469.
55. Fan, J., Gu, Z., Xiao, H., and Dong, H. (1998) Theoretical study on pyrolysis and sensitivity of energetic compounds. Part 4. Nitro derivatives of phenols. *Journal of Physical Organic Chemistry*, **11**, 177–184.
56. Murray, J.S., Lane, P., Göbel, M. *et al*. (2009) Reaction force analyses of nitro-aci tautomerizations of trinitromethane, the elusive trinitromethanol, picric acid and 2,4-dinitro-1H-imidazole. *Theoretical Chemistry Accounts*, **124**, 355–363.
57. Murray, J.S., Lane, P., Politzer, P. *et al*. (1990) A computational analysis of some possible hydrogen transfer and intramolecular ring formation reactions of o-nitrotoluene and o-nitroaniline. *Journal of Molecular Structure: Theochem*, **209**, 349–359.
58. Zeman, S., Shu, Y., and Wang, X. (2005) Study on primary step of initiation mechanisms of two polynitro arenes. *Central European Journal of Energetic Materials*, **2** (4), 47–54.
59. Gindulyte, A., Massa, L., Huang, L., and Karle, J. (1999) Proposed mechanism of 1,1-diamino-dinitroethylene decomposition: a density functional theory study. *Journal of Physical Chemistry A*, **103**, 11045–11051.
60. Storm, C.B., Ryan, R.R., Ritchie, J.P. *et al*. (1989) Structural basis of the impact sensitivities of 1-picryl-1,2,3-triazole, 2-picryl-1,2,3-triazole, 4-nitro-1-picryl-1,2,3-triazole, and 4-nitro-2-picryl-1,2,3-triazole. *The Journal of Physical Chemistry*, **93**, 1000–1007.

61. Politzer, P., Grice, M.E., and Seminario, J.M. (1997) A density functional analysis of the decomposition of 4-nitro-1,2,3-triazole through the evolution of N_2. *International Journal of Quantum Chemistry*, **61**, 389–392.
62. Fried, L.E. and Ruggiero, A.J. (1994) Energy transfer rates in primary, secondary and insensitive explosives. *The Journal of Physical Chemistry*, **98**, 9786–9791.
63. Ge, S.-H., Cheng, X.-L., Wang, X.-X. *et al*. (2007) Energy transfer rates and impact sensitivities of two classes of nitramine explosives molecules. *Structural Chemistry*, **18**, 985–991.
64. Dick, J.J. (1984) Effect of crystal orientation on shock initiation sensitivity of pentaerythritol tetranitrate explosive. *Applied Physics Letters*, **44**, 859–861.
65. Kuklja, M.M. and Rashkeev, S.N. (2009) Interplay of decomposition mechanisms at shear-strain interface. *Journal of Physical Chemistry C Letters*, **113**, 17–20.
66. Odiot, S., Blain, M., Vauthier, E., and Fliszár, S. (1993) Influence of the physical state of an explosive on its sensitivity. Is nitromethane sensitive or insensitive? *Journal of Molecular Structure: Theochem*, **279**, 233–238.
67. Tsiaousis, D. and Munn, R.W. (2005) Energy of charged states in the RDX crystal: trapping of charge-transfer pairs as a possible mechanism for initiating detonation. *Journal of Chemical Physics*, **122** (1–9), 184708.
68. Sharia, O. and Kuklja, M.M. (2012) Surface-enhanced decomposition kinetics of molecular materials illustrated with cyclotetramethylene-tetranitramine. *Journal of Physical Chemistry C*, **116**, 11077–11081.
69. Rice, B.M. and Hare, J.J. (2002) A quantum mechanical investigation of the relation between impact sensitivity and the charge distribution in energetic molecules. *Journal of Physical Chemistry A*, **106**, 1770–1783.
70. Politzer, P., Concha, M.C., Grice, M.E. *et al*. (1998) Computational investigation of the structures and relative stabilities of amino/nitro derivatives of ethylene. *Journal of Molecular Structure: Theochem*, **452**, 75–83.
71. Pospišíl, M., Vávra, P., Concha, M.C. *et al*. (2011) Sensitivity and the available free space per molecule in the unit cell. *Journal of Molecular Modeling*, **17**, 2569–2574.
72. Kuklja, M.M. and Rashkeev, S.N. (2007) Shear-strain-induced chemical reactivity of layered molecular crystals. *Applied Physics Letters*, **90** (1–3), 151913
73. Kuklja, M.M. and Rashkeev, S.N. (2010) Molecular mechanisms of shear strain sensitivity of the energetic crystals DADNE and TATB. *Journal of Energetic Materials*, **28**, 66–77.
74. Veauthier, J.M., Chavez, D.E., Tappan, B.C., and Parrish, D.A. (2010) Synthesis and characterization of furazan energetics ADAAF and DOATF *Journal of Energetic Materials*, **28**, 229–249.
75. Kunz, A.B. (1996) An *ab initio* investigation of crystalline PETN. *Materials Research Society Symposia Proceedings*, **418**, 287–292.
76. Eckhardt, C.J. and Gavezzotti, A. (2007) Computer simulations and analysis of structural and energetic features of some crystalline energetic materials. *The Journal of Physical Chemistry. B*, **111**, 3430–3437.
77. Murray, J.S., Concha, M.C., and Politzer, P. (2009) Links between surface electrostatic potentials of energetic molecules, impact sensitivities and $C-NO_2/N-NO_2$ bond dissociation energies. *Molecular Physics*, **107**, 89–97.
78. Klapötke, T.M., Martin, F., Sproll, S., and Stierstorfer, J. (2009) Azidotetrazoles: promising energetic materials or waste of time?, in 12th Seminar on New Trends in Research of Energetic Materials, Part I, University of Pardubice, Czech Republic, pp. 327–340.
79. Hollins, A.L., Merwin, L.M., and Nissan, R.A. (1996) Aminonitropyrimidines and their N-oxides. *Heterocyclic Chemistry*, **33**, 895–904.
80. Pagoria, P.F., Lee, G.S., Mitchell, A.R., and Schmidt, R.D. (2002) A review of energetic materials synthesis. *Thermochimica Acta*, **384**, 187–204.

81. Chavez, D.E., Hiskey, M.A., and Naud, D.L. (2004) Tetrazine explosives. *Propellants Explosives Pyrotechnics*, **29**, 209–215.
82. Churakov, A.M. and Tartakovsky, V.A. (2004) Progress in 1,2,3,4-tetrazine chemistry. *Chemical Reviews*, **104**, 2601–2616.
83. Politzer, P., Lane, P., and Murray, J.S. (2013) Computed characterization of two di-1,2,3,4-tetrazine tetraoxides, DTTO and iso-DTTO, as potential energetic compounds. *Central European Journal of Energetic Materials*, **10**, 17–37.
84. Stewart, R.F. (1979) On the mapping of electrostatic properties from Bragg diffraction data. *Chemical Physics Letters*, **65**, 335–342.
85. Politzer, P. and Truhlar, D.G. (eds) (1981) *Chemical Applications of Atomic and Molecular Electrostatic Potentials*, Plenum Press, New York.
86. Scrocco, E. and Tomasi, J. (1978) Electronic molecular structure, reactivity and intermolecular forces: an euristic interpretation by means of electrostatic molecular potentials. *Advances in Quantum Chemistry*, **11**, 115–193.
87. Politzer, P. and Daiker, K.C. (1981) Models for chemical reactivity, in *The Force Concept in Chemistry* (ed. B.M. Deb), Van Nostrand Reinhold, pp. 294–387.
88. Politzer, P., Laurence, P.R., and Jayasuriya, K. (1985) Molecular electrostatic potentials: an effective tool for the elucidation of biochemical phenomena. *Environmental Health Perspectives*, **61**, 191–202.
89. Naray-Szabo, G. and Ferenczy, G.G. (1995) Molecular electrostatics. *Chemical Reviews*, **95**, 829–847.
90. Murray, J.S. and Sen, K. (eds) (1996) *Molecular Electrostatic Potentials: Concepts and Applications*, Elsevier, Amsterdam.
91. Politzer, P. and Murray, J.S. (1998) Statistical analysis of the molecular surface electrostatic potential: an approach to describing noncovalent interactions in condensed phases. *Journal of Molecular Structure: Theochem*, **425**, 107–114.
92. Murray, J.S. and Politzer, P. (2011) The electrostatic potential: an overview. *WIREs Computational Molecular Science*, **1**, 153–163.
93. Politzer, P. and Murray, J.S. (2002) The fundamental nature and role of the electrostatic potential in atoms and molecules. *Theoretical Chemistry Accounts*, **108**, 134–142.
94. Politzer, P. and Murray, J.S. (2012) Molecular electrostatic potentials: some observations, in *Concepts and Methods in Modern Theoretical Chemistry, Vol. 1: Electronic Structure and Reactivity* (eds K. Ghosh and P. Chattaraj), Taylor & Francis, Boca Raton.
95. Ayers, P.W. (2007) Using reactivity indicators instead of electron density to describe Coulomb systems. *Chemical Physics Letters*, **438**, 148–152.
96. Politzer, P. (2004) Atomic and molecular energies as functional of the electrostatic potential. *Theoretical Chemistry Accounts*, **111**, 395–399.
97. Bader, R.F.W., Carroll, M.T., Cheeseman, J.R., and Chang, C. (1987) Properties of atoms in molecules: atomic volumes. *Journal of the American Chemical Society*, **109**, 7968–7979.
98. Qiu, L., Xiao, H., Gong, X. *et al*. (2007) Crystal density predictions for nitramines based on quantum chemistry. *Journal of Hazardous Materials*, **141**, 280–288.
99. Rice, B.M., Hare, J.J., and Byrd, E.F.C. (2007) Accurate prediction of crystal densities using quantum chemical molecular volumes. *Journal of Physical Chemistry A*, **111**, 10874–10879.
100. Politzer, P., Martinez, J., Murray, J.S. *et al*. (2009) An electrostatic interaction correction for improved crystal density predictions. *Molecular Physics*, **107**, 2095–2101.
101. Politzer, P., Martinez, J., Murray, J.S., and Concha, M.C. (2010) An electrostatic correction forimproved crystal density predictions of energetic ionic compounds. *Molecular Physics*, **108**, 1391–1396.
102. Politzer, P., Murray, J.S., and Lane, P. (2007) σ-Hole bonding and hydrogen bonding: competitive interactions. *International Journal of Quantum Chemistry*, **107**, 3046–3052.

103. Murray, J.S., Lane, P., Clark, T. *et al.* (2012) σ-Holes, π-holes and electrostatically-driven interactions. *Journal of Molecular Modeling*, **18**, 541–548.
104. Pauling, L. (1948) The modern theory of valency. *Journal of the Chemical Society*, 1461–1467.
105. Pauling, L. (1960) *The Nature of the Chemical Bond*, 3rd edn, Cornell University Press, Ithaca, NY.
106. Hammerl, A., Klapötke, T.M., Nöth, H., and Warchhold, M. (2003) Synthesis, structure, molecular orbital and valence bond calculations for tetrazole azide, CHN_7 *Propellants Explosives Pyrotechnics*, **28**, 165–173.
107. Hammerl, A., Klapötke, T.M., Mayer, P., and Weigand, J.J. (2005) Synthesis, structure, molecular orbital calculations and decomposition mechanism for tetrazolylazide CHN_7, its phenyl derivative $PhCN_7$ and tetrazolylpentazole CHN_9. *Propellants Explosives Pyrotechnics*, **30**, 17–26.
108. Klapötke, T.M., Nordheiter, A., and Stierstorfer, J. (2012) Synthesis and reactivity of an unexpected highly sensitive 1-carboxymethyl-3-diazonio-5-nitrimino-1,2,4-triazole. *New Journal of Chemistry*, **36**, 1463–1468.
109. Rahm, M., Dvinskikh, S.V., Furó, I., and Brinck, T. (2011) Experimental detection of trinitramide, $N(NO_2)_3$. *Angewandte Chemie-International Edition in English*, **50**, 1145–1148.
110. Montgomery, J.A. Jr. and Michels, H.H. (1993) Structure and stability of trinitramide. *The Journal of Physical Chemistry*, **97**, 6774–6775.
111. Wilson, K.J., Perera, S.A., Bartlett, R.J., and Watts, J.D. (2001) Stabilization of the pseudobenzene N_6 ring with oxygen. *Journal of Physical Chemistry A*, **105**, 7693–7699.

4

Advances Toward the Development of "Green" Pyrotechnics

Jesse J. Sabatini

US Army RDECOM-ARDEC, Pyrotechnics Technology & Prototyping Division, Pyrotechnics Research, Development & Pilot Plant Branch, USA

4.1 Introduction

Whether it is to commemorate a significant event or holiday, or at an amusement park for entertainment purposes, the fascinating field of pyrotechnics is an area capable of bringing families, large crowds, and perhaps even complete strangers closer together. Many people are naturally drawn to the beauty of fireworks displays, which frequently results in an array of colors bursting into the sky. The field of pyrotechnics has a long history dating back to the BC age when the Chinese first introduced the world to the use of black powder as a pyrotechnic material. Since that time, the field of pyrotechnics has greatly evolved. Although not obvious, the field of pyrotechnics is ubiquitous, having a daily profound impact on humankind. The use of pyrotechnics extends well beyond fireworks, with common applications in airbags, road flares, and fire extinguishers. Perhaps the most common use of pyrotechnics, though possibly overlooked by the general public, is by the militaries of the world. Military pyrotechnics encompasses many areas, including, but not limited to, illuminating charges, smokes for obscuration and signaling, delay fuzes, igniters incendiary devices, countermeasure flares, and primers. While the general public is quick to realize a pyrotechnic display when fireworks burst in the nighttime sky, it is the militaries of the world that utilize pyrotechnic munitions on a daily basis. On the battlefield and on training ranges, the area of pyrotechnics surrounds the warfighter, and in many cases, the

Green Energetic Materials, First Edition. Edited by Tore Brinck.

proper and consistent functioning of a pyrotechnic can be the difference between life and death.

Historically, when the toxicity of chemicals was not known and when regulations were relatively few in number, many pyrotechnic formulations were designed primarily to function reliably. Many of these historic formulations in the aforementioned areas are still being used today because they have already been proven-out, consistently pass quality control tests, and function very well in a wide range of temperatures. Today, however, more is known concerning the toxicity profile of chemicals found in these historic pyrotechnic formulations. Some chemicals found in these pyrotechnic formulations are no longer viewed as being acceptable due to their environmental and occupational health hazards alike.

As the toxicity profiles of pyrotechnic chemicals have become known, governments at the federal and state levels in the United States have called for increased regulations of these chemicals to address environmental issues and human health concerns. Due to the increased regulations and supposed toxicities of many traditional pyrotechnic chemicals, the abilities of military personnel to train on training ranges within or outside the continental United States has been hampered or prohibited. Because commercial fireworks companies in the United States are also coming under increasing scrutiny to "green" their fireworks, any technological breakthroughs made to generate environmentally sustainable pyrotechnics without compromising human health may also spur interest from the commercial fireworks sectors.

The United States has taken the initiative in making pyrotechnics, explosives, and propellants cleaner and "greener." Perhaps the most significant funding avenues in addressing the environmental and human health concerns in these areas are the Strategic Environmental Research & Development Program (SERDP) [1], the Environmental Security Technology Certification Program (ESTCP) [1], and the Environmental Quality Technology (EQT) program [2]. While much of the research in the area of "green" pyrotechnic development is being performed within US military defense-based federal laboratories, other defense agencies abroad, as well as academic and private sector laboratories across the globe, are also playing a significant role.

Although there is a significant interest in the development of "green" technologies for military and civilian pyrotechnics, these technologies will be of limited or no value if the performances and safeties of these new pyrotechnic formulations are compromised. Therefore, "green" pyrotechnic formulations should consist of environmentally acceptable ingredients, have equal or enhanced performances, and have identical or reduced sensitivities to ignition stimuli (i.e., impact, friction, and electrostatic discharge) compared to the environmentally questionable pyrotechnic munitions that are in existence today.

The following pages detail some of the strides made in "greening" the field of pyrotechnics. Though by no means an exhaustive list, a special emphasis will be placed on those programs performed in conjunction with US federal laboratories. As more chemicals are being called into question, and as governmental regulations increasingly crack down on what they believe are chemicals of concern, the need to develop environmentally friendly pyrotechnics for military and civilian applications is not going to go away. It is therefore imperative that environmentally sustainable formulations be developed; not only to address the challenges of today, but to address the challenges of tomorrow and in the years ahead. If those actively investigating the field of energetic materials continuously

think to "keep your chemicals green" when carrying out their research, the formulations developed will provide a great benefit to the military servicemen and servicewomen, the commercial fireworks industry, the environment, and the countries that are represented in carrying out these efforts.

4.2 The Foundation of "Green" Pyrotechnics

Although the interest in developing nontoxic pyrotechnic formulations is not an entirely new concept, perhaps the first efforts to "green" pyrotechnics stems from the use of high-nitrogen compounds in pyrotechnic illuminating compositions. The particular advantages of employing high-nitrogen compounds in pyrotechnic mixtures involves their gaseous and ashless combustion, which typically results in a larger flame plume, more brilliant colors in the form of a better dominant wavelength, and a higher spectral purity. Though never widely publicized, Douda developed the first known high-nitrogen pyrotechnic material, trisglycine strontium(II) perchlorate [3]. This compound is unique because it contains its own fuel, oxidizer, and coloring agent. Douda also proposed to make copper-glycine complexes to serve as an environmentally friendly replacement for barium-based green-light emitting pyrotechnic illuminants [4].

This initial work by Douda in the 1960s was extended by Hiskey, Chavez, and Naud at Los Alamos National Laboratory (LANL) 30 years later. Incorporation of high-nitrogen compounds into light-emitting pyrotechnic compositions dramatically improved performances and spectral purities of numerous illuminants [5,6]. Table 4.1 summarizes some common illuminant colors, light-emitting species to achieve these colors, and their associated wavelengths [7]. While there are a host of high-nitrogen compounds that can be used, tetrazole- and tetrazine-based fuels have been explored the most for pyrotechnic applications. The low carbon content of these fuel types ensures that soot production is kept to a minimum. Despite their high-nitrogen contents, the aromatic and hydrated nature of these fuels tends to increase their stabilities toward thermal conditions and various ignition stimuli. While most organic fuels derive their combustion energies from the oxidation of a carbon backbone, high-nitrogen compounds derive their energies from high heats of formation. Due to the great stability of the N≡N triple bond, lots of energy is released upon their decomposition to environmentally benign nitrogen gas.

A popular compound that the team at LANL used in low-smoke and low-ash pyrotechnics was dihydrazino tetrazine (**A**) (DHT) (Figure 4.1) [5]. Through the use of metal-free ammonium perchlorate (NH_4ClO_4) and ammonium nitrate (NH_4NO_3) oxidizers, tetrazine **A**

Table 4.1 *Light-emitting species and wavelengths of common colors in pyrotechnics.*

Color	Light-emitting species	Wavelength range [nm]
Red	SrCl, SrOH, Li	700–600
Yellow	Na	600–570
Green	BaCl, BO_2, CuOH, BaOH	570–500
Blue	CuCl	500–450

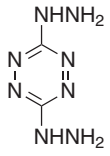

A

Figure 4.1 *Molecular structure of dihydrazino tetrazine (**A**).*

as the fuel, and a small amount of metal-based colorant, LANL was able to make smokeless pyrotechnic compositions of a variety of colors (Table 4.2).

Although these mixtures contain no binder, the NH_4ClO_4-based compositions can be wetted with water, and pressed into stars without any issues. The NH_4NO_3-based compositions are fragile, however, and need to be primed, strengthened, and waterproofed by dipping the pellets into nitrocellulose lacquer. Addition of NH_4ClO_4 to the NH_4NO_3-based compositions serves as a source of chlorine. Chlorine is widely known to deepen the color of red and green flames through the formation of metastable red-light emitting strontium(I) chloride (SrCl), and green-light emitting barium(I) chloride (BaCl) species. A source of chlorine is also needed to impart a blue flame since metastable copper(I) chloride (CuCl) is the blue-light emitting species. The addition of chlorine to yellow-light emitting formulations, however, is not beneficial because atomic sodium is the specie associated with dominant yellow-light-emission. The formation of NaCl is therefore expected to reduce atomic sodium emission, thereby reducing color quality and light intensity [8].

After their initial development of "low-smoke" pyrotechnics, the LANL team synthesized a host of high-nitrogen fuels that, when burned, produce little or no soot [6]. The two most important fuels emphasized in their study, provided in Figure 4.2, are 5,5′-bis-1*H*-tetrazole (**B**) (BT) and bis-(1(2)*H*-tetrazol-5-yl) amine monohydrate (**C**) (BTAw). The advantage of tetrazole-based fuels **B** and **C** is that many metal salt derivatives such as strontium (Sr^{2+}), copper (Cu^{2+}) and barium (Ba^{2+}) can be synthesized from these precursors (Figure 4.2).

Some tetrazole-based colorant formulations are summarized in Table 4.3. The use of high-nitrogen metal-based tetrazole salts was a novel find in pyrotechnics since these materials double as a high-energy fuel and colorant in illuminant compositions. The level of

Table 4.2 *High-nitrogen-based low-smoke pyrotechnic compositions.*

NH_4ClO_4-based compositions		NH_4NO_3-based compositions	
Components	Wt.-%	Components	Wt.-%
NH_4ClO_4	47.5	NH_4NO_3	38
Tetrazine **A**	47.5	NH_4ClO_4	8
Colorant[a–e]	5	Colorant[a–e]	8

[a] Red – $Sr(NO_3)_2$.
[b] Yellow – $NaNO_3$.
[c] Green – $Ba(NO_3)_2$.
[d] Blue – CuS.
[e] White – Sb_2S_3.

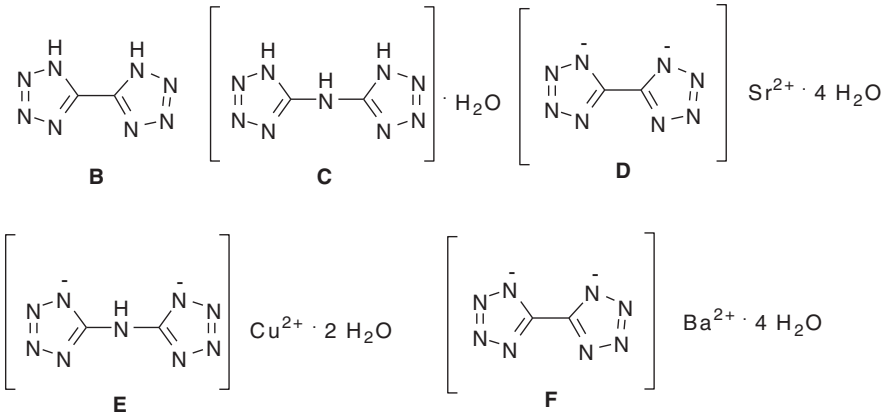

Figure 4.2 *Molecular structures of 5,5′-bis-1H-tetrazole (**B**), bis-(1(2)H-tetrazol-5-yl) amine monohydrate (**C**) and some of their metal salts (**D-F**).*

Table 4.3 *Low-smoke pyrotechnic compositions with tetrazole-based colorants.*

Components	Wt.- %
Bis-tetrazole **B**	47.5
NH_4ClO_4	47.5
Colorant **D-F**	5

Red – SrBT4w (**D**); [b)]Blue – Cu-BTA2w (**E**); [c)]Green – Ba-BT4w (**F**).

metal content needed to achieve sufficient coloration in the pyrotechnic flames is considerably less than was previously needed in traditional pyrotechnic formulations.

4.3 Development of Perchlorate-Free Pyrotechnics

4.3.1 Perchlorate-Free Illuminating Pyrotechnics

Although Douda and LANL were successful in reducing the amount of metals needed in producing a colored pyrotechnic flame, around the time the work from LANL was published, perchlorates were beginning to be viewed negatively. Historically, perchlorates were viewed as being among the ideal oxidizers due to their low moisture sensitivity, high oxidizing power, and reactivity. While NH_4ClO_4 is viewed as the ideal oxidant for propellant formulations due to its ability to produce solely gaseous products upon combustion, the use of $KClO_4$ in pyrotechnics is ubiquitous. In addition to being used in a host of colored fireworks compositions, $KClO_4$ is the oxidizer of choice in many colored military illuminants, some colored smoke formulations, a host of training simulators, incendiary compositions, and many delay fuzes.

The concern raised by environmentalists is the tendency of perchlorates to contaminate soil and public drinking supplies. As perchlorates are believed to be teratogenic, there are

concerns that unborn fetuses and newborn and infant babies could be exposed to elevated levels of perchlorates through the breast milk of women who may have unknowingly ingested perchlorates [9]. Because the ionic radii of the perchlorate polyatomic ion and iodide are similar, perchlorate has been shown to compete with iodide in binding with the thyroid gland, potentially disrupting proper functioning of this gland [9]. While it appears that the binding event between perchlorate and the thyroid gland is reversible – provided that there is a suitable uptake of iodized foods [10] – perchlorates have been regulated by the US Environmental Protection Agency (EPA). The EPA has established the federal permissible limit of perchlorates in groundwater to be 15 parts per billion (ppb) [11], with the states of California and Massachusetts setting their own respective limits of 6 ppb and 2 ppb [12,13].

In light of these regulations, the US Department of Defense spends millions of dollars annually associated with perchlorate decontamination, clean-up, and legal fees. Due to potential contamination associated with perchlorates and other suspected chemicals of concern, the commercial fireworks sector is also under scrutiny to "green" their existing pyrotechnics formulations used in fireworks and entertainment displays [14]. As a result of the aforementioned regulations, the ability of the US military to train on training ranges within and outside the continental United States has been sharply curtailed or prohibited. The inability of military personnel to properly train for combat endangers combat readiness, and puts the lives of the soldier at risk.

The seminal work performed by Douda and the team at LANL paved the way for high-nitrogen technologies to find practical applications as perchlorate replacements in red- and green-light emitting US Army military signaling flares to address the aforementioned environmental concerns. At Armament, Research, Development & Engineering Center (ARDEC), Sabatini *et al*. found that metal-based bis-tetrazolate salts **G** and **H** serve as effective $KClO_4$ replacements in pursuit of environmentally conscious M126A1 red- and M195 green-light emitting compositions (Figure 4.3) [15,16]. Although bis-tetrazolates **G** and **H** are monohydrates, outgassing does not occur when both compounds are subjected to the vacuum thermal stability (VTS) test. This is likely due to the fact that the water molecule contained in these compounds is coordinated to the metal, as has been determined by x-ray diffraction (XRD) [17]. Such an interaction allows the water molecule to remain in the crystal lattice, even at elevated temperature.

The US Army perchlorate-containing in-service M126A1 red-light and M195 green-light emitting illuminants and their replacement formulations are summarized in Table 4.4, and

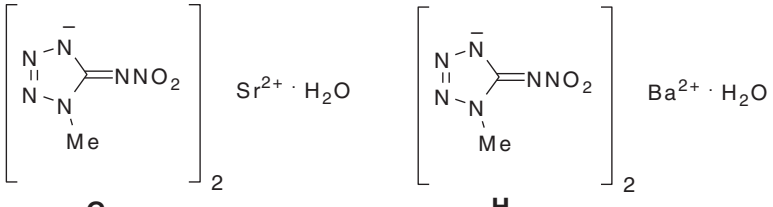

Figure 4.3 *Strontium bis-(1-methyl-5-nitriminotetrazolate) monohydrate (**G**) and barium bis-(1-methyl-5-nitriminotetrazolate) monohydrate (**H**).*

Table 4.4 *M126A1 red- and M195 green-light emitting illuminants.*

In-service M126A1		Formulation **1**		Formulation **2**	
Components	Wt.- %	Components	Wt.- %	Components	Wt.- %
$Sr(NO_3)_2$	39.3	$Sr(NO_3)_2$	39.3	$Sr(NO_3)_2$	39.3
Mg 30/50	14.7	Mg 30/50	29.4	Mg 30/50	35.4
Mg 50/100	14.7	PVC	14.7	PVC	14.7
PVC	14.7	Bis-tetrazolate **G**	9.8	Bis-tetrazolate **G**	3.8
$KClO_4$	9.8	Epon 813/ Versamid 140	6.8	Epon 813/ Versamid 140	6.8
Laminac 4116/ Lupersol	6.8				
In-service M195		**Formulation 3**		**Formulation 4**	
Components	Wt.- %	Components	Wt.- %	Components	Wt.- %
$Ba(NO_3)_2$	48	$Ba(NO_3)_2$	48	$Ba(NO_3)_2$	48
Mg 30/50	22	Mg 30/50	22	Mg 30/50	27
DP	15	DP	15	PVC	15
$KClO_4$	10	Bis-tetrazolate **H**	10	Bis-tetrazolate **H**	5
Laminac 4116/ Lupersol	5	Epon 81/ Versamid 140	5	Epon 813/ Versamid 140	5

their performances are provided in Table 4.5. In the case of the red-light emitting M126A1 illuminant, formulations **1** and **2** both exceed the military requirements and perform better than the perchlorate-containing formulation. A particular advantage of formulation **2** is its high luminous intensity; an occurrence known to happen in the presence of higher magnesium percentages that typically results in a brighter colored flame [18]. Although not occurring in these experiments, addition of too much metal can "wash out" the flame color due to excessive formation of incandescent particles. Pyrotechnicians should be mindful of this when adding metal fuels to boost the intensity of a colored flame.

For the green-light emitting M195 illuminant, formulations **3** and **4** burn longer, and with a comparable luminosity compared to the perchlorate-containing formulation. Formulation **4** is certainly the more environmentally conscious of the two newly developed formulations. This is due to the absence of dechlorane plus (DP); a chlorinated chemical that has been

Table 4.5 *Performance of M126A1 red- and M195 green-light emitting illuminants.*

Formulation	Burn time [s]	Luminous intensity [Cd]	Dominant λ [nm]	Spectral purity [%]
M126A1 military requirement	50.0	10 000.0	620 ± 20	76.0
In-service M126A1	54.0	17 194.9	613.1	88.6
1	63.3	16 285.0	612.5	89.9
2	55.1	24 490.1	612.7	91.6
M195 military requirement	50.0	5000.0	540 ± 20	50.0
In-service M195	55.3	6973.3	562.3	64.8
3	56.2	6536.7	561.9	65.3
4	59.3	6608.7	564.7	69.4

called into question by the US Army Public Health Command over concerns associated with bioaccumulation [19,20]. Interestingly, formulations **3** and **4** and the perchlorate-containing M195 formulation currently used in production have dominant wavelength values outside of the 540 ± 20 nm threshold. Sodium contamination is believed to be the culprit, and can be traced to two potential sources in these formulations; as an impurity in the $Ba(NO_3)_2$ oxidizer, and from the Kraft fiberboard tubes used to house the pyrotechnic illuminants [21]. Many of the military requirements were written decades ago, so it is possible that newer technologies today are able to offer more precise measurements. Regardless, this is an issue that is worthy of further investigation.

For these particular formulations, it is omit this noteworthy that formulations **1–4** utilize an epoxy-based binder system (Epon 813/Versamid 140) as the replacement for the Laminac 4116/Lupersol binder system. In addition to the presence of styrene monomer, which has been classified by the US Department of Health and Human Services as a potential carcinogen [22], Laminac is also a single-point-of-failure material. The aforementioned epoxy-based binder system has a proven history in many US Navy illuminating compositions. Therefore, utilization of this binder system for the US Army's signaling illuminants is a safe, viable alternative for the Laminac/Lupersol 4116 binder system. Replacement of this material with the widely available epoxy binder system not only addresses the environmental issues, but also ensures that these signaling items will remain in the arsenal of the US Army and its allied military personnel.

A final note on the development of the M126A1 red- and M195 green-light emitting illuminants is that formulations **1–4** have lower impact and friction sensitivities, omit comparable electrostatic discharge sensitivities and comparable thermal onset temperatures to the perchlorate-containing items they are replacing. As is demonstrated in the reformulation of these two items, it is possible to design pyrotechnics that are more environmentally sustainable, while having better performances and equal or lower sensitivities than the items they seek to replace.

At the Naval Surface Warfare Center (NSWC) CRANE division, Shortridge and coworkers developed perchlorate-free illuminants exceeding the military requirements of the Navy's red-, green-, and yellow-light emitting signaling flare illuminants [23–26]. Table 4.6 summarizes the formulations of the in-service Navy flares and their best performing perchlorate-free counterparts. Performances of these illuminants are detailed in Table 4.7, , and the new illuminants have low sensitivities to impact, friction, and electrostatic discharge. In designing suitable perchlorate-free formulations, the Navy's approach differs from the US Army in that high-nitrogen compounds are not needed to achieve optimal performance. However, the Army and Navy signaling illuminants differ in size and diameter, and the form, fit, and function of these two items are also quite different. Therefore, an approach that yields success in one item may not have universal success in other items when various parameters or configurations are changed.

The Navy's approach in developing the perchlorate-free green is particularly interesting in that formulation **6** consists of three potential green-light emitting sources; $Ba(NO_3)_2$, Cu powder, and amorphous boron. As discussed previously, barium combines with chlorine to generate green-light emitting metastable BaCl, while copper powder, in the presence of chlorine, forms metastable copper(I) chloride (CuCl); a blue-light emitting specie. It has been stated that CuCl is stable only up to 1200 °C, and while experimental evidenced is still needed, this claim has been disputed in a theoretical sense by Sturman after thermodynamic

Table 4.6 *In-service Navy flares and their perchlorate-free formulations.*

IS Red-2		Formulation **5**	
Components	Wt.- %	Components	Wt.- %
$Sr(NO_3)_2$	34.7	$Sr(NO_3)_2$	50.323
Gran 15 Mg	24.4	Gran 17 Mg	28
$KClO_4$	20.5	PVC	14.677
PVC	11.4	Epon 813/Versamid 140	7
Asphaltum	9		
IS G Std		**Formulation 6**	
Components	Wt.- %	Components	Wt.- %
$Ba(NO_3)_2$	22.5	$Ba(NO_3)_2$	62.75
Gran 18 Mg	21	Gran 18 Mg	9.81
$KClO_4$	32.5	Gran 15 Mg	4.89
PVC	12	PVC	8
Cu powder	7	Cu powder	6.7
Epon 813/Versamid 140	5	B (amorphous)	2.85
		Epon 813/Versamid 140	5
IS Y-2		**Formulation 7**	
Components	Wt.- %	Components	Wt.- %
$Ba(NO_3)_2$	20	$NaNO_3$	37
Gran 18 Mg	30.3	$Ba(NO_3)_2$	27.05
$KClO_4$	21	Gran 18 Mg	20.1
$Na_2C_2O_4$	19.8	PVC	10.9
Asphaltum	3.95	Epon 813/Versamid 140	4.95
Epon 813/Versamid 140	4.95		

calculations using the NASA-CEA equilibrium code [27] demonstrated that several blue-light emitting formulations had temperatures well in excess of 1200 °C [28]. According to Sturman's calculations, however, magnesium-containing blue-light emitting formulations gave poor results, an indication that CuCl dissociates in the presence of hot pyrotechnic flames. The presence of the organic-based epoxy binder presents a source of hydrogen, which can combine with copper oxide (CuO) during the combustion process to form

Table 4.7 *Performance of USNavy perchlorate-free illuminants.*

Formulation	Burn time [s]	Luminous intensity [Cd]	Dominant λ [nm]	Spectral purity [%]
In-service IS Red-2	17.5	4913.0	617.0	94.0
5	19.8	6040.0	621.0	96.0
In-service IS G Std	30.0	526.0	544.0	48.0
6	31.0	763.0	547.0	54.0
In-service IS Y 2	41.0	1199.0	587.0	78.3
7	59.0	1571.0	583.0	75.3

metastable green-light emitting copper(I) hydroxide (CuOH). Amorphous boron is a highly reactive fuel, and can be quite sensitive to ignition stimuli, especially to electrostatic discharge. However, upon combustion, amorphous boron is converted to metastable boron oxide (BO_2), another green-light emitting specie [29].

The Navy's perchlorate-free yellow flare (formulation **7**) is of particular interest due to its exceptionally long burn time and higher luminosity compared to the control. Such a phenomenon makes it more likely for the flare to be spotted from a farther distance. Curiously, formulation **7** contains chlorine, which, due to NaCl formation, is expected to reduce the color purity and light intensity of the yellow flare [8]. When chlorinated organic compounds are employed in a pyrotechnic flame, they have flame cooling tendencies, which can lengthen the burn time. It is possible that the use of sodium oxalate ($Na_2C_2O_4$) as the PVC replacement in formulation **7** may be more beneficial. NaCl would no longer be produced, the coolant properties of $Na_2C_2O_4$ would still serve to prolong burn times, and the presence of a higher concentration of atomic sodium may serve to enhance the light intensity of the yellow flare.

Aside from signaling illuminants, another area where copious amounts of perchlorates have traditionally been used is for flash-bang applications. Many flash-bang devices are employed as a nonlethal diversionary device. Through the production of intense light and concussive sound, flash-bangs are typically aimed at incapacitating personnel for a specified duration without causing injuries. One such flash-bang device that has been reformulated is the US Navy's Mk 141 40 mm flash-bang charge. The Mk 141 consists of $KClO_4$ and aluminum powder to produce an ample amount of light and sound.

In an effort to remove perchlorate from the Mk 141 formulation, ATK Launch Systems developed a fuel–air mixture in generating satisfactory light and sound [30]. They report that the use of a hot gas-generating pyrotechnic activator in the presence of magnesium powder achieves the necessary ignition temperatures to breach the grenade body and disperse the magnesium into the air, where it reacts with air to produce incandescent magnesium oxide and a bright light that is greater than commercial "off-the-shelf" flash-bang devices.

4.3.2 Perchlorate-Free Simulators

Simulators are used widely and frequently by the military on training ranges in an effort to mimic the flashes, noise, loud reports, and smoke that military personnel will experience on the battlefield. Since many simulators currently used by the US military are rich sources of $KClO_4$, reformulation of these simulators in an environmentally friendly fashion makes practical sense. Efforts at ARDEC have been successful in developing perchlorate-free variants of the M115A2 ground burst and M116A1 hand grenade simulators [31], the M274 smoke signature 2.75″ rocket simulator [32], and the battlefield effects simulator (BES) [33,34].

The purpose of the M115A1 ground burst and M116A1 hand grenade simulators is to provide a "flash-bang" effect. The in-service M115A2 ground burst and M116A1 hand grenade simulators are composed of $KClO_4$ and aluminum, though their specific percentages in the formulation are not publically known [31]. The perchlorate-free formulations for these two simulators are provided in Table 4.8. A small amount of Cab-O-Sil (fumed silica) serves as a processing aid, and is necessary for proper mixing of the materials, while sulfur is

Table 4.8 *M115A2 and M116A1 simulator formulations.*

Formulation **8**		Formulation **9**	
Components	Wt.- %	Components	Wt.- %
$Sr(NO_3)_2$	53.5	KNO_3	53.5
Al	40	Al	40
S_8	5	S_8	5
Boric acid	1	Boric acid	1
Cab-O-Sil	0.5	Cab-O-Sil	0.5

added to lower the ignition temperature of the pyrotechnic mixture. The addition of a small amount of boric acid to the composition is necessary to ensure long-term storage stability. Although aluminum-containing compositions tend to be stable and are of no general concern, the presence of nitrate salts in aluminum-based compositions can lead to a buildup of an alkaline medium, owing to the presence of aluminum hydroxide that forms over time (Eqs. (4.1) and (4.2)) in the presence of moisture [10]. The addition of weakly acidic boric acid ensures that an alkaline environment does not exist, thus side-stepping this potential incompatibility and preventing the potential autoignition of the pyrotechnic mixture that could result.

$$3\,KNO_3 + 8\,Al + 12\,H_2O \rightarrow 3\,KAlO_2 + 5\,Al(OH)_3 + 3\,NH_3 \tag{4.1}$$

$$3\,Sr(NO_3)_2 + 16\,Al + 24\,H_2O \rightarrow 3\,Sr(AlO_2)_2 + 10\,Al(OH)_3 + 6\,NH_3 \tag{4.2}$$

The visible light output and sound intensity of M115A2 and M116A1 simulator formulations **8** and **9** against the in-service perchlorate-containing formulation at ambient temperature is summarized in Table 4.9. Strontium nitrate-based formulation **8** yields considerably higher visible light output (reported in luminous efficiency) compared to the in-service simulators and potassium nitrate-based formulation **9**. Formulation **9** performs marginally better than formulation **8** in the category of sound intensity, though neither formulation provides as loud of a report as the perchlorate-containing flash-bang simulators. Despite its lower visible light output, formulation **9** is the optimal choice on the grounds of its low hygroscopicity and still decent performance. The lower hygroscopicity of formulation **9** is due to the presence of KNO_3 (water solubility = 38.3 g per 100 g of H_2O), which does not absorb water as readily as $Sr(NO_3)_2$ (water solubility = 80.2 g per 100 g of H_2O) [35].

Table 4.9 *Performance of M115A2 and M116A1 simulator formulations.*

Formulation	Luminous efficiency [[Cd.s]g^{-1}]	Sound intensity [dB@ 50 ft.]
In-service M115A2	2000.0	155.8
8-M115A2	4783.3	147.1
9-M115A2	1646.7	149.1
In-service M116A1	2116.7	151.6
8-M116A1	5166.7	144.8
9-M116A1	1676.7	150.9

Table 4.10 *Composition of the M274 2.75″ training rocket.*

In-service M274		Formulation **10**	
Components	Wt.- %	Components	Wt.- %
$KClO_4$	33	$Sr(NO_3)_2$	55
Al	67	Al	35
		Magnalium	10

The removal of $KClO_4$ from the M115A2 and M116A1 simulators is significant since these simulators account for approximately 70% of the perchlorate that is released on training ranges within the United States. The achievement of developing perchlorate-free variants of these simulators resulted in the 2007 Secretary of Defense Environmental Award [36]. Though present in a small quantity, perhaps further "greening" could be done to formulation **9** in the future through the elimination of sulfur. The burning of sulfur is known to yield toxic sulfur dioxide (SO_2), a known component of acid rain. Work by Cegiel is one particular example of a perchlorate- and sulfur-free flash-bang composition [37]. His flash-bang device contains a powdery mixture composed of a nitrate oxidizer, metal oxides, metal fuels, stabilized nitrocellulose, and graphite.

ARDEC, in conjunction with Edgewood Chemical & Biological Center (ECBC) reported success in developing a perchlorate replacement for the M274 2.75″ rocket simulator [32]. The M274 is fired from an aerial platform, and its objective is to produce a flash (detected better during nighttime operations) or smoke signature (detected better during daytime operations) on impact for the purposes of marking the strike of an intended target. The M274 is balistically similar to the M151 high explosive (HE) warhead, which is also fired from the air with the goal of striking targets on the ground. The composition of the M274 pyrotechnic charge is provided in Table 4.10.

In developing a successful M274 replacement, two formulations have been identified from previous work; ARDEC's M115A2 and M116A1 formulation **9**, and ECBC's formulation **10**. Although published data is limited, formulations **9** and **10** are both reported as having better sound and visible light output, while slightly underperforming in overall smoke output but having the same smoke burn time compared to the in-service M274 formulation. Although formulation **10** had a higher light output than formulation **9**, it failed the small-scale burn test during interim hazard classification (IHC) testing, resulting in an explosion. Formulation **9**, on the other hand, passed IHC testing (impact, friction, ESD, thermal stability, and small-scale burn tests) and has been proven to be environmentally compliant. With the perchlorate-free M274 formulation in hand, it is expected that the amount of perchlorate exposed to training ranges and manufacturing sites will decline by about one ton per year, assuming an estimated usage rate of 150 000 items per year. With the successful development of perchlorate-free variants of the M115A2, M116A1, and M274, efforts are underway at ARDEC to remove $KClO_4$ from the M117 flash, the M118 illumination and the M119 whistling booby trap training simulators.

Another ARDEC success story in the area of perchlorate remediation was the development of an environmentally conscious battlefield effects simulator (BES) to simulate force-on-force and force-on-target training exercises [33,34]. The perchlorate-free variant of the BES has been proven-out and is ready for implementation. When the BES was adopted for

Table 4.11 *Composition of the M26 target kill simulator.*

M26 Composition	
Components	Wt.- %
$KClO_4$	62
Naphthalene (**I**)	28
Laminac 4116/Lupersol	10

Table 4.12 *Composition of the perchlorate-free BES formulation.*

Formulation **11**	
Components	Wt.- %
Organic dyes	30
Sucrose	21.5
$KClO_3$	29.5
$MgCO_3$/stearic acid/VAAR	19

use, there was no environmentally friendly black smoke formulation available, as the Army-based M26 target kill black smoke simulator was removed from the inventory in 1999 due to environmental concerns associated with the pyrotechnic composition (Table 4.11). While the concerns of $KClO_4$ and Laminac binder systems have already been discussed, naphthalene is also a chemical of concern. It is believed to be a carcinogenic material, and at elevated concentrations is known to cause hemolytic anemia through the destruction of red blood cells [38]. Naphthalene, whose structure is provided in Figure 4.5, is a relatively poor combustible fuel, and the black smoke and soot observed from attempts to combust naphthalene are the result of incomplete combustion products.

In developing an environmentally compatible BES composition, a black smoke of suitable quality can be obtained through the use of a mixture of red- and green-colored organic smoke dyes. Table 4.12 summarizes ARDEC's BES composition, though the exact weight percentages of all of the individual ingredients of formulation **11** are not available at this time. Colored smoke formulations typically require cool burning temperatures to ensure that the dyes sublime instead of combust. In addition to a sublimating dye, colored smoke formulations contain $KClO_3$ as the oxidizer, sugar as the fuel, as well as carbonate or bicarbonate cooling agents to suppress flames and temperatures. A more in-depth discussion of colored smokes will be covered in Section 4.6.1.

4.4 Removal of Heavy Metals from Pyrotechnic Formulations

Another area of concern to the "green" energetic pyrotechnician is the presence of heavy metals in many currently used pyrotechnic formulations. Though the use of Paris green, copper acetoarsenite ($(CuO)_3As_2O_3{\cdot}Cu(C_2H_3O_2)$) was once used in blue-light emitting

pyrotechnics, this practice is now obsolete due to toxicity concerns associated with arsenic [10]. Today, the most common heavy metals used in various pyrotechnic munitions include barium, lead, and hexavalent chromium (Cr(VI)). Although many barium compounds are not mobile in soil, and are readily converted to the relatively nontoxic and insolube barium carbonate ($BaCO_3$) and barium sulfate ($BaSO_4$) when exposed to a water environment, the use of barium in pyrotechnics has recently drawn concerns due to its occupational health hazards. Many barium compounds and barium-based combustion products are believed to be cardiotoxic [39] and are believed to be occupational health hazards.

Lead is a known poisonous material, adversely affects the nervous system, and its neurotoxicity is known. Lead is known to cause disorders of the brain, blood, cardiovascular system, and kidneys, and can bioaccumulate in the bones and soft tissues of the human body [40]. Hexavalent chromium is a known carcinogen upon inhalation, and the US Environmental Protection Agency established a 0.10 parts per million (ppm) maximum containment level (MCL) of total chromium [41]. It is believed that the EPA will establish permissible limits in drinking water for hexavalent chromium in the near future. Therefore, when possible, the removal of these heavy metals from pyrotechnics (and energetics in general) is a judicious choice toward the "greening" of pyrotechnics.

4.4.1 Barium-Free Green-Light Emitting Illuminants

The most common practice in producing an illuminating green-light emitter is through the use of $Ba(NO_3)_2$ in the presence of chlorinated organic compounds, which forms the metastable BaCl green-light emitter. PVC is a popular chlorinated organic compound used in pyrotechnic compositions due to its high weight percentage of chlorine and low cost, though other chlorine donors such as saran, parlon, and chlorinated rubber are also used. Historically, hexachlorobenzene was used as a source of chlorine in some red- and green-light emitting pyrotechnics, but the use of this chemical has been widely discontinued due to its probable carcinogenic effects and toxicity to the aquatic environment. Hexachlorobenzene is listed as one of the "dirty dozen" by the Stockholm Convention on persistent organic pollutants [42].

Although the formation of BaCl is currently the preferred method toward generating green light in military and civilian pyrotechnics, there are alternative green-light emitters. Koch *et al*. have investigated the combustion ytterbium in oyxgen and with halocarbon-based oxidizers. Atomic ytterbium, ytterbium monoxide, (YbO), ytterbium monochloride (YbCl), and ytterbium monofluoride (YbF) all yield a brilliant green light of high purity, though applications of this technology are likely to be limited to volume restricted pyrotechnics (i.e., tracers) due to cost issues associated with ytterbium [43,44]. Another green-light emitter, metastable CuOH, forms when copper-containing compounds are combusted in the presence of a hydrogen- and oxygen-rich environment. Klapötke and Stierstorfer have synthesized a number of high-nitrogen containing copper salts and these compounds are reported to generate green light upon combustion [45,46].

An alternative way of achieving green-light emission has been through the use of boron-based compounds. When combusted in the presence of oxygen, boron-based compounds produce metastable BO_2, which is also a green-light emitter. Though not an environmentally friendly formulation by today's standards, an early barium-free green-light emitting

Table 4.13 *Composition of the M125A1 control and boron carbide-based formulation* ***12****.*

In-service M125A1		Formulation **12**	
Components	Wt.- %	Components	Wt.- %
$Ba(NO_3)_2$	46	KNO_3	83
Mg 30/50	33	B_4C	10
PVC	16	Epon 828/Epikure 3140	7
Laminac 4116/Lupersol	5		

formulation, consisting of 30% B/60% $KClO_4$/10% lactose, was investigated by Eppig in the late stages of World War II in Germany as a replacement for barium chlorate-based formulations [47]. The combustion amorphous boron in the presence of potassium nitrate (B/KNO_3) is a widely known method of generating green light, and Rusan and Klapötke have produced smokeless green flames through the combustion of NH_4NO_3/B/boron-based high-nitrogen/VAAR mixtures [48]. The sensitivities of amorphous boron-based mixtures to ignition stimuli can sometimes be a concern, however, and amorphous boron is also a fairly expensive material. While amorphous boron finds applications in some pyrotechnic delay compositions, its use in pyrotechnic illuminants is usually cost prohibitive since these illuminants are composed of substantial quantities of material.

Work by Sabatini and co-workers to eliminate heavy metal barium from one of the US Army's green-light illuminating compositions shows that boron carbide (B_4C) in the presence of KNO_3 serves as an effective green-light emitter (Table 4.13) [49]. B_4C is a known abrasive material and refractory, and is currently used for many armor-based applications. Its use in energetic materials had previously been limited to propellants as a fuel in solid fuel ramjets [50], and as a fuel in some early perchlorate-based white smoke compositions [51]. The performance of formulation **12** compared to the barium-containing M125A1 illuminant formulation is summarized in Table 4.14, while photographs of the two illuminants are provided in Figure 4.4.

It is noteworthy to mention that the sensitivity of formulation **12** is remarkably low to impact (>63.7 J), friction (>360 N), and electrostatic discharge (>9.4 J) and has a high thermal onset temperature (403.5°C). In addition to the removal of heavy metal barium, another advantage of the B_4C technology is the removal of chlorinated organic compounds from the formulation. There is some concern that the use of chlorinated organic compounds (such as PVC) in pyrotechnic compositions leads to the formation of hazardous polychlorinated biphenyls (PCBs), polychlorinated dibenzodioxins (PCDDs) and polychlorinated dibenzofurans (PCDFs) [52–54]. However, there is conflicting evidence as to whether the combustion of chlorine-containing pyrotechnics leads to these toxic

Table 4.14 *Performance of formulation* ***12*** *against the barium-containing control.*

Formulation	Burn time [s]	Luminous intensity [Cd]	Dominant λ [nm]	Spectral purity [%]
In-service M125A1	8.15	1357.40	562.29	61.50
12	9.69	1403.30	561.85	51.96

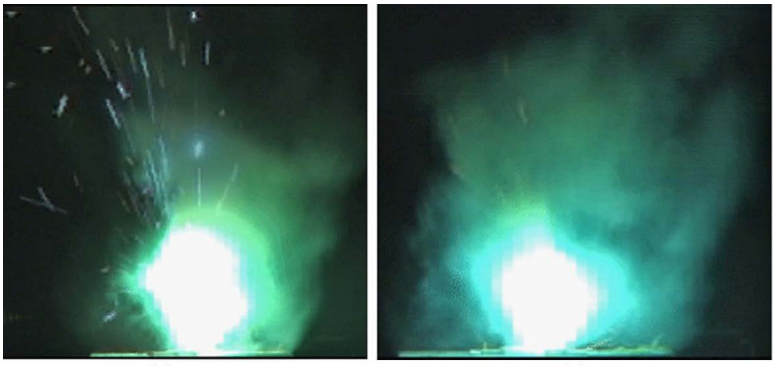

Figure 4.4 *(a) Barium-containing M125A1 control (b) Boron carbide-based formulation* ***12*** *at mid-burn.*

chemicals being produced in harmful amounts. Although Fleischer says that pyrotechnics displays account for marginal amounts of PCBs, PCCDs, and PCDFs [53], Dyke and Coleman report a fourfold increase in these chemicals following a fireworks display [54]. What is clear is that if energetic materials can be made in the absence of chlorinated organic compounds, there is no risk that these harmful chemicals will be formed.

Although the spectral purity of formulation **12** is significantly lower than the M125A1 control formulation, it is still above the 50% minimum threshold required by the US Army for this particular green-light emitting item, and efforts continue on proving-out the B_4C technology at the prototype level for implementation into military items. The reduction in spectral purity of formulation **12** can likely be traced to a substantial amount of continuum emission based on potassium hydroxide (KOH), resulting in white light and a "washing out" of the perceived green color. The use of metal-free oxidizers such as ammonium nitrate, as done by Rusan and Klapötke [48], would likely aid in increasing the spectral purity of formulation **12**, though it is likely that this approach will also affect the burn time and light output significantly.

4.4.2 Barium-Free Incendiary Compositions

The goal of pyrotechnic incendiaries, whether in the form of a grenade, a bullet, or another incendiary device, is to set fire to a given target. It is important that any incendiary composition be composed of chemicals that, upon combustion, are capable of producing high temperatures for destroying sensitive equipment, and burning through heavily armored aircraft or tanks. One of the most widely known (and environmentally friendly) incendiary compositions is the highly energetic and exothermic thermite, consisting of aluminum and red iron oxide (Eq. (4.3)). Although thermite mixtures can produce temperatures of about 2400 °C, the stability of thermite is quite high to various ignition stimuli, and it requires temperatures above 800 °C to ensure reliable ignition [10].

$$2\,Al_{(s)} + Fe_2O_{3(s)} \rightarrow Al_2O_{3(s)} + 2\,Fe_{(l)} \tag{4.3}$$

Table 4.15 *Composition of the IM-28 incendiary and formulation **13**.*

IM-28 composition		Formulation **13**	
Components	Wt.- %	Components	Wt.- %
Magnalium	50	Magnalium	48
$Ba(NO_3)_2$	40	$NaNO_3$	48
$KClO_4$	10	Calcium resinate	4

Incendiary compositions are also employed in various armor-piercing bullets. One such example is the IM-28 incendiary mix, which is a component of the M8 armor-piercing incendiary (API) bullet (Table 4.15). When an M8 is fired, the impact with which it strikes the target is to promote ignition of the IM-28 incendiary mix. This phenomenon results in the burning of the bullet inside the intended target. In addition to reaching the high temperatures required of any incendiary, it is also required that the IM-28 emit a brilliant flash of light to serve as a marking agent that the intended target has been hit.

Historically, many incendiary charges consist of large amounts of metal fuel with barium nitrate oxidizer. The resulting combustion temperatures are high, the production of metal oxides (i.e., MgO, Al_2O_3 and BaO) are good broad range molecular emitters, and are typically good generators of white light. $KClO_4$, found in the IM-28 composition, serves as a co-oxidizer, and also enhances sensitivities to ignition stimuli.

In addressing the environmental concerns associated with perchlorates and barium compounds in pyrotechnics, Griffiths developed formulation **13**, a barium- and perchlorate-free alternative to the IM-28. His mixture consists of magnalium and $NaNO_3$ with calcium resinate as a dry binder to achieve good performance [55]. Formulation **13** was reported to match the IM-28 baseline composition in flash size and duration when both formulations were subjected to gun firing trials. In addition to the environmental benefits, Griffiths' formulation is also advantageous because it burns with a higher luminosity than the IM-28 composition, undoubtedly due to the presence of atomic sodium, which is known to contribute to overall light intensity.

A potential disadvantage of formulation **13**, however, is the presence of $NaNO_3$, which is known to be quite hygroscopic (water solubility = 91.2 g/100 ml of H_2O) [35]. Although $NaNO_3$ is widely used in military yellow-light emitting compositions, hygroscopicity is always a concern, and strict humidity control is required during the manufacturing process. Long-term aging is also a concern for $NaNO_3$-based formulations that are present in high humidity environments for an appreciable amount of time.

After formulation **13** was disclosed, efforts by Moretti, Sabatini, and Chen sought to improve the formulation further, and a barium- and perchlorate-free alternative to Griffiths' IM-28 composition was developed based on the use of $NaIO_4$ as the oxidizer (Table 4.16) [56]. Compared to the control, formulation **14** has lower or equal sensitivities to various ignition stimuli, and a comparable burn time to the control formulation with a 20% brighter output (Table 4.17). Periodate salts are less water soluble and more thermodynamically stable than perchlorate salts [35,57], and although the toxicology profile of periodates needs further assessment, the larger polyatomic radius of IO_4^- compared to ClO_4^- is presumed to prohibit the competition of periodates with the thyroid gland. Though more research is needed in this area, it is possible that KIO_4 could serve as an effective

Table 4.16 *Composition of formulation* ***14****.*

Formulation **14**	
Components	Wt.- %
Magnalium	60
$NaIO_4$	40

Table 4.17 *Performance of the IM-28 control and formulation* ***14****.*

Formulation	Burn time [s]	Luminous efficiency [[Cd.s]/g]
In-service IM-28	0.109	11 294.00
14	0.090	13 545.80

$KClO_4$ replacement in a host of pyrotechnic munitions, while $NaIO_4$ could find its way into a host of other yellow- and white-light emitting pyrotechnic compositions.

4.4.3 Lead-Free Pyrotechnic Compositions

The presence of lead-based pyrotechnic formulations encompasses the areas of igniters, electric matches, some delay compositions, and primer compositions. Although the category of lead-free primer development falls into the pyrotechnic realm, it will not be discussed in this chapter. Lead-free primers are discussed in the primary explosives chapter (Chapter 5) since many compounds being evaluated for their primary explosive properties may find potential primer use.

One area in need of "greening" was the lead-based "first fire" igniter composition for the AN-M14 thermate incendiary grenade (Table 4.18) [58]. ECBC is credited with developing formulation **15**, which is free of red lead (Pb_3O_4) and has three times the heat output as the red lead-based formulation. The addition of charcoal to the formulation is essential for reliable ignition, especially at cold temperatures (i.e., below $-25\,^{\circ}C$). Charcoal has a high heat output per gram, and is used to facilitate ignition and accelerate burn rates.

Six years later, ARDEC determined that formulation **15** still exhibited ignition failures, and developed formulation **16** to mitigate this [59]. Although no calorimetric data is

Table 4.18 *Igniter compositions for the AN-M14 incendiary grenade.*

AN-M14 igniter		Formulation **15**		Formulation **16**	
Components	Wt.- %	Components	Wt.- %	Components	Wt.- %
Pb_3O_4	25	KNO_3	66	KNO_3	35
Fe_2O_3	25	Ti	11	Si	26
Si	25	Al	8	Fe_3O_4	22
Ti	25	Si	6	Al	13
Nitrocellulose	4.5	S_8	2	Charcoal	4
		Charcoal	5	Nitrocellulose	+5
		Polyacrylic rubber	2		

available in comparing the two lead-free formulations, ARDEC notes that only formulation **16** achieves reliable ignition with no failures. Although the removal of red lead in the AN-14 igniter composition represents a significant achievement, the "greening" problem is only partially resolved since the AN-M14 incendiary composition is composed of an $Al/Fe_2O_3/Ba(NO_3)_2/S_8$/binder mixture [59]. Therefore, development of an AN-M-14 incendiary composition free of barium and sulfur would represent a fully "green" version of this incendiary device.

"First fire" compositions are not the only ignition-based pyrotechnic compositions that have historically contained lead. Another source of lead-containing pyrotechnic devices is the electric match. An electric match is advantageous over a burning fuse because the match has no delay time before ignition, and it can be reliably fired over a safe distance to minimize personnel exposure to energetics. Commercial electric matches in use typically consist of three dip coat layers: a spark sensitive layer composed of lead-based tetroxide, nitroresorcinate or isocyanate compounds, a layer composed of metal fuels or a mixture of $Ti/KClO_4$ (TPP) to produce hot particles to ignite a first fire composition, and a layer of lacquer to provide water resistance and mechanical strength [60]. Upon burning of the electric match composition, lead-based smoke is produced, thus contaminating the surrounding environment and firing areas.

Scientists at LANL made a lead-free alternative to electric matches using pyrotechnic compositions based on the Al/MoO_3 nano-thermite composition known as a metastable intermolecular composite (MIC) [60]. MIC is generally known to have a high degree of thermal stability, but its compositions are highly reactive and can be quite sensitive to ESD. LANL's lead-free electric match consists of three dip coat layers: a spark sensitive layer containing MIC-based Al/MoO_3 and nitrocellulose, a layer composed of $KClO_4$/Al/Ti/nano-Fe_2O_3/Nitrocellulose, and a vinyl layer to minimize moisture sensitivity of the electric matches. The matches fire reliably, even after being submerged in water for a period of three weeks. The MIC-based matches react much faster and yield a brighter light output compared to the lead-based matches, an indication of higher combustion temperatures. While a further environmental improvement with the MIC-based electric matches would be the removal of perchlorate from the second dip coat layer, the perchlorate issue was not an environmental issue at the time the lead-free electric match technology was first being developed at LANL.

Pyrotechnic delay compositions can also be a source of lead, mainly in the form of lead oxides and lead chromates. Some of the hardware that houses pyrotechnic delays has also been composed of rolled lead tubing, though the presence of these tubes is being phased out for housings that are more environmentally compliant (i.e., brass- and aluminum-based housings). It is important that thermal conductivity differences between delay housings be considered when designing a delay for a specified burn rate. Thermal conductivity of the housing used may have a substantial influence on the burn rate of a given pyrotechnic delay mixture. Focke indicates that Si/Bi_2O_3- and Si/Sb_6O_{13}- based delay mixtures encased in aluminum housings have a reduced burn rate on the order of 20–50% compared to the burn rates observed when these mixtures burn in lead housings [61]. This phenomenon is believed to be attributed to the large thermal conductivity of aluminum, which is about six times that of lead. The higher the thermal conductivity of aluminum directs more heat toward the housing and away from the delay mixture, thus reducing the propagation rate of the pyrotechnic

4.4.4 Chromium-Free Pyrotechnic Compositions

Lead oxides and hexavalent chromium oxides are traditionally found in a host of pyrotechnic delay compositions, with barium chromate ($BaCrO_4$) and lead chromate ($PbCrO_4$) being the most common hexavalent chromium-based oxidizer used in these formulations. These oxidizers represent a "double whammy" in an environmental sense as both contain the toxic hexavalent chromium and the heavy metal hazards associated with barium and lead discussed earlier in the chapter. Therefore, successful removal of these chemicals from pyrotechnic delay mixtures would represent a significant milestone in environmental remediation technology toward the "greening" of energetic materials.

Although the full data is not publically releasable, Reimer and Mangum developed an environmentally compatible replacement for the $BaCrO_4$/B-containing T-10 delay fuze, consisting of a binary $SrMoO_4$/B pyrotechnic system [62]. They report that the $SrMoO_4$/B delay system exceeds the minimum military requirements for the T-10 item, and that use of the RAM technology [63] may further improve results by increasing the homogeneity of this pyrotechnic delay mix.

In a joint effort between the Naval Surface Warfare Center (NSWC) Indian Head Division and the South Dakota School of Mines, Rose, Bichay, and Puszynski patented non-toxic replacements for two military-related delay fuzes; the Mn/$PbCrO_4$/$BaCrO_4$ (MIL-M-21383) and the W/$BaCrO_4$/$KClO_4$/SiO_2 (MIL-T-23132) delay systems [64]. Based on thermite-based mixtures of Si/Al/Fe_3O_4, this approach has a high level of tunability since one set of chemicals is used to develop "green" replacements for multiple items.

Although a mixture of 30% Si/70% Fe_3O_4 functions well at ambient and elevated temperatures (70 °C), propagation of this mixture is problematic at cold temperatures (−65 °C), resulting in a number of misfires. Addition of a small amount of aluminum (1–7%) at the expense of silicon ensured consistent and reliable propagation of the delay mixtures at cold temperatures. Due to its high thermal conductivity and reactivity, the addition of more aluminum powder to the pyrotechnic mixture predictably results in an enhanced propagation rate. This delay system, pressed into aluminum tubes, undergoes gasless combustion, is safe to handle, has a low sensitivity to moisture, and exhibits tunable burn rates ranging from 5–20 mm/s.

Shaw and Poret report recent progress on a replacement for a variant of the M125A1 handheld signal MIL-T-23132 delay system using a ternary system of Si/Bi_2O_3/Sb_2O_3 [65]. This particular system appears to have a high degree of tunability, and consistently ignites when loaded into stainless steel or aluminum housings. The delays burn significantly longer in stainless steel housings and shorter in aluminum housings, even though aluminum has about 13 times the thermal conductivity of stainless steel. The faster burning nature of the delays encased in aluminum housings is believed to be attributed to the larger thermal diffusivity and larger thermal effusivity values of aluminum. The heat generated by the pyrotechnic reaction in aluminum tubes is transferred more rapidly down the walls of the housing, quickly affecting unburned layers of pyrotechnic material and increasing the burn rate. Since more thermal energy is confined to pyrotechnic delay mixtures encased in stainless steel housings, less energy propagates through the walls of the housing, resulting in a reduced burn rate. In improving the environmental compatibility of this formulation further, it may be advantageous to remove or replace Sb_2O_3. Sb_2O_3 has been classified as a possible human carcinogen, and antimony, like barium, is a suspected hazard to

occupational health [66]. Of course, removal or replacement of Sb_2O_3 in the aforementioned delay system would be expected to alter the burn rate.

4.5 Removal of Chlorinated Organic Compounds from Pyrotechnic Formulations

4.5.1 Chlorine-Free Illuminating Compositions

In Section 3.1, the combustion of KNO_3/B_4C to generate green light was discussed as a "green" alternative to the traditional conditions that relies on the use of barium- and chlorinated organic-containing compounds. As discussed in Section 4.4.1, the main concern with the presence of chlorinated compounds in pyrotechnic mixtures is their supposed propensity to generate PCBs, PCDDs, and PCDFs during the combustion process if organic materials are present. However, there is conflicting evidence in the literature as to the quantity of harmful chlorinated organic compounds generated during the combustion process of pyrotechnic materials [53,54]. What is not in question, however, is that if chlorine is absent from pyrotechnic mixtures, formation of PCBs, PCDDs, and PCDFs will not occur.

Traditional green-light emitting pyrotechnic mixtures are not the only colored illuminants that used chlorinated organic compounds. Red-light emitting pyrotechnic mixtures, such as those summarized in Tables 4.3 and 4.6 in Section 2.1, typically rely on a reaction between $Sr(NO_3)_2$ and a chlorinated species, such as PVC, to generate SrCl, a deep red-light emitting species. Although metastable strontium(I) hydroxide (SrOH) is known to be a red-light emitter, its "deepness" of color is not as intense as SrCl.

Though this remains a work in progress, Koch has shown that the use of strontium or chlorinated organic compounds may not be an absolute necessity toward generating an acceptable red-light emitting pyrotechnic illuminant. Koch's approach toward the development of red-light emission is focused on lithium [67]. Unlike the molecular emitter SrCl, lithium is an atomic emitter, with Li being the red-light emitting specie. Therefore, the presence of chlorine is detrimental toward the generation of lithium-based red light since LiCl is not a red-light emitter, but instead emits in the ultraviolet (UV) region.

$$LiCl_{(g)} + Al_{(g)} \rightarrow Li_{(g)} + AlCl_{(g)} \tag{4.4}$$

Koch *et al*. have reported on red-light emitting formulations (**17–20**), summarized in Table 4.19, with their dominant wavelengths and spectral purities given in Table 4.20. As observed in formulations **17–20**, the addition of aluminum to the pyrotechnic mixture effectively serves as a chlorine scavenger in the reaction (Eq. (4.4)), resulting in improved spectral purities. However, increasing amounts of Al produce more incandescent Al_2O_3 particles, leading to a downward shift in the dominant wavelength. Formulation **20** utilizes NH_4ClO_4 instead of $KClO_4$, resulting in a dramatic improvement of the spectral purity, since NH_4ClO_4 combusts to form entirely gaseous products while the combustion of $KClO_4$ leads to the formation of incandescent KOH particles that result in a deterioration of the flame purity. The dominant wavelength of formulation **20**, however, is significantly shifted to the orange-light emitting region during this process. Since chlorine is detrimental in

Table 4.19 *Koch's red-light emitting formulations based on lithium.*

Formulation **17**		Formulation **18**	
Components	Wt.- %	Components	Wt.- %
$KClO_4$	60	$KClO_4$	57.14
$Li_2C_2O_4$	25	$Li_2C_2O_4$	23.81
Dextrin	5	Al	4.76
Gummi accroides	10	Dextrin	4.76
		Gummi accroides	9.53
Formulation **19**		Formulation **20**	
Components	Wt.- %	Components	Wt.- %
$KClO_4$	54.55	NH_4ClO_4	47.62
$Li_2C_2O_4$	22.72	$Li_2C_2O_4$	19.84
Al	9.09	Al	20.63
Dextrin	4.55	Dextrin	3.97
Gummi accroides	9.09	Gummi accroides	7.94

Table 4.20 *Performance of Koch's lithium-based formulations.*

Formulation	Dominant λ [nm]	Spectral purity [%]
17	614.0	53.1
18	616.0	55.7
19	609.0	70.4
20	600.0	80.3

atomic lithium-based red flares, the use of perchlorate oxidizers is not necessary to meet the objective of a red flare based on lithium. Given the lessons learned from Koch's study, perhaps a perchlorate-free derivative of these promising formulations can be developed in the near future to meet another environmental milestone.

4.6 Environmentally Friendly Smoke Compositions

4.6.1 Environmentally Friendly Colored Smoke Compositions

A final area worthy of discussion in this chapter is the development of environmentally sustainable pyrotechnic smoke compositions. For generations, smokes have been widely used by the military for the purposes of obscuration or marking/signaling. Colored smokes in pyrotechnics can be of a multitude of colors. For example, red, green, yellow, and violet encompass the colors associated with the Army's M18 smoke grenades. Black smoke is another color commonly used in the battlefield effects simulator (BES) whose environmentally benign technologies have been described in Section 4.3.2 (see Tables 4.11 and 4.12). An example of a historically used green-colored smoke composition is provided in Table 4.21 [10].

Table 4.21 *Green-colored smoke dye composition.*

Formulation **21**	
Components	Wt %
Solvent green 3 (**J**)	40
$KClO_3$	25.4
$NaHCO_3$	24.6
S_8	10

To function reliably, colored smoke compositions are typically characterized by low ignition temperatures, and low temperatures throughout the duration of a burn. For this reason, many colored smoke mixtures based on $KClO_3/S_8$ were once commonplace due to their low ignition temperatures and low burning temperatures. Colored smoke formulations must burn in a cool manner to ensure sublimation of a smoke dye to impart the necessary color for a given smoke formulation. If a temperature is too high, the dye will decompose, resulting in poor colored smoke quality. To prevent high temperatures from being obtained in colored smoke compositions, the use of metal fuels is avoided. The chemical structures of some colored smoke dyes and smoke agents are summarized in Figure 4.5.

Significant accidents have occurred with $KClO_3/S_8$ mixtures. Unlike many oxidizers employed in pyrotechnics, $KClO_3$ undergoes exothermic decomposition. In the presence of trace amounts of acid (i.e., HCl or H_2SO_4 as found in flowers of sulfur), $KClO_3/S_8$ mixtures can ignite immediately due to the formation of metastable chloric acid and subsequent disproportionation into perchloric acid, water, and chlorine dioxide (ClO_2), a gaseous and very potent oxidizer [68]. The introduction of basic chemicals such as magnesium carbonate ($MgCO_3$) or sodium bicarbonate ($NaHCO_3$) will effectively suppress the formation of chloric acid, increasing the safety of many smoke mixtures. The aforementioned basic chemicals are deemed as "coolants" in smoke formulations. $MgCO_3$ and $NaHCO_3$ undergo endothermic decomposition, effectively minimizing the flame in a smoke mixture (Eqs. (4.5) and (4.6)). The CO_2 produced by these coolants can also aid in providing an enhanced smoke by dispersing the smoke agents and particulates during the pyrotechnic reaction.

$$MgCO_3 \rightarrow MgO + CO_2 \tag{4.5}$$

$$2\,NaHCO_3 \rightarrow Na_2CO_3 + H_2O + CO_2 \tag{4.6}$$

Although an acceptable practice in prior art smoke formulations, the presence of sulfur is now considered environmentally hazardous, as it is converted to SO_2 when burned in a pyrotechnic mixture. In the presence of atmospheric oxygen and water, SO_2 is converted to the acid rain components sulfuric acid (H_2SO_4) and sulfurous acid (H_2SO_3). US Army military personnel have also complained of a burning sensation in their lungs when breathing in the sulfur-based colored smoke clouds. Due to these environmental and human health hazards, a replacement for sulfur-based smokes is needed. Like sulfur, its fuel replacement needs to have a low ignition temperature when combined with $KClO_3$, and a low combustion energy to aid in keeping temperatures low.

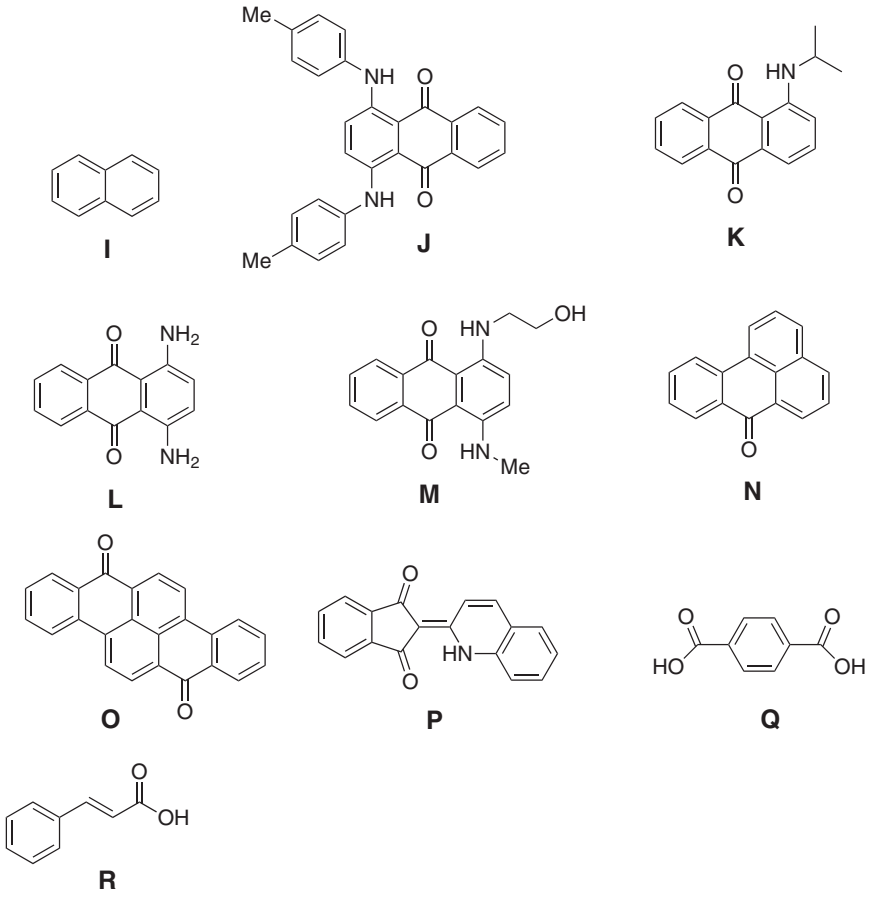

Figure 4.5 *Chemical structures of some colored smoke dyes and smoke agents in pyrotechnics.*

Many carbohydrate-based fuels have been determined to be viable replacements for sulfur in colored smoke formulations, with sucrose being a popular choice due to its low cost and low toxicity. Because of the highly oxygenated nature of sucrose, its heat output per gram is lower than organic materials that are less oxidized; an attribute which helps keep colored smoke mixtures at a cool burning temperature. To date, the US Army has reported that yellow- and green-colored M18 colored smoke grenade formulations utilizing $KClO_3$/sugar mixtures are currently being used in the field [69]. ECBC is investigating $KClO_3$/sugar mixtures as a replacement for the sulfur-containing red and violet M18 colored smokes that satisfy the color and burn time requirements (50–90 seconds) required by the US Army (Table 4.22) [70].

Red smoke formulation **22** burns for 88 seconds, and exhibits an acceptable color requirement. Addition of a small amount of violet dye **L** to the formulation is necessary to deepen the color of the smoke. In the absence of the violet dye, formulation **22** yields a light red color and thus fails the military specification.

Table 4.22 *M18 red- and violet-colored smoke formulations.*

Formulation **22**		Formulation **23**	
Components	Wt %	Components	Wt %
Sucrose (powdered 10X)	28	Sucrose (powdered 10X)	14
Solvent red 169 (**K**)	27	Sucrose (granulated)	14
$KClO_3$	21	Solvent red 169 (**K**)	15
$MgCO_3$	21	$KClO_3$	21
Solvent violet 47 (**L**)	3	$MgCO_3$	21
Nitrocellulose Binder	+2	Disperse blue 3 (**M**)	15
		Nitrocellulose Binder	+2

With a burn time of 60 seconds, and a smoke color of acceptable quality, formulation **23** has been identified to be an acceptable violet smoke. The use of granulated sucrose allows for a slower burn rate, as pyrotechnic formulations containing fuels of a larger particle size are known to burn for longer periods of time. Interestingly, the use of Solvent Violet 47, while yielding a brilliant violet smoke, results in a short burn time that fails the military specification. Employing a combination of red dye **K** and blue dye **M** to provide the purple color does afford the necessary burn time and color requirements. This result underscores the importance of dye properties in colored smoke formulations. Each colored smoke dye has a different enthalpy of sublimation that can significantly affect the behavior and performance of a colored smoke formulation. Smoke dyes with higher heats of sublimation absorb more heat than those with lower heats of sublimation, and an extended burn time is often the result.

Aside from removing sulfur from colored smoke formulations, another area of interest is the removal of some of the anthraquinone-based colored smoke dyes used. Two of these, the yellow dyes benzanthrone (**N**) and vat yellow 4 (**O**), have been identified as being carcinogenic materials. Chin and Borer state that yellow smoke containing these dyes should be considered to be among the most toxic smokes [71]. One US Army item containing these toxic dyes is the M194, a US Army yellow smoke handheld signaling device (Table 4.23). At ARDEC, Moretti reports that M194 yellow smoke signaling formulation **24** has an acceptable smoke intensity using quinoline-based solvent yellow

Table 4.23 *M194 yellow smoke handheld signal formulations.*

In-service M194		Formulation **24**	
Components	Wt %	Components	Wt %
$KClO_3$	35	$KClO_3$	29.5
Benzanthrone (**N**)	28	Sucrose	22
Vat yellow 4 (**O**)	13	Solvent yellow 33 (**P**)	32
Sucrose	20	$MgCO_3$	15.5
$NaHCO_3$	3	Stearic acid	1
VAAR	1		

33 (**P**) as the smoke dye [72]. With a burn time of 17.3 seconds, formulation **24** is within the 9–18 second range outlined in the military specification. Solvent yellow 33 is used in externally applied drugs and cosmetics, and previous research has shown that when inhaled, solvent yellow 33 is quickly removed from the lungs [73]. Interestingly, in this same toxicology study, solvent green 3 is retained in the lungs for a significant amount of time. For the sake of human health, it would be advantageous to find alternative green smoke dyes that, like solvent yellow 33, are quickly removed from the lungs upon inhalation.

4.6.2 Environmentally Friendly White Smoke Compositions

In addition to colored smoke compositions, the generation of white smoke is another area of interest for signaling and obscuration purposes. An effective way of generating white smoke is through the sublimation of sulfur by igniting fuel-rich mixtures of $KNO_3/Sb_2S_3/S_8$ [74]. However, sulfur will not undergo a "clean sublimation" in this process; toxic SO_2 vapor forms, and antimony compounds such as Sb_2S_3 have toxicity issues [66]. A more environmentally compatible way of generating white smoke is through the vaporization and recondensation of various oils and water/glycol-based mixtures in the air to create a fog. Fog machines have been deployed in battle for obscurant purposes, with the most popular choices of fog oil being SGF-2 (standard grade fuel #2) [75]. The advantage of a fog generator is that the amount of smoke generated by one of these machines is large. The disadvantages, of course, include the slow response time of these machines compared to pyrotechnic munitions that can employ smoke on demand. The limited portability of these machines is also problematic, particularly in the presence of constantly shifting winds. Fortunately, this issue can be mitigated by the use of the M56, a mechanical smoke generator system that is mounted on the M1113 high mobility multi-purpose wheeled vehicle (HMMWV) [76]. As a result, the M56 can disperse fog oil to obscure both stationary and moving targets. Despite the benefits of mechanical smoke generators like the M56, it is still advantageous that the warfighter have access to pyrotechnic white smoke compositions in order to complete the necessary tactical missions on the battlefield.

A good smoke obscurant of those in operation today is white phosphorous (WP). When kept in water, WP is quite stable and does not ignite. In fact, Koch points out that an old method of filling smoke grenades with WP was by an underwater melt-casting process [77]. As outlined in Eq. (4.7), WP readily burns when exposed to the air, first forming phosphorous pentoxide (P_4O_{10}). P_4O_{10} is a strong dessicant, which reacts with moisture in the air to form phosphoric acid (H_3PO_4) (Eq. (4.8)). H_3PO_4 is also hygroscopic and can absorb further amounts of moisture from the air. The large amounts of atmospheric water that react with WP and its combustion products make it a wonderful white smoke obscurant (and a difficult candidate to replace) for obscuration purposes. To date, the obscuring power of WP cannot be matched by any other material or formulation.

Despite its wonderful obscuration qualities, WP has the potential to cause substantial collateral damage and can also harm military personnel using the chemical for obscuration or marking purposes. Since WP is also used in incendiary munitions, its numerous combustion products can cause fires to nearby areas, and can cause severe burns upon direct exposure to human skin. Hazardous effects to the respiratory tract, mucous membranes, kidneys, liver, and heart can also result upon inhalation and oral ingestion of combustion products [78]. The quest to make an environmentally friendly smoke with the

Table 4.24 *Composition of the AN-M8 HC grenade.*

Formulation **25**	
Components	Wt %
C_2Cl_6	44.5
ZnO	46.5
Al	9

efficiency of WP is ongoing. If such a smoke could be designed that meets or exceeds the obscuration abilities of WP, it would be one of the greatest accomplishments in the history of the field of pyrotechnics.

$$P_4 + 5O_2 \rightarrow P_4O_{10} \tag{4.7}$$

$$P_4O_{10} + 6\,H_2O \rightarrow 4\,H_3PO_4 \tag{4.8}$$

The use of hexachloroethane (C_2Cl_6) as a white smoke agent for the hygroscopic chloride (HC) grenade for obscuration purposes has been a popular choice for many decades. Original HC-based smokes contained zinc metal, but these mixtures were quite sensitive to moisture and spontaneous ignition was possible. Safer HC-based compositions, such as the one outlined in Table 4.24, contain zinc oxide and aluminum [79]. Small alterations in the percentage of aluminum employed in the HC smokes have a substantial influence on the burn rate, perhaps due to its tendency to undergo a thermite-type reaction with ZnO (Eq. (4.9)). The basic chemical reaction that occurs in this HC smoke composition leads to a large production of gaseous $ZnCl_2$ (Eq. (4.10)), though small amounts of gaseous HC and $AlCl_3$ vapor are also produced, as determined by Katz and colleagues [80]. The high moisture sensitivities of $ZnCl_2$ and $AlCl_3$ allow these Lewis acids to pull moisture from the air, which further aids in smoke generation. The presence of ZnO in the composition is beneficial in whitening the smoke, as ZnO undergoes an endothermic reaction with carbon above 1000 °C to produce gaseous CO (Eq. (4.11)). Unfortunately, the high moisture sensitivities of the HC smoke-generating specie $ZnCl_2$ leads to the formation of highly corrosive zinc acid [$ZnCl_2(H_2O)_2$], $ZnCl_4$ anion, and hydrochloric acid. For this reason, the HC-based family of smokes are strong eye and respiratory irritants, can cause severe damage to military equipment, and have caused death of personnel who are in close proximity to the HC obscurant. Eaton notes that several chlorinated organic combustion products generated by HC smoke are believed to be carcinogenic [81], and Shinn has identified the HC smoke as the worst smoke in a health and environmental screening [82]. Due to the toxicity concerns associated with HC, the US Army is no longer producing these smokes for use. More benign technologies are therefore being developed in numerous laboratories to address these concerns.

$$2\,Al + 3\,ZnO \rightarrow 3\,Zn + Al_2O_3 \tag{4.9}$$

$$2\,Al + C_2Cl_6 + 3\,ZnO \rightarrow 3\,ZnCl_2 + Al_2O_3 + CO + Heat \tag{4.10}$$

$$ZnO + C \rightarrow CO + Zn \tag{4.11}$$

Table 4.25 *Krone's ammonium-based smoke formulation.*

Formulation **26**	
Components	Wt. %
NH_4ClO_4	34
ZnO	31.3
Polychloroisoprene	15
NH_4Cl	10.3
Di-octylphthalate	9.4

In an effort to address the concerns associated with the corrosive nature of HC smokes, Krone developed a series of formulations using ammonium compounds to yield zinc–ammonia complexes [83]. One representative formulation of his work is summarized in Table 4.25. The presence of ammonium chloride (NH_4Cl) effectively buffers the resulting fog, and a pH range between 5–6 is obtained. Though not environmentally hazardous at the time of the invention, it is now evident that Krone's ammonium-based smoke formulations are no longer perceived as being environmentally acceptable due to the presence of NH_4ClO_4 and di-octylphthalate plasticizer. Di-octylphthalate and other phthalate-containing plasticizers have been called into question due to concerns associated over adverse effects on the development of the reproductive system of male laboratory animals [84].

Dillehay disclosed the successful development of an HC smoke replacement consisting of a "mixed smoke cloud." This cloud combines the low toxicity of a sublimable terephthalic acid (**Q**)- or cinnamic acid (**R**)-based formulation with the high obscuration effect of a red phosphorus (RP) formulation [85]. The smoke pot consists of a center canister containing the RP-based smoke mix surrounded by a cavity containing the organic acid-based smoke mix. Upon ignition, the two smokes mix and are ejected into the atmosphere through a vent as a mixed smoke cloud. The smoke pot is designed in a way that prevents the two formulations from reacting with each other during storage of the device. Dillehay indicates that this method is effective at raising the obscuration index to 100–125% of HC smoke.

Four mixed smoke clouds have been determined as being capable of producing an obscuration index 125% of HC smoke, and these pyrotechnic smoke compositions are provided in Table 4.26. Organic acid-based formulations **27** or **28** comprise approximately 80% of the total smoke composition, and RP-based formulations **29** or **30** comprise the remaining 20% of the total smoke composition. The four mixed smoke clouds exceeding HC in obscuration performance are the result of combining formulations **27** and **29**, formulations **27** and **30**, formulations **28** and **29**, and formulations **28** and **30**. Although RP is known to produce corrosive phosphoric acid (H_3PO_4), its formation is effectively minimized by the acid scavenging metal oxides (i.e., MgO, K_2O and Na_2O) generated in the formulations to form the benign metal phosphate salts and water outlined in Eqs. (4.12)–(4.14).

Of the RP-based formulations provided in Table 4.26, formulation **30** is the preferred formulation to use in making the "mixed smoke cloud." Formulation **29** contains Viton® A, a fluoropolymer elastomer that has the potential to produce hazardous fluoride-containing

Table 4.26 *Composition of RP- and organic acid-based HC replacement formulations.*

Formulation **27**		Formulation **28**	
Components	Wt. %	Components	Wt. %
Terephthalic acid (**Q**)	50	Cinnamic acid (**R**)	45
Nitrocellulose	8	Nitrocellulose	10
Sucrose	10	Sucrose	10
$KClO_3$	27	$KClO_3$	30
$NaHCO_3$	5	$NaHCO_3$	5
Formulation **29**		Formulation **30**	
Components	Wt. %	Components	Wt. %
Red phosphorus	55	Red phosphorus	55
Pyrolusite	25	$NaNO_3$	35
Mg	15	LP/epoxy binder	5
Viton® A	5		

aerosols upon combustion [86]. Also, Mg/RP mixtures are prone to generating phosphides (i.e., Mg_3P_2), which easily hydrolyzes to give highly toxic phosphine vapor (PH_3).

$$2\,H_3PO_4 + 3\,MgO \rightarrow Mg_3(PO_4)_2 + 3\,H_2O \tag{4.12}$$

$$2\,H_3PO_4 + 3\,K_2O \rightarrow 2\,K_3PO_4 + 3\,H_2O \tag{4.13}$$

$$2\,H_3PO_4 + 3\,Na_2O \rightarrow 2\,Na_3PO_4 + 3\,H_2O \tag{4.14}$$

Another environmentally benign method of generating white smoke is the use of organic acids such as terephthalic acid (TA) as a smoke agent (**Q**). A representative TA-based smoke formulation is detailed in Table 4.27 [10]. The white smoke of this formulation is produced when the $KClO_3$/sugar pyrotechnic mixture generates enough heat to sublime TA, which then recondenses to generate smoke. Unlike HC smoke, TA smoke is not very hygroscopic, and therefore does not benefit from the ability to pull moisture from the air. TA smokes burn quite inefficiently, leaving a substantial amount of ash that does not contribute to the thickness of the smoke cloud. TA smoke formulations have shorter burn times and approximately 60% of the screening power compared to HC smoke formulations [85].

Table 4.27 *Composition of a TA smoke mixture.*

Formulation **31**	
Components	Wt %
$KClO_3$	23
Sucrose	14
Terephthalic acid (**Q**)	57
$MgCO_3$	3
Graphite	1
Nitrocellulose	2

Table 4.28 *Compositions of "Salty Dog" and "Salty Frog."*

Formulation **32**		Formulation **33**	
Components	Wt. %	Components	Wt. %
$KClO_4$	61	NaCl	30
NaCl	17	$KClO_4$	24
Mg	3	NH_4ClO_4	17
Li_2CO_3	1	Mg	6
Binder	18	Li_2CO_3	5
		Binder	18

For these reasons, the warfighter must employ multiple TA grenades to obtain the smoke output obtained with the HC grenade. Because TA smokes cannot match HC smokes in obscuration, their intended use has always been as a nontoxic HC replacement to be used on training ranges.

Another method of generating white smoke is through the sublimation of alkali metal salts. Early formulations employing this technology, such as those outlined in Table 4.28, include mixtures known as the "Salty Dog" formulation **32** and the "Salty Frog" formulation **33** [87]. Although not environmentally acceptable by today's standards, these formulations are reported to yield excellent white smoke, especially in the presence of moist atmospheres. The "Salty Frog" formulation yields a smoke of higher quality compared to the "Salty Dog" formulation due to the higher level of Li_2CO_3 in the formulation. Although Li_2CO_3 functions as a coolant, the higher lithium percentage in "Salty Frog" allows water vapor absorption to begin at a lower relative humidity. The higher magnesium levels in the "Salty Frog" formulation allow higher temperatures to be reached, resulting in smaller resultant particle sizes and a dense, stable fog.

Seven years after disclosing his ammonium-based smoke formulations (Table 4.25), Krone reported white smoke formulations suitable for training that produce calcium- and potassium-based salt aerosols [88]. When burned, the smoke formulation disclosed in Table 4.29 has a pH range of 6–9, and is also considered suitable by today's environmental standards since the metal-based combustion products from formulation **34** are macro-nutrients for plants. Sublimation of KCl is effectively achieved through the energy released when KNO_3 reacts with magnesium to yield MgO in an exothermic process. The addition of

Table 4.29 *Krone's white smoke formulation for training purposes.*

Formulation **34**	
Components	Wt. %
KCl	32
KNO_3	30
$CaCO_3$	15
Mg	15
Azodicarbonamide	8

Table 4.30 *Boron carbide-based white smoke formulation.*

Formulation **35**	
Components	Wt %
KNO_3	60
B_4C	13
KCl	25
Calcium stearate	2

azodicarbonamide is necessary to produce a continuous gas stream for better aerosol particle transport and to enhance aerosol particle yield. The gas generation prevents the slag from flowing together, thus enhancing sublimation and evaporation by means of an enlarged surface area. A more recent extension of this work is being investigated by Webb to generate various hygroscopic salts *in situ* in hopes of generating a suitable replacement for HC. His approach focuses on using mixtures of $NaClO_3$/Cellulose/$CaCO_3$/magnesium to achieve the desired smoke aerosol [89].

Work by Shaw *et al*. reports that a thick white smoke is produced when KCl undergoes sublimation in the presence of B_4C fuel and KNO_3 oxidizer (Table 4.30) [79]. This formulation also has a remarkably low sensitivity to impact (31.9 J), friction (>360 N) and electrostatic discharge (>9.4 J). The addition of a small percentage of calcium stearate is critical to minimize sparks and flames. On a mass basis, formulation **35** has a mass composition figure of merit (FOM_{mc}) of $1.80 \pm 0.05\ m^2/g$, which is comparable to HC's FOM_{mc} of $1.99 \pm 0.14\ m^2/g$. Shaw notes that the FOM_{mc} values of formulation **35** and HC are achieved in two distinct ways. As its smoke components are not very hygroscopic, formulation **35** achieves a high FOM_{mc} value from its high burning efficiency, as just 10% slag was detected. On the other hand, although half of the mass of HC smoke is not volatilized, the hygroscopic nature of $ZnCl_2$ allows moisture to be pulled from the air, thus accounting for its high obscuring potential.

Since HC smoke has a higher density ($2.43\ g/cm^3$) than formulation **35** ($1.75\ g/cm^3$), it still has the advantage of producing a more efficient smoke since many smoke munitions are volume restricted. With this being said, formulation **35** still represents a very significant achievement in the area of white smoke production, because it burns much more efficiently with a thicker smoke than TA smoke. Efforts to optimize formulation **35** to further improve obscuration may very well lead to a white smoke that can further rival or surpass the performance of HC.

4.7 Conclusions

The efforts described in this chapter detail some of the measures undertaken to "green" the area of pyrotechnics. Through the removal of perchlorates, heavy metals, suspected carcinogens, and caustic materials, the strides made in improving the environmental footprint of pyrotechnic items are significant and have the potential to benefit the public and private sectors alike. Researchers in pyrotechnic formulation development are encouraged to continue removing the materials of concern mentioned throughout this chapter.

Despite the significant progress made in the "greening" of pyrotechnics, challenges remain that need to be addressed. With many phthalates being called into question [84], removing these chemicals from pyrotechnic formulations will be a future priority. The removal of antimony from pyrotechnics is also important due to its supposed environmental and human health hazards [66]. Despite an extensive amount of research performed by the Navy, the development of a perchlorate-free, spectrally matched decoy flare remains an elusive target worthy of further investigation [26]. Passed in 2007, the European Union regulation known as Registration, Evaluation, Authorization and Restriction of Chemicals (REACH) is believed to be the strictest law to date regulating chemicals. REACH will affect industries throughout the world, and is being phased in over an 11 year period. REACH will evaluate the toxicity of combinations of chemicals, while continuing to assess and establish toxicity profiles of individual chemicals in an effort to reduce the presence of heavy metals, endocrine disruptors, and persistent organic pollutants such as PCBs, PCDD's and PCDF's [90].

Regardless of one's personal views of the regulations imposed on the field of pyrotechnics, they are here to stay, and the area of "green" pyrotechnics is not going away. Going forward, it is necessary for a scientist in the field of pyrotechnics to ask the following question: "Are the chemicals I plan to use, and is the technology I am planning to develop, environmentally friendly?" The environmental restrictions placed on in-service pyrotechnic munitions are limiting the ability of military personnel to effectively carry out their missions. With regulations seeming to evolve every year, the military personnel that rely on such items to sustain combat readiness and to stay alive on the battlefield have the most to lose if the environmental challenges are not met. It is therefore imperative that potential environmental hazards are identified early, and that environmentally benign technologies are identified and addressed before the new environmental regulations take effect.

Acknowledgments

Having the opportunity to write a chapter on "green" pyrotechnics is an honor, but would not have been possible if not for the support I received in carrying out my research programs in the area of environmentally friendly pyrotechnics. The invitation by Prof. Dr. Tore Brinck (KTH Royal Institute/Sweden) to submit this chapter is gratefully acknowledged. I thank Mrs. Rebecca Ralf, assistant editor at Wiley-Blackwell, for her hard work, cooperation, and support in publishing this chapter and book.

I thank my division chief, Mr. James L. Wejsa (ARDEC/USA) and my branch chief, Mr. Thomas J. Carney III (ARDEC/USA) for their constant support and encouragement to conduct cutting-edge research in this fascinating area of pyrotechnics. I am very grateful to Dr. Ernst-Christian Koch (MSIAC-NATO/Belgium) for his review of this chapter, and for his many helpful suggestions and comments concerning its contents. I am indebted to Prof. Dr. Thomas M. Klapötke (LMU Munich/Germany) for many insightful discussions and for his willingness to provide me with references on demand; many of which have been discussed in this chapter.

I appreciate the efforts of Mr. Erik B. Hangeland (RDECOM/USA), Mrs. Kimberly Watts (RDECOM/USA), and Mr. Noah Lieb (Hughes Associates/USA) for their financial support

and profound interest in environmental initiatives in pyrotechnics research as part of the Environmental Quality Technology Program. I wish to thank Dr. Robin A. Nissan (SERDP-ESTCP/USA) and those on the SERDP/ESTCP panel for their continued financial support and his interest in environmental programs pertaining to weapons systems and platforms.

In no particular order, I would like to extend my thanks to the following individuals for their helpful advice and/or experimental assistance that has helped me in writing this chapter.

Mr. Gary Chen (ARDEC/USA), Dr. Jared D. Moretti (ARDEC/USA), Dr. Anthony P. Shaw (ARDEC/USA), Dr. Jay C. Poret (ARDEC/USA), Dr. Reddy Damavarapu (ARDEC/USA), Mr. Eric A. Latalladi (ARDEC/USA); Mr. Stephen C. Taggart (ARDEC/USA); Dr. David E. Chavez (LANL/USA), Mr. Joseph A. Domanico (ECBC/USA); Mr. William H. Ruppert (ARL/USA); Dr. Mark S. Johnson (MEDCOM/USA); Dr. William S. Eck (MEDCOM/USA); Dr. Steven F. Son (Purdue University/USA); Mr. Rutger Webb (Clearspark/Netherlands).

Finally, I want to express a special thanks to Dr. Sara K. Pliskin (NSWC/USA) and Dr. Gregory D. Knowlton (Pyrogetics/USA) for their encouragement and invitation to become involved in the International Pyrotechnics Society. The advice they have given me and the many technical discussions that I have had with them pertaining to the field of pyrotechnics has been invaluable to my professional development.

Abbreviations

Al	Aluminum
AlCl	Aluminum monochloride
$AlCl_3$	Aluminum trichloride
Al_2O_3	Aluminum oxide
ARDEC	Armament Research, Development & Engineering Center
B	Amorphous boron
B_4C	Boron carbide
BaBT4w	Barium 5,5′-bis-1*H*-tetrazole tetrahydrate
BaCl	Barium(I) chloride
$BaCrO_4$	Barium chromate
$Ba(NO_3)_2$	Barium nitrate
BaO	Barium oxide
BaOH	Barium(I) hydroxide
BES	Battlefield Effects Simulator
Bi_2O_3	Bismuth oxide
BO_2	Boron oxide
BT	5,5′-Bis-1*H*-tetrazole
BTAw	Bis-(1(2)*H*-tetrazol-5-yl) amine monohydrate
C_2Cl_6	Hexachlorethane
$CaCO_3$	Calcium carbonate
Cd	Candela
ClO_2	Chlorine dioxide
cm	centimeter

Cu	Copper
CuBTA2w	Copper bis-(1(2)H-tetrazol-5-yl) amine dehydrate
CuO	Copper oxide
CuCl	Copper(I) chloride
CuOH	Copper(I) hydroxide
CuS	Copper sulfide
dB	decibel
DHT	Dihydrazino tetrazine
DP	Dechlorane plus
ECBC	Edgewood Chemical & Biological Center
EPA	Environmental Protection Agency
ESD	Electrostatic discharge
Fe_2O_3	Red iron oxide
Fe_3O_4	Black iron oxide
FOM_{mc}	Mass consumption figure of merit
ft.	feet
g	gram
Gran	Granulation
H_3PO_4	Phosphoric acid
H_2SO_3	Sulfurous acid
H_2SO_4	Sulfuric acid
HC	Hygroscopic chloride
HCl	Hydrochloric acid
K_2O	Potassium oxide
KCl	Potassium chloride
$KClO_3$	Potassium chlorate
$KClO_4$	Potassium perchlorate
KIO_4	Potassium periodate
KNO_3	Potassium nitrate
KOH	Potassium hydroxide
K_3PO_4	Potassium phosphate
LANL	Los Alamos National Laboratories
$Li_2C_2O_4$	Lithium oxalate
LiCl	Lithium chloride
Li_2CO_3	Lithium carbonate
Mg	Magnesium
$MgCO_3$	Magnesium carbonate
MgO	Magnesium oxide
$Mg_3(PO_4)_2$	Magnesium phosphate
mm	millimeter
Mn	Manganese
MoO_3	Molybdenum trioxide
$Na_2C_2O_4$	Sodium oxalate
NaCl	Sodium chloride
$NaClO_3$	Sodium chlorate
Na_2O	Sodium oxide

$NaHCO_3$	Sodium bicarbonate
$NaIO_4$	Sodium periodate
$NaNO_3$	Sodium nitrate
Na_3PO_4	Sodium phosphate
NH_4Cl	Ammonium chloride
NH_4NO_3	Ammonium nitrate
NH_4ClO_4	Ammonium perchlorate
nm	Nanometer
NSWC	Naval Surface Warfare Center
P_4O_{10}	Phosphorous pentoxide
Pb_3O_4	Red lead
$PbCrO_4$	Lead chromate
PCBs	Polychlorinated biphenyls
PCDDs	Polychlorinated dibenzodioxins
PCDFs	Polychlorinated dibenzofurans
PVC	Poly(vinyl chloride)
RP	Red phosphorous
s	Second
S_8	Sulfur
Sb_2O_3	Antimony oxide
Sb_6O_{13}	Antimony hexitatridecoxide
Sb_2S_3	Antimony sulfide
Si	Silicon
SiO_2	Silicon dioxide
SO_2	Sulfur dioxide
SrCl	Strontium(I) chloride
$SrMoO_4$	Strontium molybdate
$Sr(NO_3)_2$	Strontium nitrate
SrOH	Strontium(I) hydroxide
SrBT4w	Strontium 5,5′-bis-1H-tetrazole tetrahydrate
TA	Terephthalic acid
Ti	Titanium
VAAR	Vinyl alcohol acetate resin
W	Tungsten
WP	White phosphorous
λ	Wavelength
$ZnCl_2$	Zinc chloride
$[ZnCl_2(H_2O)_2]$	Zinc chloride dihydrate
ZnO	Zinc oxide

References

1. Strategic Environmental Research and Development Program (SERDP) (2013) http://www.serdp.org/About-SERDP-and-ESTCP/About-SERDP (last accessed in 2013).
2. Environmental Security Technology Certification Program (ESTCP) (2013) http://www.serdp.org/About-SERDP-and-ESTCP/About-ESTCP (last accessed in 2013).

3. Douda, B.E. (1967) Pyrotechnic Compound Tris(Glycine) Strontium(II) Perchlorate and Method for Making Same, Patent Number US 3,296,045.
4. Douda, B.E. (1969) Colored Flare Ingredient Synthesis Program, DTIC Report, Accession Number 447410.
5. Chavez, D.E. and Hiskey, M.A. (1998) High-nitrogen pyrotechnic compositions. *Journal of Pyrotechnics*, **7**, 11–14.
6. Chavez, D.E., Hiskey, M.A., and Naud, D.L. (1999) High-nitrogen fuels for low-smoke pyrotechnics. *Journal of Pyrotechnics*, **10**, 17–36.
7. Steinhauser, G. and Klapötke, T.M. (2008) Green pyrotechnics: a chemists' challenge. *Angewandte Chemie International Edition*, **47** (18), 3330–3347.
8. Douda, B.E. (1964) Theory of Colored Flame Production, DTIC Report, Accession Number 951815.
9. Sellers, K., Weeks, K., Alsop, W. *et al*. (2007) *Perchlorate Environmental Problems and Solutions*, CRC Press – Taylor & Francis Group, Boca Raton, FL.
10. Conkling, J.A. and Mocella, C.J. (2011) *Chemistry of Pyrotechnics: Basic Principles and Theory*, 2nd edn, Taylor & Francis Group, Boca Raton, FL.
11. US Environmental Protection Agency (2008) Interim Drinking Water Health Advisory for Perchlorate, 1–35: http://www.epa.gov/safewater/contaminants/unregulated/pdfs/healthadvisory_perchlorate_interim.pdf.
12. Office of Environmental Health Hazard Assessment (2004) Public Health Goals for Chemicals in Drinking Water, 1–106, http://oehha.ca.gov/water/phg/pdf/finalperchlorate31204.pdf.
13. Massachusetts Department of Environmental Protection (2008) Potential Environmental Contamination From the Use of Perchlorate-Containing Explosive Products, http://www.mass.gov/dep/cleanup/.
14. Wilkin, R.T., Fine, D.D., and Burnett, N.G. (2007) Perchlorate behavior in a municipal lake following fireworks displays. *Environmental Science & Technology*, **41** (11), 3966–3971.
15. Sabatini, J.J., Nagori, A.V., Chen, G. *et al*. (2012) High-nitrogen-based pyrotechnics: longer- and brighter burning, perchlorate-free, red-light illuminants for military and civilian applications. *Chemistry-A European Journal*, **18** (2), 628–631.
16. Sabatini, J.J., Raab, J.M., Hann, R.K. *et al*. (2012) High-Nitrogen-based pyrotechnics: development of perchlorate-free green-light illuminants for military and civilian applications. *Chemistry-An Asian Journal*, **7** (7), 1657–1663.
17. Damavarapu, R., Klapötke, T.M., Stierstorfer, J., Tarantik, K.R. (2010) Barium salts of tetrazole derivative – synthesis and characterization. *Propellants, Explosives, Pyrotechnics*, **35** (4), 395–406.
18. Dillehay, D. (2004) Illuminants and illuminant research, in *Pyrotechnic Reference Series, No. 4, Pyrotechnic Chemistry* (eds K. Kosanke, B.J. Kosanke, I.vonMaltitz, B. Sturman, T. Shimizu, M.A. Wilson, N. Kubota, C. Jennings-White, and D. Chapman), Journal of Pyrotechnics, Whitewater, CO, USA, pp. 1–8.
19. Jia, H., Sun, Y., Liu, X. *et al*. (2011) Concentration and bioaccumulation of dechlorane compounds in coastal environment of Northern China. *Environmental Science & Technology*, **45** (7), 2613–2618;
20. Hoh, E., Zhu, L. and Hites, R.A. (2006) Dechlorane plus, a chlorinated flame retardant, in the Great Lakes. *Environmental Science & Technology*, **40** (4), 1184–1189.
21. Biermann, C.J. (1993) *Essentials of Pulping and Papermaking*, Academic Press, Inc., San Diego, CA.
22. Erickson, B. (2011) Formaldehyde, styrene cancer warning. *Chemical and Engineering News*, **89** (25), 11.
23. Shortridge, R.G. and Yamamoto, C.M. (2009) Perchlorate-Free Red Signal Flare Composition, Publication Number US 2009/0320977 A1.

24. Shortridge, R.G. and Yamamoto, C.M. (2011) Perchlorate-Free Green Signal Flare Composition, Patent Number US 7,988,801 B2.
25. Yamamoto, C.M. and Shortridge, R.G. (2009) Perchlorate-Free Yellow Signal Flare Composition, Publication Number US 2009/0320976 A1.
26. Shortridge, R.G., Wilharm, C.K., and Yamamoto, C.M. (2007) Elimination of Perchlorate Oxidizers from Pyrotechnic Flare Compositions, SERDP Project–WP 1280, 1–52.
27. NASA Glenn Research Center, NASA Computer program CEA (Chemical Equilibrium with Applications) (Webpage last updated March 2010) http://www.grc.nasa.gov/WWW/CEAWeb/ceaHome.htm (last accessed in 2013).
28. Sturman, B.T. (2006) On the emitter of blue light in copper-containing pyrotechnic flames. *Propellants, Explosives, Pyrotechnics*, **31** (1), 70–74.
29. Poret, J.C. and Sabatini, J.J. (2013) Comparison of barium and amorphous boron pyrotechnics for green light emission. *Journal of Energetic Materials*, **31** (1), 27–34.
30. Newell, R.H., Liu, L.S., Blau, R.J. *et al*. (2008) Nonlethal 40 mm Flash-Bang Devices with Fuel-Rich Flash Powders, in Proceedings of the 35th International Pyrotechnic Seminars, Fort Collins, CO, USA, pp. 253–258.
31. Chen, G., Motyka, M., and Wejsa, J. (2006) Perchlorate Free Pyrotechnic Composition and its Application in M115A2 Ground Burst Simulator and M116A1 Hand Grenade Simulator, Proceedings of the 33rd International Pyrotechnic Seminars, Fort Collins, CO, USA, pp. 269–279.
32. Chen, G. (2009) Perchlorate Elimination in M274 2.75″ Practice Rocket Warhead Smoke Charge, Proceedings of the 36th International Pyrotechnic Seminars, Rotterdam, The Netherlands, 427–437.
33. Raibeck, G., Kislowski, C. and Chen, G. (2008) Demonstration of an Environmentally Benign Pyrotechnic Black Smoke in a Battlefield Effects Simulator, Proceedings of the 35th International Pyrotechnic Seminars, Fort Collins, CO, USA, pp. 95–102;
34. Chen, G., Showalter, S., Raibeck, G., and Wejsa, J. (2006) Environmentally Benign Battlefield Effects Black Smoke Simulator, DTIC Report, Accession Number 481520.
35. Lide, D.R. (2004) *CRC Handbook of Chemistry and Physics*, 85th edn, (2004–2005), CRC Press, Boca Raton.
36. The US Army Military Command (2007) http://aec.army.mil/usaec/newsroom/awards07/rdecom.pdf (last accessed in 2008).
37. Cegiel, D., Strenger, J., and Zimmermann, C. (2012) Perchlorate-Free Pyrotechnic Mixture, Publication Number US020120132328A1.
38. US Environmental Protection Agency, Technology Transfer Network: Air Toxics Web Site, Napthalene Hazard Summary - created in April 1992; revised in January 2000: http://www.epa.gov/ttn/atw/hlthef/naphthal.html (last accessed in 2013).
39. Reeves, A.L. (1979) *Handbook on the Toxicology of Metals*, Elsevier/North Holland Biomedical Press, New York, NY.
40. US Environmental Protection Agency, Air Trends 1995 Summary: Lead (Pb) (Last updated January 2012) http://www.epa.gov/airtrends/aqtrnd95/pb.html (last accessed in 2013).
41. US Environmental Protection Agency, Chromium in Drinking Water (Last updated April 2012) http://water.epa.gov/drink/info/chromium/index.cfm (last accessed in 2012).
42. Johansen, B.E. (2003) *The Dirty Dozen: Toxic Chemicals and the Earth's Future*, Praeger Publishers – Greenwood Publishing Group, Westport, CT.
43. Koch, E.-C., Weiser, V., Roth, E. *et al*. (2012) Combustion of ytterbium metal. *Propellants, Explosives, Pyrotechnics*, **37** (1), 9–11.
44. Koch, E.-C., Weiser, V., Roth, E. *et al*. (2012) Metal fluorocarbon pyrolants. XV: combustion of two ytterbium-halocarbon formulations. *Journal of Pyrotechnics*, **31**, 3–9.
45. Steinhauser, J., Tarantik, K., and Klapötke, T.M. (2008) Copper in pyrotechnics. *Journal of Pyrotechnics*, **27**, 3–13.

46. Klapötke, T.M., Radies, H., Stierstorfer, J. *et al*. (2010) Coloring properties of various high-nitrogen compounds in pyrotechnic compositions. *Propellants, Explosives, Pyrotechnics*, **35** (3), 313–319.
47. Eppig, H.J. (1945) The Chemical Composition of German Colored Signal Lights, CIOS Report, pp. 32–39.
48. Klapötke, T.M., Rusan, M.A., and Stierstorfer, J. (2012) The Synthesis and Investigation of Nitrogen-rich and Boron-based Compounds as Coloring Agents in Pyrotechnics, Proceedings of the 38th International Pyrotechnic Seminars, Denver, CO, 527–550.
49. Sabatini, J.J., Poret, J.C., and Broad, R.N. (2011) Boron carbide as a barium-free green light emitter and burn rate modifier in pyrotechnics. *Angewandte Chemie International Edition*, **50** (20), 4264–4266.
50. Natan, B. and Netzer, D.W. (1996) Boron carbide combustion in solid-fuel ramjets using bypass air. Part I: Experimental investigation. *Propellants, Explosives, Pyrotechnics*, **21** (6), 289–294.
51. Lane, G.A., Smith, W.A., and Jankowiak, E.M. (1968) Novel pyrotechnic compositions for screening smokes, Proceedings of the 1st International Pyrotechnic Seminars, Estes Park, CO, 263–292.
52. Katami, T., Yasuhara, A., Okuda, T., and Shibamoto, T. (2002) Formation of PCDDs, PCDFs, and coplanar PCBs from polyvinyl chloride during combustion in an incinerator. *Environmental Science & Technology*, **36** (6), 1320–1324.
53. Fleischer, O., Wichmann, H., and Lorenz, W. (1999) Release of polychlorinated dibenzo-p-dioxins and dibenzofurans by setting off fireworks. *Chemosphere*, **39** (6), 925–932.
54. Dyke, D. and Coleman, P. (1995) Dioxins in ambient air, bonfire night 1994. *Organohalogen Compounds*, **24**, 213–216.
55. Griffiths, T.T. (2009) Alternative for Perchlorates in Incendiary and Pyrotechnic Formulations for Projectiles, SERDP Project–WP 1424, 1–160.
56. Moretti, J.D., Sabatini, J.J., and Chen, G. (2012) Periodate salts as pyrotechnic oxidizers: development of barium- and perchlorate-free incendiary formulations. *Angewandte Chemie International Edition*, **51** (8), 6981–6983.
57. Cotton, F.A., Wilkinson, G., Murillo, C.A., and Bochmann, M. (1999) *Advanced Inorganic Chemistry*, 6th edn, Wiley, New York, NY, p. 570.
58. Tracy, G.V. (2002) High Energy, Lead-Free Ignition Formulation for Thermate, DTIC Report, Accession Number 400193.
59. Horning, J. and Chen, G. (2008) Product Improvements on the Thermate Incendiary Grenade, in Proceedings of the 35th International Pyrotechnic Seminars, Fort Collins, CO, pp. 259–267.
60. Son, S.F., Hiskey, M.A., Naud, D. *et al*. (2002) Lead-Free Electric Matches, http://library.lanl.gov/cgi-bin/getfile?00852315.pdf871–877.
61. Kalombo, L., DelFabbro, O., Conradie, C., and Focke, W.W. (2007) Sb6O13, Bi_2O_3 as oxidants for Si in pyrotechnic time delay compositions. *Propellants, Explosives, Pyrotechnics*, **32** (6), 454–460.
62. Reimer, K. and Mangum, M. (2012) New "Green" Pyrotechnic Time Delays with Strontium Molybdate, JANNAF 59th Propulsion Meeting, 41st Structures and Mechanical Behavior/37th Propellant and Explosives Development and Characterization/28th Rocket Nozzle Technology/26th Safety and Environmental Protection Joint Subcommittee Meeting, San Antonio, TX; paper is only accessible to US nationals but the work is listed as "distribution A (unlimited)."
63. Resodyn Corporation, Resonant Acoustic Mixers, Inc. (RAM) (2011–2013) http://resodyn.com/pages/29/Resodyn-Acoustic-Mixers.html (last accessed in 2013).
64. Rose, J.E., Bichay, M., and Puszynski, J. (2011) Non-Toxic Pyrotechnic Delay Compositions, Patent Number US 7,883,593 B1.
65. Poret, J.C., Shaw, A.P., Groven, L.J. *et al*. (2012) Environmentally Benign Pyrotechnic Delays, Proceedings of the 38th International Pyrotechnic Seminars, Denver, CO, pp. 494–500.

66. Sundar, S. and Chakravarty, J. (2010) Antimony toxicity. *International Journal of Environmental Research and Public Health*, **7** (12), 4267–4277.
67. Koch, E.-C. and Jennings-White, C. (2009) Is it Possible to Obtain a Deep Red Pyrotechnic Flame Based on Lithium?, Proceedings of the 36th International Pyrotechnic Seminars, Rotterdam, The Netherlands, 205–110.
68. Ellern, H. (1968) *Military and Civilian Pyrotechnics*, New York, NY, Chemical Publishing Group.
69. The US Army Military Command (2005) http://aec.army.mil/usaec/newsroom/update/sum05/sum0517.html (last accessed in 2005).
70. Diviacchi, G. (2008) Evaluation of Candidate Low Toxicity Colored Smoke Dyes, Proceedings of the 35th International Pyrotechnic Seminars, Fort Collins, CO, pp. 491–497.
71. Chin, A. and Borer, L. (1983) Identification of combustion products from colored smokes containing organic dyes. *Propellants, Explosives, Pyrotechnics*, **8** (4), 112–118.
72. Moretti, J.D., Sabatini, J.J., Shaw, A.P., and Chen, G. (2012) Environmentally Sustainable Yellow Smoke Formulations for Use in the M194 Hand Held Signal, Proceedings of the 38th International Pyrotechnic Seminars, Denver, CO, pp. 445–456.
73. Subcommittee on Military Smokes and Obscurants, National Research Council (1999) *Toxicity of Military Smokes and Obscurants Volume 3*, The National Academies Press, Washington, DC.
74. American Chemical Society (2012) ACS Webinars: http://acswebinars.org/wp-content/uploads/2012/04/Mocella-ACS-Webinar-2-Advanced-Pyrotechnics-June-2012.pdf (last accessed in 2012).
75. Haehnel, R.B. (2008) Simulation of Fog Oil Deposition During Military Training Operations, DTIC Report, Accession Number 491391.
76. http://www.sunshine-project.org/incapacitants/jnlwdpdf/smoke_m56_coyote.pdf (last accessed in 2001).
77. Koch, E.—C. (2008) Special materials in pyrotechnics: V. Military applications of phosphorus and its compounds. *Propellants, Explosives, Pyrotechnics*, **33** (3), 165–176.
78. Agency for Toxic Substances and Disease Registry (ATSDR) (1997) Toxicological Profile for White Phosphorous – Chapter 2: Health Effects: http://www.atsdr.cdc.gov/toxprofiles/tp103.pdf (last accessed in 2013).
79. Shaw, A.P., Poret, J.C., Gilbert, R.A. *et al*. (2012) Pyrotechnic Smoke Compositions Containing Boron Carbide, Proceedings of the 38th International Pyrotechnic Seminars, Denver, CO, pp. 569–582.
80. Katz, S., Snelson, A., Farlow, R. *et al*. (1980) Physical and Chemical Characterization of Hexachloroethane Smoke, DTIC Report, Accession Number 08936.
81. Eaton, J.C., Lopinto, R.J., and Palmer, W.G. (1994) Health Effects of Hexachloroethane (HC) Smoke, DTIC Report, Accession Number 277838.
82. Shinn, J.H. (1987) Smokes and Obscurants: A Guidebook of Environmental Assessment. Volume I. Method of Assessment and Appended Data, DTIC Report, Accession Number 203810.
83. Krone, U. and Moeller, K. (1983) Smoke Composition, Patent Number 4,376,001.
84. https://acc.dau.mil/adl/en-US/503526/file/63081/Risk%20Alert%20for%20Phthalates%20March%202012.pdf (last accessed in 2012).
85. Dillehay, D.R. (1996) Low Toxicity Obscuring Smoke Formulation, Patent Number 5,522,320.
86. Koch, E.—C. *Metal-Fluorocarbon-Based Energetic Materials*, Wiley, Weinheim, Germany, pp. 326–332.
87. Blomerth, E.A. (1974) Project Foggy Cloud 1, DTIC Report, Accession Number 874515.
88. Krone, U. (1990) Pyrotechnics Mixture for Producing a Smoke Screen, Patent Number 4,986,365.
89. Webb, R. (2011) Update on Development of Low-Toxicity Obscurant Material, Partners in Environmental Technology Technical Symposium & Workshop, Washington D.C.
90. http://ec.europa.eu/environment/chemicals/reach/reach_intro.htm (last accessed in 2012).

5

Green Primary Explosives

Karl D. Oyler

U.S. Army Armament Research, Development and Engineering Center (ARDEC)
Picatinny Arsenal, USA

5.1 Introduction

If the study of energetic materials is considered a niche field in the broad scope of chemical and engineering research, primary explosives themselves can be considered a niche within a niche. It's also a relatively static field; only a handful of organizations are involved in the development of new primary explosives, and the technology and materials that are most often used have changed very little since the 1960s. Annual requirements and production totals for primaries as a whole are also dwarfed by several orders of magnitude compared to explosive mainstays like RDX (1,3,5-trinitro-1,3,5-triazacyclohexane) and HMX (1,3,5,7-tetranitro-1,3,5,7-tetraazacyclooctane), but despite the apparent scarcity of primary explosives, these materials are ubiquitous and found (at least in small amounts) in a huge number of military and commercial munitions. Whether it's the lead azide-based detonator in a 40 mm mortar round or commercial blasting cap, or the lead styphnate in the primers of 5.56 mm small arms ammunition, primary explosives are vital to any military's portfolio and essential to the construction and mining industries. As such, the toxicity associated with the largely lead-based primary explosives can take a serious toll on the environment and any populations that are in close proximity to areas where explosives are set off or firearms are employed [1]. This impact is certainly not limited to soldiers on the battlefield; firing ranges, ammunition and explosives workers, miners, and construction workers are also placed at risk. For these reasons and others, a major current focus in the energetics community is the development of lead-free, environmentally acceptable alternatives to the current toxic primary explosive materials.

Green Energetic Materials, First Edition. Edited by Tore Brinck.

5.1.1 What is a Primary Explosive?

Primaries are generically defined as explosives that can be initiated through the addition of a relatively small stimulus, be it impact, friction, shock, heat, or electrostatic discharge [2]. On the whole, they tend to be less potent than the more powerful and more stable secondary explosives such as RDX; instead of causing destruction, the main purpose of a primary explosive is generally to trigger these harder to initiate energetics. One of the most important characteristics of an effective primary explosive is an extremely swift deflagration to detonation transition (DDT), meaning that once the material is initiated it quickly proceeds from a rapid combustion to a detonation (e.g., the reaction front becomes supersonic). This is a key feature because it allows the primary explosive charge (whether in a detonator, primer, or other initiator) to be kept small, an important aspect to safety and handling. From a chemical structure point of view, primary explosives tend to contain highly sensitive chemical functional groups as triggers that lead to rapid molecular decomposition; these groups include azido- (N_3), diazo- (N_2), fulminate (-NCO), furoxans, and tetrazoles [3].

Although several compounds are employed as primary explosives in commercial and military applications throughout the world, currently the most popular are lead azide and lead styphnate (both normal and basic forms), and tetrazene. With its high explosive performance, lead azide is most often implemented as the main primary explosive fill in detonators and blasting caps. Lead styphnate, on the other hand, is mainly found in primers, where a more gentle touch is required to smoothly initiate a propellant without inadvertently shattering a gun barrel. Another relatively common primary explosive is tetrazene[1] (1-(5-tetrazolyl)-3-guanyltetrazene hydrate); although relatively weak, its high sensitivity is needed to assist in the initiation of both lead azide and lead styphnate to make them reliable for use in their applications (see Table 5.1).

The first primary explosive to see widespread, practical use was mercury(II) fulminate ($Hg(CNO)_2$), adopted by Alfred Nobel for use in some of the first commercial blasting caps in 1867 (although Johann Kunckel von Löwenstern, better known for discovering phosphorus, first synthesized the compound in the 1600s) [2]. Lead azide began to replace the even more toxic mercury explosive in the early twentieth century [5], although the reasons at the time were more for cost and performance-related concerns than health or the environment: mercury fulminate was more sensitive, tended to dead-press (lost performance under higher loading pressures), and its base-metal, mercury, was more expensive and harder to obtain than lead [2]. Around the same time period, Herz reported the synthesis of normal

Table 5.1 *Basic explosive properties of lead azide and lead styphnate [4].*

Material	Impact (J)	Friction (N)	ESD (mJ)	Density (g/cc)	DSC (°C)	VOD (m/s)
Lead azide (RD1333)	0.089	<1	5.0	4.80	315	5500
Lead styphnate (basic)	0.025	<1	0.2	3.00	282	5200

[1] Numerous old references refer to this compound as "tetracene," which can lead to confusion with the completely unrelated tetracyclic aromatic compound of the same spelling.

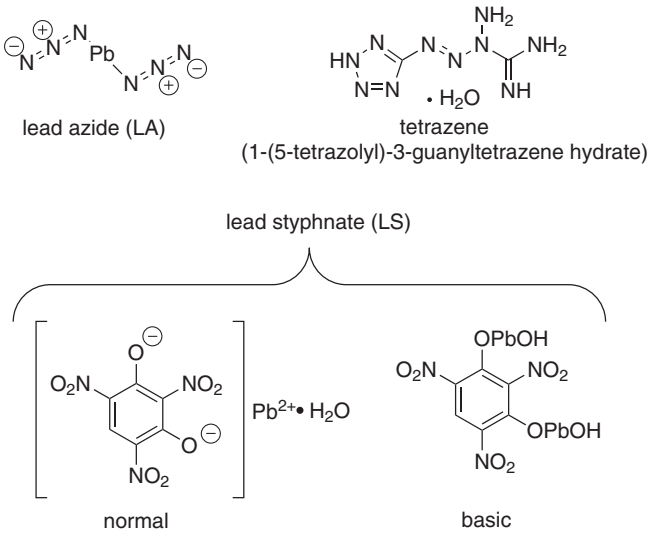

Figure 5.1 *Current common primary explosives.*

lead styphnate (lead(II) 2,4,6-trinitroresorcinate, Figure 5.1) [6], which was eventually implemented into detonator initiating mixes as well as primers. Basic lead styphnate (Figure 5.1) was also developed for similar uses. From the 1950s on, a handful of other primary explosives, such as silver azide, mercury(II) 5-nitrotetrazole (DXN-1/DXW-1), diazodinitrophenol (DDNP), lead monoresorcinate (LMNR), and potassium dinitrobenzofuroxan (KDNBF), were implemented in smaller applications.

5.1.1.1 Common Initiating Devices: Detonators/Primers/Blasting Caps

Primary explosives are typically incorporated into some sort of initiating device, depending on the application. Most often these include blasting caps, detonators, and primers, which generally consist of one or more explosive powder charges loaded into a metallic cup through mechanical pressing.

Detonators are useful for high explosive applications where a strong shockwave is needed to set off a secondary explosive charge or other energetic; they are frequently incorporated as parts of a larger fuze apparatus that may also include additional pyrotechnic delays and/or booster charges. As such, detonators are essential for a huge number of explosive munitions including grenades, mortars, rockets, artillery rounds, submunitions, and so on. The two main types of detonators are stab and electric. A stab detonator (Figure 5.2), such as the US Army M55 and M61 is designed to function by the mechanical impact of a firing pin, whereas electric detonators such as the M100 are triggered by electric impulse. The stab detonator almost always consists of three separate charges loaded into an aluminum or steel cup. The initiation charge (also called the stab mix) is typically a formulation such as NOL-130[2], which is intended to be very sensitive

[2] NOL is short for the Naval Ordnance Laboratory.

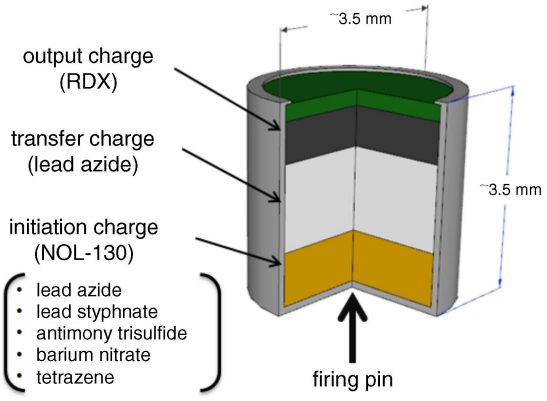

Figure 5.2 *A common stab detonator configuration.*

to impact and friction. It contains both lead azide and lead styphnate as well as tetrazene for added sensitivity; a pyrotechnic fuel/oxidizer combination of antimony trisulfide and barium nitrate is also used for its extra energy output as well as to provide an abrasive for added friction sensitivity. The initiation charge is followed by a transfer charge of RD1333 lead azide, which in turn is intended to set off an output charge consisting of a secondary explosive such as RDX or HMX. Electric detonators are configured similarly, but in place of the initiation charge they are usually set off by an electric bridgewire affixed with a small spot charge of lead styphnate.

Blasting caps come in a variety of types, but in general are similar in design to detonators. The main difference comes in that they tend to be larger and are normally electric. Instead of being incorporated into a fuze, they are standalone and most often used for directly initiating secondary energetics, such as plastic explosives used in demolition charges. The caps themselves most typically employ dextrinated lead azide (DLA) as the main primary explosive material, although diazodinitrophenol (DDNP) is frequently used also.

Primers are now largely used as the initiators in ammunition cartridges, both commercial and military. Typically, they are either percussion or electric. Percussion primers are by far the most common, and come in a variety of sizes and configurations depending on the ammunition size and requirements. They function through the impact of the firing pin on the primer, which pinches the primary explosive-containing primer formulation between the outer cup and a small metal anvil. From there, the hot gases and molten slag produced go on to initiate the propellant bed, which rapidly deflagrates and ejects the bullet from the cartridge at a high rate of speed. The primer formulation itself is generally very similar to those used in the detonator stab mixes described above; the main component is most often lead styphnate for military primers, along with other pyrotechnic additives. A common example is PA101, which contains basic lead styphnate, antimony trisulfide, barium nitrate, aluminum powder, and tetrazene (Table 5.2). Commercial green primers often contain lead-free primary explosives, such as DDNP or KDNBF, which will be discussed in more detail later. In contrast to detonators and blasting caps, the primer is usually not intended to generate a strong shock wave, but instead to produce large amounts of slag-generating heat, which is used to ignite the propellant bed without shattering the casing.

Table 5.2 *Weight percentages of components in common initiating mixes [7].*

Constituents	NOL-130	NOL-60	PA-101	FA-956
Lead azide	20			
Basic lead styphnate	40	60	53	
Normal lead styphnate				37
Barium nitrate	20	25	22	32
Tetrazene	5	5	5	4
Antimony trisulfide	15	10	10	15
PETN				7
Aluminum powder			10	

5.1.2 The Case for Green Primary Explosives

As lead azide and lead styphnate account for the vast majority of commercial and military primary explosive use, the largest environmental issue associated with primaries is their heavy metal lead content. From the time of their development through the 1960s, these materials were not thought to be major health dangers (except when exploding of course); as the venerable Picatinny Arsenal *Encyclopedia of Explosives and Related Items* stated in 1960 [8]: "LA [leadazide] is not considered particularly toxic but inhalation of its dust should be avoided as this causes headaches and distention of blood vessels." Considerable research over the last 50 years has certainly revised this assessment, and serious attention has been given to the connection between chronic, relatively low-level lead exposure and human health [9,10]. Lead is now known to drastically affect the central nervous system, the renal system, and the blood; children and unborn fetuses are particularly vulnerable in these areas, as sufficiently high doses can lead to mental impairment and behavioral issues, kidney damage, and anemia [9]. These effects are somewhat mitigated in adults, but still present significant dangers.

Because of its pronounced toxicity, lead has become one of the most highly regulated chemical substances internationally. In the USA, lead is classified as a toxic pollutant under both the Clean Air Act (CAA) of 1963 and the Clean Water Act (CWA) of 1972, and falls under Executive Order 12 856 of 1993, which requires reduction or elimination in the procurement of hazardous materials by federal facilities (including those used by the Department of Defense). Regulations on lead continue to become even more strict; the US Environmental Protection Agency (EPA) recently revised the National Ambient Air Quality Standard (NAAQS) on lead down to only 0.15 $\mu g/m^3$ (effective in 2017), which is lower than the previous standard by a factor of ten. In Europe, the Registration, Evaluation, Authorisation, and Restriction of Chemicals (REACH) Program has specifically targeted lead azide and lead styphnate for regulation. The connection between the discharge of lead explosives and increased lead levels in the blood has also been established; an often cited 1991 survey found that employees of a US Federal Bureau of Investigations (FBI) gun range had 10 times the government-recommended level of lead in their blood just after the cleaning of the site [11]. As a result, a clear need exists for environmentally acceptable primary explosive materials capable of replacing both lead azide and lead styphnate. Several US government programs have emerged in recent decades to study environmental issues such as lead replacement, among many others. These include the two major Department of

Defense (DoD) research programs: the Strategic Environmental Research and Development Program (SERDP) and the Environmental Security Technology Certification Program (ESTCP). The US Army, being one of the world's largest producers and users of military explosives, also has an environmentally dedicated initiative, the Ordnance Environmental Program (OEP), as part of the Environmental Quality Technology (EQT) Program.

Major factors that have helped spur this study of lead replacement by the US DoD in particular, include the other issues associated with lead azide. For one, the compound has a well-established tendency to decompose and release highly toxic hydrazoic acid vapors in the presence of water and CO_2. This gas not only presents a health hazard, but can readily react with copper and other metal-containing fixtures (i.e., pipes, wiring, casing) to form extremely sensitive and dangerous explosives like copper azide [12–14]. This has led to fatal accidents in the past, and was a driving reason for the US Navy to adopt the use of the even more toxic mercury(II) 5-nitrotetrazole (DXN-1) as an alternative to lead azide [12]. Also of prime importance are concerns over availability of military-qualified lead azide in the United States. During the Vietnam War era, the USA adapted the British RD1333 lead azide process to allow for large-scale production of so-called Special Purpose lead azide (SPLA, discussed in more detail later in this chapter). The SPLA process allowed for batches of up to 7.7 kg of the material to be produced; subsequent massive overproduction over the course of the war resulted in the manufacture of close to 500 000 kg of SPLA. Roughly half of this material was not consumed around the time it was made, and was instead incorporated into a stockpile at a US Army facility [15]. Since then, the US Army and its major contractors have relied upon the store to supply a huge number of items; the material has been provided essentially free of cost with the exception of shipping expenses. Therefore, little incentive has existed for other domestic facilities to maintain the production of military-qualified material, as it would be minimally profitable and constitute high risk for little reward. This system worked well enough until recently, when the stockpile inevitably began to dwindle and the quality of the material still present was called into question. Although new, qualified lead azide production is under development at several sites in the USA, the coincidence of the need for new quantities of primary explosives along with the emergence of growing environmental restrictions presents an excellent opportunity for the implementation of green alternatives.

5.1.3 Legacy Primary Explosives

5.1.3.1 Lead Azide (LA)

Lead azide ($Pb(N_3)_2$), occasionally referred to as lead hydronitride, trinitride, or nitride in some older references [16], came to prominence around the 1920s owing largely to its unique blend of performance and producibility characteristics, although it is not without its problems. The combination of its relatively long-term chemical and thermal stability, reliability, rapid build to detonation, and simple chemical synthesis are very difficult for alternative compounds to match; and from a cost and production standpoint – of vital significance to both military and commercial manufacturers – the material has historically been relatively cheap and straightforward (if sometimes dangerous) to produce in large quantities.

Like many other metal azide compounds, lead azide owes its start to the so-called grandfather of nitrogen chemistry, Theodor Curtius, following his discovery of hydrazine and hydrogen azide (more commonly known as hydrazoic acid), in the late 1880s [17]. It can form four known crystal polymorphs: α, β, γ, or δ, of which α is the most stable and the only acceptable form for explosive applications [18]. Typically prepared from a lead salt, such as lead nitrate or acetate and sodium azide in water, the synthesis appears quite simple on the surface. However, as with most primary explosives, particle size, morphology, and the presence of surfactants/coatings play a key role in determining whether the material performs well for its intended application and can also be handled safely. For this reason, a variety of lead azide types have been developed since the 1920s that are still in use today. Some of the most important types include:

Dextrinated lead azide (DLA) [8,14,15] is considered to be the safest-to-handle form and the most common type now used commercially. It was developed in the USA in 1931 [8] as a solution to the numerous accidental explosions associated with attempts to manufacture pure lead azide. The key feature is the incorporation of dextrin – a short-chained, starch-based polysaccharide – which helps to desensitize the explosive by preventing the formation of large fragile crystals, albeit at the cost of performance and added hygroscopicity [15].

Service lead azide (SLA) [8,14,15] was developed by the British and does not involve a coating agent; instead it makes use of the addition of acetic acid and sodium carbonate, which provides a nucleus to precipitate lead azide in a less-hazardous (compared to needle-shaped crystals) spherical morphology. SLA has higher explosive performance than DLA or RD1333/SPLA, but is somewhat more sensitive.

RD1333 and Special Purpose lead azide (SPLA) [8,15] Although involving somewhat different processing pathways, both British-developed RD1333 [19] and the later US-developed SPLA are similar in that they have nearly identical performance requirements/specifications and make use of the sodium salt of carboxymethylcellulose (CMC) as the desensitizing agent. As such, in the USA the two terms are often used interchangeably. The materials were developed to meet the need for LA that performed better – especially in smaller detonators – while maintaining some of the safe handling characteristics of DLA. As described above, SPLA makes up a large portion of the current US military stockpile of lead azide, which has existed since the 1960s.

On-demand lead azide (ODLA) [20] is a much more recent development compared to the others described here. It is a military-qualified process developed by the US Army ARDEC that produces lead azide that meets the RD1333 spec, and as such is considered equivalent to RD1333 and SPLA. The main advantage is that is produced in an on-demand, continuous fashion, thus avoiding the hazards associated with handling large-scale batches of the material. The small footprint and low cost of the processing equipment also means that it can be placed close to item production lines, further reducing the need for expensive and dangerous transport of lead azide on public roadways. ODLA was qualified by the US Army in 2012 and is currently being evaluated in larger-scale loading operations.

As mentioned previously, a key drawback to lead azide's use, apart from the lead content, is its tendency to slowly decompose under ambient conditions (Scheme 5.1):

$$2Pb(N_3)_2 \xrightarrow[H_2O]{CO_2} PbCO_3 \cdot Pb(OH)_2 + 4HN_3\,(g)$$

Scheme 5.1 *Decomposition reaction of lead azide in the presence of carbon dioxide and water [12].*

This process not only degrades the explosive over time, but the HN_3 generated can go on to react with other exposed metal surfaces, most notably copper contained in pipes or in brass fixtures [21]. This occurrence was blamed for several accidents associated with handling and storage of lead azide, as well as incidences of premature firings of explosive items [12].

5.1.3.2 Lead Styphnate (LS)

Lead styphnate (also known as lead trinitrorescorcinate) in both its normal (lead(II) 2,4,6-trinitro-*m*-phenylene dioxide) and basic forms started to gain serious attention around the same time as lead azide in the early twentieth century. It is noticeably less powerful than lead azide in terms of explosive force, but tends to initiate more reliably and generate a high degree of heat output. For this reason, it has found a use alongside the somewhat harder to trigger lead azide in initiating applications, including percussion primers as well as the initial explosive components in both stab and electrically initiated detonators. A major advantage of lead styphnate in primer applications is that it does not generate excessive residue, which can cause the corrosion of gun barrels. Its manufacturing takes place all over the world, including the USA and at least 14 locations in the EU; as of 2011, estimates put the total production of the material in the EU at somewhere between 10 and 100 tons per year [22].

The first form of lead styphnate to be synthesized was basic lead styphnate in 1874, which was made from magnesium styphnate and lead nitrate in acidic aqueous solution [23]. Basic lead styphnate is especially useful when incorporated into formulations with lead azide, such as the stab mixture NOL-130, as its basic nature does not encourage lead azide's tendency toward hydrolysis [24]. Normal lead styphnate was first reported in 1914 by Herz [6], who later developed a popular manufacturing method [25]. Although basic lead styphnate tends to be superior in terms of thermal stability and compatibility with lead azide, normal lead styphnate is considered to be easier to control in terms of crystal habit [26]. Both types are still in use and produced by manufacturers today.

5.2 Green Primary Explosive Candidates

To be considered an effective and practical green primary explosive, a candidate must meet a large number of criteria aside from the obvious avoidance of heavy metals and other toxins. It is generally regarded that a compound must be capable of undergoing almost instantaneous DDT on timescales of less than approximately 1 μs and over distances of less than 1 mm. It is vital that the explosive be sensitive enough to impact and friction to be considered reliable, yet capable of safe and predictable handling. It must be thermally stable (preferably with a decomposition temperature over 200 °C) as well as chemically stable, for example, capable of being stored for long periods of time across a wide temperature range

with negligible deterioration. For ammunition applications, such as lead styphnate replacement in primers, the material should not generate excessive residue, which may corrode the gun barrel. It must be compatible with common materials used in items such as detonators, primers, and blasting caps; this includes the materials the items might be constructed from, such as stainless steel and aluminum, as well as common explosives like tetrazene, RDX, HMX, PETN, and CL-20; it should also ideally be suitable to be mixed with common primer and stab initiation formulation components, such as antimony trisulfide and barium nitrate. As water is commonly used as a desensitizing agent for safe storage and handling of primary explosives, the material must be almost completely insoluble in aqueous solution to prevent unwanted recrystallization. The required synthesis reagents and solvents, along with the generated waste-stream, should be benign and environmentally acceptable. Last, but certainly not least, a candidate material must also be able to be synthesized in a simple, one- or two-step manner that can economically and safely be scaled up to at least the 0.5 kg batch size. Given this extensive list of often independent requirements, it should be clear why a century's worth of research has given few viable alternatives to lead azide or lead styphnate. However, considering that cheap price was one of the biggest advantages for these explosives in the past, newer cost-prohibitive environmental restrictions on the manufacturing, storage, and disposal/demilitarization of the materials now presents an opportunity for other candidates to be considered more competitive.

A number of prospective lead azide and lead styphnate replacement candidates will be described in this chapter, with a focus on materials that are already far enough along in development and/or practical use to be considered viable (although others will be mentioned). Table 5.3 lists a summary of these, divided into those that are likely better suited for green detonator applications (lead azide replacement) and those that are considered to have use in green primers (lead styphnate replacements).

5.2.1 Inorganic Compounds

5.2.1.1 Silver Azide (SA)

Silver azide (AgN_3) has been investigated by various organizations over the last century for primary energetic use [16,27–31], and has even been useful in less dramatic applications such as photographic emulsions [18] (which, fortunately, were not reported to be explosive). It has primarily been studied in detonator applications as a more effective alternative to lead

Table 5.3 *Summary of notable lead-free primary explosive candidates for detonators and primers.*

Detonator candidates	Primer candidates
Silver azide	KDNP
DDNP	KDNBF
NHN	MIC
DBX-1	Red phosphorus
BNCP	TTA
	DDNP

azide. When compared to that material, it possesses a number of advantages, including improved chemical stability, better explosive performance, and reportedly better applicability in microscale detonation devices [15]. A key point is that silver azide does not decompose to hydrazoic acid gas in the presence of water and CO_2, as described previously in this chapter for lead azide. By far the most studied form of silver azide is the monoazide, although the diazide anion ($Ag(N_3)_2$) was investigated more recently by Klapötke [32].

Relative to lead, silver is more environmentally and toxicologically acceptable. Although not typically harmful to humans or other vertebrates, except in large amounts, ionic silver is a well-known antimicrobial agent that has been used for its disinfection properties for centuries. Unfortunately, unchecked release of silver into the environment can likewise be extremely toxic for many freshwater aquatic micro-organisms, potentially leading to ecological damage. Therefore it's hard to describe silver as a completely "green" metal, although it is clearly superior to lead in this regard.

Its synthesis is simple and generally very similar to that of lead azide. In his original report, Curtius used his newly discovered (and highly toxic) hydrazoic acid (HN_3), bubbling the gas through an aqueous solution of silver nitrate. Attracted by its improved properties compared to lead azide, the British military developed a more practical synthesis method in the late 1940s, employing sodium azide (NaN_3) as the starting material; a key improvement was the incorporation of ammonium hydroxide into the reaction mixture, followed by slow addition of acid to encourage the formation of large-crystal, free-flowing silver azide product [31]. Later, US researchers adapted the synthesis for larger-scale batches (Scheme 5.2) [27].

Of course, if it was an ideal lead azide replacement candidate, the material likely would have been adopted for more widespread use years ago. Historically, the biggest obstacle has always been the high cost of silver compared to lead; most primary explosive producers were happy to trade off the performance advantages of silver azide for the much lower price of lead azide except in the most demanding applications. For stab-initiated detonators, silver azide also has a significant drawback in that it is incompatible with tetrazene and antimony sulfide, which are both ingredients in the most common stab initiation mixture, NOL-130, as sensitizing agents to insure reliable initiation when struck by a firing pin. In the case of tetrazene, the cause is attributed to the formation of highly sensitive silver azidotetrazole, which can lead to spontaneous explosions of both loose powder and pressed formulations [30]. As stab detonators, such as the M55 or M59, are common in a large number of US military munitions, this feature further prevents widespread use of silver azide in the absence of a suitable alternative to tetrazene (although previous reports exist that have investigated this [30]). However, as the use of lead-based materials becomes less feasible and cost-prohibitive due to environmental regulations, more consideration may be given to silver azide in the future.

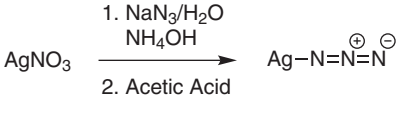

Scheme 5.2 *Synthesis of silver azide [27].*

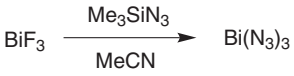

Scheme 5.3 *Synthesis of bismuth triazide.*

5.2.1.2 Other Inorganic Azides

Though numerous other metal azides have been synthesized since Curtius began his investigations with hydrazoic acid, aside from lead and silver azides most are unsuitable for use as primary explosives for various reasons, including insufficient or excessive sensitivity, toxicity, poor thermal properties, high cost, and so on. Some recently investigated compounds of note include bismuth and copper azides:

Bismuth azide. In terms of green energetics, bismuth is an appealing metal target because of its relatively low toxicity along with its high density (it sits adjacent to lead on the periodic table). One of the first (unsuccessful) reports of an attempt at a bismuth azide species was in 1927 [8,33], and some organometallic varieties were later reported [18]. It was not until much more recently, however, that researchers reported the synthesis of bismuth triazide ($Bi(N_3)_3$); first as an inseparable reaction mixture [34] and later as an isolated product (Scheme 5.3) [35,36]. Although the material was listed as being highly sensitive and explosive, no studies have yet been published on more detailed explosive properties and/or performance in any detonators or primers.

Copper azide. Owing to its reputation as an extremely ESD-sensitive, unpredictable, and dangerous explosive (even for a primary), copper azide has never seriously been considered for widespread use as a lead azide alternative. Historically, any time spent researching it has been more for purposes of preventing its accidental formation than interest in the material itself. Nevertheless, copper azide has more recently re-emerged for possible use in small-scale applications where it can, for instance, be formed *in situ* directly on items such as microelectromechanical systems (MEMS) devices and employed as an initiating charge [37]. Other intriguing developments include reports of desensitized copper azide formed inside single-walled carbon nanotubes (CNTs) using copper oxide nanoparticles as starting materials [38,39]. The resulting encapsulated copper azide particles show considerably reduced sensitivity compared to the neat material.

5.2.1.3 Nickel Hydrazine Nitrate (NHN)

NHN has recently arisen as an alternative to lead azide, with Indian and Chinese researchers in particular devoting considerable attention to the compound [14,40–42]. It is thought to be an "eco-friendly" compound in itself [14], although the presence of hydrazine is somewhat disconcerting given that the uncoordinated molecule is known to be extremely toxic. Nevertheless, in terms of properties, NHN appears to be a suitable substitute for lead azide in a number of primary explosive applications; it is reported to possess high thermal stability and relative insensitivity (for a primary) yet maintains reliability when triggered by flame, flash, or hot-wire [41]. It additionally exhibits reasonably high explosive performance (detonation velocity of 7000 m/s) [14].

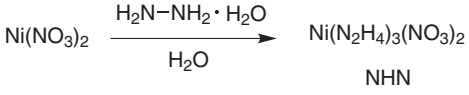

Scheme 5.4 *Synthesis of NHN [40].*

The published procedure for the synthesis of NHN is fairly straightforward, involving the reaction of nickel(II) nitrate with hydrazine hydrate in aqueous solution (Scheme 5.4). Researchers also experimented with dextrinated varieties of NHN, which was shown to significantly improve the bulk density of the compound [41]. From a green chemistry perspective, the reaction is highly atom efficient in that the only waste/by-product generated is the ejected hydrated water molecules of the reagents; recycling of the reaction medium has also been demonstrated to generate further product [40]. These environmental benefits are somewhat negated, of course, by the use of toxic hydrazine hydrate as a starting material.

5.2.1.4 Metastable Intermolecular Composites (MICs)

Traditional pyrotechnic thermites are mixtures of fuel and oxidizer particles (almost always a metal and a metal oxide) that are capable of achieving high concentrations of exothermic heat when reacted, often in the form of molten metal products. As such, they are often used for applications such as incendiaries and spot welding. A classic example is the reaction of iron(II) oxide (rust) with aluminum [43]:

$$Fe_2O_3 + 2Al \rightarrow Al_2O_3 + 2Fe$$

The generation of large amounts of heat and molten slag are highly desirable in primer applications. As described previously, toxic lead styphnate, along with environmentally undesirable metal fuel/oxidizer combinations (e.g., barium nitrate, antimony trisulfide) in formulations such FA-956, are traditionally used to accomplish this task. Provided environmentally acceptable metal/metal-oxide combinations are used, thermite-based energetics are highly appealing from a green perspective. However, in their common micron or larger particle size, thermites are unsuitable for primers as they are simply too difficult to ignite. Fortunately, the development of nanoscale particles over recent decades has opened the door for these applications. Nanoparticles can contain as few as under 1000 atoms, with the surface containing 100 or less atoms; this huge ratio of surface area to volume means that a combination of fuel and oxidizer particles can react extremely rapidly [44]. This class of thermites has wound up with a number of names, including superthermites, nanothermites, metastable interstitial composites, metastable nanoenergetic materials (MNCs), or, most commonly, as metastable intermolecular composites (MICs, pronounced "micks"). These compounds have been investigated extensively over the past decade [44–52]. Nanoaluminum is used almost exclusively as the fuel owing to its high energy content, well-established properties, and availability. Typical metal oxidizers used for MICs are bismuth(III) trioxide (Bi_2O_3) and molybdenum(VI) trioxide (MoO_3):

$$Bi_2O_3 + 2Al \rightarrow Al_2O_3 + 2Bi$$
$$MoO_3 + 2Al \rightarrow Al_2O_3 + Mo$$

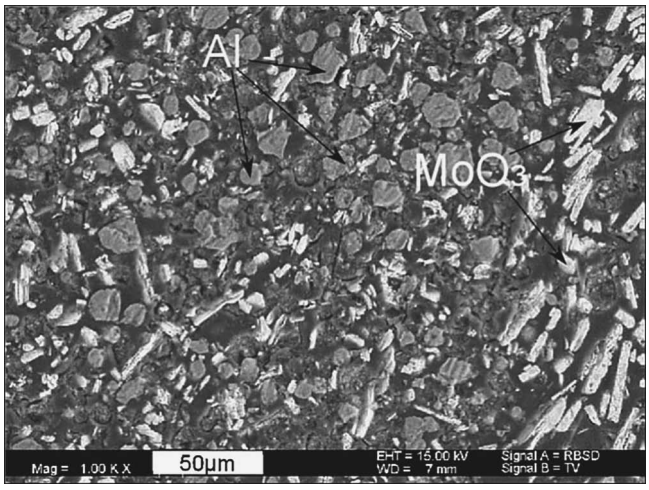

Figure 5.3 *SEM image of a typical MIC formulation. Reproduced with permission from [51] © 2006 WILEY-VCH Verlag GmbH & Co. KGaA, Weinheim.*

Proper mixing of fuel and oxidizer particles to form a homogenous blend is essential to achieve an effective MIC as maximum surface-to-surface contact is needed for the reaction to occur rapidly. On the laboratory scale, this is typically accomplished by sonicating the powders as they are suspended in an organic solvent, such as hexane or isopropanol [47], resulting in a well-mixed sample (Figure 5.3) after evaporation of the solvent. This type of procedure, however, is impractical for scaling up to production levels and safely loading into items such as primer cups. The challenges that arise include the high ESD and friction sensitivity attributed to dry MIC powders (especially when Bi_2O_3 is used) as well as the large quantities of organic solvents that would be required. Additionally, from an environmental perspective, mixing and work-up in aqueous solvent is highly desirable; but in the case of MICs, the nanoaluminum fuel and many of the possible metal oxides can be degraded by exposure to moist air and water. Aluminum slowly reacts to form aluminum hydroxide [43], while molybdenum oxide can form molybdic acid [53]. Work carried out by Puszynski related to organic acid coating agents and other additives has helped address some of these concerns and allowed for some of the first water-based processing methods for MIC-based primers that avoid the handling of hazardous dry MIC powder [54]. Further, investigations over the last decade carried out jointly by the US Army and Navy under SERDP and ESTCP programs [55,56] have extended this work, allowing for the incorporation and successful demonstration of Al/Bi_2O_3 MIC materials into common military primers, such as the Army primer #41 and the Navy PVU-1/A. As such, MICs have been shown as viable, drop-in replacements to legacy primer formulations and allow for elimination of toxic lead styphnate, antimony trisulfide, and barium nitrate.

5.2.1.5 Red Phosphorous

Phosphorus has long been a key ingredient in some energetic applications, particularly in pyrotechnics [43]. The element typically takes the form of one of two allotropes: white

phosphorus (P_4) or red phosphorus (polymeric). White phosphorus has been used in smoke formulations, among other applications, but is highly toxic in both vapor and solid forms and can also spontaneously ignite in air at temperatures of 50 °C or less, causing fires that are extremely difficult to extinguish. For these reasons, it is slowly being phased out of practical applications [57]. Red phosphorus, however, has gradually begun to see more attention. As a pure compound, red phosphorus is toxicologically and environmentally benign; it is not at all volatile, insoluble in water, and poorly absorbed by the body [58]. Unfortunately, red phosphorus can frequently be contaminated with traces of toxic white phosphorous and is notorious for its slow reaction with air and moisture to form highly toxic phosphine gas (PH_3) and corrosive phosphoric acid. This reaction can be accelerated at high temperatures and under alkaline conditions, although it is somewhat mitigated by formulating red phosphorus particles with suitable coating agents. Additionally, red phosphorus has led to several unexpected explosions when tested in confined ammunition applications, making it a risky material to work with from a handling perspective [57]. Despite these concerns, red phosphorus has been the subject of several primer inventions. The first report of its use in that application was in a 1940 patent, where it was combined with oxidizer barium nitrate as well as antimony trisulfide as a fuel/frictionating agent [59]. Later improvements were made after the discovery that copper or nickel containing primer fixtures could speed the decomposition of the formulation [60]; the incorporation of additional explosive ingredients was also explored [61]. Very recently, a patent by Busky *et al*. has brought red phosphorus primers back into the spotlight, making use of metal oxide coatings to help in the stabilization of the phosphorus particles from dangerous decomposition under aging conditions [62].

5.2.2 Organic-Based Compounds

5.2.2.1 Tetrazoles

Outside of the inorganic azides, compounds based on substituted tetrazoles have probably been the most investigated materials as alternative primary explosives. Tetrazoles are five-membered aromatic ring systems, and contain four nitrogen atoms with one carbon atom at the 5 position; in the parent tetrazole molecule, two hydrogens are present: one bound to the carbon and the other in one of two possible tautomeric locations on the ring nitrogens (Figure 5.4).

Tetrazole itself is considered far too sensitive and unstable for practical use as an explosive [63], but this can be addressed through the addition of suitable substituents at the carbon position. 5-Nitrotetrazole ($R = NO_2$) and 5-nitriminotetrazole ($R = N\text{-}NO_2$) are

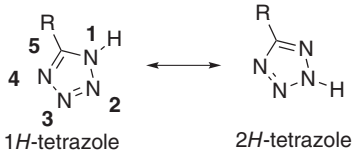

Figure 5.4 *Tetrazole and common primary explosive substituents.*

probably the most common substituents used for tetrazole-based primary explosives which will be discussed in detail below; 5-azotetrazole (tetrazole azide, R = N_3) has been studied, but is too sensitive for safe handling [64]. In addition to the 5 position, the hydrogen proton remaining on the nitrogen atom is acidic and can easily be replaced by a metal or organic cation; for explosives in general this is an advantage as salts tend to be less volatile and more thermally stable. This feature is of further importance to primaries as the metal salts also can help provide desired sensitivity to impact and friction. In fact, most practical 5-nitrotetrazole-based primary explosives are metal salts, although some purely organic varieties have also been studied [65]. Metal-based 5-nitrotetrazoles are certainly not new compounds, and have been investigated as primary explosives alternatives since not long after lead azide was adopted [66,67]. From the environmental perspective, most tetrazole compounds fall under the category of high-nitrogen materials. As such, their major decomposition product is inert and nontoxic N_2 gas. In addition to energetic uses, tetrazoles also have applications in pharmaceuticals and organic synthesis [68].

5.2.2.2 Sodium 5-Nitrotetrazolate (NaNT)

By far the most common practical use for NaNT is as a precursor to a number of other metal-based 5-nitrotetrazole explosives; the most notable of these, such as copper-based DBX-1, are shown in Figure 5.5 and discussed in more detail later in this chapter. The material itself is not a useful primary explosive as it is extremely hygroscopic and readily forms hydrates, which are relatively insensitive; the anhydrous material, in turn, is extremely sensitive and dangerous to handle. The compound was first reported during the 1930s in a patent by von

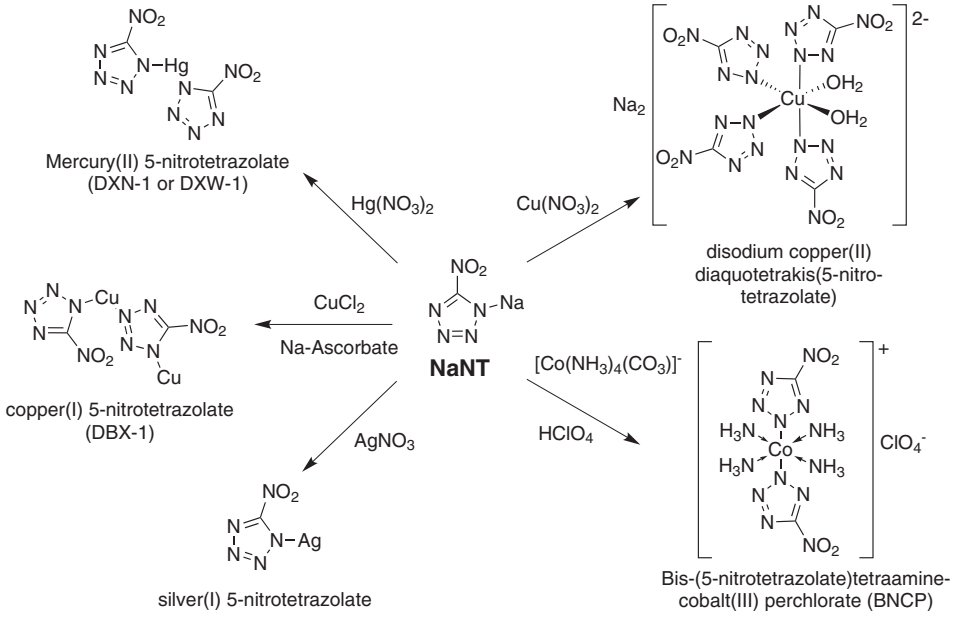

Figure 5.5 *Prominent primary explosives synthesized via sodium 5-nitrotetrazolate (NaNT).*

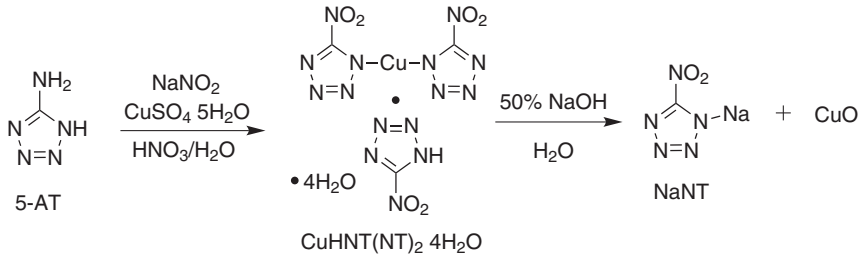

Scheme 5.5 *von Herz procedure for the synthesis of sodium 5-nitrotetrazolate (NaNT).*

Herz [66], who also applied it to synthesize silver, mercury, and basic lead 5-nitrotetrazolate compounds.

The reaction starts from 5-aminotetrazole (5-AT) and proceeds through a modified Sandmeyer reaction, oxidizing the 5-AT in an acidic solution of sodium nitrite and isolating a copper acid salt intermediate, $CuHNT(NT)_2$ as a tetrahydrate (Scheme 5.5). This salt can then be reacted with sodium hydroxide solution to precipitate CuO and leave the NaNT product in solution; solid material can be obtained by solvent evaporation and purified by recrystallization. One of the biggest issues with the process, however, is its tendency to produce microdetonations in the reaction mixture while the synthesis is taking place. Although these events are minor, they have resulted in cracked glassware on occasion and are "psychologically disturbing [12]." As the cause has been attributed to the formation of dangerous 5-diazotetrazole, the von Herz procedure was modified by Gilligan and Kamlet in the 1970s as part of their development efforts on mercury(II) 5-nitrotetrazolate (DXN-1) [12,69]. They found that adding a catalytic amount of a copper(II) salt to the 5-AT/HNO_3 feed solution prevented the occurrence of these mild detonations, presumably by rapidly converting the 5-diazotetrazole to harmless 5-hydroxytetrazole. Additionally, the researchers shifted the reaction stoichiometry towards excess sodium nitrite; this was found to improve the processing of the $CuHNT(NT)_2$, which is otherwise a slow and dangerous filtration step. Although these modifications improve the lab-scale synthesis of NaNT, the microdetonation and filtration issues reemerge as the process is scaled up, and at present no practical method exists to make large production sized batches. These problems can be exacerbated in that many of the metal-based explosives made from NaNT (e.g., DBX-1 [70], DXN-1 [12]) require that the starting material be high in purity, therefore necessitating extra purification steps. The high solubility of NaNT makes this difficult to carry out while maintaining a good yield of product.

5.2.2.3 Copper(II) 5-Nitrotetrazolate Coordination Compounds

One of the most publicized discoveries in the area of green primary explosives was reported in 2006 by Huynh and Hiskey of Los Alamos National Laboratory [71]. They synthesized a family of octahedral transition metal complexes based on 5-nitrotetrazole using both iron(II) and copper(II) and counterions such as Na^+ and NH_4^+. Although 5-nitrotetrazole complexes had been extensively investigated considerably earlier, most of these were based on known toxic materials such as the mercury content of mercury(II) 5-nitrotetrazole (DXN-1) or the perchlorate content of BNCP. Of the two metals

investigated, the copper(II) salt was found to have better performance when tested in detonators. Although it is an essential trace nutrient in both animals and plants, like silver, copper may be difficult to consider as a completely "green" metal as forms of it are known to be toxic to aquatic life. It is, of course, still considerably more toxicologically acceptable than lead.

As with the other 5-nitrotetrazole compounds discussed here, the precursor for the disodium 5-nitrotetrazolate copper(II) compound was the sodium salt, NaNT. The synthesis (Figure 5.5) was carried out in an aqueous solution using copper nitrate hydrate as the metal ion source; the blue-white product precipitates and is readily separable by filtration [72]. The authors reported the sensitivity of the compound to be comparable to lead azide, with somewhat higher values for velocity of detonation; when it was loaded into M55 stab detonators as the transfer charge in place of lead azide, the performance was found to meet the military requirements as determined by dent depths in steel witness plates. Despite this apparent success, however, the copper(II) 5-nitrotetrazolate complexes have yet to see any practical use. The main reason for this is the impracticality of the material for use in large-scale production; the as-synthesized product has a needle-like morphology and tends to manifest as a flaky powder that is wholly unsuitable for loading into detonators by traditional means, where a free-flowing, granular powder is required. Efforts to improve the particle habit in the copper(II) complex instead led directly to a much more practical compound for primary explosive use: the copper(I) salt of 5-nitrotetrazole, designated DBX-1.

5.2.2.4 Copper(I) 5-nitrotetrazolate (DBX-1)

Working under contract for the US Navy, Fronabarger and Williams of Pacific Scientific Energetic Materials Company (PSEMC) synthesized and developed DBX-1 as part of a lead azide replacement program [70]. The compound was discovered somewhat unintentionally while the researchers attempted to improve the properties of the afore-mentioned octahedral copper(II) 5-nitrotetrazolate complexes. In an effort to remove the two coordinated water molecules in that compound using reducing agents such as hydrazine, they found that the copper ion itself could be reduced, forming the entirely new copper(I) salt of 5-nitrotetrazole. The compound forms striking orange-red particles which present as free-flowing, monoclinic crystals; as such, DBX-1 is far superior in practical uses than the copper(II) nitrotetrazolate complex. The material has undergone extensive testing by the US DoD and is currently under consideration by an ESTCP program as a candidate for a "drop-in" replacement of RD1333 LA and SPLA (meaning that in most items it could simply be substituted as a volume-for-volume replacement with no major engineering modifications required) [73].

The synthetic procedure for DBX-1 is fairly simple and straightforward, which is another strong selling point when it comes to producibility (see Figure 5.6). To date, two methods have been reported: the reaction of copper(I) chloride in aqueous solution with NaNT [74] or the similar reaction using copper(II) chloride and sodium ascorbate (a form of Vitamin C) as a reducing agent to generate copper(I) *in situ* [70]. The latter method is preferred as it is more efficient and reproducible in terms of consistent particle size and morphology. The process is also environmentally benign; the reaction is carried out entirely in aqueous solution and the waste-stream consists mainly of NaCl and water. Any copper species present can be precipitated as CuO through the addition of base.

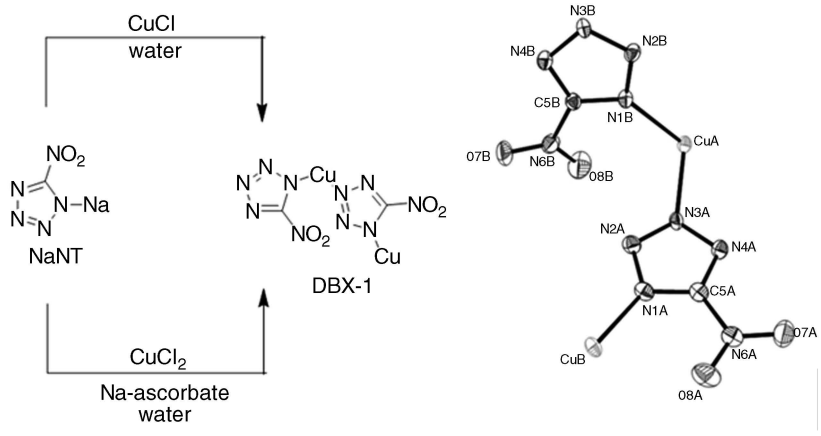

Figure 5.6 *Synthesis and crystal structure. Reproduced with permission from [70] © 2011 WILEY-VCH Verlag GmbH & Co. KGaA, Weinheim.*

Table 5.4 *Comparison between DBX-1 and legacy RD1333 lead azide.*

Compound	Friction (N)	Impact (J)	ESD (μJ)	Density (g/cc)	DSC onset (°C)
DBX-1	0.098	0.036 ± 0.012	12.00	4.80	310
LA (RD1333)	0.098	0.089 ± 0.054	6.75	2.58	320

In terms of explosive properties, DBX-1 is very similar to lead azide in terms of sensitivity to impact, friction, and ESD (Table 5.4). Its initiability and priming ability also appear comparable to lead azide in the applications that have been tested to date; these include both detonator and primer platforms [70,75], indicating that the material may have applicability as a lead styphnate alternative in some items as well. DSC compatibility studies show that DBX-1 is compatible with common detonator materials as well as typical military explosives; it also appears more resistant to oxidation than lead azide when aged under high temperatures and humidity.

Some drawbacks to DBX-1 do exist. Like lead azide, it can slowly decompose when stored in water [70]; however, instead of toxic and dangerous HN_3, it forms a soluble copper (II) nitrotetrazole complex that can be rinsed out. From a production standpoint, the current synthesis relies on the use of NaNT as the starting material; as described above, this compound currently has challenges to meet regarding safe scale-up. For DBX-1 production to reach large batch sizes, an improved process will be required for making high purity NaNT (or an alternative method that avoids isolating NaNT altogether).

5.2.2.5 Bis-(5-Nitrotetrazole)Tetraamine Cobalt(III) Perchlorate (BNCP)

BNCP (Figure 5.5) came to prominence in the 1990s as part of joint effort between Sandia National Laboratories and PSEMC to develop lead primary explosive replacements, which dates back to the 1970s. The program initially targeted a related compound, pentaamine(5-cyanotetrazole) cobalt(III) perchlorate (CP), which saw use in detonators starting in 1979

before it was abandoned due to its reliance on hazardous and scarce cyanogens, $(CN)_2$ [76]. In terms of performance, BNCP exhibits rapid DDT sufficient for primary explosive use [41]. Like DBX-1 and other 5-nitrotetrazolate explosives described here, BNCP relies on NaNT as a precursor and large-scale production is once again limited by the availability of this compound. In addition, although the toxicity of cobalt is preferable to that of lead, the material does contain perchlorate and therefore cannot be classified as a green compound. Nevertheless, BNCP continues to be produced by manufacturers and has seen use in applications such as fire suppression systems on aircraft.

5.2.2.6 Other Tetrazoles

A number of other tetrazole-based explosive compounds have been reported in the literature, but are not currently known to be in development for practical use; a handful of the more prominent of these will be briefly mentioned here (Figure 5.7). These include coordination compounds of 1,5-diaminotetrazole with metals such as copper(II) and iron(II), such as so-called DFeP and DCuP. These were investigated by Los Alamos National Laboratory [77] as well as a SERDP project [78], which found them to be promising candidates. The perchlorate content, however, makes them less appealing from the green perspective. The Klapötke group has additionally investigated a number of promising primary explosive candidates. These include nitriminotetrazoles such as copper (II) bis(1-methyl-5-nitrimiminotetrazolate) [79] and calcium 5-nitriminotetrazolate [80], the latter of which was tested successfully in a priming charge.

5.2.2.7 2-Diazo-4,6-Dinitrophenol (DDNP)

Apart from lead azide, lead styphnate, and tetrazene, DDNP (sometimes referred to as Dinol) has been one of the most widely used primary explosives for applications since the early twentieth century, and is old enough to be considered a "traditional" primary explosive. Either DDNP or KDNBF (discussed below) are considered to be the explosives of choice for commercial "green primers" due to their performance coupled with the absence of lead or other heavy metals. A flurry of patents in the 1990s was issued

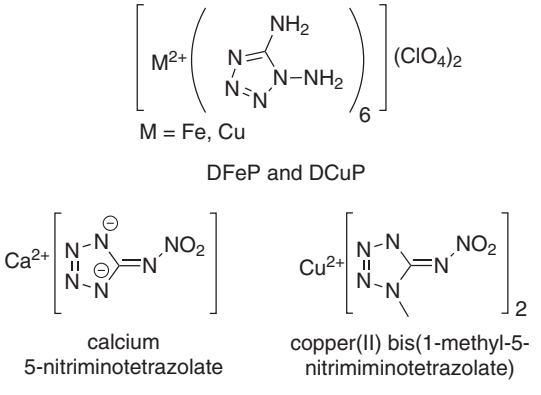

Figure 5.7 *1,5-diaminotetrazole coordination compounds (DFeP and DCuP).*

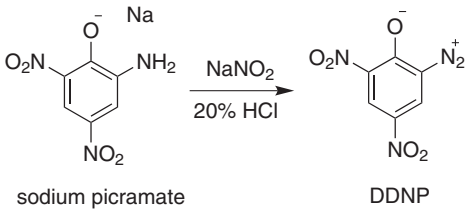

Scheme 5.6 *Synthesis of DDNP from picramate.*

for "green" DDNP-based primers, with major ammunition companies each developing their own specific formulation; see for instance: [81–84]. From the military standpoint, however, DDNP is thought to be unsuitable for demanding applications, such as reliability in extreme cold weather climates, as it is considered to have low sensitivity to friction and low flame temperature [85]. Additionally, early reports indicated that DDNP is highly incompatible with lead azide [86] and as such could not be used in place of lead styphnate in common stab mixes such as NOL-130, which rely on mixtures of lead azide and lead styphnate.

Apart from its well-established practical use as a primary explosive, DDNP also has a prominent role in chemical history, as it was first synthesized by Peter Griess in 1858 and became the basis of his first studies on the now well-known diazotization reaction [2,87]. Structurally, DDNP is a picric acid derivative and is synthesized from picramate in acidic solution with a nitrite salt (Scheme 5.6). Its exact structure has been the subject of debate over the years, with some early studies depicting the direct bonding of the diazo group with the phenolic oxygen to form a fuzed, bicyclic ring system [2]; even after the crystal structure of DDNP was finally reported in 1987 [88], discrepancy still exists over the exact resonance structure [89].

5.2.2.8 Potassium 4,6-Dinitrobenzofuroxan (KDNBF)

Potassium dinitrobenzofuroxan (potassium 4,6-dinitro-7-hydroxy-7-hydrobenzofurazan-1-oxide) is a heavy-metal-free primary explosive that dates back as far as 1899 [90]. Along with DDNP, it is the most common commercially available lead styphnate alternative used in "green" primers, and the compound and its analogues have been investigated by defense agencies [91,92] as well as having become the subject of many commercial patents and patent applications; see for instance: [81,85,93,94].

KDNBF exists as a Meisenheimer adduct between 4,6-dinitrobenzofuroxan and potassium hydroxide, synthesized by the reaction of the former compound with potassium bicarbonate; the base compound is fairly unique among explosives in that it can readily form salts despite the lack of an acidic proton. The traditional synthetic pathway (intended for manufacturing scale) is shown in Scheme 5.7, with *o*-nitroaniline as the starting material. Other metal salts also have been reported (e.g., Ag, Na, Ba, etc.) [95], but do not perform as well for practical primary explosive applications. The compound has been used in commercial and military initiating items since the 1950s [96], although its exact structure was not determined until later [96]. Despite its practical uses, KDNBF has not been adopted as a universal alternative to lead styphnate. One issue is that it is significantly less thermally

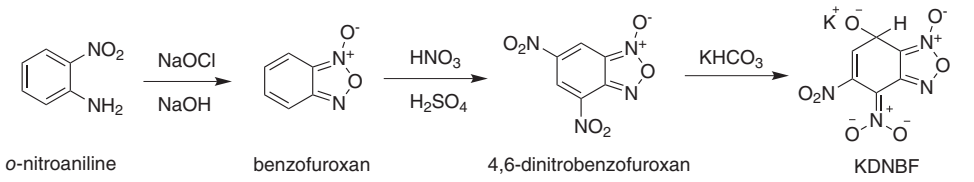

Scheme 5.7 *Synthesis of KDNBF [91].*

stable than the lead compound; the DSC decomposition point of normal lead styphnate is approximately 280 °C, while the value has been reported as being as low as 217 °C for KDNBF [97]. More recently, investigators have improved this feature through small chemical modifications, leading to the development of similar nitrobenzofuroxans, such as KDNP [98] described below.

5.2.2.9 Potassium 4,6-Dinitro-7-Hydroxybenzofuroxan (KDNP)

Although its synthesis was originally reported as far back as 1983, KDNP has only recently been looked at seriously as a possible lead styphnate alternative [97–99]. As is the case for DBX-1, KDNP is currently being developed by the US Navy in conjunction with contractor PSEMC [98]. The compound has been shown to be very comparable to lead styphnate in terms of explosive performance, and has been tested in items such as percussion primers, impulse cartridges, and other initiators [98,100].

Structurally, the compound differs from the more traditional KDNBF in the absence of a hydrogen atom; this minor change allows for the restoration of aromaticity in the benzofuroxan ring system, thus increasing the stability of KDNP relative to KDNBF. In fact, the DSC decomposition point of KDNP is reported as roughly 285 °C, considerably higher than the 217 °C for KDNBF and comparable to the 280–290 °C attributed to lead styphnate [98]. A number of synthetic methods exist for producing KDNP; the more traditional processes [101] involve water, which has been found to be retained in the product material and purportedly leads to the formation of undesirable, sensitive needles that require recrystallization. For this reason, a new method (Figure 5.8) was developed that avoids the use of water in the synthesis [98].

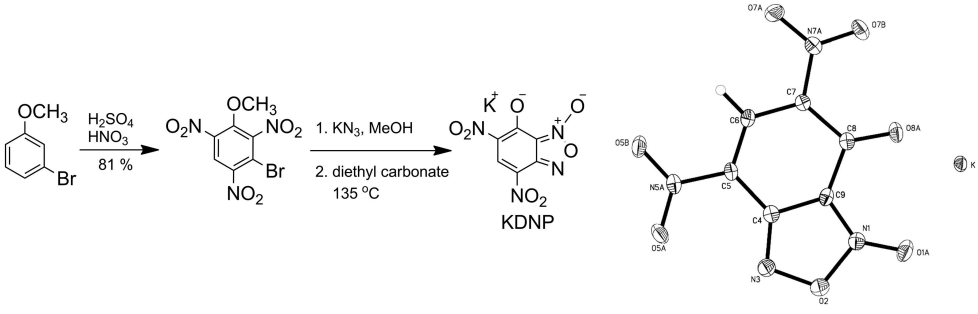

Figure 5.8 *Preferred synthetic method for the synthesis of KDNP, with crystal structure where ellipsoids represent 50% probability. Reproduced with permission from [98] © 2011 WILEY-VCH Verlag GmbH & Co. KGaA, Weinheim.*

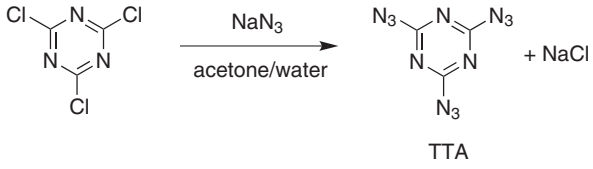

Scheme 5.8 *Synthesis of TTA.*

5.2.2.10 Cyanuric Triazide (CTA), aka Triazine Triazide (TTA)

Cyanuric triazide is another metal-free primary explosive compound that has existed for well over a century and has been the subject of several investigations since its discovery [102–105]. CTA is more powerful than lead azide in terms of explosive power, making it an effective performer for medium and large detonators. It has a somewhat slower DDT compared to lead azide, however, and therefore is not suitable for very small detonator applications. The initial reports on CTA found it to be extremely sensitive [102] and also displayed a tendency to sublime at elevated temperatures [105]. More recent investigations by the US Army ARDEC at Picatinny Arsenal have focused on the development of less sensitive CTA through improved synthetic methodologies; the older procedures tended to form large, sensitive, needle-like crystals which broke easily, whereas the newer procedure reduced the particle size to more stable ranges [106]. Despite the improved handling, the volatility of the compound is still likely to be an issue. As such, any future development of CTA will likely be restricted to its use as an ingredient in stab mix and primer formulations, where it has already shown considerable promise as an alternative to lead styphnate in primers.

In terms of synthesis, the first report on CTA is attributed to French chemist Auguste A. T. Cahours in 1847 [107] and the first patent for explosive use of the compound was in 1921 by Ott [108]. The process itself is a very simple, one-step procedure from simple cyanuric chloride and sodium azide in acetone/water (Scheme 5.8). From an environmental perspective, the waste-stream of the process is benign, as the major by-product is innocuous sodium chloride (NaCl).

5.2.2.11 Peroxide Explosives: Triacetone Triperoxide (TATP) and Hexamethylenetriperoxide Diamine (HMTD)

Virtually every organic chemistry undergraduate student is well educated in the explosive dangers associated with the inadvertent formation of peroxides. Although they may be appealing from an environmental perspective, the extreme sensitivity and tendency towards volatility of organic peroxides make most of them impractical as useful materials. The two most prominent examples of this class, which have been studied extensively, are TATP and HMTD. Unfortunately, both materials have become somewhat infamous in the recent past as they have often become terrorists' explosives of choice in suicide bombings and attempts, including suspected use as detonators in the July 7, 2005 London subway attacks. Both compounds have been known since the 1800s (HMTD was first reported in 1885 [109]), and HMTD, at least, has at one point been considered for primary explosive use [2]. Their appeal to amateurs and criminals stems from their simple synthesis from relatively available

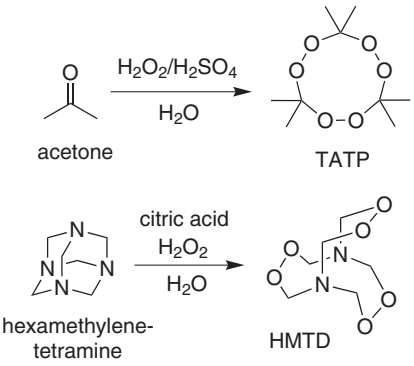

Scheme 5.9 *Syntheses of TATP and HMTD. Reproduced with permission from [111] © 2005 American Chemical Society.*

starting materials (Scheme 5.9). Although recent studies have shown suggested that TATP and HMTD are not as friction sensitive as previously thought [110], it is still unlikely that either will see official use at any time in the near future.

5.3 Conclusions

After more than a century dominated by the use of lead- or mercury-based primary explosives, the last decades have shown tremendous advances in the development of environmentally acceptable replacements. The many challenges associated with finding new materials that perform equivalently to the legacy lead azide/styphnate in the same hardware, while maintaining achievable producibility and reasonable cost, has led to a relatively small list of viable candidates, however. Of the currently available practical options, DBX-1 appears to be one of the better choices for a lead azide replacement as it matches well in terms of properties and performs equivalently to military spec lead azide in small detonators. Although the metal content is not ideal from an environmental perspective and some obstacles remain (such as the producibility of its precursor, NaNT), the developmental maturity of the material compared to other alternatives gives it a large advantage. The venerable silver azide remains an option as well given its well-established properties along with its current incorporation into some commercial and military applications; although not a purely green candidate owing to its silver content, its use may well be expanded as increasing costs make the use of traditional lead compounds less and less economically viable. In terms of lead styphnate replacement in applications such as ammunition primers, MIC technology appears to be well advanced and has been demonstrated in several common military items. For commercial purposes, it is likely that traditional "green" primer candidates, such as DDNP and KDNBF, will continue to see use, and newcomers such as KDNP may also find a role as well. Whatever direction the field of primary explosives may take, it remains vital that researchers in the area remain abreast of the always evolving environmental studies and regulations that take place worldwide and ensure supply of these essential materials remains available.

Acknowledgments

I am extremely grateful to Prof. Tore Brinck of KTH Royal Institute of Technology for his kind invitation to contribute to this important summary of advances in green energetics, as well as Prof. Thomas Klapötke of Ludwig-Maximilian University of Munich for his generous consideration and greatly appreciated efforts towards welcoming newcomers to the field of explosive chemistry. I also acknowledge Ms. Sarah Tilley and Ms. Rebecca Ralf of Wiley for their assistance and dedicated efforts in preparing this chapter.

I thank my coworkers in the Primary Explosives group at ARDEC for their hard work over the last ten years in bringing much needed attention to the necessity for environmental research in the area: in particular team leader Mrs. Neha Mehta, as well as Mr. Gartung Cheng, Ms. Emily Cordaro-Gioia, Mr. Akash Shah, and Mr. Kin Yee. I also want to acknowledge Drs. Paritosh Dave and Daniel "Dano" Stec, III of SAIC for their numerous helpful contributions to the program, in addition to Dr. Reddy Damavarapu of ARDEC for his kind mentorship and many helpful discussions. I'm further grateful to my management, including Competency Manager Mr. Steven Nicolich and Branch Chief Mr. Sanjeev Singh for their guidance and support.

I also want to recognize the dedicated efforts of the US Army RDECOM's Ordnance Environmental Program (OEP) for their advancement of not only our work, but many other researchers in the area of green energetics; in particular Mr. Erik Hangeland and Ms. Kimberly Watts of RDECOM, and Mr. Noah Lieb of Hughes Associates.

I am further grateful to valuable discussions from many other sources that helped me greatly in writing this chapter, including Dr. Jan Puszynski and Magdy Bichay of US NSWC-IH, Drs. John Fronabarger and Mike Williams of PSEMC, and Dr. William Eck of US Army Public Health Command. And finally, a sincere thanks to Dr. Monica Saumoy for her patient reading of many drafts of this chapter.

References

1. Giles, J. (2004) Collateral damage. *Nature*, **427**, 580–581.
2. Davis, T.L. (1943) *The Chemistry of Powder and Explosives*, GSG & Associates, San Pedro, CA.
3. Tarver, C.M., Goodale, T.C., Cowperthwaite, M., and Hill, M.E. (1977) Structure/property correlations in primary explosives, Stanford Research Institute, Menlo Park, CA, Final Report 76-2 for U.S. Navy NAVSEASSYSCOM Contract No. N00024-76-C-5329.
4. Klapötke, T. M. (2012) *Chemistry of High-Energy Materials*, 2nd Edition, Walter de Gruyter GmbH & Co., Berlin.
5. Hyronimus, F. (1909) Charging of Primers, US Patent 908,674.
6. Herz, E. (1915) Lead Salt of Trinitroresorcin, British Patent 17961.
7. Cooper, P.W. (1996) *Explosives Engineering*, Wiley-VCH, New York, NY.
8. Federoff, B.T. (1960) *Encyclopedia of Explosives and Related Items*, Picatinny Arsenal, Dover, NJ.
9. Committee on Measuring Lead in Critical Populations, National Research Council (1993) *Measuring Lead Exposure in Infants, Children, and Other Sensitive Populations*, The National Academies Press, Washington, D.C.
10. Committee on Lead in the Human Environment, National Research Council (1980) *Lead in the Human Environment*, The National Academies Press, Washington, D.C.

11. Barsan, M.E. and Miller, A. (1996) Lead Health Hazard Evaluation, National Institute for Occupational Safety and Health, Cincinnati, OH, HETA Report 91-0346-2572.
12. Gilligan, W.H. and Kamlet, M.J. (1976) Synthesis of Mercuric 5-Nitrotetrazole, White Oak Laboratory, Naval Surface Weapons Center NSWC/WOL/TR 76-146.
13. Meyer, R., Köhler, J., and Homburg, A. (2007) *Explosives: Sixth, Completely Revised Edition*, Wiley-VCH, Weinheim.
14. Agrawal, J.P. (2010) *High Energy Materials: Propellants, Explosives, and Pyrotechnics*, Wiley-VCH, Weinheim.
15. Costain, T. and Wells, F.B. (1977) Processes for the manufacture of lead and silver azide, in *Energetic Materials Volume 2: Technology of the Inorganic Azides* (eds. H.D. Fair and R.F. Walker), Plenum Press, New York, NY, USA, pp. 11–54.
16. Taylor, G.B. and Cope, W.C. (1917) Initial Priming Substances for High Explosives, U.S. Dept of the Interior, Bureau of Mines Technical Paper 162.
17. Bräse, S. and Banert, K. (2010) *Organic Azides Synthesis and Applications*, John Wiley & Sons Ltd., Chichester, UK.
18. Richter, T.A. (1977) Synthesis and the chemical properties, in *Energetic Materials Volume 1: Physics and Chemistry of the Inorganic Azides* (eds. H.D. Fair and R.F. Walker), Plenum Press, New York, pp. 15–86.
19. Taylor, G.W.C. and Napier, S.E. (1966) Preparation of Explosive Substances Containing Carboxymethyl Cellulose, US Patent 3,291,664.
20. Perich, A., Cordaro, E.A., Cheng, G. *et al*. (2008) On-Demand Lead Azide Production, US Patent 7,407,638.
21. Warren, K.S. and Rinkenbach, W.H. (1942) Study of the Action of Lead Azide on Copper, Picatinny Arsenal Report No. 1152.
22. European Chemicals Agency (2011) Annex XV – Identification of Lead Styphnate as SVHC.
23. Griess, P. (1874) Ueber Einwirkung von Salpeter-Schwefelsäure auf Orthonitrobenzoësäure, *Berichte*, **7**, 1223.
24. Taylor, G.W.C. and Thomas, A.T. (1962) Lead Styphnate Part 4: The Monobasic Lead Salts of Trinitroresorcinol, Polymorphic Modifications and the Development of R.D. 1346 and R.D. 1349, Explosives Research & Development Establishment Report No. 9/R/62.
25. Herz, E. (1935) Manufacture of Lead Styphnate, US Patent 1,999,728.
26. Taylor, G.W.C. and Thomas, A.T. (1975) Manufacture of Basic Lead Styphnate, US Patent 3,894,068.
27. Costain, T. (February (1974)) A New Method for Making Silver Azide in a Granular Form, Picatinny Arsenal Technical Report 4595.
28. Klapötke, T.M. and Rienacker, C.M. (2001) Drophammer test investigations on some inorganic and organic azides. *Propellants, Explosives, Pyrotechnics*, **26** (1), 43–47.
29. Millar, R.W. and Hamid, J. (2003) Lead-free initiator materials for small electro-explosive devices for medium caliber munitions, *SERDP Project PP*-1306 *Final Report.*
30. Spear, R.J., Redman, L.D., and Bentley, J.R. (1983) Sensitization of high density silver azide to stab initiation, Department of Defence Materials Laboratory Report MRL-R-881.
31. Taylor, G.W.C. (February (1950)) The Manufacture of Silver Azide R.D. 1336, Explosives Research & Development Establishment Report No. 2/R/50.
32. Klapötke, T.M., Krumm, B., and Scherr, M. (2009) The binary silver nitrogen anion [Ag(N3)2]-. *Journal of the American Chemical Society*, **131**, 72–74.
33. Vournazos, A.C. (1927) A new group of azido mixed salts. *Zeitschrift fur Anorganische und Allgemeine Chemie*, **164**, 263.
34. Klapötke, T.M. and Schulz, A. (1997) Group 15 triazides: a comprehensive theoretical study and the preparation of bismuth triazide. *Main Group Metal Chemistry*, **20**, 325–338.

35. Haiges, R., Rahm, M., Dixon, D.A. *et al*. (2012) Binary group 15 polyazides. structural characterization of [Bi(N3)4]-, [Bi(N3)5]2-, [bipy·Bi(N3)5]2-, [Bi(N3)6]3-, bipy·As(N3)3, bipy·Sb(N3)3, and [(bipy)2·Bi(N3)3]2 and on the lone pair activation of valence electrons. *Inorganic Chemistry*, **51**, 1127–1141.
36. Villinger, A. and Schulz, A. (2010) Binary bismuth(III) azides: Bi(N3)3, [Bi(N3)4]-, and [Bi (N3)6]3. *Angewandte Chemie International Edition*, **49**, 8017–8020.
37. Laib, G. (2008) Integrated Thin Film Explosive Micro-detonator, US Patent 7,322,294.
38. Forohar, F. and Bichay, M. (2011) Single Walled Carbon Nanotubes Activated with Hydrazoic Acid, US Patent 7,879,166.
39. Pelletier, V., Bhattacharyya, S., Knoke, I. *et al*. (2010) Copper azide confined inside templated carbon nanotubes. *Advanced Functional Materials*, **20** (18), 3168–3174.
40. Shunguan, Z., Youchen, W., Wenyi, Z., and Jingyan, M. (1997) Evaluation of a new primary explosive: nickel hydrazine nitrate (NHN) complex. *Propellants, Explosives, Pyrotechnics*, **22**, 317–320.
41. Talawar, M.B., Agrawal, A.P., Chhabra, J.S. *et al*. (2004) Studies on nickel hydrazinium nitrate (NHN) and bis-(5-nitro2H tetrazolato-N2)tetraamino cobalt (III) perchlorate (BNCP): potential lead-free advanced primary explosives. *Journal of Scientific & Industrial Research*, **63**, 677–681.
42. Chhabra, J.S., Talawar, M.B., Makashir, P.S. *et al*. (2003) Synthesis, characterization and thermal studies of (Ni/Co) metal salts of hydrazine: potential initiatory compounds. *Journal of Hazardous Materials*, **99**, 225–239.
43. Conklin, J.A. and Mocella, C.J. (2011) *Chemistry of Pyrotechnics: Basic Principles and Theory, Second Edition*, CRC Press Taylor & Francis Group, Boca Raton, FL.
44. Pantoya, M.L. and Granier, J.J. (2005) Combustion behavior of highly energetic thermites: nano versus micron composites. *Propellants, Explosives, Pyrotechnics*, **30** (1), 53–62.
45. Asay, B.W., Son, S.F., Busse, J.R., and Oschwald, D.M. (2004) Ignition characteristics of metastable intermolecular composites. *Propellants, Explosives, Pyrotechnics*, **29** (4), 216–219.
46. Bezmelnitsyn, A., Thiruvengadathan, R., Barizuddin, S. *et al*. (2010) Modified nanoenergetic composites with tunable combustion characteristics for propellant applications. *Propellants, Explosives, Pyrotechnics*, **35** (4), 384–394.
47. Perry, W.L., Smith, B.L., Bulian, C.J. *et al*. (2004) Nano-scale tungsten oxides for metastable intermolecular composites. *Propellants, Explosives, Pyrotechnics*, **29** (2), 99–105.
48. Shende, R., Subramanian, S., Hasan, S. *et al*. (2008) Nanoenergetic composites of CuO nanorods, nanowires, and Al-nanoparticles. *Propellants, Explosives, Pyrotechnics*, **33** (2), 122–130.
49. Yarrington, C.D., Son, S.F., Foley, T.J. *et al*. (2011) Nano aluminum energetics: the effect of synthesis method on morphology and combustion performance. *Propellants, Explosives, Pyrotechnics*, **36** (6), 551–557.
50. Bockmon, B.S., Pantoya, M.L., Son, S.F. *et al*. (2005) Combustion velocities and propagation mechanisms of metastable interstitial composites. *Journal of Applied Physiology*, **98**, 064903/1-/7.
51. Umbrajkar, S.M., Schoenitz, M., and Dreizin, E.L. (2006) Control of structural refinement and composition in Al-MoO3 nanocomposites prepared by arrested reactive milling. *Propellants, Explosives, Pyrotechnics*, **31** (5), 382–389.
52. Piercey, D.G. and Klapötke, T.M. (2010) Nanoscale aluminum - metal oxide (thermite) reactions for applications in energetic materials. *Central European Journal of Energetic Materials*, **7** (2), 115–129.
53. Puszynski, J.A., Bichay, M.M., and Swiatkiewicz, J.J. (2006) Wet processing and loading of percussion primers based on metastable nanothermite composites, US Patent 7,670,446.

54. Puszynski, J.A. (2006) MIC Water Based Loading Evaluation, Innovative Materials and Processes, LLC, Rapid City, SD, Final Report for U.S. Navy contract N00174-05-M-0141.
55. Middleton, J. (1997) Elimination of Toxic Heavy Metals from Small Caliber Ammunition, Strategic Environmental Research and Development Program (SERDP), Final Report for Project PP/1057/78.
56. Hirlinger, J. and Bichay, M. (2009) Demonstration of Metastable Intermolecular Composites (MIC) on Small Caliber Cartridges and CAD/PAD Percussion Primers, Environmental Security Technology Certification Program (ESTCP), Final Report for Project WP-200205.
57. Koch, E.-C. (2008) Special materials in pyrotechnics: V. military applications of phosphorus and its compounds. *Propellants, Explosives, Pyrotechnics*, **33** (3), 165–176.
58. Salocks, C. and Kaley, K.B. (2003) Red Phosphorus Office of Environmental Health Hazard Assessment (OEHHA), Sacramento, CA, Technical Support Document: Toxicology Clandestine Drug Labs/Methamphetamine, Volume 1, Number 12.
59. Pritham, C.H., Rechel, E.R., and Stevenson, T. (1940) Noncorrosive Priming Composition, US Patent 2,194,480.
60. Silverstein, M.S. (1953) Primer, US Patent 2,649,047.
61. Woodring, W.B. and McAdams, H.T. (1961) Priming Composition, US Patent 2,970,900.
62. Busky, R.T., Botcher, T.R., Sandstrom, J., and Erickson, J. (2010) Non-toxic, Non-corrosive Phosphorus-based Primer Compositions, US Patent 7,857,921.
63. Klapötke, T.M., Stein, M., and Stierstorfer, J. (2008) Salts of 1H-tetrazole - synthesis, characterization and properties. *Zeitschrift fur Anorganische und Allgemeine Chemie*, **634**, 1711–1723.
64. Hammerl, A., Klapötke, T.M., Nöth, H. *et al.* (2003) Synthesis, structure, molecular orbital and valence bond calculations for tetrazole azide, CHN7. *Propellants, Explosives, Pyrotechnics*, **28** (4), 165–173.
65. Spear, R.J. (1980) 1-Methyl-5-nitrotetrazole and 2-methyl-5-nitrotetrazole Part 1: Synthesis, Characterization, Detection, and Molecular Complex, Australia Department of Defence Materials Research Laboratories Report MRL-R-780.
66. von Herz, E. (1937) C-Nitrotetrazole Compounds, US Patent 2,066,954.
67. Klapötke, T.M., Sabate, C.M., and Welch, J.M. (2008) Alkali metal 5-nitrotetrazolate salts: prospective replacements for service lead(II) azide in explosive initiators. *Dalton Transactions*, 6372–6380.
68. Frija, L.M.T., Ismael, A., and Cristiano, M.L.S. (2010) Photochemical transformations of tetrazole derivatives: applications in organic synthesis. *Molecules*, **15**, 3757–3774.
69. Gilligan, W.H. and Kamlet, M.J. (1978) Method of Preparing the Acid Copper Salt of 5-Nitrotetrazole, US Patent 4,093,623.
70. Fronabarger, J.W., Williams, M.D., Bragg, J.G. *et al.* (2011) DBX-1 – a lead-free replacement for lead azide. *Propellants, Explosives, Pyrotechnics*, **36**, 541–550.
71. Huynh, M.H.V., Hiskey, M.A., Meyer, T.J., and Wetzler, M. (2006) Green Primaries: environmentally friendly energetic complexes. *Proceedings of the National Academy of Sciences of the United States of America*, **103** (14), 5409–5412.
72. Huynh, M.H.V., Coburn, M.D., Meyer, T.J., and Wetzler, M. (2006) Green primary explosives: 5-nitrotetrazolato-N2-ferrate hierarchies. *Proceedings of the National Academy of Sciences of the United States of America*, **103** (27), 10322–10327.
73. Thom, T. (2011) Demonstration of DBX-1 as an Alternative to RD-1333 Lead Azide, Environmental Security Technology Certification Program (ESTCP), Project #WP-201109.
74. Fronabarger, J.W., Williams, M.D., and Sanborn, W.B. (2010) Lead-Free Primary Explosive Composition and Method of Preparation, US Patent 7,833,330.
75. Mehta, N., Oyler, K.D., and Cheng, G. (2012) Green Replacements for Lead-based Materials and Safe Synthesis and Characterization of Primary Explosives, Proceedings of the 38th International Pyrotechnics Seminar, Denver, CO, USA, pp. 433–443.

76. Fronabarger, J.W., Sanborn, W.B., and Massis, T. (1996) Recent Activities in the Development of the Explosive BNCP, Proceedings of the 22nd Annual International Pyrotechnics Seminar, 645–652.
77. Huynh, M.H.V. (2009) Explosive Complexes, US Patent 7,592,462.
78. Bichay, M. and Hirlinger, J. (2004) Final report: new primary explosives development for medium caliber stab detonators, SERDP Project PP-1364.
79. Geisberger, G., Klapötke, T.M., and Stierstorfer, J. (2007) Copper bis(1-methyl-5-nitriminotetrazolate): a promising new primary explosive. *European Journal of Inorganic Chemistry*, 4743–4750.
80. Fischer, N., Klapötke, T.M., and Stierstorfer, J. (2011) Calcium 5-nitriminotetrazolate–a green replacement for lead azide in priming charges. *Journal of Energetic Materials*, **29** (1), 61–74.
81. Bjerke, R.K., Ward, J.P., Ells, D.O., and Kees, K.P. (1990) Primer Composition, US Patent 4,963,201.
82. Mei, G.C. and Pickett, J.W. (1992) Nontoxic Priming Mix, US Patent 5,167,736.
83. Erickson, J.A. (1998) Lead-free centerfire primer with DDNP and barium nitrate oxidizer, US Patent 5,831,208.
84. Guindon, L. and Allard, D. (1995) Low Toxicity Primer Formulation, US Patent 5,388,519.
85. Sandstrom, J., Quinn, A.A., and Erickson, J. (2011) Non-toxic, Heavy-metal Free Sensitized Explosive Percussion Primers and Methods of Preparing the Same, US Patent Publication 2011/0239887.
86. Clark, L.V. (1933) Diazodinitrophenol, a detonating explosive. *Industrial & Engineering Chemistry*, **25**, 663–669.
87. Heines, S.V. (1958) Peter Griess–Discoverer of diazo compounds. *Journal of Chemical Education*, **35** (4), 187.
88. Lowe-Ma, C.K., Nissan, R.A., and Wilson, W.S. (1987) Diazophenols–Their Structure and Explosive Properties, Naval Weapons Center, China Lake, Ca NWC TP 6810.
89. Holl, G., Klapötke, T.M., Polborn, K., and Rienäcker, C. (2003) Structure and bonding in 2-Diazo-4,6-dinitrophenol (DDNP). *Propellants, Explosives, Pyrotechnics*, **28** (3), 153–156.
90. Drost, P. (1899) III. Ueber nitroderivate des o-dinitrosobenzols. *Justus Liebigs Annalen der Chemie*, **307**, 49–69.
91. Costain, T. (1970) Investigation of Potassium Dinitrobenzofuroxan (KDNBF) to Provide Data Necessary for the Preparation of a Military Specification, Picatinny Arsenal, Picatinny, NJ Technical Report 4067.
92. Norris, W.P. and Spear, R.J. (1983) Potassium 4-hydroxyamino-5,7-dinitro-4,5-dihydrobenzofurazanide 3-oxide, the first in a series of new primary explosives, Department of Defence Support, Materials Research Laboratories, Melbourne, Victoria, Australia, MRL-R-870.
93. Pile, D.A. and John, H.J. (2012) Bismuth Oxide Primer Composition, US Patent Publication 2012/0125493.
94. Carter, G.B. (1995) Primer Compostions Containing Dinitrobenzofuroxan Compounds, US Patent 5,538,569.
95. Spear, R.J. and Norris, W.P. (1983) Structure and properties of the potassium hydroxide-dinitrobenzofuroxan adduct (KDNBF) and related explosive salts. *Propellants, Explosives, Pyrotechnics*, **8**, 85–88.
96. Brown, N.E. and Keyes, R.T. (1965) Structure of Salts of 4,6-Dinitrobenzofuroxan. *The Journal of Organic Chemistry*, **30** (7), 2452–2454.
97. Fronabarger, J.W., Williams, M.D., Sanborn, W.B. *et al.* (2007) Preparation, characterization, and output testing of salts of 7-hydroxy-4,6-dinitrobenzofuroxan. *Safe J*, **35** (1), 14–18.
98. Fronabarger, J.W., Williams, M.D., Sanborn, W.B. *et al.* (2011) KDNP – A lead free replacement for lead styphnate. *Propellants, Explosives, Pyrotechnics*, **36**, 459–470.

99. Fronabarger, J.W., Williams, M.D., and Hartman, S. (2007) Final Report on the Investigation of the Alternatives to Lead Azide and Lead Styphnate, Pacific Scientific Energetic Materials Company NSWC-IH Contract N00174-06-C-0079.
100. Fronabarger, J.W. and Williams, M.D. (2009) Lead-free primers, US Patent Application 2009/0223401.
101. Norris, W.P., Chafin, A., Spear, R.J., and Read, R.W. (1984) Synthesis and thermal rearrangement of 5-chloro-4,6-dinitrobenzofuroxan. *Heterocycles*, **22**, 271.
102. Taylor, C.A. and Rinkenbach, W.H. (1923) Preparation and detonating qualities of cyanuric triazide, U.S. Bureau of Mines Reports of Investigation Report No. 2513.
103. Mehta, N., Cheng, G., Cordaro, E.A. *et al*. (2011) Lead free detonator and composition, US Patent 7,981,225.
104. Gillan, E.G. (2000) Synthesis of nitrogen-rich carbon nitride networks from an energetic molecular azide precursor. *Chemistry of Materials*, **12**, 3906–3912.
105. Kast, H. and Haid, A. (1924) The explosive properties of the most important initiating explosives. *Angewandte Chemie*, **38**, 43–52.
106. Mehta, N., Cheng, G., Cordaro, E.A. *et al*. (2009) Modified ARDEC Triazine Triazide (TTA) Synthesis, U.S. Army ARDEC Technical Report ARMET-TR-09019.
107. Headquarters, U.S. Department of the Army (1984) *Military Explosives, Department of the Army Technical Manual TM 9-1300-214*, U.S. Department of the Army, Washington, D.C.
108. Ott, E. (1921) Explosive (tritriazotriazine), US Patent 1,390,378.
109. Legler, L. (1885) Ueber producte der langsamen verbreunnung des aethylathers. *Berichte der deutschen chemischen Gesellschaft*, **18** (2), 3343–3351.
110. Matyas, R., Selesovsky, J., and Musil, T. (2012) Sensitivity to friction for primary explosives. *Journal of Hazardous Materials*, **213–214**, 236–241.
111. Dubnikova, F., Kosloff, R., Almog, J. *et al*. (2005) Decomposition of triacetone triperoxide is an entropic explosion. *Journal of the American Chemical Society*, **127**, 1146–1159.

6

Energetic Tetrazole *N*-oxides

Thomas M. Klapötke and Jörg Stierstorfer

Department of Chemistry and Biochemistry, Energetic Materials Research, Ludwig-Maximilian University of Munich, Germany

6.1 Introduction

This review aims to give an oversight in the recent advances in the chemistry of energetic tetrazole *N*-oxides. It is therefore only concerned with tetrazole *N*-oxides which have been reported in the literature showing the properties which are prerequisites for energetic materials. It does not consider tetrazole *N*-oxides which do not show energetic properties – these compounds have been covered in a very recent review [1]. The synthetic routes for the preparation of tetrazole *N*-oxides as well as the properties of tetrazole *N*-oxides in comparison with the corresponding tetrazole compounds are presented and discussed using both experimental and computational data. Furthermore, the reasons for the current interest in the synthesis of a wide range of tetrazole *N*-oxide compounds and their related derivatives are given.

6.2 Rationale for the Investigation of Tetrazole *N*-oxides

The synthesis of modern energetic materials is an area of intense research both in terms of synthetic investigations as well as computational work [2]. Modern state-of-the-art explosives should have low sensitivity, high performance, and high thermal stability as well as being environmentally friendly [3–5]. However, RDX, which is currently used as a secondary explosive in many energetic formulations, shows very good energetic properties, but is toxic. Therefore, one strategy that has been employed in the search for new energetic materials is to

Green Energetic Materials, First Edition. Edited by Tore Brinck.

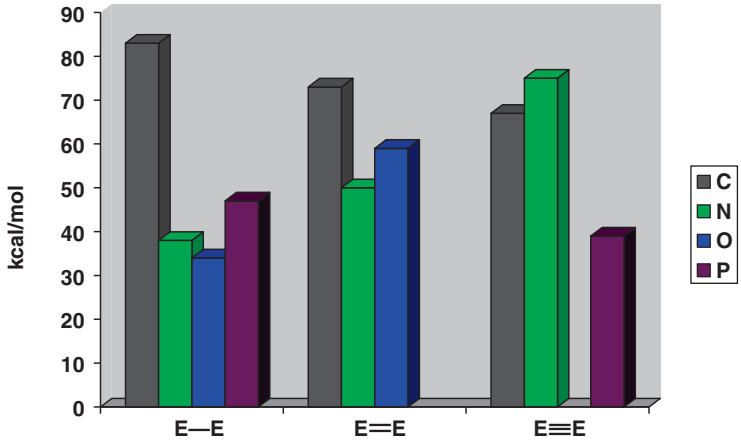

Figure 6.1 *Comparison of the formal average bond energies per 2-electron bond of N–N, N=N, and N≡N.*

synthesize nitrogen-rich compounds that have a high (positive) heat of formation, so that on detonation, a large amount of energy will be released. Another advantage of such energetic materials is that a large volume of nontoxic dinitrogen (N_2) gas is produced on detonation rather than environmentally hazardous and toxic detonation products. The reason that these nitrogen-rich materials have high positive heats of formation is due to the fact that the N≡N triple bond (which is present in the N_2 gas that is formed on detonation) is much more stable than either the N–N single bond or N=N double bond (Figure 6.1).

Since N–N single bonds are less stable than the N=N or N≡N bonds, long chains of the type $(-N-N-N-)_x$ cannot be isolated at room temperature [6]. Even monomethyl hydrazine $Me(H)NNH_2$, which contains only an N_2 chain, decomposes slowly in air at room temperature [7]. Therefore, the preparation of pseudo-aromatic heteronuclear rings incorporating as many nitrogen atoms as possible is probably the best strategy for synthesizing room temperature stable compounds that have many nitrogen atoms directly connected to one another. This approach results in aromatic rings in which the N–N bonds have relatively low bond orders, but are stabilized by π-electron delocalization. If we look at the series pyrrole, pyrazole, triazole, tetrazole, and pentazole, we can see that on moving from left to right through the series, one –CH group is substituted by an isolobal and isosteric N atom (Figure 6.2).

By calculating the heats of formation, we can see that they increase on increasing the number of nitrogen atoms present in the ring. It has also been shown that, in such systems, the explosive performance is correlated to the heat of formation, which means that compounds of this type with larger positive heats of formation show increasing explosive performance [8]. It would therefore seem simple that all new energetic materials should then be based on the pentazole ring [9], however this is not the case, since pentazole itself has not been isolated in macroscopic quantities, and organic derivatives of the type $R-N_5$ are either thermally not very stable, are extremely sensitive to detonation stimuli, or require large, bulky R- groups for stabilization, which then reduce the energy content of the compound. For example, whereas *p*-$Me_2N-C_6H_4-N_5$ is stable at room temperature [10], $C_6H_5-N_5$ decomposes at −50 °C [11,12].

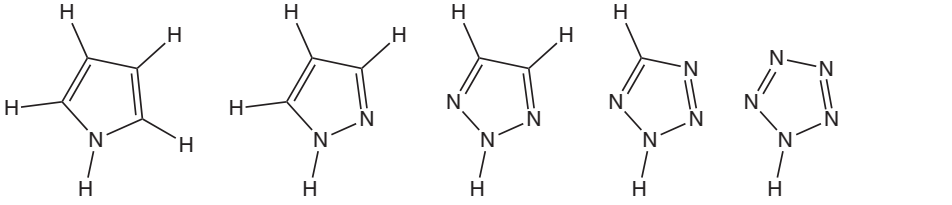

Figure 6.2 *Five-membered C–N rings from (left to right): pyrrole, pyrazole, 1,2,3-triazole, tetrazole, and pentazole. The calculated* $\Delta_f H°$(g,M) heats of formation values are given in kcal mol^{-1} below.

As a compromise between excellent explosive performance (i.e., very high positive heats of formation) and good thermal and mechanical stability, the triazole and tetrazole rings have proven so far to be the most promising backbones. A large number of 1,2,3-triazole, 1,2,4-triazole, and 1,2,3,4-tetrazole derivatives have now been prepared. Not only have tetrazole derivatives been prepared in which the R group connected to the carbon atom has been substituted by a number of other – often nitrogen-rich – groups, but also compounds have been prepared in which two tetrazole rings are joined by –NH–, –N=N– or –NH–N=N– bridges. Also bis(tetrazole) in which the two tetrazole rings are directly attached to one another either by one C atom (5,5′-bistetrazole) from each tetrazole ring or one C atom and one N atom (1,5′-bistetrazole) from the other tetrazole ring have been described. Furthermore, salts containing the deprotonated corresponding tetrazolate anions have also been prepared in large numbers (Figure 6.3).

Recently, it has been shown that many of the energetic properties of tetrazole-containing compounds can be improved by forming the corresponding *N*-oxide. The difference between a tetrazolate anion and a tetrazolate-*N*-oxide anion is simply the oxidation of the N1 or N2 atom

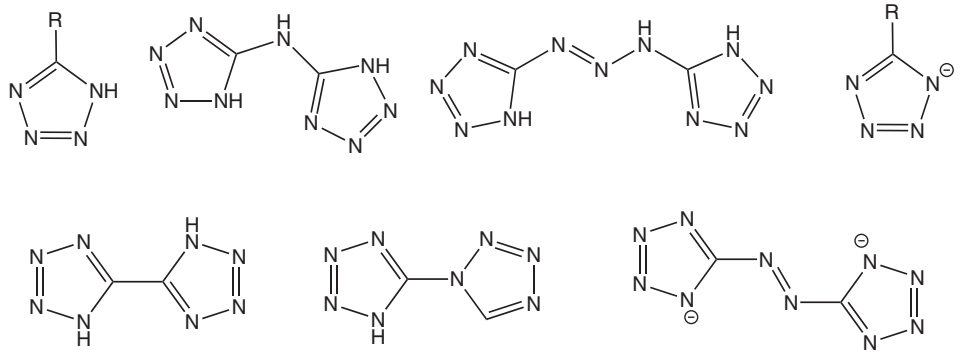

Figure 6.3 *Examples of tetrazole derivatives: 1*H*-tetrazole (top far left), bis(tetrazolyl)amine (top second left), bis(tetrazolyl)triazene (top second right), and tetrazolate anions (top far right), 5,5'-bis(tetrazoles) (bottom left), 1,5'-bis(tetrazoles) (bottom middle) as well as 5,5′-azobistetrazolate anions (bottom right).*

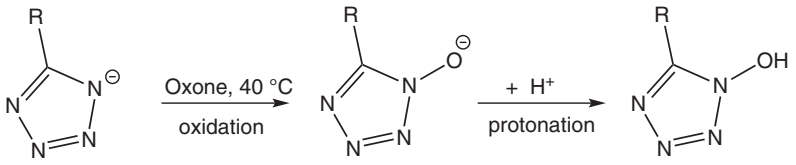

Figure 6.4 *Scheme showing an example of the generation of tetrazolate* N*-oxide anions by oxidation of the corresponding tetrazolate anion. The oxidation of the 5-R-tetrazolate anion forming the corresponding tetrazolate* N*-oxide species and its subsequent protonation forming the 1-hydroxy-5-R-tetrazole molecule is shown.*

by the formation of an N → O group. The N → O group can be subsequently protonated to form neutral hydroxytetrazole, (Figure 6.4).

Although the introduction of oxygen does not increase the percentage nitrogen content of the tetrazole, it increases the oxygen balance Ω in comparison with the nonoxidized tetrazole species. Furthermore, the tetrazole *N*-oxides have been shown to usually result in an increased density (the detonation pressure scales with the square of the density and the detonation velocity scales with the density of the energetic material) and performance of the energetic material in comparison with the corresponding nonoxidized tetrazole, but at the same time also lower its sensitivity to mechanical friction (i.e., shock, impact). Interestingly, although the tetrazole *N*-oxides are usually less endothermic than their nonoxidized tetrazole counterparts, this disadvantage is more than compensated for by their higher densities. There are two disadvantages, however, with the tetrazole *N*-oxide compounds, which are: (i) they often (but not always) have slightly decreased thermal stability in comparison with the nonoxidized tetrazole and (ii) they do not have one generally applicable synthetic route, since different tetrazole derivatives must be oxidized using different routes depending on which functional groups are present in the original tetrazole-containing compound. Therefore, obviously, interest in the conversion of tetrazole compounds into their tetrazole *N*-oxide derivatives for application as energetic materials such as secondary explosives is considerable.

6.3 Synthetic Strategies for the Formation of Tetrazole *N*-oxides

As was mentioned above, there is not one universal approach that can be used for the conversion of a tetrazole into the corresponding tetrazole *N*-oxide compound, largely because of the different functional groups that are present in energetic tetrazoles – usually located at the 5-position of the ring (C atom). Therefore, we are going to look at the different strategies that use different oxidizing reagents to prepare tetrazole *N*-oxides in the following section and discuss the general advantages and disadvantages of each method.

6.3.1 HOF·CH_3CN

HOF (hypofluorous acid) has the connectivity H−O−F. As a consequence of this, the O atom is bonded directly to an F atom making the O atom highly electrophilic, since F is the only element that has a higher Pauling electronegativity than oxygen. A consequence of this is that it is one of the best oxygen transfer reagents known [13]. HOF·CH_3CN is an easy and safe

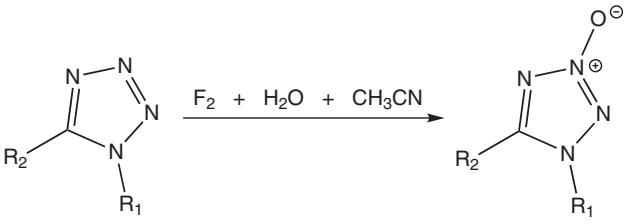

Figure 6.5 *General reaction showing the formation of a 1-substituted 5-alkyl-tetrazole 3N-oxide by the oxidation of the corresponding 1-substituted 5-alkyl-tetrazole.*

reagent to prepare and can be prepared in large quantities. A gaseous mixture of 10–20% F_2 in N_2 is passed through a cold (*ca.* −15 °C) CH_3CN/H_2O mixture. The reaction of the dilute F_2 gas with H_2O results in the formation of HOF and HF as the by-product (Eq. (3.1)). This results in typical concentrations of 0.4–0.6 molar of the oxidizing reagent. Since dilute difluorine gas and ambient and not elevated pressure are used, it is safe to use. Moreover, the excess HOF and HF can be easily and safely removed by the addition of $NaHCO_3$ [13].

$$F_2 + H_2O \xrightarrow{CH_3CN} HOF + HF \tag{3.1}$$

The general procedure for the formation of 1- or 2-substitued 5-alkyl-tetrazole-3*N*-oxides is to dissolve the 1- or 2-substitued 5-alkyl-tetrazole that is to be oxidized in CH_2Cl_2 and after cooling this mixture to 0 °C, the $HOF{\cdot}CH_3CN$ oxidizing agent is added. After only a few minutes the reaction is usually complete and the 1- or 2-substituted 5-alkyl-tetrazole-3*N*-oxide can be worked-up and isolated and the HOF and HF removed using $NaHCO_3$ (Figure 6.5) [13]. Previously it was thought that the tetrazole rings could not be oxidized, since even very strong oxidizers had failed in attempts to prepare the corresponding tetrazole *N*-oxide [14]; however, later it was found that $HOF{\cdot}CH_3CN$ could be successfully used for the preparation of the tetrazole *N*-oxides [13].

The advantages of this method are that the $HOF{\cdot}CH_3CN$ is cheap and easy to prepare, it uses only mild conditions for oxidation, and it delivers products in high yields. Furthermore, this method is reported to form the tetrazole *N*-oxide even if electron withdrawing groups are located at the tetrazole ring C atom or if sterically hindered tetrazoles are used [13].

6.3.2 Oxone®

The first tetrazole-*N*-oxide with respect to energetic background was prepared by Bottaro et. al. [15]. They described the reaction of ammonium nitrotetrazolate with Oxone forming nitrotetrazolate-2*N*-oxide. Oxone® is the commercial name for an oxidizing agent that has the formula $2\ KHSO_5{\cdot}KHSO_4{\cdot}K_2SO_4$ and contains the active oxidizing ingredient potassium peroxymonopersulfate, $KHSO_5$. Oxone is a useful oxygen transfer reagent since – amongst many other examples – it has been found to convert trialkyl amines into their corresponding trialkylamineoxide (R_3NO) compounds, R_3B into $(RO)_3B$ compounds, and R_3P into R_3PO compounds [16]. Furthermore, it is commercially available and cheap, it is thermally stable as long as it is stored at ambient temperatures with the exclusion of moisture, it can be added directly as a solid to aqueous reactions mixtures, or stored in acidic aqueous solution, and since it is nontoxic it is easy to handle. Furthermore, it usually shows good regioselectivity in the synthesis of 5-nitrotetrazolate-*N*-oxide in which the

5-nitrotetrazolate-2*N*-oxide is produced and not a mixture of the 5-nitrotetrazolate-1*N*-oxide and 5-nitrotetrazolate-2*N*-oxide. Furthermore, due to the simple work-up for the above reaction, yields of over 90% were reported for certain 5-nitrotetrazolate-2*N*-oxide salts.

Oxone has unfortunately one major disadvantage in the synthesis of energetic tetrazole-based *N*-oxides, and that is that it is unsuitable for oxidation reactions involving tetrazole rings that contain other oxidizable N atoms in the molecule. For example, salts containing the 5-cyanotetrazolate anion can be easily and efficiently oxidized to form salts containing the 5-cyanotetrazolate-2*N*-oxide ion [17]. However, Oxone cannot be used for the formation of the nitriminotetrazolate-*N*-oxide anion from the corresponding nitriminotetrazole, since the nitrimino group contains N atoms, which can also be relatively easily oxidized by Oxone. Therefore, Oxone cannot be used in every system and other oxygen transfer reagents are required for tetrazoles containing additional oxidizable N atoms.

6.3.3 CF_3COOH/H_2O_2

The addition of anhydrous trifluoroacetic acid (CF_3COOH) to a dichloromethane/H_2O_2 mixture has been shown to act as an effective oxidizer. Although there are no reports in the literature for the preparation of tetrazole *N*-oxides using this method, several other nitrogen-rich energetic materials containing the *N*-oxide functional group have been prepared using CF_3COOH/H_2O_2 as the oxidizer. Therefore, in the future it may also be used for the preparation of tetrazole *N*-oxide derivatives. Two important examples of the use of this oxidizing mixture for the preparation of energetic materials are the preparation of 1-oxide 3,5-dinitro-2,6-pyrazinediamine 1-oxide (LLM-105), which is obtained in the final step by the reaction of 3,5-dinitro-2,6-diaminopyrazine (Figure 6.6) [18–20], and the N-oxide derivative of 3,3′-azobis(6-amino-1,2,4,5-tetrazine), which is obtained by the oxidation of 3,3′-azobis(6-amino-1,2,4,5-tetrazine) [21] (Figure 6.6).

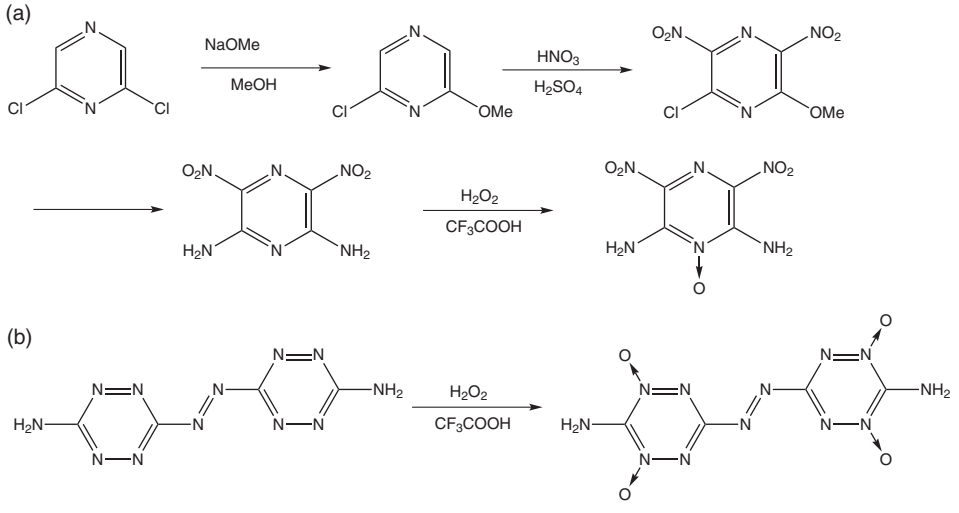

Figure 6.6 *The use of CF_3COOH/H_2O_2 as the oxidizer in the preparation of two nitrogen-rich energetic materials: (a) preparation of 3,5-dinitro-2,6-pyrazinediamine 1-oxide (LLM-105) and (b) the* N*-oxide derivative of 3,3′-azobis(6-amino-1,2,4,5-tetrazine).*

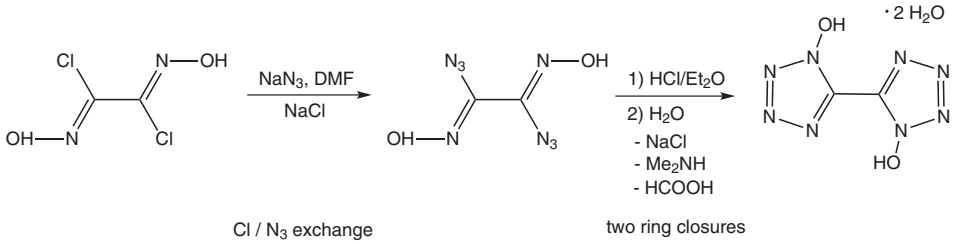

Figure 6.7 *Dichloroglyoxime can be converted into the friction and impact sensitive diazidoglyoxime by reaction with NaN_3 in DMF. Passing HCl gas through diazidoglyoxime suspended in diethylether results in cyclization forming 5,5′-bis(1-hydroxytetrazole).*

6.3.4 Cyclization of Azido-Oximes

Another possible strategy for the formation of tetrazole *N*-oxides is through the cyclization of azido-oximes. In such a method, an azidoglyoxime is prepared, often by the chloro-/azido-exchange of the corresponding chloroglyoxime with NaN_3 in DMF, and is then isolated and subsequently added to diethylether to form a suspension through which HCl gas is bubbled. After leaving the reaction mixture overnight, cyclization is complete and the tetrazole *N*-oxide can be recovered from the solution (Figure 6.7) [22].

Although, in principle, this is a useful method and has been used in the preparation of, for example, 5,5′-bis(1-hydroxytetrazole), which can then be deprotonated using a variety of Brønsted bases to form salts containing the corresponding 5,5′-bis(tetrazolate-1-oxide) anion, it has two major drawbacks. One is that not many of the azido-oximes that are required for the final cyclization step are known. A second problem is that many of the azido-oximes that are known are compounds that are highly sensitive to mechanical friction and are therefore hazardous to handle. For example, diazidoglyoxime, which is necessary for the cyclization step for the formation of 5,5′-bis(1-hydroxytetrazole), is highly friction and impact sensitive [23,24]. This second problem has been improved upon to some extent by a new one-pot synthesis for the synthesis of hydroxylammonium 5,5′-bis(tetrazolate *N*-oxide) by using DMF solution and reacting the diazidoglyoxime generated *in situ* further without isolating the diazidoglyoxime itself and forming a suspension of it in diethylether [23,24].

6.4 Recent Examples of Energetic Tetrazole *N*-oxides

In this section we are going to look at specific examples of energetic tetrazole *N*-oxides and salts containing tetrazolate *N*-oxide anions, and give an overview of their synthesis and structures as well as their stability and energetic properties. Most of the compounds discussed are not neutral tetrazole *N*-oxides with the zwitterionic unit described by Harel and Rozen [13], but are salts containing a tetrazolate anion in which one of the tetrazolate ring N atoms has been oxidized and exhibits the $N \rightarrow O$ functionality. First of all *N*-oxides based on tetrazoles will be discussed followed by *N*-oxide derivatives of bistetrazoles, 5,5′-azobistetrazoles, and finally tetrazine bridges bistetrazoles.

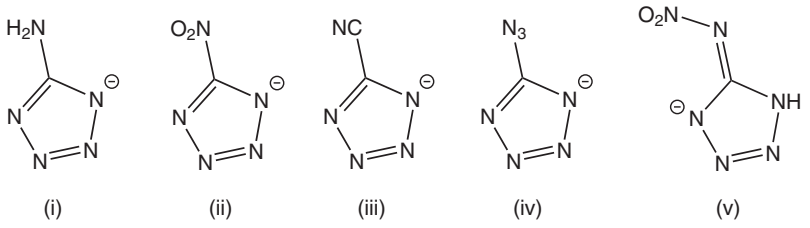

Figure 6.8 *Structures of the 5-aminotetrazolate (i), 5-nitrotetrazolate (ii), 5-cyanotetrazolate (iii) 5-azidotetrazolate (iv), and 5-nitriminotetrazolate (v) anions.*

6.4.1 Tetrazole *N*-oxides

There are three main classes of energetic tetrazole *N*-oxides, that is those based on 5-aminotetrazolate, 5-nitrotetrazolate, 5-cyanotetrazolate, and 5-azidotetrazolate anions (Figure 6.8). Each of the tetrazoles differs only on the functional group, which is located at the C atom of the tetrazole ring (5-position).

5-Aminotetrazole is one of the most important starting materials in tetrazole chemistry, and has been used extensively to prepare a large number of nitrogen-rich energetic materials that contain the tetrazole group [25]. Furthermore, 5-aminotetrazole has the advantage of being commercially available and is not sensitive, and is therefore easy to handle. The preparation of the *N*-oxide derivative would therefore be of considerable interest – also for use in the synthesis of *N*-oxide derivatives analogously to those that can be obtained from 5-aminotetrazole. However, the simple oxidation of the N1 ring atom using an oxidizer such as Oxone is not possible, since the $-NH_2$ group is present that can also be oxidized. Instead, 1-hydroxy-5-aminotetrazole was prepared by the reaction of the cyanogen azide intermediate (generated by the reaction of BrCN with NaN_3) with an excess of hydroxylamine followed by acidification [26]. The location of the $-OH$ group is at the N1 ring atom. (Figure 6.9). If acidification is not performed, then the tetrazolate *N*-oxide anion is obtained as its hydroxylammonium salt. However, generation of 1-hydroxy-5-aminotetrazole is an important step, since deprotonation of the $-OH$ group by nitrogen-rich Brønsted bases is possible and forms many nitrogen-rich salts containing the 1-*N*-oxide-5-aminotetrazolate anion (Figure 6.9). For example, reaction of 1-hydroxy-5-aminotetrazole with ammonia results in the formation of the corresponding ammonium salt (Figure 6.9). In contrast to the tetrazole 3*N*-oxides prepared by Harel and Rozen, which contain the zwitterionic N^+-O^- group [13], no zwitterionic N^+-O^- center is present in these tetrazolate *N*-oxide anions.

It was found that the hydroxylammonium 5-aminotetrazolate-1*N*-oxide crystallizes in two different polymorphs: orthorhombic with a density of $1.664\,g\,cm^{-3}$ and monoclinic with a higher density of $1.735\,g\,cm^{-3}$. In both polymorphs there is an extensive hydrogen bonding network between the NH_3OH^+ cations and the $N_5CH_2O^-$ anion in which each of the atoms on the $N_5CH_2O^-$ anion (except the C atom) participate in at least one hydrogen bond with a NH_3OH^+ cation. Whereas the ring N atoms only participate in one significant hydrogen bond in both polymorphs, the O atom of the *N*-oxide group of the orthorhombic polymorphs participates in three hydrogen bonds, whereas the O atom of the *N*-oxide group of the monoclinic polymorph participates in two (Figure 6.10) [26].

Interestingly, although the corresponding NH_4^+ salt ammonium 5-aminotetrazolate-1 *N*-oxide also shows a significant intermolecular hydrogen bonding network, it has a relatively

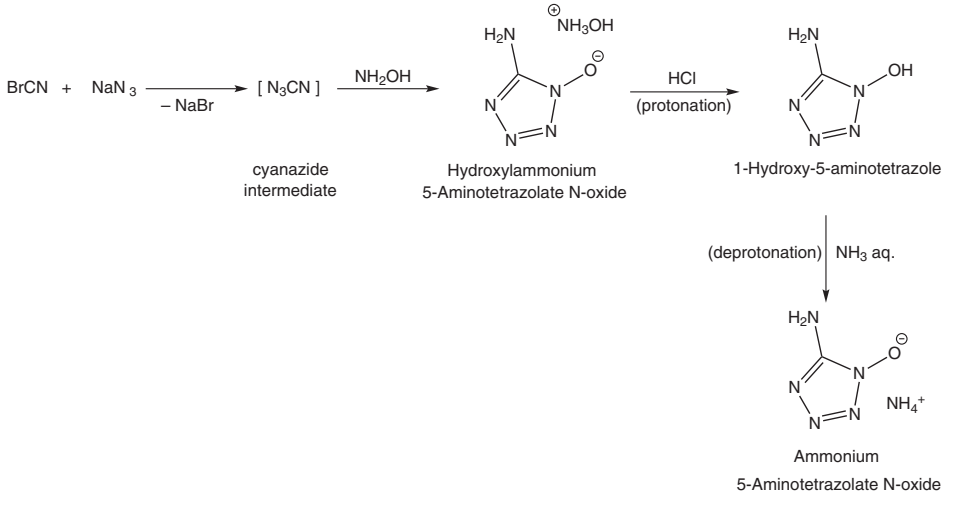

Figure 6.9 *The preparation of 1-hydroxy-5-aminotetrazole via the acidification of hydroxylammonium 5-aminotetrazolate-N-oxide formed from the reaction of BrCN with NaN_3 generating the N_3CN intermediate, which is then reacted with hydroxylamine. Deprotonation of 1-hydroxy-5-aminotetrazole by the Brønsted base NH_3 results in the formation of the corresponding ammonium salt. Reproduced with permission from [26] © 2012 WILEY-VCH Verlag GmbH & Co. KGaA, Weinheim.*

low density in the solid state ($\rho = 1.530\,\mathrm{g\,cm^{-3}}$) [26], which is considerably lower than the densities of both polymorphs of the hydroxylammonium 5-aminotetrazolate-1*N*-oxide ($\rho_{(\mathrm{orthorhombic})} = 1.664\,\mathrm{g\,cm^{-3}}$; $\rho_{(\mathrm{monoclinic})} = 1.735\,\mathrm{g\,cm^{-3}}$) [26]. This is reflected in the calculated detonation velocities that are much higher for the two hydroxylammonium 5-aminotetrazolate-1*N*-oxide polymorphs (orthorhombic = 9056 $\mathrm{ms^{-1}}$; monoclinic = 9312 $\mathrm{ms^{-1}}$) than for the NH_4^+ salt (8225 $\mathrm{ms^{-1}}$), which is a result of the low crystalline density of the ammonium salt [26].

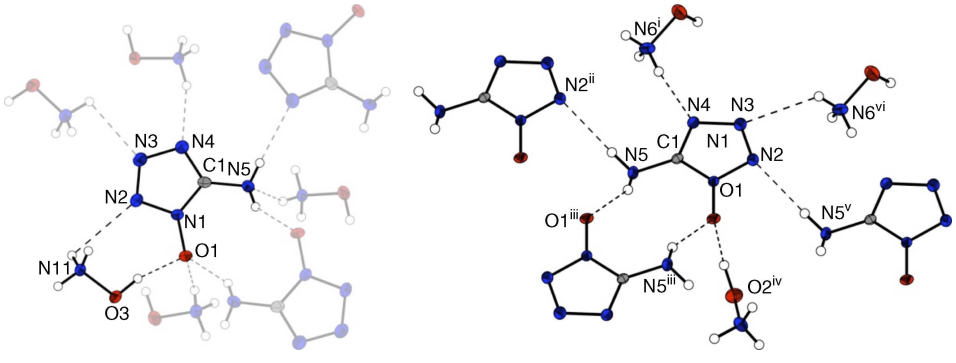

Figure 6.10 *Hydrogen bonding between one $CH_2N_5O^-$ anion and the NH_3OH^+ cations in the orthorhombic (left) and monoclinic (right) polymorphs of hydroxylammonium 5-aminotetrazolate-1N-oxide.*

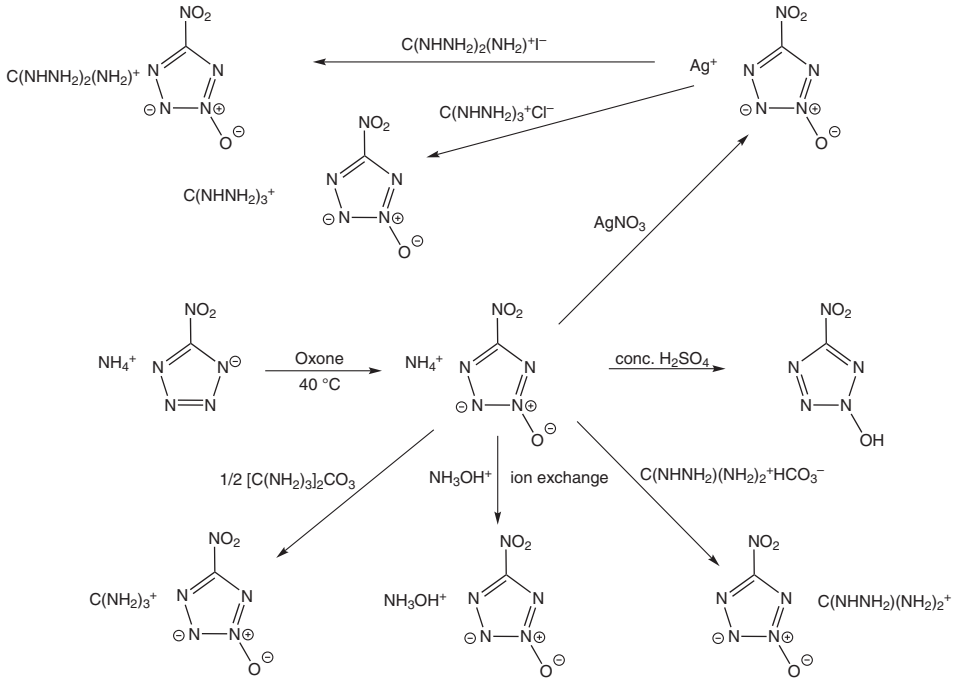

Figure 6.11 *Scheme showing the preparation of ammonium nitrotetrazolate-2*N*-oxide by oxidation of ammonium 5-nitrotetrazolate using Oxone and the subsequent use of ammonium nitrotetrazolate-2*N*-oxide as a starting material for the synthesis of a wide range of salts containing nitrogen-rich cations obtained by different cation exchange methods.*

If we now change the functional group located at the C-atom of the tetrazole ring (5-position) from $-NH_2$ to $-NO_2$, then another large number of salts containing the 2-hydroxide-5-nitrotetrazolate anion that shows the N → O functionality at the N2 position can be prepared. The most convenient method was to oxidize the ammonium salt of the 5-nitrotetrazolate anion using Oxone as the oxidizer (Figure 6.11) [15,27]. The ammonium as well as the silver nitrotetrazolate-2*N*-oxide salt was then used as the starting material for the preparation of other salts using different methods of cation exchange, which are summarized in Figure 6.11.

It would be futile here to give an in-depth discussion of the different characterization methods used and sensitivity data obtained for each individual salt, but we will focus on a few selected examples. If we compare the sensitivity data of silver 5-nitrotetrazolate-2*N*-oxide with that of the closely related nonoxidized silver 5-nitrotetrazolate, then we can see that the introduction of the *N*-oxide moiety has a considerable stabilizing effect. Whereas silver nitrotetrazolate is a highly sensitive primary explosive (IS < 1 J, FS < 5 N), silver nitrotetrazolate-2*N*-oxide is not a real primary explosive (IS = 5 J, FS = 120 N), (Table 6.1) [27]. A comparison of the multinuclear NMR data of ammonium nitrotetrazolate and ammonium nitrotetrazolate-2*N*-oxide proved interesting (Table 6.1) [27,28]: the ^{13}C chemical shift for the ring C atom in ammonium nitrotetrazolate ($\delta = 169.5$ ppm) is significantly shifted to low field in comparison with the corresponding signal for ammonium nitrotetrazolate-2*N*-oxide

Table 6.1 *Comparison of selected properties of salts containing the 5-nitrotetrazolate (5-NT) anion with those containing the 5-nitrotetrazolate-2N-oxide (5-NT2O) anion. Values marked with * were calculated using EXPLO5.04.*

Property	5-NT salt	Value	Property	5-NT2O salt	Value
$\delta/^{13}$C NMR	NH_4^+	169.5 ppm	$\delta/^{13}$C NMR	NH_4^+	158.4 ppm
$\delta/^{14}$N NMR	NH_4^+	19 (N2/N3), −22 (N5), −62 (N1,N4), −359 ($NH4^+$)	$\delta/^{15}$N NMR	NH_4^+	−28.8, −30.1, −33.3, −75.6 ($-NO_2$), −103.4, −360.3 (NH_4^+)
ρ/cm^{-3}	NH_4^+	1.637	ρ/cm^{-3}	NH_4^+	1.7304
	$C(NH_2)_3^+$	1.644		$C(NH_2)_3^+$	1.6978
	$C(NHNH_2)_3^+$	1.601		$C(NHNH_2)_3^+$	1.6391
	NH_3OH^+	–		NH_3OH^+	1.850
BAM impact/J	Ag^+	<1	BAM impact/J	Ag^+	5
	NH_4^+	<120		NH_4^+	7
	$C(NH_2)_3^+$	30		$C(NH_2)_3^+$	>40
	$C(NHNH_2)_3^+$	2		$C(NHNH_2)_3^+$	25
BAM friction/N	Ag^+	<5	BAM friction/N	Ag^+	120
	NH_4^+	<4		NH_4^+	120
	$C(NH_2)_3^+$	360		$C(NH_2)_3^+$	252
	$C(NHNH_2)_3^+$	48		$C(NHNH_2)_3^+$	72
ESD/mJ	Ag^+	<50	ESD/mJ	Ag^+	50
	NH_4^+	–		NH_4^+	250
	$C(NH_2)_3^+$	–		$C(NH_2)_3^+$	200
	$C(NHNH_2)_3^+$	–		$C(NHNH_2)_3^+$	200
T_{dec}/°C			T_{dec}/°C		
	NH_4^+	210		NH_4^+	173
	$C(NH_2)_3^+$	217		$C(NH_2)_3^+$	211
	$C(NHNH_2)_3^+$	191		$C(NHNH_2)_3^+$	153
$\Delta_f U°$/kJ kg^{-1}			$\Delta_f U°$/kJ kg^{-1}		
	NH_4^+	1413		NH_4^+	1135
	$C(NH_2)_3^+$	961		$C(NH_2)_3^+$	830
	$C(NHNH_2)_3^+$	2334		$C(NHNH_2)_3^+$	2126
V_{Det}/ms^{-1} *			V_{Det}/ms^{-1} *		
	NH_4^+	8328		NH_4^+	8767
	$C(NH_2)_3^+$	7895		$C(NH_2)_3^+$	8270
	$C(NHNH_2)_3^+$	8396		$C(NHNH_2)_3^+$	8617

($\delta = 158.4$ ppm). The ^{15}N NMR spectra were also recorded. Although ^{14}N NMR spectra would be more convenient to record due to the much higher natural abundance of the ^{14}N isotope (99.7%) in comparison with the ^{15}N NMR isotope (0.3%), the quadropolar moment of the ^{14}N nucleus ($I = 1$) results in broad signals for tetrazole ring N atoms (^{15}N: $I = ½$). In the ^{15}N NMR spectrum of ammonium nitrotetrazolate [28], due to the location of the $-NO_2$ group on the ring at the 5-position (C-atom), there are only two ^{15}N signals to be expected for the tetrazole ring N atoms. In contrast, the location of the *N*-oxide group at the N2 position of the tetrazole ring in ammonium nitrotetrazolate-2*N*-oxide results in four signals for the tetrazole ring N atoms since they are all now nonequivalent. Finally, the largest change in the chemical shift in the ^{15}N NMR spectrum is that for the signal, which corresponds to the N2 ring N atom

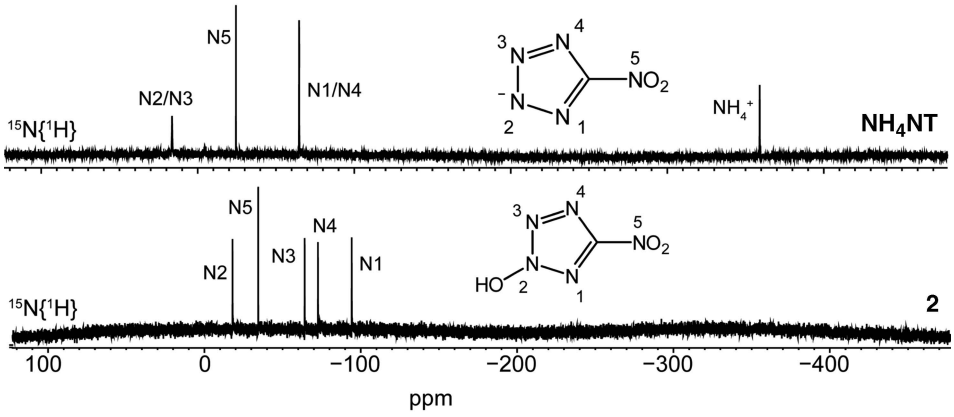

Figure 6.12 *Comparison of the $^{15}N\{^1H\}$ NMR spectra of ammonium nitrotetrazolate (top) and 2-hydroxy-nitrotetrazolate (bottom). Reproduced with permission from [27] © 2010 American Chemical Society.*

in ammonium nitrotetrazolate-2*N*-oxide [27]. In both the nitrotetrazolate salts and the nitrotetrazolate-2*N*-oxide salts, the chemical shift of the $-NO_2$ group remains similar (Figure 6.12). Therefore, from the NMR spectra in solution, the formation of the *N*-oxide derivative is supported. The additional use of ^1H NMR spectroscopy to determine the site of protonation of the nitrotetrazolate-2*N*-oxide anion forming the free acid nitrotetrazole-2*N*-oxide in solution was also successful, since the very high chemical shift observed for the free acid ($\delta = 12.99$ ppm) is not in the range expected for the $-N-H$ group if protonation of one of the ring N atoms had occurred and is indicative of the presence of an $-OH$ group and, furthermore, no $^{15}N-^1H$ coupling was observed in the ^{15}N NMR spectrum, which would be expected if the $-NH$ functional group was present, but not if the $-OH$ group was present [27]. In addition, calculation of the four tautomers of the acid of the nitrotetrazolate-2*N*-oxide anion showed that the tautomer with $O-H$ connectivity should be the lowest in energy, with the tautomers with N1-H, N3-H and N4-H being higher in relative energy by 7.6, 4.2, and 4.6 kcal mol^{-1} respectively [27].

Furthermore, in the crystalline state, the structure of the acid of the 5-nitrotetrazolate-2*N*-oxide anion was shown to exhibit $-OH$ connectivity (Figure 6.13) [27]. The solid state structures of the salts investigated that contain the nitrotetrazolate-2*N*-oxide anions show that the crystal density is higher in comparison with the corresponding nonoxidized salts of the 5-nitrotetrazolate anion (Table 6.1). This has been shown to be the result of the 5-nitrotetrazolate-2*N*-oxide anion being able to participate in more intermolecular hydrogen bonding interactions in comparison with the 5-nitrotetrazolate anion (Figure 6.13).

Despite the presence of the strong intermolecular interactions, the triaminoguanidinium salt has a low decomposition of only 153 °C, whereas the ammonium salt decomposes thermally at 211 °C. The decomposition temperature was reported to decrease with increasing numbers of amino substituents on the guanidinium cation. However, the ammonium salt shows a violent thermal decomposition. Table 6.1 shows that the nitrogen rich salts containing the 5-nitrotetrazolate-2*N*-oxide anions decompose at lower temperatures than the corresponding 5-nitrotetrazolate salts, leading to the general statement that the *N*-oxide compounds are thermally less stable.

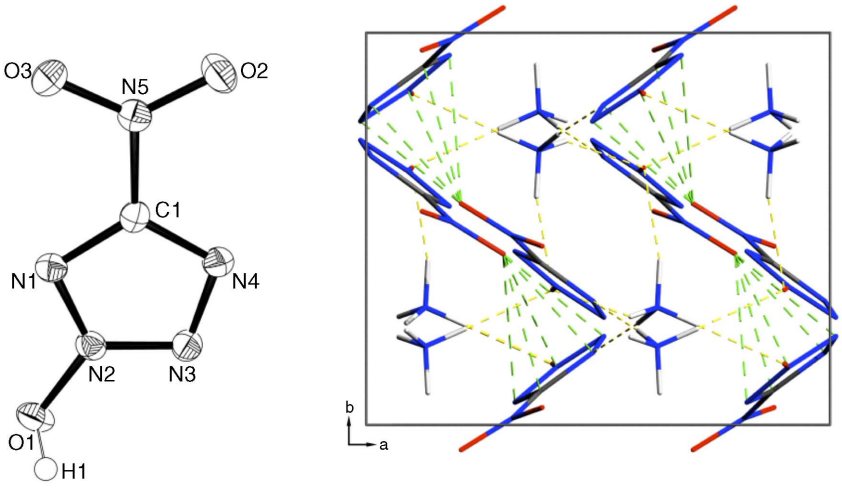

Figure 6.13 *ORTEP representation of the molecular structure of 2-hydroxy-5-nitrotetrazole (left) and the unit cell packing of ammonium 5-nitrotetrazolate-2N-oxide viewed along the c axis (right). Dashed lines indicate intermolecular hydrogen bonding. Reproduced with permission from [27] © 2010 American Chemical Society.*

Computational work showed that the calculated heats of formation of the salts containing the 5-nitrotetrazolate-2*N*-oxide anion were lower (i.e., the compound is less endothermic) than the corresponding 5-nitrotetrazolate salt [27]. Despite this disadvantageous property (in terms of desired properties for an energetic material), the NH_4^+, $C(NHNH_2)_2NH_2^+$ and $C(NHNH_2)_3^+$ salts of the 5-nitrotetrazolate-2*N*-oxide anion have detonation velocities and pressures that are similar to those of RDX [29], whereas the hydroxylammonium salt has detonation properties that are better than those of β-HMX [30]. Furthermore, the detonation velocities of the 5-nitrotetrazolate-2*N*-oxide salts are significantly higher than for the 5-nitrotetrazolate salts – despite the larger positive heats of formation for the 5-nitrotetrazolate salts – which is a consequence of the higher densities of the 5-nitrotetrazolate-2*N*-oxide salts, which more than compensate for their lower heats of formation [27]. Finally, the measured sensitivities of the 5-nitrotetrazolate-2*N*-oxide salts were shown to be lower than the corresponding 5-nitrotetrazolate salts (with the exception of the $C(NHNH_2)NH_2^+$ salt) and the guanidinium and substituted guanidinium salts were found to have lower sensitivities and therefore to be less sensitive than RDX – a property that is important for improved insensitive munitions (IMs).

Related compounds have also been prepared in which the electron withdrawing $-NO_2$ group at the 5-position of the 5-nitrotetrazolate-2*N*-oxide anions was replaced by the electron withdrawing $-CN$ group resulting in 5-cyanotetrazolate-*N*-oxides [17]. In contrast to the 5-nitrotetrazolate-*N*-oxide anions in which the *N*-oxide functional group was found at the 2-position [15], for the 5-cyanotetrazolate-*N*-oxides the $N \rightarrow O$ functional group could be located either at the 1-position or at the 2-position, depending on the synthetic route used for the formation of the 5-cyanotetrazolate-*N*-oxide [17].

The sodium salt of the cyanotetrazolate-2*N*-oxide anion was prepared in the same way as the 5-nitrotetrazolate-2*N*-oxide salts, namely by the reaction of sodium 5-cyanotetrazolate with Oxone [17]. The silver salt could then be prepared by reaction of the sodium salt with

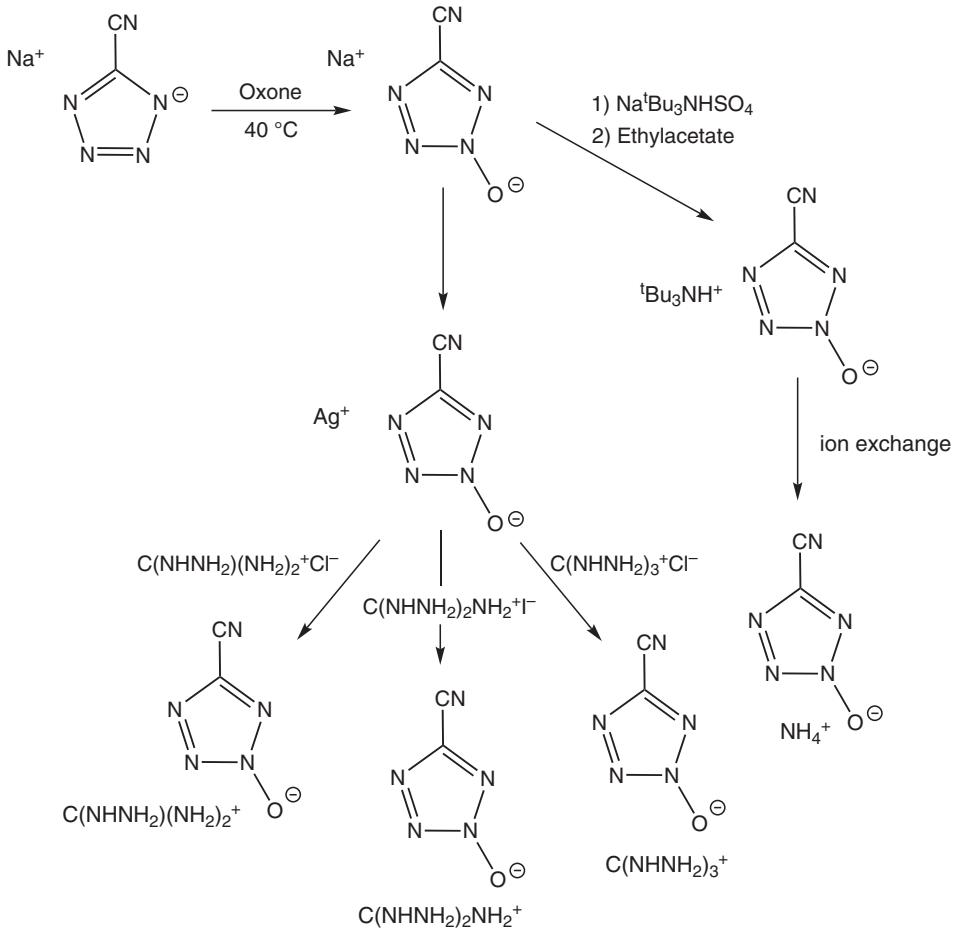

Figure 6.14 *Scheme showing the formation of the 5-cyanotetrazolate-2*N*-oxide anion and its nitrogen-rich salts.*

$AgNO_3$ [17]. The silver salt was particularly useful in metathesis reactions with salts containing nitrogen-rich cations (Figure 6.14) [17].

The sodium salt of the cyanotetrazolate-1*N*-oxide anion was prepared very differently. Azidoaminofurazane was reacted with $NaNO_2$ and HOAc forming the sodium salt of 5-cyanotetrazolate-1*N*-oxide [31]. This salt could then either be protonated to form the corresponding acid with the −OH functional group, or it could be reacted with $AgNO_3$ to form the silver 5-cyanotetrazolate-1*N*-oxide, which could then be used in metathesis reactions to form salts containing nitrogen-rich cations instead of nonenergetic Na^+ or Ag^+ cations (Figure 6.15) [17].

^{15}N NMR and IR spectroscopy clearly showed the presence of one noncyclized −CN group in both the 1*N*-oxide and 2*N*-oxide salts. The ν(CN) stretch at high wavenumbers about 2255 cm^{-1} in the IR spectra of all of the 5-cyanotetrazolate-*N*-oxide compounds was observed

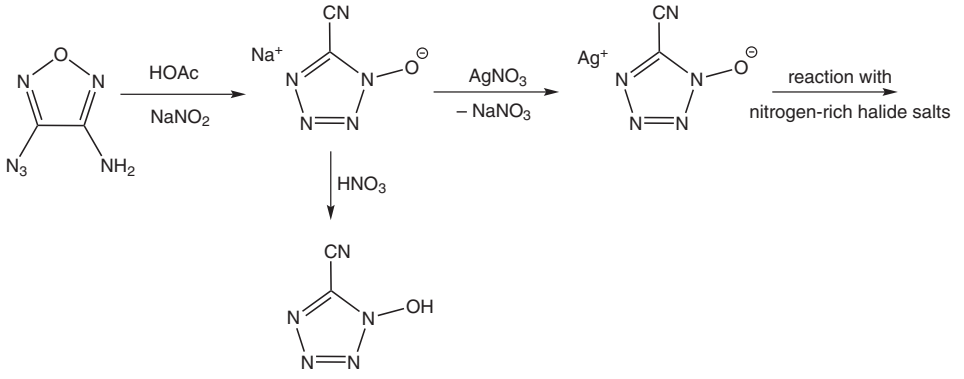

Figure 6.15 *Scheme showing the formation of the 5-cyanotetraolate-1N-oxide anion and its acid and silver salt.*

as a strong peak and the N−O functional group showed the characteristic band in the region between 1430 and 1674 cm^{-1} [17]. The planar 5-cyanotetrazolate-*N*-oxide rings (1*N*-oxide or 2*N*-oxide) observed in the anions, however, do not result in high densities for the nitrogen-rich salts, which were measured experimentally to be only in the range of 1.504–1.583 g cm^{-3}. The resulting calculated detonation velocities are therefore disappointing, reaching a maximum value of 8214 m s^{-1} for triaminoguanidinium 5-cyanotetrazolate-1*N*-oxide (8044 m s^{-1} for the corresponding 2*N*-oxide salt) [17] corresponding to a comparable or slightly higher performance than TNT [32], but lower than the minimum desired values that are observed for RDX [29] and β-HMX [30], which are currently in use. Finally, the sensitivities of the nitrogen-rich salts of the 5-cyanotetrazolate-N-oxide anions were determined to lie in the range, which would classify them as less sensitive to sensitive energetic materials [33–38].

Replacing the cyano group (−CN is a pseudohalogen) at the 5-position by the azide group ($-N_3$ is also a pseudohalogen) results in quite a different story, however. The nonoxidized salts containing the 5-azidotetrazolate anion are treacherously explosive [39] as is the corresponding acid [40], which should only be prepared in small quantities with stringent adherence to safety requirements. Due to their extremely high sensitivities, the salts containing the 5-azidotetrazolate anion are extremely difficult to handle. Since it has been shown that, in general, the formation of an *N*-oxide derivative of tetrazolate anions reduces the sensitivity of tetrazolates to mechanical stimuli, the preparation of the *N*-oxide derivatives of the 5-azidotetrazolate anion were investigated, with the hope that the sensitivities of the resulting salts would be reduced in comparison with the nonoxidized salts, and in addition, even although they would possess lower heats of formation, due to the higher densities they would be expected to show in the crystalline state they would show higher performances. This would mean that the danger in handling would be reduced, but the performance would be increased – a win, win situation.

Unfortunately the synthetic route started from 5-azido-1*H*-tetrazole, which is so explosive that it has to be weighed out multiple times in small quantities to avoid handling a dangerous quantity at one time [41]. After deprotonation and *in situ* reaction oxidation of the 5-azidotetrazolate, which was generated using Oxone, the corresponding 5-azidotetrazolate-2*N*-oxide anion was formed *in situ* and protonated with concentrated H_2SO_4 to generate the corresponding acid. This acid was then deprotonated to give the pure ammonium

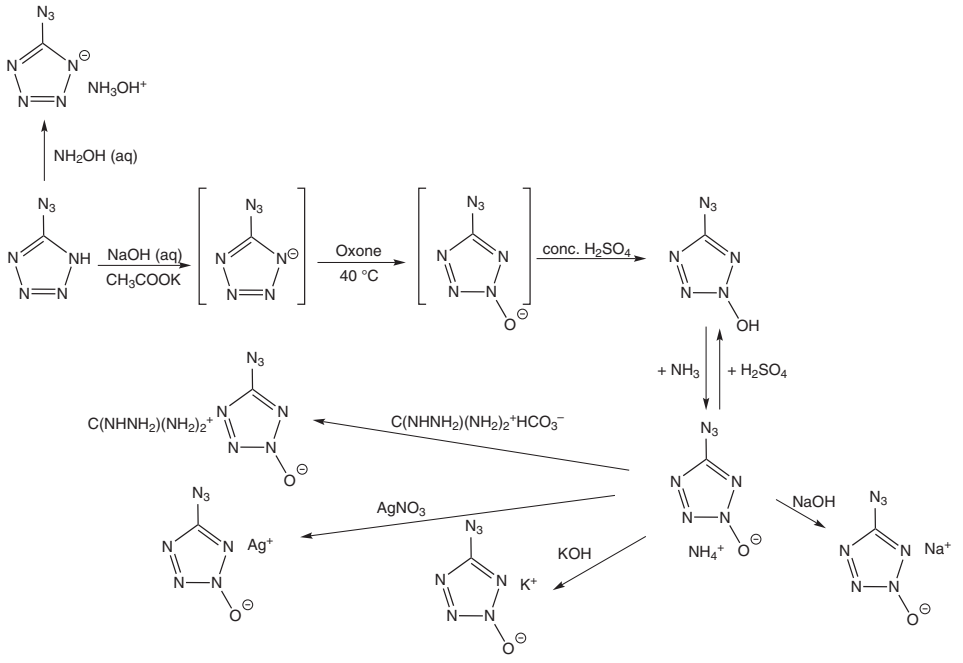

Figure 6.16 *Scheme showing the generation of $NH_4^+CN_7O^-$ via oxidation of the 5-azidotetrazolate anion using Oxone and subsequent cation exchange reactions.*

5-azidotetrazolate-2*N*-oxide salt. Not only was this salt interesting as it was a constitutional isomer of hydroxylammonium 5-azidotetrazolate, it was also a good starting material for cation exchange reactions. Furthermore, acidification of the pure $NH_4^+CN_7O^-$ salt resulted in pure HCN_7O (Figure 6.16) [40].

Whereas the $Na^+CN_7O^-\cdot 2H_2O$ salt was described as being safe to handle, the anhydrous potassium salt and silver salt were both described as being highly sensitive. In fact, $Ag^+CN_7O^-$ is so sensitive, that it frequently explodes in the solid state when dry on attempts to manipulate it [41]. To determine the effect of the *N*-oxide on the properties of the CN_7^- ring, the ammonium salts of CN_7^- and CN_7O^- can be compared (Table 6.2). Although the introduction of the *N*-oxide group reduces the sensitivity (higher impact sensitivity, friction sensitivity, and ESD values), it also results in a decrease in the thermal stability, whereby $NH_4^+CN_7^-$ decomposes in an exothermic manner at 157 °C [39], whereas $NH_4^+CN_7O^-$ decomposes already at 145 °C [41], and a decreased value for the heats of formation, thereby making it a less endothermic compound. Despite this, again the higher density of the *N*-oxide ($\rho = 1.689\ g\ cm^{-3}$) [41] derivative in the solid state ($NH_4^+CN_7^-$: $\rho = 1.61\ g\ cm^{-3}$) [39] results in a higher performance for $NH_4^+CN_7O^-$ than for $NH_4^+CN_7^-$ such that $NH_4^+CN_7O^-$ has a higher calculated heat of explosion, detonation pressure, and detonation velocity than $NH_4^+CN_7^-$. In addition, the oxygen balance is, of course, better in $NH_4^+CN_7O^-$ than in $NH_4^+CN_7^-$. This is an excellent example that shows that a compound that is less endothermic can still show a higher performance and better sensitivity than a more endothermic compound. Compounds that show this combination of higher performance but less sensitivity are often extremely difficult to achieve, but

Table 6.2 *Experimentally determined and calculated values for ammonium 5-azidotetrazolate ($NH_4^+CN_7^-$) [39] and ammonium 5-azidotetraozlate-2<fiN</i-oxide ($NH_4^+CN_7O^-$) [41]. Values marked * were calculated using EXPLO5.04.*

Property	Ammonium 5-azidotetrazolate-2*N*-oxide, $NH_4^+CN_7O^-$	Ammonium 5-azidotetrazolate, $NH_4^+CN_7^-$
Impact sensitivity/J	1	<1
Friction sensitivity/N	10	<5
ESD/J	30	10
$T_{dec.}$/°C	151	157
$\Delta_f H°$(s)/kJ mol^{-1}	534	544
$\Delta_f U°$(s)/kJ kg^{-1}	3817	4360
Ω (oxygen balance)/%	−33.3	−50.0
ρ/g cm^{-3}	1.69	1.61
*T_E/K	3960	3498
*ρ_{C-J}/g cm^{-3}	325	287
*D/ms^{-1}	8926	8917

show that careful and clever modification of seemingly "*untamable*" compounds can result in more "*tame*" compounds but with superior performance. It is worthwhile pointing out here that $NH_3OH^+CN_7^-$ is a constitutional isomer of $NH_4^+CN_7O^-$. Not only is the nonoxidized $NH_3OH^+CN_7^-$ more sensitive [41] than $NH_4^+CN_7O^-$ [39], it also has a second disadvantage of a lower density in the crystalline state.

If we now briefly look at the structure of $NH_4^+CN_7O^-$ in the crystalline state, we can see that the CN_7O^- anions are essentially planar and that the O atoms of the *N*-oxide groups participate in hydrogen bonding with the NH_4^+ cations, thus stabilizing the salt in the solid state and reducing its sensitivity to mechanical stimuli. In fact, one NH_4^+ cation shows hydrogen bonding to four separate CN_7O^- anions: three of these hydrogen bonds involve the O atoms of the *N*-oxide groups, whereas only one involves a ring N atom (Figure 6.17) [41]. If a closer look is taken at the structure of one CN_7O^- anion in, for example, $NH_4^+CN_7O^-$, then we can see that a covalent azide group is present in which the $N_\alpha-N_\beta$ bond length (1.253(2) Å) is longer than the $N_\beta-N_\gamma$ (1.118(2) Å) bond length and the $C-N_\alpha-N_\beta$ angle is bent (113°) and the $N_\alpha-N_\beta-N_\gamma$ angle is nonlinear (173°). These characteristics are typical for a covalent azide and not for an ionic azide. It is worthwhile mentioning, however, that whereas in the $NH_4^+CN_7O^-$ salt the azide and the N−O group are pointing away from each other [41], in some other salts, such as $K^+CN_7O^-$, the azide and N−O groups are pointing in the same direction [41]. Another important feature is the d(N−O) bond length of the *N*-oxide group, which is found in the region of 1.280–1.311 Å. These values lie between the common bond lengths that are observed for N−O single bonds (d(N−O) = 1.45 Å) and N=O double bonds (d(N=O) = 1.17 Å) [42,43], which indicates that the *N*-oxide group in these compounds shows considerable multiple bond character.

At this stage it would be useful to summarize the important properties of the 5-substitued tetrazolate-*N*-oxide salts that have been discussed so far, before moving on to consider the *N*-oxide derivatives of bistetrazoles. As we can see in Table 6.3, the functional group at the 5-position of the tetrazole ring has a marked effect on the energetic properties of the corresponding NH_4^+ salt containing the tetrazolate anion. However, the introduction of an

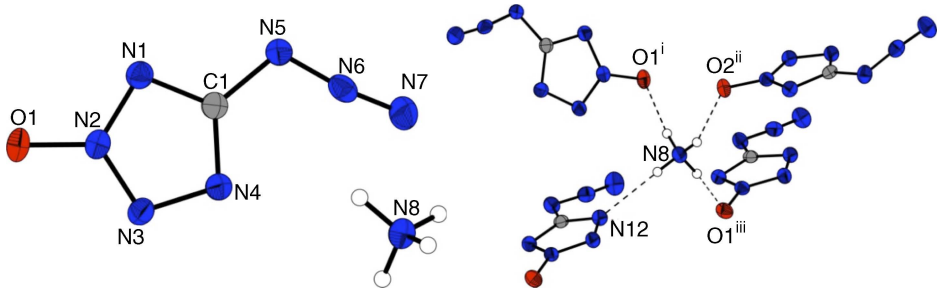

Figure 6.17 *Molecular structure of $NH_4^+CN_7O^-$ in the crystalline state (left) and the hydrogen bonding between the NH_4^+ cations and four CN_7O^- anions (right). Reproduced with permission from [41] © 2011 WILEY-VCH Verlag GmbH & Co. KGaA, Weinheim.*

N-oxide group usually results in lower thermal stabilities, higher densities, higher detonation velocities, and lower sensitivities. Particularly for tetrazolate salts, which are highly sensitive are very difficult to handle, the introduction of the *N*-oxide group can be hugely beneficial in (usually) lowering the sensitivities of the salts thereby making them often easier to work with.

6.4.2 Bis(tetrazole-*N*-oxides)

Bis(tetrazoles) are compounds in which two tetrazole rings are directly bonded to one another either through the C atoms of each tetrazole ring, through one ring N atom from each ring, or through the C atom of one tetrazole ring with the N atom of the other tetrazole ring [50]. So far, *N*-oxide derivatives have only been prepared of the bistetrazoles in which the tetrazole rings are joined through two C atoms. The site of the N → O functional groups on each tetrazole ring, however, can be either 1,1′ or 2,2′ or less importantly 1,2′ depending on other substituents on the tetrazole ring systems.

Energetic salts containing the 1,1′-bis(tetrazolate-1*N*-oxide) anion with the empirical formula $C_2N_8O_2^{2-}$ have been extensively investigated in recent years. Not only have salts of the type $(Cat^+)_2C_2N_8O_2^{2-}$ been prepared in which two N−O groups are present in the anion and two countercations are present (2 : 1 salts), but also salts of the type $(Cat^+)C_2HN_8O_2^-$ in which one protonated *N*-oxide group N−OH is present as well as one N−O group (1 : 1 salts), as well as salts of the type $(Cat^{2+})C_2N_8O_2^{2-}$ in which two N−O groups are present and a counteraction that has +2 charge (1 : 1 salts) [51]. In addition, the neutral $C_2H_2N_8O_2$ molecule has been prepared and isolated [51]. The neutral molecule 5,5′-bis(1-hydroxytetrazole) dihydrate ($C_2H_2N_8O_2$) was prepared in accordance with the reaction shown in Figure 6.18 above, by the ring closing reaction of diazidoglyoxime. Since diazidoglyoxime is a covalent diazide, the ring closure can occur twice to form two tetrazole-1*N*-oxide rings.

First of all, if we look at the neutral molecule 5,5′-bis(1-hydroxytetrazole) dihydrate, we can see that the two tetrazole rings are joined via the two carbon atoms and the N−OH groups are located in the 1-position of the tetrazole rings, but in a trans arrangement. The acidic proton of the −OH group forms hydrogen bonds with the two water molecules present, which stabilizes the molecule. The free acid dihydrate can be dehydrated if heated

Table 6.3 *Overview of selected properties of the ammonium salts of 5-substituted tetrazolates and of 5-substituted tetrazolate* N*-oxides. Values marked with * were calculated using EXPLO5.04 [44–48].*

Property	NH_4_ATX [26]	NH_4_CNT [49]	NH_4_CNT2X [17]	NH_4_CNT1X [17]	NH_4_NT [28]	NH_4_NT2X [15,27]	NH_4_AZT [39]	NH_4_AZT [41]
IS/J	>40	<25	15	35	1	7	<1	1
FS/N	>360	>360	216	360	120	120	<5	10
ESD/J	1.5	–	0.30	0.75	–	0.25	10	30
$T_{dec.}$/°C	195	191	184	172	210	173	157	151
$\Delta_f H°$(s)/kJ mol^{-1}	227	313	326	355	172	152	534	544
$\Delta_f U°$(s)/kJ kg^{-1}	2056	2796	2543	2770	1413	1135	3817	4360
Ω/%	−54.19	−45.3	−62.45	−62.45	−24.2	−10.80	−50.0	−33.31
ρ/g cm^{-3}	1.530	1.499	1.554	1.526	1.637	1.730	1.61	1.689
*T_E/K	3007	3277	3288	3412	3678	4218	3498	3960
*$p_{C\text{-}J}$/kbar	245	176	222	220	274	322	287	325
*D/ms^{-1}	8225	7138	7749	7730	8328	8885	8917	8926

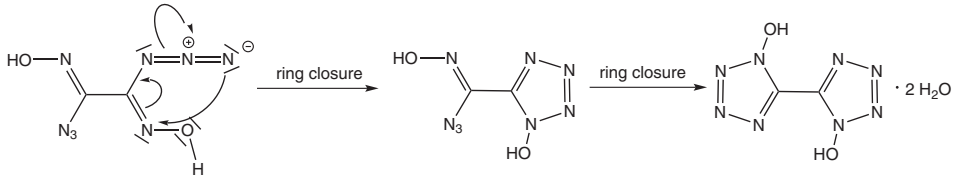

Figure 6.18 *Scheme showing a mechanism for one ring closure in diazidoglyoxime forming a tetrazole ring. A second ring closure also occurs involving the second azide group to form 5,5′-bis(1-hydroxytetrazole).*

to 140 °C for 24 h; however, by doing this the sensitivity of the molecule is increased considerably. DSC measurements have shown that the free acid loses water at 115 °C and subsequent decomposition of the dehydrated material occurs at 214 °C. The two H atoms of the −OH groups can be removed when a sufficiently strong Brønsted base is used (Figure 6.19), forming nitrogen-rich salts containing the 5,5′-bis(tetrazolate-1*N*-oxide) dianion. The two tetrazole rings are planar with respect to one another and the density of the dihydrate is 1.81 g cm^{-3} in the crystalline state [51].

The 5,5′-bis(1-hydroxytetrazole) dihydrate molecule is the starting material for a large number of derivatives (mainly salts), which can be grouped into four different classes. In the first class, the −OH groups of the 5,5′-bis(1-hydroxytetrazole) molecule have both been deprotonated, resulting in an anion with a −2 charge. Two cations each with a +1 charge are present resulting in a 2 : 1 salt (2 cations : 1 anion). In the second class, again both −OH groups have been deprotonated, however in these salts only one countercation is present, which has a +2 charge, resulting in 1 : 1 salts (1 cation : 1 anion). The third class shows a −1 anion present, which is the result of only one of the two −OH groups in the 5,5′-bis(1-hydroxytetrazole) molecule being deprotonated. Again a countercation with +1 charge is present resulting also in salts of the type 1 : 1, but this time with only +1/−1 charged ions present. Finally, the 5,5′-bis(1-hydroxytetrazole) molecule can also form a Lewis acid-base adduct with the Lewis base 2-methyl-5-aminotetrazole, which is neutral (Figure 6.20) [51].

The bond lengths observed in the neutral 5,5′-bis(1-hydroxytetrazole) molecule, singly deprotonated and doubly deprotonated anions, show essentially no significant differences in

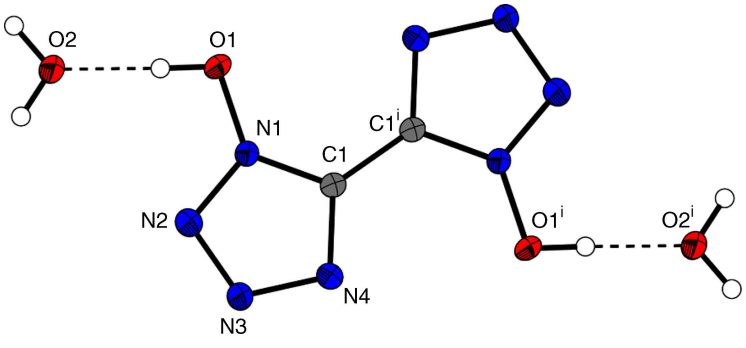

Figure 6.19 *Molecular structure of 5,5′-bis(1-hydroxytetrazole) dihydrate in the crystalline state showing hydrogen bonding interactions between the two −OH groups and the two water molecules.*

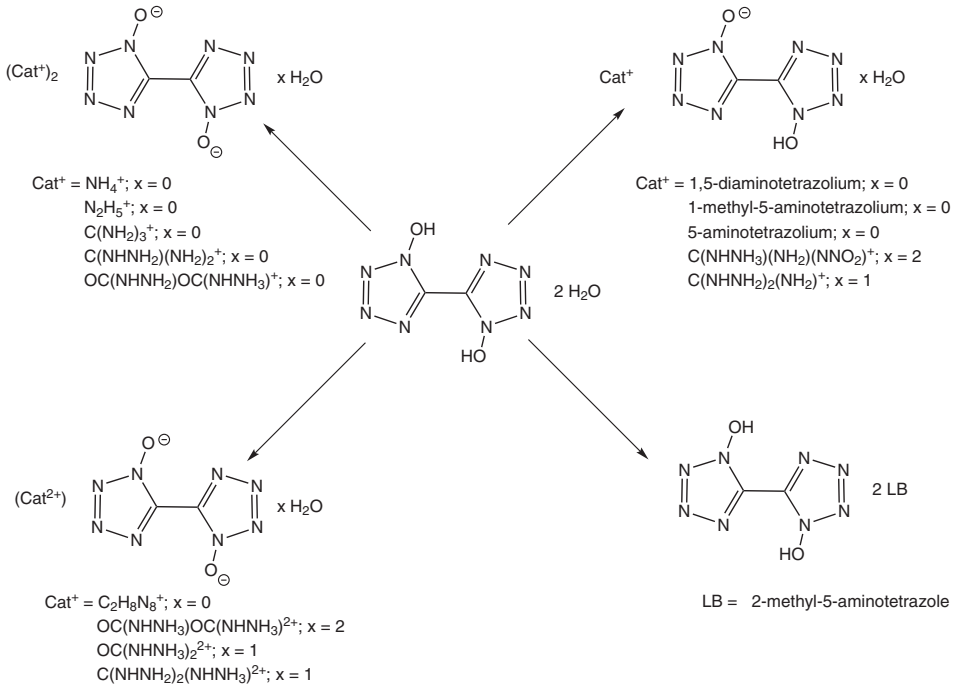

Figure 6.20 *Scheme showing the reactivity of 5,5′-bis(1-hydroxytetrazole) dihydrate towards nitrogen-rich compounds.*

bond lengths within the anions. The molecular structure of the guanidinium salt of the doubly deprotonated 5,5′-bis(1-hydroxytetrazole) molecule shows two planar rings that are coplanar with respect to each other. The bond lengths within the two tetrazole rings are in the region between C−N/N−N single bond and C=N/N=N double bonds and are indicative of the presence of multiple bond character and delocalization of the 6π electrons within the ring. The N−O bonds are shorter than the values expected for N−O single bonds and therefore also indicate multiple bond character, as does the C−C bond connecting the two tetrazole rings, which is also shorter than a C−C single bond but longer than a C=C double bond. Two guanidinium cations are present per molecular unit and form strong hydrogen bonds with both ring N atoms as well as the oxygen atoms of the N−O groups (Figure 6.21) [51]. Despite this, the guanidinium salt $(C(NH_2)_3^{+})_2C_2N_8O_2^{2-}$, also described in another crystallographic study this year [24], shows a relatively low density in the crystalline state for a 2 : 1 salt ($\rho = 1.639\ g\ cm^{-3}$) and is considerably lower than the densities observed for the bis(oxalyldihydrazinium) ($\rho = 1.828\ g\ cm^{-3}$), diammonium ($\rho = 1.800\ g\ cm^{-3}$), and dihydrazinium ($\rho = 1.725\ g\ cm^{-3}$) salts, but higher than that observed for the bis(aminoguanidinium) salt ($\rho = 1.596\ g\ cm^{-3}$). Here it is worth pointing out that all of the $(Cat^{+})_2C_2N_8O_2^{2-}$ salts, which were structurally characterized in the solid state, did not show the presence of crystal water.

If the sensitivities of these salts (X_2_BT1O) are compared with those of salts of 5,5′-bistetrazole (X_2_55BT), for example ammonium and guanidinium, interestingly the *N*-oxides have slightly higher sensitivities, but also significantly better performances

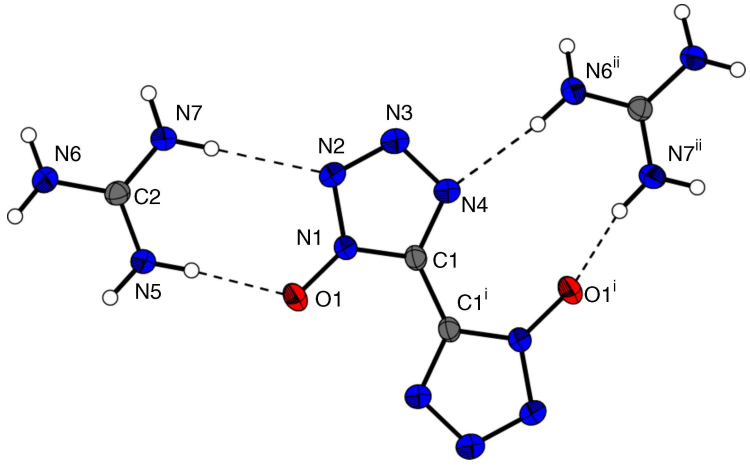

Figure 6.21 *Molecular structure of the bis(guanidinium) salt of 5,5′-bis(1-hydroxytetrazole), showing the strongest hydrogen bonding present between the cations and anions.*

($(NH_4)_2$_55BT: $IS > 40$ J, $FS > 360$ N, $D = 7417$ m s^{-1}; $(NH_4)_2$_BT1O: $IS = 35$ J, $FS = 360$ N, $D = 8817$ m s^{-1}; G_2_55BT: $IS > 40$ J, $FS > 360$ N, $D = 7199$ m s^{-1}; G_2_BT1O: $IS > 40$ J, $FS > 360$ N, $D = 7917$ m s^{-1}).

Salts were also isolated containing the doubly deprotonated $C_2N_8O_2^{2-}$ anion but only 1 : 1 salts since a +2 charged cation, such as the triaminoguanidinium cation, $C(NHNH_2)_2NHNH_3^{2+}$ is present as the countercation. This salt could be easily prepared by the reaction of the neutral 5,5′-bis(hydroxytetrazole) dihydrate with an aqueous solution of triaminoguanidinium chloride under reflux. Other salts, such as the diaminouronium salt were prepared in the same way from the reaction of 5,5′-bis(hydroxytetrazole) dihydrate with the Brønsted base diaminourea. A 1 : 1 salt arises from the double deprotonation of the diaminourea base, whereby both protons are abstracted from the −OH groups of 5,5′-bis (hydroxytetrazole) dihydrate (Eq. (6.1)) [51].

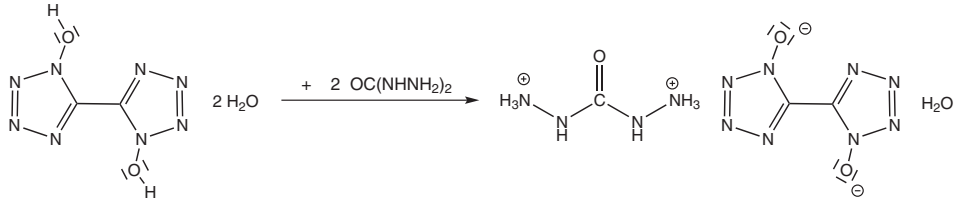

(6.1)

The decomposition temperatures of the $Cat^{2+}A^{2-}$ salts that were investigated are all over 200 °C [51] and higher than the decomposition temperature for RDX (205 °C) [29], but lower than that for β-HMX ($T_{dec.} = 275$ °C) [30] except for the 3,6-bishydrazino-1,2,4,5-tetrazinium salt, which has a disappointingly low decomposition temperature of 180 °C. Despite the high density of the oxalyldihydrazinium (dihydrate) salt ($\rho = 1.885$ g cm^{-3}), which is higher than that reported for RDX (ρ at 90 K = 1.858 g cm^{-3}) [29], the detonation velocity of this salt ($D = 8203$ ms^{-1}) and all of the other $Cat^{2+}A^{2-}$ salts that were

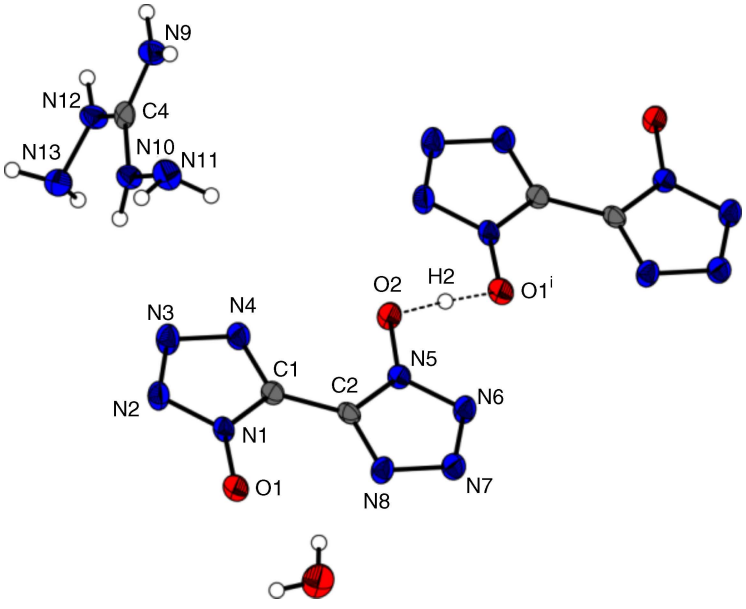

Figure 6.22 *Molecular structure of the hydrate of the diaminoguanidinium salt of 5,5′-bis(1-hydroxytetrazole), showing the almost symmetrical hydrogen bridge between the −OH group of one anion and the N−O group of another anion. Reproduced with permission from [23] © 2013 WILEY-VCH Verlag GmbH & Co. KGaA, Weinheim.*

investigated (8028–8788 ms^{-1}) [51] are significantly lower than that observed for RDX ($D = 8983\ ms^{-1}$) [29] and much lower than the detonation velocity of β-HMX ($D = 9221\ ms^{-1}$) [30].

The molecular structure of the 1 : 1 salts in which the anion has only been deprotonated at one −OH group combined with the 5-aminotetrazolium cation shows only strong hydrogen bonding between the H atoms of the N−H and $-NH_2$ groups of the tetrazolium cation and the ring N atom and N−O group of the bistetrazolate anion, the diaminoguanidinium salt shows the presence of an almost symmetrical hydrogen bridge between the −OH group of one monoanion with the N−O group of a second monoanion (Figure 6.22). The densities of the 1 : 1 salts of the singly deprotonated 5,5′-bis(1-hydroxytetrazole) molecule also show significant variation from 1.729 $g\,cm^{-3}$ for the diaminoguanidinium salt to a density of 1.839 $g\,cm^{-3}$ for the 5-aminotetrazolium salt – a range of 0.11 $g\,cm^{-3}$.

If the densities of the 1 : 1 salts containing the monodeprotonated anions are compared, the salt with the highest density was the 5-aminotetrazolium salt ($\rho = 1.839\ g\,cm^{-3}$), however the densities for these salts were all below 1.80 $g\,cm^{-3}$ except for the 5-aminotetrazolium and 1,5-diaminotetrazolium salts ($\rho = 1.828\ g\,cm^{-3}$). Two of the five Cat^+A^- salts studied show detonation velocities above 9000 ms^{-1}, namely the 5-aminotetrazolium salt ($D = 9097\ ms^{-1}$) and the 1,5-diaminotetrazolium salt ($D = 9160\ ms^{-1}$) [51], which are approaching the value of β-HMX ($D = 9221\ ms^{-1}$) [30] and higher than that of RDX ($D = 8983\ ms^{-1}$) [29].

At the start of this section, it was mentioned that salts containing the 5,5′-bis(tetrazolate-1*N*-oxide) dianion or the 5,5′-bis(tetrazolate-2*N*-oxide) dianion are known. For the tetrazolate-*N*-oxide anion, the 1*N* as well as the 2*N* anion has been observed in salts. A recent study is particularly interesting since it allows a direct comparison between salts containing the 5,5′-bis(tetrazolate-1*N*-oxide) dianion and 5,5′-bis(tetrazolate-2*N*-oxide) dianion, since the anhydrous diammonium, bisguanidinium, and bisaminoguanidinium salts of both anions have been prepared, structurally characterized, the sensitivity values measured, and the explosive values calculated [51].

In contrast to 5,5′-bis(1-hydroxytetrazole), which was prepared by the cyclization of azidoglyoxime, 5,5′-bis(2-hydroxytetrazole) was prepared by the oxidation of the N2 atoms of each tetrazole ring by the reaction of 5,5′-bistetrazole using a buffered Oxone suspension at 45 °C, followed by acidification of the product and extraction (Eq. (6.2)) [51].

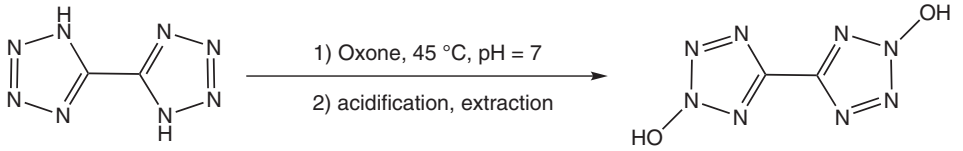

(6.2)

Again, as with the salts of 5,5′-bis(1-hydroxytetrazole), the 5,5′-bis(2-hydroxytetrazole) molecule is a Brønsted acid, which can be deprotonated by nitrogen-rich Brønsted bases. Furthermore, the nitrogen-base 3-amino-1-nitroguanidine has been introduced to improve the oxygen balance of the salts that it forms. Finally, the bis(5-aminotetrazolium) salt was formed in which both the cations and anion are based on the tetrazole ring system. The salts that were isolated and characterized are shown in Figure 6.23 [51].

Before considering any of the salts that are formed, it is worth considering the structure of the neutral 5,5′-bis(2-hydroxytetrazole) molecule, since it is anhydrous and has a very high density of 1.953 g cm^{-3} [51]. A closer look at the solid state structure shows that all of the bond lengths lie in the range between CC, CN, NN, NO single and double bonds, showing a delocalized π-system is once again present. Particularly interesting is the fact that, just as in the 5,5′-bis(1-hydroxytetrazole) molecule, the 5,5′-bis(2-hydroxytetrazole) molecule shows two coplanar tetrazole rings, however, the hydrogen atoms of the −OH groups do not lie within this plane (Figure 6.24). As the result of a strong unsymmetrical hydrogen bond involving the −OH group and a ring N atom, a 3D-network is observed in the solid state.

Despite this strong hydrogen bonding, the neutral molecule has a disappointingly low decomposition temperature of 165 °C, which discounts it from being a possible candidate for replacing the high explosives RDX or β-HMX, which is frustrating considering its high density and very high detonation velocity (9364 ms^{-1}) [51], which is much higher than that of RDX ($D = 8983$ ms^{-1}) [29] and higher even than that of β-HMX ($D = 9221$ ms^{-1}) [30]. It also shows a very high detonation pressure ($P_{C\text{-}J} = 409$ kbar), which is again higher than RDX ($P_{C\text{-}J} = 380$ kbar) [29] and comparable with that of the commonly used high explosive β-HMX ($P_{C\text{-}J} = 415$ kbar) [30]. Another disadvantageous property of 5,5′-bis(2-hydroxytetrazole) is its very high impact sensitivity of 3 N, which means it must be classified as very sensitive, and its friction sensitivity (<5 N) means that it has to be

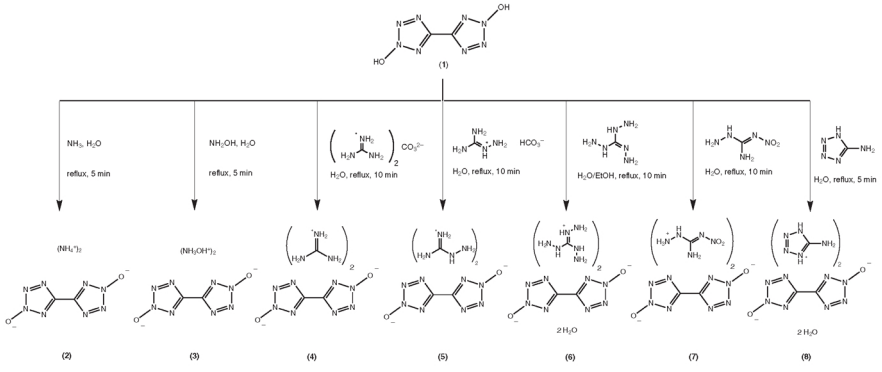

Figure 6.23 *Scheme showing the reactivity of 5,5′-bis(2-hydroxytetrazole) towards nitrogen-rich compounds. Reproduced with permission from [51] © 2013 Elsevier.*

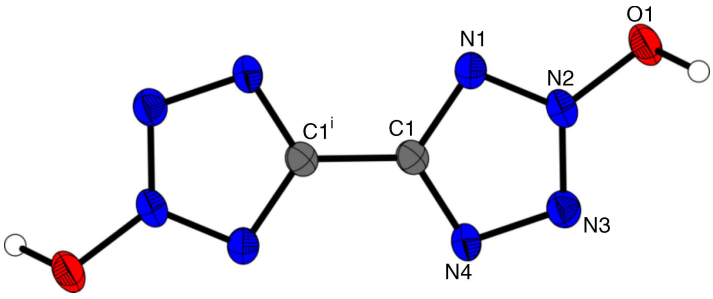

Figure 6.24 *Molecular structure of 5,5′-bis(2-hydroxytetrazole) in the crystalline state.*

classified as extremely sensitive [33–38] therefore excluding it being a possible candidate for application as an insensitive munitions.

The 5,5′-bis(2-hydroxytetrazole) can form salts of the type $(Cat^{+})_2A^{2-}$ as either anhydrous compounds or as hydrates. It is worthwhile mentioning that in contrast to the salts of 5,5′-bis(-hydroxytetrazole), which were reported with the general formulae $Cat^{2+}A^{2-}$, $(Cat^{+})_2A^{2-}$, $Cat^{+}A^{-}$, only $(Cat^{+})_2A^{2-}$ salts of the 5,5′-bis(2-hydroxytetrazole) have been reported so far [51]. Figure 6.23 shows which salts were prepared and the synthetic route used. The bisguanidinium salt shows $C_2N_8O_2^{2-}$ anions and $C(NH_2)_3^{+}$ cations, which show hydrogen bonding between the H atoms of the guanidinium $-NH_2$ groups and the tetrazolate ring N atoms and O atoms of the *N*-oxide groups (Figure 6.25).

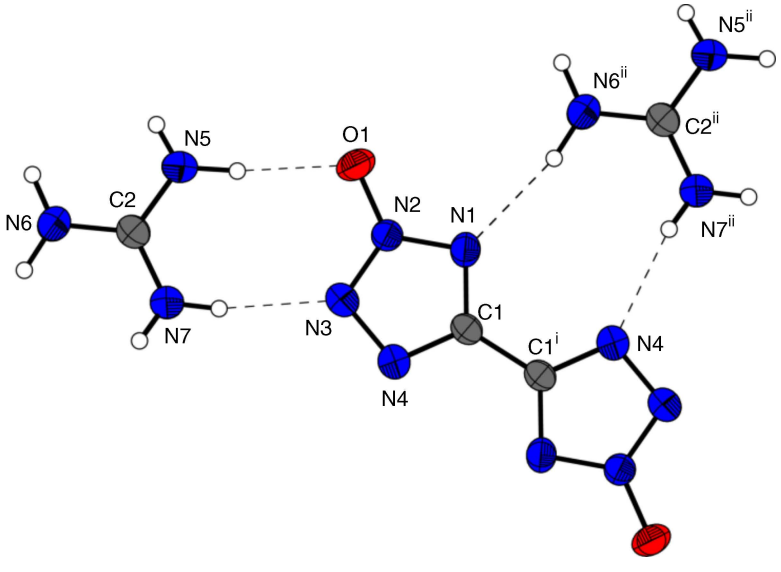

Figure 6.25 *Molecular structure of bisguanidinium 5,5′-bis(tetrazolate-2N-oxide) in the crystalline state showing hydrogen bonding interactions between the cations and anions. Reproduced with permission from [51] © 2013 Elsevier.*

The two tetrazolate rings within one dianion are coplanar and the N−O groups point in opposite directions. The structures of the other salts are all very similar, the main difference being which atoms are involved in intermolecular hydrogen bonding, and are therefore not discussed further here.

If the properties of the salts derived from 5,5′-bis(tetrazole-2*N*-oxide) are compared, several compounds show very good properties [51]. However, none of the compounds show good values for all of the properties, which are essential for a new compound to replace RDX and β-HMX. A good example is the neutral molecule 5,5′-bis(2-hydroxytetrazole), which has a very high density of 1.953 g cm^{-3} and detonation velocity of 9364 ms^{-1} – both of which are higher than the values reported for RDX and β-HMX. However, its very low decomposition temperature of 165 °C makes it useless as a replacement for RDX or β-HMX since decomposition temperatures of around 200 °C are required for such candidates. If the bisguanidinium salt is then considered, it has a very high decomposition temperature of 331 °C, which is excellent and much higher than those observed for RDX and β-HMX. However, although it has the highest decomposition temperature out of the 5,5′-bis(tetrazolate-2*N*-oxide) salts that were investigated, it has one of the lowest densities ($\rho = 1.633$ g cm^{-3}) and consequently a detonation velocity of 7752 ms^{-1}, which is much lower than that of RDX (8983 ms^{-1}) [29] and β-HMX (9221 ms^{-1}) [30] meaning it is also not a possible candidate for replacing RDX or β-HMX. In those salts that were studied, it appears to be a trend that the compounds that have the high densities of $\rho > 1.820$ g cm^{-3} have the lowest decomposition temperatures (< 200 °C), whereas the compounds with the lower densities have the higher decomposition temperatures. Here it is worthwhile mentioning that the salt that has the lowest decomposition temperature is the bis(3-amino-1-nitroguanidinium) salt, which decomposes already at 163 °C, however, very low decomposition temperatures appear to be a characteristic of salts that contain this cation. At the opposite end of the scale, the bisguanidinium salt has a decomposition temperature of 319 °C, which is close to that of hexanitrostilbene ($T_{dec.} = 320$ °C) [52] that is used in applications where a highly thermally stable explosive is required, such as in the deep oil drilling industry.

The sensitivities of the compounds show large ranges. For example, within the series of salts, the impact sensitivities range from the very sensitive bishydroxylammonium salt (3 J) to the insensitive bisguanidinium salt (> 40 J). The friction sensitivities also range from the very sensitive bis(3-amino-1-nitroguanidinium) salt (48 N) to the insensitive bisguanidinium salt (>360 N). However, the only compound that was highly sensitive towards electrical discharge was the neutral acid 5,5′-(2-hydroxytetrazole) (ESD = 0.03 J) [33–38,51].

Interestingly, the bisammonium, bisguanidinium, and diaminoguanidinium salts containing the 5,5′-bis(tetrazolate-2*N*-oxide) dianion can be directly compared with the corresponding salts of the 5,5′-bis(tetrazolate-1*N*-oxide) dianion since all of these salts were obtained as anhydrous materials [51]. Apart from the impact sensitivities of the salts containing the 5,5′-bis(tetrazolate-1*N*-oxide) dianion being higher than for the salts containing the 5,5′-bis(tetrazolate-1*N*-oxide) dianion, there are no trends to be observed that are valid for all of the compounds shown in Table 6.4. For example, whereas all of the salts containing the 5,5′-bis(tetrazolate-2*N*-oxide) dianion are more friction sensitive than the corresponding salts containing the 5,5′-bis(tetrazolate-1*N*-oxide) dianion, the decomposition temperature of the bisguandinium salt of the 5,5′-bis(tetrazolate-2*N*-oxide) dianion is

Table 6.4 *Overview of selected properties of the nitrogen-rich salts containing the bis(tetrazolate-*N*-oxide) anions [51]. Values marked with * were calculated using either Explo5 or EXPLO5.04 [44–48].*

Property	Bisammonium 5,5′-bis(tetrazolate-1*N*-oxide)	Bisammonium 5,5′-bis(tetrazolate-2*N*-oxide)	Bisguanidinium 5,5′-bis(tetrazolate-1*N*-oxide)	Bisguanidinium 5,5′-bis(tetrazolate-2*N*-oxide)	Bisaminoguanidinium 5,5′-bis(tetrazolate-1*N*-oxide)	Bisaminoguanidinium 5,5′-bis(tetrazolate-2*N*-oxide)	RDX [29]	β-HMX [30]
IS/J	35	10	>40	>40	40	30	7.5	7
FS/N	360	360	>360	>360	324	>360	120	112
ESD/J	0.25	0.75	0.50	0.15	0.25	0.20	0.2	0.2
Ω/%	47.02	−47.02	−66.60	−66.60	−65.35	−65.35	−21.61	−21.61
T_{dec}/°C	290	265	274	331	228	255	205	275
ρ/g cm^{-3}	1.800	1.664	1.639	1.633	1.596	1.637	1.858	1.944
T_E/K *	2939	2903	2606	2481	2852	2698	4232	4185
P_{C-J}/kbar *	316	258	233	221	243	247	380	415
D/MS^{-1} *	8817	8212	7917	7752	8111	8137	8983	9221

higher than for the bisguanidinium 5,5′-bis(tetrazolate-1*N*-oxide) salt, but is lower for the bisammonium 5,5′-bis(tetrazolate-2*N*-oxide) in comparison with the bisammonium 5,5′-bis (tetrazolate-1*N*-oxide) salt. The two neutral compounds 5,5′-bis(1-hydroxytetrazole) and 5,5′-bis(2-hydroxytetrazole) cannot be compared since the former is a dihydrate, whereas the latter is anhydrous [51].

Two further compounds containing the 5,5′-(tetrazolate-*N*-oxide) dianion must be mentioned here and compared, namely bishydroxylammonium 5,5′-(tetrazolate-1*N*-oxide), which is also known as TKX-50, and the corresponding isomer bishydroxylammonium 5,5′-(tetrazolate-2*N*-oxide) [51]. These two compounds are discussed in this section at the end, since TKX-50 shows outstanding properties and, when compared with the 1*N*-oxide isomer, the huge difference a seemingly small change can make with respect to the energetic properties of a substance is illustrated.

TKX-50 (bishydroxylammonium 5,5′-(tetrazolate-1*N*-oxide)) can be prepared on a multi-gram scale (extreme caution though has to exercised when handling this compound) by the reaction of *in situ* prepared 5,5′-(1-hydroxytetrazole) with dimethyl amine to form the bis (dimethylammonium) 5,5′-(tetrazolate-1*N*-oxide) salt, which is then isolated, purified, and subsequently reacted on boiling water with two equivalents of hydroxylammonium chloride to form TKX-50, dimethylammonium chloride and HCl. TKX-50 crystallizes out of solution first as a pure material [51]. The advantage of this method is that it avoids isolating the highly explosive diazidoglyoxime, since the diazidoglyoxime precursor is cyclized *in situ* (without isolating it as in previous synthetic routes) and then directly converted into the dimethylammonium salt in DMF solution. The dimethylamine arises from the hydrolysis of DMF (Figure 6.26). The dimethylammonium salt can then be isolated as a pure substance. Here it is worth stressing that whereas TKX-50 can be prepared by a cheap and easy method that uses easily obtained starting materials, energetic materials such as octanitrocubane [53] – which shows some excellent energetic properties – involve difficult and expensive synthetic routes and often require the handling of hazardous materials.

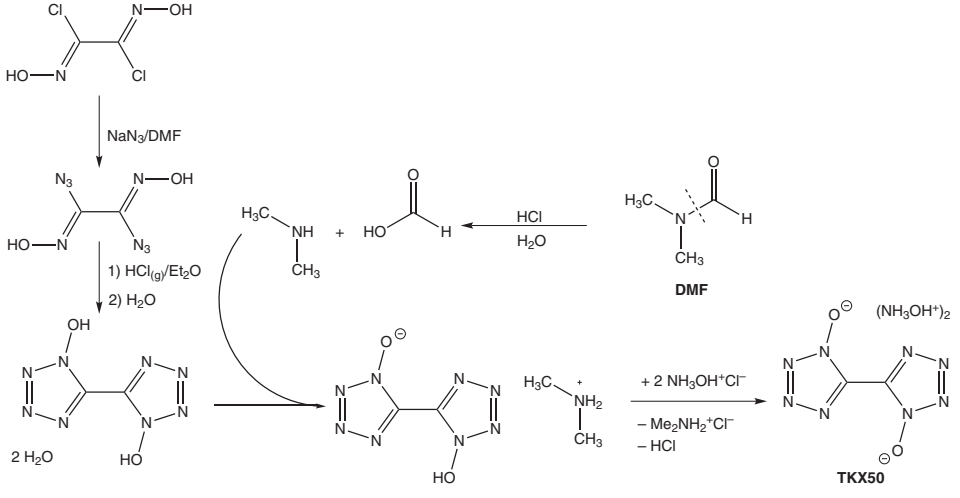

Figure 6.26 *Synthetic route to TKX-50 as a pure 1,1′-isomer avoiding the isolation of sensitive intermediates [51].*

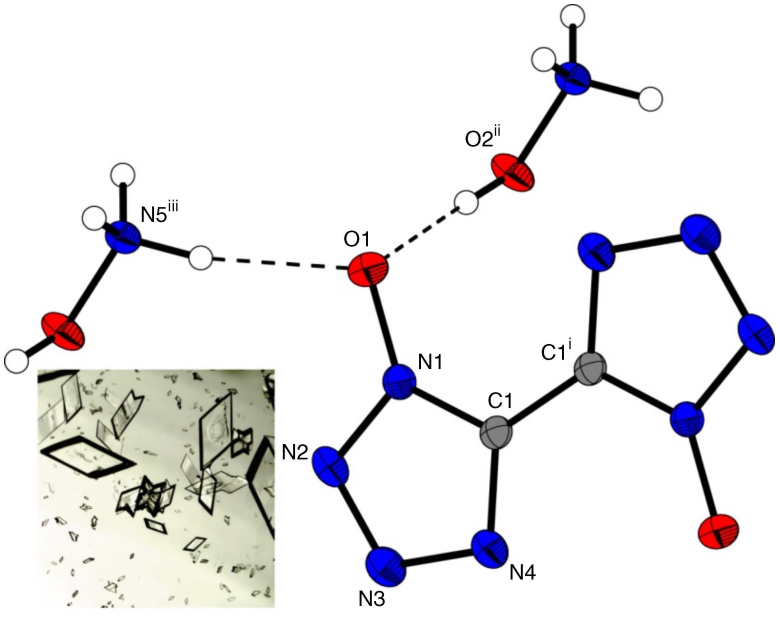

Figure 6.27 *Molecular structure of bis(hydroxylammonium) 5,5′-bis(tetrazolate-1*N*-oxide) (also referred to as TKX-50) in the crystalline state showing hydrogen bonding interactions between the cations and anions.*

In contrast, the corresponding 2*N*-oxide compound can be more easily prepared simply by the deprotonation of the 5,5′-(2-hydroxytetrazole) by hydroxylamine in aqueous solution. This compound is more easily prepared since it does not involve the use of the hazardous diazidoglyoxime to prepare the acid, but instead is prepared by the oxidation of bistetrazole by Oxone in a buffered solution at elevated temperature [51].

The structure of TKX-50 shows cations and anions that exhibit hydrogen bonding interactions between the −OH group of the hydroxylammonium cations and the O atoms of the N−O group of the anion. The bistetrazolate rings are coplanar and show similar structural parameters with those of the other salts containing this anion (Figure 6.27) [51].

The density of TKX-50 is, however, very high ($\rho = 1.918\ \mathrm{g\,cm^{-3}}$) [51] and is higher than both the bis(hydroxylammonium) bis(tetrazolate-2*N*-oxide) salt ($\rho = 1.822\ \mathrm{g\,cm^{-3}}$) [51] and the related nonoxide salt bis(hydroxylammonium) 5,5′-bistetrazolate ($\rho = 1.742\ \mathrm{g\,cm^{-3}}$) [51]. The higher densities of both of the *N*-oxide salts in comparison with the nonoxidized bistetrazolate salt is in agreement with the findings for the tetrazolate *N*-oxide salts, which were also shown to have higher densities than the corresponding nonoxidized tetrazolate salts. The very high density of the 1*N*-oxide salt means that it has a very high detonation velocity of $9698\ \mathrm{ms^{-1}}$, which is not only higher than that of β-HMX [30] ($D = 9221\ \mathrm{ms^{-1}}$) but also of ε-CL20 ($D = 9455\ \mathrm{ms^{-1}}$) [54], even although ε-CL20 has a higher density ($\rho = 2.083$ at 100 K) than TKX-50 ($\rho = 1.918\ \mathrm{g\,cm^{-3}}$). In fact, in comparison with the common mass-produced explosives, which are used today, TKX-50 has the highest detonation velocity. By comparison, the 2*N*-oxide salt still has a high detonation velocity ($D = 9264\ \mathrm{ms^{-1}}$) [51], which is higher than those of 2,4,6-TNT ($D = 7459\ \mathrm{ms^{-1}}$) [32] and RDX ($D = 8983\ \mathrm{ms^{-1}}$) [29] and

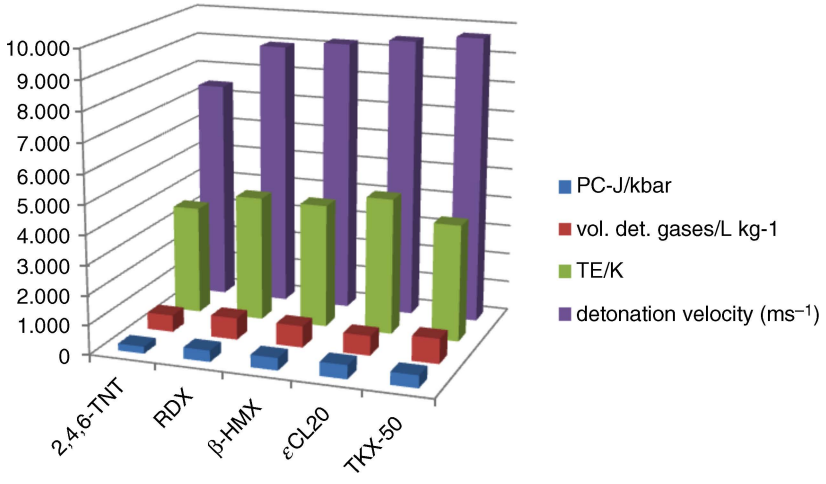

Figure 6.28 *Graph comparing the energetic properties (detonation pressure* $P_{C\text{-}J}$*, volume of detonation gases* V_0*, explosion temperature* T_E*, and detonation velocity* D *of 2,4,6-TNT [32], RDX [29], β-HMX [30], ε-CL-20 [54], TKX-50 [51], and bis(hydroxylammonium) bis(tetrazolate-2N-oxide) [51].*

comparable with β-HMX ($D = 9221\ \text{ms}^{-1}$) [30], but which is lower than both ε-CL20 [54] and TKX-50 [51] (Figure 6.28).

The explosive performance of TKX-50 was further investigated using a small-scale reactivity test (SSRT), which showed that, after initiation, TKX-50 produced a dent in a steel block of a larger volume than RDX did and was comparable to that generated by ε-CL20 [51]. Although the performance of an energetic material is of utmost importance, it is also important that the explosive nature of the compound can be utilized when required but safely handled when initiation is not wanted. For example, if a compound shows excellent explosive performance, but is too sensitive to impact and friction sensitivity then it will not be a suitable replacement for RDX or ε-CL20. The impact sensitivity is obviously important because explosives that are transported and manipulated in large quantities should not detonate if they are exposed to impact stress. TKX-50 is not very sensitive to impact with an impact sensitivity value of 20 J [51], which is much less sensitive than for RDX (7.5 J) [29], β-HMX (7 J) [30], and ε-CL20 (4 J) [54], which require the addition of desensitizing components in order to be used in practical situations. Also, the friction sensitivity is important since, during the preparation of large quantities of the explosive material, it must be safe to handle. Again, the friction sensitivity of TKX-50 (120 N) [51] in comparison with the values for RDX (120 N) [29], β-HMX (112 N) [30], and ε-CL20 (48 N) [54] means that is less sensitive to friction than β-HMX or ε-CL20 and similar to RDX. A final practical requirement is that the energetic material should be thermally stable, ideally up to temperatures over 200 °C since an energetic material may be exposed to high temperatures if left in the sun. The excellent thermal stabilities of 2,4,6-TNT ($T_{\text{dec.}} = 290\,^{\circ}\text{C}$) [32] and β-HMX ($T_{\text{dec.}} = 279\,^{\circ}\text{C}$) [30] are not matched by TKX-50 ($T_{\text{dec.}} = 221\,^{\circ}\text{C}$) [51], however this value is still high and is comparable with those for RDX ($T_{\text{dec.}} = 210\,^{\circ}\text{C}$) [29] and ε-CL20 ($T_{\text{dec.}} = 215\,^{\circ}\text{C}$) [54]. This is another major disappointment with respect to the 2*N*-oxide salt, since it has a decomposition temperature

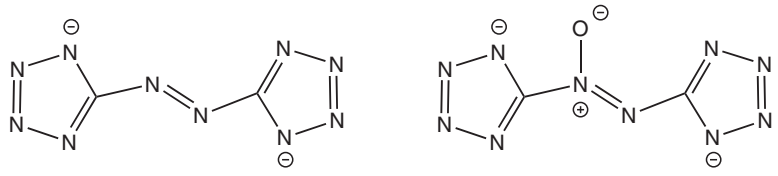

Figure 6.29 *Comparison of the connectivities of the 5,5′-azotetrazolate (left) (also referred to as zT) and 5,5′-azoxytetrazolate (also referred to as zTO) dianions.*

of only 172 °C, which is almost 50 °C lower than the 1*N*-oxide salt (TKX-50) and rules out further investigation. TKX-50 is an excellent example of where the introduction of *N*-oxide groups increases the oxygen balance of a compound, the density, and the safety of handling the compound and is a promising strategy for the synthesis of further energetic materials of this type.

6.4.3 5,5′-Azoxytetrazolates

Salts containing the 5,5′-azotetrazolate dianion are compounds in which the anion consists of two tetrazole rings that are linked to one another through a –N = N– bridge. If one of the bridging N atoms is changed into an *N*-oxide group, then the corresponding 5,5′-azoxytetrazolate dianion is formed (Figure 6.29).

The idea of forming compounds in which two tetrazole rings are linked by a diazo bridge is very old. As far back as 1898, $Na_2zT{\cdot}5H_2O$ was prepared by Thiele in a simple one-step reaction in which 5-aminotetrazole is oxidized using $KMnO_4$ in alkaline conditions (Eq. (6.3)) [55].

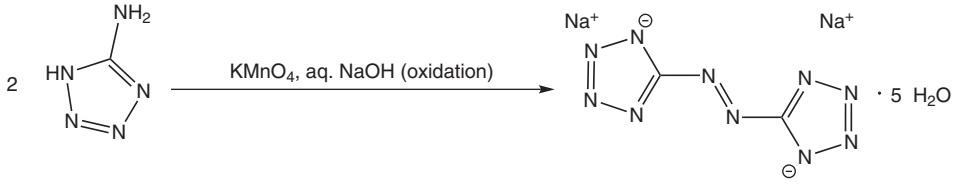

(6.3)

The proposed mechanism for this reaction involves oxidation of the 5-aminotetrazole to form 5-hydroxyaminotetrazole, which then undergoes a condensation reaction with another 5-hydroxyaminotetrazole molecule and deprotonation in alkaline aqueous NaOH solution to form the $Na_2zT{\cdot}5H_2O$ (Figure 6.30). The aminotetrazole is not initially oxidized further, since the oxidizing agent ($KMnO_4$) is added to an excess of the tetrazole [26].

Salts containing the 5,5′-azotetrazolate dianion have been well investigated as energetic materials – particularly in recent times – since they have a high nitrogen content, often relatively low sensitivity, and good thermal stability [56–65]. One particularly good example is the use of the recently synthesized bis(triaminoguanidinium) 5,5′-azotetrazolate salt [56–65] as a nitrogen-rich gas generating additive in the propellant NILE [66]. However, many have been prepared such as ammonium, the hydrazinium and guanidinium salt.

Surprisingly, by simply altering the order in which the reagents used to prepare the 5,5′-bisazotetrazolate salts are added, the *N*-oxide derivative of the anion can be prepared,

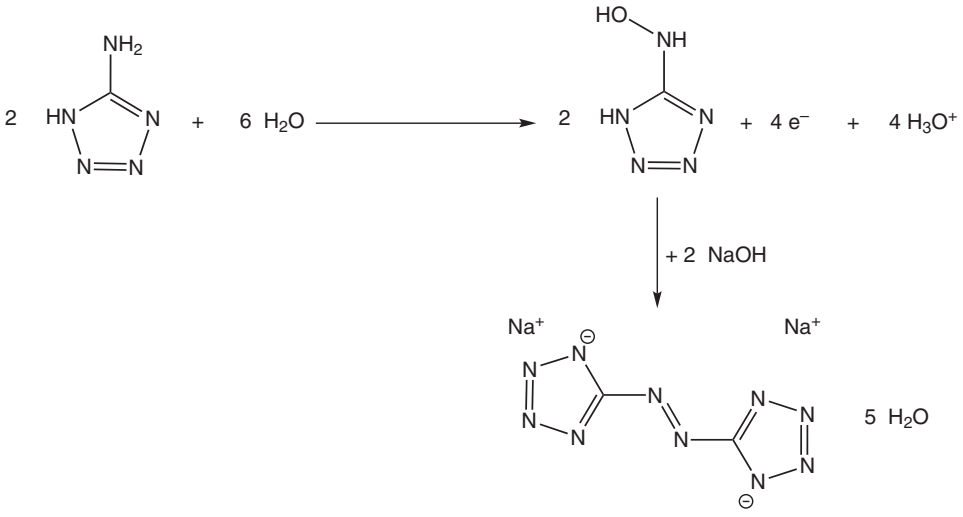

Figure 6.30 *Proposed mechanism for the formation of the sodium salt of 5,5′-azotetrazolate starting from 5-aminotetrazole. Reproduced with permission from [26] © 2012 WILEY-VCH Verlag GmbH & Co. KGaA, Weinheim.*

namely the 5,5′-azoxytetrazolate dianion in which one of the bridging N atoms has been oxidized to form the *N*-oxide group [67]. To form the 5,5′-azoxytetrazolate salts it is important that the oxidizing agent is in excess, so that the oxidation of the 5-aminotetrazole starting material does not only stop at the formation of 5-hydroxyaminotetrazole, but continues in part to form 5-nitrosotetrazole, which can then react with the incompletely oxidized 5-hydroxyaminotetrazole molecules in a condensation reaction in alkaline solution forming the 5,5′-azoxytetrazolate anion (Figure 6.31).

For the generation of salts containing nitrogen-rich cations, usually the sodium salt is first of all converted into the corresponding barium salt by cation exchange of the sodium salt with barium dichloride hydrate. The reason for doing this is that sulfate salts containing the

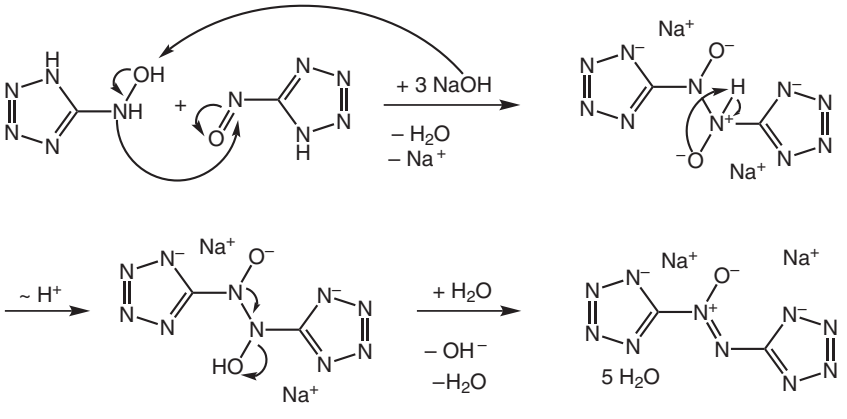

Figure 6.31 *Proposed mechanism for the formation of the sodium salt of 5,5′-azoxytetrazolate starting from 5-aminotetrazole. Reproduced with permission from [67] © 2012 by MDPI AG.*

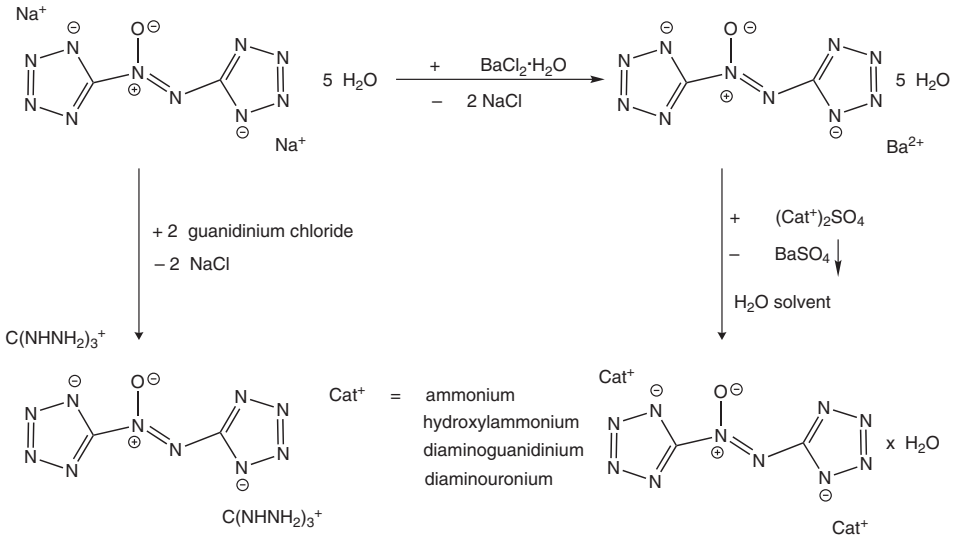

Figure 6.32 *Scheme showing the synthetic routes used for the synthesis of nitrogen-rich salts containing the 5,5′-azoxytetrazolate dianion. Reproduced with permission from [67] © 2012 by MDPI AG.*

nitrogen-rich cations are either commercially available or can be conveniently prepared and barium sulfate is highly insoluble, meaning that the reaction of the barium 5,5′-azoxytetrazolate salt with, for example, ammonium sulfate in water results in the formation of the water soluble ammonium 5,5′-azoxytetrazolate, which can be easily separated from the insoluble barium sulfate precipitate and isolated after evaporation of the water (Figure 6.32) [67].

The structure of the zTO^{2-} anion in the salts that were investigated shows a very similar structure to that observed for the zT^{2-} anion in related salts and shows only small deviation from planarity. Despite the addition of oxygen to one of the diazo-bridge N atoms, the *d*(NN) of the diazo-bridge in the bis(ammonium) salt (1.27 Å) is slightly shorter than is observed in the corresponding $(NH_4)_2zT$ salt ($d(NN)_{azo\text{-}bridge} = 1.36(1)$ Å) [56–65]. The dihydroxylammonium dihydrate salt shows the most significant hydrogen bonding between the crystal water molecules and the N atoms of the tetrazole rings as do the hydroxylammonium cations. In contrast to what was observed for other hydroxylammonium tetrazolate-based salts, the $(NH_3OH)_2zTO{\cdot}2H_2O$ salt has a lower density in the crystalline state ($\rho = 1.596\ g\ cm^{-3}$) [67] than the corresponding nonoxidized $(NH_3OH)_2zT{\cdot}2H_2O$ salt ($\rho = 1.612\ g\ cm^{-3}$) [56–65]. If we simply change the cation, however, then it is observed that $(NH_4)_2zTO$ has a higher density ($\rho = 1.592\ g\ cm^{-3}$) [67] than $(NH_4)_2zT$ ($\rho = 1.562\ g\ cm^{-3}$) [56–65]! Furthermore, unexpectedly the thermal stability of the two salts is the opposite of what would have been predicted, whereby the decomposition temperature of $(NH_3OH)_2zTO{\cdot}2H_2O$ ($T_{dec.} = 175\ °C$) is higher than that of $(NH_3OH)_2zT{\cdot}2H_2O$ ($T_{dec.} = 130\ °C$) and $(NH_4)_2zTO$ ($T_{dec.} = 222\ °C$) has a higher decomposition temperature than $(NH_3OH)_2zT$ ($T_{dec.} = 195\ °C$). However, it is not always the case that the zTO^{2-} salts have higher decomposition temperatures than the zT^{2-} salts [56–65,67].

Calculation of the heats of formation at CBS-4M for selected compounds have shown that the *N*-oxide salt $(NH_4)_2zTO$ has a lower heat of formation ($524\ kJ\ mol^{-1}$, i.e., less

endothermic) in comparison with $(NH_4)_2zT$ (551 kJ mol^{-1}). In terms of the sensitivity of the compounds, again there is no apparent trend. Whereas $(NH_4)_2zTO$ (1 J) is much more impact sensitive than $(NH_4)_2zT$ (3 J) and shows a similar friction sensitivity (40 and 42 N), $(NH_3OH)_2zTO$ has a lower impact sensitivity than $(NH_3OH)_2zT{\cdot}2H_2O$ and a significantly lower friction sensitivity (160 N) than $(NH_4)_2zT$. Finally, both the ammonium and hydroxylammonium salts containing the zTO^{2-} anion [67] have higher detonation temperatures and detonation velocities than the corresponding zT^{2-} salts [56–65], however the detonation velocity values of 8054 ms^{-1} ($(NH_4)_2zTO$) and 8224 ms^{-1} ($(NH_3OH)_2zTO$) are much lower than the values reported for the commonly used energetic materials RDX ($D = 8983$ ms^{-1}) [29] and β-HMX ($D = 9221$ms^{-1}) [30].

Other *N*-oxide derivatives of previously synthesized 5,5′-azobistetrazole have also been reported in the literature in which the N−O group is not located at one of the bridging azo-N atoms, but is instead in the 1-position of each of the tetrazole rings [26] – which is more similar to the *N*-oxides that were reported for the tetrazole and bis(tetrazoles) discussed above. Equation (6.4) showed the formation of the sodium salt of the bisazotetrazolate dianion by the azo-coupling of aminotetrazole in aqueous alkaline solution and, in exactly the same way, 1-hydroxy-5-aminotetrazole can be azo-coupled using $KMnO_4$ in basic solution to form the corresponding azotetrazole-1,1′dioxide anion.

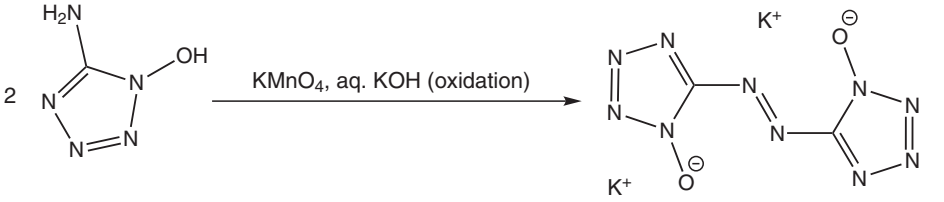

(6.4)

This dianion can then be subsequently protonated in acidic media to form the corresponding neutral molecule 1,1′-dihydroxy-5,5′-azobistetrazole, which is an orange solid at room temperature [26]. Obviously, for new energetic materials that are nitrogen-rich, the formation of the potassium salt is not particularly promising. However, using the neutral acid, other salts can easily be prepared by reaction with a nitrogen-rich Brønsted base, which results in deprotonation of the acid. For example, the reaction of 1,1′-dihydroxy-5,5′-azobistetrazole with ammonia results in the formation of the bisammonium salt of the doubly deprotonated acid, and with hydroxylammonia or hydrazine hydrate the corresponding bis(hydoxylammonium) or bis(hydrazinium) salts (Figure 6.33) [26].

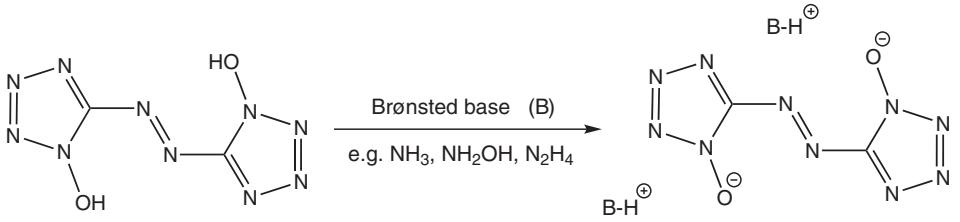

Figure 6.33 *Scheme showing the synthetic routes used for the synthesis of nitrogen-rich salts containing the 5,5′-azoxytetrazolate dianion.*

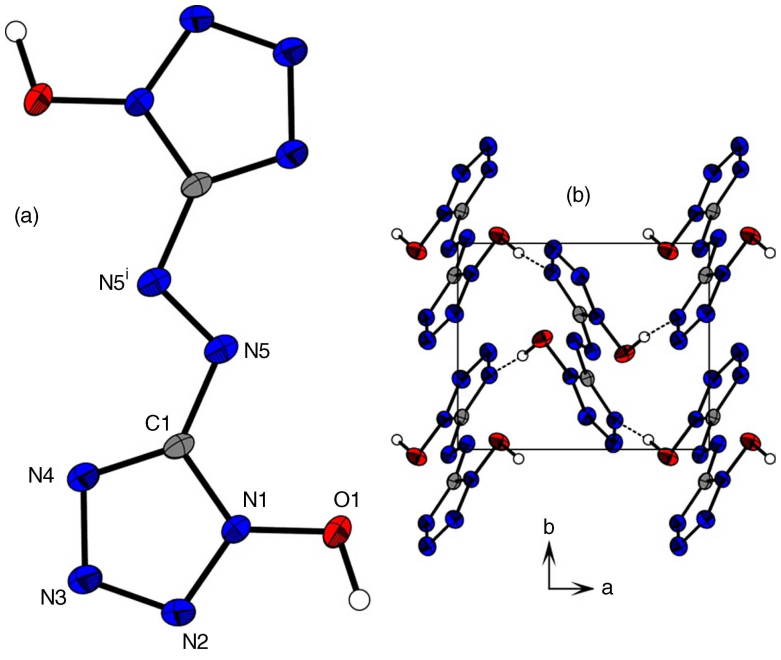

Figure 6.34 *Molecular structure of 1,1′-dihydroxy-5,5′-azobistetrazole in the crystalline state (a) showing hydrogen bonding interactions between the molecules (b). Reproduced with permission from [26] © 2012 WILEY-VCH Verlag GmbH & Co. KGaA, Weinheim.*

The structure of the neutral 1,1′-dihydroxy-5,5′-azobistetrazole molecule shows an almost coplanar arrangement of the two tetrazole rings and the diazo bridge. The H atoms of the −OH groups, however, do not lie in the molecular plane and are twisted out of the ring plane, forming hydrogen bonds with the ring N atoms of other 1,1′-dihydroxy-5,5′-azobistetrazole molecules (Figure 6.34) [26].

The hydroxylammonium, ammonium, and hydrazinium salts that contain the doubly deprotonated dianions show a coplanar arrangement of the two tetrazole rings. In both the hydroxylammonium and ammonium salts the O atoms (and ring N atoms in the hydroxylammonium salt) are involved in hydrogen bonding, but the azo bridge N atoms are not involved in hydrogen bonding. The hydrazinium salt shows two polymorphs. In one, the $-NH_3^+$ group of the hydrazinium cations forms hydrogen bonds with the NO group of the anion and the $-NH_2$ group of the hydrazinium cations forms hydrogen bonds with the ring N atom of the anion, whereas in the other polymorph it is the other way around and the $-NH_3^+$ group forms hydrogen bonds with the ring N atoms of the anion whereas the $-NH_2$ group forms hydrogen bonds with the N−O group of the anions (Figure 6.35) [26].

The densities of the nitrogen-rich salts are all considerably lower than the high density observed for the neutral 1,1′-dihydroxy-5,5′-azobistetrazole molecule, which has a density of 1.902 g cm^{-3}. In addition, the neutral molecule has a very high heat of formation of 883 kJ mol^{-1}, which results in it possessing an excellent detonation velocity of 9548 ms^{-1}. It also exhibits a remarkably high specific impulse of 271 s and has a very good detonation

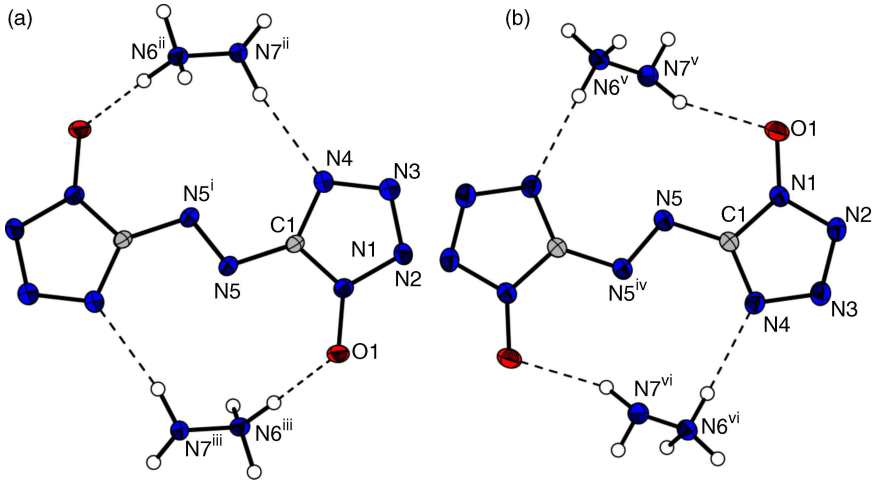

Figure 6.35 *Molecular structure of the two polymorphs of hydrazinium 5,5′-azotetrazole-1,1′-dioxide in the crystalline state showing the strongest hydrogen bonding interactions between the cations and anion: lower density polymorph (a) and higher density polymorph (b). Reproduced with permission from [26] © 2012 WILEY-VCH Verlag GmbH & Co. KGaA, Weinheim.*

pressure of 424 kbar. Furthermore, it even shows smokeless combustion. However, disappointingly it shows a low thermal stability, decomposing at a temperature of only 170 °C, which is considerably lower than the desired value of over 200 °C. In addition, it is very sensitive towards impact and friction (Table 6.5) [26].

Out of the nitrogen-rich salts that were investigated, the salt containing the ammonium cations shows the highest density ($\rho = 1.800\ \mathrm{g\,cm^{-3}}$) – slightly higher than the value observed for the hydroxylammonium salt ($\rho = 1.778\ \mathrm{g\,cm^{-3}}$) and significantly higher than

Table 6.5 *Overview of selected properties of the neutral 1,1′-dihydroxy-5,5′-azobistetrazole (HAZTO) molecule and its hydroxylammonium (Hx_2AZTO) and ammonium (A_2AZTO) salts [26] as well as of ammonium 5,5′-azobistetrazolate (A_2AZT), bis(1-hydroxytetrazolyl)hydrazine (BTOH) and bis(tetrazolyl)hydrazine (BTH) [56–65]. Values marked with * were calculated using EXPLO5.04 [44–48].*

Property	HAZTO	Hx_2AzTO	A_2AzTO	A_2AzT	BTHO	BTH
IS/J	<1	15	3	6	1	4
FS/N	<5	54	160	44	<5	24
ESD/J	0.01	0.2	0.2	0.18	0.007	0.25
Ω/%	−24.23	−24.22	−41.34	−63.94	−28.17	−57.1
$T_{dec.}$/°C	170	190	250	190	120	212
ρ/g cm^{-3}	1.902	1.778	1.800	1.562	1.707	1.841
T_{det}/K	4973	4310	3313	2565	3851	4672
P_{C-J}/kbar	424	375	338	216	312	343
V_o/l kg^{-1}	733	841	837	823	833	759
D/ms^{-1}	9548	9348	9032	7788	8711	9019

the values observed for the two hydrazinium polymorphs ($\rho = 1.673$ and $1.725\ \mathrm{g\,cm^{-3}}$) (Table 6.5). Despite these disappointingly low densities, all three salts show detonation velocities of over $9000\ \mathrm{ms^{-1}}$ – with the detonation velocity of the bishydroxylammonium salt ($9348\ \mathrm{ms^{-1}}$) [26] being higher than that of RDX ($D = 8983\ \mathrm{ms^{-1}}$) [29] or β-HMX ($D = 9221\ \mathrm{ms^{-1}}$) [30]. This salt also has a slightly higher decomposition temperature than the neutral molecule of 190 °C. Although the ammonium salt has a slightly lower detonation velocity ($D = 9032\ \mathrm{ms^{-1}}$) than the hydroxylammonium salt ($D = 9348\ \mathrm{ms^{-1}}$), it has a much higher thermal stability, not decomposing until 250 °C (Table 6.5). If the data for the bisammonium salt is compared with that for the bisammonium 5,5′-azotetrazolate [56–65] in which no *N*-oxide groups are present, then not only has the density been improved with the formation of the *N*-oxide derivative, but also the oxygen balance, decomposition temperature, detonation temperature, detonation pressure, volume of detonation gases, and detonation velocity. In addition, the ammonium salt of the *N*-oxide derivative is much easier to prepare than ammonium bistetrazolate containing the nonoxidized anion.

A final derivative from 1,1′-dihydroxy-5,5′-azobistetrazole is 1,1′-dihydroxy-5,5′-bistetrazolylhydrazine sesquihydrate. This molecule can be prepared according to Eq. (6.5) by the reaction of 1,1′-dihydroxy-5,5′-azobistetrazole with Mg at elevated temperature followed by addition of HCl [26].

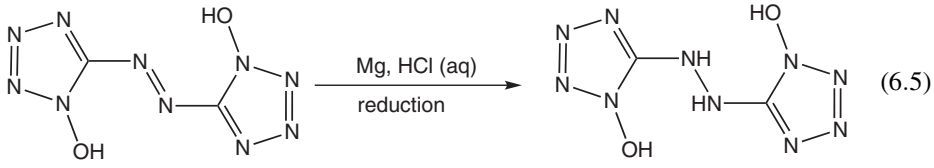

(6.5)

The reduction of the azo-bridged salt results in the formation of the hydrazine bridge connecting two tetrazole rings. The tetrazole rings both have the −OH group again in the 1-position. The colorless hydrazine derivative shows a much longer bridging N−N bond, which is the result of the formation of two −NH− groups. As a result, the two tetrazole rings in this molecule are not coplanar (Figure 6.36). This compound does not have much promise of finding application as an energetic material, though, since it is relatively easily oxidized back to the azo-bridged anion in alkaline media and has a low decomposition temperature of only 120 °C, which is much lower than that of the bistetrazolylhydrazine molecule that doesn't decompose until 207 °C [26].

6.4.4 Bis(tetrazole)dihydrotetrazine and Bis(tetrazole)tetrazine *N*-oxides

A final class of energetic compounds that contain both the tetrazole and *N*-oxide groups is that containing bridging tetrazine units (Figure 6.37). Many tetrazine compounds have been investigated both synthetically and computationally [68] and compounds that contain two tetrazole rings linked by a tetrazine group have been investigated. However, recently it has been possible to modify such compounds such that *N*-oxide groups are also included [17]. Two examples are the dihydrotetrazines 3,6-bis(2-hydroxytetrazole)-dihydro-1,2,4,5-tetrazine dihydrate and 3,6-bis(1-hydroxytetrazole)-dihydro-1,2,4,5-tetrazine dihydrate and their related nitrogen-rich salts as well as the tetrazine-based compound 3,6-bis(2-

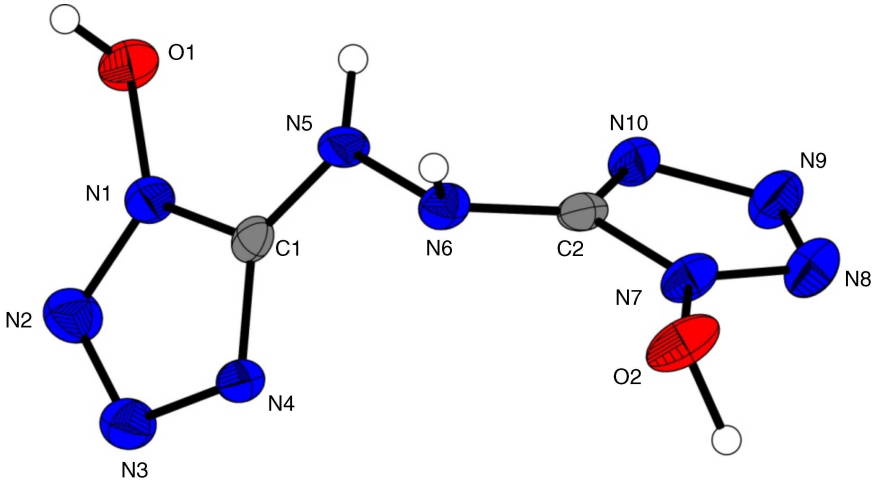

Figure 6.36 *Molecular structure of the 1,1′-dihydroxy-5,5′-bistetrazolylhydrazine sesquihydrate in the crystalline state. The crystal water molecules are not shown for clarity.*

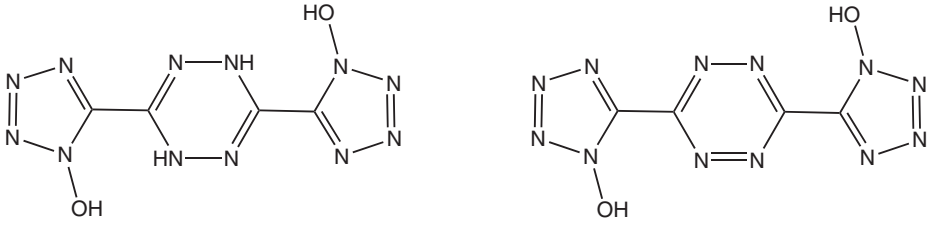

Figure 6.37 *Structures of 3,6-bis(1-hydroxytetrazole)-dihydro-1,2,4,5-tetrazine (left) and 3,6-bis(1-hydroxytetrazole)-1,2,4,5-tetrazine (right).*

hydroxytetrazole)-1,2,4,5-tetrazine and its related nitrogen-rich salt ammonium 3,6-bis (tetrazolate-2-oxide)-1,2,4,5-tetrazine monohydrate [17].

The formation of a dihydrotetrazine by the reaction of 5-cyanotetrazole with hydrazine in ethanol results in the formation of a dihydrotetrazine compound in which the dihydrotetrazine group bridges two tetrazole rings, which are each attached to the dihydrotetrazine group via the 5-position, meaning that no cyano group is present in the resulting compound [69]. If the same reaction is carried out using the 5-cyano-1-hydroxytetrazole or 5-cyano-2-hydroxytetrazole (which were mentioned earlier) instead of the nonoxidized 5-cyanotetrazole, the corresponding dihydrotetrazine compound is prepared in which the dihydrotetrazine group bridges two *N*-oxide tetrazole rings. In these compounds, however, the neutral compound is not isolated, but rather the deprotonated hydrazinium salts (Figure 6.38) [17].

The corresponding neutral 1- and 2-hydroxy molecules could then be prepared from the corresponding dihydrazinium salt by protonation in acidic media, which then allows the possibility of deprotonation using a different Brønsted base (such as NH_3) to form

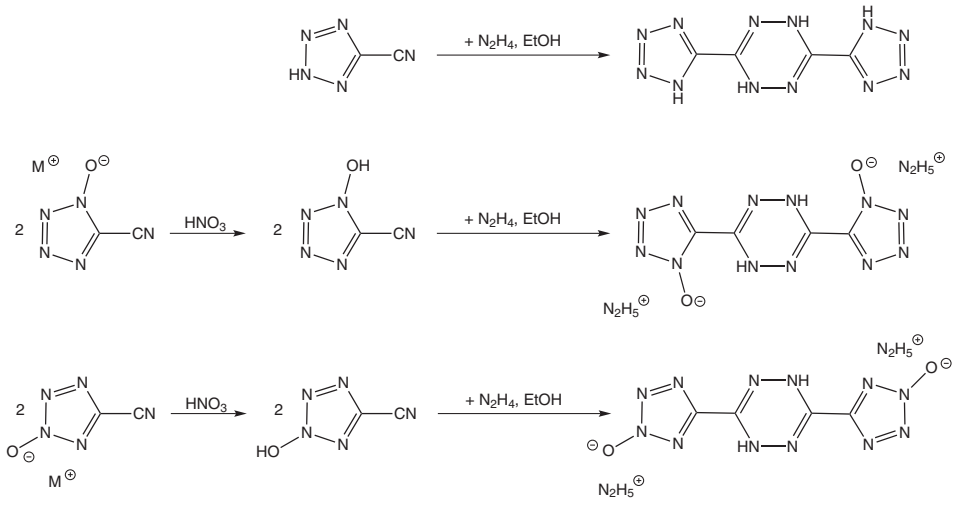

Figure 6.38 *Reaction of 5-cyanotetrazole with hydrazine forming the dihydrotetrazine bridging derivative (above) and the formation of the hydrazinium salts of the* N*-oxide derivatives (1*N*-oxide derivative (middle) and 2*N*-oxide derivative (bottom)) starting from the corresponding 5-cyano-*N*-oxide-tetrazolate.*

the corresponding salt. Unfortunately, for all of these compounds, no density was able to be determined experimentally using single crystal X-ray diffraction, which therefore meant that the explosive properties of the compounds could not be calculated using the EXPLO5.04 code [44–48], since this requires the enthalpy of formation of the compound and the density as its input. However, the impact, friction, and electrostatic sensitivities of the compounds were measured experimentally and show that both compounds are very sensitive when dry.

Finally, the 2-hydroxytetrazole derivative of the dihydrotetrazine could be oxidized by using a dilute MeCN solution of NO_2 to form the corresponding tetrazine derivative as a deep red, hygroscopic, and highly impact sensitive solid. This material was further deprotonated using aqueous ammonia to form the corresponding ammonium salt hydrate, which could be isolated as a crystalline substance. Surprisingly, the oxidation of the 1-hydroxytetrazole derivative of the dihydrotetrazine did not result in the formation of a pure compound (Figure 6.39) [17].

In the solid state, the ammonium salt hydrate shows the strongest hydrogen bonds between the water molecules and an N atom of the tetrazole or tetrazine rings, whereas the NH_4^+ cations show the strongest hydrogen bonding with either the water molecules or with the O atom of the 2*N*-oxide group (Figure 6.40).

The ammonium salt is less impact and friction sensitive in comparison with the neutral molecule prior to deprotonation. But again it shows a low density of only 1.627 g cm^{-3} and a thermal decomposition temperature of 189 °C. Furthermore, it also shows a low detonation temperature of 2746 K and a low detonation velocity of only 7999 ms^{-1} [17]. Despite these disappointing values, the combination of the 3,6-bis(tetrazolate-2-oxide)-1,2,4,5-tetrazine anion with other energetic nitrogen-rich cations, may lead to compounds with improved energetic properties in the future.

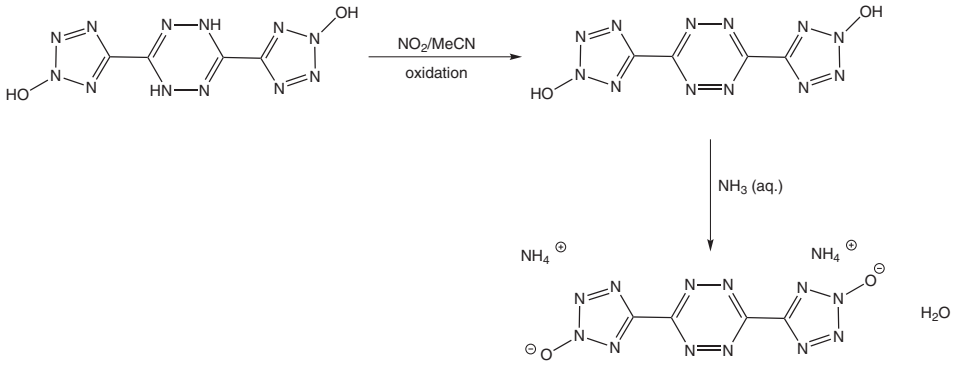

Figure 6.39 *Formation of the tetrazine derivative 3,6-bis(2-hydroxytetrazole)-1,2,4,5-tetrazine by oxidation of 3,6-bis(2-hydroxytetrazole)-dihydro-1,2,4,5-tetrazine and its deprotonation forming ammonium 3,6-bis(2-N-oxidotetrazolate)-1,2,4,5-tetrazine monohydrate.*

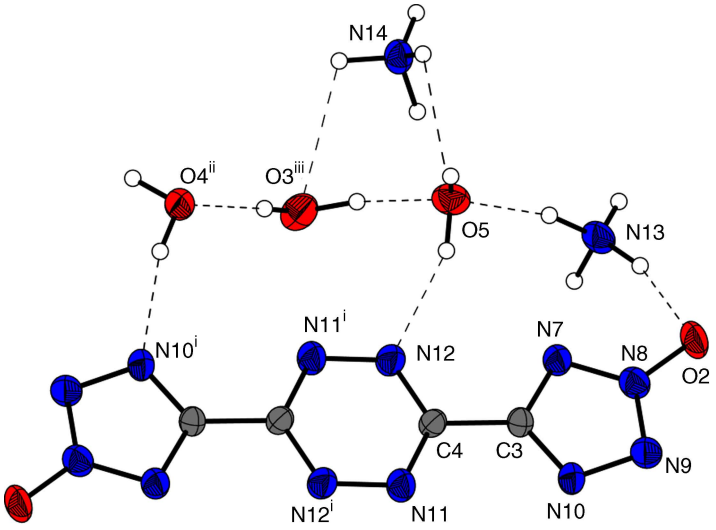

Figure 6.40 *Molecular structure of bisammonium 3,6-bis(tetrazolate-2-oxide)-1,2,4,5-tetrazine trihydrate in the crystalline state. The crystal water molecules are not shown for clarity. Reproduced with permission from [17] © 2012 WILEY-VCH Verlag GmbH & Co. KGaA, Weinheim.*

6.5 Conclusion

In this review, the chemistry of new tetrazole-containing compounds that also contain the *N*-oxide group have been discussed and the difficulties of synthesizing new energetic compounds that have the desired properties of a high density and thermal stability combined with a very high detonation velocity have been highlighted. All of the compounds that have

been discussed are examples of compounds that belong to the "green energetic" class of compounds since they only contain combinations of the elements C, H, N, and O and no heavy metals, aluminum or halides are present – all of which are hazardous to the environment. Despite the excellent energetic properties of RDX, it is toxic to the environment and human beings and therefore developing new compounds, which have energetic properties equal to or superior to RDX, but which are less environmentally hazardous, is a target. Another commonly used explosive is ε-CL-20, however it necessitates a synthetic route that involves many steps and the straightforward synthetic procedures used in the preparation of the *N*-oxide compounds discussed in this review is advantageous since less chemicals are involved in the synthetic routes, offering a more environmentally compatible process if produced on a large scale. The synthesis and characterization of TKX-50, in particular, has shown that this area offers potential for the synthesis of energetic materials that are not only environmentally compatible but which have some energetic properties that surpass even those of ε-CL-20. Only subsequent work in this area will determine whether tetrazole compounds containing *N*-oxide groups are the green explosives of the future.

Acknowledgments

Financial support of this work by the Ludwig-Maximilian University of Munich (LMU), the US Army Research Laboratory (ARL) under grant no. W911NF-09-2-0018, the Armament Research, Development and Engineering Center (ARDEC) under grant nos. R&D 1558-TA-01 and W911NF-12-1-0467, W911NF-12-1-0468, and the Office of Naval Research (ONR) under grant nos. ONR.N00014-10-1-0535 and ONR.N00014-12-1-0538 is gratefully acknowledged. The authors acknowledge collaborations with Dr. Mila Krupka (OZM Research, Czech Republic) in the development of new testing and evaluation methods for energetic materials and with Dr. Muhamed Sucesca (Brodarski Institute, Croatia) in the development of new computational codes to predict the detonation and propulsion parameters of novel explosives. We are indebted to and thank Drs. Betsy M. Rice and Brad Forch for many inspired discussions (ARL, Aberdeen, Proving Ground, MD).

References

1. Begtrup, M. (2012) Diazole, triazole and tetrazole N-Oxides. *Advances in Heterocyclic Chemistry*, **106**, 1–109.
2. Gao, H. and Shreeve, J.M. (2011) Azole-based energetic salts. *Chemical Reviews*, **111**, 7377–7436.
3. Klapötke, T.M. (2011) *The Chemistry of Energetic Materials*, 1st edn, Walter de Gruyter, Berlin.
4. Klapötke, T.M. and Holl, G., (2001) *Green Chemistry*, **G75**.
5. Agrawal, J.P. (2010) *High Energy Materials*, John Wiley & Sons, Weinheim.
6. Holleman, A.F., Wiberg, E. and Wiberg, N. (2007) Chapter XIV, *Lehrbuch der Anorganischen Chemie*, 102th edn, Walter de Gruyter, Berlin, New York.
7. Schmidt, E.W. (2001) *Hydrazine and its Derivatives*, vol. 1 and 2, 2nd edn, John Wiley & Sons, New York, Chichester.
8. Klapötke, T.M., Stierstorfer, J., Fischer, N. *et al*. (2011) *Strategies for the Development of RDX Replacements*, ARL-CECD Workshop, College Park, MD, April 3–6.

9. Huisgen, R. and Ugi, I. (1956) Zur Lösung eines klassischen problems der organischen stickstoffchemie. *Angewandte Chemie*, **68**, 705–706.
10. Wallis, J.D. and Dunitz, J.D. (1983) An all-nitrogen aromatic ring system: structural study of 4-dimethyl-aminophenylpentazole. *Journal of the Chemical Society. Chemical Communications*, 910–911.
11. Biesemeier, F., Müller, U. and Massa, W. (2002) Die Kristallstruktur von Phenylpentazol $C_6H_5N_5$. *Zeitschrift Fur Anorganische und Allgemeine Chemie*, **628**, 1933–1934.
12. Ugi, I. and Huisgen, R. (1957) Die Zerfallsgeschwindigkeit der Arylpentazole. *Chemische Berichte*, **91**, 531–537.
13. Harel, T. and Rozen, S. (2010) The tetrazole 3-*N*-oxide synthesis. *The Journal of Organic Chemistry*, **75**, 3141–3143.
14. Eicher, T. and Hauptmann, S. (1995) *The Chemistry of heterocycles*, Thieme, New York, p. 212.
15. Bottaro, J.C., Petrie, M., Penwell, P.E. *et al*. (2003) Nano/HEDM technology: late Stage Exploratory effort, SRI international chemical science and technology, 333, Ravenswood Ave, Menlo Park, CA 9402, Oct. 9th.
16. Travis, B.R., Sivakumar, M., Hollist, G.O. and Borhan, B. (2003) Facile oxidation of aldehydes to acids and esters with oxone. *Organic Letters*, **5**, 1031–1034.
17. Boneberg, F., Kirchner, A., Klapötke, T.M. *et al*. (2012) A study of cyanotetrazole oxides and derivatives thereof. *Chemistry - An Asian Journal*. 2013, **8**, 148–159.
18. Tran, T.D., Pagoria, P.F., Hoffman, D.M. *et al*. (2002) *Proceedings of International Annual Conference of ICT*, **33**, 45-1–45-16.
19. Hoffman, D.M., Lorenz, K.T., Cunningham, B. and Gagliardi, F. (2008) *Proceedings of International Annual Conference of ICT*, **39**, V29/1–V29/11.
20. Tarver, C.M., Urtiew, P.A. and Tran, T.D. (2005) Sensitivity of 2,6-Diamino-3,5-Dinitropyrazine-1-Oxide. *Journal of Energetic Materials*, **23**, 183–203.
21. Klapötke, T.M. (2012) *Chemistry of High Energy Materials*, 2nd edn, de Gruyter, Berlin, p. 17.
22. Tselinskii, I.V., Mel'nikova, S.F. and Romanova, T.V. (2001) Synthesis and reactivity of carbohydroximoyl azides: I. Aliphatic and aromatic carbohydroximoyl azides and 5-Substituted 1-Hydroxytetrazoles based thereon. *The Journal of Organic Chemistry*, **37**, 430–436.
23. Fischer, N., Klapötke, T.M., Reymann, M. and Stierstorfer, J. (2013) Nitrogen-Rich Salts of 5,5′-Bis(1-hydroxytetrazole) – energetic materials combining low sensitivities with high thermal stability. *European Journal of Inorganic Chemistry*, 2167–2180.
24. Fan, R., Li, P. and Ng, S.W. (2012) Bis[(diaminomethylidene)azanium] 5-(1-oxido-1H-1,2,3,4-tetrazol-5-yl)-1H-1,2,3,4-tetrazol-1-olate. *Acta Crystallographica*, **E68**, o1376.
25. Roh, J., Vávrová, K. and Hrabálek, A. (2012) Synthesis and functionalization of 5-substituted tetrazoles. *European Journal of Organic Chemistry*, 6101–6118.
26. Fischer, N., Izsak, D., Klapötke, T.M. *et al*. (2012) Nitrogen-rich 5,5′-Bistetrazolates and their potential use in propellant systems: A comprehensive study. *Chemistry - A European Journal*, **18** (13), 4051–4062.
27. Göbel, M., Klapötke, T.M., Piercey, D.G. *et al*. (2010) A general approach to next generation energetic materials: Nitrotetrazolate-2N-oxides, and the strategy of N-oxide introduction. *Journal of the American Chemical Society*, **132**, 17216–17226.
28. Sabate, C.M., Klapötke, T.M. and Rasp, M. (2009) Pyrotechnics, propellants and explosives: bridged 5-nitrotetrazole derivatives, in *New Trends in Research of Energetic Materials, Proceedings of the Seminar*, vol. 2, 12th, Pardubice, Czech Republic, pp. 627–646.
29. Mayer, R., Köhler, J. and Homburg, A. (2002) *Explosives*, 5th edn, Wiley VCH, Weinheim, pp. 174–177.
30. Mayer, R., Köhler, J. and Homburg, A. (2002) *Explosives*, 5th edn, Wiley VCH, Weinheim, pp. 237–239.

31. Churakov, A.M., Ioffe, S.L., Kuz'min, V.S. *et al.* (1988) Unusual conversion of Aminoazidofurazan into 1-Hydroxy-5-cyanotetrazole sodium salt. *Khimiya Geterotsiklicheskikh Soedineni*, **12**, 1666–1669.
32. Mayer, R., Köhler, J. and Homburg, A. (2002) *Explosives*, 5th edn, Wiley VCH, Weinheim.
33. Sućeska, M. (1995) *Test Methods for Explosives*, Springer, New York, p. 21 (impact); p. 27 (friction).
34. www.bam.de.
35. NATO (1999) NATO standardization agreement (STANAG) on explosives, impact sensitivity tests, no. 4489, Ed. 1, Sept. 17 (1999).
36. WIWEBStandardarbeitsanweisung 4-5.1.02, Ermittlung der Explosionsgefährlichkeit, hier der Schlagempfindlichkeit mit dem Fallhammer, Nov. 8 (2002).
37. http://www.reichel-partner.de.
38. NATO (2002) NATO standardization agreement (STANAG) on explosives, friction sensitivity tests, no. 4487, Ed. 1, Aug. 22 (2002).
39. Klapötke, T.M. and Stierstorfer, J. (2009). The CN_7^- Anion. *Journal of the American Chemical Society*, **131** (3), 1122–1134.
40. Hammerl, A., Klapötke, T.M., Nöth, H. *et al.* (2003). Synthesis, structure, molecular orbital and valence bond calculations for tetrazole azide, CHN_7 *Propellants, Explosives, Pyrotechnics*, **28** (4), 165–173.
41. Klapötke, T.M., Piercey, D.G. and Stierstorfer, J. (2011). The taming of CN_7^-: The azidotetrazolate-2N-oxide anion. *Chemistry: A European Journal*, **17**, 13068–13077.
42. Ganguli, P.S. and McGee, H.A. Jr. (1972) Synthesis and stability of nitrogen-oxygen-fluorine compounds from a MINDO [modified intermediate neglect of differential overlap] molecular orbital perspective. *Inorganic Chemistry*, **11**, 3071.
43. Huheey, J., Kreiter, E. and Kreiter, R. (1995) *Anorganische Chemie*, 2nd edn, Walter de Gruyter, Berlin, New York, appendix Table E.1.
44. Sućeska, M. (2010). *EXPLO5.4 program*, Zagreb, Croatia.
45. Sućeska, M. (1991) *Propellants, Explosives, Pyrotechnics*, **16**, 197–202.
46. Sućeska, M. (2004) *Materials Science Forum*, **465–466**, 325–330.
47. Sućeska, M. (1999) *Propellants, Explosives, Pyrotechnics*, **24**, 280–285.
48. Hobbs, M.L. and Baer, M.R. (1993) Proceedings of the 10th Symp. on Detonation, ONR 33395-12, Boston, MA, July 12–16, 409.
49. Crawford, M.-J., Klapötke, T.M., Martin, F.A. *et al.* (2011). Energetic salts of the binary 5-Cyanotetrazolate anion ($[C_2N_5]^-$) with Nitrogen-rich cations. *Chemistry: A European Journal*, **17** (5), 1683–1695.
50. Sabate, C.M. and Klapötke, T.M. (2009) Azole-based energetic materials: advances in nitrogen-rich chemistry, New Trends in Research of Energetic Materials, Proceedings of the Seminar, 12th, Pardubice, Czech Republic, **1**, p. 172–194.
51. Fischer, N., Gao, L., Klapötke, T.M. and Stierstorfer, J. (2013). Energetic Salts of 5,5′-Bis(tetrazole-2-oxide) in a Comparison to 5,5′-Bis(tetrazole-1-oxide) Derivatives. *Polyhedron*, **51**, 201–210.
52. Mayer, R., Köhler, J. and Homburg, A. (2002) *Explosives*, 5th edn, Wiley VCH, Weinheim, p. 174.
53. Zhang, M.-Xi, Eaton, P.E. and Gilardi, R. (2000). Hepta- and octanitrocubanes. *Angewandte Chemie-International Edition in English*, **39**, 401–402.
54. Bircher, H.R., Maeder, P. and Mathieu, J. (1998). Proceedings of the International Annual Conference of ICT, 29th, 94.1–94.14.
55. Thiele, J. (1888). Ueber Azo- und Hydrazoverbindungen des Tetrazols. *Justus Liebigs Annalen der Chemie*, **303**, 57–75.
56. Hammerl, A., Holl, G., Kaiser, M. *et al.* (2001). Methylated ammonium and hydrazinium salts of 5,5′-Azotetrazolate. *Zeitschrift für Naturforschung*, **56b**, 847–856.

57. Hammerl, A., Holl, G., Kaiser, M. *et al*. (2001) New Hydrazinium salts 5,5′-Azotetrazolate. *Zeitschrift für Naturforschung*, **56b**, 857–870.
58. Hammerl, A., Holl, G., Kaiser, M. *et al*. (2002) Salts of 5,5′-Azotetrazolate. *European Journal of Inorganic Chemistry*, 834–845.
59. Hiskey, M.A., Hammerl, A., Holl, G. *et al*. (2005) Azidoformamidinium and guanidinium 5,5′-Azotetrazolate salts. *Chemistry of Materials*, **17**, 3784–3793.
60. Klapötke, T.M. and Miró Sabaté, C. (2008) Nitrogen-rich tetrazolium azotetrazolate salts: a New family of insensitive energetic materials. *Chemistry of Materials*, **20**, 1750–1763.
61. Eberspächer, M., Klapötke, T.M. and Miro Sabate, C. (2009) Nitrogen-rich salts based on the energetic 5,5′-Hydrazinebistetrazolate anion. *Helvetica Chimica Acta*, **92**, 977–996.
62. Klapötke, T.M. and Miró Sabaté, C. (2009) New energetic compounds based on the Nitrogen-rich 5,5′-Azotetrazolate anion ($[C_2N_{10}]^{2-}$). *New Journal of Chemistry*, **33** (7), 1605–1617.
63. Tremblay, M. (1965) Synthesis of some tetrazole salts. *Canadian Journal of Chemistry*, **43**, 1230.
64. Hiskey, M.A., Goldman, N. and Stine, J.R. (1998) High-nitrogen energetic materials derived from azotetrazolate. *Journal of Energetic Materials*, **16**, 119.
65. Tappan, B.C., Ali, A.N., Son, S.F. and Brill, T.B. (2006) Decomposition and ignition of the high-nitrogen compound triaminoguanidinium azotetrazolate (TAGzT). *Propellants, Explosives and Pyrotechnics*, **31**, 163–168.
66. Michienzi, C.M., Campagnuolo, C.J., Tersine, E.G. and Knott, C.D. (2010) NDIA IM/EM Symposium, October 11–14, Munich, Germany, http://www.imemg.org.
67. Klapötke, T.M., Stierstorfer, J., Fischer, N. *et al*. (2012). Synthesis and crystal structures of new 5,5′-Azotetrazolates. *Crystals*, **2**, 127–136.
68. Churakov, A.M. and Tartakovsky, V.A. (2004). Progress in 1,2,3,4-Tetrazine Chemistry. *Chemical Reviews*, **104**, 2601–2616.
69. Sauer, J., Pabst, G.R., Holland, U. *et al*. (2001). 3,6-Bis(2H-tetrazol-5-yl)-1.2.4.5-tetrazine: A versatile bifunctional building block for the synthesis of linear oligoterocycles. *European Journal of Organic Chemistry*, **4**, 1666–1669.

7

Green Propellants Based on Dinitramide Salts: Mastering Stability and Chemical Compatibility Issues

Martin Rahm[1] *and Tore Brinck*[2]

[1]*Loker Hydrocarbon Research Institute and Department of Chemistry, University of Southern California, USA*
[2]*Applied Physical Chemistry, School of Chemical Science and Engineering, KTH Royal Institute of Technology, Sweden*

7.1 The Promises and Problems of Dinitramide Salts

The need to find a replacement for the environmentally hazardous ammonium perchlorate (AP, $NH_4^+ClO_4^-$) in solid rocket propellants is the main reason for the increasing interest in dinitramides, and ammonium dinitramide (ADN, $NH_4^+N(NO_2)_2^-$) in particular [1]. This chapter reviews the most up-to-date knowledge of the chemical and thermal stability of the dinitramide anion (DN) and its salts. It mainly focuses on ADN (Figure 7.1), but also touches on various metal and organic salts. Several of the different theoretical models that have been applied in explaining the behavior of solid and liquid dinitramide salts are covered, including discussions on thermal stability, decomposition routes, reactivity, and stabilization of DN salts. Spectroscopic investigations of ADN and potassium dinitramide (KDN) are also presented.

Aside from their potential in rocket propellants, explosives, and pyrotechnics, dinitramide salts are also considered for a wide range of other applications [2]. The potassium salt of dinitramide (KDN) is due to the high electrical conductivity of its combustion products,

Green Energetic Materials, First Edition. Edited by Tore Brinck.

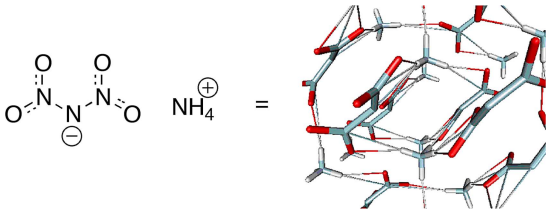

Figure 7.1 *Ammonium dinitramide (ADN).*

considered a possible plasma-forming fuel in future magnetohydrodynamic (MHD) generators [3]. Lithium dinitramide (LiDN) is reported to be an effective electrolyte additive in electrochemical cells (batteries), using lithium cathodes, where it significantly reduces self-discharge rates [4]. Due to a high solubility in lipophilic media, the use of dinitramide salts of biologically active cations holds promise in a variety of medical fields including pharmaceuticals, drug delivery, medical imaging, and diagnostics [5]. There are also synthetic possibilities, in which the dinitramide molecule can be used as a reagent in pursuit of new compounds [6–8].

The first commercial use of dinitramides was in gas generators for air bags [9–12]. In this application, the ADN precursor guanylurea dinitramide (GUDN) is used. More recently, an extra pure ADN-synthesis has enabled the development of a liquid ADN-based monopropellant [13]. The propellant, which significantly outperforms corresponding hydrazine-based formulations, is currently being tested in the navigational thrusters of the Swedish PRISMA satellite, now in low Earth orbit. The satellite's mission is to demonstrate green propellant technology and formation flying in space [14].

Unfortunately, the development of a solid ADN-based propellant has proved a considerable challenge. This is primarily due to ADNs reactivity towards many commonly used polymer binder systems, as well as its anomalous solid-state behavior [15–18].

ADN is in many respects a green oxidizing agent. Contrary to AP it does not contain chlorine, and as such does not produce hazardous chlorinated combustion products, such as hydrochloric acid (HCl). Given that a suitable fuel is chosen, ADN also enables a low-signature (no smoke) combustion. Finally, the dinitramide anion is slightly more energetic than perchlorate, which leads to a better performance (higher specific impulse). It has been estimated that, if a propellant formulation based on ADN were to replace today's AP-based propellants, the lift capacity of space launchers would increase by approximately 8% [19,20].

ADN is a colorless salt that becomes yellowish when non-dry. α-ADN has a monoclinic crystal structure in the $P2_1/c$ space group [21]. A second monoclinic high-pressure phase, β-ADN, has been reported over 2 GPa [22]. ADN is highly soluble in polar solvents while being nonsoluble in most low-polarity solvents [23]. Due to its high hygroscopicity, ADN dissolves if the relative humidity exceeds 55% [24,25]. Similar to all dinitramide salts, ADN is photosensitive and should not be subjected to excessive UV light [26,27]. The relevant properties of ADN are summarized in Table 7.1.

There are several ways of synthesizing ADN, using standard industrial chemicals. For instance, nitration of primary amines, or ammonia, using mixed acids or other nitration agents, such as NO_2BF_4 or N_2O_5 [26,28]. Since 1996 ADN has been produced on a larger scale at a pilot plant operated by SNPE Eurenco in Karlskoga, Sweden.

Table 7.1 *Properties of ADN. Reproduced with permission from [1] © 2010 M. Rahm, Stockholm, Royal Institute of Technology (KTH).*

Molecular weight	124.07 g/mol
Density of solid (25 °C)	1.81 g/cm [23]
Density of liquid (100 °C)	1.56 g/cm [27]
Melting point	93 °C [26]
Heat of formation	−35.4 kcal/mol [26]
Heat of combustion	101.3 kcal/mol [23]
Heat capacity	1.8 J/g [27]
Oxygen balance	+25.79%
Critical relative humidity	55.2% [23]
Friction sensitivity	72 N [29]
Impact sensitivity	5 J [29]
Electrostatic discharge sensitivity	0.45 J [28]
UV absorption maxima in water	214 and 284 nm [26,30]
Solubility in water at 20 °C	357 g in 100 g solvent [23]
Solubility in butyl acetate at 20 °C	0.18 g in 100 g solvent [23]
Solubility in dichloromethane at 20 °C	0.003 g in 100 g solvent [23]

7.2 Understanding Dinitramide Decomposition

Many dinitramide salts exhibit an anomalous solid-state decomposition, meaning faster decomposition in the solid state compared to liquid state, acceleration of decomposition within a small temperature range corresponding to the melting point of the eutectic mixture with the nitrate salt, and instantaneous inhibition of accelerated decomposition with the addition of water [31–33]. The behavior has been reported for a range of compounds, including salts of metal ions such as Li^+, Na^+, K^+, Rb^+, and Cs^+ [31]. Interestingly, the dinitramide salts of guanidine [21,31] and guanylurea [34] show no anomalous behavior.

One example of a metallic dinitramide, which will be discussed in parallel with ADN, is KDN. The simplicity of the potassium cation makes KDN a less complicated compound to analyze, compared to ADN. Hydrogen bonding and proton transfer, possible in ADN, cannot exist in KDN. However, extensive differential scanning calorimetry (DSC) studies have shown that KDN exhibits complicated eutectic, fusion, and liquefaction processes in the solid state [35]. It has been concluded that KDN's decomposition processes are highly topochemical, with accelerated decomposition following smaller particle sizes and cracking of crystals [35]. This is indicative of surface chemistry and similar to observations on ADN [31].

The activation barrier for decomposition of KDN under moist air has been estimated to 41 kcal/mol using a manometric procedure [31]. KDN's initial decomposition barrier (1 % decomposed) under closed vacuum has been reported to be 37.5 kcal/mol when using thermobalance measurements [36]. In its solid state, KDN primarily breaks down into KNO_3 and N_2O. NO and NO_2 have also been observed [35,37].

In contrast to KDN, ADN holds an intermediate position with regard to the anomalous decomposition behavior, exhibiting accelerated decomposition only close to the melting point of the eutectic with nitrate at 60 °C [32,33]. Its decomposition is also considerably

more complex. The initial activation energy for ADN is highly dependent on experimental conditions and is typically reported to be between 29–42 kcal/mol [26,28,31,33,38,39]. This corresponds to a span in possible reaction rates of about nine orders of magnitude. Under vacuum or after significant drying (<0.1% water) decomposition accelerates, and the activation barrier is around 30 kcal/mol. A barrier close to 40 kcal/mol is usually seen in non-dry samples, and at atmospheric pressure [31,33,38,39]. ADN has been reported to decompose into numerous products, such as N_2O, NO_2, NO, NH_4NO_3, HNO_3, N_2, HONO, H_2O, and NH_3 [22,28,33,38,40,41]. The relative amounts of these products vary depending on the extent of reaction, temperature, and pressure. Reported products also depend on the detection capacity of the instruments used in each study.

Initial ADN decomposition gases have been analyzed with time resolved transmission FT-IR spectroscopy at low and high temperatures [39]. It has been proposed that decomposition occurs mainly through two pathways [39,42], one that operates at low temperatures and produces NO_2 as the initial product,

$$N(NO_2)_2^- \rightarrow NO_2^{\bullet} + NNO_2^{\bullet -} \tag{7.1}$$

and another that becomes important at higher temperatures (≈150 °C) and produces mainly N_2O,

$$N(NO_2)_2^- \rightarrow NO_3^- + N_2O \tag{7.2}$$

Surface effects and dinitramide distortions have been speculated to provide an explanation for the anomalous decomposition of ADN and dinitramide metal salts. The dinitramide anion, which is typically semi-planar and resonance stabilized, was suggested to be less stable in the solid state due to a nonsymmetrical geometric and electronic structure [33]. The structural and electronic distortions of the dinitramide anion in different salts have been analyzed by spectroscopic and theoretical methods [15,17,43–45].

It is clear that ADN's decomposition is strongly dependent on the nature of its chemical surroundings. In principle there are three forms in which molecular ADN can exist; free isolated ions – DN^- and NH_4^+, complexed ions – $[DN^-NH_4^+]_n$, or as the conjugated acid/base pair – HDN and NH_3. A quantum chemical study has provided an estimate to this equilibrium in different media (Figure 7.2) [1]. It was found that solid-state like clusters are thermodynamically favored in all but the most polar solvents. Free ions are unlikely in nonpolar solvents, and highly unfavorable in the gas phase. The formation of dinitraminic acid (HDN) from ADN also appears unfavorable, even in the gas phase. In light of the study illustrated in Figure 7.2 we now proceed to discuss the different possible decomposition mechanisms in more detail.

7.2.1 The Dinitramide Anion

If one considers the isolated dinitramide anion (DN^-) in gas phase, the best *ab initio* estimate of its enthalpic decomposition barrier is 46.1 kcal/mol. The reaction proceeds through an internal transition state (**TS 1**, Figure 7.3), which transforms the dinitramide anion into an NO_3^- anion and nitrous oxide (**2**). Several groups have previously reported calculations on this transition state, at lower levels of theory [46–48].

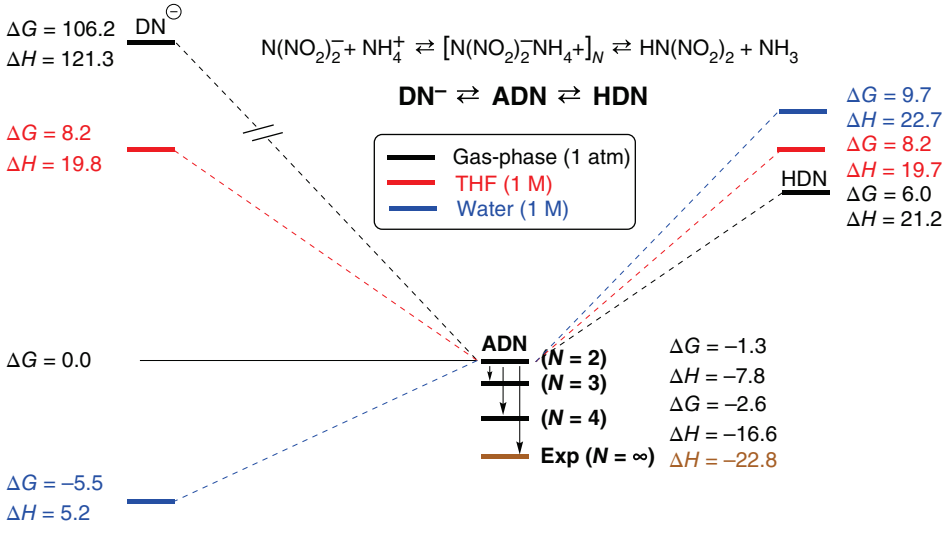

Figure 7.2 *The acid-base equilibrium of ADN in different media, calculated at the PCM-B3LYP/6-31 + G(d,p) level. N = 2,3 and 4 denotes ADN clusters of increasing size in the gas-phase. Reproduced with permission from [1] © 2010 M. Rahm, Stockholm, Royal Institute of Technology (KTH).*

The dissociation enthalpy for homolytic cleavage of the nitrogen–nitrogen bond (Eq. (2.1)) is as high as 49.7 kcal/mol at the CBS-QB3 level [20]. The corresponding energy barriers for both reactions are 44.8 (Eq. (7.1)) and 47.0 kcal/mol (Eq. (7.2)) at the B2PLYP/aug-cc-pVTZ level [20].

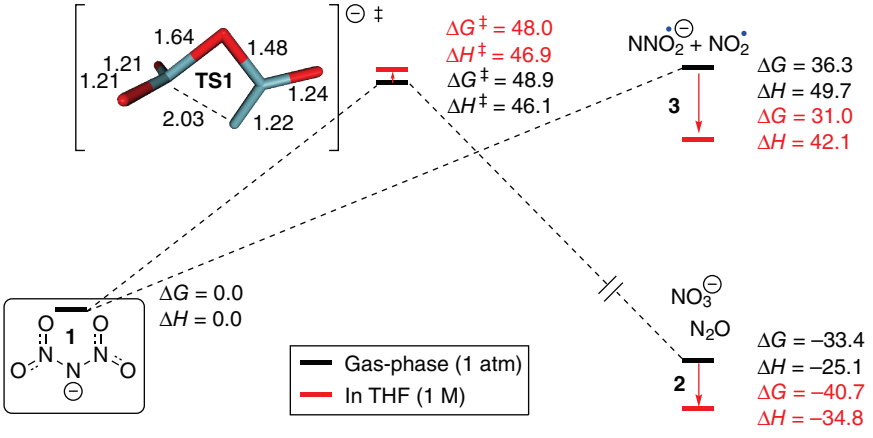

Figure 7.3 *Decomposition of the free dinitramide anion (**1**) in gas-phase and in THF solution. Concerted NO_2-transfer, (**TS1**). Homolytic bond fission (**3**). Energies in kcal/mol are calculated at the CBS-QB3 level [1, 20]. Bond lenghts are shown in Å. Reproduced with permission from [1] © 2010 M. Rahm, Stockholm, Royal Institute of Technology (KTH).*

It is clear that using a single dinitramide anion for modeling ADN stability results in unrealistically high decomposition barriers, and that the model is insufficient for describing proper kinetics of solid-state dinitramide salts. This is also in accordance with x-ray diffraction data and computational work, which has shown a single ion to be an insufficient model for recreating experimental dipole moments [44].

To improve on the single-molecule model, the effect of a more polar surrounding was investigated using implicit solvation models [20]. The effect of a low polarity solvent (THF) proved significant. The lowest decomposition route changed to a homolytic bond cleavage reaction (Eq. (7.1)), in which NO_2 radicals and NNO_2^- radical anions were formed (Figure 7.3). The enthalpy of activation for this process was estimated to 42 kcal/mol, which is in close agreement with experimental data available for several non-dry dinitramide solids, as well as dinitramide melts [31]. However, these calculations do not explain the anomalous behavior, that is even lower barriers at low humidity and pressure.

7.2.2 Dinitraminic Acid

In an effort to combine experimentally determined activation energies and final products in a viable theoretical explanation, several groups have invoked the conjugate acid of the dinitramide anion (HDN) [46–51]. On the basis of comparison with ammonium nitrate, it was argued that ADN could decompose via HDN, which forms through sublimation of the salt, or proton transfer in the crystal.

The most accurate calculations on the gas-phase stability of HDN give an enthalpy of activation of 36.5 kcal/mol for its decomposition (Figure 7.4) [51]. In comparing the obtained activation energies with experiments, HDN appears inadequate in explaining the energetics of solid-state dinitramide salt decomposition (which should be in the vicinity of $\Delta H^{\ddagger} \approx 30$ kcal/mol).

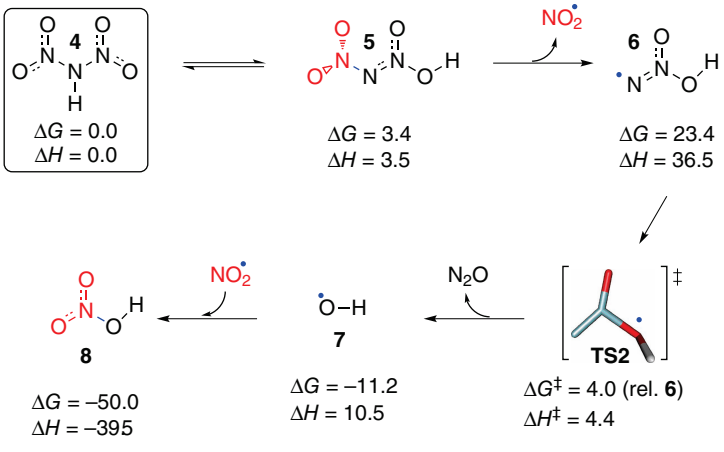

Figure 7.4 *Self-decomposition of HDN (**4**) can proceed through homolytic nitrogen–nitrogen bond cleavage in an HDN proton transfer isomer (**5**). The process generates HNO_3 and N_2O (**8**). Energies in kcal/mol are calculated at the CBS-QB3 level. Reproduced with permission from [1] © 2010 M. Rahm, Stockholm, Royal Institute of Technology (KTH).*

In addition to its high activation barrier, there are several other facts that argue against the importance of HDN formation [15,17]. Firstly, HDN has a reported pK_a of -4.9 [52], a value in good agreement with earlier theoretical estimates ($pK_a \approx -5.6$ [53]). Consequently, it is highly acidic and unlikely to exist in any but very harsh conditions, for example strong acids or vacuums. Secondly, the sublimation enthalpy of ADN has been indirectly obtained from experimental data and found to be 44 kcal/mol [46]. This significant energy barrier likely negates the possibility for HDN formation in a solid–gas interface. Thirdly, the kinetic isotope effect for the decomposition of ADN has been measured to 1.38 [33]. This low value, which corresponds to a nonprimary kinetic isotope effect, proves that the process does not include proton transfer in the rate-determining step. Figure 7.2 illustrates HDN's high energy relative to ADN in different media. Finally, the characteristic anomalous behavior of metal dinitramides (such as KDN) cannot be explained by the existence of HDN, since such compounds do not contain any hydrogen atoms.

7.2.3 Dinitramide Salts

In order to properly capture the complexity of solid-state dinitramide decomposition, the theoretical model needs to go beyond isolated molecules. Several conformers of the ADN and KDN dimer have been investigated by DFT methods, and already for these smaller clusters large differences from isolated molecules have been observed [17]. The ADN dimer proved to be the smallest gas-phase system where the salt can exist in ionic form (no spontaneous HDN formation). Due to the high surface to volume ratio in the dimer, the dinitramide anions experience a lower degree of coordination than in bulk solid-state ADN. It is important to realize that this is a similar situation to dinitramide anions situated on the surface of a crystal.

Interestingly, conformations that have one dinitramide anion coordinated at only one NO_2 group are energetically favored over conformations with a more symmetrical coordination. Dinitramide anions that have an unsymmetrical coordination of counterions become polarized. The polarization reduces the electron resonance stabilization of the anion, which results in partial weakening of one nitrogen–nitrogen bond (Figure 7.5). As a consequence, the dinitramide anion becomes distorted and transforms from a semi-flat structure into a twisted conformation. Despite being lower in energy (i.e., more thermodynamically favored), the elongated nitrogen–nitrogen bonds in the less symmetrical conformers of ADN and KDN have proved to be significantly weaker [17].

Even though KDN is known to exhibit the same anomalous solid-state behavior as ADN (and many other dinitramide salts), it is a more stable compound. That is, it has a higher activation barrier for its decomposition. When comparing calculations on ADN with those on KDN, it is clear that the difference in stability is correlated with the level of distortion. Distorted structures (like **10** for ADN and **16** for KDN) are considerably more prone to decomposition than their more symmetric analogues. The generally less distorted KDN structures also correspond to higher activation barriers, compared to ADN.

7.2.3.1 Potassium Dinitramide (KDN)

Figure 7.6 shows a proposed mechanism for the decomposition of KDN in the solid state. The initial decomposition step is the dissociation of a polarized (distorted) dinitramide anion

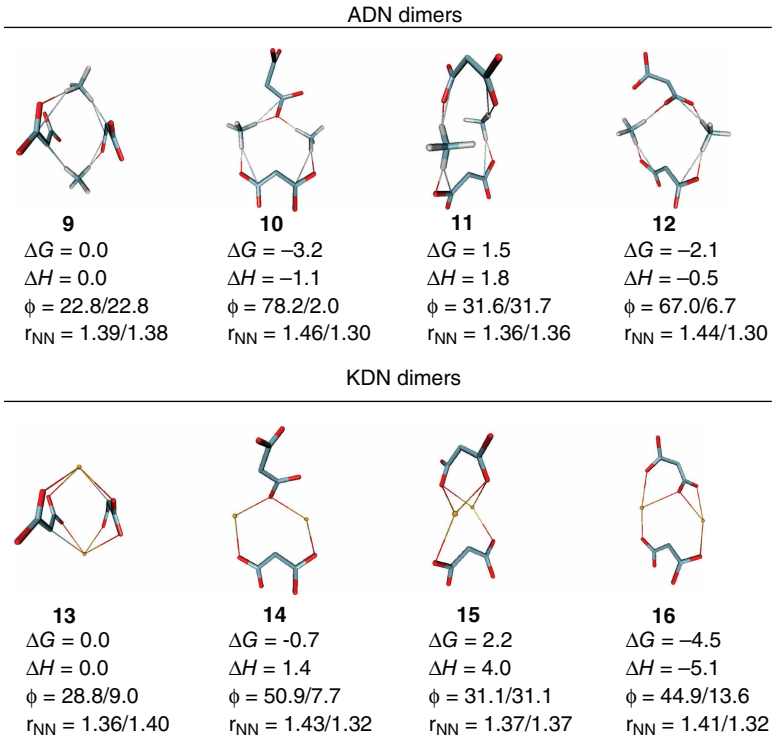

Figure 7.5 *Some conformers of the ADN and KDN dimer. Relative enthalpies (ΔH) and Gibbs free energies (ΔG) are calculated at the B2PLYP/aug-cc-pVTZ//B3LYP/6-31 + G(d,p) level for ADN and B2PLYP/TZV(2d) + //B3LYP/6-31 + G(d) level for KDN. ϕ denotes the dihedral twist angles of the two nitro groups in the most distorted dinitramide. r_{NN} are the corresponding nitrogen–nitrogen bond lengths. Reproduced with permission from [17] © 2010 American Chemical Society.*

into NO_2 and an NNO_2 radical anion (Eq. (7.1)). The enthalpy of activation for this step equals 36.0 kcal/mol when calculated at the B2PLYP/TZV(2d)+ level.

The first step (**16** → **17** + NO_2) is rate determining if it is assumed irreversible (NO_2 leaves). This is likely the case under an open atmosphere or low-pressure conditions. The second step is the homolytic cleavage of the NNO_2 radical anion, via **TS3**, with an enthalpy of activation of 17.7 kcal/mol (relative **17**). This step produces N_2O and leaves an anionic oxygen radical bound to the metallic surface (**18**). At thermodynamic equilibrium, assuming a pressure of 1 atm, **17** and **18** exist in equal quantities ($\Delta\Delta G^0 = 0$). Furthermore, the driving force for the combination of **18** with NO_2 radicals (**18** + NO_2 → **19**) is very large ($\Delta G^0 = -68.9$ kcal/mol; $\Delta H^0 = -75.0$ kcal/mol). Thus, NO_2 radicals that are not driven off by the low-pressure conditions are likely to be instantaneously scavenged by **18** upon formation, rendering the initial step irreversible. A combination of **18** and NO_2 leads to the formation of the nitrate salt, KNO_3 (**19**). As a whole, the reaction is greatly exothermic ($\Delta H^0 = -39.0$ kcal/mol) and produces N_2O and NO_3^- as final products, in good agreement with experimental observations [35,37].

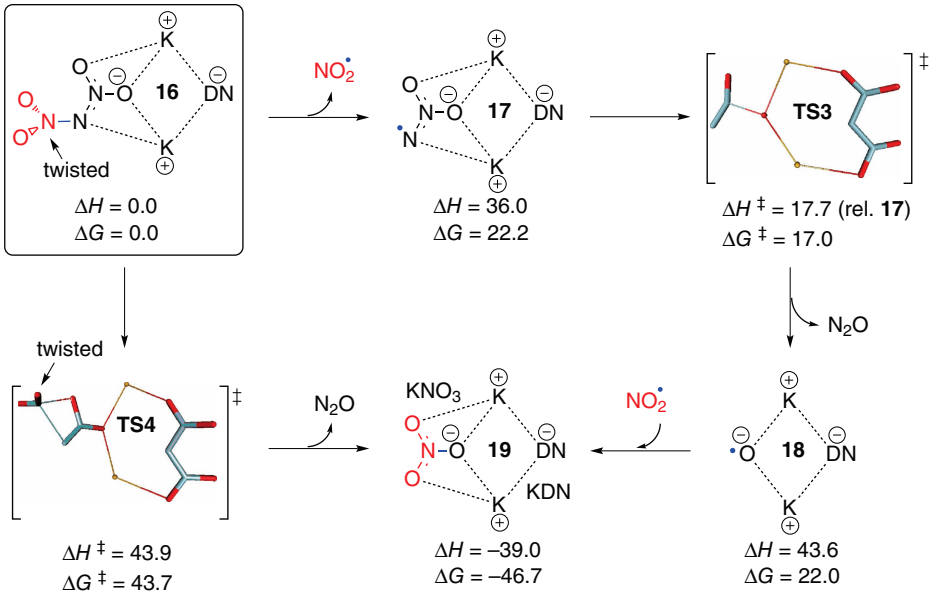

Figure 7.6 *Proposed decomposition mechanisms for solid-state KDN. Energies in kcal/mol are relative to* ***16*** *unless otherwise stated and calculated at the B2PLYP/TZVP(2d)+ level. Reproduced with permission from [17] © 2010 American Chemical Society.*

In order to better address issues such as long range coulombic interactions on real crystal surfaces and the effect of increased ion coordination for the critical rate-determining step, the calculations were expanded to larger clusters containing 12 dinitramide anions (this was also done for ADN) [15,17]. The 12-mer geometry was obtained through optimization from KDN's experimentally obtained crystal structure [21]. However, the lowering of the dissociation barrier due to a presumed increased stabilization of the formed NNO_2 radical anion was found to be minor.

The transformation of KDN into N_2O and NO_3^- can also occur in a direct pathway through **TS4** (Figure 7.6, Eq. (7.2)). **TS4**, which is the analogue to **TS1** for the free dinitramide anion, corresponds to an enthalpy of activation of 43.9 kcal/mol. It is likely that the two processes compete, depending on the temperature and pressure. It is noteworthy that both competing processes proceed through a twisted conformation of the dinitramide anion ($\Phi = 90$), and that both are greatly favored by surface polarization.

7.2.3.2 Ammonium Dinitramide (ADN)

Because of the greater complexity of ADN's decomposition, compared to KDN, an initial model based on the dimer was scaled up to the tetramer [15,17]. Figure 7.7 shows the proposed decomposition mechanism for solid-state ADN, occurring at the surface of a tetramer cluster. The barrier for dissociation of a dinitramide anion into an NO_2 radical and an NNO_2^- radical anion (Eq. (7.1)) is lowered by a staggering 19.0 kcal/mol compared to the same reaction for the lone dinitramide anion in the gas phase. This corresponds to a rate

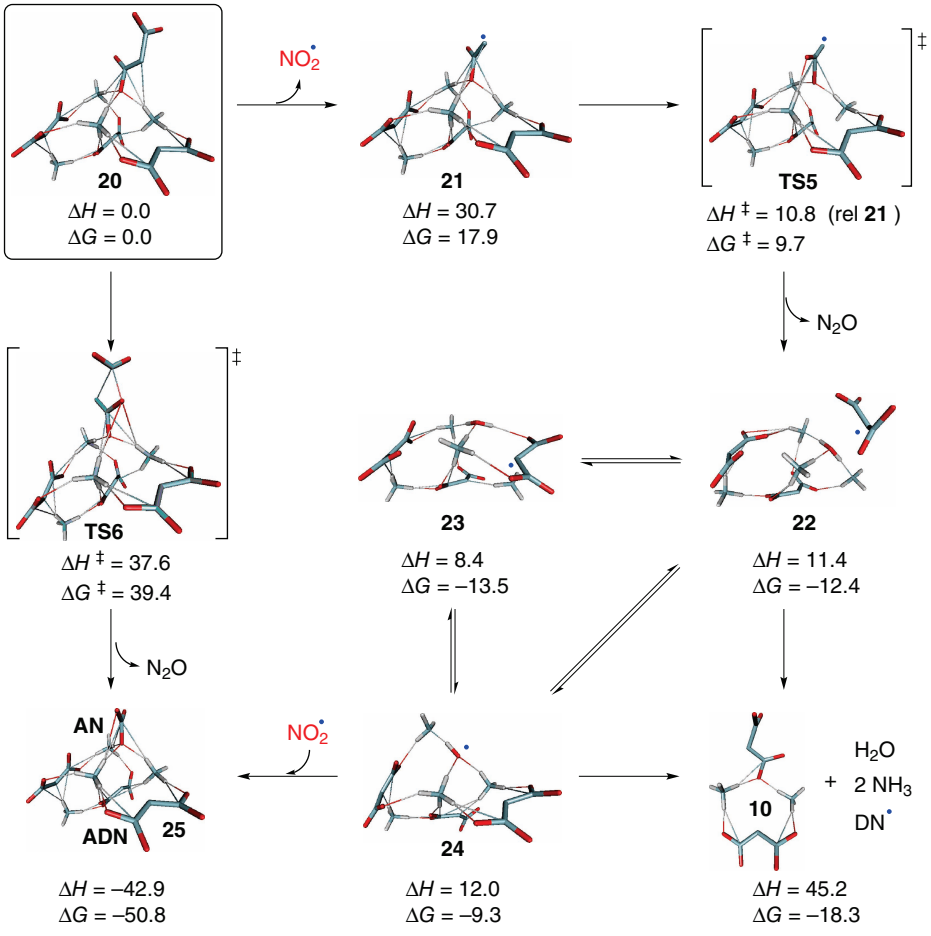

Figure 7.7 *Proposed decomposition pathways for solid-state ADN. Energies in kcal/mol are relative to* ***20*** *unless otherwise stated and calculated at the B2PLYP/TZV(2d,2p)+ level. Reproduced with permission from [17] © 2010 American Chemical Society.*

difference of close to 14 orders of magnitude. Modeling of the initial step on the surface of an ADN 12-mer did not reduce the barrier significantly compared to the tetramer. It did, however, contrary to the case of KDN, lower it markedly compared to the dimer model.

If one assumes the first step (**20** → **21**) to be irreversible (due to loss of NO_2), it becomes rate determining. The initial step is quickly followed by the release of N_2O through **TS5**, and the likely formation of a mixture of OH radicals, dinitramine radicals, water, and ammonia in **22**, **23**, and **24**. At this point the OH radicals will act as scavengers of NO_2 radicals (making the initial step irreversible). The combination of **24** and NO_2 produces the final decomposition product: ammonium nitrate (NH_4NO_3) in **25**.

The dinitramine radical, which is formed in this process (seen in **22**), was predicted to decompose primarily through homolytic bond dissociation of its nitrogen–nitrogen single

bond requiring an enthalpy of activation of 20.1 kcal/mol [17]. The dinitramine radical can also decompose in the presence of other radicals through the formation of various trinitroamine ($N(NO_2)_3$) isomers. The stability and experimental detection of trinitroamine (trinitramide) is addressed in detail elsewhere [8]. The formation and decomposition of the dinitramine radical (Figure 7.7) helps to explain the formation of water, as well as ammonia and several NO_X species that have been observed experimentally [33,38,39,42,54,55]. Over all, the proposed decomposition mechanism is greatly thermodynamically favored, with a relative Gibbs free energy of close to −50 kcal/mol.

The direct formation of nitrate through a concerted process, analogous to **TS1** and Eq. (7.2), was also investigated in the tetramer model (**TS6**). The polarization of the perturbed anion had the effect of lowering **TS1** by almost 9.5 kcal/mol, giving an enthalpy of activation of 37.6 kcal/mol and a free energy barrier of 39.4 kcal/mol.

It is concluded that, analogous to what is observed in the dimer models, distorted and polarized dinitramide conformations also form spontaneously on the surface of larger, more realistic, clusters. Due to the larger number of coordinating cations in these systems, the polarization effect is enhanced, which can be seen when observing the dihedral twist angles.

For KDN, the polarization phenomenon appears to reach its maximum already in the dimer model, as further expansion into larger clusters has limited effect. Thus, the initial decomposition barrier for KDN is estimated to 36 kcal/mol. In contrast, for ADN, the initial dissociation (likely to be rate-determining) is treated accurately first when the size of the system is expanded into the tetramer. The barrier does not change with further expansion of the system into the 12-mer. The difference relative to the alternate higher energy pathway (direct N_2O formation, Eq. (7.2)) is unlikely to shrink below 6 kcal/mol. This is in agreement with experimental results, which detect NO_2 at considerably lower temperatures than N_2O [39,42]. Hence, our best estimate of ADN's initial decomposition barrier is approximately 30 kcal/mol. This is in very good agreement with what is seen experimentally, in the case of dry samples or vacuum conditions [33,38,39].

7.3 Vibrational Sum-Frequency Spectroscopy of ADN and KDN

As it is likely that surface chemistry plays an important role in the chemical reactivity and stability of both ADN and KDN, detailed knowledge of their molecular surface structure is important. To verify the theoretical predictions regarding polarized dinitramide anions, described in the previous section, both salts were investigated using Vibrational Sum-Frequency Spectroscopy (VSFS) [45]. The details of this study will not be reiterated here; instead the main conclusions will be summarized.

VSFS is a coherent second-order nonlinear laser spectroscopy technique, which can be used to investigate the molecular structure of interfaces that are accessible by a laser. The second-order nature of VSFS enables it to only detect molecules with a net orientation. Thus, it only probes the very few molecules residing at the interface between two centrosymmetric media, such as a gas–liquid or a liquid–solid boundary. The technique involves a visible laser beam at a fixed frequency and a tunable infrared (IR) laser beam, which results in the generation of a beam having a frequency equal to the sum of the frequencies of the incident beams. The beam induces IR and Raman anti-Stokes transitions in the surface molecules, which require the molecular vibrations to be both IR and Raman

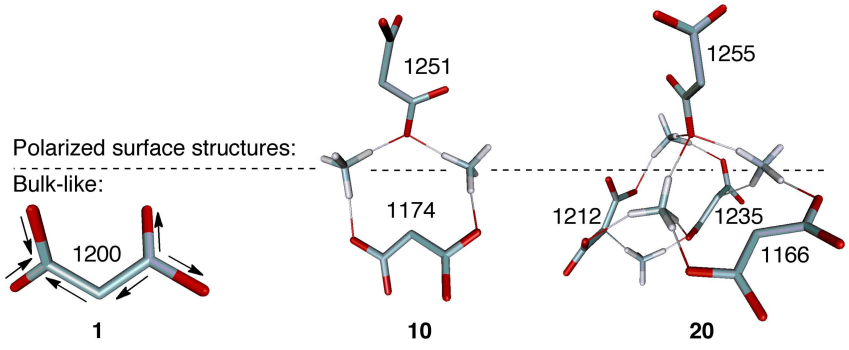

Figure 7.8 *The frequency of the symmetric and out of phase NO_2 stretching mode of the dinitramide anion is blue shifted when the anion is polarized (twisted). Harmonic vibrational frequencies have been calculated at the B3LYP/6-31 + G(d,p) level, and scaled by 0.97 to fit experimental data of the 1200 cm^{-1} band. Reproduced with permission from [45] © 2010 American Chemical Society.*

active in order to generate a signal in the sum-frequency spectrum. The underlying theories behind VSFS are outlined elsewhere [56–60].

In order to enable a clear identification of polarized surface dinitramides, a large frequency shift of the vibrational mode compared to the corresponding signal originating from nonpolarized molecules is preferable. Furthermore, the vibrational mode(s) used for identification should not be close to, or overlap, bands from the nitrate decomposition products, which are presumed to partly occupy the surface. The vibrational mode most suitable for this purpose is the symmetric and out-of-phase NO_2 stretch, $\nu_s(NO_2)$, of the dinitramide anion (Figure 7.8). Since this mode includes a significant amount of anti-symmetric N–N–N stretching, it is sensitive to changes in the N–N bond strength. As demonstrated in the previous sections of this chapter, the N–N bond strength changes dramatically in going from a nonpolarized to a polarized dinitramide anion. Consequently, a relative shift of approximately $+55\,cm^{-1}$ can be expected for the $\nu_s(NO_2)$ mode in ADN (Figure 7.8).

Initially, theoretical orientation-averaged VSFS-like spectra were calculated for a large number of ADN, KDN, NH_4NO_3, and KNO_3 clusters by multiplying IR and Raman intensities obtained at the B3LYP/6-31 + G(d,p) level [45]. The average sum frequency intensity of the $\nu_s(NO_2)$ stretch of polarized dinitramide anions was estimated to be significantly higher than most other bands.

Crystals of ADN and KDN were obtained after crystallization in 2-propanol. Some crystals were stored in saturated solution, whereas others were stored in air. Different conditions (such as ambient and N_2 atmosphere) were also tried during VSFS acquisition. In addition to the VSFS studies, bulk IR and Raman measurements were made on ADN, KDN, NH_4NO_3, and KNO_3 crystals (Figure 7.9). Published experimental IR and Raman data was also used to facilitate the assignment of the VSFS peaks [61,62].

The surface of KDN was found to be rough and predominantly covered with a thin layer of KNO_3, which due to its low thickness was not detectable by infrared and Raman spectroscopy [45]. This is in agreement with observations done by XPS [35]. The presence

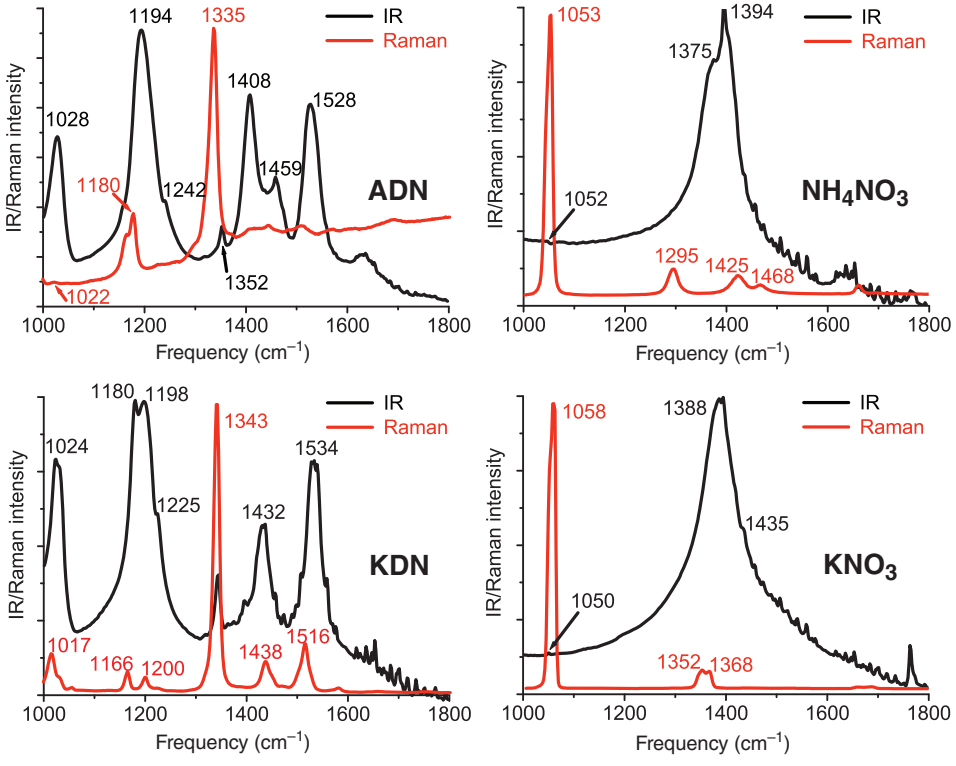

Figure 7.9 *Bulk Raman and IR spectra of ADN, KDN, NH_4NO_3, and KNO_3 crystals. Reproduced with permission from [45] © 2010 American Chemical Society.*

of distorted dinitramides could not be ascertained due to the large presence of nitrate, and the overlap of several relevant dinitramide and nitrate VSFS peaks. In contrast, no conclusive signature of NH_4NO_3 was observed on the surface of ADN. Instead, ADN exhibits an extremely inhomogeneous surface on which polarized dinitramide anions were detected (Figure 7.10). However, as it is well established that the main solid-state decomposition product of both ADN and KDN is nitrate [22,33,38,41] the observed peaks (1348 and 1044 cm^{-1} in Figure 7.10) are likely to originate at least partly from nitrate.

Due to the random nature of the ADN surfaces, quantitative measurements were impossible to perform. No correlation between preparatory methods and peaks were found, and the spectra in Figure 7.10 have been chosen to show all encountered signals. The peaks at ~1180 and ~1210 cm^{-1} originate from the symmetric NO_2 stretching vibration (out-of-phase) of ADN, $\nu_s(NO_2)$ [61,62]. Good agreement with the computed spectra indicates that the peaks at ~1243 and ~1271 cm^{-1} originate from the same vibration in polarized anions. A thorough discussion surrounding the peak assignments for both ADN and KDN is given elsewhere [45].

The theoretical and experimental observations of polarized dinitramide anions on disordered surfaces of ADN are of importance for understanding the chemical stability and reactivity of the ADN salt. As unwanted decomposition is likely to be topochemical,

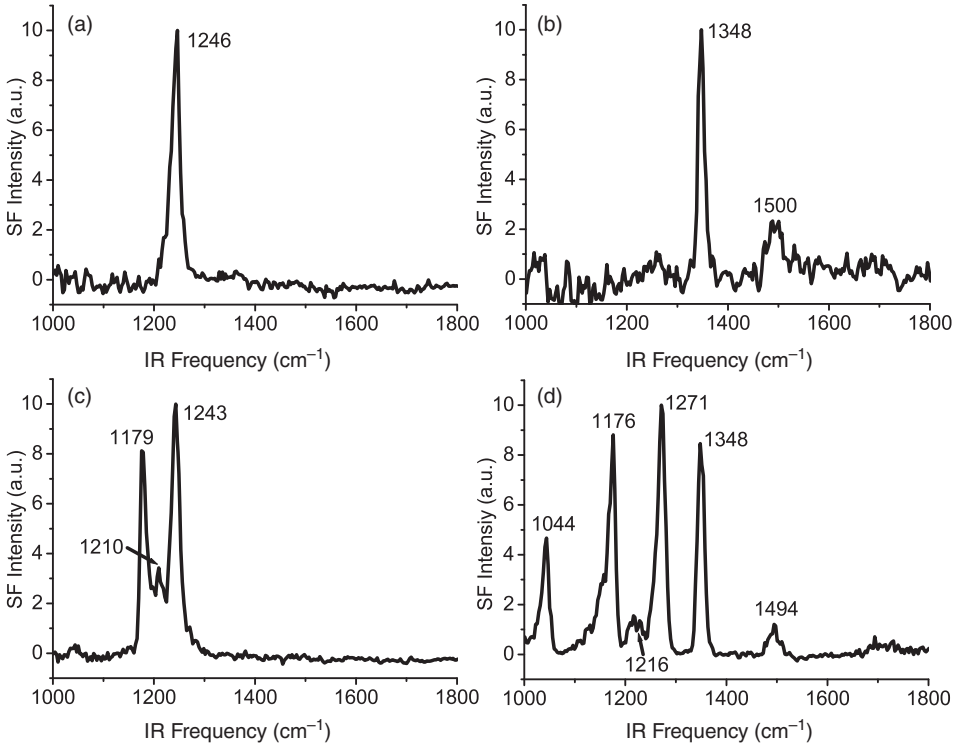

Figure 7.10 *Four selected VSFS spectra of ADN that show proof of a highly disordered surface, where polarized dinitramide anions are present in different conformations. Reproduced with permission from [45] © 2010 American Chemical Society.*

these results will hopefully facilitate a more efficient tailoring of surface-active polymer support, stabilizers, and/or coatings for ADN.

7.4 Anomalous Solid-State Decomposition

The so-called anomalous behavior of dinitramide salts has long puzzled researchers. It is loosely defined as faster decomposition of the salts in the solid state compared to liquid state, acceleration of decomposition at the melting point of the eutectic mixture with nitrate, and instantaneous inhibition of accelerated decomposition with the addition of water [31–33].

There is irrefutable experimental evidence showing the existence of surface processes in dinitramide decomposition. For instance, the decomposition rates of dinitramide salts are known to accelerate with grinding of crystals [31,35]. Grinding increases the overall surface area, and creates new nondecomposed surfaces of dinitramide. As speculated in earlier work [31], the formation of eutectic mixtures is also accompanied by an increased number of crystal defects. This will likely reduce the stability of the regions bordering such defects.

The dependence on pressure and the stabilizing effect of water vapor also supports the importance of surface processes.

Our computational studies have revealed that the decomposition barrier of an unperturbed dinitramide anion is around 40–42 kcal/mol in polar and nonpolar solvents. This value for the barrier is similar to that for symmetric nonpolarized (i.e., bulk-like) clusters of ADN and KDN in gas phase. The average value of 41 kcal/mol is in agreement with the values experimentally obtained for several dinitramide metal salts, both in the solid state, and in the molten state [31]. The value is also in agreement with non-dry ADN under atmospheric conditions [33,38].

As discussed in the previous sections, an accelerated decomposition, with activation barriers of approximately 30 and 36 kcal/mol for ADN and KDN, respectively, is explained by a situation where the dinitramide ion is polarized due to favorable interactions with its surrounding counterions. This effect is especially pronounced when the respective solids are subjected to a surrounding with weak interactions to the surface, such as a vacuum or a nonpolar environment. Our VSFS studies have revealed that polarized structures do exist even under ambient conditions [45]. With this in mind, the known stabilizing effect of water is easily understood. Water molecules coordinating to protruding dinitramide anions effectively counteract the polarization through hydrogen bonding. Implicit and explicit solvation modeling of dinitramide clusters have shown that water reduces decomposition rates by several orders of magnitude [15,17]. This is in excellent agreement with experimental findings [33].

Because both theoretical modeling and spectroscopic measurements suggest that the surfaces of ADN and KDN are complex in nature, pure dinitramide covered surfaces are unlikely to exist for longer time periods, especially under drying conditions. Instead, a pacifying layer of nitrate appears to cover the surface of KDN, whereas ADN appears to have both nitrate and dinitramide present on its irregular surface. As speculated in earlier literature [31,33], the occurrence of nitrate–dinitramide eutectic mixtures is a likely explanation for the accelerated decomposition of ADN at 60 °C, and KDN at 109 °C. However, as bulk and sub-surface Raman and IR measurements show no sign of nitrate in either salt, the anomalous acceleration likely arises due to melting processes on the surfaces of the salt particles.

In this context it is also worth mentioning the charge-topological similarity between the nitrate ion and the NNO_2^- radical anion, which is formed in the initial steps of KDN's and ADN's decomposition (and likely many other dinitramide salts). An ADN-NNO_2NH_4 mixture is likely to exhibit similar physical properties to ADN-NO_3NH_4 (e.g., close to identical melting points). Since the NNO_2^- radical anion is significantly less stable than both nitrate and dinitramide (see **17** and **21** in Figures 7.6 and 7.7), it will greatly affect the overall decomposition rate. During its short existence, it and its immediate surroundings constitute an ADN-NO_3NH_4 imitating ADN-NNO_2NH_4 mixture. As such regions are likely to melt close to the eutectic point, they will add to the overall acceleration of decomposition in this temperature range. However, it should be noted that no experimental data is known for NNO_2NH_4, and that its physical properties and importance are purely speculative.

The anomalous acceleration at the eutectic temperature only occurs at that specific temperature, and not above. The constitution of ADN and NO_3NH_4 at the eutectic point is reported to be a 1 : 2 ratio [33]. Thus, by omitting the many phase changes inherent to pure

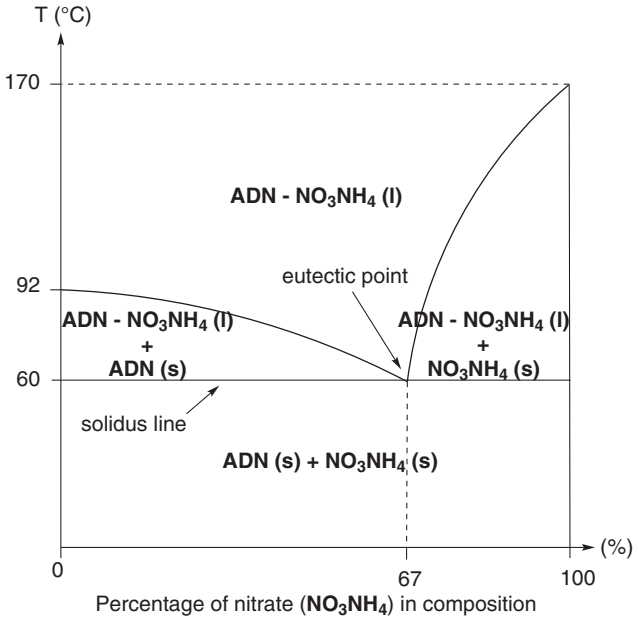

Figure 7.11 *An estimate of the ADN-NO_3NH_4 eutectic system. Accelerated decomposition at specifically 60°C is explained by melting processes. A pacifying NO_3NH_4-phase is expected to form if the concentration of nitrate in the surface composition exceeds ~67%.*

NO_3NH_4, a crude sketch of the binary eutectic system can be devised from the melting points of ADN and NO_3NH_4 (Figure 7.11). The accelerated decomposition at the eutectic temperature is likely due to the necessary phase changes (melting) that need to occur when the system resides in this temperature (see horizontal solidus line in Figure 7.11). Such processes will create new interfacial surfaces and crystal defects where polarized dinitramides can form and accelerate decomposition. Because nitrate is generated during decomposition, such an effect should be observable regardless of the initial concentration of NO_3NH_4 in the system. The decrease in rate, when increasing the temperature above the eutectic temperature, is explained by a system in equilibrium (no phase changes). Crystallization of ammonium nitrate on the surface of ADN should also act stabilizing. The decomposition barrier for any co-existing liquid ADN-NO_3NH_4 phase will be similar to that for bulk ADN, that is approximately 40–42 kcal/mol.

7.5 Dinitramide Chemistry

7.5.1 Compatibility and Reactivity of ADN

The ambivalent reactivity of dinitramide salts has long plagued efforts directed towards ADN-based solid rocket propulsion. For example, the polymer matrix of choice in most state-of-the-art AP-based propellants is based on hydroxyl-terminated polybutadiene.

This polymer is in itself sufficiently compatible with ADN. However, it typically requires the use of isocyanate containing cross-linking (curing) agents to formulate the propellant. There are reports of ADN-based propellants prepared in such a manner [63–65]. However, as isocyanates are toxic, as well as incompatible with ADN [66], the use of such conventional cure chemistry is far from ideal. Similarly, many other conventional polymer matrices have been tried with little success.

Recent systematic heat-flow calorimetric (HFC) studies [1,16,18] have confirmed the high ambivalence of ADN's reactivity, and we have on occasion referred to it as the Dr. Jekyll and Mr. Hyde of molecules.

To name a few examples, the energetic polymers poly(glycidyl azide) polymer (GAP) and poly-3-methyl-3-(nitratomethyl)oxetane (poly-NIMMO) are known to be ADN compatible. In addition to these materials, hyperbranched poly-3-ethyl-(hydroxymethyl)oxetane (poly-TMPO) has been shown to be surprisingly compatible. A number of different copolymers of TMPO and THF also exhibit good stability towards ADN [18]. The ether functionality is deemed stable when present in a small molecule in solution, and when incorporated into polymers such as GAP, NIMMO, and poly-TMPO. In contrast it is furiously incompatible when present in a larger polyethylene glycol (PEG) chain [18].

It is noteworthy that carboxylic acid groups appear thermally stable with ADN, when present in solution. This goes against the premise that acidity (although weak in this case) is of importance for ADN's stability. It can also be concluded that hydroxyl groups, which are present in various alcohols and polymers, work well with ADN.

Amines have been shown to be incompatible in several cases. However, the amine functionality is also present in several stable dinitramide salts, such as guanylurea dinitramide (GUDN), as well as known ADN stabilizing agents, such as 2-methyl-4-nitroaniline (MNA). Dimethyl amines have proved exceedingly stable when present in the solvent DMF, while incompatible when situated on a phenyl group, such as N-dimethyl aniline. Azides are undoubtedly thermally stable together with ADN, while carbonyl groups can be both stable (e.g., in carboxyl groups) and unstable (e.g., in ketones).

We can conclude that the ADN-compatibility of several functional groups depends heavily on their physical environment. For instance, hydroxyls, amines, and ethers behave differently when present in a small molecule in solution, compared to when embedded in a macromolecule. One likely cause for the wide range of incompatibility issues is the ammonium cation. The surrounding environment needs to discourage exchange of protons, by strongly binding to the surface of ADN. To facilitate this, the surrounding should preferably be polar in nature, and capable of hydrogen bond donation. This will stabilize surfaces of ADN, and discourage the formation of HDN and ammonia. At the same time the surroundings should not enable ADN to become partly solvated, as this likely creates new reaction centers at the ADN-polymer interface. As ADN predominantly exists as clusters in medium and low-polarity solvents (that have surfaces), the above reasoning also applies to such solutions.

There are several types of reaction mechanism that can explain some of the dinitramide's reactivity. These include 1,3-dipolar cycloadditions and 1,4-conjugate addition of HDN to various olefinic double bonds, the presence of radical decomposition intermediates, and ammonium mediated conjugate additions of the dinitramide anion to unsaturated moieties [1]. These will now be discussed.

7.5.2 Dinitramides in Synthesis

To date, the published use of dinitramide moieties in synthesis is limited. A fairly large number of organic and inorganic dinitramide salts have been reported. However, as the dinitramide anion is in principal chemically unchanged between different salts, varying only in the dihedral twist angle of its NO_2 groups, these will not be addressed here.

We recently reported the experimental detection of trinitroamine (trinitramide, TNA), which was prepared through metathesis reactions, melting KDN and ADN acetonitrile solutions over NO_2BF_4 at −40 °C [8]. Being the largest nitrogen oxide to date, with an outstanding energy content, estimated density, and oxygen balance, it could prove useful as a high-performance oxidizer in cryogenic rocket engines. Unfortunately, TNA is of limited stability in solution, and will decompose rapidly at ambient temperatures. Future studies will hopefully reveal its properties in its cryogenic solid state.

Another example of utilizing the dinitramide moiety in synthesis is dinitramide substituted borates, that is $BH_{(4-x)}(DN)_x^-$. Several such compounds have recently been prepared in solution and characterized by $^{11}B/^{14}N$-NMR [67].

Earlier literature has reported on the addition of HDN to activated olefinic double bonds through Michael-type reactions in benzene [68]. 2-Propenal, methyl vinyl ketone, and phenyl vinyl ketone were shown to react rapidly, but the more electron-poor double bonds of acrylonitrile and methyl acrylate proved nonreactive [68].

In an attempt to explain this reactivity, and clarify the ambivalent reactivity of dinitramides in general, a number of model compounds were analyzed in gas-phase using B3LYP/6-31 + G(d,p) and basis set extrapolated CCSD(T) calculations. The reactions were found to proceed through a type of concerted 1,4-conjugate addition, in which the carbonyl oxygen of the olefin accepts a proton from HDN, as the center nitrogen of the dinitramide attacks the β-carbon (Figure 7.12). Subsequent keto-enol tautomerization gives the final products, which have been identified by ^{1}H-NMR [68].

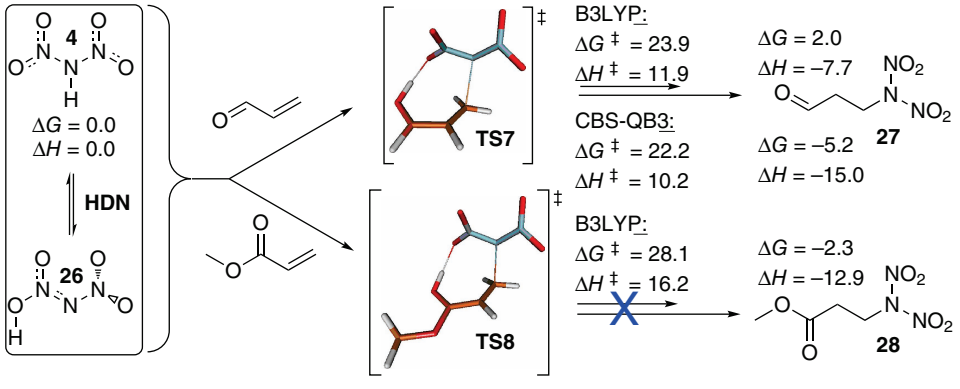

Figure 7.12 *Reactions between HDN and electron-poor olefinic double bonds are possible via concerted conjugate addition, provided that the bond is neighbored by a sufficiently basic carbonyl group. Energies in kcal/mol (1 M) are calculated at the B3LYP/6-31 + G(d,p) level. X means no reaction at room temperature [68].*

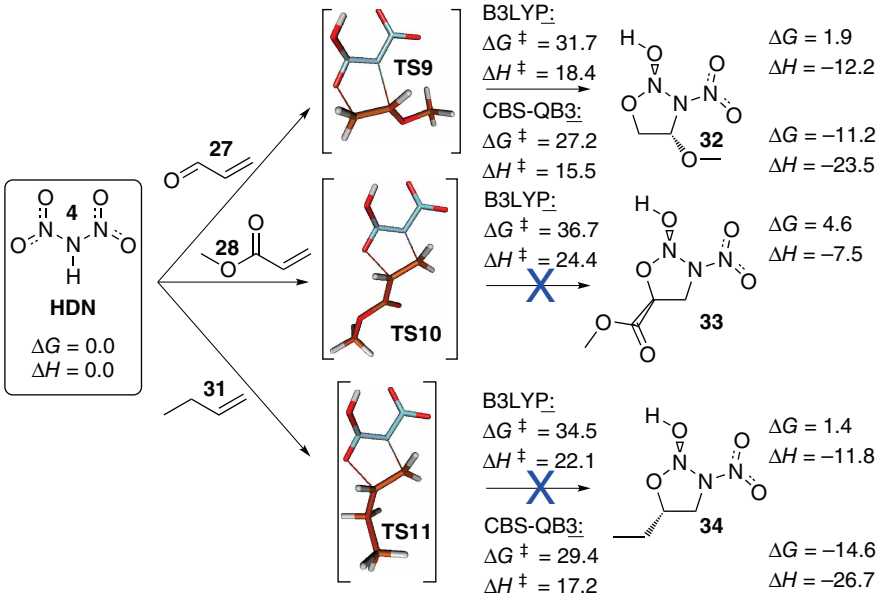

Figure 7.13 *Reactions between HDN and electron-rich olefinic double bonds are possible through 1,3-dipolar cycloadditions. Energies in kcal/mol (1 M) are calculated at the B3LYP/6-31 + G(d,p) level. X means little or no reaction predicted after 19 days at 75 °C.*

When a lone aldehyde or ketone neighbors the double bond, the basicity of the carbonyl is sufficient to make the reaction proceed rapidly. However, when an electronegative group or element, such as oxygen, neighbors the carbonyl the activation barrier rises significantly, and hinders the reaction (Figure 7.12).

Our theoretical studies have also suggested that HDN can react in hitherto unknown 1,3-dipolar cycloaddition reactions with olefinic double bonds (Figure 7.13). The reactivity of eight different double bonds, with varying electron affinity, was modeled with HDN, and compared to the known 1,3-dipoles azide and nitrile oxide. Electron-rich double bonds, such as vinyl ethers, were predicted to be substantially more reactive than more electron-poor ones, such as acrylates [7].

One explanation for the wide range of compatibility issues of ADN is realized when considering conjugate additions of the ammonium–dinitramide ion pair to various double bonds. Figure 7.14 shows some of the investigated reactions with vinyl and carbonyl double bonds. Nonsubstituted alkenes are predicted to be kinetically stable with respect to dinitramide addition, with free energy activation barriers exceeding 40 kcal/mol. This is in agreement with our HFC study. The reactivity between ADN and electron-poor double bonds, such as acrylates, can be understood by ammonium-mediated 1,4-conjugate addition of the dinitramide anion to the β-carbon (**TS13**, Figure 7.14). The observed reactivity of ADN towards ketones can also be explained by a similar 1,2-addition to the carbonyl carbon (**TS15**, Figure 7.14). For clarity, energies in Figure 7.14 are shown relative HDN and ammonia. However, the free energy activation barriers are very similar to when ADN clusters are used as references, due to their lower entropy.

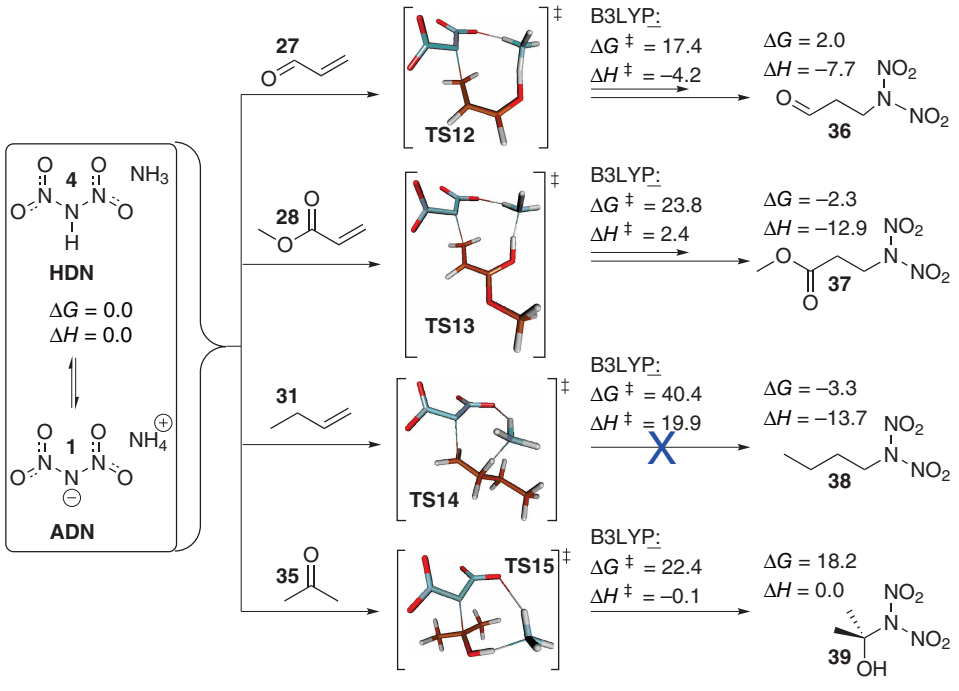

Figure 7.14 *Conjugate additions of the ammonium-dinitramide ion pair to vinyl and carbonyl carbons explain much of ADN's reactivity. Energies in kcal/mol (1 M) are calculated at the B3LYP/6-31 + G(d,p) level. X means little or no reaction after 19 days at 75 °C.*

Some of the reactivity of HDN and ADN, which is now rationalized by theoretical models, is intriguing and can possibly be utilized in synthesizing a range of new organic dinitramide derivatives.

7.6 Dinitramide Stabilization

The most important aspect for stabilization of dinitramide salts is maintaining electron delocalization in the anion. Polarized dinitramides, which are primarily present at interfaces, reduce the stability of ADN under nonpolar, dry, and vacuum conditions. We have explained the known stabilizing effect of small amounts of water by implicit and explicit solvation of ADN clusters [15,17]. Higher activation barriers in dinitramide melts and solutions, compared to the solid state, support this conclusion.

The importance of maintaining resonance stabilization of dinitramide anions, for example by hydrogen bond donation, indicates that surface-active species can act as stabilizing agents for dinitramide salts, and especially ADN. Amines and compounds containing hydroxyl groups are predicted to generally function towards this end. Suitably unreactive compounds with strong polar or ionic character likely assist in a similar manner. This is in agreement with the known pacifying effect of nitrate on the surface of solid ADN and KDN, as well as the effect of potassium phosphate and ammonium fluoride [33], to name a few.

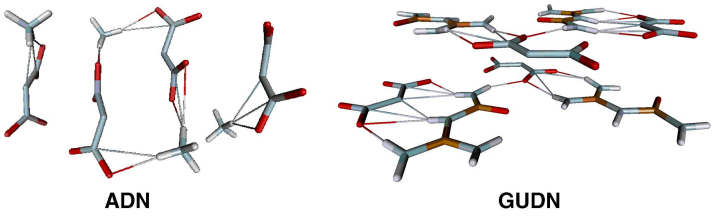

Figure 7.15 *Destabilization and stabilization of the dinitramide anion through crystal lattice effects is clearly illustrated in the crystal unit cells of ADN and GUDN, respectively.*

One effective way of removing the issue of polarization is to change the cationic counterion. If chosen carefully, this can also remove many ammonium-catalyzed reaction pathways, described in the previous section. If the dinitramide anion is strongly locked in a flat geometry, for example through hydrogen bonding from a matching counterion, the stability of the anion increases significantly. One example of this is realized when comparing the crystal structures of ADN and guanylurea dinitramide (GUDN), shown in Figure 7.15. The stabilization of the dinitramide anion in GUDN is impressive, and the activation energy has been measured at 66.2 kcal/mol [34]. This value should be compared with the approximately 40 kcal/mol seen in most moist, solvated, or otherwise stabilized forms of metal and ammonium dinitramides, or 30 kcal/mol in dry ADN.

The activation barrier for molten dinitramide salts, that is of anions devoid of crystal effects, is approximately 40 kcal/mol [31]. Compared to this base value, dinitramide anions in solid ADN can experience a destabilization due to polarization of up to 10 kcal/mol [15,17]. In the same fashion, metal dinitramides, such as KDN are destabilized by roughly 4 kcal/mol. As already mentioned, polarization-negating counterions, such as guanyl urea (GU), act in the opposite way, and can stabilize dinitramide anions by as much as 26 kcal/mol [34]. Because the nature of the counterion is paramount for the stability of the dinitramide anion, future research into novel dinitramide counterions could result in materials that surpass ADN in both performance and stability.

When considering the stability of ADN, it is also advisable to consider the formation of radicals. It is clear from the mechanistic investigations on ADN's decomposition, that many different radical species can be formed. This suggests that antioxidants should be potent as ADN stabilizers.

Finally, one can consider basicity, which by many is assumed the most important property of an ADN stabilizer [32,33]. However, as already discussed at length in this chapter, the justification for HDN formation from ADN is poor, and possible base stabilization of ADN is only deemed relevant in the most nonpolar of environments.

Several compounds have been tried experimentally with ADN in efforts aimed at finding suitable stabilizers [32,33,69,70]. Different amines, such as hexamine, diphenylamine, 2-nitro-diphenylamine, 2-methyl-4-nitroaniline (MNA), and ammonia have all generated positive effects [32,33,70]. Amides as well as various inorganic salts have been shown to be effective in the molten [70] and in the solid state [33]. Perhydro-1,3,5-triazine-2,4,6-trion, commonly known as Verkades superbase, [71,72] is reported to be a good stabilizer for ADN [32]. Methyldiphenyl urea (Akardit II) has also shown stabilizing properties [73].

One plausible explanation for the stabilizing effect of these compounds is that they can form complexes with free radicals, i.e. act as radical-traps, or "radical-stabilizers." This has already been demonstrated as theoretically possible for ammonia (e.g., **23** in Figure 7.7).

We have investigated several compounds theoretically for their ability to complex the dinitramine radical. Interestingly, hexamine and MNA, two of the most successful ADN stabilizers, proved among the best in this respect [1]. Adduct formation enthalpies, calculated at the B3LYP level, were between 12 and 14 kcal/mol, and effectively raise the decomposition barrier for the dinitramine radical above 30 kcal/mol.

Aside from the theoretical justification for the radical-trap nature of these stabilizers, there is also experimental evidence. MNA is known to stabilize nitrocellulose, which decomposes through the formation of NO_X gases (radicals). Furthermore, the depletion of MNA has been reported to track decomposition of ADN, while pushing the decomposition onset to a higher temperature [74]. It is also known that nitrogen oxides can oxidize amines [70]. Consequently, it is reasonable to assume that the ADN-stabilizing effect of amines [32,33,69,70] is due to their reducing ability, rather than their basicity.

It is concluded that dinitramide salts, and in particular ADN, can be stabilized in several different ways:

1. By mitigating the polarization of dinitramides at surfaces and interfaces. Suggestively by using surface-active species that can adhere to protruding dinitramides using dipolar, ionic, or hydrogen bond interactions.
2. By changing the cationic counterion to one that does not aid the reactivity of the dinitramide anion, and preferably reduces the polarization effect.
3. By the pacification of formed free radicals, using radical-complexation and reducing agents.

7.7 Conclusions

Mastery of dinitramide salts requires the intertwined use of experimental compatibility testing, surface sensitive spectroscopy, and quantum chemical calculations. When combined, these approaches have provided atomistic and fundamental understanding of the complex processes that govern decomposition, reactivity, and, in the end, the usefulness of dinitramide-based materials.

Polarized dinitramide anions residing on the surface of dinitramide salts are theoretically predicted to exist, and act to dramatically accelerate decomposition. Such structures have been observed on the outmost monolayers of ADN crystals using surface sensitive Vibrational Sum-Frequency Spectroscopy. Stabilization of ADN is realized by hindering the polarization of DN-anions by surface-active stabilizing agents. The full mechanisms for the self-decomposition of solid-state ADN and KDN have been presented and discussed. Radical decomposition intermediates stress the necessity of using anti-oxidants as stabilizers. The anomalous solid-state behavior of many dinitramide salts has also been discussed and explained. Finally, the use of the dinitramide moiety in synthesis has been briefly reviewed, and several mechanisms for its reactions with various olefinic double bonds discussed.

In view of these insights, as well as the recent use of an ADN-based monopropellant in satellite maneuvering (Chapter 1), the development of ADN-compatible polymeric materials (Chapter 8), and recent improvements in sustainable manufacturing and purification of ADN (Chapter 9), the future of ADN-based rocket propulsion is deemed promising.

References

1. Rahm, M. (2010) *Green Propellants. [dissertation] Stockholm*, Royal Institute of Technology (KTH), Stockholm, Sweden.
2. Vandel', A.P., Lobanova, A.A., and Loginova, V.S. (2009) Application of dinitramide salts (Review). *Russian Journal of Applied Chemistry*, **82** (10), 1763–1768.
3. Luk'yanov, O.A. and Tartakovskii, V.A. (1997) Chemistry of dinitramine and its salts. *Rossiiskii Khimicheskii Zhurnal*, **41** (2), 5–13.
4. Gorkovenko, A. and Jaffe, S. (2006) Novel enhanced electrochemical cells with solid-electrolyte interphase promoters. [patent] *US Pat Appl Publ*, 2006–328759, 20 pp.
5. Bottaro, J.C., Petrie, M.A., Penwell, P.E., and Bomberger, D.C. (2003) N,n-dinitramide salts as solubilizing agents for biologically active agents. [patent] *PCT Int Appl*, 2002-US21802, 41 pp.
6. Luk'yanov, O.A., Shlykova, N.I., and Tartakovsky, V.A. (1994) Dinitramide and its salts. 5. Alkylation of dinitramide and its salts. *Izvestiya Akademii Nauk, Seriya Khimicheskaya*, **10**, 1775–1778.
7. Rahm, M. and Brinck, T. (2008) Novel 1,3-dipolar cycloadditions of dinitraminic acid: Implications for the chemical stability of ammonium dinitramide. *Journal of Physical Chemistry A*, **112** (11), 2456–2463.
8. Rahm, M., Dvinskikh, S.V., Furo, I., and Brinck, T. (2011) Experimental detection of trinitramide, N(NO(2))(3). *Angewandte Chemie (International Edition in English)*, **50** (5), 1145–1148.
9. Blomquist, H.R. (2000) Guanylurea dinitramide-based gas-generating compositions for inflation of vehicle airbags. [patent] *US*, 99-359248, 9 pp., Cont.-in-part of U.S. Ser. No. 123,821.
10. Persson, S. and Sjöqvist, C. (2000) Guanyl urea dinitramide-based solid propellants with adjustable burning rate for vehicle airbag inflation. [patent] *PCT Int Appl*, 2000-SE864, 26 pp.
11. Persson, S. and Sjöqvist, C. (2001) Gas-generating composition for automobile airbags. [patent] *Swed*, 98-4610, 15 pp.
12. Sjöberg, P. (2000) Guanidine dinitramide-guanylurea dinitramide mixture for acutation of vehicle safety devices. [patent] *PCT Int Appl*, 99-SE2496, 16 pp.
13. Wingborg, N., Eldsäter, C., and Skifs, H. (2004) Formulation and characterization of ADN-based liquid monopropellants. Eur Space Agency, [Spec Publ] SP, **SP-557**(Space Propulsion 2004), 94–99.
14. Anflo, K. and Möllerberg, R. (2009) Flight demonstration of new thruster and green propellant technology on the PRISMA satellite. *Acta Astronaut*, **65** (9–10), 1238–1249.
15. Rahm, M. and Brinck, T. (2009) The anomalous solid state decomposition of ammonium dinitramide: a matter of surface polarization. *Chemical Communications*, **20**, 2896–2898.
16. Rahm, M., Westlund, R., Eldsäter, C., and Malmström, E. (2009) Tri-block copolymers of polyethylene glycol and hyperbranched poly-3-ethyl-3-(hydroxymethyl)oxetane through cationic ring opening polymerization. *Journal of Polymer Science Part A: Polymer Chemistry*, **47** (22), 6191–6200.
17. Rahm, M. and Brinck, T. (2010) On the anomalous decomposition and reactivity of ammonium and potassium dinitramide. *Journal of Physical Chemistry A*, **114** (8), 2845–2854.

18. Rahm, M., Malmström, E., and Eldsäter, C. (2011) Design of an ammonium dinitramide compatible polymer matrix. *Journal of Applied Polymer Science*, **122** (1), 1–11.
19. Talawar, M.B., Sivabalan, R., Mukundan, T. *et al*. (2009) Environmentally compatible next generation green energetic materials (GEMs). *Journal of Hazardous Materials*, **161** (2–3), 589–607.
20. Rahm, M. and Brinck, T. (2010) Kinetic stability and propellant performance of green energetic materials. *Chemistry - A European Journal*, **16**, 6590–6600.
21. Gilardi, R., Flippen-Anderson, J., George, C., and Butcher, R.J. (1997) A new class of flexible energetic salts: The crystal structures of the ammonium, lithium, potassium, and cesium salts of dinitramide. *Journal of the American Chemical Society*, **119** (40), 9411–9416.
22. Russell, T.P., Piermarini, G.J., Block, S., and Miller, P.J. (1996) Pressure, temperature reaction phase diagram for ammonium dinitramide. *The Journal of Physical Chemistry*, **100** (8), 3248–3251.
23. Eldsäter, C., deFlon, J., Holmgren, E. *et al*. (2009) ADN prills: production, characterization and formulation. Int Annu Conf ICT 40th (Energetic Materials), 24/1-24/10.
24. Wingborg, N. (2006) Ammonium dinitramide-water: Interaction and properties. *Journal of Chemical and Engineering Data*, **51** (5), 1582–1586.
25. Cui, J., Han, J., Wang, J., and Huang, R. (2010) Study on the crystal structure and hygroscopicity of ammonium dinitramide. *Journal of Chemical and Engineering Data*, **55** (9), 3229–3234.
26. Östmark, H., Bemm, U., Langlet, A. *et al*. (2000) The properties of ammonium dinitramide (ADN): part 1, basic properties and spectroscopic data. *Journal of Energetic Materials*, **18** (2–3), 123–138.
27. Hahma, A., Edvinsson, H., and Östmark, H. (2010) The properties of ammonium dinitramine (ADN): Part 2: Melt casting. *Journal of Energetic Materials*, **28** (2), 114–138.
28. Venkatachalam, S., Santhosh, G., and Ninan, K.N. (2004) An overview on the synthetic routes and properties of ammonium dinitramide (ADN) and other dinitramide salts. *Propellants, Explosives, Pyrotechnics*, **29** (3), 178–187.
29. Teipel, U., Heintz, T., and Krause, H.H. (2000) Crystallization of spherical ammonium dinitramide (ADN) particles. *Propellants, Explosives, Pyrotechnics*, **25** (2), 81–85.
30. Bottaro, J.C., Penwell, P.E., and Schmitt, R.J. (1997) 1,1,3,3-Tetraoxo-1,2,3-triazapropene Anion, a new oxy anion of nitrogen: The dinitramide anion and its salts. *Journal of the American Chemical Society*, **119** (40), 9405–9410.
31. Babkin, S.B., Pavlov, A.N., and Nazin, G.M. (1997) Anomalous decomposition of dinitramide metal salts in the solid phase. *Russian Chemical Bulletin*, **46** (11), 1844–1847.
32. Mishra, I.B. and Russell, T.P. (2002) Thermal stability of ammonium dinitramide. *Thermochimica Acta*, **384** (1–2), 47–56.
33. Pavlov, A.N., Grebennikov, V.N., Nazina, L.D. *et al*. (1999) Thermal decomposition of ammonium dinitramide and mechanism of anomalous decay of dinitramide salts. *Russian Chemical Bulletin*, **48** (1), 50–54.
34. Östmark, H., Bemm, U., Bergman, H., and Langlet, A. (2002) N-guanylurea-dinitramide: a new energetic material with low sensitivity for propellants and explosives applications. *Thermochimica Acta*, **384** (1–2), 253–259.
35. Lei, M., Zhang, Z.-Z., Kong, Y.-H. *et al*. (1999) The thermal behavior of potassium dinitramide. Part 1. Thermal stability. *Thermochimica Acta*, **335** (1–2), 105–112.
36. Dubovitskii, F.I., Volkov, G.A., Grebennikov, V.N. *et al*. (1996) Thermal decomposition of potassium dinitramide in solid state. *Doklady Akademii Nauk SSSR*, **348** (2), 205–206.
37. Lei, M., Liu, Z.-R., Kong, Y.-H. *et al*. (1999) The thermal behavior of potassium dinitramide Part 2. Mechanism of thermal decomposition. *Thermochimica Acta*, **335** (1–2), 113–120.
38. Tompa, A.S. (2000) Thermal analysis of ammonium dinitramide (ADN). *Thermochimica Acta*, **357–358**, 177–193.

39. Vyazovkin, S. and Wight, C.A. (1997) Ammonium dinitramide: Kinetics and mechanism of thermal decomposition. *Journal of Physical Chemistry A*, **101** (31), 5653–5658.
40. Brill, T.B., Brush, P.J., and Patil, D.G. (1993) Thermal decomposition of energetic materials 58. Chemistry of ammonium nitrate and ammonium dinitramide near the burning surface temperature. *Combustion and Flame*, **92**, 178–186.
41. Löbbecke, S., Krause, H.H., and Pfeil, A. (1997) Thermal analysis of ammonium dinitramide decomposition. *Propellants, Explosives, Pyrotechnics*, **22** (3), 184–188.
42. Vyazovkin, S. and Wight, C.A. (1997) Thermal decomposition of ammonium dinitramide at moderate and high temperatures. *Journal of Physical Chemistry A*, **101** (39), 7217–7221.
43. Pinkerton, A.A. and Ritchie, J.P. (2003) Structural trends and variations in dinitramide salts - a balance between resonance stabilization and steric repulsion. *Journal of Molecular Structure*, **657** (1–3), 57–74.
44. Ritchie, J.P., Zhurova, E.A., Martin, A., and Pinkerton, A.A. (2003) Dinitramide Ion: Robust molecular charge topology accompanies an enhanced dipole moment in its ammonium salt. *The Journal of Physical Chemistry. B*, **107** (51), 14576–14589.
45. Rahm, M., Tyrode, E., Brinck, T., and Johnson, C.M. (2011) The molecular surface structure of ammonium and potassium dinitramide: a vibrational sum frequency spectroscopy and quantum chemical study. *The Journal of Physical Chemistry C*, **115** (21), 10588–10596.
46. Politzer, P., Seminario, J.M., and Concha, M.C. (1998) Energetics of ammonium dinitramide decomposition steps. *Theochem*, **427**, 123–130.
47. Alavi, S. and Thompson, D.L. (2003) Decomposition pathways of dinitramic acid and the dinitramide ion. *Journal of Chemical Physics*, **119** (1), 232–240.
48. Michels, H.H. and Montgomery J Jr., J.A. (1993) On the structure and thermochemistry of hydrogen dinitramide. *The Journal of Physical Chemistry*, **97** (25), 6602–6606.
49. Doyle J Jr., R.J. (1993) Sputtered ammonium dinitramide: tandem mass spectrometry of a new ionic nitramine. *Organic Mass Spectrometry*, **28** (2), 83–91.
50. Politzer, P. and Seminario, J.M. (1993) Computational study of the structure of dinitraminic acid, HN(NO2)2, and the energetics of some possible decomposition steps. *Chemical Physics Letters*, **216** (3–6), 348–352.
51. Rahm, M. and Brinck, T. (2008) Dinitraminic acid (HDN) isomerization and self-decomposition revisited. *Chemical Physics*, **348** (1–3), 53–60.
52. Kazakov, A.I., Rubtsov, Y.I., Manelis, G.B., and Andrienko, L.P. (1997) Kinetics of thermal decomposition of dinitramide 1. Decomposition of different forms of dinitramide. *Russian Chemical Bulletin*, **46** (12), 2015–2020.
53. Brinck, T., Murray, J.S., and Politzer, P. (1991) Relationships between the aqueous acidities of some carbon, oxygen, and nitrogen acids and the calculated surface local ionization energies of their conjugate bases. *The Journal of Organic Chemistry*, **56** (17), 5012–5015.
54. Oxley, J.C., Smith, J.L., Zheng, W. *et al.* (1997) Thermal decomposition studies on ammonium dinitramide (ADN) and 15N and 2H isotopomers. *Journal of Physical Chemistry A*, **101** (31), 5646–5652.
55. Yang, R., Thakre, P., and Yang, V. (2005) Thermal decomposition and combustion of ammonium dinitramide (review). *Combustion, Explosives, and Shock Waves*, **41** (6), 657–679.
56. Bloembergen, N. and Pershan, P.S. (1962) Light waves at the boundary of nonlinear media. *Physical Review*, **128**, 606–622.
57. Wang, H.F., Gan, W., Lu, R. *et al.* (2005) Quantitative spectral and orientational analysis in surface sum frequency generation vibrational spectroscopy (SFG-VS). *International Reviews in Physical Chemistry*, **24** (2), 191–256.
58. Bain, C.D. (1995) Sum-frequency vibrational spectroscopy of the solid/liquid interface. *Journal of the Chemical Society-Faraday Transactions*, **91** (9), 1281–1296.

59. Zhuang, X., Miranda, P.B., Kim, D., and Shen, Y.R. (1999) Mapping molecular orientation and conformation at interfaces by surface nonlinear optics. *Physical Review B: Condensed Matter and Materials Physics*, **59** (19), 12632–12640.
60. Miranda, P.B. and Shen, Y.R. (1999) Liquid interfaces: A study by sum-frequency vibrational spectroscopy. *The Journal of Physical Chemistry. B*, **103** (17), 3292–3307.
61. Christe, K.O., Wilson, W.W., Petrie, M.A. *et al*. (1996) The dinitramide anion, N(NO2)2-. *Inorganic Chemistry*, **35** (17), 5068–5071.
62. Shlyapochnikov, V.A., Tafipolsky, M.A., Tokmakov, I.V. *et al*. (2001) On the structure and spectra of dinitramide salts. *Journal of Molecular Structure*, **559** (1–3), 147–166.
63. Chakravarthy, S.R., Freeman, J.M., Price, E.W., and Sigman, R.K. (2004) Combustion of propellants with ammonium dinitramide. *Propellants, Explosives, Pyrotechnics*, **29** (4), 220–230.
64. Hinshaw, C.J., Wardle, R.B. and Highsmith, T.K. (1998) Propellant formulations based on dinitramide salts and energetic binders. [patent] *US*, 96-614303, 7 pp., Cont.-in-part of U.S. 5,498,303.
65. Hinshaw, C.J., Wardle, R.B. and Higshsmith, T.K. (1994) Propellant formulations based on dinitramide salts and energetic binders. [patent] *PCT Int Appl*, 94-US4270, 16 pp.
66. Johansson, M., DeFlon, J., Petterson, Å. *et al*. (2006) Spray Prilling of ADN and Testing of ADN Based Solid Propellants, 3rd International Conference on Green Propellants for Space Propulsion, France.
67. Chabot, G.B., Haiges, R., Rahm, M., and Christe, K.O. (2012) High-oxygen Borates: Potential Green Replacements for AP in Rocket Propellants, 243rd ACS National Meeting, San Diego.
68. Luk'yanov, O.A., Konnova, Y.V., Klimova, T.A., and Tartakovsky, V.A. (1994) Dinitramide and its salts. 2. Dinitramide in direct and reverse Michael-type reactions. *Izvestiya Akademii Nauk, Seriya Khimicheskaya*, **7**, 1264–1266.
69. Manelis, G.B. (1995) Thermal Decomposition of AND, Int Annu Conf ICT 26th (Pyrotechnics), Karlsruhe 15/1-15/17.
70. Andreev, A.B., Anikin, O.V., Ivanov, A.P. *et al*. (2000) Stabilization of ammonium dinitramide in the liquid phase. *Russian Chemical Bulletin*, **49** (12), 1974–1976.
71. Lensink, C., Xi, S.K., Daniels, L.M., and Verkade, J.G. (1989) The unusually robust phosphorus-hydrogen bond in the novel cation [cyclic] HP(NMeCH2CH2)3N+. *Journal of the American Chemical Society*, **111** (9), 3478–3479.
72. Tang, J., Mohan, T. and Verkade, J.G. (1994) Selective and efficient syntheses of Perhydro-1,3,5-triazine-2,4,6-triones and carbodiimides from isocyanates using ZP(MeNCH2CH2)3N catalysts. *The Journal of Organic Chemistry*, **59** (17), 4931–4938.
73. Löbbecke, S., Krause, H., and Pfeil, A. (1997) Thermal decomposition and stabilization of ammonium dinitramide, Int Annu Conf ICT 28th (Energetic materials), Karlsruhe, 112.
74. Clubb, J.W. (2007) 3rd Dinitramide and Fox 7 Seminar, San Remo.

8

Binder Materials for Green Propellants

Carina Eldsäter[1] *and Eva Malmström*[2]

[1]*Swedish Defence Research Agency, FOI, Sweden*
[2]*School of Chemical Science and Engineering, KTH Royal Institute of Technology, Sweden*

'Green' is a wide definition and there are several aspects of how to define 'green' in the context of green propellants. The mostly used definition is that the propellant itself should not be harmful to the environment and that no environmentally unfriendly/hazardous combustion products should be formed.

If the definition is stretched further, the environmental impact of the whole lifecycle of the propellant should be considered, such as the synthesis and production of raw materials, manufacturing of the propellant, storage, handling and use, combustion, ageing and recycling.

The reason for discussing 'green' solid propellants is that the most commonly used solid propellants are based on the oxidiser ammonium perchlorate or lead-containing nitrocellulose/nitroglycerin (so called double-base propellants) of which none can be considered environmentally friendly.

Ammonium perchlorate (AP) has, for at least 50 years, been the solid oxidiser of choice due to its high performance, relative low hazardness and the possibility of tailoring its ballistic properties. However, AP has a negative impact on the environment and on personal health. Perchlorate anions (ClO_4^-) have been found in drinking water supplies throughout the southwestern United States [1]. At high enough concentrations, perchlorate can affect thyroid gland functions, where it is mistakenly taken up in place of iodide. Based on current information, perchlorate may be a problem for water supplies in some regions of the USA [1].

Recently, the US Department of Defence organised workshop on advanced strategy for environmentally sustainable energetics identified AP as one of the key environmental, safety and occupational health issues [2]. Apart from impacting thyroid activity in humans,

Green Energetic Materials, First Edition. Edited by Tore Brinck.

AP forms a vast amount of hydrochloric acid on combustion. For instance, the space shuttle and the Ariane 5 generated 580 and 270 tons of concentrated hydrochloric acid respectively per launch.

Double-base propellants do not contain a solid oxidiser since the main ingredients – nitrocellulose and nitroglycerin – by themselves constitute the oxidiser and fuel. These propellants do not have as good a performance as AP-based propellants, but they are used when minimal smoke is required. In order to tune their ballistic properties, lead compounds are added. Lead compounds are well known to be toxic and environmentally unfriendly and researchers are striving to find suitable alternatives [3]. Efforts to replace nitroglycerin are also being conducted to reduce the environmental impact of double-base propellants [4,5].

In this chapter we discuss binder materials for green solid composite and homogeneous rocket propellants in four sections: binder properties, inert polymers, energetic polymers and energetic plasticisers. The last part of the chapter is an outlook on how to design binders for green propellants.

Solid *composite* rocket propellants contain a crystalline oxidiser, an energetic filler, embedded in an elastic polymer matrix, also called the binder. The binder constitutes only a small part of these propellants. Typically, a solid composite propellant constitutes 70–90% of the solid filler and 10–30% of the binder, and the binder may therefore not play such an important role when defining 'green' in discussions on combustion. However, when discussing manufacturing and recycling, the binder and its ingredients will be more important, even though the final concentration in the propellant is low. For nitrocellulose-based (*homogeneous*) propellants, on the other hand, the polymer constitutes 40–70% of the propellant [6].

During the last 15 years, several propellant compositions have been proposed. We will, however, restrict ourselves to discussing binders for those solid propellants that are discussed most frequently as 'green' in the open literature. The solid green propellants considered here are, therefore, based on ammonium dinitramide, hydrazinium nitroformate, ammonium nitrate, guanyl urea dinitramide or diamino-dinitroethylene. 'Greener' double-base propellants will also be discussed.

Ammonium dinitramide, ADN, is perhaps the most interesting ingredient for propellants due to its high energy content and high oxygen balance, Figure 8.1. ADN was first synthesised in Russia in the 1970s but the dinitramide technology was strictly classified and unknown to the rest of the world until 1988 when it was 're-invented' at SRI International, USA [7,8]. In

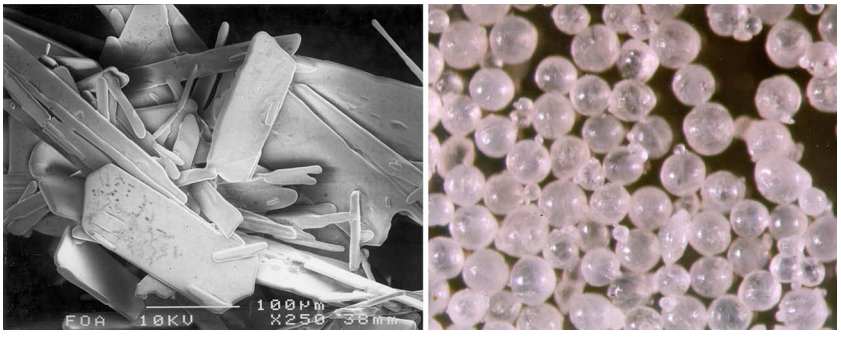

Figure 8.1 *Crystals (left) and spherical particles (right) of ammonium dinitramide, ADN. Pictures from FOI.*

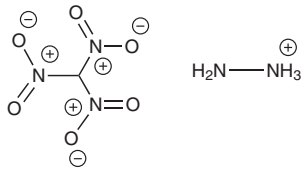

Figure 8.2 *Chemical structure of hydrazinium nitroformate, HNF.*

the beginning of the 1990s, the Swedish Defence Research Establishment (FOA) in Sweden initiated research on ADN in order to develop minimum-smoke propellants for tactical missile applications. For many years, the work was focused on preparing suitable crystals or particles [9–21]. Since 2006, spherical particles of good quality have been produced by the Swedish Defence Research Agency (FOI), Sweden [22], and these were commercialised during 2011 by EURENCO Bofors, Sweden. The major challenge in the development of ADN-based solid propellants is currently to find binder ingredients that will give an ADN-based solid propellant with good curing properties and good mechanical and ballistic properties. ADN is also a hygroscopic compound.

Hydrazinium nitroformate, HNF, has been considered the major competitor to ADN when considering performance, Figure 8.2. HNF has been proposed as an oxidiser in solid propellants since at least 1972 [23,24]. The challenges with HNF are to improve its thermal stability and its sensitivity to friction [23,25]. HNF is considered less thermally stable than un-stabilised nitrocellulose and ADN [26]. Whether HNF can be considered 'green' could be discussed, since it is a salt of hydrazine. Hydrazine is highly toxic and a suspected carcinogen and special protective gear is necessary when working with it. In 2011, hydrazine was registered on the European Chemicals Agency's candidate list of chemicals as carcinogenic [27,28].

Ammonium nitrate, AN, is the third oxidiser that is considered for green solid propellants. It has been mentioned as a propellant ingredient in the literature since at least 1896 [29]. AN is not as energetic as ADN or HNF but has a reasonably good oxygen balance (Table 8.1) and is also relatively insensitive compared to both ADN and HNF. The major challenge of AN is its phase transition at 32 °C resulting in volumetric expansion [30]. AN is therefore phase-stabilised using different additives, for example KNO_3 [30–33], NiO [33] and ZnO [34].

1,1-Diamino-2,2-dinitroethylene, FOX-7 (Figure 8.3), is a low-sensitivity explosive with a performance very close to that of hexogen, RDX. FOX-7 is also insensitive, stable and compatible with most binder ingredients, which makes it very well suited for applications where insensitivity is important [37]. FOX-7 was first prepared in 1998 by Latypov *et al.* [38].

Table 8.1 *Data on important oxidisers. ADN = ammonium dinitramide. HNF = hydrazinium nitroformate. AN = ammonium nitrate. AP = ammonium perchlorate (added as reference). Values from the ICT thermodynamic database if not stated otherwise [35].*

Oxidiser	Formula	M_w (g/mol)	Ω (%)	ΔH_f (kJ/mol)	ρ (g/cm^3)
ADN	$NH_4N(NO_2)_2$	124	+25.8	−135 [36]	1.81
HNF	$N_2H_5C(NO_2)_3$	183	+13.1	−72	1.87
AN	NH_4NO_3	80.0	+20.0	−367	1.72
AP	*NH_4ClO_4*	*118*	*+34.0*	*−283*	*1.95*

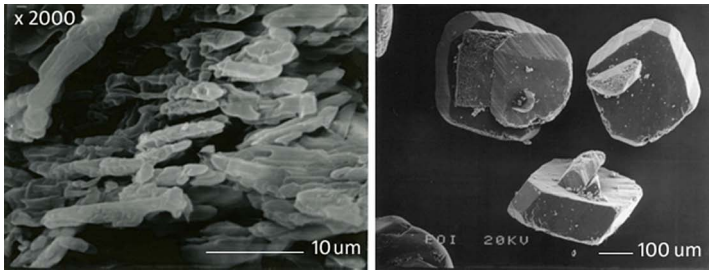

Figure 8.3 *Crystals of 1,1-diamino-2,2-dinitroethylene, FOX-7, from synthesis (left) and after recrystallisation (right). Pictures from FOI.*

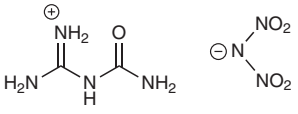

Figure 8.4 *Chemical structure of* N*-guanylurea dinitramide, GUDN.*

Table 8.2 *Data on explosives used in solid green propellants. GUDN = N-guanylurea dinitramide. FOX-7 = 1,1-diamino-2,2-dinitroethylene. Values from the ICT thermodynamic database if not stated otherwise [35].*

Explosive	Formula	M_w (g/mol)	Ω (%)	ΔH_f (kJ/mol)	ρ (g/cm^3)
GUDN	$C_2H_7N_7O_5$	209	−19.1	−356	1.75
FOX-7	$C_2H_4N_4O_4$	148	−21.6	−359	1.89

N-Guanylurea dinitramide, GUDN (Figure 8.4), is a dinitramide salt, like ADN. In contrast to ADN it is not hygroscopic and is also extremely insensitive [39]. The energetic properties of FOX-7 are well suited for propellant applications due to the low sensitivity and its relatively good oxygen balance (Table 8.2). The challenge with GUDN, as well as with FOX-7, is to achieve high enough performance of the rocket propellant.

'Green' double-base propellants will also be discussed in this chapter. Double-base propellants do not usually contain any solid oxidiser since the main ingredients, nitrocellulose and nitroglycerin, by themselves constitute the oxidiser and fuel. This type of propellant has been in use for a long time and is used in applications where minimum smoke is required. The challenges with these propellants are to raise their performance, tailor their ballistic properties and to improve their storage stability without the need for hazardous additives.

8.1 Binder Properties

The purpose of the binder, or the polymer matrix, is to form a solid, elastic body of the propellant ingredients with sufficient mechanical properties. The binder is also used as fuel since it mainly contains hydrogen and carbon. Good mechanical properties are essential to ensure that the rocket will perform as intended and to provide sufficient storage stability. In fact, the major cause of failures of solid rocket motors is linked to the

Figure 8.5 *Example of propellant grain profiles. Pictures from FOI.*

structural integrity of the propellant [40]. In some cases, the binder may stabilise the oxidiser.

The main part of a binder in a solid propellant is constituted by a polymer which has to be stable towards the oxidiser. It may be a thermo-setting polymer, that is it is crosslinked during the propellant manufacturing process; a thermoplastic elastomer, that is a polymer that is melted or dissolved in solvent during the propellant manufacturing process; or a thermoplastic polymer. In addition to the polymer, several additives are present in a solid propellant. Typically, plasticisers and bonding agents are added to obtain suitable mechanical properties. Metal powder and ballistic modifiers are used to tailor combustion properties, and stabilisers are used to maintain long-term storability.

The binder is an essential part of a solid propellant. It enables the propellant to be shaped in a suitable geometry to obtain the desired ballistic properties and performance of a rocket motor. Examples of grain profiles are shown in Figure 8.5. The most important properties of the binder are its mechanical properties and its ability to adhere to the energetic filler and to the case. The mechanical properties and the adherence will directly affect the safety of a propellant. If a propellant is brittle, cracks may form and, when ignited, this will result in an uncontrolled burning area expansion that may cause a rocket motor explosion.

From a manufacturing point of view, the rheological properties of a binder are important. Thermo-setting pre-polymers are typically liquids at room temperature and are mixed together with the energetic filler, the curing agent and other additives in a batch mixer or extruder, Figure 8.6. If the viscosity of the mixture is too high, casting is difficult and may result in voids in the final propellant grain. If, on the other hand, the viscosity is too low, the energetic filler may sediment, which will result in a composition gradient. Both these manufacturing errors will affect the safety and performance of the propellant.

Thermoplastic elastomers are, in contrast to the liquid thermo-set pre-polymers, solid at room temperature and are typically triblock copolymers, based on soft (amorphous) and hard (semi-crystalline) components. They do not contain chemical crosslinks, as the thermo-set polymer matrix do. Instead they contain physical crosslinks, that is parts of the polymer chain that are held together by attractive forces, for example hydrogen bonds, forming crystalline regions. In order to process these elastomers into a propellant, these crystalline domains must be broken which is typically accomplished either by heat or solvent. In the case of melting, the melting temperature must not be too high, typically between 60–120 °C [41], since decomposition or physical changes of other ingredients may start at

Figure 8.6 *Propellant processing in a batch mixer. Pictures from FOI.*

higher temperatures. The strength of the thermoplastic elastomeric block copolymers depends on phase separation and it is therefore desirable to have some immiscibility between the blocks. They should not, however, be completely immiscible because this may affect the processability negatively due to high viscosity [41].

Another important aspect of the binder is that it needs to be chemically and thermally stable. It must not react with the other ingredients in the propellant during storage. If it does so, it may cause an accelerated self-heating which might result in a thermal explosion, or degradation of the binder, resulting in poor mechanical properties and, in the long run, cracks or voids.

Finally, binders used for solid propellants may either be inert or energetic. The performance of a rocket propellant is of major importance and it has therefore been the driving force behind the development of binders that will contribute to the specific impulse, rather than diluting the energy content of the propellant. In order to increase the energy content of a binder, energetic polymers have been developed, which contain functional groups, such as azido, nitro (*C*-nitro, *O*-nitro (nitrate esters) and *N*-nitro (nitramines)) and difluoramine groups, along the polymer backbone. Incorporation of these functional groups increases the performance of the formulation, in addition to improving the overall oxygen balance [42]. Another way of increasing the energy content of a binder, based on an inert polymer, is to add an energetic plasticiser.

8.2 Inert Polymers for Binders

The following subsections aim at introducing the various polymers that have been used as binders for propellants.

8.2.1 Polybutadiene

The most well-known polymer used in composite solid propellants is hydroxyl-terminated polybutadiene, HTPB [43]. HTPB (R45M) has a density of 0.95 g/cm^3 and an oxygen balance

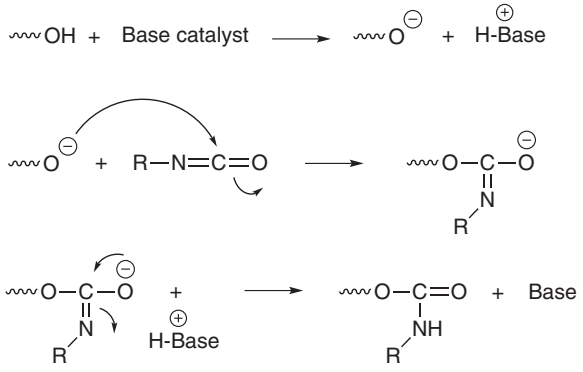

Figure 8.7 *Schematic reaction between a hydroxyl group and an isocyanate group to give an isocyanate-containing compound.*

of −318% [35]. HTPB has excellent mechanical properties and a very low glass transition temperature, which is favourable for use as binder in solid propellants. Depending on molecular weight and functionality of HTPB, tensile strengths of 0.4–1.0 MPa and strains at max stress of 250–1200% can be obtained [44,45]. The glass transition of cured HTPB is approx. −80 °C.

HTPB has been investigated as a binder in ADN- [46–50], HNF- [51], AN- [52] and FOX-7-based [53,54] propellants and is cured by isocyanates, compounds containing the functional group –NCO). 3-Isocyanatomethyl-3,5,5-trimethylcyclohexyl isocyanate (isophoron diisocyanate or IPDI) [46,49], 4,4′-di(isocyanatocyclohexyl)methane (H_{12}MDI or Desmodur W) [46,50], Desmodur N3300 [46] and toluene 2,4-diisocyanate (TDI) [52] have been used to cure ADN/HTPB-based propellants. ADN-based propellants, using coated ADN particles, were cured with dimeryldiisocyanate (DDI) [48]. The general reaction between the hydroxyl-terminated polymer and the isocyanate is shown in Figure 8.7. Isocyanates are classified as potential human carcinogens and are known to cause cancer in animals. They are also known to give rise to lung conditions and acute irritation of eyes, nose, throat and skin. Safety precautions have to be undertaken when handling isocyanates. It is noteworthy that the formed urethane linkage is heat sensitive and the reaction may reverse at temperatures above 150 °C to give the corresponding isocyanate.

Even though the mechanical properties of HTPB-based propellants are very good, results indicate that HNF/HTPB propellants have poorer mechanical properties than GAP/HNF, due to particle/binder debonding [51].

Copolymers of butadiene and acrylonitrile, PBAN, have also been used together with ADN [49]. PBAN, in this study, was cured using an epoxy curing agent.

Combustion studies of HNF/HTPB-based propellants show that the burn rate of these was high (20–25 mm/s at 7 MPa) and the pressure exponent was, unfortunately, also high (0.78–1.12), unless burn rate modifiers were employed [55]. Small particles of HNF resulted in a lower pressure exponent, whereas large particles resulted in higher values [51]. Combustion studies of ADN/Al/HTPB-based propellants point in the same direction as for HNF/HTPB. High pressure exponents were observed (0.87–0.91) [46]. Van der Heijden *et al.* [51] discussed this phenomenon and compared the results with GAP-based counterparts, which exhibited lower pressure exponents. They proposed several explanations, such as that the bonding to the particles was better with GAP than with HTPB causing voids in the

propellant, where burning could occur at higher rates. Another explanation was that GAP contributes to the heat generation during decomposition more efficiently than HTPB does. A lower flame temperature was observed for HNF/HTPB compared to pure HNF and HNF/GAP. The latter suggestion was also given by Chakravarthy *et al.* [49] when studying combustion of ADN in PBAN matrices. It is clear that further combustion studies are needed to fully understand this phenomenon.

AN-based propellants have very low burn rates compared to ADN- and HNF-based propellants. AN/HTPB-based propellants have burn rates in the order of 1–3 mm/s at 7 MPa and a pressure exponent of approx. 0.6 [52,56]. Burn rate studies of FOX-7-based propellants are rare in literature but Sinditskii *et al.* [57] have measured the burn rate of pressed FOX7. It was in the order of 12 mm/s at 7 MPa and the pressure exponent was 0.85–0.91, which is rather high. Sinditskii *et al.* claimed that the burn rate of FOX-7 is slightly lower than that of hexogen, RDX [57]. Florczak *et al.* showed that an FOX-7 addition to an AP-based propellant reduced the burn rate, as compared to an addition of octogen, HMX [54]. Vörde *et al.* [58] have developed a FOX-7-based gas generator composition and the burn rate was studied. It was shown that an addition of co-oxidisers, such as MnO_2 and Al_2O_3, reduced the pressure exponent to 0.68.

8.2.2 Polyethers

Several polyethers have been used as binders in solid propellants, such as polyethylene glycol (PEG), polypropylene glycol (PPG) and poly(tetrahydrofurane) (PTHF), Table 8.3. Some of these have also been used together with 'green' energetic fillers. The polyethers are interesting from a propellant view, especially since they have low glass transition temperatures and, due to their oxygen content, higher oxygen balance than, for example, HTPB.

Hydroxyl-terminated polyethers are crosslinked with isocyanates. Hexadiisoxyanate (HDI) has been used to cure a polyether used as a binder of FOX-7/GUDN-based propellants [61]. PEG has, besides being curable with isocyanates, been crosslinked using a curing system based on propargyl bromide, THF as solvent and potassium *tert*-butoxide as catalyst [62]. In this binder system, the PEG was alkyne-terminated.

ATK, USA, has together with DuPont developed a block copolymer of PEG and PTHF called TPEG. A propellant based on AP/AN/TPEG has been developed and one of its

Table 8.3 *Data on polyethers used in solid green propellants. PEG = poly(ethylene glycol). PPG = poly(propylene glycol). PTHF = poly(tetrahydrofurane). Values from the ICT thermodynamic database if not stated otherwise [35].*

Polymer	Formula	Ω (%)	*Tg* (°C)	ρ (g/cm^3)
PEG	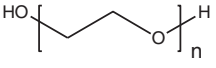	−182	−60 [59]	1.13
PPG	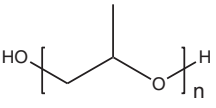	−218	−45 to −65[a]	1.00
PTHF	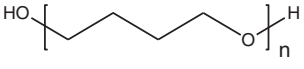	−244	−60 to −70 [60]	0.99

[a] measured at FOI (unpublished).

advantages is that it contributes to insensitive propellants better than HTPB [33]. A copolymer of PEG and PTHF, cured with Desmodur N3200, has also been used in propellant studies by Caro *et al*. [34]. The propellants had low glass transition temperatures (−76 to −62 °C). Interestingly, addition of AN to the propellant increased the glass transition temperature by 15 °C.

A series of multifunctional copolymers of PEG and PPG has been synthesised by Reed *et al*. [63] and energetic compositions based on HMX had excellent tensile properties, stresses ranging from 0.37–0.64 MPa and strains between 473 to 972%. These were cured using isocyanates such as Desmodur N100. One of these polymers, a four-chain polyether, has been used in ADN-based propellants. Small motor tests with these propellants resulted in specific impulses between 230–240 s [64]. The burn rate of this propellant was high, 19 mm/s at 7 MPa, and the pressure exponent was 0.64.

8.2.3 Polyesters and Polycarbonates

Polyesters and polycarbonates have also been used as binders in propellants using 'green' oxidisers or energetic fillers. Examples of these are poly(ε-caprolactone) and Desmophen, an aliphatic polycarbonate [65], poly(ethylene-*co*-vinylactetate) and poly(di(ethylene glycol) adipate). The oxygen balance, density and glass transition temperature of typical polyesters are shown in Table 8.4.

Table 8.4 *Data on polyesters and polycarbonates used in solid green propellants. PCL = polycaprolactone. Desmophen 2200 = aliphatic polycarbonate. EVA = poly(ethylene-co-vinylacetate). PGA = poly(di(ethylene glycol) adipate). Values from the ICT thermodynamic database [35].*

Polymer	Formula	Ω (%)	*Tg* (°C)	ρ (g/cm^3)
PCL	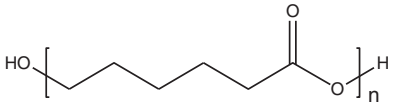	−201	−60	1.07
Desmophen 2200	Aliphatic polycarbonate diol [65]	−167	n.a.	n.a.
EVA	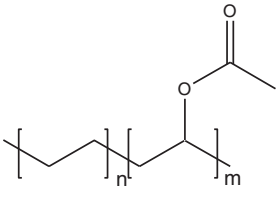	−266	−30[a]	1.01
PGA	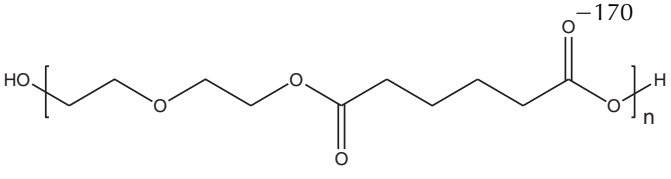	−170	n.a.	1.19

[a] measured at FOI (unpublished)
n.a. = not available

Table 8.5 *Tensile properties of polyurethane-based propellants at 20 °C. σ_m = max stress. ε_m = elongation at max stress. E = elastic modulus. Tensile testing was conducted at a rate of 50 mm/min using JANNAF Class C dog-bones if not otherwise stated.*

Propellant	σ_m (MPa)	ε_m (%)	*E* (MPa)	Comment
ADN/Desmophen 2200/TMETN/Al/Desmodur N3400 [66]	0.54[a]	7[a]	11.2[a]	66% solids
ADN/Desmophen 2200/TMETN/HMX/ Desmodur N3400 [66]	0.6[a]	26[a]	13.6[a]	66% solids
FOX7/AP/Desmophen 2200/Lupranol3300 2200/TMETN/BTTN/isocyanate [67]	0.52	12.8	6.97	28% FOX-7 42% AP
FOX7/AP/Desmophen 2200/Lupranol3300 2200/BDNPA-F/isocyanate [67]	0.83	10.1	13.95	28% FOX-7 42% AP

[a] approximate values as estimated from a graphic presentation of the tensile test.

Hydroxyl-terminated polyesters are crosslinked with isocyanates. Desmophen 2200 has been used in ADN-based propellants and was cured with Desmodur N3400 [66], Desmodur W and IPDI [67]. An unknown polyester, cured with Desmodur N3400, has been proposed as a binder of GUDN-based propellants [61].

The mechanical properties of polyester urethanes are in general very good. Depending on the adhesion to the crystalline energetic filler, the tensile properties of the resulting propellant might, however, vary. Table 8.5 shows tensile properties of some examples of green solid propellants.

Poly(ε-caprolactone) (PCL) has been used in combustion studies of ADN-based propellants [68]. Two different molecular weights of PCL were used in the study, 10 000 and 1250 g/mol. The compositions studied had high pressure exponents, which makes them difficult to use in rocket propellant applications. With an addition of CuO to the low molecular-weight PCL-based propellant, the pressure exponent decreased from 0.70 to 0.44, which is a very positive result. These low pressure exponents were, however, not achieved for the high molecular-weight PCL-based ADN propellant. It should, however, be noted that the binders in this study were uncured and, at least the low molecular-weight PCL, needs to be crosslinked in order to achieve acceptable mechanical properties.

PCL was also used in ADN-based propellants developed by Chan *et al*. [69]. The polymer binder was cured using the curing agent Desmodur N100 and the curing catalyst triphenyl bismuth. Initial measurements showed that the mechanical properties were good, a stress of 0.5 MPa and a strain of 58% at ambient conditions. The propellants had burn rates of 16–19 mm/s at 7 MPa, and pressure exponents of 0.65–0.68.

Poly(di(ethylene glycol) adipate), PGA, has been used together with AN in solid propellants. The propellants had excellent mechanical properties, a strain of 51% at 24 °C, 48% at −40 °C and 16% at −53 °C. Corresponding values of the maximum stresses were 1, 3 and 7.7 MPa. The burn rate of these propellants was in the range of 3.3 mm/s at 7 MPa and the pressure exponent was approximately 0.7 [70].

A poly(vinyl ester), poly(ethylene-vinyl acetate) (EVA), has been proposed and tested as a binder in ADN-based propellants [71]. EVA has excellent mechanical properties, a tensile stress of 8 MPa and a strain at max stress of 500%. Sandén [71] used the thermoplastic EVA elastomer Escorene UL 15 019, that melted at 70 °C, which enabled blending with ADN below its melting point at approx. 90 °C.

Fujisato *et al*. have studied the combustion of ADN-based propellants, with 70–90% ADN, and they used an inert, low melting, thermoplastic elastomer. Unfortunately, no chemical details of the binder were given in the paper. As for many ADN-based propellants using inert binders, the pressure exponents of these propellants were high if no burning rate catalyst was used. Using nano-CuO or nano-sized aluminium (Alex), the pressure exponent was decreased to 0.54 and 0.76 respectively [72].

8.3 Energetic Polymers

8.3.1 Nitrocellulose

Nitrocellulose (Figure 8.8) is the oldest energetic polymer used in solid propellants. It was first discovered in 1846 by Schönbein and Böttger [73,74] and it is still used in gun propellants and in minimum-smoke rocket propellants. Nitrocellulose is processed by swelling cellulose in organic solvent or nitroglycerine combined with kneading and calendering techniques [6]. One of the major drawbacks of nitrocellulose is its poor thermal stability, and stabilisers are therefore necessary to store the propellant. Nitrocellulose has a density of 1.65 g/cm^3 and an oxygen balance varying between −24 and −85% depending on the degree of nitration [35].

Nitrocellulose (NC) is often used together with a plasticiser to aid the processing and improve the properties of the final propellant. Traditionally, nitroglycerin, NG, has been and is still used as plasticiser in many applications. NG has, however, a strong effect on the human health and is considered toxic in many countries [4]. Attempts have been made to replace NG in NC-based propellants and thereby produce a less toxic and thus greener propellant [5].

Barium nitrate (BaN), dibutyl phthalates (DBP) and diphenyl amine (DPA) are other ingredients commonly used in nitrocellulose-based propellants but also they are toxic and/or potentially carcinogenic [75]. Manning *et al*. have developed a nitrocellulose-based propellant, in which the toxic compounds have been removed and the manufacturing process has been improved with respect to volatile organic compounds, such as ether and ethanol [75].

In order to tailor the ballistic properties of double-base propellants, lead salts are used. Several attempts at research level have been made to replace them [76] but successful results are scarce in the literature.

The mechanical properties of double-base propellants are rather poor, compared to composite solid propellants using an elastic polymer matrix as binder. Typical tensile properties have been given by Hervé and are summarised in Table 8.6 [6].

NC has also been used together with crystalline energetic fillers and this type of propellant is called composite modified double-base propellants (CMDB). Zhao *et al*. have reported on an

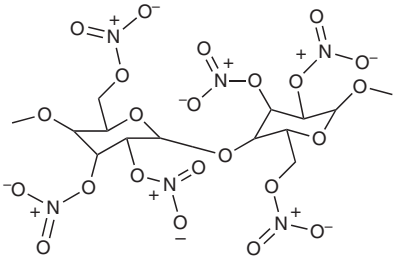

Figure 8.8 *Repeating unit of nitrocellulose.*

Table 8.6 *Tensile properties of double-base propellants at different temperatures from Hervé [6]. EDB = extruded double-base. CDB = cast double-base. σ_m = max stress. ε_m = elongation at max stress. E = elastic modulus.*

Propellant type	−40 °C	+20 °C	+60 °C
EDB, σ_m(MPa)	51	11	2
EDB, ε_m(%)	2.8	2.5	8.0
EDB, E (MPa)	1835	439	21
CDB, σ_m(MPa)	33	11	3
CDB, ε_m(%)	1.0	2.0	10.7
CDB, E (MPa)	3279	555	27

insensitive and minimum-smoke propellant containing FOX-7 as the energetic filler [77]. FOX-7 contributed to increased specific impulse but the pressure exponent was too high. Müller *et al*. have patented a composition containing NC and FOX-7 [78]. Müller *et al*. report that NC/FOX-7 base propellants, plasticised with a dinitro-diaza-type plasticiser instead of NG, have excellent thermal stability and a high performance as a gun propellant [79].

NC has been investigated as a binder for ADN-based propellants by Pontius *et al*. and they found that ADN and nitrocellulose are not chemically compatible [80].

8.3.2 Poly(glycidyl azide)

Poly(glycidyl azide) or glycidyl azide polymer, GAP, is perhaps the energetic polymer that has been most widely reported by propellant researchers. GAP is a polyether, synthesised using epichlorohydrin monomer or the corresponding polymer [81,82]. It was first synthesised in 1972 by Vandenberg [83], and in 1976 Frankel *et al*. at Rocketdyne synthesised the GAP-triol and later the GAP-diol [84].

The advantages of GAP are that it has a high heat of formation, 1172 kJ/kg [85], and produces low molecular-weight combustion products, such as N_2, CO, CH_4 and NH_3 [86]. GAP also has a high oxygen balance of −118%, as compared to HTPB. GAP has a glass transition temperature of approximately −35 °C [87] and at lower operating temperatures, such as −40 °C or −50 °C, plasticisers are needed in order to maintain elasticity of the binder.

The high heat of formation of GAP results in propellants with a maximum specific impulse comparable to propellants using inert binders, such as HTPB. The GAP-based propellant results, however, in a maximum specific impulse at a substantially lower amount of oxidiser, for example AP. The benefit of having a lower amount of solid filler is that the propellant mixture is easier to cast and this, in some cases, may positively affect the sensitivity of the propellant due to improved mechanical properties. The sensitivity is also dependent on the type of oxidiser used. Figure 8.9 shows the theoretical specific impulse of AP-based propellants using GAP or inert binders.

Hydroxyl-terminated GAP is normally chemically crosslinked using isocyanates, following a similar strategy as for HTPB. Polyfunctional isocyanates, such as Desmodur N100, have been used to cure, for example, ADN-based propellants [89] and GUDN-based propellants [3,61]. Curing catalysts, such as dibutyltin dilaurate, triphenylbismuth, zinc octoate and Desmorapid PP, have been used together with Desmodur N100 [90,91]. Reed *et al*. [90] showed that a mixture of dibutyltin dilaurate and triphenylbismuth was preferable, since dibutyltin dilaurate alone resulted in tacky surfaces. By varying the ratio between the two, the cure rate and the cure quality could be tailored.

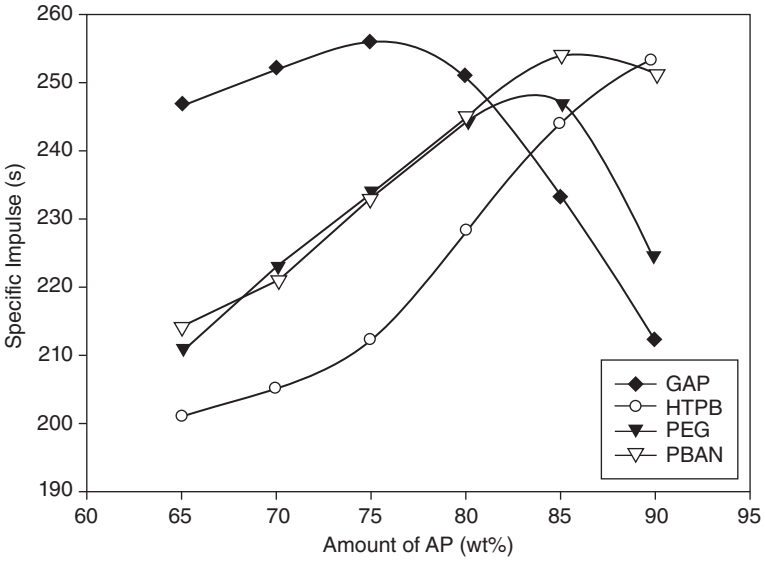

Figure 8.9 *Calculated specific impulse of AP-based propellants using different binders.* $P_e = 1$ *atm.* $P_c = 68$ *atm. Cheetah 2.0 Code [88].*

Depending on the molecular weight of the GAP diol, the resulting polymer network will be more or less rigid, when using trifunctional isocyanates. A typical molecular weight of commercial GAP diol is approximately 2000 g/mol and this will result in a rigid polymer matrix unless chain extenders or long-chain isocyanates are used.

Difunctional isocyanates, such as Desmodur W and IPDI, have been used in FOX-7/GAP-based solid propellants [67]. In order to achieve a polymer matrix, polyfunctional diols are used together with the diisocyanate and the difunctional GAP (Figure 8.10). 1,2,5-Hexanetril was used when curing the FOX-7/GAP-based solid propellants [67].

Propellants based on GAP, Desmodur W and 1,2,5-hexanediol had acceptable mechanical properties, where the maximum stress was 0.48–0.85 MPa and the elongation at max stress was 17–22% at room temperature [67]. It should, however, be mentioned that these propellants contain 20–42% of AP and will therefore not be considered 'green', but the authors claim that they have developed similar propellants without AP as well.

Because of the incompatibility between isocyanates and ADN, the search for alternative curing agents has been on-going for some time. In 2001, Sharpless *et al.* first reported on a highly efficient 1,3-dipolar cycloaddition reaction between an alkyne moiety and an azide, catalysed by a Cu(II) salt [92]. The reaction can also be conducted without the addition of Cu(II)-salt. GAP has the advantage of having pendant azide groups and these can undergo the 1,3-dipolar cycloaddition reaction together with acetylene compounds, forming a triazole crosslink, Figure 8.11. The challenge with this curing system is to control the number of crosslinks per GAP chain and the amount of the acetylene compounds must therefore be low in order to form a thermoset with appropriate mechanical properties [93]. Eldsäter *et al.* developed alkyne-functional hybrid dendritic-linear polyethers that showed excellent compatibility with ADN, and rapid curing with GAP was demonstrated through 1,3-dipolar cycloaddition [94].

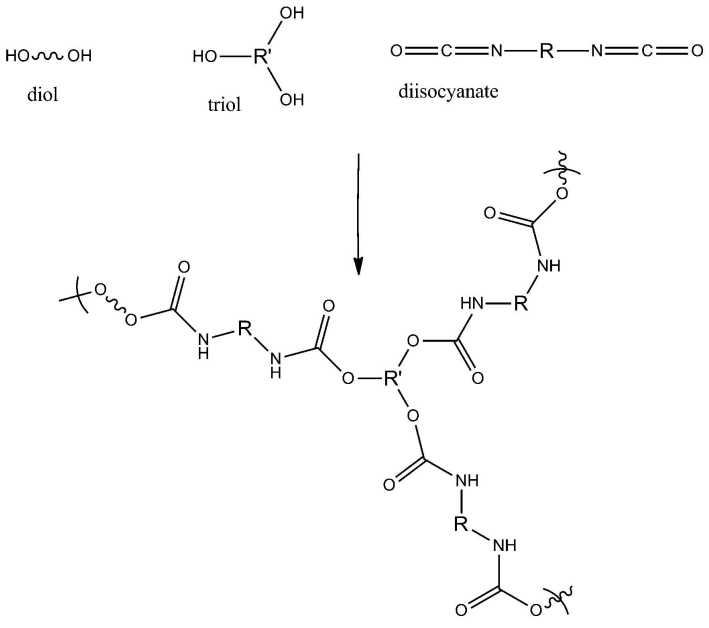

Figure 8.10 *Schematic reaction between a difunctional polyol, a difunctional isocyanate and a triol.*

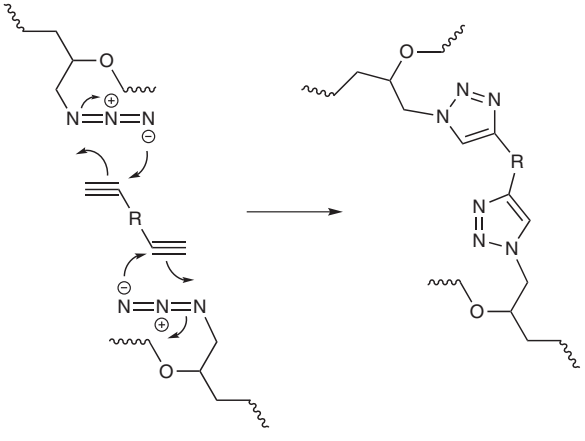

Figure 8.11 *Schematic reaction between GAP and a difunctional acetylene compound.*

Different acetylenic compounds have been used to cure GAP. Min *et al*. [95] used bispropargyl succinate, BPS, to cure di- and trifunctional GAP and mixtures of the two. Triphenyl bismuth was used as the curing catalyst. The resulting polymer matrices had maximum stresses between 0.06 and 0.69 MPa. Trifunctional GAP gave the highest values and difunctional GAP the lowest. The strains at max stress were in the range of 34 to 178%. GAP cured with BPS and 3,6,9-trioxaundecanedioic acid bispropargyl ester has also been investigated by Keicher *et al*. [96]. The pure binder showed strains between 47 and 95% and the max stress was in the range of 0.05 to 0.32 MPa. A mixture of di- and trifunctional

short-chain GAP, cured with BPS, resulted in slightly lower stress (0.05–0.21 MPa) and slightly higher strain (45–124%) [97]. ADN/GAP-based propellants, cured with BPS, had a max stress in the range of 0.2–0.3 MPa and the strain at max stress was in the range of 10–24% [66]. These propellants also contained 10% of HMX or aluminium. Since GAP, cured with BPS, has a higher glass transition than GAP, cured with isocyanate, plasticisers are needed to meet the low temperature requirements. Menke *et al*. used trimethylolethane trinitrate TMETN as a plasticiser in their ADN/GAP-propellant [89]. The advantage of BPS in relation to ADN is that they are chemically compatible with each other, contrary to ADN and isocyanates. It has, however, been shown that when hydroxyl-terminated GAP has been cured with isocyanate, no compatibility issues remain [98].

Min *et al*. have also used 1,4-bis(1-hydroxypropargyl)benzene, BHPB, to crosslink GAP [95]. GAP cured with BHPB had similar mechanical properties as GAP cured with BPS.

Manzara *et al*. [99] have crosslinked GAP successfully with different acrylates, such as pentaerythritol triacrylate (PE3A) and hexandiol diacrylate (HDDA). GAP, cured with these acrylates, had a broad range of mechanical properties depending on the type and amount of acrylate added. Cunliffe *et al*. [50] investigated PE3A, HDDA and tetra(ethylene glycol) diacrylate (TEGDA) together with difunctional GAP. The materials cured very well and the material with the longest pot life was selected for compatibility studies with ADN. Unfortunately, ADN and GAP/TEGDA were strongly incompatible.

Compared to crosslinked HTPB, GAP-based binders have less good mechanical properties. In a recent paper by Min *et al*. [95], the mechanical properties of difunctional GAP were largely improved, using a combined curing system, consisting of both an isocyanate and an acetylene compound. Difunctional GAP, cured with IPDI and 0.5 pph of BPS, resulted in a max stress of 0.55 MPa and a strain of 588%. Difunctional GAP, cured with Desmodur N100 and no acetylene component added, had a stress of 0.71 MPa and a strain at break of only 50%.

It has been demonstrated that the type of filler will affect the mechanical properties of GAP-based propellants [66] and therefore it may be difficult to judge the GAP-based binder by studying only results from propellants containing 'green' oxidisers. Results from Nguyen *et al*. show that an AP-based aluminised solid GAP-based propellant had strains ranging between 30 and 52% at 20 °C [100], which are acceptable mechanical properties for many applications [40,101,102]. Data are summarised in Table 8.7.

A few combustion studies of GAP-based propellants have been performed. ADN/GAP-based propellants have high burn rates and pressure exponents ranging between 0.42 and 0.54 [50,89,103]. In the study of Wingborg *et al*. [103], the specific impulse in a motor experiment, using an un-optimised nozzle, was determined to 233 s of a propellant containing 70% of ADN (Figure 8.12).

Wingborg *et al*. have also presented a GAP-based propellant containing a mixture of ADN and GUDN [104]. This propellant had a burn rate of 15 mm/s at 7 MPa and a pressure exponent of 0.55.

GAP has also been used in ammonium nitrate-based propellants [105].

Various GAP/HNF-based propellants have been developed by TNO, NL [106]. These had acceptable mechanical properties, a propellant denoted K-1 which had a maximum stress of 0.69 MPa and a strain of 27% at 20 °C. The burn rate of this propellant was 17.7 mm/s at 7 MPa. The pressure exponent was high, 0.89, but values of 0.64 could be reached for other compositions.

Table 8.7 *Tensile properties of GAP-based green propellants at 20 °C. σ_m = max stress. ε_m = elongation at max stress. E = elastic modulus. Tensile testing is done at a rate of 50 mm/min using JANNAF Class C dog-bones unless otherwise stated.*

Propellant [ref]	σ_m (MPa)	ε_m (%)	*E* (MPa)	Comment
ADN/HMX/GAP/BDNPA-F [66]	00.25[a]	14[a]	3.6[a]	BPS, 66% solids
ADN/Al/GAP/BDNPA-F [66]	0.23-0.27[a]	12[a]	3.6[a]	BPS, 66% solids
ADN/HMX/GAP/TMETN [89]	0.27	15.7	5.4	N100, 66% solids
ADN/HMX/GAP [89]	0.25	23.9	1.6	BPS, 70% solids
ADN/HMX/GAP/TMETN [89]	0.22	10.9	2.8	BPS, 69% solids
FOX-7/AP/GAP/TMETN/BTTN [67]	0.48	11.3	6.83	48% FOX-7 20% AP
FOX-7/AP/GAP/TMETN/BTTN [67]	0.83	16.2	6.57	33% FOX-7 36% AP
FOX-7/AP/GAP/TMETN/BTTN [67]	0.55	29.8	3.4	28% FOX-7 42% AP
FOX7/AP/GAP/BDNPA-F [67]	0.85	20.9	5.6	38% FOX7 30% AP

[a] approximate values as estimated from a graphic presentation of the tensile test.

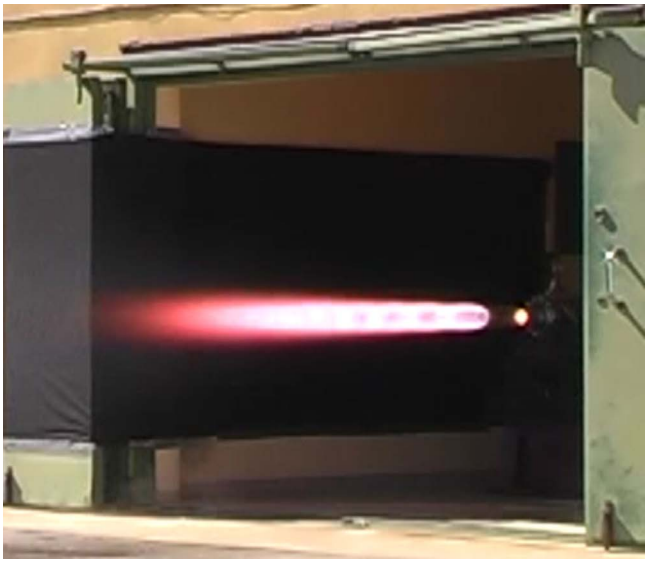

Figure 8.12 *Test firing of a 3 kg ADN/GAP rocket motor. Reproduced with permission from [103] © 2010 the American Institute of Aeronautics and Astronautics.*

8.3.3 Poly(3-nitratomethyl-3-methyloxetane)

Poly(3-nitratomethyl-3-methyloxetane), polyNIMMO, was developed in the 1980s by Manser [107,108]. PolyNIMMO has a much lower heat of formation than GAP (−2290 kJ/kg [109] compared to +1172 kJ/kg for GAP), but is also not classified as an explosive material or a propellant. This is an advantage from a manufacturing point of view,

but will of course lower the performance of the propellant. The density of polyNIMMO is 1.26 g/cm^3 [35], which is higher than for inert polymers.

PolyNIMMO has a glass transition temperature of approximately −30 °C [50] and plasticisers are thus almost always necessary to improve the low temperature properties of these binders. A mixture of difunctional and trifunctional polyNIMMO has been cured with the diisocyanate Desmodur W using dibutyl tin dilaurate as a cure catalyst [50]. The mechanical properties of the resulting polymer matrix were very good. The max stress was 1.6 MPa and the strain at max stress was 700%. The strain decreased to 500% when the plasticiser dioctyl sebacate was added to the binder. The glass transition temperature was, however, improved.

PolyNIMMO has been investigated as a binder of ADN- [50,80], AN- [110] and FOX-7/GUDN-based [3] propellants. Pontius *et al.*, however, found that ADN and polyNIMMO are not chemically compatible [80]. Cunliffe *et al.* [50] also found that the uncured polyNIMMO showed borderline incompatibility with ADN, but when cured the propellant was chemically stable. ADN/polyNIMMO-based propellants had rather low tensile strength, 0.1 MPa, but the tensile stain was acceptable (40%) [50].

Burn rate studies showed that ADN/polyNIMMO, plasticised with BTTN/TMETN, had a high burn rate (28 mm/s at 7 MPa of a propellant containing 75% ADN) and an acceptable pressure exponent (0.5) [50].

PolyNIMMO has also been used as a binder of HNF/Al-based propellants [106]. Mixtures of polyNIMMO diols and triols, or triols alone, have both been used. Propellants using the polyNIMMO triol only resulted in somewhat lower tensile stresses but higher strain than the propellants using a mixture of diol and triol. The stresses at 20 °C were 0.44–0.48 MPa and the strains were 21–23%. The burn rate of HNF/Al/polyNIMMO-based propellants was high, 19 mm/s at 7MPa, and so was the pressure exponent, 0.9. Burn rate modifiers were therefore investigated and it was possible to reduce the pressure exponent to 0.68, but this also raised the burn rate to 24 mm/s at 7 MPa.

8.3.4 Poly(glycidyl nitrate)

Poly(glycidyl nitrate), polyGLYN, belongs to the same polymer family as GAP, the polyoxiranes, and was commercialised in the 1990s by ICI Nobel Enterprises, UK. Glycidyl nitrate (GLYN) is prepared by the nitration of glycidol, and is polymerised to give a hydroxyl terminated prepolymer. PolyGLYN has a glass transition temperature of −32 °C [111] and plasticisers are thus needed to improve the low temperature properties of polyGLYN-based binders [50]. The density of polyGLYN is 1.47 g/cm^3 [35].

Early batches of cured polyGLYN had poor long-term stability and became soft with time. DERA and ICI, UK, therefore modified the primary end groups and the stability was largely improved [112–115]. The mechanical properties of polyGLYN are not as good as those of HTPB. PolyGLYN is softer and has less strength. Provatas has studied the effect of using mixtures of isocyanates on the mechanical properties of polyGLYN [111]. Desmodur N3400 and Desmodur N100 were mixed with IPDI at various ratios, and it was shown that the hardness of the materials decreased with increasing amount of IPDI. The highest value of maximum tensile stress (approx. 0.65 MPa) was obtained using a mixture of 75% Desmodur N100 and 25% IPDI.

PolyGLYN has been investigated as a binder for ADN-based propellants by Pontius *et al.*, and they found that ADN and PolyGLYN are not chemically compatible [80]. This

has also been shown by Cunliffe *et al.* [50], and they proposed that it may be the modified end group of polyGLYN (1,2-hydroxy [112]) that interacts negatively with ADN. Shang *et al.* have, however, performed a combustion study of ADN/Al/polyGLYN-based propellants with interesting results concerning the burn rate and pressure exponent [116]. Chan *et al.* [69] have also used polyGLYN, cured with Desmodur N100, in ADN-based propellants. The propellants had high burn rates, 20–23 mm/s at 7MPa, and pressure exponents of 0.59–0.71.

PolyGLYN has also been used together with AN [117] in propellants. AN/polyGLYN-based propellants were cured using a mixture of Desmodur N100 and HMDI [117]. The tensile stresses of these propellants were in the range of 1–2 MPa and the strains were 13–33%, indicating good mechanical properties. The burn rate of these was 14–19 mm/s at 28 MPa and they had pressure exponents of 0.45–0.82.

Propellants based on polyGLYN and HNF have also been investigated, but it was found that HNF was incompatible with polyGLYN [106].

8.3.5 Poly[3,3-bis(azidomethyl)oxetane]

Poly[3,3-bis(azidomethyl)oxetane], polyBAMO was developed in the 1970s by Manser [118]. PolyBAMO has a higher content of azido groups than GAP and therefore offers an enhanced kinetic and thermodynamic advantage for propellants [119,120]. The disadvantages of the homopolymer of BAMO are a high melting point (60–80 °C) [35,121], a high glass transition temperature (−39 °C) and poor processability in comparison to GAP. BAMO has therefore been used as a building block in copolymers.

Several examples of copolymers of BAMO exist, both as thermoplastic elastomers and thermo-set polymers. Kimura *et al.* have evaluated copolymers of BAMO and NIMMO, in propellants based on AN, with respect to burning behaviour and sensitivity [120]. The propellant was less sensitive than AP- and HMX-based propellants, using the same binder.

Wardle *et al.* have developed block copolymers of BAMO and 3-azidomethyl-3-methyloxethane (AMMO) crystalline below 60 °C and amorphous above −20 °C [122]. They have acceptable mechanical properties but somewhat low densities (1.2 g/cm^3) compared to, for example GAP. Sanderson *et al.* therefore exchanged the AMMO-blocks with GAP. The authors also suggested polyGLYN as an alternative to GAP, but no data on these polymers were available in the patent [41] (Table 8.8).

A copolymer of BAMO and GAP has also been chemically crosslinked with the isocyanate Desmodur N100 to form a polymer matrix of a composite propellant, Figure 8.13 [123]. This was, however, not a green propellant, since AP was the main ingredient. The polymer, containing approximately 30–40% polyBAMO, had very interesting properties, such as a low viscosity at room temperature and a low glass transition temperature of −55 °C.

Table 8.8 *Tensile properties of copolymers of polyBAMO at 20 °C. σ_m = max stress. ε_m = elongation at max stress. E = elastic modulus. Data from reference [41].*

Polymer binder	σ_m (MPa)	ε_m (%)	*E* (MPa)
Poly(BAMO-AMMO)	1.3	251	3.5
Poly(BAMO-NIMMO)	1.3	325	4.0
Poly(BAMO-GAP)	0.7	161	1.9

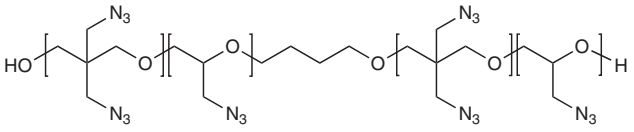

Figure 8.13 *Structure of the copolymer used by Menke* et al. *[123, 124].*

Reed used compounds such as 1,4-bis(ethylcarbonyl)benzene and 1,3-bis(cyanoethynyl) benzene to crosslink copolymers of BAMO and NIMMO [93]. The latter resulting polymer matrix had excellent elasticity with an elongation at max stress above 800%. When evaluating the binder, cured with 1,4-bis(ethylcarbonyl)benzene, together with HMX as a filler, the max stress was 0.7 MPa and the elongation at max stress was 315%.

8.4 Energetic Plasticisers

Plasticisers are often an important part of the binder in solid propellants and they are used to improve the low temperature properties of the binder and the processing of the propellant. Inert plasticisers have been used in the plastics industry for a long time and have also played an important role in the production of propellants.

Energetic plasticisers are similar to energetic polymers in the sense that they contain energetic functional groups, and were developed for the same reason as energetic polymers were, that is to bring more energy into the binder.

A good plasticiser should have a low glass transition temperature, a low viscosity and a low ability to migrate [115]. An energetic plasticiser should also have a high oxygen balance, low impact sensitivity and a high thermal stability. These demands are in many cases contradictory and it is thus not easy to find the ultimate energetic plasticiser. Several energetic plasticisers, such as nitratoethyl nitramines (NENAs) [115,125–128], nitrate esters (e.g. nitroglycerine, butanetriol trinitrate (BTTN) and trimethylolethane trinitrate (TMETN)) [129], azido compounds [129–131], bis(2,2-dinitropropyl)acetal/bis(2,2-dinitropropyl)formal (BDNPA/F) [115,127,128,132], nitroaromatic compounds (e.g. 2,4-/2,6-dinitroethylbenzene/2,4,6-trinitroethylbenzene) [115,127,128], nitrato and azido oligomers (GLYN, NIMMO and GAP oligomers) [133–139], have been developed worldwide for use in solid propellants and plastic bonded explosives. The major share of these is commercialised.

8.5 Outlook for Design of New Green Binder Systems

The rapid expansion of the chemical toolbox available for the polymer chemist to synthesise polymers with tailored properties will bring about new possibilities for designing suitable binder polymers for green propellants. However, it should be kept in mind that it is a true challenge to design polymers for such demanding conditions as for a green propellant system, to fulfil all the boundary conditions that apply.

Obviously, the oxidiser/s has to be inert towards the binder polymer and, depending on the choice of oxidiser/s, a range of chemical functional groups have to be discarded. Unfortunately, it has been shown to be difficult to fully predict appropriate combinations of oxidisers and functional groups from (quantum) modelling, since parameters such as concentration of functional groups, presence of trace amounts of water (or humidity), as well

as particle size and morphology of the oxidiser will play a major role in the stability of the final composition. Modelling can provide guidance but has to be complemented with experiments.

The dispersion of the oxidiser in the binder polymer is a science in itself. Bonding agents can be utilised to provide adhesion and/or to tailor the oxidiser's reactivity. However, with nanotechnology as an emerging area, there has been an immense interest in how to optimise dispersion of nanoparticles efficiently to give stable nanocomposites; it may be well worth studying the latest developments in this field [140].

Apart from the stability aspect, several other aspects have to be considered in order to develop a binder with appropriate properties. One of the most demanding criteria is the temperature span at which the binder has to be mechanically stable; with small variations in different countries the relevant temperature interval is −40 °C to +60 °C, where especially the elasticity is the key parameter. Also, the mechanical stress that the propellant is subjected to during launch requires binder materials that have high creep strength.

The final, crosslinked, binder system must have good mechanical properties; max stress above 0.7 MPa and elongations higher than approximately 300%. If one of those boundary conditions has to be sacrificed it is crucial that the elongation is high enough to give good performance.

The glass transition of the crosslinked system must be sufficiently low, below −40 °C, to allow for sufficient molecular mobility. This criterion necessitates that the major part of the binder has to be based on flexible polymers, typically having −C−C− or −C−O−C− bonds in the backbone, which the reported systems also typically have.

Provided that the key requirements above can be met, there are several design features that can be considered when designing green polymeric binders for propellants, of which some will be briefly discussed below.

8.5.1 Architecture of the Binder Polymer

The binder should, apart from being miscible with the oxidiser, provide a suitable mixing viscosity allowing for facile manufacturing of the propellant into, for example, pellets. Traditionally, linear polymers have been used as binders for propellants which, when high molecular-weight polymers are used, bring about high viscosity in the melt with challenging dispersion as a consequence. However, the recent years of development of dendritic, or tree-like, polymers bring about possible advantages in that they give rise to a lower viscosity than corresponding linear polymers, due to the absence of chain entanglements as observed for molecular weights below 20 000 g/mol [141]. This suggests that a promising binder backbone architecture contains both linear and highly branched segments, where the linear parts provide mechanical/elastic properties and the branched part acts as a rheology modifier, Figure 8.14.

8.5.2 Chemical Composition and Crosslinking Chemistries

Depending on what kind of binder that is aimed for – crosslinked (thermo-setting polymer) or thermoplastic elastomer – different design options apply for the polymer composition.

The development of new reversible-deactivation radical polymerisations (RDRP) [142] for example atom transfer radical polymerisation (ATRP) [143], nitroxide-mediated polymerisation (NMP) [144] and reversible addition-fragmentation chain-transfer

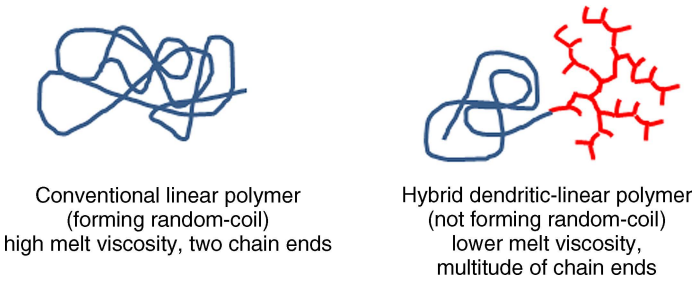

Figure 8.14 *Schematic illustrations showing a linear polymer chain (left) and a hybrid dendritic-linear polymer (right).*

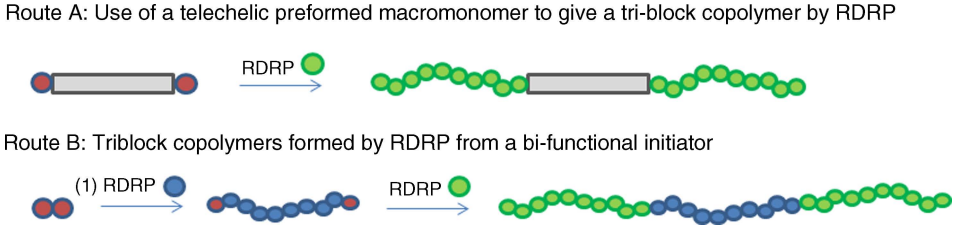

Figure 8.15 *New block copolymers can be synthesised by controlled radical polymerisation techniques (RDRP) and combined with new polymer architectures.*

(RAFT) polymerisation [145], allows for the synthesis of novel block-copolymers. These new polymerisations enable the synthesis of new thermoplastic elastomeric binders, rendering it possible to utilise new polymer combinations, Figure 8.15. For instance, one can make use of a telechelic isocyanate-block onto which polymer blocks of suitable composition can be polymerised. Another possibility is synthesising a telechelic block by RDRP and then growing a second block by the addition of a second monomer.

The development of RDRPs has also made it possible to use a large number of different vinyl monomers, which have historically been difficult to incorporate in block copolymers.

Traditionally, the majority of propellant systems rely on a thermo-setting binder that undergoes chemical crosslinking reactions during and/or after the processing into the final propellant. Typically, linear, telechelic, flexible polymers have been crosslinked with reactive species such as di- or polyfunctional isocyanates. Again, the binder architecture can be utilised as a tool to improve the crosslinking efficiency; if one of the components is branched, crosslinking will be more efficient. However, this requires that the functional group in excess is unreactive towards the oxidiser/s, though some other prerequisites regarding the polymer system have to be fulfilled: (i) no condensation by-products can be formed during the crosslinking reaction since these may remain in the solid propellant and eventually react with the oxidiser. This would significantly hamper the storage stability (and safety) of the processed propellant. (ii) The crosslinking reaction itself may, depending on the curing chemistry, give rise to shrinkage of the binder system as well as changes in polarity during cure, which may result in dewetting of the solid oxidiser to give voids in the final propellant with decreasing storage stability and safety during use as a consequence.

The curing reaction is essentially always triggered by temperature; during crosslinking the temperature is raised to initiate the crosslinking reaction. Today, there are several photochemically induced reactions that may hold interest in the attempt to develop green binders for propellants; compounds containing double bonds or thiols can be readily crosslinked by irradiation by UV-light, under certain circumstances even in the absence of a photoinitiator which most likely is beneficial for a propellant system. A challenge for UV-curable systems is, of course, that the optical transparency of the irradiated system must be sufficient. However, in the coatings industry dispersions are often photochemically cured. Another interesting alternative may be to use electron beam curing, which is less specific but extremely powerful and therefore also less sensitive to the thickness of the curing sample. Given that the oxidiser is stable, EB curing may be an interesting pathway towards green propellants. Photochemically induced curing also allows for the separation between the mixing step and the curing step in the manufacturing process. In a temperature-triggered crosslinking system there will always be a risk that the crosslinking reaction occurs during the mixing step.

References

1. Urbansky, E.T. (2002) Perchlorate as an environmental contaminant. *Environmental Science and Pollution Research*, **9** (3), 187–192.
2. DoD Workshop Advanced Strategy for Environmentally Sustainable Energetics. Rockaway, NJ, USA (2009)
3. Dawley, S.K. and Friedlander, M.P. (2012) End-burning propellant grain with area-enhanced burning surface for rockets and missiles. Patent No. WO2012047322A2.
4. Vogelsanger, B., Schädeli, U. and Antenen D. (2007) ECL - A New Propellant Family With Improved Safety and Performance Properties, in Proceedings of the 38th International Annual Conference of ICT, Karlsruhe, Germany, pp. V15/1–V15/12.
5. Vogelsanger, B., Schädeli, U. and Antenen, D. (2011) ECL - A new propellant technology has reached maturity, in Proceedings of the 42nd International Annual Conference of ICT, Karlsruhe, Germany, pp. 33/1–33/9.
6. Hervé, A. (1993) Double-base propellants, in *Solid Rocket Propulsion Technology* (ed. A. Davenas), Pergamon Press, Oxford, pp. 369–413.
7. Bottaro, J.C. (1991) Dinitramide salts and method of making same. Patent No. WO9119669.
8. Bottaro, J.C., Penwell, P.E. and Schmitt, R.J. (1997) 1,1,3,3-Tetraoxy-1,2,3-triazapropene Anion, a new oxy anion of nitrogen: The dinitramide anion and its salts. *Journal of the American Chemical Society*, **119**, 9405–9410.
9. Langlét, A., Wingborg, N. and Östmark, H. (1996) ADN: a new high performance oxidizer for solid propellants, in *Challenges in Propellants and Combustion 100 Years After Nobel (International Symposium on Special Topics in Chemical Propulsion, 4th, Stockholm, May 27–31, 1996)* (ed. K.K. Kuo), Begell House, New York, pp. 616–626.
10. Chan, M.L., Turner, A., Merwin, L. *et al.* (1997) ADN propellant technology, in *Challenges in Propellants and Combustion 100 Years After Nobel (International Symposium on Special Topics in Chemical Propulsion, 4th, Stockholm, May 27–31, 1996)* (ed. K.K. Kuo), Begell House, New York, pp. 627–635.
11. Östmark, H., Bemm, U., Langlét, A. *et al*. (2000) The properties of ammonium dinitramide (ADN): Part 1, basic properties and spectroscopic data. *Journal of Energetic Materials*, **18**, 123–128.

12. Teipel, U., Heintz, T. and Krause, H.H. (2000) Crystallization of spherical ammonium dinitramide (ADN) particles propellant explosives pyrotechnics. *Propellants, Explosives, Pyrotechnics*, **25** (1), 81–85.
13. Ramaswamy, A.L. (2000) Energetic-material combustion experiments on propellant formulations containing prilled ammonium dinitramide. *Combustion, Explosion and Shock Waves*, **36** (1), 119–124.
14. Heintz, T. and Fuchs, A. (2010) Continuous production of spherical ammonium dinitramide particles (ADN-Prills) by microreaction technology, in Proceedings of the 41th International Annual Conference of ICT, pp. 100/1–100/11.
15. Muscatelli, F., Renouard, J. and Bouchez, J.-M. (2010) Crystallization of ADN (ammonium dinitramide) by crystallization in protic viscous solvent. Patent No. WO 2010031962, A1.
16. Eldsäter, C., deFlon, J., Holmgren, E. *et al*. (2009) ADN prills: production, characterization and formulation, in Proceedings of the 40th International Annual Conference of ICT, pp. 24/ 1–24/10.
17. Heintz, T., Pontius, H., Aniol, J. *et al*. (2009) Ammonium dinitramide (ADN) - prilling, coating, and characterization. *Propellants, Explosives, Pyrotechnics*, **34** (3), 231–238.
18. Heintz, T., Pontius, H., Aniol, J. *et al*. (2008) ADN - prilling, coating and characterization, in Proceedings of the 39th International Annual Conference of ICT, pp. V11/1–V11/14.
19. Fuhr, I. and Reinhard, W. (2007) Crystallization of Ammonium Dinitramide - Part 1: Solvent Screening, in Proceedings of the 38th International Annual Conference of ICT, pp. 73/1–73/6.
20. Benazet, S. and Jacob, G. (2006) Process for production of ammonium dinitroamide (ADN) crystals, the obtained ADN crystals and energetic composites containing them. Patent No. FR 2884244A1.
21. Heintz, T., Leisinger, K. and Bohn, M. (2012) Advanced stabilization of ADN-prills by preparation of raw materials by means of fluidized bed technology, in Proceedings of the 43rd International Annual Conference of ICT, Karlsruhe, Germany, pp.
22. Johansson, M., Flon, J.d., Petterson, Å. *et al*. (2006) Spray prilling of ADN and testing of ADN-based solid propellants, in Proceedings of the 3rd Int. Conf. on Green Propellant for Space Propulsion and 9th Int. Hydrogen Peroxide Propulsion Conference, Poitiers, France, pp. ESA SP-635.
23. Haury, V.E. (1972) Hydrazinium nitroformate propellant stabilized with nitroguanidine. Patent No. US 3658608, A.
24. Flynn, J.P., Lane, G.A. and Plomer, J.J. (1975) Plasticized nitrocellulose propellant compositions containing hydrazinium nitroformate and aluminum hydride. Patent No. US 3862864, A.
25. Brown, J.A. and Knapp, C.L. (1968) Stabilization of nitroform salts. Patent No. US3384675A.
26. Bohn, M. (2005) Thermal stability of Hydrazinium Nitroformate (HNF) Assessed by Heat Generation Rate and Heat Generation and Mass Loss, in Proceedings of the International Symposium on the Heat Flow Calorimetry of Energetic Material Indiana, USA, pp.
27. European Chemicals Agency ECHA (2011) Inclusion of substances of very high concern in the candidate list (Decision of the European Chemicals Agency). Vol. ED/31/2011.
28. European Chemicals Agency ECHA (2011) Member state committee support document for identification of hydrazine as a substance of very high concern because of its CMR properties.
29. Munroe, C.E. (1896) On the development of smokeless powder. *Journal of the American Chemical Society*, **18** (9), 819–846.
30. Oommen, C.J. and R, S. (1999) Ammonium nitrate: a promising rocket propellant oxidizer. *Journal of Hazardous Materials*, **A67**, 253–281.
31. Talley, S.K. (1961) Ammonium nitrate rocket-fuel compositions. Patent No. US 2984556.
32. Bice, C.C. and Reynolds, W.B. (1961) Solid propellants. Patent No. US 2993769.

33. van Zyl, G.J. (2011) Insensitive composite propellants based on a HTPE binder, in Proceedings of the 42nd International Annual Conference of the Fraunhofer ICT, Karlsruhe, Germany, pp. 48/1–48/9.
34. Caro, R.I. and Bellerby, J.M. (2008) Preparation of hydroxy terminated polyether (HTPE) composite rocket propellants, in Proceedings of the 39th International Annual Conference of ICT, Karlsruhe, Germany, pp. 78/1–78/12.
35. Bathelt, H. and Volk, F. (2004) Thermochemical database of ICT, 7.0; Fraunhofer Institut für Chemiche Technologie: Germany.
36. Kon'kona, T.S., Matsyushin, Y.N., Miroshnichenko, E.A. and Vorob'ev, A.B. (2009) Thermochemical properties of dinitramidic salts. *Russian Chemical Bulletin, International Edition*, **58** (10), 2020–2027.
37. Kjellström, A. (2003) 'The insensitive energetic material FOX-7', FOI-R–0916–SE.
38. Latypov, N.V., Bergman, J., Langlét, A. *et al*. (1998) Synthesis and reactions of 1,1-Diamino-2,2-dinitroethylene. *Tetrahedron*, **54** (38), 11525–11536.
39. Östmark, H. (2002) N-guanylurea-dinitramide: a new energetic material with low sensitivity for propellants and explosives applications. *Thermochimica Acta*, **384**, 253–259.
40. Davenais, A. (1993) *Solid Rocket Propulsion Technology*, Pergamon Press., Oxford.
41. Sanderson, A.J., Edwards, W.W., Cannizzo, L.F. and Wardle, R.B. (2000) Synthesis of thermoplastic polyoxirane-polyoxetane block copolymers as energetic binders for propellants and explosives. Patent No. WO 2000034209, A2.
42. Provatas, A. (2000) 'Energetic polymers and plasticisers for explosive formulations - A review of recent advances', DSTO-TR-0966.
43. Sutton, G.P. and Biblarz, O. (2001) *Rocket Propulsion Elements*, John Wiley & Sons, Inc., New York.
44. Rama Rao, M., Scariah, K.J., Varghese, A. *et al*. (2000) Evaluation of criteria for blending hydroxy terminated polybutadiene (HTPB) polymers based on viscosity build-up and mechanical properties of gumstock. *European Polymer Journal*, **36**, 1645–1651.
45. Wingborg, N. (2002) Increasing the tensile strength of HTPB with different isocyanates and chain extenders. *Polymer Testing*, **21**, 283–287.
46. Andreasson, S., de Flon, J., Liljedahl, M. *et al*. (2010) 'Initial evaluation of ADN as an oxidizer in solid propellants for large space launcer boosters', FOI-R–2988–SE.
47. de Flon, J., Andreasson, S., Liljedahl, M. *et al*. (2011) Solid Propellants based on ADN and HTPB, in Proceedings of the 47th AIAA/ASME/SAE/ASEE Joint Pro-pulsion Conference, San Diego, USA, pp. AIAA2011-6136.
48. Heintz, T., Leisinger, K. and Pontius, H. (2006) Coating of spherical ADN particles, in Proceedings of the 37th International Annual Conference of ICT, Karlsruhe, Germany, pp. 150/1–150/12.
49. Chakravarthy, S.R., Freeman, J.M., Price, E.W. and Sigman, R.K. (2004) Combustion of propellants with ammonium dinitramide. *Propellants, Explosives, Pyrotechnics*, **29** (4), 220–230.
50. Cunliffe, A., Eldsäter, C., Marshall, E. *et al*. (2002) 'United Kingdom/Sweden Collaboration on ADN and PolyNIMMO/PolyGLYN Formulation Assessment', FOI-R–0420–SE.
51. van der Heijden, A.E.D.M. and Leeuwenburgh, A.B. (2009) HNF/HTPB propellants: Influence of HNF particle size on ballistic properties. *Combustion and Flame*, **156**, 1359–1364.
52. Pandey, M., Jha, S., Kumar, R. *et al*. (2012) The pressure effect study on the burning rate of ammonium nitrate-HTPB-based propellant with the influence catalysts. *Journal of Thermal Analysis and Calorimetry*, **107** (1), 135–140.
53. Chen, Z.-e., Li, Z.-y., Yao, N. *et al*. (2010) Safety property of FOX-7 and HTPB propellants with FOX-7 (chinese, abstract in english). *Hanneng Cailiao*, **18** (3), 316–319.

54. Florczak, B. (2008) A comparison of properties of aluminized composite propellants containing HMX and FOX-7. *Central European Journal of Energetic Materials*, **5** (3–4), 103–111.
55. Tummers, M.J., van der Heijden, A.E.D.M. and van Veen, E.H. (2012) Selection of burning rate modifiers for hydrazinium nitroformate. *Combustion and Flame*, **159**, 882–886.
56. Sinditskii, V., Egorshev, V., Tomasi, D. and DeLuca, L. (2008) Combustion mechanism of ammonium-nitrate-based propellants. *Journal of Propulsion and Power*, **24** (5), 1068–1078.
57. Sinditskii, V.P., Levshenkov, A.I., Egorshev, V.Y. and Serushkin, V.V. (2003) Study on combustion and thermal decomposition of 1,1-diamino-2,2-dinitroethylene (FOX-7) International Pyrotechnics Seminar, Volume: 30th, 1, 299–311.
58. Vörde, C., Roestlund, S., Sjöqvist, C. and Klaw, Å. (2007) Development of a moisture insensitive gas generating composition, 38th International Annual Conference of ICT, 11/1–11/7.
59. Törmälä, P. (1974) Determination of glass transition temperature of poly(ethylene glycol) by spin probe technique. *European Polymer Journal*, **10** (6), 519–521.
60. Shirasaka, H., Inoue, S.-i., Asai, K. and Okamoto, H. (2000) Polyurethane urea elastomer having monodisperse Poly(oxytetramethylene) as a soft segment with a uniform hard segment. *Macromolecules*, **33**, 2776–2778.
61. Menke, K. and Eisele, S. (2012) Gas generators and propellants based on guanylurea dinitramide with additional energetic components. Patent No. DE 102011100113, A1.
62. Qu, Z., Zhai, J., Zhang, H. and Yang, R. (2010) XX (chinese, abstract in english). *Huozhayao Xuebao*, **33** (6), 61–64.
63. Reed, R. (1989) Multifunctional polyalkylene oxide binders. Patent No. US 4799980, A.
64. Reed, R. (2003) High-energy propellant with reduced hydrogen chloride pollution containing ammonium dinitramide oxidizer and energetic binders and plasticizers. Patent No. US 20030024617, A1.
65. Bayer Material Science, Product information Desmophen C2200 http://www.bayermaterialsciencenafta.com (2012-07-17).
66. Cerri, S. and Bohn, M.A. (2011) Ageing behaviour of rocket propellant formulations with ADN as oxidiser, in Proceedings of the 14th Seminar 'New Trends in Research of Energetic Materials', Pardubice, Czech Republic, pp. 88–105.
67. Lips, H., Helou, S., Kentgens, H. *et al.* (2012) Less Sensitive Smoke Reduced Rocket Propellants based on FOX 7, in Proceedings of the 43rd International Annual Conference of the Fraunhofer ICT, Karlsruhe, Germany, pp. 22/1–22/11.
68. Korobeinichev, O.P., Paletsky, A.A., Tereschenko, A.G. and Volkov, E.N. (2003) Combustion of ammonium dinitramide/polycaprolactone propellants. *Journal of Propulsion and Power*, **19** (2), 203.
69. Chan, M.L. and Turner, A. (2005) Minimum signature propellant. Patent No. US 6863751, B1.
70. Fleming, W., McSpadden, H. and Olander, D. (2000) Phase stabilized ammonium nitrate propellants, in Proceedings of the 36th AIAA/ASME/SAE/ASEE Joint Propulsion Conference and Exhibit, Huntsville, AL, USA, pp. AIAA-2000-3179.
71. Sandén, R. (2007) Composite gunpowder based on ammonium dinitramide and ethene-vinyl-acetate copolymer. Patent No. SE 529096, C2.
72. Fujisato, K., Habu, H., Hori, K. *et al.* (2012) Combustion mechanism of ADN-based composite propellant, in Proceedings of the 43rd International Annual Conference of the Fraunhofer ICT, Karlsruhe, Germany, pp.
73. Schönbein, C.F. (1846)
74. Urbansky, E.T. (1965) *Chemistry and Technology of Explosives*, Pergamon Press, New York.
75. Manning, T.G., Rozumov, E., Adam, C.P. *et al.* (2011) The system level approach final assessment of insensitive munitions (IM) response of deterred double base propellant through

optimized ignition and venting, in Proceedings of the 42nd International Annual Conference of ICT, pp. 67/1–67/12.
76. Pi, W.-f., Song, X.-d., Zhang, C. *et al.* (2011) Combustion performance of double-based propellant with a lead-free catalyst Gal-BiCu (chinese, abstract in english). *Hanneng Cailiao*, **19** (4), 405–409.
77. Zhao, F., Gao, H., Xu, S. *et al.* (2010) Energy parameters and combustion characteristics of the insensitive and minimum smoke propellants containing 1,1-diamino-2,2-dinitroethylene (FOX-7) (Chinese, abstract in English). *Huozhayao Xuebao*, **33** (4), 1–4.
78. Müller, D. and Langlotz, W. (2011) Double-base gun propellants containing nitrocellulose and cellulose acetate butyrate. Patent No. EP 2388244, A1.
79. Bohn, M.A. and Mueller, D. (2006) Insensitivity aspects of NC bonded and DNDA plasticizer containing gun propellants, in Proceedings of the 37th International Annual Conference of ICT, Karlsruhe, Germany, pp. 47/1–47/11.
80. Pontius, H., Aniol, J. and Bohn, M.A. (2004) Compatibility of ADN with components used in formulations, in Proceedings of the 35th International Annual Conference of ICT, Karlsruhe, Germany, pp. 169/1–169/19.
81. Frankel, M.B., Witucki, E.F. and Woolery, E.O. (1983) Aqueous process for the quantitative conversion of polyepichlorohydrin to glycidyl azide polymer. Patent No. US 4379894, A.
82. Earl, R.A. (1984) Use of polymeric ethylene oxides in the preparation of Glycidyl azide polymer. Patent No. US 4486351, A.
83. Vandenberg, E.J. (1972) Polyethers containing azidomethyl side chains. Patent No. US 3645917, A.
84. Frankel, M.B., Grant, L.R. and Flanagan, J.E. (1992) Historical development of glycidyl azide polymer. *Journal of Propulsion and Power*, **8**, 560–563.
85. Finck, B. and Graindorge, H. (1996) New molecules for high energetic materials, in Proceedings of the 27th International Annual Conference of ICT, Karlsruhe, Germany, pp.
86. Arisawa, H. and Brill, T.B. (1998) Thermal decomposition of energetic materials 71: Structure-decomposition and kinetics relationships in flash pyrolysis of glycidyl azide polymer (GAP). *Combustion and Flame*, **112**, 533–544.
87. Materials, M.S. GAP-5527 Polyol - Product Information http://www.machichemicals.com/pdf/3M_GAP-5527.pdf (2012-07-05).
88. Energetic Materials Center Cheetah 2.0, Lawrence Livermore National Laboratory.
89. Menke, K., Heintz, T., Schweikert, W. *et al.* (2009) Formulation and properties of ADN/GAP propellants. *Propellants, Explosives, Pyrotechnics*, **34** (3), 218–230.
90. Reed, R. and Chan, M.L. (1983) Propellant binders cure catalyst. Patent No. US 4379903.
91. Bayer Material Science, Product information Desmodur N100 http://www.bayermaterialscien-cenafta.com (2012 -07-17).
92. Kolb, H.C., Finn, M.G. and Sharpless, K.B. (2001) Click Chemistry: Diverse chemical function from a few good reactions. *Angewandte Chemie International Edition*, **40** (11), 2004–2021.
93. Reed, R. (2000) Triazole crosslinked polymers. Patent No. US 6103029, A.
94. Rahm, M., Malmström, E. and Eldsäter, C. (2011) Design of an Ammonium Dinitramide Compatible Polymer Matrix. *Journal of Applied Polymer Science*, **122**, 1–11.
95. Min, B.S., Park, Y.C. and Yoo, J.C. (2012) A study on the triazole crosslinked polymeric binder based on glycidyl azide polymer and dipolarophile curing agents. *Propellants, Explosives, Pyrotechnics*, **37** (1), 59–68.
96. Keicher, T., Kuglstatter, W., Eisele, S. *et al.* (2010) Isocyanate-free curing of glycidyl-azide-polymer (GAP), in Proceedings of the 41st International Annual Conference of ICT, pp. 12/1–12/10.

97. Keicher, T., Kuglstatter, W., Eisele, S. *et al*. (2008) Isocyanate-free curing of glycidyl-azide-polymer (GAP) with bis-propargyl-succinate, in Proceedings of the 39th International Annual Conference of ICT, Karlsruhe, Germany, pp. 66/1–66/13.
98. Pontius, H., Bohn, M.A. and Aniol, J. (2008) Stability and compatibility of a new curing agent for binders applicable with ADN evaluated by heat generation rate measurements, in Proceedings of the 39th International Annual Conference of ICT Karlsruhe, Germany, pp. 129/1–129/34.
99. Manzara, A.P. (1997) Azido polymers having improved burn rate. Patent No. US 5681904,A.
100. Nguyen, C., Morin, F., Hiernard, F. and Guengant, Y. (2010) High Performance Aluminized GAP-based Propellants – IM Results, in Proceedings of the 2010 Insensitive Munitions & Energetic Materials Technology Symposium, Munich, Germany, pp.
101. (1971) Solid propellant selection and characterization. NASA Space Vehicle Design Criteria (Chemical Propulsion), National Aeronautics and Space Administration (NASA): Vol. SP-8064.
102. Bivin, R.L., Johnson, J.T., Markovitch, I.L. and Mehrotra, A.K. (1992) Development of a class 1.3 minimum smoke propellant, in Proceedings of the 28th AIAA/ASME/SAE/ASEE Joint Propulsion Conference and Exhibit, Nashville, TN, USA, pp. AIAA-1992-3724.
103. Wingborg, N., Andreasson, S., de Flon, J. *et al*. (2010) Development of ADN-based Minimum Smoke Propellants, in Proceedings of the 46th AIAA/ASME/SAE/ASEE Joint Propulsion Conference Exhibit, Nashville, TN, USA, pp. AIAA2010-6586.
104. de Flon, J., Johansson, M., Liljedahl, M. *et al*. (2012) Overview of ADN propellants development, in Proceedings of the Space Propulsion 2012, Bordeaux, France, pp. SP2394088.
105. Oyumi, K.E. (1996) Insensitive munitious and combustion characteristics of GAP/AN composition propellant. *Propellant Explosives Pyrotechnics*, **121** (5), 271–276.
106. Schöyer, H.F.R., Korting, P.A.O.G., Veltmans, W.H.M. *et al*. (2000) An overview of the development of HNF and HNF-based propellants, in Proceedings of the 36th AIAA/ASME/SAE/ASEE Joint Propulsion Conference and Exhibit, Huntsville, AL, USA, pp. AIAA-2000-3184.
107. Manser, G.E. (1984) Energetic copolymers and method of making same. Patent No. US 4483978, A.
108. Manser, G.E. (1987) Nitramine oxetanes and polyethers formed therefrom. Patent No. US 4707540, A.
109. Diaz, E., Brousseau, P., Ampleman, G. and Prud'homme, R.E. (2003) Heats of combustion and formation of new energetic thermoplastic elastomers based on GAP, polyNIMMO and polyGLYN. *Propellant Explosives Pyrotechnics*, **28** (3), 101–106.
110. Powell, I. (2005) Reduced Vulnerability Minimum Smoke Propellants For Tactical Rocket Motors, in Proceedings of the 41st AIAA/ASME/SAE/ASEE Joint Propulsion Conference and Exhibit, Tucson, Arizona, USA, pp. AIAA-2005-3615.
111. Provatas, A. (2001) 'Characterisation and Polymerisation Studies of Energetic Binders', DSTO-TR-1171.
112. Leeming, W.B.H., Marshall, E., Bull, H. and Rodgers, M.J. (1996) An investigation into polyGLYN cure stability, in Proceedings of the 27th International Annual Conference of ICT, Karlsruhe, Germany, pp. 99/1–99/5.
113. Bunyan, P.F., Clements, B.W., Cunliffe, A.V. *et al*. (1997) Stability studies on end-modified polyGLYN, in Proceedings of the Insensitive Munitions and Energetic Materials Technology Symposium, Tampa, Florida, USA, pp. 1–6.
114. Cumming, A.S. (1995) Characteristics of novel United Kingdom energetic materials, in Proceedings of the International Symposium in Energetic Materials Technology, Phoenix, USA, pp. 69–74.

115. Flower, P. and Garaty, B. (1994) Characterisation of PolyNIMMO and Polyglycidyl Nitrate Energetic Binders, in Proceedings of the 25th International Annual Conference of ICT, Karlsruhe, Germany, pp. 70/71-78.
116. Shang, D.-q. and Huang, H.-y. (2010) Combustion properties of PGN/ADN propellants (chinese, abstract in english). *Hanneng Cailiao*, **18** (4), 372–376.
117. Willer, R.L. and McGrath, D.K. (1997) Clean space motor/gas generator solid propellants. Patent No. US 5591936.
118. Manser, G.E. (1983) Cationic polymerization. Patent No. US 4393199, A.
119. Oyumi, Y., Inokami, K., Yamazaki, K. and Matsumoto, K. (1994) Burning rate augmentation of BAMO based propellants. *Propellant Explosives Pyrotechnics*, **19** (4), 180.
120. Kimura, E. and Oyumi, Y. (1996) Insensitive munitions and combustion characteristics of BAMO/NMMO propellants. *Journal of Energetic Materials*, **14** (3–4), 201–215.
121. Colclough, M.E., Desai, H., Millar, R.W. *et al.* (1993) Energetic polymers as binders in composite propellants and explosives. *Polymers for Advanced Technologies*, **5**, 554–560.
122. Wardle, R.B. (1989) Method of producing thermoplastic elastomers having alternate crystalline structure for use as binders in high-energy compositions. Patent No. US 4806613, A.
123. Menke, K., Kempa, P.B., Keicher, T. *et al.* (2007) High energetic composite propellants based on AP and GAP/BAMO copolymers, in Proceedings of the 38th International Annual Conference of ICT, Karlsruhe, Germany, pp. 82/1–82/10.
124. Kawamoto, A.M., Barbieri, U., Polacco, G. *et al.* (2007) Synthesis and characterization of glycidyl azide-r-(3,3-bis(azidomethyl)oxetane) copolymers, in Proceedings of the 38th International Annual Conference of ICT, Karlsruhe, Germany, pp. 71/1–71/11.
125. Arber, A., Bagg, G., Colclough, E. *et al.* (1990) Novel Energetic Polymers Prepared Using Dinitrogen Pentoxide Chemistry, in Proceedings of the 21st International Annual Conference of ICT, Karlsruhe, Germany, pp. 3/1–3/11.
126. Licht, H.-H. and Ritter, W.B. (1996) NENA-sprengstoffe, 28th International Annual Conference of ICT, 28/21-29.
127. Mäder, P. (1997) Polymere Binder für Zukünftige Treibmittel, in Proceedings of the 28th International Annual Conference of ICT, Karlsruhe, Germany, pp. 49/41-47.
128. Bunyan, P., Cunliffe, A. and Honey, P. (1998) Plasticizers for New Energetic Binders, in Proceedings of the 29th International Annual Conference of ICT, Karlsruhe, Germany, pp. 86/1-14.
129. Drees, D., Löffel, D., Messmer, A. and Schmid, K. (1999) Synthesis and characterization of azido plasticizer. *Propellant Explosives Pyrotechnics*, **24**, 159–162.
130. Ou, Y., Chen, B., Yan, H. *et al.* (1995) Development of energetic additives for propellants in china. *Journal of Propulsion and Power*, **4**, 838–847.
131. Rindone, R.R., Huang, D.-S. and Hamel, E.E. (1996) Energetic azide plasticizer. Patent No. US 5532390, A.
132. Hamel, E.E. (1982) Research in Polynitroaliphatics for Use in Solid Propellants, in Proceedings of the Internationale Jahrestagung ICT, Karlsruhe, Germany, pp. 69–84.
133. Flanagan, J.E. and Wilson, E.R. (1990) Glycidyl azide polymer diacetate. Patent No. US 4970326, A.
134. Flanagan, J.E. and Wilson, E.R. (1990) Glycidyl azide polymer esters. Patent No. EP 0403727, A2.
135. Ampleman, G. (1992) Synthesis of a diazido terminated energetic plasticizer. Patent No. US 5124463, A.
136. Ampleman, G. (1993) Glycidyl azide polymer. Patent No. US 5256804, A.
137. Desai, H., Cunliffe, A.V., Honey, P.J. and Stewart, M.J. (1994) Synthesis and characterisation of a,w-nitrato telechelic oligomers of 3,3-(nitratomethyl)-methyl oxetane (NIMMO) and glycidyl

nitrate (GLYN), in Proceedings of the International Symposium on Energetic Materials Technology, pp. 272–301.
138. Desai, H., Cunliffe, A.V., Hamid, J. *et al*. (1996) Synthesis and characterisation of a,w-nitrato telechelic oligomers of 3,3-(nitratomethyl)-methyl oxetane (NIMMO) and glycidyl nitrate (GLYN). *Polymer*, **37**, 3461–3469.
139. Cliff, M.D. and Cunliffe, A.V. (1999) Plasticised polyGLYN binders for composite energetic materials, in Proceedings of the 29th International Annual Conference of ICT, Karlsruhe, Germany, pp. 85/1-14.
140. Hussain, F., Hojjati, M., Okamota, M. and Gorga, R.E. (2006) Review article: Polymer-matrix nanocomposites, processing, manufacturing and application: An overview. *Journal of Composite Materials*, **40** (17), 1511–1575.
141. Tonhauser, C., Wilms, D., Korth, Y. *et al*. (2010) Entanglement transition in hyperbranched polyether-polyols. *Macromolecular Rapid Communications*, **31**, 2127–2132.
142. Jenkins, A.D., Jones, R.G. and Moad, G. (2010) Terminology for reversible-deactivation radical polymerization previously called "controlled" radical or "living" radical polymerization (IUPAC Recommendations 2010). *Pure and Applied Chemistry*, **82** (2), 483–491.
143. Matyjaszewski, K. and Tsarevsky, N.V. (2009) Nanostructured functional materials prepared by atom transfer radical polymerization. *Nature Chemistry*, **1**, 276–288.
144. Hawker, C.J., Bosman, A.W. and Harth, E. (2001) New polymer synthesis by nitroxide mediated living radical polymerizations. *Chemical Reviews*, **101**, 3661–3688.
145. Moad, G., Rizzardo, E. and Thang, S.H. (2008) Radical addition-fragmentation chemistry in polymer synthesis. *Polymer*, **49**, 1079–1131.

9

The Development of Environmentally Sustainable Manufacturing Technologies for Energetic Materials

David E. Chavez

WX Division, Los Alamos National Laboratory, USA

9.1 Introduction

The development of novel and usable energetic materials has never been more difficult in the history of the field, due in large part due to the multiple restricting factors that have been placed on these materials. In addition to the standard quest of higher performing, safer energetic materials, the materials and the process to make them must not be harmful to the environment. Because energetic materials are tested and used in the open environment, these materials, their residues and the decomposition products are exposed to natural conditions. Some, such as perchlorate or RDX, can enter water systems, where they are persistent. Lead primers used in some ammunition also collect and contaminate the environment with lead, especially in areas such as shooting ranges, both military and civilian.

The manufacturing processes for preparing energetic materials are also an area where environmentally friendly methods could have a major impact on minimizing the production of hazardous waste-streams. Of particular importance is the fact that often energetic materials are produced on extremely large scales. As such, the ability to develop environmentally friendly processes to make standard energetics, or the development of novel replacement materials, could have a tremendous impact on the reduction of hazardous waste-streams attributed to energetic materials.

Green Energetic Materials, First Edition. Edited by Tore Brinck.

Rarely are energetic molecules used exactly as they are prepared. Often, the molecules are incorporated into formulations. An example of a formulation is a propellant, a pyrotechnic composition or a plastic bonded explosive. Each of these materials require some form of processing, which may or may not involve organic solvents. The development of processes that reduce the need for the use of organic solvents in formulation steps would also have an impact in reducing the amount of waste-stream created by the production of energetic materials.

When addressing the goal of sustainable manufacturing processes for energetic materials, the precursor chemicals for any process must also be taken into consideration. If a precursor chemical is available and inexpensive, yet is produced through a hazardous process or generates a hazardous waste-stream, then any production methods relying on the precursor chemical will likely not be sustainable in the long run. Thus, sustainable manufacturing of precursor chemicals is also an important aspect for the development of sustainable energetic materials technologies. Preferably, the precursor chemical would be available from renewable resources, minimizing the use of organic solvents, and having nonexistent or at least nonhazardous waste-streams.

In the United States the Strategic Environmental Research and Development Program (SERDP) [1] and the Environmental Security Technology Certification Program (ESTCP) [1] are two sources of funding looking to develop new technologies that will support the development of environmentally sustainable technologies for energetic materials. However, as the importance of this concept continues to grow, technologies are being developed throughout the world that are also contributing to the advancement of sustainable processes.

This chapter will provide some details of the development of different sustainable manufacturing technologies as they apply to explosives, propellants, pyrotechnics, and their precursor chemicals. Additionally, examples of sustainable energetic material formulation technologies will be discussed. Although process chemistry equipment and techniques, such as continuous processes and microreactor technology, are important components of the development of sustainable manufacturing processes for energetic materials, these will not be covered in detail in this chapter.

9.2 Explosives

9.2.1 Sustainable Manufacturing of Explosives

The synthesis of 3,3′diamino-4,4′azoxyfurazan (DAAF) was first reported in the literature by Solodyuk in 1981 [2]. Although DAAF was not described as an energetic material in the original publication, it was subsequently tested as an energetic material by Hiskey and coworkers [3,4]. Interestingly, DAAF displayed some very unique safety properties, yet showed impressive performance properties given its somewhat low density of 1.75 g/cm^3 under ambient conditions (Tables 9.1 and 9.2). The material was found to be insensitive to impact, spark, and friction, yet it had a shock sensitivity similar to that of HMX. Explosive materials with these types of safety and performance properties can be considered outliers when compared to conventional energetic materials. As such, the interest in the further testing of the molecule increased as did the requirement for the preparation of more material.

Table 9.1 *Explosive properties of DAAF.*

Explosive properties of DAAF
$D_v = 7.93$ km/s at $\rho = 1.685$
$P_{cj} = 306$ kbar at $\rho = 1.685$
Critical diameter <3 mm
Run to detonation distance similar to HMX
$\Delta H_f = 106$ kcal/mol
Density = 1.747 g/cm^3

Table 9.2 *Small-scale sensitivity sata for DAAF.*

Sensitivity data
DSC onset @ 220 °C (Peak exotherm @ 260 °C)
Drop weight impact = >78 J (PETN = 3.7 J)
Friction = >360 N (PETN = 80 N)
Spark TIL = 0.0625 J (PETN = 0.0625 J)

The original procedure described an oxidation of 3,4-diaminofurazan (DAF, **1**) using 96% sulfuric acid and 30% hydrogen peroxide to produce DAAF (**2**) (Scheme 9.1). Although this process could be scaled-up, the waste produced represented two significant hazards. The first hazard was that the waste-stream was highly acidic and was also strongly oxidizing. The second hazard was that the waste-stream could not be stored in sealed containers, as the hydrogen peroxide remaining continues to decompose to molecular oxygen and builds up pressure over time. In addition to the waste-stream issues, the material produced by this method contained minor quantities of varying amounts of impurities that decreased the overall thermal stability and thermal safety properties of DAAF. These impurities included 3-amino-4-nitrofurazan, 3-amino-4-nitrosofurazan and its dimer, in addition to other unidentified impurities. These impurities appeared to be occluded in the isolated product. This required a subsequent purification step that produced significant amounts of organic solvent waste-streams.

In 2010, a new process for the synthesis of DAAF was reported [5]. The oxidizer chosen to perform the oxidation of DAF was Oxone, a readily available oxidizer commonly used in the swimming pool sanitation industry. Oxone is a mixture of K_2SO_4, $KHSO_4$, and two equivalents of $KHSO_5$. When dissolved in water, the pH of the Oxone solution becomes quite acidic, but the solutions can be buffered up to slightly above neutral conditions and still maintain their oxidizing capability to a certain degree. Under conditions where no buffer was used, the results were very similar to those from the original Solodyuk method,

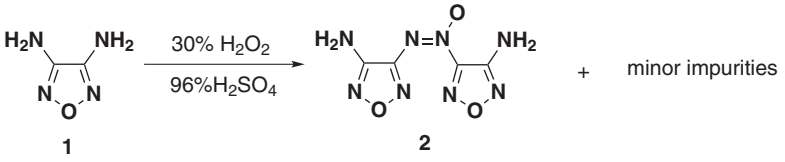

Scheme 9.1 *Original synthesis of DAAF (**2**).*

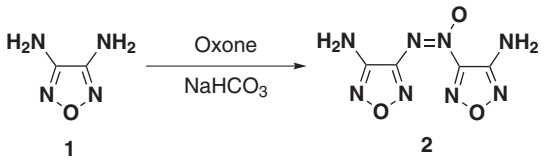

Scheme 9.2 *Oxidation of DAF using Oxone at pH = 7.*

however, as the Oxone solutions were buffered up pH 7, the results improved dramatically (Scheme 9.2). Overall, the isolated product was obtained in good yield (>80%) and in a very pure form as evidenced by the large improvements in thermal stability observed in the final product as displayed in Figure 9.1. Additionally, the particle size of the material was such that no further modification was necessary in order to proceed with subsequent performance testing and characterization.

An additional benefit to the process was that the waste-stream became nonhazardous. After isolating the product, the filtrate is essentially neutral water containing sulfate salts. Overall the process involves the use of water as the solvent, under neutral conditions, and employs an oxidizer that is used commercially on a large scale.

The Oxone method for synthesizing DAAF has also been investigated at the process scale [6]. The original batch process presented some engineering challenges that required further study. These included foaming that occurred upon neutralization on Oxone with sodium bicarbonate, heat flow management, large volumes of water, and particle size control of the product. The use of a continuous process offered several advantages over the batch process, including removal of the operator from the process, elimination of pH variations observed in the batch process, ease of heat flow management, tighter control of

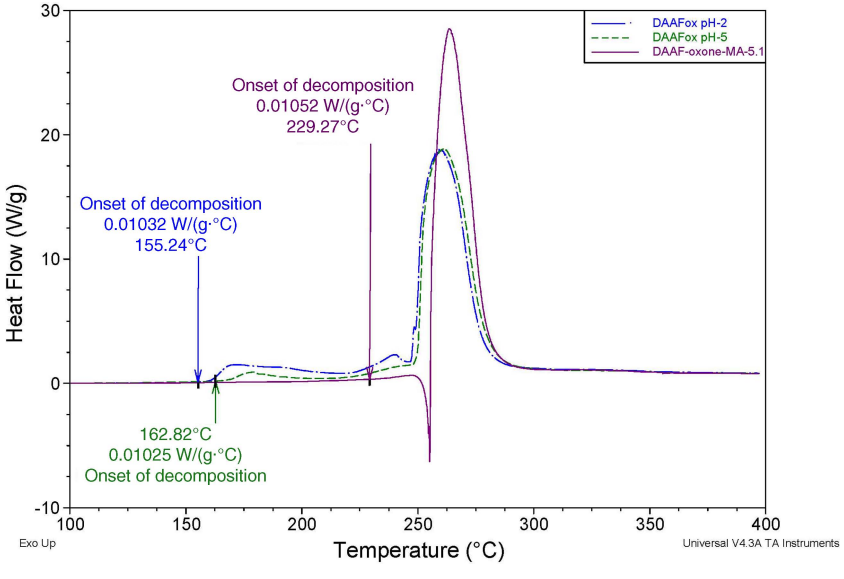

Figure 9.1 *Thermal stability of DAAF produced by Oxone at pH = 2, 5, and 7.*

particle size distribution, and providing a lower cost product. In order to develop a continuous process for the synthesis of DAAF, reactor design must take place. This effort includes the development of mixing models and kinetic models.

Tools to develop these models included Visimix and Dynochem products [7,8], as well as the use of reaction calorimetry to determine the heat flow for the process. The Visimix software allows for mixing challenges to be identified and resolved early in development. Some of the key issues that were addressed using this software were the position of the pH probe and the impeller design. Dynochem is also a software tool that uses a visualization tool to help model certain aspects of the kinetics of reactions of interest. This tool was also used for the development of the continuous process for DAAF. Overall, these tools help to create a more efficient, safe, and ecologically friendly process development for the scale-up of chemical products.

Some of the alterations investigated included the addition of reagents as solutions in water, and the use of sodium carbonate as a base rather than sodium bicarbonate. Through optimization of the continuous process, the foaming could be reduced and more product could be produced per volume of solvent used. Additionally, the pH control of the process could be controlled to a higher level and this also resulted in increased yield and reduced lot-to-lot variability. Overall, the continuous process was able to reduce the total production time by a factor of 4 compared to the original batch production process.

Another interesting aspect of Oxone chemistry is its versatility with respect to oxidation. For example, Oxone can employed in the presence of the chloride ion, which then undergoes *in situ* oxidation to become available for further oxidation chemistry on substrates [9]. This property of Oxone can be utilized in the oxidation of DAF to obtain 3,3′diamino-4,4′azofurazan (DAAzF, **3**).

DAAzF has also been described in the literature by Solodyuk [2] and Hiskey [3,4]. It is an explosive material with an excellent thermal stability (decomposes at 315 °C) and performance greater than hexanitrostilbene (HNS) (DAAzF: Detonation Velocity, 7.42 km/s, Detonation Pressure, 26.2 GPa; HNS: Detonation Velocity, 6.8 km/s, Detonation Pressure, 200 GPa). Interestingly, this material is also insensitive to impact, spark, and friction, yet displays a small failure diameter [3,4]. Unfortunately, methods to synthesize DAAzF suffer from being inefficient or require multiple steps to obtain high purity product.

By employing Oxone in the presence of sodium chloride, DAF can be oxidized to DAAzF in an efficient manner, as displayed in Scheme 9.3. The product is obtained in pure form and requires no further manipulation with respect to particle size (Chavez, D.E., unpublished results).

An interesting approach to the manufacture of environmentally friendly explosives is the development of self-remediating energetic materials. In both training situations and in live combat scenarios, unexploded ordinance (UXO) issues always arise. The energetic materials in the UXO not only present a safety hazard, but may also present an environmental

Scheme 9.3 *The synthesis of* ***3*** *using Oxone in the presence of NaCl.*

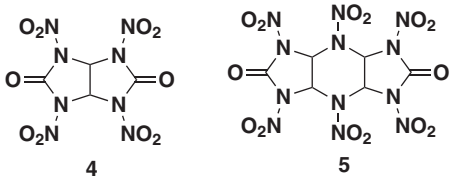

Figure 9.2 *Chemical structure of TNGU and HHTDD.*

hazard. One such energetic material is RDX. RDX is known to enter water systems such as streams or aquifers. Its natural biodegradation is very slow, yet it has moderate to high mobility in soil. The EPA limit for RDX in drinking water is 2 μg/l (ppb).

A report from 2009 describes an effort to prepare explosives for self-remediating munition charges [10]. The objective of the work was to prepare energetic materials that would undergo degradation upon exposure to environmental conditions, while remaining stable under controlled storage prior to use. An important aspect for the design of molecules to meet these requirements is that the materials must be stable enough for use, but must undergo degradation on a reasonable time-scale upon exposure to the environment.

The materials chosen for study in this report included tetranitroglycouril (TNGU, **4**) and hexanitrohexaazatricyclododecane-dione (HHTDD, **5**) (Figure 9.2). These materials are known in the literature. These materials are much more hydrolytically reactive than simple nitramines such as HMX or RDX.

TNGU and HHTDD were both exposed to a variety of different environmental conditions including moist (85% relative humidity) and dry air (28% relative humidity) as well as moist and dry soil. Under the dry air and dry soil conditions, the TNGU and HHTDD were found to degrade rather slowly. TNGU reaches half of its original concentration (t_{50}) at 240 days while the t_{50} for HHTDD was 217 days under the dry air conditions. Under the dry soil conditions, TNGU took longer to degrade ($t_{50} = 294$ days), while HHTDD degraded slightly faster ($t_{50} = 202$ days) in the dry soil experiments.

Both TNGU and HHTDD degraded much more rapidly under the moist air and soil conditions. TNGU displayed a t_{50} of 3.67 days, whereas HHTDD displayed a t_{50} of 0.95 days under the moist air conditions. In the moist soil conditions, degradation occurred to a more rapid extent (TNGU $t_{50} = 1.73$ hours, HHTDD $t_{50} = 0.384$ hours).

9.2.2 Environmentally Friendly Materials for Initiation

Environmentally friendly replacements for lead azide, lead styphnate, and mercury fulminate have been a focus of attention in the energetic materials community in recent years [11–14]. Mercury fulminate is currently banned, essentially worldwide, in commercial primers and blasting caps due to the effects it has on the environment. For example, mercury and its derivatives have negative effects on many biological systems, and are particularly toxic to warm-blooded animals. Mercury salts also have the tendency to form organomercury compounds in aquatic systems, which also present significant environmental and health problems. A significant quantity of lead is added to the environment each year from the use of lead styphnate and lead azide in primers and detonators through industrial and military applications. Lead and its compounds also pose a significant environmental threat.

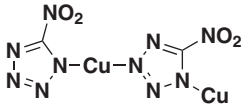

6

Figure 9.3 *The structure of DBX-1 (**4**).*

Children and young adults are particularly susceptible to lead, which can lead to mental development issues. Lead can also have an effect on the blood, bones, and sulfur containing enzymes of the human body.

Of particular interest for the replacement of lead azide in stab detonators is the copper (I) 5-nitrotetrazolate salt (**6**), known as DBX-1 (Figure 9.3). This material was developed at Pacific Scientific, Inc. and has been described as a drop in replacement for lead azide [12].

DBX-1 is made by a condensation reaction of a copper(II) salt with the sodium salt of 5-nitrotetrazolate, followed by an *in situ* reduction using ascorbic acid, to reduce the copper (II) salt to copper(I). Unfortunately, there are some drawbacks to the synthesis process. First, there is no commercially available source for sodium 5-nitrotetrazolate. Second, the literature method for the synthesis of sodium 5-nitrotetrazolate suffers from the isolation of a hazardous intermediate, which limits the utility and scale of the traditional sodium 5-nitrotetrazolate procedure. Additionally, the synthesis process for sodium 5-nitrotetrazolate produces unknown impurities that interfere with DBX-1 production and make the overall process much more complicated.

Recently, Nalas Engineering and Pacific Scientific, along with the Klapoetke group in Germany, developed a new synthesis procedure for the preparation of sodium 5-nitrotetrazolate (**8**) [15]. The researchers first identified one of the key impurities, 5-aminotetrazole (**7**), in the NaNT synthesis process that led to reproducibility problems in the synthesis of DBX-1. The researchers then removed the need to isolate the hazardous Cu(II) 5-nitrotetrazolate/5-nitrotetrazole complex, using *in situ* treatment of this complex with strong base (NaOH) to ultimately provide NaNT as a solution in water. The water could then be evaporated and the salts extracted with acetone to provide NaNT in 80% yield (Scheme 9.4). The DBX-1 produced by this method was equivalent to the DBX-1 produced

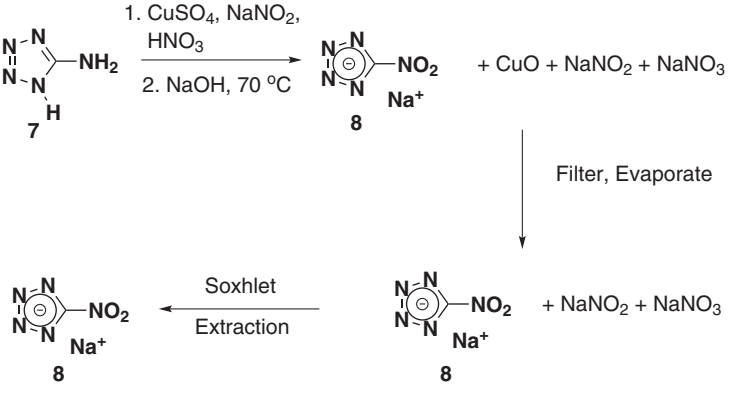

Scheme 9.4 *Improved synthesis process for NaNT.*

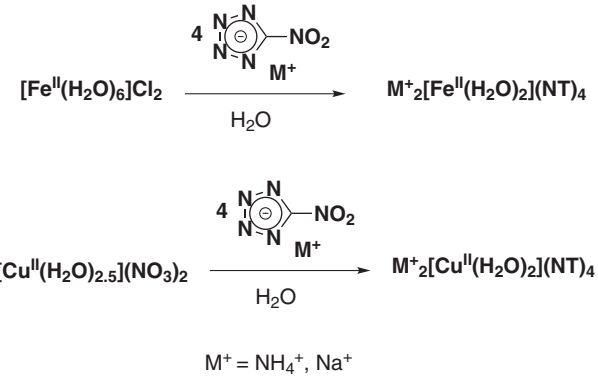

Scheme 9.5 *Synthesis of Cu(II) and Fe(II) 5-nitrotetrazolate salts.*

by the original process. Overall, the new process should allow for larger scale manufacture of DBX-1 and NaNT for future efforts at lead azide replacement applications.

With an improved synthesis of NaNT in place, other technologies dependent on NaNT could also become viable candidates as lead-free initiator type materials. One such technology was described by Huynh and coworkers in 2006 [13]. The materials developed under this project included both copper(II) and iron(II) salts containing the 5-nitrotetrazolate ion as a ligand. Both the corresponding ammonium and sodium salts were investigated (Scheme 9.5). Both the copper(II) and the iron(II) 5-nitrotetrazolate salts were isolated as the dihydrate complexes. No crystal structures have been reported for these complexes. The density of each of these materials was determined using gas pycnometry.

The ammonium and sodium salts displayed similar thermal stabilities and impact sensitivities. They differed significantly with respect to sensitivity to friction. The sodium salts displayed friction sensitivities similar to lead styphnate. All of the salts studied were insensitive to spark, whereas lead azide (LA) and lead styphnate (LS) are quite sensitive to spark initiation. The characterization data is displayed in Table 9.3.

Fronabarger and coworkers also developed a lead-free replacement for lead styphnate [16]. The compound is the potassium salt of 5,7-dinitro-[2,1,3]-benzoxadiazol-4-olate-3-oxide (KDNP) (Figure 9.4). Lead styphnate is used in a variety of applications, including bridgewire detonators, stab detonators, and percussion primers. Lead styphnate use and production both lead to lead contamination in the environment.

Table 9.3 *Characterization data for Cu(II) and Fe(II) 5-nitrotetrazolate salts.*

Explosive	DSC exo °C	Impact (cm)	Friction (g)	Spark (J)	Density (g/cm^3)	V_D (km/s)
NH_4Fe(5NT)	255	12	2800	>0.36	2.2	7.7
NaFe(5NT)	250	12	20	>0.36	2.2	N/A
NH4Cu(5NT)	265	12	500	>0.36	2.0	7.4
NaCu(5NT)	259	12	40	>0.36	2.1	N/A
LA	315	10	6	0.0047	4.8	5.5
LS	282	14	40	0.0002	3.0	5.2

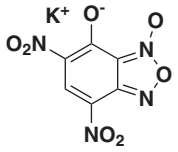

9

Figure 9.4 *The structure of KDNP.*

As a material, KDNP has good thermal stability (differential scanning calorimetry exotherm, 558 K). It is prepared using a straightforward nitration of 3-bromo-anisole, followed by treatment with potassium azide and heating. It has a crystal density of 1.945 g/cm^3. KDNP has been studied in a variety of different tests, including strong confinement testing, hot wire initiation testing, closed bomb testing, and also as a component in a number of different initiator applications. Each of these studies, when combined, lead to the conclusion that KDNP can be used as a drop-in replacement for lead styphnate. Overall, the material does not contain lead and is an improvement over the lead styphnate synthesis process with respect to environmental exposure, in terms of manufacture, use, and disposal of KDNP. Unfortunately, a potential drawback of KDNP as a lead-based primary explosive replacement in primers and detonators is the ability to function well at the low temperatures required for military implementation (−65 °F).

An additional application employing lead-based primary explosives is in primers. Lead azide, lead styphnate, lead thiocyanate, mercury fulminate, and potassium perchlorate are all components in primer compositions and each of these materials exhibits harmful environmental effects. Additionally, some compositions contain red phosphorus, which can release phosphine gas. This occurs when red phosphorus reacts with moisture and oxygen. A possible solution to the problem of elimination of these hazardous materials is through the use of metastable interstitial composites (MICs). MIC materials are essentially thermite-like materials, comprising a fuel (e.g., aluminum) and an oxidizer (e.g., molybdenum trioxide). One of the drawbacks of MIC materials in primer applications is that they do not generate sufficient volumes of gas to effect proper performance in medium caliber cartridges, especially under cold conditions [17]. An important aspect to consider regarding MIC materials is their use of nano-sized chemical particles. The environmental and occupation risk of regarding these materials has not been fully elucidated or characterized.

Seminal work done in the development of MIC-containing primers has been reported [18,19]. In 2012 a patent was granted to a technology that developed a MIC-containing electric primer [20]. Overall the invention incorporates pentaerythritol tetranitrate (PETN) with a MIC composition and gum Arabic as a binder. An anti-oxidant coating, composed of ammonium diphosphate is also used (0.5 weight percent). The use of this anti-oxidant coating was originally developed by Pusynski and Swiatkiewicz to coat nano-aluminum so that it can be processed in water-based MIC formulation processes [21]. Without the coating, the nano-aluminum is too water reactive. Organic solvents can be used, but the overall process is less environmentally friendly. Additionally, current lead-based primer processes are performed in water and any replacement technology would likely require a water-based process as well.

9.2.3 Synthesis of Explosive Precursors

Precursor chemicals for use in the manufacture of energetic materials are an important lynchpin in the development of environmentally sustainable manufacturing processes for energetic materials. If the precursor chemicals are not manufactured in a sustainable fashion, environmentally friendly energetic material processes may ultimately fail. Chemical precursors derived from renewable resources, and manufactured using sustainable methods, will continue to be highly sought after not only for the energetic materials industry, but also for the chemical industry in general for years to come.

9.2.3.1 The Use of Oxone

Oxone can be used for the chlorination of aromatic derivatives that are precursors to energetic materials. As described above, Oxone used in the presence of the chloride ion can be an effective way to promote alternative oxidation pathways involving the chlorine atom. These methods have been described in the literature [9]. Interestingly, the chlorination of aniline using Oxone and chloride ion has not been described in the literature. Chlorination of aniline (**10**) to 2,4,6-trichloroaniline (**11**) is a key step in the synthesis of 1,3,5-trichlorobenzene, a precursor in the synthesis of 1,3,5-triamino-2,4,6-trinitrobenzene (TATB, **12**).

Oxone, in the presence of chloride ion, was found to chlorinate aniline (**10**) to 2,4,6-trichloroaniline (Scheme 9.6) (Chavez, D.E., unpublished results). The reaction proceeds in acetonitrile as the solvent, but other solvents, such as methanol, can be used as well. Although, the reaction cannot be performed in water, the method is still potentially useful for the synthesis of 2,4,6-trichloroaniline. The overall benefit that makes this chlorination method environmentally sustainable, is that the source of chlorine for the chlorination reactions is a nontoxic chloride salt. Although the same transformation can be accomplished just as effectively with chlorine gas, this method suffers from the extreme reactivity and toxicity of chlorine gas.

In 2004, Frost and coworkers reported a biosynthetic pathway for the conversion of glucose (**13**) to phloroglucinol (**14**) [22], a precursor chemical for 1,3,5-triamino-2,4,6-trinitrobenzene (TATB). Phlorogluincol is present in the environment as a substituent in several natural products [23]. Frost found that *P.fluorescens* Pf-5/pME6031 produced phloroglucinol in the culture supernatants. Frost then optimized for the production of phloroglucinol through modification of *P. fluorescens* Pf-5, with the eventual use of *E. coli* JWF1(DE3)pJA3.131A as the final source of reasonable production of phloroglucinol from glucose as the starting material (Scheme 9.7). Overall the method represents an environmentally sustainable manufacturing process of an energetic material precursor from nontoxic glucose, which can be derived from plants. Subsequently, Frost and coworkers

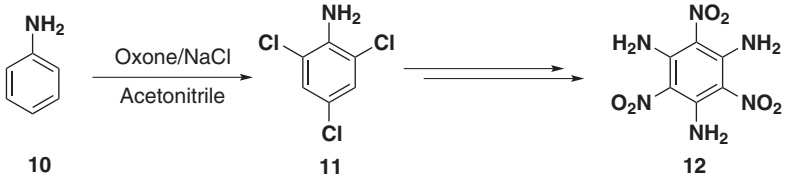

Scheme 9.6 *Chlorination of aniline using Oxone and NaCl.*

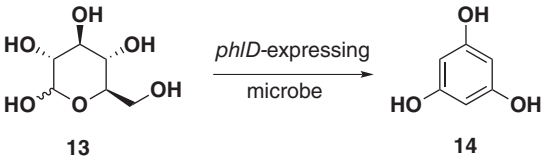

13 **14**

Scheme 9.7 *The synthesis of phloroglucinol from glucose.*

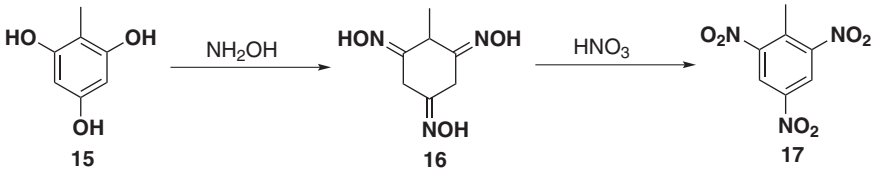

15 **16** **17**

Scheme 9.8 *Synthesis of TNT from 2,4,6-trihydroxytoluene.*

demonstrated that phloroglucinol and phloroglucinol derivatives (**15**) could be transformed to TNT (**17**) and TATB [24]. The TNT synthesis process demonstrated was claimed to be a red-water free approach to the preparation of TNT (Scheme 9.8).

Frost also developed a microbial synthesis of 1,2,4-butanetriol, a precursor chemical to the energetic material 1,2,4-butanetriol trinitrate (BTTN, **18**) (Figure 9.5) [25]. BTTN is an important ingredient in propellant compositions as it is less shock sensitive, more thermally stable, and less volatile than nitroglycerin. Unfortunately, due to the limited availability of 1,2,4-butanetriol, other sources of this chemical have been sought. The main commercial methods to produce 1,2,4-butanetriol involve borohydride reductions and generate a significant quantity of waste.

An interesting problem that is present within this particular task, is the fact that the BTTN used in propellant formulations is employed as a racemic mixture. The use of a single enantiomer of BTTN would behave differently in the propellant formulations relative to racemic BTTN. However, microbial synthesis of the BTTN precursor is likely to be selective for one enantiomer over the other, necessitating the development of microbial synthesis processes that produce both enantiomers.

Frost solved this overall problem related to stereochemistry by starting with two different starting material sources, D-xylose (**19**) and L-arabinose (**20**). In a 4 step, enzymatic process, the two starting material sugars are converted to D and L 1,2,4-butanetriol (**24**) (Scheme 9.9). Although further work is needed to optimize the process, this in another example of the application of biosynthesis to the preparation of an energetic material precursor using nontoxic and renewable starting materials in a sustainable and environmentally friendly process.

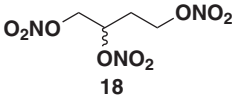

18

Figure 9.5 *The structure of BTTN.*

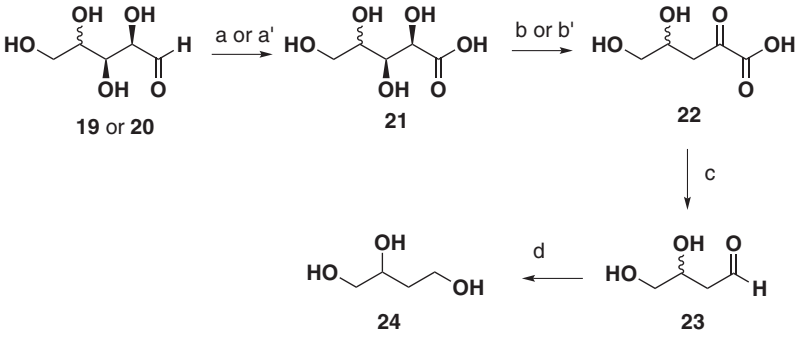

Scheme 9.9 *Biosynthesis of 1,2,4 butanetriol (a)* D*-xylose dehydrogenase (*P. fragi*); (a′)* L*-arabinose dehydrogenase (*P. fragi*); (b)* D*-xylonate dehydratase (*E. coli*); (b′)* L*-arabinonate dehydratase (*P. fragi*); (c) benzoylformate decarboxylase (*P. putida*); (d) dehydrogenase (*E. coli*).*

9.3 Pyrotechnics

9.3.1 Commercial Pyrotechnics Manufacturing

Commercial pyrotechnics used in indoor facilities must produce minimal amounts of smoke and hazardous combustion products, both to improve visual effects as well as to reduce the exposure of combustion products to audience members. In 2002, a patent by Hiskey and Naud was granted that described their efforts at producing low-smoke pyrotechnic compositions [26].

The main components of their compositions were nitrocellulose, nitroguanidine, an oxidizing agent, a flame coloring agent, and, in some cases, a metal powder. There are some key components of this patent that should be considered as applicable to the topic of this chapter. The first is that the patent claims to produce low-smoke pyrotechnics based on novel formulations. This factor is important in that the formulations are more environmentally friendly than traditional formulations. A second, and very important, factor to consider is that the patent describes a process for making the formulations that only requires water as a solvent, and no organic solvents are used in the overall processing technique. Equally important is the secondary effect of using water as the solvent for pyrotechnic formulation manufacture: the safety improvement of the manufacture of the pyrotechnic products. The water reduces the flammability issues and improves the safety of the formulations with respect to impact, spark, and friction. Finally, a water soluble binder is used in the development of the pyrotechnic formulations. One of the binders chosen is polyvinyl alcohol, which is a nonhazardous, nontoxic binder that is soluble in water and does not require organic solvents for processing.

Interestingly, all of the examples provided in the patent use ammonium perchlorate as the oxidizer and chlorine donor for flame color enhancement. However, the patent also claims that other oxidizers are just as effective, including alkali metal nitrates. Formulations employing alkali metal nitrates as the oxidizing agent would be perchlorate-free as well as having the low-smoke characteristic. This technology is currently employed to manufacture commercial low-smoke pyrotechnics on a large scale (Personal communication with M. A.

Hiskey). These devices are used in many indoor commercial pyrotechnic displays (Personal communication with M. A. Hiskey).

In 2012, a patent application was published describing a method for preparing a pyrotechnic composition and a charge [27]. The invention comprises the use of a water-soluble cellulose ether binder in pyrotechnic compositions. The method involves mixing fibrous nitrocellulose in wet form, with one or more water soluble cellulose ether binders. These binders include hydroxyethyl cellulose, hydroxypropyl cellulose, hydroxypropyl-methyl cellulose, among others.

The patent application claims that cellulose ether binders are suitable for low-smoke pyrotechnics. The patent application refers to the Hiskey patent as suffering from the use of nitroguanidine and perchlorate ingredients. The aim of the invention is to allow for a water soluble binder as the choice of solvent to dissolve the cellulose ether binders. The advantages given include the nonflammability of water, and the cheap and environmentally friendly nature of this solvent. Additionally, it was found that the residual water in the cellulose ether binders allows for the manufacture of pyrotechnic charges with desired porosity and high mechanical strength. Overall the binder concentration is typically 1–5 wt%.

In addition to the environmental friendliness of the work, the authors also claim enhancements in the safety of producing the pyrotechnic compositions. The flammability of the nitrocellulose is moderated as it is worked with while wet with water, and any risks during subsequent processing are similarly mitigated in much the same way as described by the Hiskey patent. A typical pyrotechnic composition is provided in Table 9.4. It is worth noting that a common drawback of employing nitrocellulose, despite its smokeless combustion behavior, is its long-term storage or shelf-life issues. The material tends to decompose over time to release acidic by-products. The technology presented in the patent helps to address acid generation by employing basic metal salts as the coloring agents. However, these bases will not hinder the decomposition of nitrocellulose. A future direction may be the investigation of low-smoke formulations employing more stable binders or the development of binder free formulations.

In 2012, the US Navy was granted a patent for the development of a perchlorate-free signal flare composition [28]. The composition is composed of magnesium, strontium nitrate, polyvinyl chloride, and a two-part curable binder. The binder is composed of an epoxy and a curing agent.

The compositions were used for either linear burning, 0.75 inch diameter, free-standing red signal flare candles, or as 1.2 inch diameter, linear burning red flare candles. The flares

Table 9.4 *Example pyrotechnic composition using cellulose ethers as binder.*

Component	Wt%
Fibrous nitrocellulose (13.5%N)	85
Methyl-2-hydroxyethyl cellulose	3.5
$Ba(ClO_3)_2$	4.5
$Ba(NO_3)_2$	4.5
Polyvinylchloride	2.5
Total	100

Table 9.5 *Pyrotechnic color compositions.*

Ingredient	Formulation 1 (%)	Formulation 2 (%)
Ammonium nitrate	83	
Barium 5-AT + 5-AT-HCl	6	
Nitrocellulose	11	94.8
Ammonium chloride		0.2%
Strontium 5-AT		5

produced are claimed to provide equal or superior luminous intensities, burn times, dominant wavelengths, and color purity compared to the red flares currently in use.

Another important factor in this invention is that the formulations do not appear to have a negative effect on the sensitivity properties compared to the in-service materials. Overall, these compositions have reduced potential for accidental initiation of a signal flare.

In 2010, a patent application was published describing a pyrotechnic color composition [29]. The overall goal of the invention was to reduce the environmental impact of fireworks by providing low-smoke and perchlorate-free formulations for use in large scale production of fireworks. The invention disclosure refers to prior art [26] where several new high-nitrogen, low-carbon content fuels were used to produce low-smoke pyrotechnics. The main drawback mentioned about the prior art was that the high-nitrogen materials were not commercially available, and some of the fuels were produced using toxic or environmentally problematic chemical precursors.

In order to overcome these challenges, the inventors employed 5-aminotetrazole as a potential source for preparing a variety of metal salts. Some examples of the salts prepared include the strontium and barium salts of 5-aminotetrazole(5-AT). These salts were claimed to be safe to handle, having no risk of self-combustion. The typical procedure for producing the metal salts includes treatment of 5-aminotetrazole with a metal hydroxide compound in water as the solvent.

These pyrotechnic compositions also rely on the incorporation of a chlorine donor in the formulation. The chlorine donor can include standard materials, such as polyvinyl chloride. Alternatively, the authors claim that the 5-aminotetrazole can be used as a chlorine donor source if it is first treated with hydrochloric acid, to make the 5-aminotetrazolium hydrochloride salt. A typical formulation is seen in Table 9.5. Although the authors claim the use of the hydrochloride salt of 5-AT as a chlorine donor component, it is very likely that this material is incompatible with the alkali and alkaline salts of 5-AT, through the pathway of acid/base reaction chemistry. Unfortunately, no data was given on the long-term stability of these types of formulations in the patent application disclosure.

9.3.2 Military Pyrotechnics

Over the past decade, many efforts have been undertaken to improve the environmental sustainability of pyrotechnic materials and devices manufactured for the US military. Many of these efforts have already been described in the Chapter 4 of this book, authored by Dr. Jesse Sabatini.

9.4 Propellants

9.4.1 The "Green Missile" Program

In 2001, the US completed a report on the "Green Missile" program [30]. The ultimate objective of the "Green Missile" program was the elimination of toxic/hazardous materials in solid rocket propulsion systems. The goals included lead-free castable propellants for minimum smoke systems, lead-free extrudable propellant for minimum smoke systems, complete and clean HCl-free combustion of propellants, and solventless methods for processing energetic oxidizers.

In the area of lead-free castable propellants, the US Army developed two bismuth containing compounds for replacement of the lead compounds used in solid propellant formulations for use in ballistic control. The two bismuth compounds included bismuth salicylate and bismuth citrate. Both of the bismuth compounds displayed excellent ballistic properties, burning rate, burning rate exponent, and temperature sensitivity properties (Table 9.6).

Efforts to produce lead-free extrudable propellants were also undertaken. Double-base propellants are often processed using solvent-based systems for producing cast propellants. Alternatively, a solventless extrudable process can be employed. A third method was investigated in the "Green Missile" program, which is known as the Alternative Feedstock (AF). The advantage of AF is the production of double-base propellants without the use of solvents for both extrusion and cast applications. AF uses nitrocellulose/nitrate ester formulations. The nitrocellulose used is in a plastisol form often referred to as PNC. PNC propellants are not crosslinked, which allows for more flexibility in the extrusion process.

Formulations using PNC and BTTN were developed. These formulations also used copper- or bismuth-based ballistic modifiers. Unfortunately, there are some issues that are present with these types of formulations. BTTN is significantly more expensive than nitroglycerin and PNC is also somewhat expensive due to the associated labor costs. However, there is significant interest is these types of formulation processes because they can produce a high energy, low sensitivity minimum smoke propellant. From an environmental aspect, the solventless extrusion process and lead-free ballistic modifiers make the overall process an attractive and environmentally sustainable method.

An alternative method for obtaining lead-free propellants is to use propellant ingredients that do not require lead-based ballistic modifiers. Ammonium dinitramide-based propellants do not require lead compounds for good combustion. Ammonium dinitramide (ADN) is an interesting oxidizer for many reasons, but in particular, the material is thought to be more environmentally friendly than ammonium perchlorate (AP) as it degrades naturally to

Table 9.6 *Comparison of lead-free propellant vs. state-of-the-art lead-based propellants.*

Catalyst	Bismuth salicylate	Lead citrate	Lead oxide
Burn rate	0.46	0.35	0.35
Burn rate/pressure	0.3	0.3	0.45
Density (lb/in^3)	0.0609	0.062	0.0614
Thrust (lb-sec/lb)	248	246	246
Thrust density	15.1	15.3	15.1

ammonium nitrate. One study in the "Green Missile" program found that ADN propellants displayed enhancements in burn rate. Good propellant formulations were found using both glycidyl azide polymer (GAP) and Formrez. Unfortunately, GAP/ADN formulations displayed friction sensitivities that were unacceptable. The Formrez-based formulation showed reduced friction sensitivity and promising performance.

There is also a need to find an alternative to the GAP polymer system. This system, and others like it, relies on toxic isocyanate curing agents. A SERDP statement of need was released recently calling for the elimination of these curing agents in energetic binder systems [31].

A separate study of ADN formulations was also conducted to prepare both lead-free and HCl-free combustion product formulations. This study made use of ADN and ADN/CL-20 formulations. The study found that ADN and CL-20 were compatible with each other, as evidenced by differential scanning calorimetry and vacuum thermal stability tests. Burn rate studies showed that the propellant mixes burned at 0.6–0.7 in/s at 1000 psi. These formulations did show some sensitivity to pressure that was attributed mainly to CL-20 combustion properties. Additional positive properties of these formulations included low shock sensitivity (<70 cards, NOL card gap test), good processing properties, and no pressure slope breaks.

9.4.2 Other Rocket Propellant Efforts

Aluminum is a common ingredient in rocket propellants. Often, aluminum is used in combination with strong oxidizers, such as ammonium perchlorate, to provide the propulsive energy required in applications such as solid rocket boosters. In the past decade, there has been an increase in efforts to commercially manufacture nano-sized aluminum particles. With this increase in availability of nanoaluminum has come an increase in the study of its applications in solid rocket propellants.

Nanoaluminum is generally more reactive than micron sized aluminum and this property lead to the study of its reactivity with oxidizers less reactive than perchlorates. One such oxidizer is water. Nanoaluminum, in contact with water, is oxidized to Al_2O_3 with the production of hydrogen gas. Son *et al.*, studied this process in detail to determine the viability of the manufacture of aluminum/water rockets, or more specifically, aluminum/ice rockets [32].

Nanoaluminum is known to degrade over time in the presence of water, with a shelf-life of a few weeks. However, if the water/nanoaluminum mixture is stored at −25 °C, the active aluminum content is retained for 40 days with additional data showing that the active aluminum content remained stable up to 6 months. In addition to the stability of the mixture at cold temperatures, the nanoaluminum/ice (ALICE) mixtures displayed excellent resistance to spark, impact, and shock initiation.

The ALICE mixture was subjected to burn rate measurements between 4 and 30 MPa. These studies showed that the mixture had a pressure exponent of 0.57 over the pressure range studied, with the burn rate varying from 1 to 3 cm/s over this pressure range. Additional studies included motor performance prediction, static thrust stand experiments, rocket design and launch.

The development of environmentally friendly oxidizers for use in propellants is currently of high interest in the United States. Specifically, replacements for ammonium perchlorate

are desired due to the detrimental biological and ecological effects attributed to the perchlorate anion. The most well-known and studied oxidizer that meets the requirements to replace AP is ammonium dinitramide [33]. Ammonium dinitramide is a promising oxidizer with respect to environmentally sustainability for many reasons. ADN decomposes to ammonium nitrate and N_2O over time, thus leaving behind relatively benign by-products. Secondly, ADN has excellent oxidizer capability.

ADN is often manufactured using the sulfamate process. This method involves the fuming nitric acid/sulfuric acid nitration of sulfamate. The reaction is quenched with water and neutralized with potassium hydroxide to obtain a potassium dinitramide solution that is later converted to the ammonium salt through the use of ion exchange resins. Overall, the process generates a considerable amount of waste. Recently, a more environmentally friendly process was developed for the manufacture of ADN [34,35]. This process involves quenching the reaction mixture with minimal amounts of water and obtaining the dinitramide anion by neutralization with guanyl urea. Overall, this new process makes it possible to recover high concentrations of spent acid, which was not possible using the earlier method, and this results in reduction of waste by up to 75%.

The use of solutions of ADN for use as liquid propellant replacements for hydrazine has been reported [36]. Hydrazine is a liquid propellant fuel used in many applications, however it is quite toxic. The ADN solutions often contain a fuel, such as methanol or ammonia, and outperform hydrazine-based propellants.

9.4.3 Gun Propellants

In 2006, a report was published on efforts by the US Army to develop an environmentally friendly "green" propellant for medium caliber training rounds [37]. Of the many components comprising medium caliber gun propellants, barium nitrate, dibutyl phthalate, and diphenyl amine are some of the ingredients that are particularly problematic when it comes to environmental and human exposure. Each of these materials is toxic, hazardous, and carcinogenic.

Specifically, dibutyl phthalate, a known carcinogen, is used for its plasticizer properties. During the manufacture of the gun propellant, workers are continuously exposed to this compound. Phthalates are currently under heavy scrutiny due to the REACH (Registration, Evaluation, Authorization, and Restriction of Chemical Substances) regulations in the European Union [38]. The Office of the Undersecretary of Defense has recently called for their removal, and issued a risk alert in March 2012 on phthalates [39]. Phthalates are also suspected endocrine disruptors. Diphenylamine is used as a stabilizer against nitrate ester degradation, but is a known toxin. Interestingly, diphenyl amine also contains a carcinogenic impurity, 4-aminobiphenyl, which can be absorbed through the skin or by inhalation during the propellant manufacturing process. Barium nitrate is a heavy metal compound that displays some toxicity and can cause dermatitis, as well as irritation of mucosal membranes.

In addition to worker exposure during manufacture, the environment is also exposed to these materials at testing grounds. Firing ranges can become increasingly contaminated over time. Environmental cleanup is further complicated by the hazards associated with aging propellant rounds.

The approach to solving the environmental problems associated with the gun propellant was to use a solventless propellant manufacturing process. This process relies on nitrate

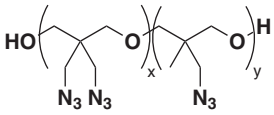

Figure 9.6 *Chemical structure of BAMO-AMMO copolymer.*

ester plasticizers, such as nitroglycerine or diethylene glycol dinitrate, in conjunction with nitrocellulose. A formulation known as PAP-8386 was developed based upon these principles. Unfortunately, the report did not describe the exact composition of the formulation. This formulation was studied using closed bomb characterization techniques, which led to the use of a deterrent coating being added to the formulation to improve the interior ballistic efficiency. The formulation was also subjected to sensitivity and compressive mechanical testing.

Overall, the PAP-8386 formulation showed promise as a propellant for medium caliber applications. The hazardous ingredients were removed from the formulation and the solventless manufacturing process eliminated the use of volatile solvents. The formulation was also superior to the JA2 formulation with respect to mechanical properties, in addition to the impact response.

A similar effort to remove diphenyl amine and barium nitrate for medium caliber gun propellants was undertaken, however this approach involved the use of energetic thermoplastic elastomers in place of nitrate ester-based formulations [40]. The overall objective of this effort was an environmentally friendly gun propellant with improved safety properties, good performance, and low cost.

One of the key characteristics of the thermoplastic elastomer approach over the nitrocellulose approach is the potential for the manufacture of advanced propellant grain geometries. Additionally, nitrocellulose-based systems often require nitrate ester plasticizers in order to obtain the appropriate mechanical properties. Unfortunately, there can be issues of plasticizer migration over time in these types of formulations. Nitrate esters also require stabilizers, whereas energetic thermoplastic elastomers do not. Additionally, energetic thermoplastics can be recycled, thus minimizing propellant waste.

The energetic thermoplastic elastomers chosen for study were based on copolymers of poly[3,3-(bisazidomethyl)oxetane] (BAMO) and poly[3-(azidomethyl)-3-(methyl)oxetane] (AMMO) (Figure 9.6) and copolymers of BAMO and glycidy-azide polymer (GAP) (Figure 9.7). The BAMO segments serve as the "hard" segments of the elastomer, while the AMMO segments serve as the "soft" segments of the polymer.

Two different propellant formulations were prepared for further study: TGD-043 (70.75% RDX, 14.625% BAMO-AMMO, 14.625% BAMO-GAP) and TGD-044 (75% RDX, 25% BAMO-AMMO). The calculated performance values of these formulations are shown in Table 9.7. Compared to traditional nitrocellulose formulations, these new

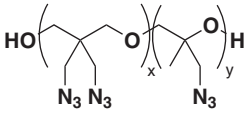

Figure 9.7 *Chemical structure of BAMO-GAP copolymer.*

Table 9.7 *Calculated performance of TGD-043 and TGD-044.*

Propellant	TGD-043	TGD-044
Caliber (mm)	25/30	25/30
Density (g/cm^3)	1.592	1.5901
Impetus (J/g)	1177	1175
Flame temperature (°K)	2800	2800
Ballistic energy (J/g)	4259	4268
25 mm charge (g)	77	77
30 mm charge (g)	122	122

Table 9.8 *Safety data for TGD-043, TGD-044.*

	TGD-043	TGD-044	044 ribbons
ABL impact (cm)	21	33	26
ABL friction (lbs)	800	800	800
ESD unconfined (J)	>8	>8	>8
SBAT onset (°F)	307	313	315
TC impact (in)	31.6	28.6	25.1
TC friction (lbs)	>64	>64	

formulations show improved performance in addition to a 16–22% reduction in propellant mass required. Maximum pressure and muzzle velocity calculation were also performed and the data show that the new formulations fell within the range required according to the military specifications MIL-PRF-71140A and MIL-P-3984J.

One of the important aspects of gun propellants is the propellant grain design. After optimization, it was determined that the best design was a colayered ribbon grain design (044 ribbons). This design includes a fast-burning component and a slow-burning component. New calculations were determined for muzzle velocity based on the colayered ribbon grain for both TGD-043 and TGD-044. The data showed that the performance was acceptable for the application.

The safety properties of the formulations were also determined and the data is displayed in Table 9.8. When compared to standard nitrocellulose-based propellants, the thermoplastic elastomer formulation showed improved safety properties. The colayered grains also showed similar safety properties compared to the propellants.

Further performance testing was completed in this project and the data showed that the TGD-044 propellant was an excellent candidate as a medium caliber gun propellant, particularly for the 25 mm M-39 application. The processing, safety, performance, and environmental properties of these propellants were very favorable.

9.5 Formulation

Formulation of energetic materials is often a key process in which a raw explosive ingredient or ingredients are mixed with inert or energetic binders to create a product for end use. Formulation technologies often require the use of an organic solvent to dissolve

the binder followed by coating of the energetic material by direct evaporation of the lacquer on the energetic particles or by crash precipitation of the lacquer onto a slurry of the energetic material. Both of these methods produce significant amounts of solvent wastes.

One new technique for preparing formulation mixes is through the use of resonance acoustic mixing. Mixers have been developed by Resodyne Acoustic Mixers, Inc. that make use of acoustic energy to mix a wide variety of materials, such as powders, pastes, and slurries [41]. This technology is capable of formulation of mixes with potential elimination of significant quantities of the organic solvents required using traditional formulation technologies.

9.6 Conclusions

The creation of novel, environmentally friendly energetic materials is only one aspect of the lifecycle that must be taken into account in the development of environmentally sustainable manufacturing technologies for energetic materials. The cost and availability of environmentally sustainable precursors is also of importance. The use of nonhazardous solvents and reagents is also a critical component. Finally, the amount and type of waste produced during a process can also have a huge impact on the sustainability of an overall process. This chapter has described several approaches aimed at the development of environmentally sustainable manufacturing technologies for energetic materials that cover each of these areas. As in other chapters of this book, most of these approaches are aimed at the removal of hazardous or toxic components in the manufacture or use of energetic materials. Examples have been taken from the three main areas of energetic material, namely explosives, propellants, and pyrotechnics.

Looking toward the future, governmental regulations will continue to become more and more restrictive, not only with respect to end product energetic materials, but also with respect to the availability and use of chemicals (solvents, precursors, reagents) required for manufacturing technologies currently in use. It is very likely that old processes will no longer be viable due to the inability to obtain or use key chemicals. A primary example of this is the manufacture of TATB in the United States. The precursor chemical required for the Benziger TATB synthesis process, 1,3,5-trichlorobenzene, is not produced domestically due to environmental concerns, necessitating a new environmentally friendly route to this compound. Challenges such as these will continue into the future. In the end, it is critical for scientists and engineers to continue to develop new environmentally sustainable processing and manufacturing technologies in order to meet the challenges of energetic material production in the future.

Acknowledgments

It is a great honor to have the opportunity to write this chapter. The invitation by Prof. Dr. Tore Brinck (KTH Royal Institute/Sweden) is gratefully acknowledged. I am indebted to Dr. Michael A. Hiskey (Univ. Colorado, Colorado Springs), Dr. Jesse Sabatini (ARDEC/USA), Dr. Jamie Neidert (AMRDEC/USA), Chris Csernica (ARDEC/USA), and Prof. Dr. Tore Brinck for providing useful and invaluable feedback on this chapter.

Abbreviations and Acronyms

ABL	Aberdeen Ballistics Lab
ADN	ammonium dinitramide
AF	alternative feedstock
ALICE	nano-aluminum/ice mixture
AMMO	3-amino-3-methyl-oxetane
5-AT	5-aminotetrazole
$Ba(ClO_3)_2$	barium chlorate
BAMO	3,3 bisazidomethyl-oxetane
$Ba(NO_3)_2$	barium nitrate
BTTN	1,2,4-butanetriol trinitrate
CL-20	2,4,6,8,10,12-hexanitro-2,4,6,8,10,12-hexaazaisowurtzitane
DAF	3,4-diaminofurazan
DAAF	3,3′diamino-4,4′azoxyfurazan
DAAzF	3,3′diamino-4,4′azoxyfurazan
DBX-1	copper (I) 5-nitrotetrazolate
DSC	differential scanning calorimetry
EPA	environmental protection agency
ESD	electrostatic discharge
ESTCP	Environmental Security Technology Certification Program
g	grams
GAP	glycidyl azide polymer
GPa	gigaPascal
HCl	Hydrogen chloride
HHTDD	hexanitrohexaazatricyclododecane-dione
HMX	octahydro-1,3,5,7-tetranitro-1,3,5,7-tetrazocine
HNS	hexanitro-stilbene
J	joules
KDNP	potassium 5,7-dinitro-[2,1,3]-benzoxadiazol-4-olate-3-oxide
$KHSO_4$	potassium hydrogen sulfate
K_2SO_4	potassium sulfate
K_2SO_5	potassium hydrogen peroxysulfate
LA	lead azide
LS	lead styphnate
MIC	metastable interstitial composite
mm	millimeter
MPa	megaPascal
N_2O	nitrous oxide
NaCl	sodium chloride
NaNT	sodium 5-nitrotetrazolate
NaOH	sodium hydroxide
NH_4^+	ammonium
NH_2OH	hydroxylamine
NOL	Naval Ordnance Laboratory
Oxone	$K_2SO_4 \cdot KHSO_4 \cdot 2KHSO_5$

PBXN-5	95% HMX, 5% fluoroelastomer
P_{CJ}	detonation pressure
PETN	pentaerythritol tetranitrate
PNC	plastisol nitrocellulose
RDX	1,3,5-trinitro-hexahydro-1,3,5-triazine
SERDP	Strategic Environmental Research and Development Program
t_{50}	half life
TATB	1,3,5-triamino-2,4,6-trinitrobenzene
TIL	threshold initiation level
TNGU	tetranitroglycouril
TNT	2,4,6-trinitrotoluene
UXO	unexploded ordnance
V_D	detonation velocity
Wt%	weight percent
ΔH_f	enthalpy of formation

References

1. www.serdp.org/ (last accessed in May 2013).
2. Solodyuk, G.D., Boldyrev, M.D., Gidaspov, B.V., and Nikolaev, V.D. (1981) Oxidation of 3,4-Diaminofurazan by some peroxide reagents. *Zhurnal Organicheskoi Khimii*, **17**, 1756.
3. Chavez, D., Hill, L., Hiskey, M., and Kinkead, S. (2000) Preparation and properties of azo- and azoxy-furazans. *Journal of Energetic Materials*, **8**, 219.
4. Hiskey, M.A., Chavez, D.E., Bishop, R.L. *et al.* (2000) US Patent 6358339.
5. Francois, E.G., Chavez, D.E., and Sandstrom, M.M. (2010) The development of a new synthesis process for 3,3′-diamino-4,4′-azoxyfurazan (DAAF). *Propellants, Explosives, Pyrotechnics*, **35**, 529.
6. Francois, E. and Hanson, K. (2013) Task 09-2-29 Insensitive explosive formulations containing diaminoazoxyfurazan (DAAF) as replacements for PBXN-7 http://www.osti.gov/scitech/biblio/1080346 (last accessed May 2013).
7. Salan, J. and Jorgensen, M. (2013) Utilizing Visimix to assist energetic materials process development http://www.visimix.com/wp-content/uploads/2011/07/VisiMix-2011-Boston-Salan-Chemical-Processing-in-the-Energetic-Community.pdf (Last accessed May 2013).
8. Hanson, K., Salan, J.S., Pearsall, A.G. *et al.* and (2011) Automated pilot plant system producing 3,3-diamino-4,4-azoxyfurazan 11th American Institute of Chemical Engineers Conference Proceedings, Particle Technology Forum.
9. Narender, N., Srinivasu, P., Kulkarni, S.J., and Raghavan, K.V. (2002) Para-selective oxychlorination of aromatic compounds using potassium chloride and Oxone. *Synthetic Communications*, **32**, 279.
10. Chapman, R.D., Quintana, R.L., Baldwin, L.C., and Hollins, R.A. (2009) Cyclic dinitroureas as self-remediating munition charges, Final Report, SERDP Project WP-1624.
11. For a review, see: Ilyushin, M.A., Tselinksy, I.V., and Shugalei, I.V. (2012) Environmentally friendly energetic materials for initiation devices. *Central European Journal of Energetic Materials*, **9**, 293.
12. Fronabarger, J.W., Williams, M.D., Sanborn, W.B. *et al.* (2011) DBX-1 – A lead free replacement for lead azide. *Propellants, Explosives, Pyrotechnics*, **11**, 36.

13. Huynh, M.H.V., Hiskey, M.A., Meyer, T.J., and Wetzler, M. (2006) Green primaries: Environmentally friendly energetic complexes. *PNAS*, **103**, 5409.
14. Huynh, M.H.V., Coburn, M.D., Meyer, T.J., and Wetzler, M. (2006) Green primary explosives: 5-Nitrotetrazolato-N^2-ferrate hierarchies. *PNAS*, **103**, 10322.
15. Klapotke, T.M., Piercey, D.G., Mehta, N. *et al.* (2013) Preparation of high purity sodium 5-nitrotetrazolate (NaNT): An essential precursor to the environmentally acceptable primary explosive, DBX-1. *Zeitschrift fur Anorganische Und Allgemeine Chemie*, **639**, 681–688.
16. Fronabarger, J.W., Williams, M.D., Sanborn, W.B. *et al.* (2011) KDNP- A lead free replacement for lead styphnate. *Propellants, Explosives, Pyrotechnics*, **36**, 459.
17. Dixon, G.P., Martin, J.A., and Thompson, D. (1998) US Patent 5717159.
18. Hirlinger, J. and Bichay, M. (2009) Demonstration of Metastable Interstitial Composites (MIC) on Small Caliber Cartridges and CAD/PAD Percussion Primers, ESTCP Project WP-200205.
19. Ellis, M. (2007) Environmentally Acceptable Medium Caliber Ammunition Percussion Primers, SERDP Project WP-1308.
20. Yalamanchili, R., Hirlinger, J., and Csernica, C. (2012) US Patent 8277585.
21. Puszynski, J. and Swiatkiewicz, J.J. (2008) Low Cost Production of Nanstructured Superthermites, SBIR Final Report, Contract No. N68939-08-C-0046.
22. Achkar, J., Xian, M., Zhao, H., and Frost, J.W. (2005) Biosynthesis of Phloroglucinol. *Journal of the American Chemical Society*, **127**, 5332.
23. Yang, F. and Cao, Y. (2012) Biosynthesis of phloroglucinol compounds in microorganisms-review. *Applied Microbiology and Biotechnology*, **93**, 487.
24. Frost, J.W. (2010) Manufacture of TATB and TNT from biosynthesized phloroglucinols, Final Report SERDP Project WP-1582.
25. Nie, W., Molefe, M.N., and Frost, J.W. (2003) Microbial synthesis of the energetic material precursor 1,2,4-butanetriol. *Journal of the American Chemical Society*, **125**, 12998.
26. Hiskey, M.A. and Naud, D.L. (2003) US Patent 6599379.
27. Van Rooijen, M.P., Webb, R., and Zebregs, M. (2012) EP2526077 A1.
28. Shortridge, R.G. and Yamamoto, C.M. (2012) US Patent 82777583 B2.
29. Van Rooijen, M.P., Webb, R., and Zevenbergen, J.F. (2010) EP2155631 A2.
30. Stanley, R., Melvin, W., McDonald, J. *et al.* (2001) Elimination of toxic materials and solvents from solid propellant components, SERDP Project PP-1058.
31. http://www.serdp.org/Funding-Opportunities/SERDP-Solicitations/SEED-SONs-FY14 (Last accessed May 2013).
32. Pourpoint, T.L., Wood, T.D., Pfeil, M.A. *et al.* (2012) Feasibility Study and demonstration of an aluminum and ice solid propellant. *International Journal of Aerospace Engineering*, Article ID 874076.
33. Nagamachi, M.Y., Oliveira, J.I.S., Kawamoto, A.M., and de Dutra, R.C.L. (2009) ADN-The new oxidizer around the corner for an environmentally friendly smokeless propellant. *Journal of Aerospace Technology and Management*, **1**, 153.
34. Skifs, H., Stenmark, H. and Thormaehlen, P. (2012) Development and scale-up of a new process for production of high purity ADN. International Conference of ICT, 43rd (Energetic Materials) 6/1-6/4, Karlsruhe, Germany.
35. Stenmark, H., Skifs, H., and Voerde, C. (2010) Environmental improvements in the dinitramide production process, International Conference of ICT, 41st (Energetic Materials: for High Performance, Insensitive Munitions and Zero Pollution) 1/1-1/5, Karlsruhe, Germany.
36. Sjoberg, P. and Skifs, H. (2009) A stable liquid monopropellant based on ADN, Proceedings of the 40th International Annual Conference of ICT, Karlsruhe, Germany.
37. Manning, T.G., Thompson, D., Ellis, M. *et al.* (2006) Environmentally friendly "green" propellant for the medium caliber training rounds, DTIC report, Accession number ADA481741.

38. http://ec.europa.eu/environment/chemicals/reach/reach_intro.htm (Last accessed May 2013).
39. https://acc.dau.mil/adl/en-US/503526/file/63081/Risk%20Alert%20for%20Phthalates%20March%202012.pdf (last accessed May 2013).
40. Cramer, M. and Akester, J. (2004) Environmentally friendly advanced gun propellants, SERDP Project PP-1363.
41. www.resodynmixers.com/ (Last accessed May 2013).

10

Electrochemical Methods for Synthesis of Energetic Materials and Remediation of Waste Water

Lynne Wallace

UNSW Canberra, University of New South Wales at the Australian Defence Force Academy, Canberra, Australia

10.1 Introduction

Electrochemistry has a great deal to offer in the creation of greener energetic materials (EMs). Electrochemical methods in general have been investigated widely for synthesis of new and existing materials, for remediation of waste from established manufacturing processes, and also for analysis of environmental samples and waste streams. While such techniques in general have so far been exploited to a relatively limited extent on the industrial scale, research continues to demonstrate the utility of the approach and to extend the possibilities for further applications of this technology [1–5].

Electrosynthesis has for many years been considered an environmentally benign methodology, embodying many of the 12 Principles of Green Chemistry [6]. The electron represents a clean and efficient reagent for direct oxidation or reduction, particularly when used instead of hazardous oxidising or reducing agents [2–4]. It has been estimated that in many cases the electron offers greater economy over chemical redox reagents, in terms of reagent cost per mole of substrate oxidised or reduced [3,4]. Control of the cell voltage can offer greater selectivity in product formation compared to conventional syntheses, and aqueous solvent systems are commonly used. Mild conditions are possible because energy supplied to the system is controlled by the applied potential or current density, rather than by the application of

Green Energetic Materials, First Edition. Edited by Tore Brinck.

heat or high pressure. In addition, different types of transformation may be possible in electrochemical reactions, which might facilitate the synthesis of a given product from an alternative feedstock or in a reduced number of steps. The electrode surface may catalyse some processes, facilitating nonstoichiometric reactions and increasing efficiency and economy. In indirect processes, a reactive intermediate is generated electrochemically and may be utilised *in situ*, eliminating the need for storage and transport of hazardous reagents.

As yet, electrosynthesis has not yet been extensively used to produce EM, aside from the well-established industrial production of perchlorate salts. However, there are several examples of laboratory-scale procedures that encompass a range of chemical transformations. Remediation methods involving electrochemistry have been used much more commonly for treating waste resulting from the manufacture and use of EM. An impressive array of both direct and indirect methods has been brought to bear on this important environmental problem, extending to pilot-scale treatment and field use. This chapter will give an overview of some of the different ways in which electrochemical methods have been utilised in the synthesis of EM, and in the remediation of wastes resulting from the manufacture and use of EM. Some more recent developments are briefly discussed, for example the use of reaction media such as ionic liquids and novel electrode materials that offer improved efficiency or economy.

10.2 Practical Aspects

There are many excellent and detailed accounts of the practical aspects of electrochemical technology, which demonstrate the importance and promise of this approach. A brief summary is presented here outlining some of the main considerations, while the reader is directed to one of these reviews for a comprehensive account of the methodology in general [2,4,7].

The simplest arrangement is a galvanic cell comprising two electrodes immersed in a conducting medium, usually an electrolyte solution, between which the current flows (Figure 10.1, left panel). Electron transfer occurs at the surface of the electrodes, reducing or oxidising the substrate(s), and further chemical transformations may then occur to form the final products. In this basic set-up, a galvanostat controls the cell current and the cell

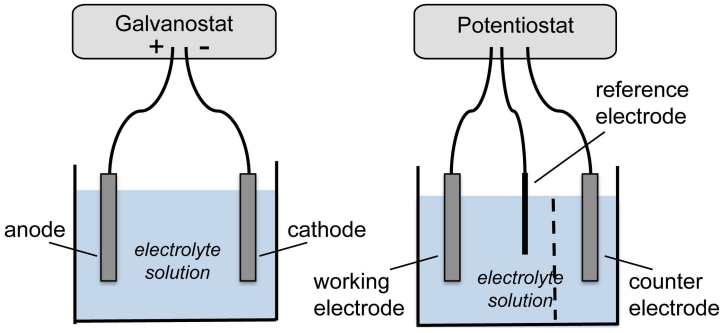

Figure 10.1 *Simple representations of (left) galvanostatic, undivided cell electrolysis and (right) potentiostatic, divided cell electrolysis.*

potential is not fixed. The electrode at which the desired reaction occurs is termed the working electrode; the other is the counter (or auxiliary) electrode. Often it is necessary to employ a divided cell, in which the electrodes are separated by a barrier to avoid interfering reactions at the counter electrode. The barrier must permit charge to pass and can take several forms, such as porous frit, salt bridge or semi-permeable membrane. In other situations an undivided cell may be used, which will have lower resistance and therefore greater energy efficiency.

The more common and useful approach in laboratory synthesis is potentiostatic electrolysis, which utilises a three-electrode system (Figure 10.1, right panel). The voltage of the working electrode is controlled relative to a reference electrode using a potentiostat. The counter electrode completes the circuit as usual, and its voltage is not controlled. This arrangement allows control over the degree of oxidation or reduction of the substrate, and hence greater selectivity. Divided or undivided cell arrangements can again be employed. For industrial scale synthesis, this set-up is usually less economical than a galvanostatic cell due to equipment cost [2].

One of the main potential problems with an electrochemical system regards mass transfer, since electron transfer occurs at the electrode surface. Reagents are transported to the electrode surface by a combination of migration, diffusion and convection [4,7], with mechanical agitation often employed to assist these processes. The larger the scale of the electrolysis, the more significant the mass transfer problems can be; however, a range of techniques have been developed to address this issue. Different electrode configurations can be employed, such as concentric electrodes and moving electrodes; and 3-dimensional electrodes (mesh, cloth, foam or packed particles) offer a large surface area for reaction. Moving bed electrodes consist of particulates that are mobilised by the flow of the electrolyte, and also offer a large surface area. The efficiency of the electrochemical process is also affected by the cell resistance, which in turn depends on factors such as the conductivity of the medium and the nature of the separator dividing cathode and anode compartments, if one is used.

Before adopting an electrochemical procedure there are many factors to be considered [7]. One important parameter is the current efficiency (CE), defined in Eq. (10.1).

$$\mathrm{CE} = \frac{\text{charge consumed in forming product}}{\text{total charge consumed}} \tag{10.1}$$

The electrode material can be critical in determining the efficiency of the reaction. Usually, cheap and robust electrodes are preferred (e.g. carbon) but in other cases more expensive materials might be preferred due to the different chemistry that might pertain. In any solvent, the limits of the potential window for electrochemical transformations are determined by the oxidation and reduction potentials of the solvent: if electrolysis of the solvent starts to occur as a side-reaction it may reduce the current efficiency of the process.

One of the main factors in aqueous media is the overpotential, that is the difference between the thermodynamically expected voltages at which water oxidation (Eq. (10.2)) or reduction (Eq. (10.3)) occurs, and the experimentally observed values.

$$2\mathrm{H_2O} \rightarrow \mathrm{O_2} + 4\mathrm{H^+} + 4\mathrm{e^-} \tag{10.2}$$

$$2\mathrm{H_2O} + 2\mathrm{e^-} \rightarrow \mathrm{H_2} + 2\mathrm{OH^-} \tag{10.3}$$

The overpotentials are strongly dependent on the electrode material, and this is related to the ability of the material to catalyse some of the steps. Thus it may be necessary to select a material with a high overpotential, to avoid water discharge. But in many other cases, reactive intermediates generated from water electrolysis may be exploited in the overall process.

10.3 Electrosynthesis

Electrosynthesis has not at this stage been used very widely in the production of EM, but the examples available do illustrate several of the approaches that are possible. Direct electrosynthesis of EM has been reported, utilising alternative feedstocks to the conventional synthetic route and even using wastewater as a precursor. Starting materials for existing procedures have been prepared by alternative electrochemical routes, and the electrosynthesis of reagents for nitration has had a major impact on synthetic strategies for EM.

In direct electrosynthesis, the desired product is prepared by electrolytic oxidation or reduction of a substrate. Usually, this is carried out in a divided cell, to avoid back reactions at the counter electrode. However, it is possible in some cases to design paired electrosyntheses, in which the processes at both electrodes contribute to the formation of the final product. These processes offer greater efficiency and economy, and contribute to the green nature of the synthesis [2]. Indirect, or mediated, electrosynthesis involves the generation of a reactive species within the cell that acts as a redox catalyst.

10.3.1 Electrosynthesis of EM and EM Precursors

Nitroorganic compounds feature extensively in the current range of EM. A variety of products are possible upon electrochemical reduction of nitroorganics, depending upon the particular substrate and on parameters such as applied potential, solution pH and electrode material [8]. Nitroso compounds, hydroxylamines and amines may be formed, and bimolecular coupling of initial electrode products (nitroso and hydroxylamine) can produce azoxy, azo and hydrazo derivatives (Figure 10.2).

A recent example is the laboratory electrosynthesis of the high-nitrogen compound azoxytriazolone (AZTO) by reductive electrolysis of aqueous acidic solutions of nitrotriazolone (NTO), in a divided cell [9]. High-nitrogen compounds are themselves considered to be green [10,11]. These materials contain a higher proportion of nitrogen by mass, compared to conventional explosives, and they derive their energy output from this factor, rather than via the oxidation of fuel elements (carbon, hydrogen) by oxygen. Nitrogen gas (N_2) is the major product of explosion, so high-nitrogen compounds burn more cleanly than other organic explosives.

In the case of NTO, the coupling is very efficient and AZTO precipitates in good yield, leaving the solution phase largely free of organic material (Figure 10.3, reaction 1). Further electrochemical reduction of AZTO under aqueous alkaline conditions (Figure 10.3, reaction 2) gives azotriazolone (azoTO), which has greater thermal stability but is slightly less energetic than AZTO.

The starting material NTO is itself an insensitive high explosive (IHE) with potential as a replacement for RDX in some applications, but its high water solubility poses challenges in

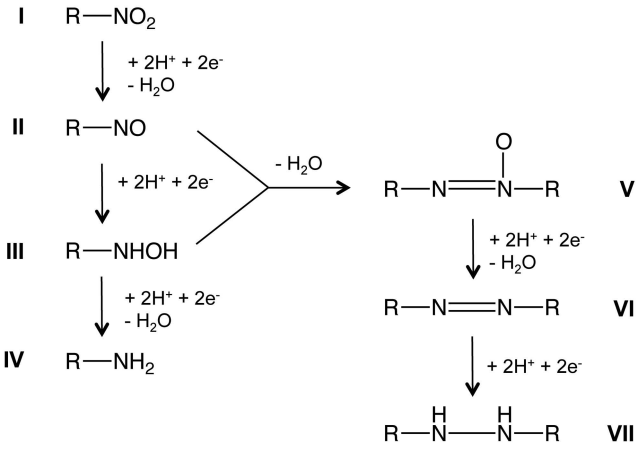

Figure 10.2 *Possible products formed upon reduction of nitroaromatic compounds (I) include nitroso (II), hydroxylamine (III), amine (IV), azoxy (V), azo (VI) and hydrazo (VII) derivatives.*

the treatment of manufacturing wastewater. The electrochemical conversion to insoluble AZTO may therefore represent an economical solution to this problem, as well as creating a new green energetic material. This reaction also demonstrates the different reactivity that can be obtained using electrochemistry, since chemical reduction of NTO gives aminotriazolone as the product instead of AZTO [9].

Since many azo and azoxy compounds have been investigated for their potential as EM [12–15], this electrochemical approach might prove very useful in the synthesis of these materials. However, the yield of the electrosynthesis depends on the propensity of the initial reduction products to undergo coupling: under similar conditions to NTO bulk electroreduction, 3-nitrotriazole formed only a little azo- and azoxytriazole, with the major product being hydroxylaminotriazole [9].

Hexanitrostilbene (HNS) is traditionally prepared by oxidative coupling of trinitrotoluene (TNT) in organic solvent, using NaOCl [16]. Although the yield is low (40%), this is still considered to be the most economical route [17]. Much improved yields of HNS were reported via isolation of the intermediate 2,2′,4,4′,6,6′-hexanitrobibenzyl (HNBB), followed by chemical oxidation to HNS [18]. A number of oxidising agents were tested, with yields ranging from 0–92%; however it was later demonstrated that this latter oxidation could be carried out electrochemically (Figure 10.3, reaction 3). Oxidative electrolysis of HNBB in dimethylsulfoxide (DMSO) generated HNS in near quantitative yield [19], although the product was not isolated from solution. The potential for scale-up was considered, with several suggestions offered for improving the cost efficiency of the electrochemical procedure.

The feasibility of electrosynthesis of another azo explosive, hexanitroazobenzene (HNAB) has also been considered [20]. Evidence was presented for the electrochemical oxidation of hexanitrohydrazobenzene (HNHB) in DMSO to generate HNAB, though again this species was not isolated from solution. HNAB is normally prepared from

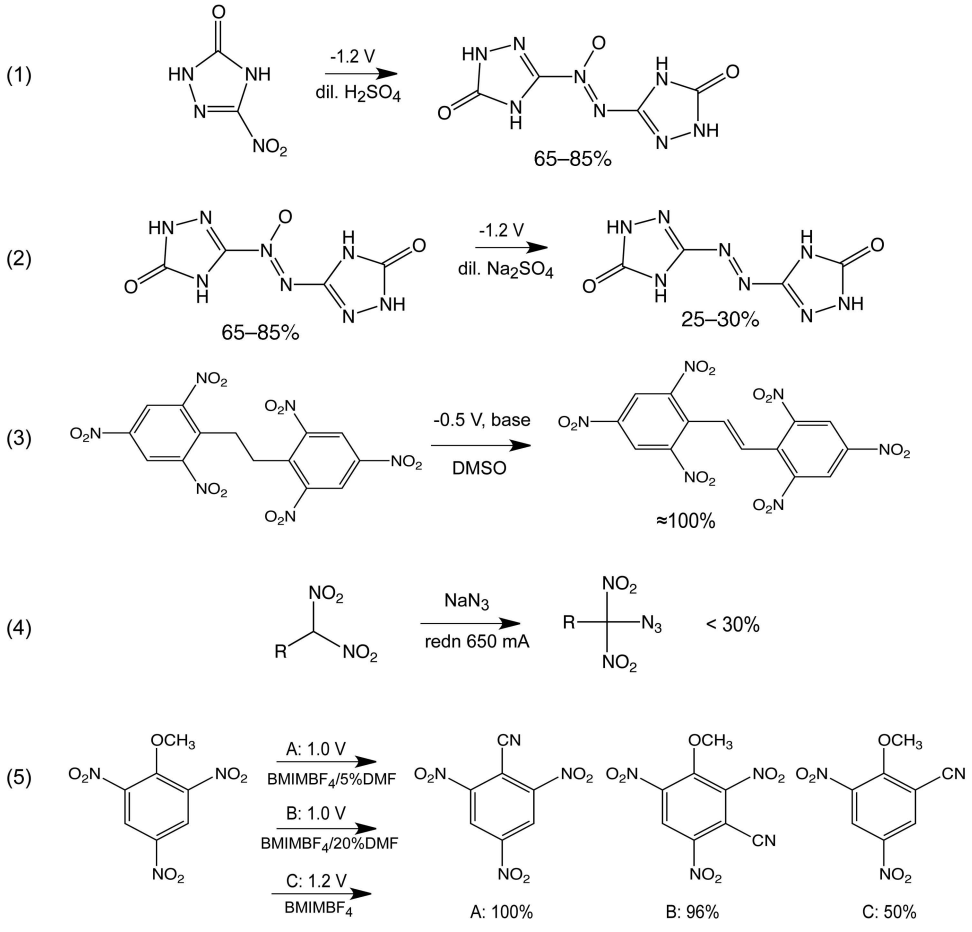

Figure 10.3 *Electrochemical synthesis of some organic EM.*

dinitrochlorobenzene and hydrazine to give tetranitrohydrazobenzene, which is then simultaneously oxidised and further nitrated with mixed acids [21]. HNHB, an alternative feedstock, can be obtained from picryl chloride and hydrazine [22], though the comparative toxicity and availability of these starting materials would need to be considered when assessing for overall environmental impact.

Azidodinitroalkanes, reported to be useful in propellant compositions, can be prepared by galvanostatic oxidation of 1,1-dinitroalkanes in aqueous solution, in the presence of sodium azide (Figure 10.3, reaction 4) [23]. A divided cell was used, and yields were low (<30%). This work was later extended to the preparation of alcohol and ester derivatives [24].

Electrochemical synthesis has generally been more common in the preparation of inorganic compounds, and there are several examples of industrial-scale procedures for inorganics. Perchlorate salts, used extensively in propellants and pyrotechnics, are prepared industrially via a series of electrochemical steps based on the chlor-alkali process [4]. The chlor-alkali process is one of the most significant industrial electrochemical processes, in

which brine is electrolysed to produce sodium hydroxide at the cathode and chlorine at the anode (Eq. (10.4)).

$$2NaCl + 2H_2O \rightarrow 2NaOH + H_2 + Cl_2 \tag{10.4}$$

A membrane usually separates the anode and cathode compartments, to prevent reaction of chlorine with hydroxide ion. If the membrane is removed, a disproportionation reaction occurs and sodium hypochlorite is produced (Eq. (10.5)); at higher cell temperatures, sodium chlorate can be formed instead (Eq. (10.6)). Sodium perchlorate is then obtained by anodic oxidation of sodium chlorate (Eq. (10.7)).

$$2NaOH + Cl_2 \rightarrow NaCl + NaOCl + H_2O \tag{10.5}$$

$$6NaOH + 3Cl_2 \rightarrow NaClO_3 + 5NaCl + 3H_2O \tag{10.6}$$

$$NaClO_3 + H_2O \rightarrow NaClO_4 + 2H^+ + 2e^- \tag{10.7}$$

From sodium perchlorate a range of other perchlorate salts are prepared, including ammonium perchlorate, which is used extensively as a rocket propellant. Other perchlorate salts are employed in pyrotechnic formulations. The apparatus and conditions for the chlor-alkali process have been modified over the years, incorporating advances that improve efficiency and reduce environmental impact [5].

Another large-scale electrosynthesis was reported for the liquid propellant ingredient hydroxylammonium nitrate (HAN). Reductive electrolysis of nitric acid in a divided cell gave the desired product in one step and in high purity (Eq. (10.8)), and the pilot plant was able to generate the product safely and reliably at the rate of 70 000 kg/year [25].

$$2HNO_3 + 6H^+ + 6e^- \rightarrow NH_3OH \cdot NO_3 + 2H_2O \tag{10.8}$$

Some precursor materials used in EM synthesis have been prepared electrochemically. For example mannitol, subsequently nitrated to give the explosive hexanitromannitol, was previously prepared from sugars (dextrose) via electroreduction [26], though this process is now obsolete. Now, advances in technology and understanding have led to a new wave in electrochemical synthesis, and further processes have been introduced or are in testing in pilot plants. Ethylene glycol, used to prepare ethylene glycol dinitrate (EGDN), can be prepared by electrolysis of formaldehyde in a process that offers several advantages over the traditional method, including the use of an alternative and less hazardous feedstock, in formaldehyde [5]. EGDN is prepared industrially from ethylene oxide, a highly toxic and flammable compound, but pilot-scale production via the cleaner electrosynthetic route has been trialled.

10.3.2 Electrosynthesis of Useful Reagents

A widely used electrochemical method in EM synthesis has been the generation of N_2O_5 for use in nitration. N_2O_5 has been shown to be a versatile and relatively benign nitrating agent, and is considered to be a greener alternative to mixed acids in some situations [27,28]. In organic solvents, N_2O_5 is a mild, selective nitrating agent, while the N_2O_5/HNO_3 system has

similar nitrating power to mixed acids but without the disadvantage of containing sulfuric acid. Thus, nitration by N_2O_5/HNO_3 can be used to prepare substrates such as nitramines, which are sensitive to decomposition by sulfuric acid.

N_2O_5 can be generated via oxidation of N_2O_4 in nitric acid [29] and the reactions at the anode and cathode are shown below (Eqs. (10.9)–(10.11)):

$$\text{Anode:} \quad N_2O_4 + 2HNO_3 \rightarrow 2N_2O_5 + 2H^+ + 2e^- \tag{10.9}$$

$$\text{Cathode:} \quad 2HNO_3 + 2H^+ + 2e^- \rightarrow N_2O_4 + 2H_2O \tag{10.10}$$

$$\text{Overall:} \quad 4HNO_3 \rightarrow 2N_2O_5 + 2H_2O \tag{10.11}$$

The N_2O_4 generated at the cathode can be recycled into the anode compartment to improve overall efficiency. N_2O_5/HNO_3 solutions can be prepared in a range of concentrations and can be stored indefinitely below 0 °C [30].

Nitration with N_2O_5/HNO_3 has been used to prepare several explosives, mainly nitramines such as RDX and HMX [28,30]. Higher yields can be obtained compared to conventional nitration methods, and by-products are often reduced or eliminated. For example, in the industrial synthesis of HMX from hexamethylenetetramine, the desired product is formed only in moderate yield, and RDX is produced in higher quantities. Separation of the two is difficult. However, using N_2O_5 either material can be prepared without formation of the other, greatly aiding purification.

N_2O_5 can also be prepared by oxidation of N_2O_4 with ozone, and this method has typically been used to prepare the solid material to be used in organic solvents. However, methods have also been developed for extraction of pure N_2O_5 from the nitric acid mixture [31]. In this way, the electrochemical synthesis could form the basis of either reagent system: the powerful, unselective N_2O_5/HNO_3 mixture; or the mild, selective N_2O_5/organic solvent system. An assessment of the relative production costs has been carried out [27] and this analysis predicted that for relatively small-scale production, the ozonation process would be more economical, due partly to the cost of extracting N_2O_5 from nitric acid. But for large-scale production (upwards of ≈100 tonnes/year), the much lower cost of the nitric acid feedstock for electrolysis, compared to N_2O_4 for ozonation, made the electrolytic method the preferred option.

Many more novel and improved syntheses have been reported that involve the use of N_2O_5 in organic solvents, and a great number of EM have been prepared in this way [27,28]. A cleaner synthesis of TNT was reported, via nitration of toluene using N_2O_5 in dichloromethane, which limits the formation of unsymmetrical TNT isomers to less than 2%. These by-products must normally be removed via a sulfitation process that generates the notorious red water waste from TNT production, but it is possible that this step could be eliminated in the N_2O_5 process [32].

10.4 Electrochemical Remediation

For EM, electrochemical methods have more commonly been applied in the remediation of waste and environmental residues. Remediation is a significant issue for the EM industry [33], and a great deal of research has been carried out into methods for the treatment or

recycling of manufacturing waste; and for the decontamination of polluted environments resulting from testing and use of EM. Most EM are toxic to at least some degree, and many are slow to degrade in the environment, so that the contaminants persist or accumulate in soil and groundwater. For munitions wastewater, three major components are RDX, TNT and dinitrotoluene (DNT) [34], and much of the reported work focuses on these species. DNT in particular is highly toxic and carcinogenic. In addition, soil and groundwater can become contaminated with EM residues following leaching from waste storage pits or via field use in testing ranges. The main EM wastes that have been under research are:

1. Spent nitrating acid.
2. Wastewater from washing.
3. Red and pink water from TNT production.
4. Contaminated soil and groundwater.

Many electrochemical techniques are available for remediation of both organic and inorganic pollutants [1,35–38]. As in any remediation technique, pollutants can be removed by different means: complete degradation to innocuous materials; transformation to less toxic species or species that are more amenable to further treatment; or conversion to different physical forms (e.g. solids) that may be more easily removed. Relevant parameters for assessing the efficiency of the remediation process include the current efficiency, percentage removal of the target pollutant and the total organic carbon content (TOC) or chemical oxygen demand (COD) of the waste.

Direct electrochemical remediation involves either cathodic reduction or anodic oxidation of the target (or both, in an undivided cell), while indirect methods involve *in situ* electrogeneration of an active redox agent that acts upon the target. Both approaches have been used in the treatment of EM waste. Many laboratory-scale studies have been reported, and in some cases pilot plant and field-scale treatments have also been carried out. In several cases the electrochemical methods have been found superior to existing treatments such as incineration.

10.4.1 Direct Electrolysis

This is effective for substrates that can undergo relatively facile oxidation or reduction within the solvent window. The majority of treatment methods based on direct electrochemical transformations have tended to involve cathodic reduction, since the nitro compounds that are the main pollutants are highly oxidised species. In other cases, a combination of reduction and oxidation (either sequentially or simultaneously) has been applied.

10.4.1.1 Cathodic Reduction

In the case of nitroaromatic compounds, such as TNT and DNT, cathodic reduction generally converts the nitro to the corresponding amine derivatives (see Figure 10.2). The aromatic amines, although often still toxic, are more susceptible to further degradation than the parent nitro compounds which are usually quite resistant to aerobic biodegradation [33].

Rodgers and Bunce [39] showed that in acidic solution DNT is reduced to diaminotoluene, with hydroxylamines and aminonitrotoluenes observed as intermediates. Various solid azoxy compounds were also formed in the later stages of electrolysis, but this took place by aerial oxidation of the aminotoluene products rather than via an electrochemical

transformation. Complete reduction of TNT proved to be more difficult, as triaminotoluene (TAT) represented a minor product regardless of electrolysis time, but 80% reduction of TNT (to aminonitrotoluenes) was still achieved within 2.5 h. These authors suggested a combined reduction–oxidation approach for treatment of wastewater containing these nitrotoluenes, based on oxidation of resulting amino derivatives to insoluble oligomers in the same cell as the reduction occurred. Electrochemical oxidation was found to be more efficient for removal of the amino compounds than either aerial or enzymatic oxidation, and it was also estimated to be more economical.

Reactors based on the reduction of EM have been trialled at bench scale and pilot scale. Simulated munitions wastewater, containing TNT, DNT and RDX, was treated in a divided cell, demonstrating that all three contaminants could be converted effectively [40]. This process was then scaled up for DNT, in pilot-scale reactors that were trialled in batch mode and flow-through mode [34]. A molar balance of 100% was achieved; 80% of the product comprised solid azoxy species, with around 20% of aminotoluenes remaining in solution. The flow-through reactor was able to maintain an 80% level of reduction of DNT over 14 days, before cleaning was required to remove the solids. A bench-scale reactor for TNT [41] employed the same approach, but with sodium sulfite added to the solution to help maintain oxygen-free conditions. This largely prevented aerobic oxidation, and TAT was the only solution phase product observed.

For aliphatic nitro compounds, such as nitramines and nitrate esters, cathodic reduction is more likely to result in degradation. Bonin *et al*. [42] showed that RDX is readily decomposed to small molecules upon galvanostatic reduction in acetonitrile/water solutions. A flow-through divided cell reactor was employed, with a membrane as separator between anode and cathode, and the test solution was passed through several times until the substrate was consumed.

FOX-7 (1,1-diamino-2,2-dinitroethene) undergoes degradation upon bulk electrochemical reduction in aqueous media, forming ammonium and nitrate ions as the main solution products, plus gases [43]. This was not reported specifically as a remediation technique, but serves to illustrate that bulk electrolysis may give products different to those observed analytically (analytical electrochemistry indicated that 1,2-diaminoethane was the reduction product under these conditions, but in bulk electrolysis a different mechanism operated and degradation occurred). Nitroglycerine and other nitrate esters have also been converted via electrochemical reduction in aqueous media [44]. The reduction occurred with elimination of nitrite ions, forming the corresponding alcohols.

Cathodic reduction has been used to recover lead from lead azide, commonly used in detonators. During electrolysis of aqueous alkaline solutions of lead azide at around 80 °C, lead metal is deposited on the cathode with high electrical efficiency [45]. In large-scale (18 gallon) tests, 97% recovery of lead was achieved, and the reagent cost was estimated at only one-tenth that of standard chemical disposal methods.

10.4.1.2 Combined Reduction and Oxidation

While cathodic reduction may be effective in transforming nitro compounds, it often does not eliminate all toxic organics. An approach that combines oxidation and reduction can often be more effective, since organic compounds remaining after reduction might be decomposed upon oxidation.

An approach of sequential oxidative and reductive electrolysis has been applied to aqueous phase energetic compounds, in a method applicable to *in situ* remediation of groundwater [46]. The contaminated water flowed through a series of sand columns equipped with electrodes, and was subjected to alternate oxidative and reductive applied potentials. Under a positive–negative sequence (oxidation–reduction) 97% TNT removal and 93% RDX removal was achieved. As well as direct redox processes, oxidation by electrogenerated intermediates and alkaline hydrolysis were thought to contribute to the process. Later work on the electrolytic degradation of RDX in sand columns demonstrated that most degradation (75%) occurred in the vicinity of the cathode, while alkaline hydrolysis accounted for a further 23% in the area between the electrodes [47].

Red water is one of the most problematic waste-streams resulting from EM manufacture. It is produced during the purification of TNT and contains many different species, including nitroaromatic compounds and their soluble sulfonate salts. The organic content is considered to be high, at around 8%, and the COD can reach 120 000 mg/L [48]. Li *et al*. reported on an electrochemical method for treatment of red water [48]. A divided cell was used, in which batches of diluted red water (COD = 1300 mg/L) were electrolysed using various electrodes and with either an anion- or a cation-exchange membrane separating the anode and cathode compartments. The COD of both anolyte and catholyte was then determined. In the optimum conditions, 99% colour removal was achieved in 6 h, and 52% reduction in COD was found for the anolyte. Addition of a small amount of hydrogen peroxide to the cell improved the efficiency, so that a lower cell voltage (3 V) could be used to achieve the same COD removal efficiency. It was proposed that the pollutants are oxidised by a combination of direct anodic oxidation and indirect oxidation by electrochemically-generated oxidants such as hydroxyl radicals (see below).

10.4.1.3 Anodic Oxidation

For organic materials, direct oxidation very often leads to mineralisation of the substrate; that is breakdown into inorganic materials. This approach has therefore been used successfully in many instances for remediation of organic pollutants.

NTO can be completely mineralised, even in very high concentrations (up to 6 g/L), by anodic oxidation in acidic aqueous solution [49]. As mentioned above, NTO has very high water solubility of up to 15 g/L at 20 °C, which causes problems in treatment of the wastewater by conventional methods such as carbon filters. However, controlled potential electrolysis in a divided cell caused complete degradation of NTO, with ammonium and nitrate ions as the only solution products. All carbon was discharged as gas (CO_2, CO) at the working electrode.

However, many other nitro-organics are quite resistant to direct oxidation, due to their highly oxidised nature, and in this case it is usually more effective to employ indirect oxidative methods.

10.4.2 Indirect Electrolytic Methods

In this approach the active redox agent is generated electrochemically and this then reacts with the substrate. Most commonly, strong oxidising agents such as hydrogen peroxide or the hydroxyl radical are generated; these particular electrochemical methods therefore constitute one of the Advanced Oxidation Processes (AOPs) that are used widely for

mineralisation of organic pollutants [50,51]. AOPs are particularly useful for the treatment of recalcitrant organic wastes that are not easily degraded by conventional methods. Other non-electrochemical methods of generating peroxide/hydroxyl radicals include UV photolysis, TiO_2-catalysed photodegradation, Fenton's reagent, ozonation and sonolysis [51]. A recent review covered the application of AOPs in general for the removal of TNT [50]. Active oxidising species that can be electrogenerated include hydrogen peroxide, hypochlorite, chlorine, ozone and hydroxyl radical [37].

H_2O_2 can be formed by cathodic reduction of dissolved O_2 gas in acidic solution (Eq. (10.12)). This process takes place more easily ($E^0 = 0.70$ V vs. standard hydrogen electrode; SHE) than reduction of O_2 to water in the same medium ($E^0 = 1.23$ V vs. SHE).

$$O_2 + 2H^+ + 2e^- \rightarrow H_2O_2 \tag{10.12}$$

Hydrogen peroxide is a moderate oxidising agent, and may itself act upon some organic pollutants. A much more powerful oxidising agent is the hydroxyl radical, and this may be formed on the anode (A) during oxidation of water (Eq. (10.13)):

$$A + H_2O \rightarrow A\text{-}OH^{\bullet} + H^+ + e^- \tag{10.13}$$

The extent to which adsorbed hydroxyl radical is formed depends on the anode material. Anodes having a high overpotential for oxygen discharge tend to promote the formation of adsorbed hydroxyl radicals; thus organic species are more likely to undergo complete (unselective) oxidation to CO_2 on these anodes. On anodes with low oxygen overpotential, selective oxidation of organics is more likely [37].

Indirect electrochemical oxidation of several nitramine explosives has been demonstrated [52]. RDX, HMX and CL-20 were completely degraded to small molecules in aqueous solution, via galvanostatic oxidation on boron-doped diamond electrodes. These electrodes offer a wide potential window and electro-active species such as hydroxyl radical are generated efficiently at the surface. More recently, electrogenerated hydrogen peroxide has been used to degrade several different nitroaromatics, present in spent acid from nitration of toluene [53]. DNT isomers and TNT were completely mineralised via electrolysis in an undivided cell on platinum electrodes. At the highest electrode potential used, TOC was reduced to almost zero in 12 hours, with the main products being carbon dioxide, nitrate ion and water.

Indirect electrochemical methods can be augmented with other treatments, including photolysis, ultrasound and biodegradation. A method for degradation of TNT in aqueous acidic solution has been reported, based on a hybrid approach combining electrogenerated hydrogen peroxide and enzymatic degradation [54]. In other work, electrochemical degradation of dinitrobenzene and DNT was enhanced by application of ultrasound and ozone [55]. Wastewater from RDX manufacture has been subjected to electrocatalytic degradation as a pre-treatment for biodegradation [56]. This work showed that the biodegradability of the wastewater was greatly improved following electrolysis.

One of the most widely used electrochemical remediation technologies is the electro-Fenton (EF) method. The traditional Fenton's reagent consists of hydrogen peroxide in the presence of a ferrous salt, and has been used in the treatment of a very wide range of

chemical species and industrial wastes, including some energetic materials such as nitramines [57–59], nitroaromatics [58,59], NTO [60], and TNT wastewater [61] and pink water [62]. The reagent system generates several active chemical oxidants, including the hydroxyl radicals and complexes of the ferric ion. Hydroxyl radicals, more strongly oxidising than hydrogen peroxide, are formed by reaction of hydrogen peroxide with the ferrous ion (Fenton's reaction, Eq. (10.14))

$$Fe^{2+} + H_2O_2 \rightarrow Fe^{3+} + OH^- + HO^{\bullet} \tag{10.14}$$

At optimum pH, regeneration of Fe^{2+} occurs via interaction of Fe^{3+} with intermediates such as peroxy and superoxide radicals, and the process can become catalytic.

In the EF method, hydrogen peroxide is generated electrochemically via reduction of oxygen gas (Eq. (10.12)). In addition, Fe^{2+} is continuously regenerated at the cathode. Oxygen is usually introduced directly at the cathode for conversion into hydrogen peroxide. In a divided cell, hydroxyl radicals generated at appropriate anodes may also contribute to the degradation of organics [35]. With oxidants being generated at both electrodes, this 'paired electrocatalysis' approach may significantly increase electrical efficiency.

The EF method offers several advantages over the traditional Fenton reaction that are relevant to green chemistry. Hydrogen peroxide, a hazardous reagent, is produced *in situ* so that the need for transport and storage is eliminated. The electrochemical regeneration of the ferrous ion reduces reagent requirements – one study has shown that the EF method required one-fifth of the amount of iron to react with the same quantity of hydrogen peroxide as traditional Fenton [63] – and also increases the rate of degradation of organics [63,64]. The EF method has been very widely applied to industrial wastewaters [35,65].

Spent acid from TNT manufacture, which contains mainly DNT isomers, has been treated by an EF laboratory method [66]. Under best conditions, near complete removal of TOC was achieved. Importantly, the overall process resulted in a reduction of the water content and an increase in sulfuric acid concentration of the spent acid, thus it may allow recycling of this problematic waste. The same method was also applied to wastewater from the purification stages of nitrotoluene manufacture [67]. After 5 h, TOC removal was 100% complete at 303 K but only around 50% complete at 343 K, attributed to lower solubility of O_2 at the higher temperature.

Ayoub *et al*. [68] also studied the EF process for removal of TNT, in a cell utilising a carbon felt cathode and platinum anode. This work showed that TNT was completely removed within 20 min, with the formation of multiple aromatic intermediates. Many of these appeared to be formed via direct cathodic reduction processes. Further degradation to short-chain carboxylic acids occurred, and after 12 h the TOC had been reduced by over 90%, though residual organic species remained.

Other remediation techniques can be been used in conjunction with EF to increase the rate or extent of the degradation. For example, EF has been combined with UV photolysis (photo-assisted EF) and heterogeneous photocatalysis [35], and zero-valent iron [69]. It has been noted that approaches incorporating photolysis could become very cost-effective if a solar light source were to be utilised [70], and particularly so if solar energy could be used to provide the cell current as well. Several pilot-scale operations based on EF have been reported; for example, a combined process based on EF and sunlight exposure gave almost complete mineralisation of aromatic pollutants, including nitrobenzene [71].

10.4.3 Electrokinetic Remediation of Soils

One of the most promising electrochemical technologies for treatment of pollutants is electrokinetic remediation of contaminated soil [72–74]. This is a significant issue for EM, as there are many manufacturing sites and military training areas that have become heavily polluted with hazardous residues [33]. The electrokinetic method is included on the United States Environmental Protection Agency (US EPA) list of remediation technologies [75] and has been applied successfully to soils contaminated with nitroaromatic compounds, including DNT. It has the great advantage that it can potentially be applied *in situ*, without the need for removal or incineration of the contaminated soil layers, significantly reducing costs associated with transport.

In the technique, a low-level direct current is passed between electrodes embedded in the soil, with the groundwater often acting as the conducting medium (Figure 10.4). Contaminants are mobilised and transformed via several different processes that can occur as a result of the current flow, including ion transport, dissolution, electroosmosis, electrodeposition, direct or indirect redox reactions and precipitation. External fluids can be added to assist the processes taking place, and this is termed enhanced electrokinetic remediation. If the contaminants are not actually degraded by the process, then they are still mobilised from the soil and concentrated into zones where they can be removed by other techniques. A very wide range of contaminants has been treated using this method [72], and pilot-scale operations have also been established, for example for removal of plutonium [76] and nitrate [77] from soils.

There are some examples of soil contaminated with explosives, or compounds representative of explosives, being decontaminated by electrokinetic treatment. Ho *et al*. [78] demonstrated on the laboratory scale the feasibility of *in situ* remediation of soils containing a nitroaromatic compound, *p*-nitrophenol. Their method, 'The Lasagna Process', employed a layered arrangement of electrodes and treatment zones. Granular carbon or solid graphite electrodes were situated to either side (or above and below) a volume of contaminated soil, and a treatment zone was sandwiched between each electrode and the contaminated soil. The treatment zones comprised a sand/activated carbon mixture designed to collect organic contaminants. Upon application of the current, the contaminants were transported from the contaminated zone and moved through the treatment zones, where organic species were collected. Over 99% of *p*-nitrophenol was removed from the contaminated zone, and 90% was collected in the treatment zones. The Lasagna technology was subsequently applied in a

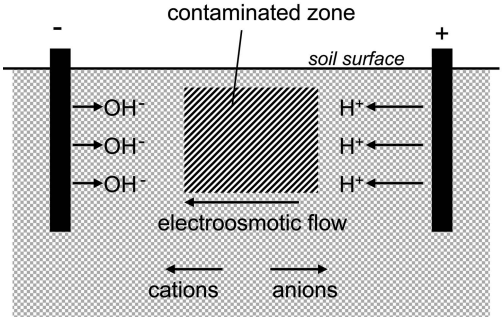

Figure 10.4 *Schematic representation of an* in situ *electrokinetic treatment.*

large-scale field test, achieving 95–99% removal of the persistent pollutant trichloroethylene [79], and further applications have followed [74]. More recently, soils contaminated with DNT have been treated by an electrokinetic method [80]. The treatment resulted in around 40% removal of DNT, mainly occurring via direct electrochemical reduction to aminotoluenes. Inorganic species can also be treated; for example, a pilot-scale experiment has investigated the clean up of soil contaminated with lead at a military facility [81]. The soil was processed for several months, after which time the lead concentration was reduced by 70–85% depending on the soil type, and the cost for electrical energy was estimated at $15–20 per cubic metre of soil per month.

There are several methods used to enhance EK techniques, which generally have the aim of solubilising contaminants or increasing the efficiency of the process in low permeability soils that are otherwise more difficult to treat [82,83]. Given the extent of the problem of soil contaminated with explosives, EK remediation might have an important role to play in the future.

10.4.4 Electrodialysis

Electrodialysis is another method that may be useful in treating wastewater and recovering useful reagents. In this technique, at least one ion-selective membrane separates the cathode and anode compartments. The membrane allows passage of either cations or anions and facilitates separation of one species from another. For example sulfuric acid can be recovered from solutions of sodium sulfate by electrolysis in a cell divided by a cation exchange membrane [4].

Nitric and sulfuric acids remain important reagents in EM manufacture, and a large amount of spent acid is generated every year [84]. Although spent nitrating acid from EM manufacture is not currently recycled, recovery of spent acid has been investigated more extensively in other industries. For example, effluent from uranium oxide waste has been treated by electrodialysis to recover nitric acid [85]. Ammonium nitrate waste has also been treated by membrane electrolysis and electrodialysis to recover ammonium nitrate and nitric acid [86].

10.5 Current Developments and Future Directions

There have been many recent advances in technology that suggest electrochemistry will be a major contributor to green chemistry in the future. Some of this methodology has already been applied in the field of energetic materials.

One of the most rapidly developing areas is the application of electrochemistry in room temperature ionic liquids (RTILs). RTILs have been utilised in many areas of synthesis, but their inherent conductivity makes them a natural choice as an electrolytic medium [87]. Most are quite resistant to oxidation and reduction, and therefore offer a wide solvent window for electrochemistry. In addition, they possess many other desirable properties, including low vapour pressure, nonflammability and air- and water-stability that facilitate safer and greener processes, and a wide range of organic and inorganic substances can be solubilised despite the ionic nature of the medium. Electrochemical reactivity in RTILs may differ significantly to that occurring in aqueous electrolytes, raising the possibility of

exploiting different (and sometimes unexpected) electrosynthetic pathways that may be possible in RTILs.

Liquid perchlorate salts form the basis of a proposed electrochemical route for remediation of ammonium perchlorate (AP) waste [88], which is generated in large quantities from demilitarisation of rocket fuels. Perchlorate is a toxic and hazardous substance, noted as an emerging contaminant by the US EPA [89]. The addition of AP to a phosphonium chloride liquid salt produces a second RTIL, the phosphonium perchlorate, by metathesis. Electrolysis of this RTIL converts all of the perchlorate to innocuous chloride, regenerating the original chloride salt for re-use. The RTIL acts as both substrate and conducting medium in this electrolysis. One drawback was that oxidation of the platinum anode also occurred, but the authors suggested that inexpensive nickel could be used as a sacrificial anode instead.

Efficient derivatisation of nitroaromatic compounds can be achieved in RTILs, in a new environmentally benign approach involving electrochemically assisted nucleophilic aromatic substitution [90]. This synthetic strategy might well serve in developing new nitroaromatic EM. For example, regioselective cyanation could be achieved by electrolysis of trinitroanisole in the presence of cyanide in RTILs based on 1-butyl-3-methylimidazolium cation (BMIM) [90], with different products being obtained depending on the medium employed (Figure 10.3, Reaction 5). Electrochemical oxidative coupling of toluene derivatives has also been demonstrated on the analytical scale [91], in a process analogous to the synthesis of HNBB from TNT. As described above, HNBB might be used in the electrosynthesis of HNS [19].

Different reactive intermediates may be electrogenerated in RTILs, such as reduction of oxygen to superoxide radical and oxidation of chloride ion to Cl_3^-, rather than Cl_2 [87]. The electrosynthesis of hydrogen peroxide in RTIL has been reported and the reagent was used *in situ* for the epoxidation of alkenes [92]. The RTIL could be recovered for use several times before the efficiency of H_2O_2 generation was compromised.

New electrode materials are being developed, and existing ones improved. Advanced carbon materials have been received particular attention [93], such as boron-doped diamond (BDD), microfabricated carbon films and carbon composite materials. BDD electrodes have been extensively investigated [94], due to their mechanical and chemical robustness, and wide potential window even in aqueous media.

It has been demonstrated that on BDD anodes, electrochemical synthesis of perchlorates can be achieved directly from chloride salts [95]. This reduces the number of steps in the synthesis compared to the current industrial electrosynthesis described above, and could form the basis of a more efficient and green route to AP.

Photochemically active electrodes can be prepared by coating conventional materials with photocatalysts such as TiO_2, and RDX has recently been mineralised with such a system [96]. Photolytic and solar methods of degradation are increasingly used in conjunction with electrochemical treatment, to give more efficient and cost-effective processes.

Electrochemical methods have for some time been considered as potentially important contributors to the creation of greener synthetic processes and a cleaner environment. Many of these techniques have been applied in the EM area, and research continues to reveal new possibilities. There are of course practical aspects to be considered, but there are also significant advantages to be realised. This is a rapidly developing area of research, and the

continuing improvements in technology and cell design serve to make electrochemical processes ever more viable on the larger scale.

References

1. Chen, G.H. (2004) Electrochemical technologies in wastewater treatment. *Separation and Purification Technology*, **38**, 11–41.
2. Frontana-Uribe, B.A., Little, R.D., Ibanez, J.G. *et al*. (2010) Organic electrosynthesis: a promising green methodology in organic chemistry. *Green Chemistry*, **12**, 2099–2119.
3. Schäfer, H.J. (2011) Contributions of organic electrosynthesis to green chemistry. *Comptes Rendus Chimie*, **14**, 745–765.
4. Scott, K. (1995) *Electrochemical Processes for Clean Technology*, The Royal Society of Chemistry, Cambridge.
5. Sequeira, C.A.C. and Santos, D.M.F. (2009) Electrochemical routes for industrial synthesis. *Journal of the Brazilian Chemical Society*, **20**, 387–406.
6. Anastas, P.T. and Warner, J.C. (1998) *Green Chemistry: Theory and Practice*, Oxford University Press, Oxford.
7. Pletcher, D. (1982) *Industrial Electrochemistry*, Chapman and Hall Ltd, London.
8. Lund, H. (1973) *Cathodic reduction of nitro groups*, in *Organic Electrochemistry* (ed. M.M. Baizer), Marcel Dekker Inc., New York, pp. 315–345.
9. Wallace, L., Underwood, C.J., Day, A.I. and Buck, D.P. (2011) Electrochemical reduction of nitrotriazoles in aqueous media as an approach to the synthesis of new green energetic materials. *New Journal of Chemistry*, **35**, 2894–2901.
10. Steinhauser, G. and Klapötke, T.M. (2008) "Green" pyrotechnics: A chemists' challenge. *Angewandte Chemie-International Edition in English*, **47**, 3330–3347.
11. Talawar, M.B., Sivabalan, R., Mukundan, T. *et al*. (2009) Environmentally compatible next generation green energetic materials (GEMs). *Journal of Hazardous Materials*, **161**, 589–607.
12. Chavez, D., Hill, L., Hiskey, M. and Kinkead, S. (2000) Preparation and explosive properties of azo- and azoxyfurazans. *Journal of Energetic Materials*, **18**, 219–236.
13. Liu, Y., Gong, X.D., Wang, L.J. *et al*. (2011) Substituent effects on the properties related to detonation performance and sensitivity for 2,2′,4,4′,6,6′-hexanitroazobenzene derivatives. *Journal of Physical Chemistry A*, **115**, 1754–1762.
14. Oxley, J.C., Smith, J.L. and Moran, J.S. (2009) Decomposition of Azo- and Hydrazo-Linked Bis Triazines. *Journal of Energetic Materials*, **27**, 63–93.
15. Sivabalan, R., Anniyappan, M., Pawar, S.J. *et al*. (2006) Synthesis, characterization and thermolysis studies on triazole and tetrazole based high nitrogen content high energy materials. *Journal of Hazardous Materials*, **137**, 672–680.
16. Shipp, K.G. and Kaplan, L.A. (1966) Reactions of alpha-substituted polynitrotoluenes .2. Generation and reactions of 2,4,6-trinitrobenzyl anion. *The Journal of Organic Chemistry*, **31**, 857–861.
17. Bellamy, A.J. (2010) Identification of α-chloro-2,2′,4,4′,6,6′-hexanitrobibenzyl as an impurity in hexanitrostilbene. *Journal of Energetic Materials*, **28**, 1–16.
18. Gilbert, E.E. (1980) The preparation of hexanitrostilbene from hexanitrobibenzyl. *Propellants Explosives, Pyrotechnics*, **5**, 168–172.
19. Firsich, D.W. (1986) "An electrochemical preparation of hexanitrostilbene (HNS) from hexanitrobibenzyl (HNBB)" Report.
20. Firsich, D.W. (1985) "The electrochemistry of hexanitroazobenzene: reactivity with metals and synthetic implications" Report.

21. Meyer, R., Köhler, J. and Homburg, A. (2002) *Explosives*, 5th edn, Wiley-VCH, Weinheim.
22. Badgujar, D.M., Talawar, M.B., Harlapur, S.F. *et al*. (2009) Synthesis, characterization and evaluation of 1,2-bis(2,4,6-trinitrophenyl) hydrazine: A key precursor for the synthesis of high performance energetic materials. *Journal of Hazardous Materials*, **172**, 276–279.
23. Wright, C.M. (1975) 1 Azido-1,1-dinitroalkanes, useful as propellants, United States Patent 3883377.
24. Weber, J.E. and Frankel, M.R. (1990) Synthesis of novel energetic compounds. 8. Electrosynthesis of azidodinitromethyl compounds. *Propellants, Explosives, Pyrotechnics*, **15**, 26–29.
25. Dotson, R.L. (1994) Electrosynthesis of HAN-liquid propellants. *Electrochemical Society Interface*, **3**, 35–37.
26. Killeffer, D.H. (1937) Alcohols from sugar by electrolytic reduction. *Industrial & Engineering Chemistry*, **15**, 489–490.
27. Millar, R.W., Colclough, M.E., Arber, A.W. *et al*. (2010) Clean nitrations using dinitrogen pentoxide - a UK perspective, in *Energetic Materials* (eds J. Howell, T.E. Fletcher), Nova Science, New York, pp. 77–106.
28. Talawar, M.B., Sivabalan, R., Polke, B.G. *et al*. (2005) Establishment of process technology for the manufacture of dinitrogen pentoxide and its utility for the synthesis of most powerful explosive of today - CL-20. *Journal of Hazardous Materials*, **124**, 153–164.
29. Harrar, J.E. and Pearson, R.K. (1983) Electrosynthesis of N_2O_5 by controlled-potential oxidation of N_2O_4 in anhydrous HNO_3. *Journal of the Electrochemical Society*, **130**, 108–112.
30. Fischer, J.W. and Atkins, R.L. (1986) Direct preparation of 1,3,5- triaza-1,3,5-trinitrocyclohexane from hexamethylenetetramine. *Organic Preparations and Procedures International*, **18**, 281–283.
31. Bagg, G.E.G., Salter, D.A. and Sanderson, A.J. (1992) Method of extracting dinitrogen pentoxide from its mixture with nitric acid, United States Patent 5266292.
32. Millar, R.W., Arber, A.W., Endsor, R.M. *et al*. (2011) Clean manufacture of 2,4,6-trinitrotoluene (TNT) via improved regioselectivity in the nitration of toluene. *Journal of Energetic Materials*, **29**, 88–114.
33. Chen, J.P., Zou, S., Pehkonon, S.O. *et al*. (2007) Explosive waste treatment, in *Hazardous Industrial Waste Treatment* (ed. L.K. Wang), Taylor & Francis, Boca Raton, pp. 429–440.
34. Doppalapudi, R., Palaniswamy, D., Sorial, G. and Maloney, S. (2003) Electrochemical pilot scale study for reduction of 2,4-DNT. *Water Science and Technology: A Journal of the International Association on Water Pollution Research*, **47**, 173–178.
35. Brillas, E., Síres, I. and Oturan, M.A. (2009) Electro-fenton process and related electrochemical technologies based on fenton's Reaction Chemistry. *Chemical Reviews*, **109**, 6570–6631.
36. Martínez-Huitle, C.A. and Brillas, E. (2009) Decontamination of wastewaters containing synthetic organic dyes by electrochemical methods: A general review. *Applied Catalysis B*, **87**, 105–145.
37. Panizza, M. and Cerisola, G. (2009) Direct and mediated anodic oxidation of organic pollutants. *Chemical Reviews*, **109**, 6541–6569.
38. Rajeshwar, K., Ibanez, J.G. and Swain, G.M. (1994) Electrochemistry and the environment. *Journal of Applied Electrochemistry*, **24**, 1077–1091.
39. Rodgers, J.D. and Bunce, N.J. (2001) Electrochemical treatment of 2,4,6-trinitrotoluene and related compounds. *Environmental Science & Technology*, **35**, 406–410.
40. Doppalapudi, R.B., Sorial, G.A. and Maloney, S.W. (2002) Electrochemical reduction of simulated munitions wastewater in a bench-scale batch reactor. *Environmental Engineering Science*, **19**, 115–130.
41. Palaniswamy, D.K., Sorial, G.A. and Maloney, S.W. (2004) Electrochemical reduction of 2,4, 6-trinitrotoluene. *Environmental Engineering Science*, **21**, 203–218.

42. Bonin, P.M.L., Bejan, D., Schutt, L. *et al*. (2004) Electrochemical reduction of hexahydro-1,3, 5-trinitro-1,3,5-triazine in aqueous solutions. *Environmental Science & Technology*, **38**, 1595–1599.
43. Simková, L., Klíma, J., Sazama, P. and Ludvík, J. (2011) Electrochemical investigation of 2,2-dinitroethene-1,1-diamine (FOX-7) in aqueous media. *Journal of Solid State Electrochemistry*, **15**, 2133–2139.
44. Miles, M.H. and Fine, D.A. (1981) The reduction of propylene-glycol dinitrate and other related nitrate esters on silver electrodes. *Journal of Electroanalytical Chemistry*, **127**, 143–155.
45. Polson, J.R. (1980) Electrolysis of lead azide, United States Patent 4236982.
46. Gilbert, D.M. and Sale, T.C. (2005) Sequential electrolytic oxidation and reduction of aqueous phase energetic compounds. *Environmental Science & Technology*, **39**, 9270–9277.
47. Gent, D.B., Wani, A.H., Davis, J.L. and Alshawabkah, A. (2009) Electrolytic redox and electrochemical generated alkaline hydrolysis of hexahydro-1,3,5-trinitro-1,3, 5 triazine (RDX) in sand columns. *Environmental Science & Technology*, **43**, 6301–6307.
48. Li, Y.P., Lu, Z.Y., Mu, J.H. *et al*. (2007) Treatment of TNT red-water by electrolytic method. *Progress in Environmental Science and Technology*, **I**, 1133–1136.
49. Wallace, L., Cronin, M.P., Day, A.I. and Buck, D.P. (2009) Electrochemical method applicable to treatment of wastewater from nitrotriazolone production. *Environmental Science & Technology*, **43**, 1993–1998.
50. Ayoub, K., vanHullebusch, E.D., Cassir, M. and Bermond, A. (2010) Application of advanced oxidation processes for TNT removal: A review. *Journal of Hazardous Materials*, **178**, 10–28.
51. Wang, J.L. and Xu, L.J. (2012) Advanced oxidation processes for wastewater treatment: formation of hydroxyl radical and application. *Critical Reviews in Environmental Science and Technology*, **42**, 251–325.
52. Bonin, P.M.L., Bejan, D., Radovic-Hrapovic, Z. *et al*. (2005) Indirect oxidation of RDX, HMX, and CL-20 cyclic nitramines in aqueous solution at boron-doped diamond electrodes. *Environmental Chemistry*, **2**, 125–129.
53. Chen, W.S. and Liang, J.S. (2009) Electrochemical destruction of dinitrotoluene isomers and 2,4,6-trinitrotoluene in spent acid from toluene nitration process. *Journal of Hazardous Materials*, **161**, 1017–1023.
54. Lee, K.B., Gu, M.B. and Moon, S.H. (2001) In situ generation of hydrogen peroxide and its use for enzymatic degradation of 2,4,6-trinitrotoluene. *Journal of Chemical Technology and Biotechnology (Oxford, Oxfordshire: 1986)*, **76**, 811–819.
55. Abramov, V.O., Abramov, O.V., Gekhman, A.E. *et al*. (2006) Ultrasonic intensification of ozone and electrochemical destruction of 1,3-dinitrobenzene and 2,4-dinitrotoluene. *Ultrasonics Sonochemistry*, **13**, 303–307.
56. Chen, Y., Hong, L., Han, W.Q. *et al*. (2011) Treatment of high explosive production wastewater containing RDX by combined electrocatalytic reaction and anoxic-oxic biodegradation. *Chemical Engineering Journal*, **168**, 1256–1262.
57. Zoh, K.D. and Stenstrom, M.K. (2002) Fenton oxidation of hexahydro-1,3,5-trinitro-1,3, 5-triazine (RDX) and octahydro-1,3,5,7-tetranitro-1,3,5,7-tetrazocine (HMX). *Water Research*, **36**, 1331–1341.
58. Liou, M.J., Lu, M.C. and Chen, J.N. (2003) Oxidation of explosives by Fenton and photo-Fenton processes. *Water Research*, **37**, 3172–3179.
59. Oh, S.Y., Chiu, P.C., Kim, B.J. and Cha, D.K. (2003) Enhancing Fenton oxidation of TNT and RDX through pretreatment with zero-valent iron. *Water Research*, **37**, 4275–4283.
60. LeCampion, L., Giannotti, C. and Ouazzani, J. (1999) Photocatalytic degradation of 5-nitro-1,2,4-triazol-3-one NTO in aqueous suspention of TiO_2. Comparison with Fenton oxidation. *Chemosphere*, **38**, 1561–1570.

61. Barreto-Rodrigues, M., Silva, F.T. and Paiva, T.C.B. (2009) Combined zero-valent iron and fenton processes for the treatment of Brazilian TNT industry wastewater. *Journal of Hazardous Materials*, **165**, 1224–1228.
62. Oh, S.Y., Cha, D.K., Chiu, P.C. and Kim, B.J. (2004) Conceptual comparison of pink water treatment technologies: granular activated carbon, anaerobic fluidized bed, and zero-valent iron-Fenton process. *Water Science and Technology: A Journal of the International Association on Water Pollution Research*, **49**, 129–136.
63. Le, T.G. and Bermond, A. (2006) Experimental and modelling approach for the comparison of Fenton and Electro-Fenton processes - Preliminary results. *Journal of Advanced Oxidation Technologies*, **9**, 35–42.
64. Oturan, M.A., Oturan, N., Edelahi, M.C. *et al*. (2011) Oxidative degradation of herbicide diuron in aqueous medium by Fenton's reaction based advanced oxidation processes. *Chemical Engineering Journal*, **171**, 127–135.
65. Rosales, E., Pazos, M. and Sanromán, M.A. (2012) Advances in the Electro-Fenton process for remediation of recalcitrant organic compounds. *Chemical Engineering & Technology*, **35**, 609–617.
66. Chen, W.S. and Liang, J.S. (2008) Decomposition of nitrotoluenes from trinitrotoluene manufacturing process by Electro-Fenton oxidation. *Chemosphere*, **72**, 601–607.
67. Chen, W.S. and Lin, S.Z. (2009) Destruction of nitrotoluenes in wastewater by Electro-Fenton oxidation. *Journal of Hazardous Materials*, **168**, 1562–1568.
68. Ayoub, K., Nelieu, S., vanHullebusch, E.D. *et al*. (2011) Electro-Fenton removal of TNT: Evidences of the electro-chemical reduction contribution. *Applied Catalysis B*, **104**, 169–176.
69. Zhu, X.P. and Ni, J.R. (2011) The improvement of boron-doped diamond anode system in electrochemical degradation of p-nitrophenol by zero-valent iron. *Electrochim Acta*, **56**, 10371–10377.
70. Flox, C., Cabot, P.L., Centellas, F. *et al*. (2007) Solar photoelectro-Fenton degradation of cresols using a flow reactor with a boron-doped diamond anode. *Applied Catalysis B*, **75**, 17–28.
71. Casado, J. and Fornaguera, J. (2008) Pilot-scale degradation of organic contaminants in a continuous-flow reactor by the Helielectro-Fenton method. *Clean-Soil Air Water*, **36**, 53–58.
72. Acar, Y.B., Gale, R.J., Alshawabkeh, A.N. *et al*. (1995) Electrokinetic remediation - basics and technology status. *Journal of Hazardous Materials*, **40**, 117–137.
73. Acar, Y.B. and Alshawabkeh, A.N. (1993) Principles of electrokinetic remediation. *Environmental Science & Technology*, **27**, 2638–2647.
74. Huang, D.Q., Xu, Q., Cheng, J.J. *et al*. (2012) Electrokinetic remediation and its combined technologies for removal of organic pollutants from contaminated soils. *International Journal of Electrochemical Science*, **7**, 4528–4544.
75. Superfund, US Environmental Protection Agency (2013) Remediation technologies:, http://www.epa.gov/superfund/remedy/tech/remed.htm (accessed C 9 Sept 2013).
76. Agnew, K., Cundy, A.B., Hopkinson, L. *et al*. (2011) Electrokinetic remediation of plutonium-contaminated nuclear site wastes: Results from a pilot-scale on-site trial. *Journal of Hazardous Materials*, **186**, 1405–1414.
77. Lee, Y.J., Choi, J.H., Lee, H.G. *et al*. (2011) Pilot-scale study on in situ electrokinetic removal of nitrate from greenhouse soil. *Separation and Purification Technology*, **79**, 254–263.
78. Ho, S.V., Sheridan, P.W., Athmer, C.J. *et al*. (1995) Integrated in-situ soil remediation technology - the lasagna process. *Environmental Science & Technology*, **29**, 2528–2534.
79. Ho, S.V., Athmer, C., Sheridan, P.W. *et al*. (1999) The Lasagna technology for in situ soil remediation. 2. Large field test. *Environmental Science & Technology*, **33**, 1092–1099.
80. Reddy, K.R., Darko-Kagya, K. and Al-Hamdan, A.Z. (2011) Electrokinetic remediation of chlorinated aromatic and nitroaromatic organic contaminants in clay soil. *Environmental Engineering Science*, **28**, 405–413.

81. Alshawabkeh, A.N., Bricka, R.M. and Gent, D.B. (2005) Pilot-scale electrokinetic cleanup of lead-contaminated soils. *Journal of Geotechnical and Geoenvironmental Engineering*, **131**, 283–291.
82. Gomes, H.I., Dias-Ferreira, C. and Ribeiro, A.B. (2012) Electrokinetic remediation of organochlorines in soil: Enhancement techniques and integration with other remediation technologies. *Chemosphere*, **87**, 1077–1090.
83. Yeung, A.T. and Gu, Y.Y. (2011) A review on techniques to enhance electrochemical remediation of contaminated soils. *Journal of Hazardous Materials*, **195**, 11–29.
84. Paul, N.C. (1997) Modern explosives and nitration techniques, in *Explosives in the Service of Man* (eds J.E. Dolan and S.S. Langer), The Royal Society of Chemistry, Cambridge, pp. 79–91.
85. Kim, K.W., Hyun, J.T., Lee, K.Y. *et al.* (2012) Recycling of acidic and alkaline solutions by electrodialysis in a treatment process for uranium oxide waste using a carbonate solution with hydrogen peroxide. *Industrial & Engineering Chemistry Research*, **51**, 6275–6282.
86. Gain, E., Laborie, S., Viers, P. *et al.* (2002) Ammonium nitrate wastewater treatment by coupled membrane electrolysis and electrodialysis. *Journal of Applied Electrochemistry*, **32**, 969–975.
87. Hapiot, P. and Lagrost, C. (2008) Electrochemical reactivity in room-temperature ionic liquids. *Chemical Reviews*, **108**, 2238–2264.
88. Cordes, D.B., Smiglak, M., Hines, C.C. *et al.* (2009) Ionic liquid-based routes to conversion or reuse of recycled ammonium perchlorate. *Chemistry-A European Journal*, **15**, 13441–13448.
89. Federal Facilities Restoration and Reuse Office, US Environmental Protection Agency (2013) Emerging contaminants: http://www.epa.gov/fedfac/documents/emerging_contaminants.htm (accessed 9 Sept 2013).
90. Cruz, H., Gallardo, I. and Guirado, G. (2011) Electrochemically promoted nucleophilic aromatic substitution in room temperature ionic liquids-an environmentally benign way to functionalize nitroaromatic compounds. *Green Chemistry*, **13**, 2531–2542.
91. Evans, R.G. and Compton, R.G. (2006) A kinetic study of the reaction between N, N-dimethyl-p-toluidine and its electrogenerated radical cation in a room temperature ionic liquid. *Chemphyschem*, **7**, 488–496.
92. Tang, M.C.Y., Wong, K.Y. and Chan, T.H. (2005) Electrosynthesis of hydrogen peroxide in room temperature ionic liquids and in situ epoxidation of alkenes. *Chemical Communications*, 1345–1347.
93. McCreery, R.L. (2008) Advanced carbon electrode materials for molecular electrochemistry. *Chemical Reviews*, **108**, 2646–2687.
94. Luong, J.H.T., Male, K.B. and Glennon, J.D. (2009) Boron-doped diamond electrode: synthesis, characterization, functionalization and analytical applications. *Analyst*, **134**, 1965–1979.
95. Sánchez-Carretero, A., Saez, C., Cañizares, P. and Rodrigo, M.A. (2011) Electrochemical production of perchlorates using conductive diamond electrolyses. *Chemical Engineering Journal*, **166**, 710–714.
96. Tian, F., Hitchman, M.L. and Shamlian, S.H. (2012) Photocatalytic and photoelectrocatalytic degradation of the explosive RDX by TiO_2 thin films prepared by CVD and anodic oxidation of Ti. *Chemical Vapor Deposition*, **18**, 112–120.

Index

Green Energetic Materials, First Edition. Edited by Tore Brinck.